

HYDRAULIC TURBINES

Their Design and Equipment

HYDRAULIC TURBINES
Their Design and Equipment

HYDRAULIC TURBINES

Their Design and Equipment

by

MIROSLAV NECHLEBA, Dr. Techn., M. E.,

*Correspondent Member of the Czechoslovak Academy of Science,
State Prize Laureate, Professor of Hydraulic Machines
at the Slovak Technical University in Bratislava*

ARTIA - PRAGUE

CONSTABLE & CO LTD

10-12 ORANGE STREET, LONDON, W.C.2

HYDRAULIC TURBINES

Their Design and Equipment

by

MIROSLAV NECHLEBA, Dr Techn., M.E.

Translated from the Czech edition by

CHARLES MAYER, CH.E. and A. G. EVANS

Copyright 1957 by ARTIA Prague

Printed in Czechoslovakia

This book presents a treatise on the design of hydraulic turbines of the Francis, Kaplan and Pelton types, their control and accessories. In places where the solution of designing problems requires special calculations in the field of hydraulics, the basic assumptions for this purpose are attached to the description of the individual plants, to facilitate the designer's work and save time.

The book is intended for designers, plant engineers as well as for students at universities and technical schools, and is an efficient aid in the erection of hydraulic power stations. The author has been awarded a State Prize Laureateship for outstanding theoretical and practical work in the field of construction and control of hydraulic turbines.

CONTENTS

Contents	5
Symbols	11

Part I

INTRODUCTION TO THEORY OF HYDRAULIC TURBINES

I. Hydraulic Energy, Hydraulic Motors, Classification of Turbines	15
II. Relations between Head, Flow Rate and Output. - Efficiency	24
1. Output and Efficiency	24
2. Total or Gross and Effective or Net Head	26
III. Action of the Flow on the Duct	30
1. Flow in the Stationary Duct, Moment of the Duct	30
2. Moment with which the Flow acts upon a Revolving Duct - Energy Equation	36
3. Hydraulic Efficiency	43
4. Flow Rate Equation; Overpressure of the Runner	45
IV. Reaction (Overpressure) and Impulse (Constant-Pressure) Turbines	49
V. Draft Tube; Cavitation	50
1. Draft Tube	50
2. Cavitation	54
VI. Examples of Turbine Designs and Output Control Methods	57
VII. Hydraulic Similarity	64
1. Influence of Head Variations	65
2. Influence of Size	68
3. Unit Values	69
VIII. Specific Speed of the Turbine and Specific Velocities	70
1. Specific Speed from Reference Values	70
2. Specific Velocities	71
3. Specific Speed Determined by Design Data	74
IX. Efficiency Variations in Dependence on the Dimensions of the Machine	81
X. Turbine Performance at Operation Variations	86
1. Turbine Performance at Constant Head and Speed and Varying Flow Rate	86
2. Behavior of the Turbine at Speed Variations	92

XI. <i>Characteristic of a Turbine</i>	97
1. Normal Characteristic	97
2. Influence of Efficiency Variations upon the Unit Values	103
XII. <i>Braun's Diagrams</i>	106
1. Derivation of the Diagram	106
2. Influence of Filling Variations in the Francis Turbine	112
3. Influence of Filling Variations in the Kaplan Turbine	116
4. Axial-Flow Propeller Turbine with Adjustable Runner and Stationary Guide Wheel Blades	117
XIII. <i>Application of Hydraulic Similarity in Turbine Manufacture</i>	118
1. General Requirements of Manufacture.	118
2. Selection of the Type Series according to Specific Speeds and the Diameter Series according to Flow Rates	119

Part II

TURBINE DESIGN

1. FRANCIS TURBINES

A. Hydraulic Investigation.

I. <i>Runner Design</i>	123
1. Elementary Turbines; Meridional Flow Field	123
2. Shape of the Turbine Space	131
3. Flow without Extraction of Energy	138
4. Position of the Inlet and Outlet Edges of the Blade; Increase in Meridional Velocities due to the Thickness of the Blade	140
5. Representation of the Blade Cross Sections on the Flow Surfaces and Representation of the Blade	145
6. Shape of the Blade Duct.	152
7. Interrelation of the Velocity Diagrams on the Flow Surfaces; Oblique Discharge from the Guide Apparatus	157
8. Measurable Widths at the Outlet Edge	162
9. General Hydraulic Design of the Runner of the Francis Turbine	163
10. Control of the Cavitation Coefficient	176
11. Strength Control of the Runner Blades	179
12. Hydraulic Load of the Runner	189
II. <i>Design of the Guide Wheel</i>	200
1. Hydraulic Design of the Guide Wheel	200
2. Forces Acting upon the Guide Blade	204
III. <i>Hydraulic Design of the Spiral</i>	209
IV. <i>Hydraulic Design of a Draft Tube</i>	218

B. Actual Design

I. <i>Design of the Machine and Construction Units</i>	224
II. <i>Runner and Shaft</i>	225
1. Runner	225
2. Cavitation and Material of the Runner	235
3. Recalculation of the Cavitation Coefficient	239
4. Sealing of the Runner Gaps	241
5. Shaft	242
III. <i>Guide Apparatus</i>	250
1. Guide Blades and Their Seating	250
2. Regulating Mechanism, Links, Regulating Ring	259
IV. <i>Extension of the Regulation</i>	278
V. <i>Spiral with Stay Blade Ring</i>	284
VI. <i>Top and Bottom Lids of the Turbine</i>	293
1. Lids	293
2. Parts of the Lids	296
VII. <i>Draft Tube and Air Supply Valves</i>	305
VIII. <i>Gear Case with Auxiliary Drives.</i>	309
C. General Remarks on Assembly Work	309

2. PROPELLER AND KAPLAN TURBINES

A. Hydraulic Investigation

I. <i>Runner Design</i>	312
1. Theoretical Introduction.	312
2. Equation for the Application of Airfoils to the Design of Turbine Blades	322
3. Aerodynamic Properties of Airfoils	328
4. Variation of the Lift Coefficient for Wings arranged into a Lattice System	340
5. Shape of the Space of the Turbine, Meridional Flow Field and Interrelation of the Velocity Diagrams on the Flow Surfaces	342
6. General Procedure in Designing the Runner of a Propeller (Kaplan) Turbine	344
7. Control of the Cavitation Coefficient	345
8. Stability of the Flow along the Blade	354
9. Strength Control of the Runner Blade	355
10. Hydraulic Load of the Runner	358
II. <i>Design of the Runner, Spiral and Draft Tube</i>	359

B. Actual Design

I. <i>Layout of the Machine and Constructional Units</i>	359
II. <i>Runner and Shaft</i>	359
1. Runner	359
2. Shaft	363

III. Inner Lid	371
C. General Assembly Procedure	372

3. PELTON TURBINES

A. Hydraulic Investigation	
I. Water Jet	374
1. Free Jet	374
2. Diameter of the Jet	380
II. Runner	381
1. Diameter of the Runner	381
2. Velocity Diagrams	384
3. Number of Blades	389
4. Inclination of the Blade to the Radius	392
5. Notch of the Blade and Blade Dimensions	396
6. Force Acting upon the Bucket	401
III. Output Regulation	411
1. Deflector and Deviator	411
2. Nozzles and Needle	415
3. Forces acting upon the Needle	417
B. Actual Design	
I. Francis or Pelton?	423
II. Arrangement of Pelton Turbines	425
III. Parts	426
1. Casing	426
2. Runner	427
3. Nozzles - Needles	431
4. Deflector	432

Part III

EQUIPMENT OF HYDRAULIC TURBINES

A. CONTROLLERS

I. Basic Principles of Controllers	433
II. Particulars of Design	439
1. Oil Pumps	439
2. Unloading Valve (Controller of Oil Pressure in the Air Vessel)	443
3. Pressure Tank	445
4. Controller of Air Content in the Pressure Tank	445
5. Control Valve	446
6. Servomotor	449

7. Receiver Tank	450
8. Governor	450
III. General Lay-Out of Controllers	458
IV. Calculation of Controllers	466
V. Checking of Controllers	475

B. THRUST BEARINGS

I. Purpose and Location of Thrust Bearings	476
II. The Hydrodynamic Theory	481
1. Viscosity of Oil	481
2. Hydrodynamic Theory of Bearings	484
III. Design of Thrust Bearings	507
1. Methods of Supporting the Segments	507
2. Material of Segments and Adhesion	512
IV. Guide Bearings and Their Location	516
V. General Lay-Out of Thrust Bearings	521
VI. Hanger structure	526
VII. Lubricating and Cooling Installations	529

C. CONDUITS

I. Pipes	535
1. Generally	535
2. Seating of Pipes	539
3. Calculation of Stability of Anchor Blocks	545
4. Calculation of Wall Thickness	549
5. Pipes for Extremely High Heads	552
II. Water Hammer	554
1. Basic Relations and Calculation	554
2. Graphical Method of Water Hammer Analysis	568
III. Surge Tanks	578
1. Purpose of Surge Tanks and Stability	578
2. Dimensioning of Surge Tanks	582
3. More Complicated Surge Tanks	583
4. Graphical Method to Determine Level Changes	585
5. Stability in Case of Great Level Oscillations	590
6. The Safety Factor	591
IV. Closing Organs for Conduits	591
1. Quick-Closing Device	591
2. Quick-Closing Gates	593
3. Quick-Closing Devices for Pipes	598
4. High-Pressure Inlet Valves	607
V. Pressure Regulators	611

STARTING OPERATION AND GUARANTEE MEASUREMENTS

I. Starting Operation	618
II. Guarantee Measurements	623
Literature	628
Index	633

SYMBOLS

A	controller capacity
a	acceleration, cross section of blade ducts on flow surfaces, velocity of pressure wave in pipes
a^{\times}	measurable cross section of blade ducts
B	face of guide wheel
C	absolute velocity of flow in turbine, flow velocity in piping or around immersed bodies
$c_i = \sqrt{1 - q} + v$	specific indicated velocity
D, d	diameter (D in particular diameter of runner and piping)
E	modulus of elasticity
F	area
f	coefficient of friction, also area
G	weight
g	gravitational acceleration
H	head in metres of water column, pressure head in metres of water column
H_B	barometric pressure in metres of water column
H_t	tension of water vapour in metres of water column
$H_b = H_B - H_t$	barometric pressure less tension of water vapour in metres of water column
H_s	suction head
H_z, h_z	losses in metres of water column
$h = \frac{p}{\gamma}$	water column corresponding to pressure p
I	Coriolis force
K, k	constants
L, l	length
m	mass
N	output
N_{ef}	effective output
N_{th}	theoretical output

N_1 output under head of 1 m
 $N'_1 = \frac{N}{D^2 \sqrt{H^3}}$ unit output
 n speed
 n_n normal (rated) speed
 n_p runaway speed
 n_1 speed under head of 1 m
 $n'_1 = \frac{nD}{\sqrt{H}}$ unit speed
 $n_s = \frac{n}{H} \sqrt{\frac{N}{H}}$ specific speed of turbine
 O Centrifugal force
 P force
 p pressure in kg/cm²
 Re Reynolds number
 Q flow-rate, through-flow
 Q_η flow-rate at best efficiency
 Q_{\max} maximum flow-rate of turbine
 Q_1 flow-rate under head of 1 m
 $Q'_1 = \frac{Q}{D^2 \sqrt{H}}$ unit flow-rate
 R, r radius
 s thickness of blade or pipe wall
 T time constants
 $T_a = \frac{GD^2 n^2}{270,000 N_{hp}}$ starting time of machine
 T_i falling time of isodrome
 $T_L = \frac{L}{a}$ half-time of one interval of the pressure wave
 $T_{2L} = \frac{2L}{a}$ time of one interval of the pressure wave
 $T_l = \frac{\Sigma L C}{gH}$ starting time of the pipe
 T_n half starting time of the revolving mass
 $T_s(T_0)$ time of closure (opening) of the controller
 t spacing, time

U peripheral velocity of turbine
 V flow velocity
 W relative velocity of flow in turbine
 z number of blades
 $c = \frac{C}{\sqrt{2gH}}$ specific absolute velocity of flow in turbine
 $u = \frac{U}{\sqrt{2gH}}$ specific peripheral velocity of turbine runner
 $w = \frac{W}{\sqrt{2gH}}$ specific relative velocity of flow in turbine
 w_z specific shock velocity
 \circ in connection with turbine subscript for conditions immediately in front of inlet into runner
 1 similarly immediately in back of inlet into runner
 2 similarly immediately in front of outlet from runner
 3 similarly immediately after discharge from runner and at the beginning of draft tube
 4 similarly at end of draft tube
 $'$ similarly at outlet from guide apparatus
 $''$ similarly at inlet into guide wheel
 $'''$ similarly at outlet from stay blades of spiral
 iv similarly at inlet into stay blades of spiral
 s similarly for inlet into draft tube $C_s \doteq C_3$
 $\alpha = c_2^2$ relative discharge loss from runner
 α angle between velocities c and u
 β angle (blade) of the velocities w and u , acceleration coefficient of the stabilisator
 γ specific gravity of water
 Γ circulation
 δ droop of the governor
 δ_i permanent droop
 $\eta = \eta_h \cdot \eta_v \cdot \eta_m$ total efficiency of turbine
 $\eta_h = 1 - \varrho + \nu - \alpha - \zeta = c_i^2 - c_2^2 - w_z^2$ hydraulic efficiency of turbine
 η_m mechanical efficiency
 η_s efficiency of draft tube
 η_v volumetric efficiency of turbine

φ coefficient of through-flow restriction by blades, outflow coefficient, relative velocity increase

$\psi = \Delta\beta$ deviation angle of blade

μ viscosity

ν kinematic viscosity

$\nu = \eta_s \frac{C_2^2 - C_4^2}{2gH}$ relative regain of draft tube

ϱ relative losses in turbine, also characteristic of piping

$\sigma = \frac{H_b - H_s}{H}$ Thoma cavitation coefficient

ξ loss coefficient

$\zeta = w_z^2$ relative shock loss

$\omega = \frac{n}{9.55}$ angular velocity

PART I

INTRODUCTION TO THE THEORY OF HYDRAULIC TURBINES

I. HYDRAULIC ENERGY, HYDRAULIC MOTORS, CLASSIFICATION OF TURBINES

Hydraulic motors utilize the energy of water ways. The water moves from higher positions – from places of higher energy – to lower positions – to places of lower

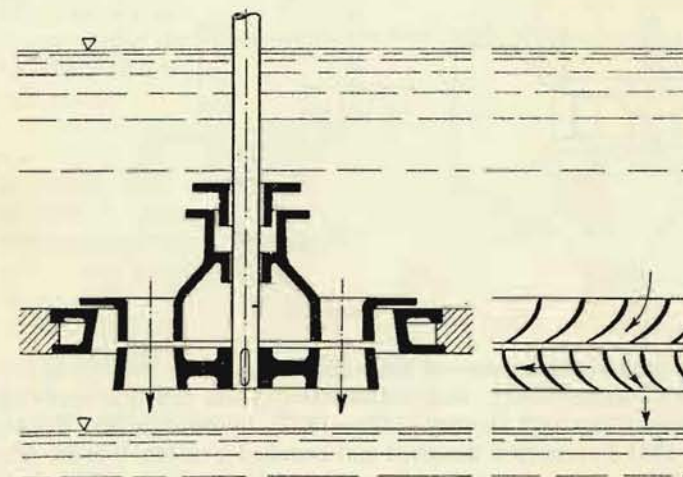


Fig. 1

energy – and its original potential energy is converted into kinetic energy at the shaft of the machine. From the place of the lowest potential energy – from the sea – the water returns to places of higher energy by the action of solar heat, which maintains the circulation of water in the nature. Hydraulic motors, therefore indirectly utilize the energy of the sun.

In ancient times hydraulic energy was utilized by means of water-wheels, the origin of which is very old. According to rather unreliable sources the first blade-fitted water-wheel was invented by Ctebios as early as 135 B. C. At the beginning

of the Christian era, the water-wheel was coming into use for driving mills in the Near East, this previously had been done by the slaves.

From 260 to 300 A. D. there was already in use a complete large-scale mill in France, near Arles¹⁾, utilizing a head of 18 m by a total of eighteen water-wheels arranged in two parallel channels.

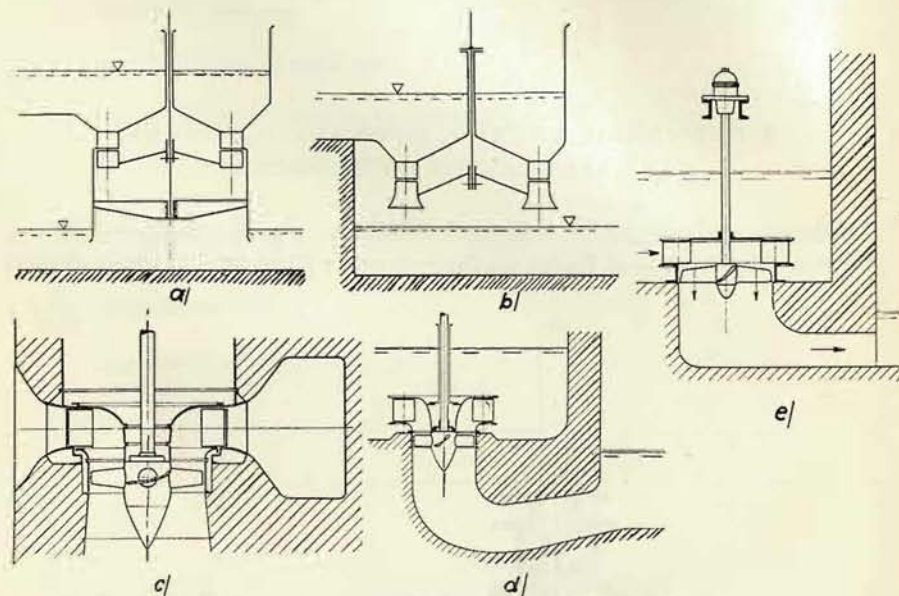


Fig. 2

Turbines in the modern sense of the word, based on the theoretical foundations developed by Leonard Euler, were not introduced into practical application, until the beginning of the 19th century (1826—1827), by Bourdin and Fourneyron in France. In 1835 Fourneyron designed and installed a turbine²⁾ at St. Blasien, for a head of 108 m and a maximum flow rate of 30 litres/sec. which had a speed of 2300 r. p. m., and an output of 40 h. p., and was in operation until 1865.

Water-wheels are for the greater part driven by the weight of water.³⁾ It must be also mentioned that there existed also hydraulic motors driven by the pressure energy of water; these were hydraulic piston motors. The pressure head of the water was alternately distributed by means of a slide valve to either side of the

¹⁾ Sylvestre V.: Contribution a l'histoire de la houille blanche..., La Houille Blanche (1946), p. 293.

²⁾ Lectures of Prof. Ing. L. Grimm at the Technical University, Brno.

³⁾ For more details regarding water-wheels see Hýbl J.: Vodní motory, 1. díl (Hydraulic Motors, Part 1), Prague ČMT 1922, pp. 152—170.

piston, and put the latter into a straight, reciprocating motion which by a crank mechanism was converted into rotary motion. It is also possible to employ directly a rotary piston. These motors were clumsy and are no longer used.

Hydraulic turbines, which have displaced both earlier types of machines, are driven by the kinetic energy of water. The water first flows through stationary, guide ducts (Fig. 1), where either the total pressure energy, or only part of it, is converted into kinetic energy. The water flows from the guide ducts into the runner ducts which are curved in an opposite direction to that of the guide ducts; the pressure of the flow on the curved blades rotates the runner.

When the total pressure energy of water, expressed in metres of water column along the head H , turns into kinetic energy in the guide ducts, the water will emerge from the latter under zero pressure at a theoretical velocity of $C = \sqrt{2gH}$. Then the water pressure will not change during the flow through the runner ducts

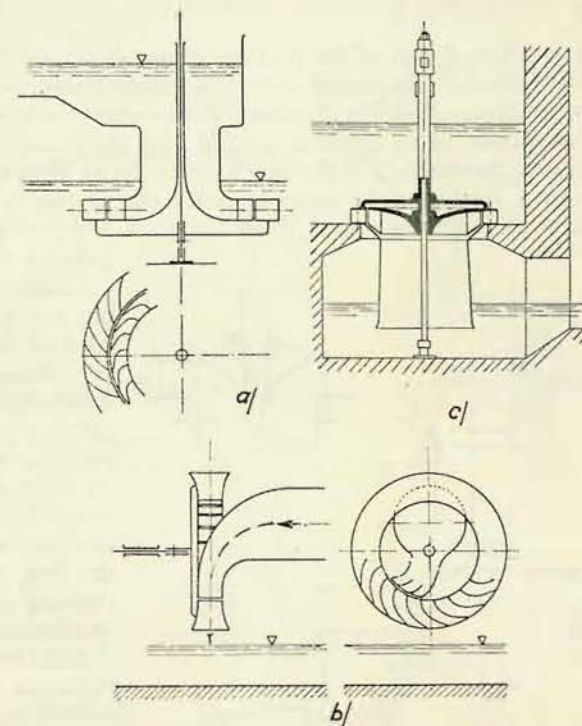


Fig. 3

and so when discharged from the runner will be at the same pressure as at the inlet. Therefore, these turbines are named constant-pressure or impulse turbines. During its flow through the runner, the water presses on the blade, the blade moves and so operates. Therefore the energy of the water leaving the runner must be lower than the energy of the water entering the runner. For this reason the velocity of the water discharging from the runner should be lower than the velocity at the inlet. Here, the absolute velocity is meant, as appearing to an observer located outside the runner. The velocity of the water along the blade, i. e. the relative velocity, as would appear to an observer moving with the runner, is the same from the inlet into the runner to the outlet, for there is no overpressure between the beginning and the end of the blade duct that would accelerate

it. The relative velocity changes its direction only owing to the curvature of the blade.

If, however, only part of the pressure energy in the guide ducts is converted into kinetic energy, the outlet velocity of the water leaving the guide ducts will

be $C < \sqrt{2gH}$. This water will, therefore, still have a static head of $\gamma \left(H - \frac{C^2}{2g} \right)$.

This residual part of the pressure energy is converted during the passage of the water through the runner ducts into kinetic energy, so that the static head of the water decreases in the direction of the outlet; the relative velocity, however – as determined by an observer moving with the runner ducts – increases from the inlet to the outlet. The absolute velocity (for an observer outside the runner) is, of course, smaller at the outlet from the runner than at the inlet. Since the water flows through the runner ducts under an overpressure, this type of turbine is called a pressure turbine.

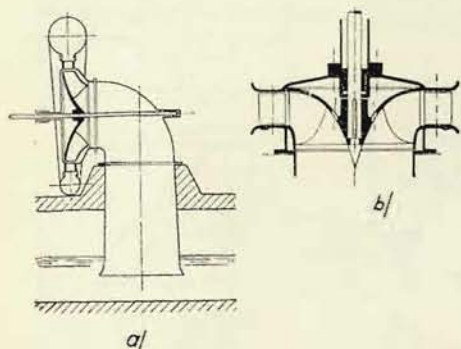


Fig. 4 (a, b)

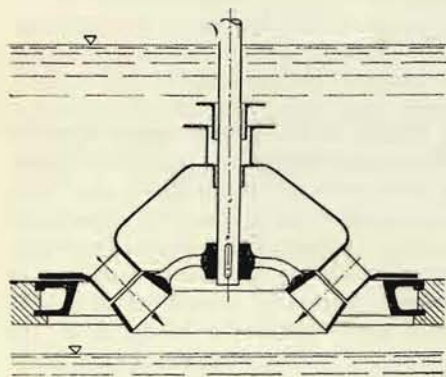


Fig. 5

Constant-pressure or impulse turbines are also termed action turbines, whereas pressure turbines are known as reaction turbines; the latter term is derived from the fact that in pressure turbines the water flow in the runner ducts is accelerated, by which a reaction on the runner blades is created. As, however, a reaction on the blades can also be caused by a mere curvature of the flow, as in the case of constant-pressure turbines, these terms cannot be considered correct.

Apart from the above classification, hydraulic turbines are also distinguished by the direction in which the water flows into and out of the runner in relation to the turbine shaft, no regard being taken to the circular flow of the water around the shaft. When the water flows through the runner parallel to the axis of the shaft, the turbine is called an axial-flow turbine (Fig. 2a—c). When the water flows through the runner in a direction perpendicular to the shaft, the turbine is known as a radial flow turbine (Fig. 3a—c); when the direction of the flow changes in the space of the runner from radial to axial, the turbine

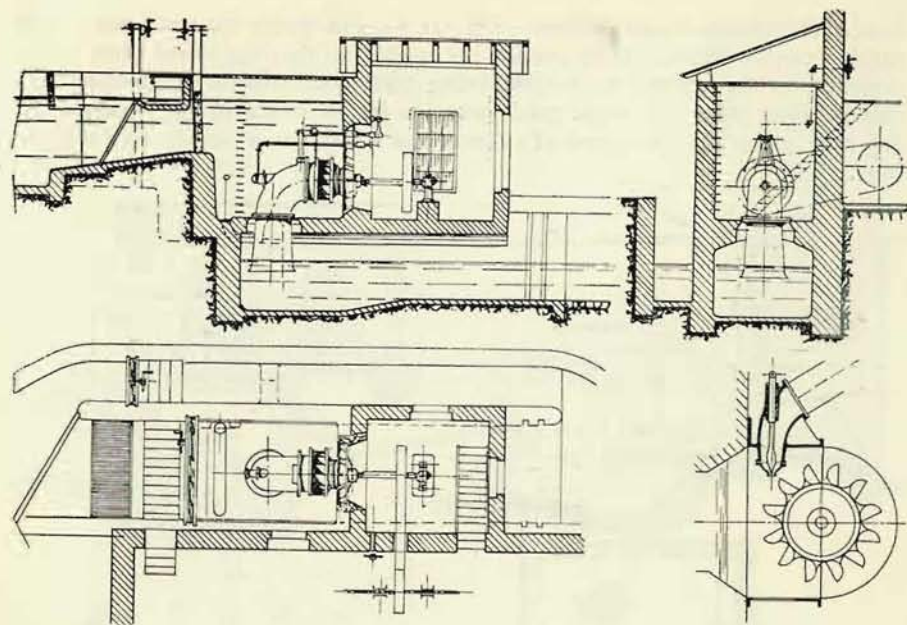


Fig. 7

Fig. 6

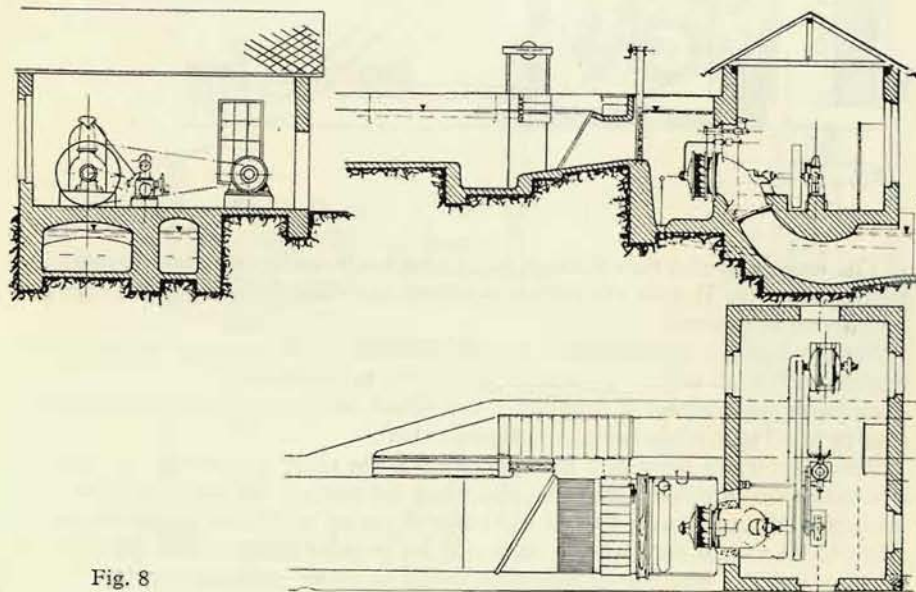


Fig. 8

is termed radial or mixed flow (Fig. 4a, b). The guide wheel of a radial-flow turbine can be located either outside the runner, so that the water flows in the direction to the centre, the turbine being termed centripetal or turbine with external inlet (Fig. 3c), or the guide wheel is placed inside of the runner (Fig. 3a), and in this case we speak of a centrifugal turbine or a turbine with internal inlet.

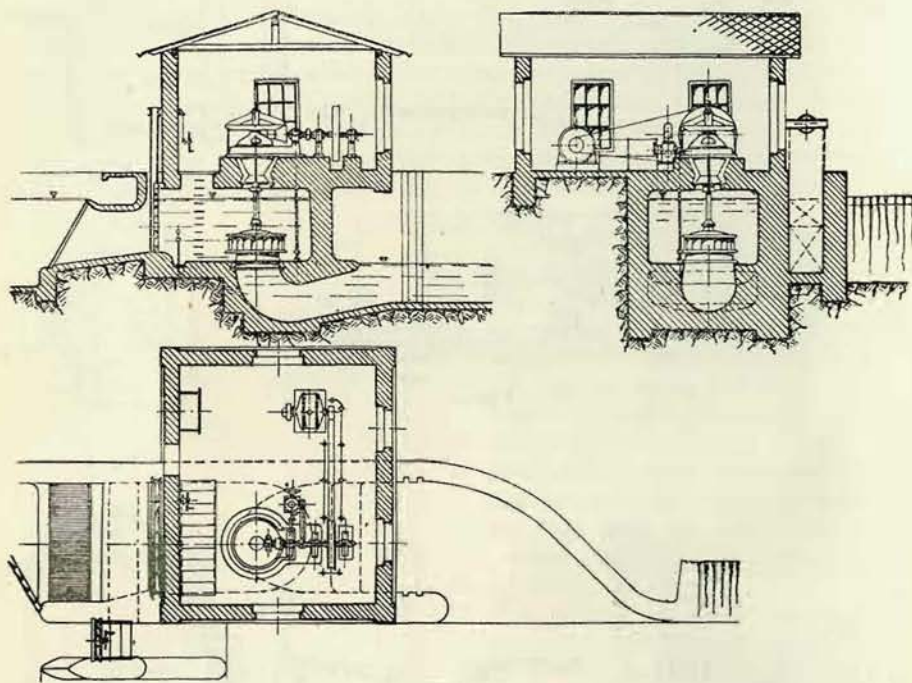


Fig. 9

The water may also flow through guide wheel and runner in a direction inclined to the shaft (Fig. 5), then the turbine is known as a conical; here also the inlet can be internal or external.

Fig. 6 indicates a tangential flow turbine, where the water impinges on the runner blades as a free jet in the direction of the tangent to the runner.

As far as the position of the shaft is concerned, all types of turbines mentioned may be fitted with a horizontal or a vertical shaft.

When the water flows into the runner along the entire periphery, we speak of a turbine with complete admission, and when the water is fed to only a part of the periphery, the machine is termed turbine with partial admission or partial turbine (Figs. 6, 3b). Partial admission is used only for impulse turbines; the efficiency of pressure turbines with partial admission would be rather unsatisfactory.

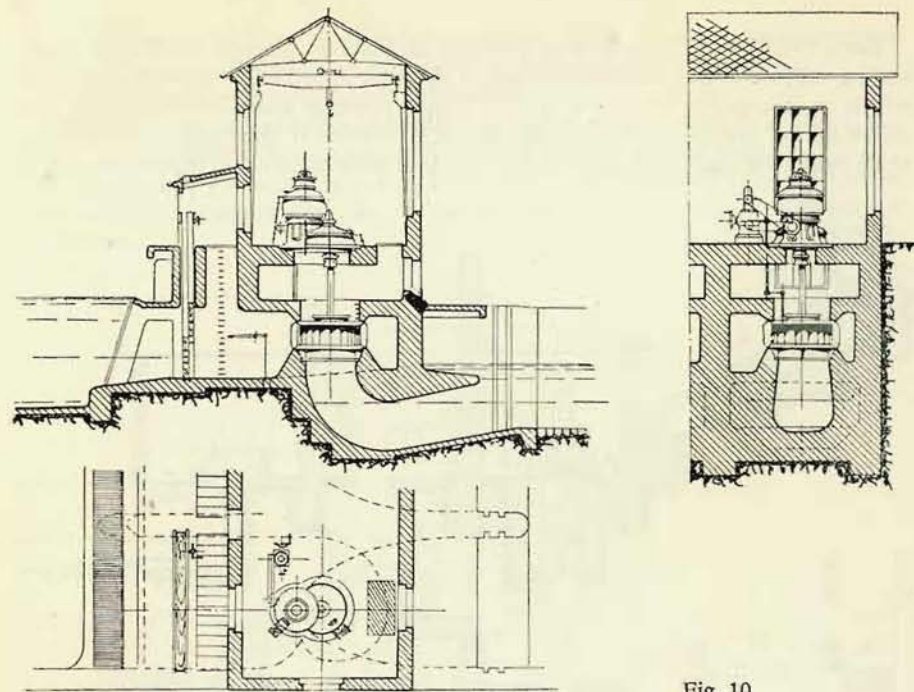


Fig. 10

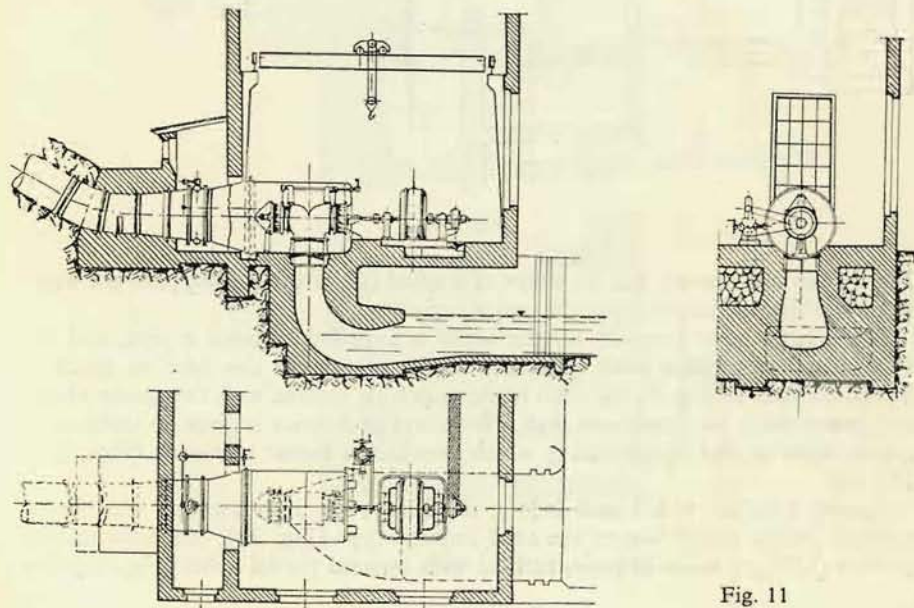


Fig. 11

For a small head the turbine is placed in an open or concrete pit. Fig. 7 shows such a turbine with a horizontal shaft. The water is led away through an elbow which in this case is located in the pit. Fig. 8 presents a similar design with the elbow on dry ground – the discharge elbow is directed to the engine room and the shaft passes through it. Fig. 9 shows a vertical turbine in a half-open pit, and in

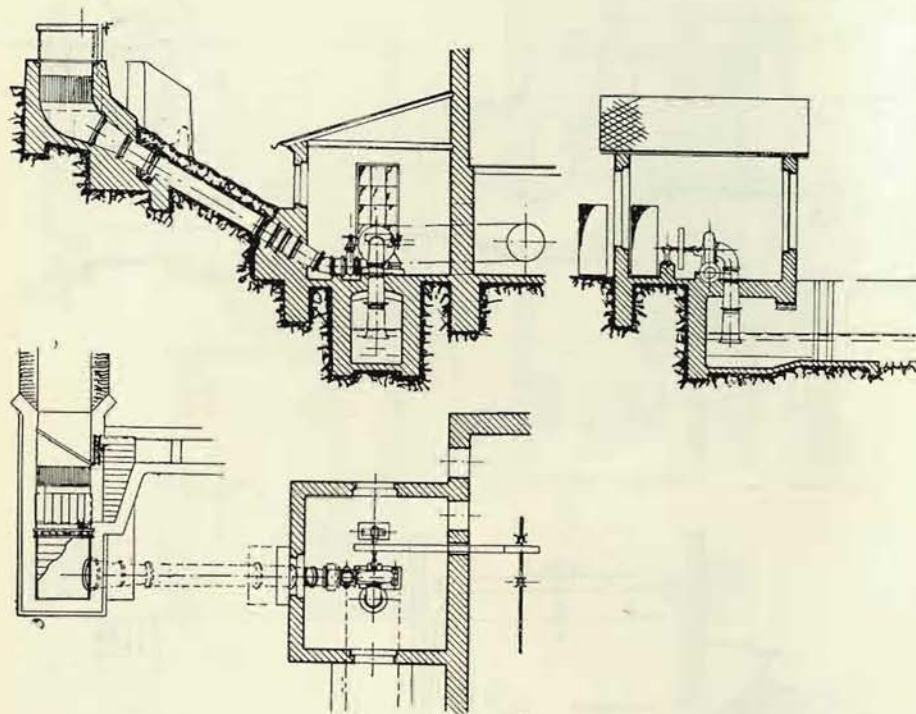


Fig. 12a

Fig. 10 the concrete pit has the shape of a spiral (see plan) and supplies the water to the turbine uniformly along the entire periphery.

For a large head (over 20 m) the water is supplied through a pipe, and the turbine is located in a shell connected to the piping. In this case we speak of a shell turbine. In Fig. 11 the shell houses a double turbine with two guide wheels and two runners on a common shaft. Nowadays preference is given to turbines in a plate-type or cast spiral casing which provides a better efficiency (Figs. 12a, 12b, 4a).

Among turbines which now belong to history, we must mention the Girard turbine (1851), which was of the axial impulse type (Fig. 2b); the Schwamkrug turbine (1858), a radial impulse turbine with internal partial influx (Fig. 3b); the

Jonval turbine (1837), an axial pressure turbine (Fig. 2a); and the Fourneyron turbine (1827), a radial pressure turbine with internal admission (Fig. 3a).

The types mostly constructed at present are:

The Francis turbine (1849) a centripetal, radial pressure turbine (Figs. 4a, b, 3c), the Pelton turbine (1880), a tangential, partial impulse turbine (Fig. 6), the propeller turbine and the Kaplan turbine (1919), an axial pressure turbine with radial guide wheel (Figs. 2c, d), and the less common turbines of Bánki and Reiffenstein.

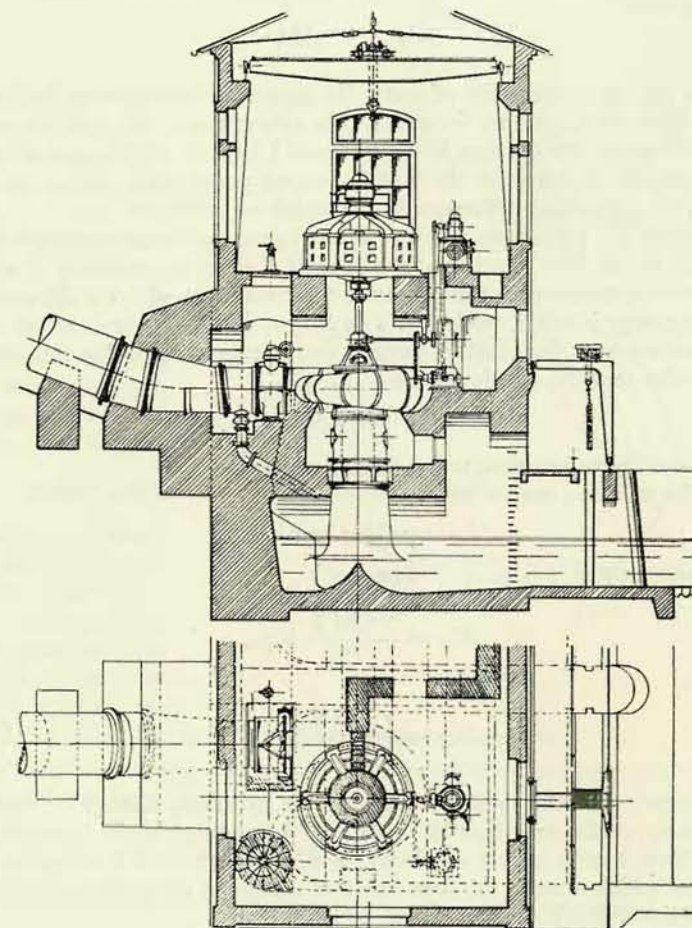


Fig. 12b

II. RELATIONS BETWEEN HEAD, FLOW RATE AND OUTPUT; EFFICIENCY

1. Output and Efficiency

When a quantity of water weighing 1 kg falls H metres in such a way that it reaches its lower position at zero velocity, the work done by this quantity of water in its fall is $1 \text{ kg} \cdot H \text{ m} = 1 \cdot H \text{ kgm}$. When during every second the quantity of water Q travels along the height difference H in the sense of gravitation, it does every second the work – or delivers the output (i. e. work per second) – of N_{th} in kgm per second:

$$N_{th} = \gamma \cdot QH, \quad (1)$$

where γ is the specific gravity of water (in general of the passing liquid) in kg, related to that unit of volume in which Q is given; hence this specific gravity of water is 1000 kg/m^3 for Q given in m^3/sec ., and 1 kg/litre for Q given in litres/sec. Q is the quantity of water (or the liquid) passing per second, briefly termed flow rate, and H is the height difference in m, which we call head.

This output N_{th} represents the theoretical value, and is the output which can be delivered by the flow rate Q and the head H if there are no losses. A hydraulic motor, however, cannot give this output as the conversion of hydraulic energy into mechanical energy is subject to losses. The output which we obtain at the coupling of the motor we term the effective output, and is expressed by the symbol N_{ef} ; it will be smaller than N_{th} , so it applies

$$N_{ef} = \eta \cdot N_{th},$$

where η is coefficient less than unity, termed efficiency.

Hence, the effective output will be

$$N_{ef} = \gamma QH\eta \text{ kgm/sec.},$$

in metric horsepower (1 h. p. = 75 kgm/sec.)

$$N_{ef} = \frac{\gamma QH\eta}{75} \text{ h.p.}, \quad (2)$$

in kilowatts

$$N_{ef} = \frac{\gamma QH\eta}{102} \text{ kw.}$$

The efficiency η is the total efficiency of the hydraulic motor; for turbines it amounts to approximately from 0.75 to 0.9, depending on the type of turbine (larger turbines have a higher efficiency) and varies with the load on the motor.

The losses which arise in the conversion of energy in the hydraulic motors, are included in the total efficiency η and are of three kinds:

a) The total flow rate Q , supplied to the turbine, does not actually pass through the runner. Part of the water by-passes the runner through the gaps between the

runner and the guide wheel, another part of the water escapes through the stuffing box around the shaft, and both of these proportions of the total flow rate produce no work. The quantity of water flowing through the runner is therefore smaller; in order to obtain the actual flow rate through the runner, Q_{ef} , the only work-producing part, we must multiply the flow rate Q by a number less than unity which we term the volumetric efficiency of the turbine, η_v .

$$Q_{ef} = \eta_v Q.$$

b) Of the head H , at disposal for the turbine, a certain part is consumed for overcoming the flow resistances within the turbine; these are resistances caused by the friction of the water on the walls of the turbine ducts, by the change of the direction of the water flow, and by the whirling of the water. The utilizable head will also be smaller by the velocity

head $\frac{C_2^2}{2g}$ corresponding to the velocity C_2 at which the water discharges from the runner. The coefficient, less than unity by which we must multiply the head H in order to obtain this smaller, so-called hydraulic head H_h , we term the hydraulic efficiency η_h .

The hydraulic output N_h , i. e. the power transmitted to the blades of the runner, will therefore be in kgm/sec.

$$N_h = \gamma Q_{ef} H_h = \gamma \eta_v Q \eta_h H.$$

c) But a further part of this output is consumed for overcoming mechanical losses; these are losses in the bearings of the turbine, in the stuffing boxes of the turbine shaft, and losses caused by the friction between the outer surfaces of the rotating runner wheel and the surrounding water. The effective output N_{ef} at the coupling

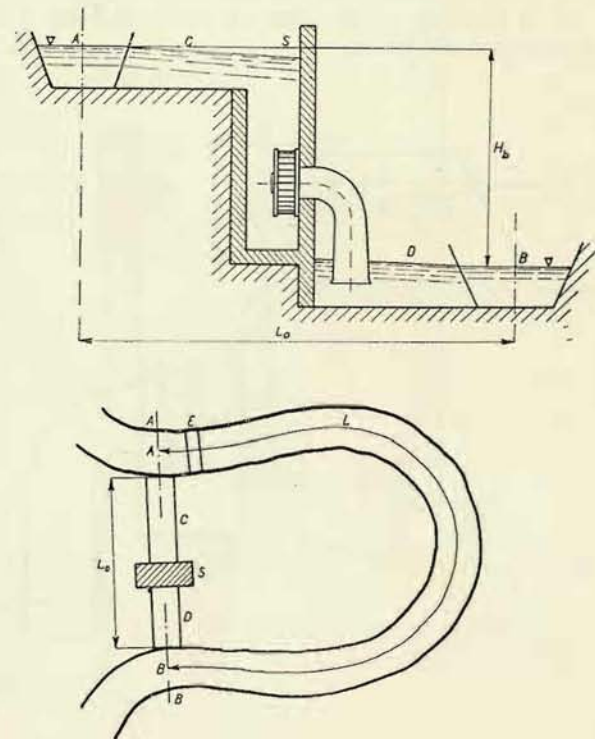


Fig. 13

will hence be smaller than the hydraulic output N_h , and we must multiply the latter by the mechanical efficiency η_m to obtain the effective output:

$$N_{ef} = \eta_m N_h,$$

so that

$$N_{ef} = \gamma Q H \eta_v \eta_h \eta_m = \eta Q H.$$

It is therefore evident that the total efficiency η is the product of the three enumerated efficiencies

$$\eta = \eta_v \eta_h \eta_m. \quad (3)$$

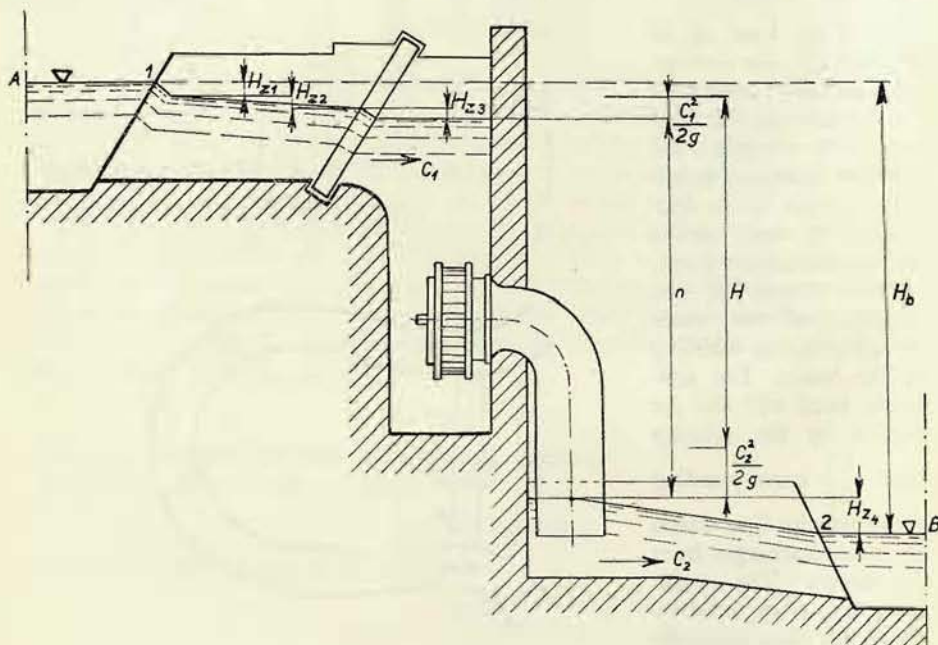


Fig. 14

2. Total or Gross and Effective or Net Head

The term head still requires further explanation. In every hydraulic power station the operator is permitted to utilize the head between the points A and B stipulated by the pertinent legal provisions (Fig. 13). This is the so-called total¹⁾ or gross head H_b . However, the turbine cannot fully utilize this head as part of it is consumed to overcome the flow resistances in the head race or pipe and in the tail race. It is clear that we are not allowed to include these losses into the

¹⁾ According to Czechoslovak Standard ČSN 085010-1951.

efficiency of the turbine because one and the same turbine would have different efficiencies depending on the losses arising in the head and tail races. We must therefore deduct these losses from the total (gross) head and thus define the effective²⁾ or net head at the disposal of the motor.

This effective or net head is not only the difference of the levels after deducting the mentioned losses, but it is defined as the difference between the total energy

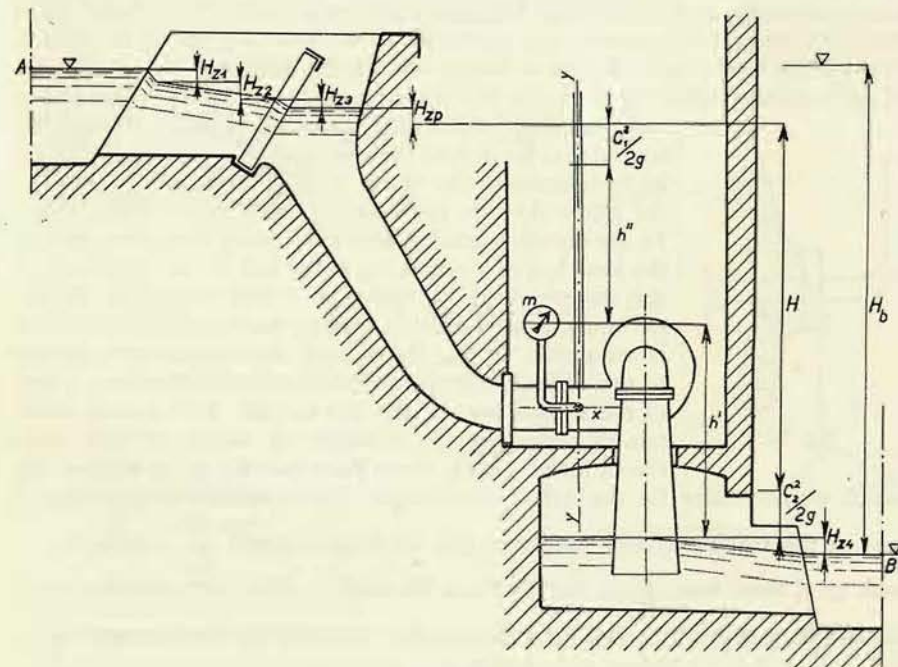


Fig. 15

of the water flowing into the turbine system and the total energy of the water discharging from it.

The effective head is hence given by the expression

$$H = \left(H_1 + h_1 + \frac{C_1^2}{2g} \right) - \left(H_2 + h_2 + \frac{C_2^2}{2g} \right), \quad (4)$$

where H with the pertinent subscript is positional energy, h pressure energy, and $\frac{C^2}{2g}$ kinetic energy. The subscript 1 relates to the input into the turbine system, the subscript 2 to the discharge from the turbine. Only in this way it is possible to arrive at a correct definition of the net head if we consider that a hydraulic motor

²⁾ According to Czechoslovak Standard ČSN 085010-1951.

has to convert the total energy of the water into mechanical energy at the shaft.

Smaller variations introduced in practical operation (see Czechoslovak Standard ČSN 085010-1951 and the following paragraphs here) are substantiated by practical requirements. Let us now see how in three most important cases we ascertain this net head:

a) *For a turbine in an open pit* (Fig. 14): From the gross head H_b we first deduct the head loss H_{z1} at the inlet to the head race; this loss is caused by the bend in the flow to the head race, by contraction in the inlet to the head race, and by the passage through the coarse grid. We must further deduct the head loss H_{z2} at the end of the head race caused by the losses in the head race (friction of the water on the walls, whirling). After the passage of the water through the

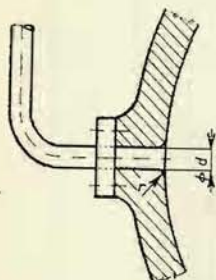


Fig. 16

second grid we deduct the head loss H_{z3} caused by the velocity increase of the water passing between the rods of the grid and by the subsequent velocity drop behind them. In the direction leading back from point B we must deduct the head loss H_{z4} pertaining to the loss in the tail race. In this way we obtain the difference h between the level in the pit and the level close behind the turbine. This difference is sometimes termed the geodetic net head and corresponds to the difference in the potential energy of the water ahead of the turbine and behind the turbine. This we can ascertain by measuring the difference in height of both mentioned levels. As the water flows into the pit at velocity C_1 , which we determine for the inflow into the pit, if we consider the pit itself as part of the turbine system, we must add the kinetic energy $\frac{C_1^2}{2g}$, belonging to each kg of water flowing into the pit. From the outlet tube of the turbine the water discharges at velocity C_2 , and we must therefore deduct¹⁾ the kinetic energy $\frac{C_2^2}{2g}$.

The net head for a turbine in an open pit will therefore be

$$H = H_b - \Sigma H_z + \frac{C_1^2}{2g} - \frac{C_2^2}{2g} = h + \frac{C_1^2}{2g} - \frac{C_2^2}{2g}.$$

b) *Turbine in spiral casing* (Fig. 15): In this case also, we must from the gross head H_b deduct the losses, which are: loss in the flow into the head race H_{z1} , loss within the head race H_{z2} , loss in the grid H_{z3} , and loss H_{z4} caused by friction of the water on the walls of the inlet tube, by whirling, by the curvature of the tube, variations in diameter, etc. At a lower water level we must again deduct the loss in the tail race H_{z4} . For these turbines we usually measure the pressure energy of the water

¹⁾ The discharge loss is involved in the hydraulic efficiency and should be calculated with the velocity in the tail race. Since this velocity does not markedly differ from the discharge velocity, the Standard introduces the discharge velocity from the outlet tube, and the deviation from the original definition is hence only small.

by means of a manometer m located in the inlet into the spiral casing. In order to obtain the net head, we must add to the metre reading of water column $h'' = 10 \cdot p$, p being given in atm. gauge pressure, the difference in the positional energies h' (the tube of the manometer is filled with water), and the difference between the kinetic energy $\frac{C_1^2}{2g} - \frac{C_2^2}{2g}$. C_1 is the mean velocity of the water in the cross section in which the manometer measurement is taken, and we obtain this value as the quotient of the flow rate Q by the area F of this flow cross section $y-y$, so that $C_1 = \frac{Q}{F}$. C_2 is again the velocity at which the water leaves the turbine

system through the last cross section of the discharge tube, and we determine it similarly. The net head in this case will be

$$H = h' + h'' + \frac{C_1^2}{2g} - \frac{C_2^2}{2g}.$$

Note: The manometer must only measure pressure energy without any components of velocity energy. The axis of the orifice where the manometer tube is inserted into the wall of the inlet tube must be absolutely perpendicular to the axis of the inlet tube, and the internal diameter of the connecting orifice should be 3 mm. The mouth of the orifice in the wall of the inlet tubes should not have a rounded edge at all, or rounded with only a small radius $r = 1$ mm (Fig. 16). Details are contained in the Czechoslovak Standard ČSN 085010-1951.

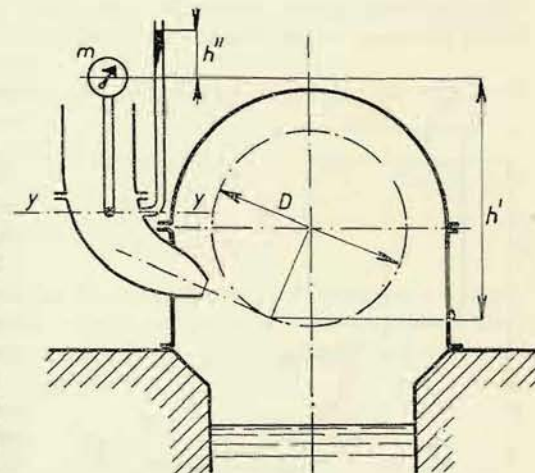


Fig. 17

c) *For tangential-flow Pelton turbines* (Fig. 17): The same holds good for these turbines as in case b), with a modification that the term $\frac{C_2^2}{2g}$ is omitted and that the height to the centre of the manometer dial is measured from the point at which the centre of the water jet contacts the pitch circle of the wheel. Hence applies

$$H = h' + h'' + \frac{C_1^2}{2g}.$$

Here we see a deviation from the originally stipulated definition. We do not take into consideration the distance of the contact point of the jet from the lower level and, furthermore, we neglect the kinetic energy of the discharge. This is certainly not quite correct, because if we should use a Francis turbine in a spiral casing,

we would reckon according to b) with these values. On the other hand, an argument in favour of the simplified form is the fact that the distance of the contact point of the jet from the lower level is also influenced by factors which are beyond the designer's control, such as variations of the lower level (the wheel must never run in water!). Details are to be found in the Czechoslovak Standard ČSN 085010-1951.

III. ACTION OF THE FLOW ON THE DUCT

1. Flow in the Stationary Duct, Moment of the Duct

The turbines extract energy from the water by changing the direction of the flow of the water in the runner. To deflect the water from its original direction it

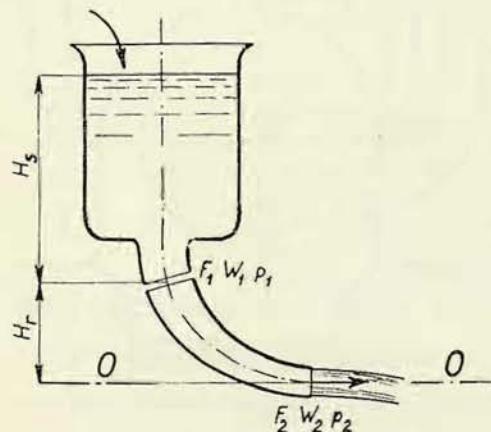


Fig. 18

must be subjected to the action of forces; this is, the forces with which the runner blades act upon the streaming water. According to the principle of action and reaction, the water, in turn, acts with the same force on the runner blades. The latter give way under the pressure of the water, turn the wheel, and thus the water produces work.

The effect of the water will be proportional to the quantity of water passing through the ducts of the runner. This flow rate is determined by the flow cross section of the duct, i. e. by the dimensions, and the velocity of the flow. Therefore we must know this velocity in

order to determine the necessary dimensions of the ducts. The corresponding calculation is termed voluminal calculation. The effect of the water upon the blades depends on the way in which the blades deflect the flow and change the velocity.

The determination of the most advantageous deflection of the flow is the task of the energy calculation, from which we ascertain how the blades must be curved.

First we shall deal with the effect of streaming water on the walls of a stationary, immovable duct. This case is simpler but we must be familiar with it as a turbine also contains stationary ducts and we must know how to ascertain the forces with which the water acts upon these stationary ducts.

a) *Voluminal calculation.* Let us assume that the vessel (Fig. 18) in which we maintain a constant level is connected to a curved duct in such a way that the latter adheres impermeably to the vessel but is otherwise freely movable. Its outlet cross

section F_2 is smaller than the inlet cross section F_1 , so that the water flowing through the duct will fill it up entirely and hence $p_1 > p_2$ will apply.

To the inlet and outlet cross sections we apply Bernoulli's theorem, taking as reference level the plane 0—0, passing through the centre of the cross section F_2 ; the head loss due to the flow through the duct being h_z :

$$\frac{p_1}{\gamma} + \frac{W_1^2}{2g} + H_r = \frac{p_2}{\gamma} + \frac{W_2^2}{2g} + h_z. \quad (5)$$

We express this head loss h_z in dependence on the higher velocity in the smaller (outlet) cross section

$$h_z = \xi \frac{W_2^2}{2g}.$$

(For well-designed turbine ducts we can assume the value ξ to be within the range $\xi = 0.06 - 0.1$.)

Thus we can transform Equation (5) to the expression

$$(1 + \xi) \frac{W_2^2}{2g} = H_r + \frac{W_1^2}{2g} + \frac{p_1 - p_2}{\gamma}. \quad (6)$$

This equation is termed the flow rate equation. Since the velocities are inversely proportional to the areas of the cross-sections, we can determine them if we know the difference $p_1 - p_2$. In the present case, for p_1 (the small velocity within the vessel not being taken into account), will apply

$$\begin{aligned} \frac{p_a}{\gamma} + H_s + 0 &= \frac{p_1}{\gamma} + \frac{W_1^2}{2g} + \xi_1 \frac{W_1^2}{2g}, \\ \frac{p_1}{\gamma} - \frac{p_a}{\gamma} &= H_s - \frac{W_1^2}{2g} - \xi_1 \frac{W_1^2}{2g}, \end{aligned}$$

where the last term expresses the losses only to the outlet from the vessel. These will be mainly caused by contraction of the flow.

(Rounding the edge of the inlet by a greater radius, we obtain $\xi_1 = 0.01 - 0.06$.)

$$\frac{p_1}{\gamma} = H_s + \frac{p_a}{\gamma} - (1 + \xi_1) \frac{W_1^2}{2g}.$$

Substituting this expression into (6), we obtain

$$\begin{aligned} (1 + \xi) \frac{W_2^2}{2g} &= H_r + \frac{W_1^2}{2g} + H_s + \frac{p_a}{\gamma} - \frac{W_1^2}{2g} - \xi_1 \frac{W_1^2}{2g} - \frac{p_2}{\gamma}, \\ (1 + \xi) \frac{W_2^2}{2g} + \xi_1 \frac{W_1^2}{2g} &= H_r + H_s + \frac{p_a}{\gamma} - \frac{p_2}{\gamma}. \end{aligned}$$

Now according to the continuity equation

$$W_1 = W_2 \frac{F_2}{F_1},$$

we obtain

$$\left(1 + \xi + \xi_1 \frac{F_2^2}{F_1^2}\right) \frac{W_2^2}{2g} = H_r + H_s + \frac{p_a}{\gamma} - \frac{p_2}{\gamma}. \quad (7)$$

When water discharges into a space of atmospheric pressure and when the same pressure acts upon the level in the vessel, $p_2 = p_a$, as the pressures on the outlet and on the water surface in the vessel cancel each other. If we further define $H_r + H_s = H$ as the total head, we obtain

$$\left(1 + \xi + \xi_1 \frac{F_2^2}{F_1^2}\right) \frac{W_2^2}{2g} = H. \quad (8)$$

We see from Equation (8) that with a given shape of the duct, we can determine the discharge velocity W_2 ; and from this value for a given flow rate Q the necessary cross section $F_2 = \frac{Q}{W_2}$, and from the continuity equation the other cross sections, too.

b) *Energy calculation.* The forces acting upon the duct we calculate by Newton's equation. By this equation the elementary force dP is given, which acts upon the mass element (particle of the water flow) dm and is required for the velocity variation dW during the time dt :

$$dP = dm \frac{dW}{dt},$$

so that

$$dP dt = dm dW.$$

also applies

This equation holds good for a straight motion. For a motion along a curved path we must only take into account the variation of the component of the velocity W in the direction of the force P , and this component we denominate W_p . Thus we obtain

$$dP = \frac{dm}{dt} dW_p. \quad (9)$$

But $\frac{dm}{dt}$ is the mass of water passing through the duct per second, because

$$\frac{Q\gamma}{g} dt = \frac{\gamma}{g} F W dt.$$

$W \cdot dt$ is, as we see from Fig. 19, a part of the length of the duct, and hence

$$\frac{Q\gamma}{g} dt = F \frac{\gamma}{g} W dt = dm.$$

Consequently applies

$$\frac{dm}{dt} = \frac{Q\gamma}{g},$$

and we can transcribe Equation (9)

$$dP = \frac{Q\gamma}{g} \cdot dW_p$$

and after integration from the duct cross section 1 to cross section 2 (Fig. 19) we obtain

$$P = \frac{Q\gamma}{g} (W_{p2} - W_{p1}).$$

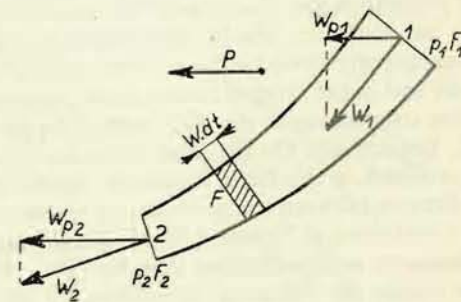


Fig. 19

W_{p1} denotes the velocity component in cross section 1 in the direction in which we seek the force, and similarly W_{p2} denotes the corresponding velocity component in cross section 2.

The formula determines the force necessary for changing the flow of the liquid, i. e. the force with which the duct acts upon the water flow. The force with which the water flow acts upon the duct is of the opposite sense

$$P = \frac{Q\gamma}{g} (W_{p1} - W_{p2}). \quad (10)$$

Since no assumptions, whatever, have been made as to the direction of the force P , Equation (10)

holds good for any arbitrarily selected direction of the force P , and, therefore, also for the determination of the forces in the directions of the axes of coordinates X and Y (Fig. 20). Giving to the force, by which the water acts upon the ducts in the direction of the axis X , the symbol P_x and to the force in the

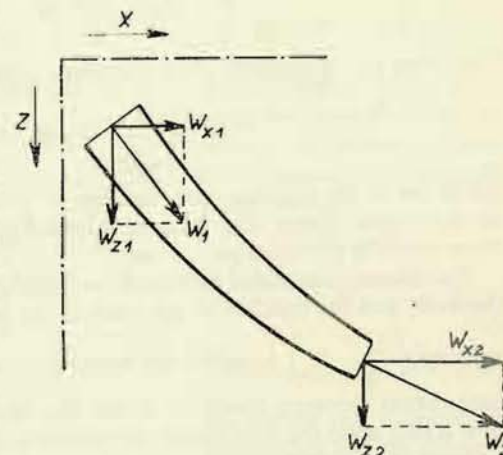


Fig. 20

direction Z the symbol P_z , we clearly see that

$$P_x = \frac{Q\gamma}{g} (W_{x1} - W_{x2}) \quad (11)$$

$$P_z = \frac{Q\gamma}{g} (W_{z1} - W_{z2}).$$

These forces are created, as is evident from the derivation, only from the change of magnitude and direction of the velocity of water. The expressions (10) and (11) do not, therefore, involve the weight of the water contained in the duct, which consequently should still be added to the force P_z , nor the static pressure on the inlet and outlet cross sections; these pressures must be determined separately and their components in the directions of the axes X and Z added to the forces P_x and P_z , respectively. On the other hand, no special regard to the friction of the water is required, as this factor is already expressed in the velocities W_1 and W_2 , or in the difference between the pressures on the extreme cross sections of the duct.

Combining in Equation (11) the components placed above each other into the resultants, and considering that $Res(W_{x1}, W_{z1}) = W_1$ and $Res(W_{x2}, W_{z2}) = W_2$, we obtain the following expression for the force with which the water acts on the duct:

$$R = Res\left(\frac{Q\gamma}{g} W_1, \frac{Q\gamma}{g} W_2\right). \quad (12)$$

The force acting upon the duct, therefore, equals the resultant of the forces

$$P_1 = \frac{Q\gamma}{g} W_1, P_2 = \frac{Q\gamma}{g} W_2,$$

which act in the extreme cross sections of the duct in the direction of the tangent to the central stream line, as indicated in Fig. 21. This theorem holds good also for a specially curved duct.

The theorem expressed by Equations (10), (11) and (12) is termed the momentum theorem, and the product of the mass of the through-flow and the corresponding velocity $\left(\frac{Q\gamma}{g} W\right)$ is called the momentum of the through-flowing liquid. The momentum theorem, therefore, states that the force of the dynamic effect of the flow acting upon the duct equals the resultant of the momentum of the liquid in the extreme cross sections, the momenta in both cross sections being taken as acting towards the centre of the duct.

We are also interested in the question as to what moment in relation to a point selected outside the duct belongs to the force with which the passing liquid acts upon the duct. This question is of interest because the resultant solution can be applied to a duct revolving around an axis to which the moment has been determined. This will be shown later.

It is clear that we can determine this moment in such a way that according to the theorem of the momentum we determine the force acting upon the duct, i. e. its magnitude, direction and position; its magnitude we multiply by the perpendicular distance from the point to which the moment is sought. More conveniently, however, we determine this moment by means of the theorem of the moment of momentum, which we shall derive in the following paragraphs.

In Fig. 22 a duct is shown through which a liquid flows at an inlet velocity W_1 at point 1 and an outlet velocity W_2 at point 2. The total force acting upon the duct is the result of the forces $P_1 = \frac{Q\gamma}{g} W_1$ and

$$P_2 = \frac{Q\gamma}{g} W_2,$$

which are also indicated in the figure. Since the moment to point O equals the sum of the moments of the components, we can express it as (subscripts 1, 2 denote that the moment arises between points 1 and 2 of the duct)

$$M_{1,2} = P_1 r_1 \cos \beta_1 - P_2 r_2 \cos \beta_2 = \frac{Q\gamma}{g} (W_1 r_1 \cos \beta_1 - W_2 r_2 \cos \beta_2).$$

Since, however, $W_1 \cos \beta_1 = W_{u1}$ and $W_2 \cos \beta_2 = W_{u2}$, where the index u denotes the components of the velocity perpendicular to the line of action of the moment, it follows that

$$M_{1,2} = \frac{Q\gamma}{g} (r_1 W_{u1} - r_2 W_{u2}). \quad (13)$$

The expressions $\frac{Q\gamma}{g} r W_u$ are named the moments of momentum and the theorem expressed in Equation (13) is termed the theorem of the moment of momentum. This theorem states that the moment of the force by which the liquid acts upon the duct is equal to the dif-

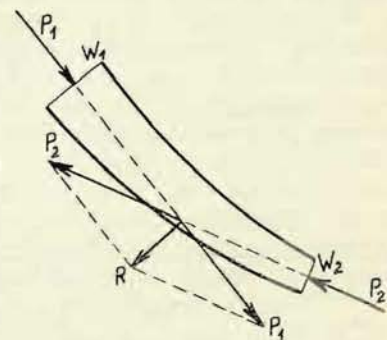


Fig. 21

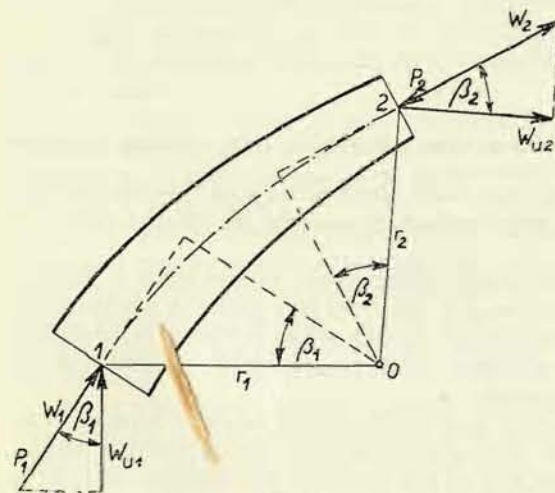


Fig. 22

ference of the moments of momentum in the extreme cross sections of the duct.

The moment for the unit weight of flow rate (i. e. for each kg of weight of the liquid flowing through the duct per one second), i. e. for $Q\gamma = 1$, will be

$$M_{1,2} = \frac{1}{g} (r_1 W_{u1} - r_2 W_{u2}). \quad (13a)$$

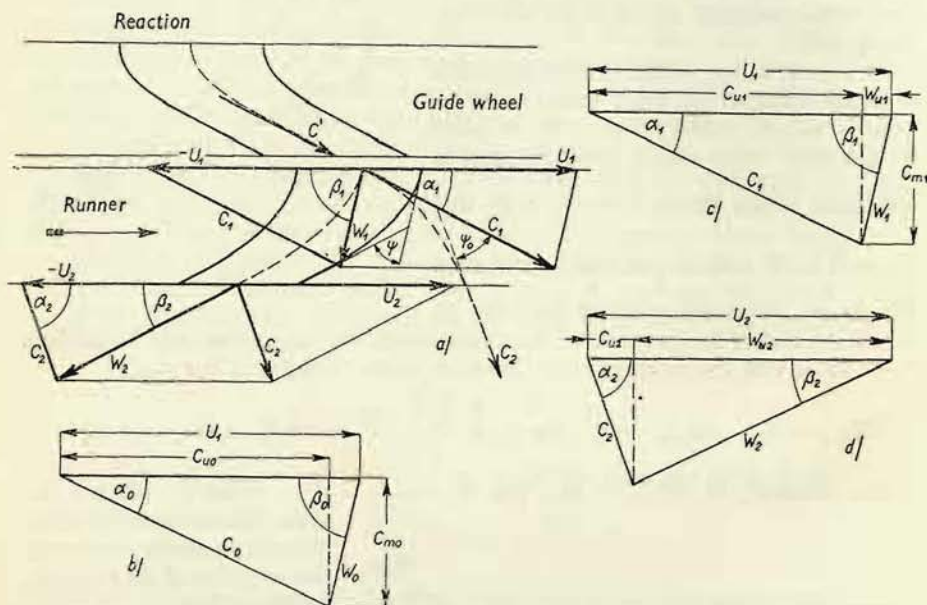


Fig. 23

2. Moment with which the Flow acts upon a Revolving Duct - Energy Equation

So far we have considered stationary ducts which do no work; the relative velocity within the duct conforms with the absolute one, and the effect, therefore, is conformable, too.

Now we shall deal with a moving duct. Here appear various kinds of velocity. There is, for instance, a relative velocity at which the flow moves in relation to the duct, and, also an absolute velocity at which the flow moves in relation to the stationary space outside the duct - and finally, there is displacement velocity at which the duct moves in the stationary space.

First of all, we must have a clear idea of the mutual relations between these velocities; they are shown in Fig. 23. Fig 23a presents a circumferential section of a duct of the guide wheel and a duct of the runner of an axial-flow turbine, as diagrammatically indicated in Fig. 2a.

The water leaves the guide duct at velocity C' . In the bladeless space between the guide wheel and the runner the velocity will somewhat differ; its magnitude immediately ahead of the runner is denoted by C_0 . In this space there are no blades, so the through-flow area will be larger by the sum of the thickness of all guide blades, and velocity C_0 will be somewhat smaller than the velocity C' . The inclination of velocity C' to the direction of rotation (to the peripheral velocity U) is denoted by α' , whilst the inclination of velocity C_0 will be termed α_0 . The water enters the duct of the runner at absolute velocity C_1 , which again will be somewhat greater than velocity C_0 , because the through-flow area is contracted by the runner blades; approximately we can say $C_1 \doteq C'$. The runner duct, however, revolves, i. e. in relation to the guide duct it moves at peripheral velocity U . The inlet cross section of the runner we denote again by subscript 1 and the outlet cross section by subscript 2 (in an axial-flow turbine the value of the peripheral velocity is the same in both these cross sections). We must, therefore, combine velocity C_1 with the negative velocity U_1 in order to obtain the relative velocity W_1 at which the water enters the runner duct under angle β_1 to the peripheral velocity.

The water leaves the runner duct at the velocity W_2 under angle β_2 to the peripheral velocity. The duct itself moves at the peripheral velocity U . For this reason we must combine the relative velocity W_2 with the displacement velocity U_2 in order to obtain the absolute inlet velocity C_2 , which is inclined to the peripheral velocity under the angle α_2 .

This resolving and eventually combining of velocities is illustrated by complete diagrams in Fig. 23. In practical application we do not draw these diagrams in full, but only sections of them, the so-called inlet and outlet velocity triangles, as indicated in Figs. 23b, c, d. Fig. 23b shows the velocity triangle for the bladeless space immediately ahead of the runner, where the water flows at absolute velocity C_0 , which by combining with the (negative) displacement velocity U_1 gives the relative velocity W_0 at which the water approaches the runner. Fig. 23c illustrates the conditions for the inlet cross section of the runner, and Fig. 23d for the outlet profile.

The symbols C , W and U with the appropriate subscripts denote the absolute, relative and peripheral velocities, and are used internationally. Similarly, the inclination of absolute velocity is marked with the letter α and that of relative velocity with the letter β .

In Fig. 23a the absolute path of a water element is also indicated (by a dashed line) as it appears to an observer standing outside the runner. It is evident that the path of the water deviates from the original direction of velocity C_1 to the direction of the velocity C_2 at an angle ψ_0 . This deflection of the absolute flow, which results in a pressure on the blade, is brought about by the deflection of the relative flow by the angle τ , which is given by the deflection of the relative outlet velocity W_2 from the relative inlet velocity W_1 , i. e. by the angle enclosed by the directions of the inlet and outlet ends of the blade. This angle is known as the efficient angle of the blade or the angle of deviation of the blade.

Note: We assume that the water flow absolutely follows the path determined by

the shape of the blade. This assumption only holds good for a great number of blades; with a small number of blades the path of the flow does not coincide with the shape of the blade, and this must be taken into account when designing the blade.

After this survey of velocities connected with a moving duct we can now start

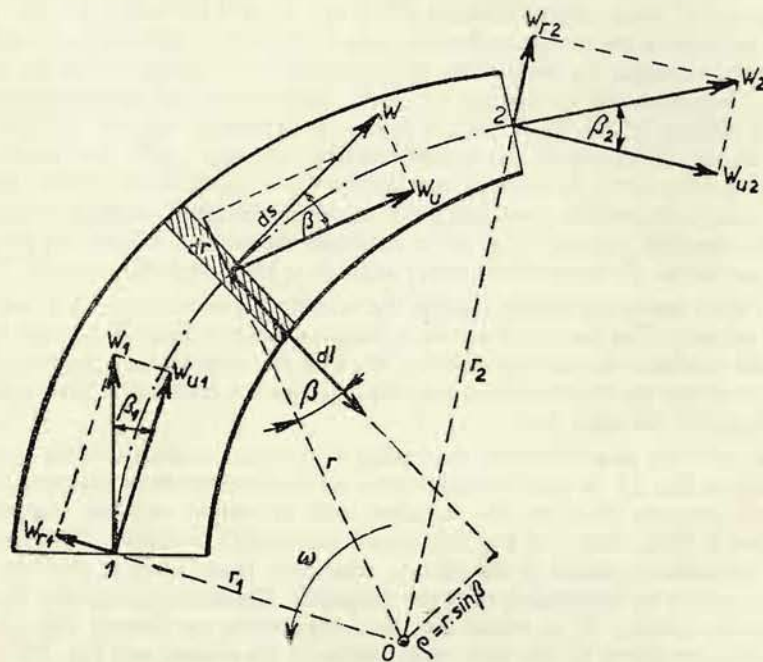


Fig. 24

to determine the moment of the force with which the flow of the water acts upon the duct.

We refer now to Fig. 24. Here we found that when this duct is at rest and a liquid flows through it, it is subjected to the action of the moment to point O ; the magnitude of this moment is according to Equation (13):

$$M = \frac{Q\gamma}{g} (r_1 W_{u1} - r_2 W_{u2}). \quad (13)$$

So far we have considered that one direction of the moment (or force in the momentum equation) to be positive which coincides with the direction of the velocity W_{u1} . Since in the ducts of turbine runners velocity W either increases in

the direction of the flow (reaction turbines), or at least remains constant (impulse turbine), but never decreases, we can transcribe (Fig. 24) as

$$r_2 W_{u2} > r_1 W_{u1}$$

and the sense of the moment, according to the given definition, will be negative against the direction of the component W_{u1} . (I. e., if we allow the duct to revolve around point O , it will do so in an anti-clockwise direction.)

The work done by the moment in revolving the duct, we shall consider as positive, and, therefore, with a revolving duct we must consider the positive moment to be that which acts in the direction of the rotary motion. For this reason the signs on the right side of Equation (13) are changed and the duct is then subjected to the action of a positive moment in the direction of the revolution of the duct

$$M = \frac{Q\gamma}{g} (r_2 W_{u2} - r_1 W_{u1}). \quad (14)$$

In a rotary motion of the duct, however, inertia forces are also manifested: centrifugal force and Coriolis force. So we must determine their moments to point O and then add them to the moment by which the water flow acts upon the duct.

The direction of the centrifugal force passes through the axis of the revolution and, therefore, creates no moment to axis O ; hence it need not be taken into account.

The Coriolis force, denoted by I , arises from the fact that the mass in changing its position in the revolving space must change its peripheral velocity, too; this force is generally defined by the expression

$$dI = 2 dm \omega W, \quad (15)$$

where dm is the mass element of the flowing medium, ω the angular velocity of the displacement motion, and W is the relative flow velocity in the duct. The Coriolis force is perpendicular to the relative velocity W , i. e. its deviation from the direction of the radius pertaining to the considered point in Fig. 24 is equal to the angle β . Its moment to the point O is

$$dM_I = dI \varrho = 2 dm \omega W \varrho,$$

where ϱ is the perpendicular distance of the direction of the force I from the axis of rotation: $\varrho = r \sin \beta$, so that

$$dM_I = 2 dm \omega W r \sin \beta. \quad (16)$$

Generally, the relative velocity W is dependent on radius r , so for the following integration we must find the relation between W and r . We obtain it by considering

$$W = \frac{ds}{dt},$$

where s is the path of the particle in the direction of velocity W . However, it further applies

$$ds \cdot \sin \beta = dr, \quad ds = \frac{dr}{\sin \beta},$$

so that

$$W = \frac{dr}{dt} \frac{1}{\sin \beta};$$

and, substituting this expression into Equation (16), we obtain

$$dM_I = 2 \frac{dm}{dt} \omega r dr,$$

and since $\frac{dm}{dt} = \frac{Q\gamma}{g}$ (see Eq. 9 and further) and $r dr = \frac{1}{2} d(r^2)$

$$dM_I = \frac{Q\gamma}{g} \omega d(r^2),$$

and because ω is constant, we can include it into the differential and apply the relation $U = r\omega$, whereby we obtain

$$dM_I = \frac{Q\gamma}{g} d(\omega r^2) = \frac{Q\gamma}{g} d(U \cdot r)$$

For the effect along the entire path of the duct between points 1 and 2, it therefore holds good that

$$M_{I,2} = \frac{Q\gamma}{g} \int_1^2 d(Ur) = \frac{Q\gamma}{g} (U_2 r_2 - U_1 r_1). \quad (17)$$

As the liquid during its passage through the duct acquires a higher peripheral velocity (it must be accelerated by the duct in the direction of the displacement motion), the Coriolis force acts on the duct against the sense of rotation; for this reason we substitute it in the following operation with the negative sign. Hence, the total moment with which the liquid flowing through acts upon the duct, will be:

$$\begin{aligned} M_{1,2} &= \frac{Q\gamma}{g} (r_2 W_{u2} - r_1 W_{u1} - U_2 r_2 + U_1 r_1) = \\ &= \frac{Q\gamma}{g} [r_1 (U_1 - W_{u1}) - r_2 (U_2 - W_{u2})]. \end{aligned}$$

From the inlet and outlet triangles, however, it is evident that holds good (Figs. 23 and 24):

$$U_1 - W_{u1} = C_{u1} \text{ and } U_2 - W_{u2} = C_{u2}.$$

As the region of action of the moment is evident from the subscripts of the velocities, we further dispense with marking the moment with subscripts 1, 2, and hence we write

$$M = \frac{Q\gamma}{g} (r_1 C_{u1} - r_2 C_{u2}). \quad (18)$$

This is the resultant moment which acts upon the revolving duct with the flow rate Q .

If we consider such a flow rate where the weight of the liquid passing in one second equals 1, then $Q\gamma = 1$, and the pertinent moment M_1 will have the value

$$M_1 = \frac{1}{g} (r_1 C_{u1} - r_2 C_{u2}). \quad (19)$$

By multiplying this moment by the angular velocity of the rotary motion of the duct we obtain the work done by the duct during its rotation:

$$M_1 \omega = \frac{1}{g} \omega (r_1 C_{u1} - r_2 C_{u2}) = \frac{1}{g} (U_1 C_{u1} - U_2 C_{u2}).$$

This work, however, equals the energy lost by each kg of the through-flowing water multiplied by the efficiency of conversion (losses within the duct) η_h , so that we can write

$$\frac{1}{g} (U_1 C_{u1} - U_2 C_{u2}) = H \eta_h. \quad (20)$$

This equation, which was published in a somewhat modified form in 1734 by Leonhard Euler, we call Euler's energy equation.

Static overpressure on the inlet cross section does not appear in this equation. To make a rotary motion possible, the inlet cross section must lie in the direction of velocity U . The resultant of the pressure acts perpendicularly to this cross section, i. e., in the direction of the radius, and therefore creates no moment to the axis of rotation. This equation holds good (similarly as the momentum theorem) also for a through-flow connected with losses, for the losses appear in the values of the velocities.

The equation was derived for a duct lying in a plane perpendicular to the axis of rotation. It is also valid for any position of the duct. This follows from Fig. 25. Velocity C which passes through point 1 may take any direction whatsoever. We project it into the plane perpendicular to the axis of rotation. To this projection of velocity, C' , we can apply the Euler equation.

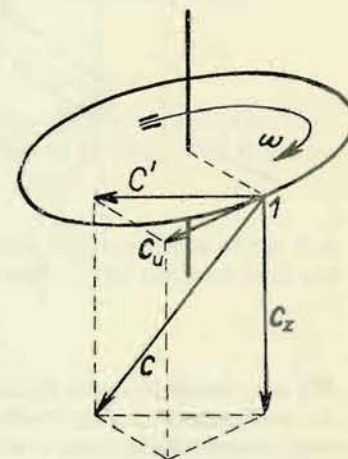


Fig. 25

tion. As, however, the peripheral component C_u of this projection of velocity coincides with the peripheral component of the original general velocity C , it is evident that we can calculate directly with the peripheral components of velocities of a general direction.

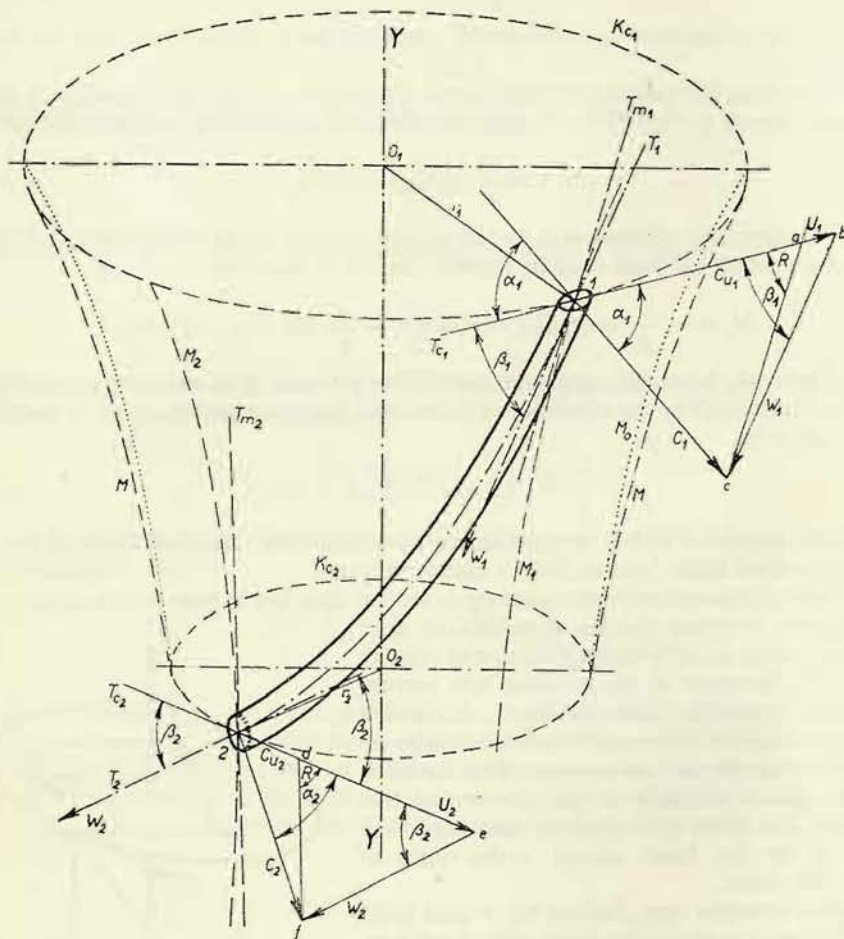


Fig. 26

We can, therefore, apply Equation (20) also to a duct with a space curve as axis, e. g., as illustrated in Fig. 26. Both velocity triangles (inlet and outlet) are drawn here in perspective in order to show the peripheral components C_{u1} and C_{u2} .

The equation holds good for any liquid if it fulfils the condition of incompress-

sibility which we have assumed; therefore even for gases, provided that the pressure variation is small enough to neglect the variations of volumes caused by them.

The equation only contains values at the beginning and the end of the duct. The progress of the flow between these two points is, therefore, of no account; we must only take care to keep the losses connected with the passage through the duct as small as possible.

The equation connects the inlet triangle with the outlet triangle and thus defines the relation between the blade angles β_1 and β_2 . Here we must introduce for η_h a reliably attainable (according to experience) value of hydraulic efficiency. We must avoid to introduce a value higher than actually attainable (with regard to the higher actual losses arising during the passage through the duct); in such a case Equation (20) would not be satisfactory and a further lowering of efficiency would occur. If we introduce a lower value than the actually efficiency attainable, the latter will also drop, but at the most to the value which we have selected for Equation (20) and for which this equation applies.

In order to attain a high output, the negative term must have the smallest possible value. We shall therefore endeavour to have $C_{u2} = 0$, i. e. that the water leaves the duct at an absolute velocity in a direction in which there are no peripheral velocity components. C_{u1} must be positive, that means that we must supply the water to the runner in the direction of its rotation.

3. Hydraulic Efficiency

Hydraulic efficiency has already been mentioned. It now appears in the principal energy equation and so it must be dealt with in more detail. As already said, hydraulic efficiency must take into account the losses in the water flow during passage through the turbine. In general, hydraulic efficiency can be expressed:

$$\eta_h = \frac{H - \sum H_z}{H},$$

where H_z represents the individual losses arising along the path of the water flow.

Hydraulic efficiency varies according to losses in the turbine, and, therefore, depends on the size, type and arrangement of the turbine.

The losses coming into consideration are:

1. Losses caused by friction, curvature of the flow, and variations of the flow cross sections; to overcome this requires a certain part H_{z1} of the total head and can be expressed as:

$$H_{z1} = \rho H; \quad \rho = \frac{H_{z1}}{H}.$$

2. H_{z2} these are losses caused by the fact that the water discharges from the runner a velocity C_2 (Fig. 27), which for a given discharge from the runner must have a certain magnitude. Together with the water, unutilized energy to the value

of $\frac{C_2^2}{2g}$ (for each kg of the flow rate through the turbine) escapes from the runner and can be expressed as relative value by

$$H_{z2} = \frac{C_2^2}{2g} = \alpha \cdot H, \quad \alpha = \frac{H_{z2}}{H}.$$

α is the coefficient of the discharge loss. That the outlet velocity need not be completely lost for energy conversion will be shown later when discussing the draft tube.

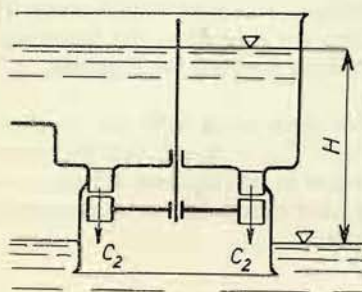


Fig. 27

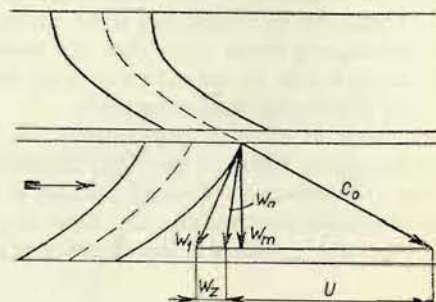


Fig. 28

When only these two types of losses occur in the turbine, hydraulic efficiency will be given by the expression

$$\eta_h = \frac{H - H_{z1} - H_{z2}}{H} = \frac{H - \rho H - \alpha H}{H} = 1 - \rho - \alpha. \quad (21)$$

3. When the water flow approaches the runner in an incorrect way connected with impacts, losses will occur due to shocks, the separation of the flow from the surface of the blade at the inlet, and by the resulting turbulence. These losses will arise when the direction of the incoming flow is not in accordance with the inlet end of the blade. Such a flow is illustrated in Fig. 28. Here we see that the relative velocity W_0 of the incoming water flow does not coincide with the direction of velocity W_1 which is determined by the inlet end of the blade. The component W_m of both velocities is termed meridional velocity because it lies in the meridional plane of the turbine; the component W_m must be the same for both velocities (W_0 and W_1). This is calculated from the continuity equation by dividing the flow rate Q by the flow cross section perpendicular to it, i. e. for velocity W_{m0} at the flow through the area immediately ahead of the inlet into the runner, and for the velocity W_{m1} at the flow through the area immediately behind this inlet; these velocities are approximately the same. We may therefore convert the velocity W_0 into W_1 by the vectorial addition of the velocity W_z , which is parallel to the horizontal velocity U .

The turbulence caused by the shock will be more intense, the greater W_z is, and so the loss arising will be proportional to the velocity head of W_z :

$$H_{z3} = k \frac{W_z^2}{2g}.$$

According to measurements carried out by several authors, mainly Oesterlen¹⁾, we can put $k = 1$ and thus write:

$$H_{z3} = \frac{W_z^2}{2g} = \zeta H.$$

In an abnormal operation, where the flow conditions do not agree with those assumed in the design of the turbine, hydraulic efficiency will be:

$$\eta_h = 1 - \rho - \alpha - \zeta. \quad (22)$$

In this case the energy equation (20), will undergo a change. The expression $\frac{1}{g} (U_1 C_{u1} - U_2 C_{u2})$ on the left should indicate the work which the wheel assumes when the velocity component C_{u1} at the radius r_1 is changed into the component C_{u2} at radius r_2 . When water contacts the blade in a direction deviating from the direction of the inlet blade end and enters the runner at velocity C_0 with the peripheral component C_{u0} , this must first be converted by shock into C_1 with the component C_{u1} , and the work performed must also be included in the work transmitted to the runner; in this case, however, according to the momentum equation, it is of no account in which way the velocity change has been brought about, as it only influences efficiency. In this case we must transcribe the energy equation:

$$\frac{1}{g} (U_1 C_{u0} - U_2 C_{u2}) = H \eta_h = H (1 - \rho - \alpha - \zeta). \quad (20a)$$

Hydraulic efficiency changes when a so-called draft tube is employed as will be explained in the pertinent chapter.

4. Flow Rate Equation; Overpressure of the Runner

From the inlet and the outlet triangles (Fig. 23c, d), applying the cosine rule, we can derive the relations:

$$W_1^2 = C_1^2 + U_1^2 - 2 U_1 C_1 \cos \alpha_1$$

$$W_2^2 = C_2^2 + U_2^2 - 2 U_2 C_2 \cos \alpha_2.$$

Subtracting the first equation from the second and dividing by two, we obtain

$$U_1 C_1 \cos \alpha_1 - U_2 C_2 \cos \alpha_2 = \frac{1}{2} (W_2^2 - C_2^2 - U_2^2 - W_1^2 + C_1^2 + U_1^2).$$

¹⁾ See, Thomann R.: Die Wasserturbinen und Turbinenpumpen, Part 1, Stuttgart, K. Wittwer 1924, p. 64.

Since $C_1 \cos \alpha_1 = C_{u1}$ and $C_2 \cos \alpha_2 = C_{u2}$, we can by the right side of this equation replace the expression in brackets ($U_1 C_{u1} - U_2 C_{u2}$) in energy equation (20), whereby we obtain

$$\frac{C_1^2 - C_2^2}{2g} + \frac{W_2^2 - W_1^2}{2g} + \frac{U_1^2 - U_2^2}{2g} = H \eta_h. \quad (23)$$

This is the so-called flow rate equation. It is a mere modification of the energy equation, but shows us another side of conditions in the runner. We now substitute for η_h according to Equation (21):

$$\frac{C_1^2 - C_2^2}{2g} + \frac{W_2^2 - W_1^2}{2g} + \frac{U_1^2 - U_2^2}{2g} = H - \varrho H - \frac{C_2^2}{2g},$$

the terms $\frac{C_2^2}{2g}$ cancel each other, and so there remains

$$\frac{C_1^2}{2g} + \frac{W_2^2 - W_1^2}{2g} + \frac{U_1^2 - U_2^2}{2g} = H - \varrho H = H(1 - \varrho). \quad (24)$$

From the flow rate equation in this form we see that the head, reduced by the losses due to friction and curvature of the flow within the turbine, $H - \varrho H = H - H_{z1}$, is divided into three parts. The first is consumed to create the inlet velocity C_1 into the runner and is defined by the first expression; the second is consumed to increase the relative velocity of the water in the duct from the value W_1 to W_2 and is expressed by the second term which presents the difference between the pertinent velocity heads and finally, the third part is consumed to overcome the centrifugal force if we consider that the water approaches the runner at the outer diameter and discharges at the inner diameter, as it usually is the case.

Note: The centrifugal force encountered here, is inherent, to the water which rotates with the runner. This will be clear if we realize that water rotating in a vessel assumes the shape of a paraboloid of revolution, the height of which equals $\frac{U^2}{2g}$ (Fig. 29).

If in Equation (24) we shift the first term to the other side, we obtain

$$\frac{W_2^2 - W_1^2}{2g} + \frac{U_1^2 - U_2^2}{2g} = H - H_{z1} - \frac{C_1^2}{2g} = h_p = \frac{p_p}{\gamma}. \quad (25)$$

The expression $H - H_{z1} - \frac{C_1^2}{2g} = h_p$ represents the head after subtracting the loss head H_{z1} and the velocity head $\frac{C_1^2}{2g}$, i. e. it expresses the pressure head of the water on entering the runner. On the discharge side we have so far assumed atmospheric pressure (discharge into the atmosphere), and the sum of the 2nd and 3rd terms of the flow rate equation is therefore the pressure difference – expressed

as water column – between the inlet and the outlet of the runner and is termed the overpressure of the runner.

These conditions are generally valid, even when the pressure at the outlet from the runner differs from the atmospheric pressure, as illustrated in Fig. 30. This figure presents a diagrammatic picture of a turbine with a runner, immersed down to the depth H_2 below the lower water level. If we neglect the height of the runner H_0 the pressure on the outlet from the runner, expressed as water column,

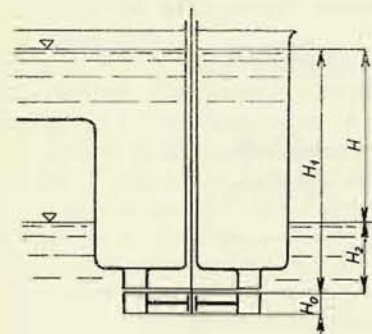


Fig. 29

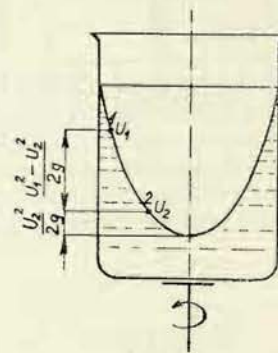


Fig. 30

will be $\frac{p_2}{\gamma} = H_2$. The pressure on the inlet into the runner (likewise expressed as water column) will be

$$\frac{p_1}{\gamma} = H_1 - H_{z1} - \frac{C_1^2}{2g},$$

and hence the overpressure

$$\frac{p_1 - p_2}{\gamma} = H_1 - H_{z1} - \frac{C_1^2}{2g} - H_2 = H - H_{z1} - \frac{C_1^2}{2g} = H(1 - \varrho) - \frac{C_1^2}{2g}.$$

It is evident that we have thus obtained the same expression as before. The sum of the 2nd and 3rd terms of the flow rate equation therefore actually expresses overpressure of the runner (in terms of water column).

Should the water enter the runner with shock, we must start again from triangles $C_0 W_0 U_1$ and $C_2 W_2 U_2$, and after substitution into Equation (20a) we obtain the corresponding flow rate equation for a flow approach subject to shocks

$$\frac{C_0^2 - C_2^2}{2g} + \frac{W_2^2 - W_0^2}{2g} + \frac{U_1^2 - U_2^2}{2g} = H \eta_h, \quad (23a)$$

where

$$\eta_h = 1 - \varrho - \alpha - \zeta.$$

In this case, all other considerations and deductions also apply to the same extent.

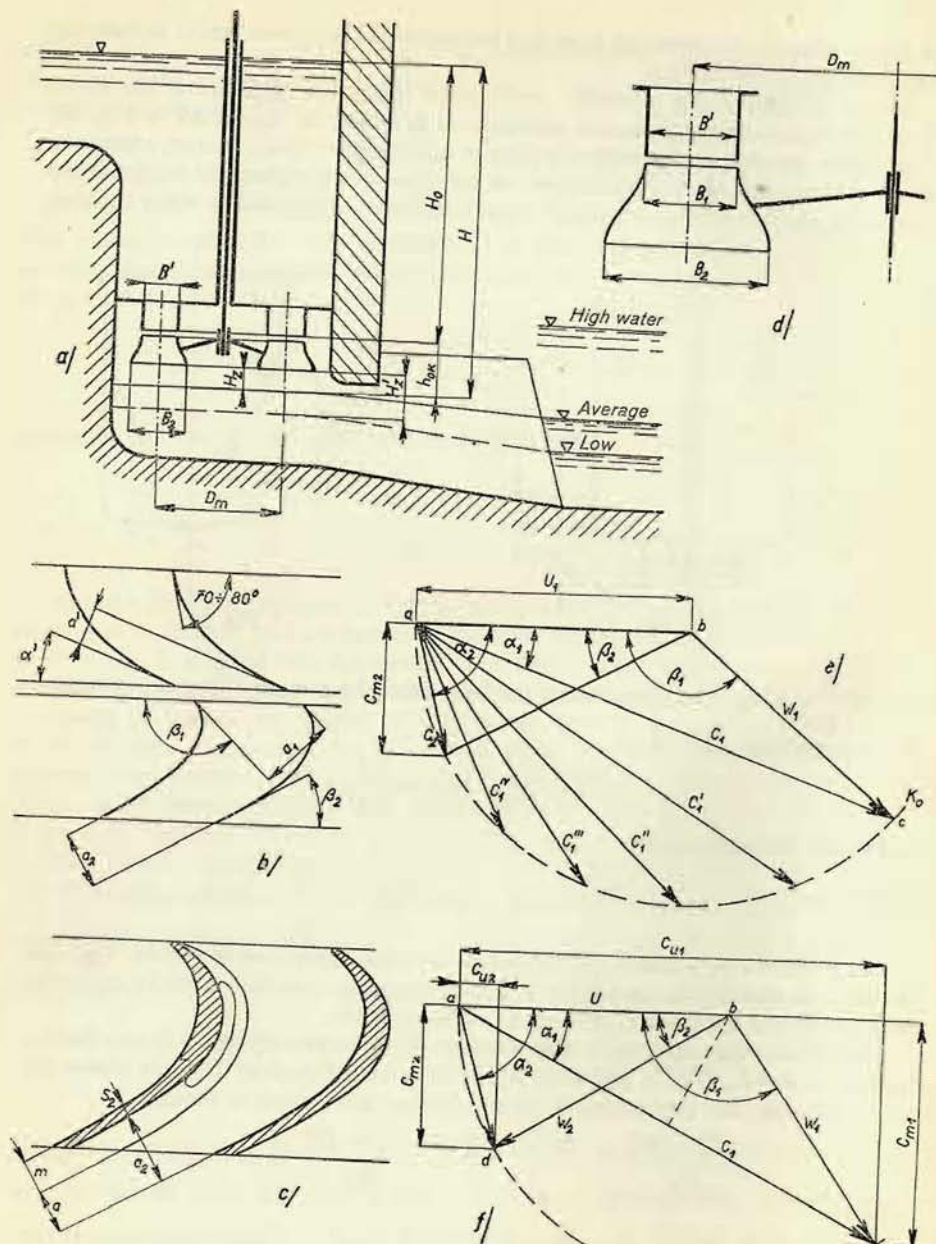


Fig. 31

IV. REACTION (PRESSURE) AND IMPULSE (CONSTANT-PRESSURE) TURBINES

In the foregoing chapter we defined overpressure of the runner as the difference between the pressure immediately in front of the inlet cross section and immediately at the back of the outlet cross section of the runner. This overpressure, as stated before, need not occur in all turbines. As it is evident from Equation (25) it will e. g. equal zero for an axial-flow turbine, where $U_1 = U_2$, provided that the inlet cross sections of the runner ducts are the same as the outlet cross sections. In this case, from the requirement of continuity, $W_1 = W_2$, and the overpressure of the runner equals zero.

Turbines, where overpressure equals zero are termed constant-pressure or impulse turbines. This name is derived from the fact that the pressure of the liquid at the front and at the back of the runner is the same. In this case we take care to prevent variations of the pressure of the liquid even during passage through the runner duct. This can be done by allowing the liquid to flow through the runner duct in such way that the level is always maintained free, i. e., the liquid does not completely fill up the duct.

As an example we mention the Girard turbine, which now belongs to the past, but offers a distinct picture of the conditions described. It is diagrammatically shown in Fig. 31a. Fig. 31b is a diagram of a peripheral section through the guide duct and the runner duct. Fig. 31c illustrates the design of the duct, and Fig. 31d shows a meridional section of the guide wheel and the runner. In this figure we can see that the rim of the runner is broader in the direction of the outlet to enable the water to spread freely across the blade (see Fig. 31c). The space between the trailing edge of the runner blade and the free water surface is filled with air through orifices in the rims of the runner. In consequence of this feature, the turbine had a good efficiency only when the tail race level was lower than the runner; when (at periods of high water) the tail race level rose to such an extent that the wheel was running in water, efficiency was lowered; i. e. the runner ducts were completely filled with water and therefore the progress of relative velocities W did not satisfy the requirements. This phenomenon is also encountered in all impulse turbine installations.

The Pelton turbine is a modern example (Fig. 6), in which a free jet impinges on the ladle-shaped blades, or buckets, and flows through them at a free level.

Turbines where h_p is larger than zero, i. e. where the pressure of the fluid at the beginning of the runner duct is higher than at the end, are termed pressure (or reaction) turbines. Here the liquid completely fills up the duct and the flow cross section decreases in the direction of the outlet, so that relative velocity W , at which the liquid flows through the duct, increases. The runner ducts are completely filled with water; therefore, it does not matter if the runner is located below the tail race level. Modern types of pressure (or reaction) turbines are e. g. the Francis turbine and the Kaplan turbine.

In summarizing, we can enumerate the following features of constant-pressure (or impulse) and pressure (or reaction) turbines:

1. In impulse turbines the total effective head is converted in the guide wheel itself into velocity of the water flow which emerges from the guide wheel. This flow then only changes direction in the runner, the magnitude of relative velocity remaining constant. The magnitude of absolute velocity C and in particular that of its peripheral component C_u decrease (see Fig. 31e). The overpressure of the runner equals zero. This must be ensured by such an arrangement so that a free surface of the water is maintained during passage through the runner.

2. In reaction turbines only part of the effective head is converted in the guide wheel into velocity at which the liquid discharges from the guide wheel; part of the head acts as pressure upon the liquid under which the liquid enters the runner. This residual pressure is only converted into velocity in the runner itself, so that the relative velocity, at which the water flows through the duct, increases towards the outlet. There is an overpressure in the runner ducts and consequently they are completely filled with water.

It is important to note, here, that impulse turbines with the same head and the same diameter of the runner have a lower speed than the reaction turbines. This follows from the energy equation:

$$\frac{1}{g} (U_1 C_{u1} - U_2 C_{u2}) = H \eta_h.$$

As already pointed out, we must endeavour to have $C_{u2} = 0$. Hence, in the equation the first term in brackets will be most important. In impulse turbines the total head is converted into velocity in the guide wheel; for this reason, C_1 and also C_{u1} , will be larger. U_1 must, therefore, be smaller than in a reaction turbine, where only part of the head is converted into velocity C_1 in the guide wheel. Since in pressure turbines velocity C_1 , and consequently its component C_{u1} , will be smaller than in impulse turbines, the value U_1 must be larger in order to obtain the same value of the product $U_1 C_{u1}$. Impulse turbines will, therefore, have a smaller peripheral velocity and consequently with the same runner diameter a lower speed. U_1 will here be smaller than C_{u1} , so that the inlet and outlet triangles will have approximately the shape indicated in Fig. 31f. A characteristic feature is given by the relation between $C_{u1} > U_1$ and $W_2 = W_1$. The triangles of a reaction turbine are indicated in Figs. 23b—d. Here applies $C_{u1} < U_2$ and $W_2 > W_1$.

V. DRAFT TUBE, CAVITATION

1. Draft Tube

We have just seen that the runner of an impulse turbine must be placed above the tail race level, and this at such a height, that even at more frequently occurring higher tail race levels, the wheel does not run in water. These turbines, therefore, require the arrangement indicated in Fig. 2b. But in this design we lose part of the head, and this loss corresponds to height of the outlet cross section above the tail race level, since along this part of its path the water falls freely without doing any

useful work. For this reason it is more advantageous to employ reaction turbines particularly, in those cases, where the head is small and the part lost in the described way comparatively large in relation to the total head.

These latter turbines can be placed below the tail race level (as approximately indicated in Fig. 3a), and then no loss of head will be encountered. Such a turbine, however, is always immersed in water and not easily accessible. In order to eliminate this drawback, the so-called draft tube has been introduced; its use is diagrammatically indicated in Fig. 2a. The turbine with runner is located above the tail race level, but the runner is surrounded by a tube which is hermetically connected with the guide wheel and extends down below the tail race level. The turbine is now easily accessible and yet no head loss is encountered, as the tube during operation is filled with water, the weight of which reduces the pressure in the outlet cross section of the runner.

The modern draft tube, however, fulfils an even more important task. It reduces the discharge loss from the runner, $\frac{C_2^2}{2g} = \alpha H$. Here the water leaves the runner at the absolute velocity C_2 . That is to say that each kilogram of the through-flow of the liquid per second takes with it an energy of $\frac{C_2^2}{2g} = \alpha H$. This energy could not be utilized by the runner, but it can be made use of, at least partially, in the draft tube by a gradual reduction of the velocity to a smaller value.

In the example just described, according to Fig. 2a, this will not be the case, for the water discharging from the runner here suddenly enters the large cross-section of the draft tube, so that velocity C_2 is destroyed by whirling.

When, however, the mouth of the draft tube has approximately the same cross section as the outlet from the runner, as e. g. in Figs. 3c, 4a and 2d, velocity C_3 at the beginning of the draft tube will be approximately the same as velocity C_2 at which the water leaves the runner (a certain difference will only occur due to the fact that the cross section of the outlet from the runner is restricted by the blades). When the draft tube diverges only gradually, thus enabling the water to fill the cross section up to the walls, the velocity of the water C_4 in the discharge end of the draft tube will be smaller than velocity C_3 . Hence the discharge loss $\frac{C_4^2}{2g}$ will be smaller and the difference in comparison with the original loss represents the theoretical regain of the draft tube: $\frac{C_3^2 - C_4^2}{2g}$. As the flow in the draft tube and

the velocity drop are connected with losses owing to the friction of the water on the walls of the tube, whirling, and the escape of air (because there is a vacuum at the beginning of the draft tube), the actual gain will be smaller. We must multiply the theoretical gain by the efficiency of the draft tube $\eta_s < 1$, whereby we obtain the actual regain, which we can express as part of the total head

$$\eta_s \cdot \frac{C_3^2 - C_4^2}{2g} = \nu H.$$

The best efficiency is offered by straight, conical draft tubes, i. e. approximately 0.9 — 0.85 — 0.7; efficiency of draft tubes having an elbow is less and amounts to about 0.6 — 0.85.¹⁾

The regain is caused by the fact that the draft tube converts velocity into pressure and so causes a pressure drop at the entrance.

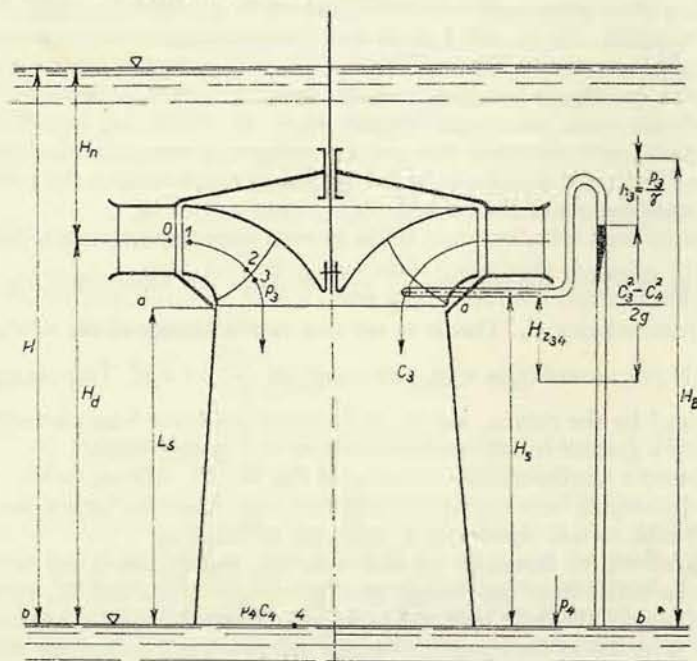


Fig. 32

When defining hydraulic efficiency, we have, apart from other factors, also taken into account the discharge loss from the runner, and so we write:

$$\eta_h = 1 - \varrho - \alpha = \frac{H - \varrho H - \frac{C_2^2}{2g}}{H}.$$

When a turbine is equipped with a draft tube, the discharge loss is no longer $\frac{C_2^2}{2g}$, but smaller by the value which is gained in the draft tube; hence:

$$\frac{C_2^2}{2g} - \eta_s \frac{C_3^2 - C_4^2}{2g} = H(\alpha - \nu).$$

¹⁾ Thomann: Wasserturbinen u. Turbinenpumpen, Part 2, p. 160, K. Wittwer, Stuttgart 1931.

Hydraulic efficiency of a turbine with a draft tube will, therefore, be:

$$\eta_h = 1 - \varrho - \alpha + \nu,$$

and this value must be taken into account in the energy and the flow rate equations, so that e. g. the flow rate equation for a turbine with draft tube reads as follows:

$$\frac{C_1^2}{2g} + \frac{W_2^2 - W_1^2}{2g} + \frac{U_1^2 - U_2^2}{2g} = H(1 - \varrho + \nu). \quad (25a)$$

The magnitude of the vacuum at the beginning of the draft tube can be determined by applying the Bernoulli equation to the cross sections *a* and *b* in Fig. 32. When we select the plane *b* — *b* as the base for position energy, the following relation will hold good:

$$H_s + \frac{p_3}{\gamma} + \frac{C_3^2}{2g} = \frac{p_4}{\gamma} + \frac{C_4^2}{2g} + H_{z3,4}.$$

Here, $H_{z3,4}$ represents the sum of the losses along the path 3 — 4, which are due to friction, shocks, and whirling in the draft tube and to the conversion of kinetic energy into pressure; p_3 and C_3 are pressure and velocity respectively in the plane *a* — *a*, and hence in the point 3, too; the subscripts 4 relate to the cross section *b* — *b*.

From this it follows that:

$$\frac{p_3}{\gamma} = \frac{p_4}{\gamma} + H_{z3,4} - H_s - \frac{C_3^2 - C_4^2}{2g}.$$

The value of the last fraction is the theoretical regain, no regard being paid to the loss of pressure head due to flaring of the draft tube. As already pointed out, this theoretical regain will be reduced by losses arising to $\eta_s \frac{C_3^2 - C_4^2}{2g}$, so that the losses will be

$$H_{z3,4} = (1 - \eta_s) \frac{C_3^2 - C_4^2}{2g}.$$

If we include in this loss the loss due to the velocity change from C_2 to C_3 , we arrive at the relation

$$\frac{p_3}{\gamma} = \frac{p_4}{\gamma} + (1 - \eta_s) \frac{C_2^2 - C_4^2}{2g} - H_s - \frac{C_2^2 - C_4^2}{2g},$$

and hence

$$\frac{p_3}{\gamma} = \frac{p_4}{\gamma} - H_s - \eta_s \frac{C_2^2 - C_4^2}{2g}.$$

We assume that velocities C_2 , C_3 and C_4 have a meridional direction, or we take

into account only their meridional components, because the peripheral component of velocity C_3 is not decreased by the draft tube and not utilized.

Pressure p_4 in the cross section $b-b$ equals barometric pressure, and we can, therefore, substitute $\frac{p_4}{\gamma} = H_B$, where H_B is the barometric pressure expressed as water column, so it applies

$$\frac{p_3}{\gamma} = H_B - H_s - \eta_s \frac{C_2^2 - C_4^2}{2g}. \quad (26)$$

Hence it is evident that the pressure at the back of the runner equals barometric pressure minus the static suction head H_s and the pressure gain of the draft tube $\eta_s \frac{C_2^2 - C_4^2}{2g} = \nu H$.

2. Cavitation

Pressure p_3 is not the lowest pressure which occurs along the passage of the liquid through the turbine. It is the pressure directly at the ends of the blades at the beginning of the draft tube. In some places within the ducts of the runner, pressure will be still lower. Since the water acts upon the blades in a peripheral direction, the pressure on the blade from one side (the so-called pressure side) must be higher (the so-called driving pressure on the blade), and the pressure from the other side (suction side) must be lower (the so-called driving underpressure on the blade). At the end of the blade, both pressures have the same value p_3 , and so within the duct, on the suction side of the blade, the pressure must be lower. The maximum difference from pressure p_3 is denominated $\Delta h'$.

Hence the lowest pressure on the blade will be

$$\frac{p_{2\min}}{\gamma} = \frac{p_3}{\gamma} - \Delta h' = H_B - H_s - \eta_s \frac{C_2^2 - C_4^2}{2g} - \Delta h'. \quad (27)$$

This pressure can have various magnitudes according to the values on the right side of the equation. When it is lower than the tension of the vapours corresponding to the temperature of the liquid flowing through the turbine (the tension of water vapour at 15°C is 0.174 m, at 20°C, 0.238 m of water column), the liquid begins to evaporate at these points in the form of bubbles. These vapour bubbles, forming on the suction side of the blade in the place of the lowest pressure, are entrained by the flow of the liquid along the suction side of the blade, i. e. they are carried to places where the pressure is higher than $p_{2\min}$. In places where pressure is higher than the vapour tension, the vapour condenses and the bubbles collapse. This collapsing of the bubbles proceeds very rapidly, so that the surrounding liquid, filling up the empty spaces thus created, impinges very violently on the blade, thereby producing audible shocks and even vibrations of the machine.

This phenomenon is called cavitation. By the impacts of the liquid the surface of the blade is subjected to heavy strain; when the blade is not made of particularly resistant material, its surface will be corroded within a short period of a few weeks, or even the blade will get holes. The cause of this rapid deterioration of the material will be explained later (in the second part of this book).

If cavitation is to be avoided, the pressure $p_{2\min}$ must be higher than the vapour tension. We express this condition, denominating the vapour tension H_t , by:

$$\frac{p_{2\min}}{\gamma} = H_B - H_s - \eta_s \frac{C_2^2 - C_4^2}{2g} - \Delta h' > H_t,$$

from which follows that the static suction head H_s must not exceed the value:

$$H_s \leq H_B - H_t - \eta_s \frac{C_2^2 - C_4^2}{2g} - \Delta h'. \quad (27a)$$

Barometric pressure minus the vapour tension is $H_b = H_B - H_t$. The expression $\eta_s \frac{C_2^2 - C_4^2}{2g} - \Delta h'$ will have a higher magnitude, the greater the flow rate through the turbine; for a certain flow rate, however, this expression is proportional to the head, so that, giving the coefficient of proportionality the sign σ , we can write

$$H_s \leq H_b - \sigma H. \quad (28)$$

The coefficient σ we call the Thoma cavitation parameter. For a given turbine its value will be the higher, and hence the permissible suction head will be the lower, the greater the flow rate through the turbine. It will assume the highest value for the maximum flow rate, and the suction head must be adjusted to these conditions.

The suction head is according to Equation (28) also dependent on barometric pressure and thus on the altitude above sea level in which the turbine has to be installed, for barometric pressure is dependent on the altitude above sea level h (m) and can be expressed with sufficient accuracy by the relation:

$$H_b = 10 - \frac{h}{900}.$$

With various types of turbines the coefficients σ differ, and according to Prof. Thoma the value of σ for the maximum flow rate may be approximately expressed on the base of the specific speed n_s (see further) by means of the following table:

n_s	50	100	200	300	400	500	600	700	800
σ	0.02	0.05	0.11	0.2	0.35	0.57	0.81	1.45	2.15

Example: We have to ascertain the suction head for a turbine determined for a head $H = 5$ m, at $n_s = 430$, will be about 0.406. The turbine has to be installed in an altitude of 900 m above sea level.

First we determine

$$H_b = 10 - \frac{900}{900} = 9 \text{ m},$$

so that:

$$H_s \geq H_b - \sigma H = 9 - 5 \cdot 0.406 = 6.97 \text{ m}.$$

Hence the runner must be placed up to 6.97 m above the tail water level.

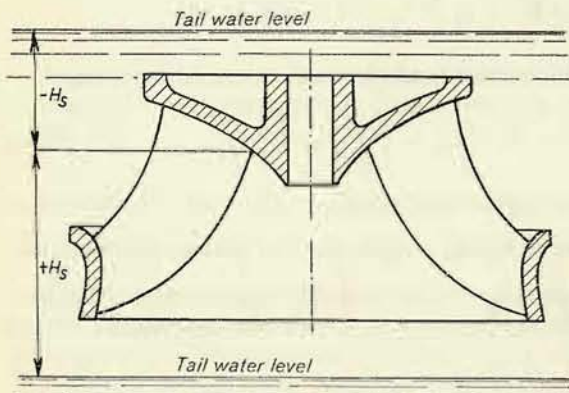


Fig. 33

If we would employ, in the same case, a turbine with a specific speed $n_s = 550$ (propeller turbine), σ would be 0.735, and therefore

$$H_s = 9 - 25 \cdot 0.735 = -9.4 \text{ m},$$

from which is evident that the demands of cavitation restrict the selection of the specific speed and also the type of turbine.

Note: In our investigations carried out so far we have seen that the energy and flow rate equations, too, under different conditions assume different forms.

Generally, we may write the energy equation as follows:

$$U_1 C_{u0} - U_2 C_{u2} = g H \eta_h = g H (1 - \varrho - \alpha - \zeta + \nu),$$

which is the energy equation in general, where the flow approach subject to shock is encountered and the turbine is fitted with a draft tube.

For shockless entrance of the water, there will hold good $C_{u0} = C_{u1}$ and $\zeta = 0$, and the equation will read:

$$(U_1 C_{u1} - U_2 C_{u2}) = g H \eta_h = g H (1 - \varrho - \alpha + \nu),$$

and for a turbine without a draft tube we further reckon

$$\nu = 0.$$

In a similar way we write the flow rate equation in this form:

$$\frac{C_0^2 - C_2^2}{2g} + \frac{W_2^2 - W_0^2}{2g} + \frac{U_1^2 - U_2^2}{2g} = H \eta_h = H (1 - \varrho - \alpha - \zeta + \nu),$$

which is the flow rate equation in general, where the flow approach with shock is encountered and the turbine is equipped with a draft tube.

For a shockless entrance of the water, $C_0 = C_1$, $W_0 = W_1$, and $\zeta = 0$, and hence the equation will assume the form

$$\frac{C_1^2 - C_2^2}{2g} + \frac{W_2^2 - W_1^2}{2g} + \frac{U_1^2 - U_2^2}{2g} = H \eta_h = H (1 - \varrho - \alpha + \nu),$$

and for a turbine without a draft tube we must reckon with $\nu = 0$.

VI. EXAMPLES OF TURBINE DESIGNS AND OUTPUT CONTROL METHODS

In the foregoing chapters we have learnt about the various arrangements of hydraulic turbines, such as turbines placed in pits, in boiler-type shells, and spiral casings. Now we shall learn about the internal arrangement of turbines, their design, by a few typical examples.

Fig. 34 presents a section through a pit-type turbine.¹⁾ This is suitable for a small output. We have here a Francis reaction turbine, i. e. with a runner of the mixed-flow type, for a head of $H = 2.5$ m, a flow rate of $Q = 0.5$ m³/sec., a speed of $n = 230$ rpm and an output of $N = 13$ metric horse-power (75 kgm/sec.).

The runner consists of an outer rim and a hub extending into a disc. Between them are the runner blades.

The runner is only keyed-on to the shaft. For such a small turbine keying is quite sufficient for transmitting both the torque and the arising axial force (directed into the elbow of the discharge tube) due to the overpressure of the runner. Since this is a pressure turbine, the water has a higher pressure in the front of the runner than in the draft elbow. In order to reduce the quantity of water which unutilized by-passes the runner between the rim and the rear cover (volume efficiency), the clearance between the rim and the cover is only small. The same is the case between the front cover and the disc of the runner. As, in spite of this arrangement some water penetrates through this gap into the space between the disc of the runner and the front cover, an additional axial load of the runner would be created by the fact that in this space the water pressure would be higher than at the other side of the disc, at the beginning of the draft elbow, just by the overpressure of the runner. For this reason the disc near the hub is provided with relief orifices by

¹⁾ From Hýbl J.: Vodní motory (Hydraulic Motors, Part 3, Tables), Prague; Česká matice technická, 1928.

which the pressure from both sides is partly equalized. These orifices – as we shall see later – should be as far away as possible from the shaft of the turbine, but not mouth into the runner ducts, because the water emerging from these relief orifices would disturb the flow in the ducts. The front cover is fastened by means of a flange to the wall ring, which in turn is concreted to the wall between the pit and the engine room. The rear cover is held by both the elbow and the bolts of the guide blades, which are for this purpose stepped on both ends.

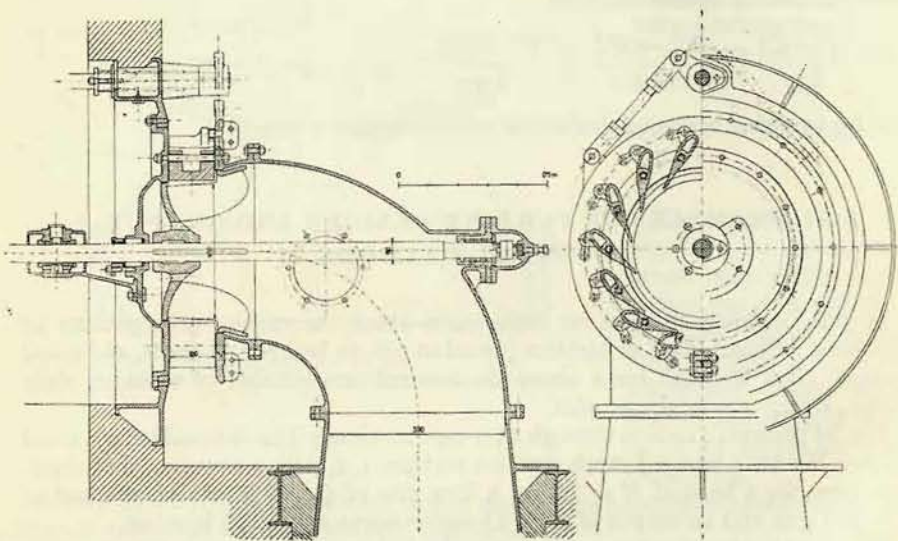


Fig. 34

Between both covers are the blades of the guide wheel. Their task is to supply the water to the runner in the correct direction and at the correct velocity, as we have already seen. At the same time, they regulate the quantity of water which must flow through the turbine and thus they also regulate the output of the turbine. For this reason they are pivoted on the already mentioned bolts, which at the same time firmly connect both covers. The blades are mounted by means of bronze sleeves, so that they can be adjusted from the open position to the fully closed position (the so-called Fink regulation). When they are put into a position other than assumed in designing the runner – on the base of the inlet velocity triangle – the water will enter the ducts of the runner at an incorrect angle, giving rise to the previously mentioned shock. The adjustment of the blades is performed by means of regulating pins and pull rods from the shifting ring, as indicated in Fig. 34. The shifting ring is shifted by means of regulating pull rods and a regulating frog actuated by a regulating shaft which proceeds through a bearing and a stuffing box in the wall ring into the engine room. The regulating shaft is shifted by means of a governor

or manually by a gear. The control mechanism in this case is in water and we speak of a so-called inside regulation.

The shaft is mounted on two bearings. One is located in the elbow of the draft tube and connected to the pin bearing to counteract the axial force. It is lubricated with lubricating grease supplied from the Stauffer lubricator in the engine room through a tube which is not indicated in the figure. This means that the shaft extends through the draft elbow and disturbs the flow in it; for this reason, the bearing is often omitted, and the runner is mounted on the shaft in an overhung arrangement, as will be shown in the following examples. The other bearing is a bracket-type, fitted with ring lubrication, and fastened to the outer cover of the turbine.

The shaft is led through the cover by means of a soft stuffing box fitted with hemp cords. The stuffing box prevents the water from penetrating to the outside when the turbine is fully opened and there is a moderate overpressure under the cover; on the other hand, it prevents the air from penetrating into the turbine through the small openings, when the vacuum prevailing in the draft tube advances through the relief orifices into the space under the cover. In order to improve this effect, the stuffing box is usually subdivided by a ring which is filled with water from the pit.

Fig. 35 shows a vertical Francis turbine in a spiral concrete pit, with a gear box for transmitting the output to a horizontal-shaft generator; the turbine is designed for a head $H = 2.17$ m, a flow rate $Q = 22$ m³/sec., a speed range $n = 38.7/215$ r. p. m. and an output of 532 h. p.¹⁾ It is important to note that this turbine differs

¹⁾ From Hýbl J.: *Vodní motory* (Hydraulic Motors, Part 3, Tables), Prague; Česká matice technická, 1928.

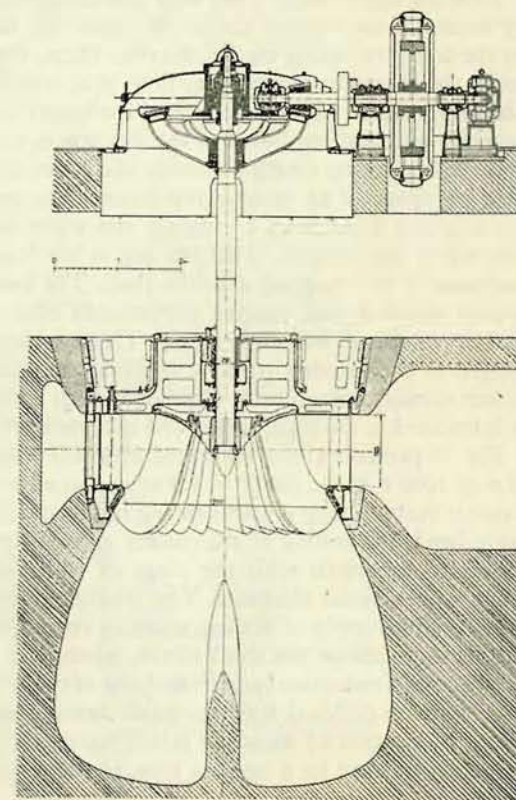


Fig. 35

from the installation described in the foregoing example particularly by the following features: The runner is placed on the shaft with sliding tolerance, whilst it is secured against rotary shift by a key and against axial forces by a split ring which fits into a groove; this ring is held together by the runner hub which is put over it.

Here the upper cover is not kept at a constant distance from the lower blade ring by means of the bolts of the guide blades but by special bolts which are covered by the freely revolving blades slid over them; these guide blades are automatically set in the direction of the water flow, thus offering the least resistance. The guide blades are fitted with cast-on pins, the upper row of which extends through the bearings and stuffing boxes to the dry space, so that the control levers, pull rods and the regulating ring are outside the water and can be well lubricated; in this case we speak of an outside regulation. The shaft extends again through a soft stuffing box fitted with a ring for the water seal and is mounted in the guide bearing of the turbine. This bearing is lubricated with oil from a vessel placed underneath and rotating with the shaft. The bearing is fitted with a tube the free end of which is bent against the sense of rotation and immersed into the vessel, and draws the oil into the bearing. The axial load due to hydraulic forces and the weight of the rotating parts is supported on the gear box by a segment bearing which rotates in an oil bath. Connected with it there is another guide bearing which is lubricated in the same way as the turbine bearing.

Fig. 36 presents a cross section of a turbine with an output of 5180 h. p. at a speed of $n = 1000$ r. p. m., for $Q = 1.9$ m³/sec. at a head $H = 220$ m. This is a horizontal Francis turbine with a spiral casing reinforced by stay blades. With regard to the large head, the sealing of the runner gaps is carried out more efficiently, i. e. by means of labyrinth seals the rings of which interlace in a comb-like arrangement with a small clearance. The stuffing box of the shaft is also of the labyrinth type, with a supply of sealing water as required for the high speed. The shifting ring is mounted on the draft elbow, where it is more accessible, and at the same time allows a reduction in the overhang of the runner. The thrust bearing is placed in a common pedestal with the guide bearing, and both are equipped with circulating lubrication by means of an oil pump, the oil passing through a cooler. The runner is relieved by a by-pass pipe, as there is no place in the hub for relief orifices.

Francis turbines are built for large heads, up to about 400 m, and for the largest output, up to 150,000 kw per unit. With small heads they are only employed for small output because of their comparative simplicity.

For small heads, up to about 60 m, and also the largest output, up to about 150,000 kw¹⁾, Kaplan Turbines are usually employed, which compared with Francis turbines have the advantage that the curve of their efficiency plotted as function of their filling (and of the head, too, should the latter be variable) has a flatter shape. That means that their efficiency does not decrease so much when the turbine is operated with a flow rate (or head) other than that for which the

¹⁾ The Kaplan turbines in the Kuibyshev power station on the Volga river have the largest output in the world, i. e. 126,000 kw.

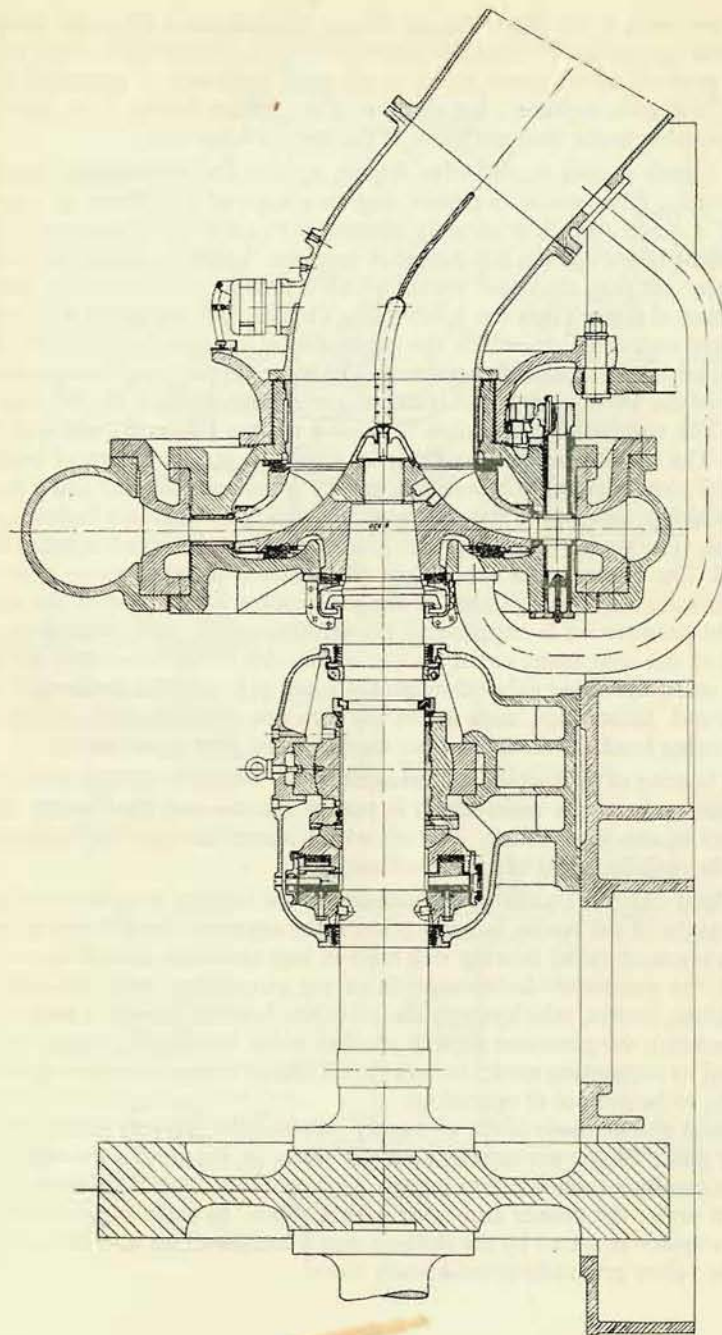


Fig. 36

runner was designed, as the shock loss at fillings differing from the rated value is smaller. This is carried out by a special feature so that at the variation of the filling not only the position of the guide blades is adjusted (by means of the usual Fink regulation as in Francis turbines), but also that of the runner blades. This allows to adjust their position to the changed angle of the approaching flow.

Appendix I gives a cross section of a Kaplan turbine for a maximum head of 20 m, a maximum flow rate of 75 m³/sec. and an output of 12,800 kw at a speed of $n = 166.7$ r. p. m., which is directly connected to an electric generator. The spiral steel casing of the turbine is mounted in concrete. The steel part of the casing is riveted to the cast ring, the upper part of which is held in position by the cast-on blades at a fixed distance from the lower part. To this ring the upper and lower blade rings are connected, in which the guide blades are arranged, in this case (a large installation) with outside regulation. The inner (upper) and bottom covers lead the flow of the water to the axial intake of the runner which is in the shape of a propeller. The turbine described has 6 pivoted runner blades mounted in the runner hub. The blades are set according to requirements by means of cranks, seated on their pins, between the bearings, and by means of pull rods and a regulating head which is fastened to the piston-rod extending through the hollow shaft of the turbine. The runner hub, in which the mechanism described is housed, is filled with oil. The piston-rod is actuated by the piston of the servomotor which is driven by pressure oil; the cylinder of the servomotor forms half of the shaft coupling. The pressure oil is supplied to the servomotor by pipes located in the hollow shaft of the alternator, either on the upper side of piston – through the outer pipe – or on the lower side – through the inner pipe and the perforated end of the piston-rod. Either pipe leads at the top into one chamber each, in the so-called distributing head. To each chamber another fixed pipe is connected.

The guide bearing of the turbine is lubricated by oil. The gear pump is driven by a toothed gearing from the main shaft; it pumps the oil into the bearing from a tank located in the inner cover. The oil which passes through the bearing is returned to the tank by means of a spray-off ring.

The axial load exerted by the water pressure on the runner, as well as the load due to the weight of the rotors, is supported on the segment thrust bearing combined with a segment radial bearing and built-in into the eight-spoked spider on the stator of the generator. Lubrication is of the circulation type, actuated by electrically driven pumps, which supply the oil to the bearing through a cooler and a filter. Underneath the generator there is another radial bearing, lubricated in the same way, and its supporting spider houses the oil brakes to stop the slowing-down turboset when to be put out of operation.

Mention must also be made of the air supply valves of the turbine, located in the cover. If the guide blades are rapidly shut the water in the draft tube will have a tendency to continue to flow due to inertia. This could lead to a disruption of the water column under the runner and cause a back shock. In such an event the air supply valves open – actuated by the shifting ring – and admit air into the turbine. After this, the valves gradually automatically close.

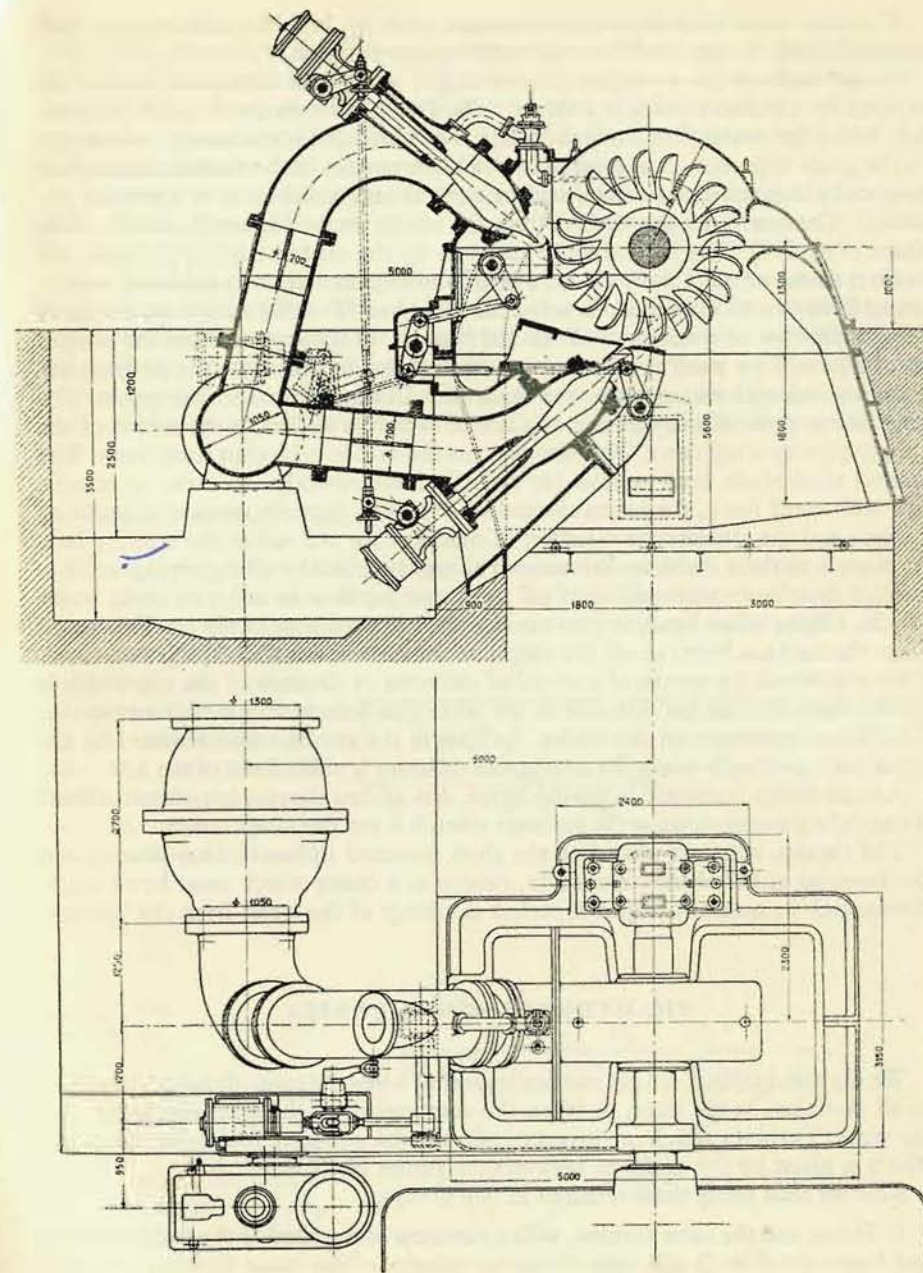


Fig. 37

Turbines with propeller-shaped runners, such as Kaplan turbines, but with non-adjustable runner blades are termed propeller turbines.

Pelton turbines are employed for the largest heads (the maximum head so far utilized by a Pelton turbine is 1747 m). The Pelton turbines are impulse turbines, i. e. with a free water flow along the blade. The total head is converted into velocity in the guide apparatus consisting of one or more nozzles (in horizontal installations maximally 2 nozzles per wheel, and in vertical arrangements 4 to 6 nozzles per wheel). The free water jet emerges from the nozzle on the blades of a double-ladle shape (Fig. 297). The jet is divided into two by the central edge of the blade (or bucket) along which it flows freely. Fig. 37 shows plan and cross section of a horizontal Pelton turbine with two nozzles, for a head of $H = 553$ m and an output of $N = 33,000$ kw at a speed of 420 to 500 r. p. m. In the cross section the nozzles can be seen; they must not enclose too small an angle, otherwise the jet from the second nozzle will encounter on the blade the still water from the first nozzle. The flow rate is controlled by means of a needle which is shifted in the socket of the supply pipe by a regulator. This also permits the nozzle to be shut completely. The control shaft shifts both needles (or spears) simultaneously. In order to achieve this with small force, the forces created by the water flow are counterbalanced by springs and the appropriate selection of diameter for the rod in the stuffing box. As regards to these turbines, the water is always supplied by a long piping, and the needles must only gradually shut off the incoming flow in order to avoid water shocks. On the other hand, to prevent an excessive overshoot of the machine speed when the load has been cut off, the output of the turbine must be rapidly decreased. This is achieved by means of a so-called deflector or deviator of the jet, which is quickly inserted into the direction of the latter and deflects it in such a way so that it no longer impinges on the blades. As soon as the needle – also actuated by the regulator – gradually opens the nozzle, the deflector is shifted out of the jet.

A small nozzle, indicated in the top figure, acts against the rotation of the turbine; it stops the slowing-down at the turboset when it is put out of operation.

The runner, which is placed on the shaft mounted in one turbine bearing and the bearings of the electric alternator, rotates in a casing which must be of ample dimensions so as not to impair a perfect discharge of the water from the buckets.

VII. HYDRAULIC SIMILARITY

We say that turbines are geometrically similar when the ratio of their dimensions in all directions is the same, or when the corresponding characteristic angles are the same. Turbines which are geometrically similar also have hydraulic similarity, which is given by the relations between the values H , Q , n , N , D .

Now we shall study these relations in two groups:

1. In one and the same turbine, with a variation of the head H the flow velocities and hence the flow Q will vary. Since the velocity of the water flow has changed,

the turbine speed, too, must change if the same inlet and outlet conditions on the blades (the same angles) are to be maintained. Since H has changed and with it Q , there must also be a change in N . The diameter D of the turbine remaining constant, we have thus given the relationship between the values H , Q , n , N . The appropriate relationship will, therefore, be valid for two individual turbines of the same size and shape, working under different heads.

2. For turbines of the same geometric shape and different diameters D , working under the same head H , we obtain the relationship between D , Q , n , and N , when $H = \text{const}$.

The relation mentioned fulfils the requirement that the Froude number must be the same. If we change the head and thus also the flow velocity in the turbine, or if we change the dimensions of the turbine, the Reynolds number of the through-flow, will also change. Thereby hydraulic losses in the turbine are also changed, and consequently the efficiency. In the first step of our investigation we shall disregard this point but special attention will be given to this in Chapters IX and XI/2.

1. Influence of Head Variations

When geometrically similar turbines of the same dimensions (i. e. the same turbines) work with the same filling (opening) under different heads H and H' , the through-flow velocities will be different, but the inlet and outlet angles of the blades and hence also the angles of the relative velocities will be the same, and the velocity triangles (inlet and outlet) may be similar. Both turbines may therefore, work under the same conditions (Fig. 38)

$$\frac{C_{u1}}{U_1} =$$

$$= \xi_1, \frac{C_{u2}}{U_2} = \xi_2. \quad (29)$$

In order to achieve this and to obtain similar flow conditions, we must appropriately adjust the peripheral velocities U_1 and U_2 , i. e. the speeds of the machines.

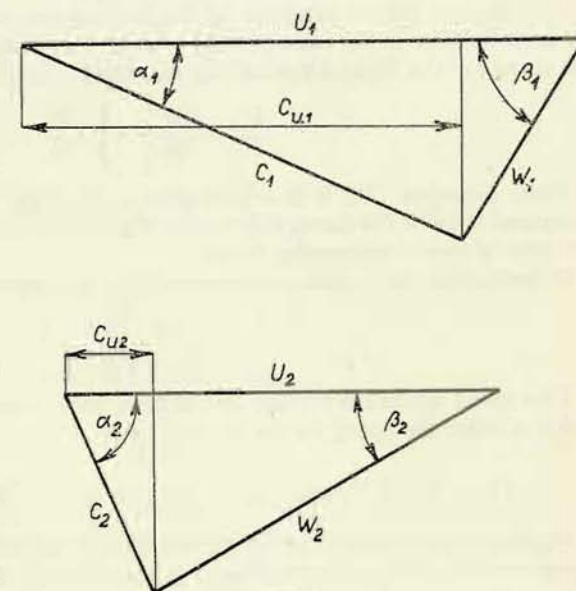


Fig. 38

α. Speed Variation with Head Variation

For these turbines the energy equation (20) applies:

$$\frac{1}{g} (U_1 C_{u1} - U_2 C_{u2}) = H \eta_h.$$

Using Equations (29), which determine the similarity of flow conditions, we can write

$$U_1^2 \xi_1 - U_2^2 \xi_2 = g H \eta_h.$$

Velocity U_2 , however, is always at a fixed ratio to velocity U_1 (in the ratio of the radii), so that $U_2 = k \cdot U_1$, so we can write

$$U_1^2 (\xi_1 - k^2 \xi_2) = g H \eta_h.$$

However, the expression in brackets is for a given turbine and a given flow rate a constant, so that we obtain

$$U_1^2 K = g H \eta_h.$$

If we denote for one of the compared turbines the peripheral velocity by U_1 , the proportional speed to this velocity by n , and the head by H , and for the corresponding characteristics of the second turbine the symbols U'_1 , n' and H' , we can write

$$U_1^2 K = g H \eta_h \text{ and } U'^2_1 K = g H' \eta_h.$$

Dividing the second equation by the first one and assuming that the efficiency for both turbines is the same (for the present we disregard the variation caused by the change of the Reynolds number), we obtain

$$\frac{U'_1}{U_1} = \frac{n'}{n} = \sqrt{\frac{H'}{H}}. \quad (30)$$

From Equation (30) it is evident that if the flow condition in the machines compared is to be the same, the ratio of their speed must equal the square root of the ratio of the corresponding heads.

If the head of the turbine compared is $H' = 1$ m, there will be

$$n_1 = \frac{n}{\sqrt{H}}. \quad (31)$$

This speed which the turbine should have under a head of 1 m, we denote by n_1 and it is called the speed for the head of 1 m.

β. Flow Rate Variation in Dependence on Head Variation

Since the cross sections of the turbine remain unchanged, flow rate Q according to the relation $FW = Q$ will change proportionally with the through-flow velocities and hence also proportionally with the angular velocities (with regard to the

already previously mentioned similarity of the triangles), and consequently with the speed, too,

$$\frac{Q'}{Q} = \frac{W'}{W} = \frac{U'_1}{U_1} = \sqrt{\frac{H'}{H}} = \frac{n'}{n}.$$

If the head of the compared turbine is $H' = 1$ m, there will be

$$Q_1 = \frac{Q}{\sqrt{H}}. \quad (32)$$

The flow rate which the turbine would have under a head of 1 m, we denote by Q_1 and it is termed the flow rate under a head of 1 m.

γ. Output Variation with Head Variation

The output of the turbine is determined by Equation (2):

$$N = \frac{1000 Q H \eta}{75}$$

for a head of H metres and a flow rate of Q m³/sec. For a flow rate of Q' and a head of H' the output will similarly be given by

$$N' = \frac{1000 \cdot Q' \cdot H' \cdot \eta}{75}.$$

Under the assumption of identical efficiencies, hence will apply

$$\frac{N'}{N} = \frac{Q' H'}{Q H},$$

and as according to previous considerations $\frac{Q'}{Q} = \sqrt{\frac{H'}{H}}$, there will be

$$\frac{N'}{N} = \frac{H' \sqrt{H'}}{H \sqrt{H}} \sqrt{\frac{H'}{H}} = \left(\frac{H'}{H} \right)^{\frac{3}{2}}.$$

If the head of the turbine discussed is 1 m, we obtain

$$N_1 = \frac{N}{\sqrt{H^3}}, \quad (33)$$

i. e. the output for the head of 1 m.

Example: If a turbine working under a head of $H = 9$ m, having a maximum flow rate of $Q = 2$ m³/sec. and a speed of $n = 600$ r. p. m., is transferred to another plant, where it works under a head of $H' = 3$ m, at what speed must the turbine run in order to attain approximately the same efficiency as in the original place, and what will be the maximum flow rate?

We apply the relation

$$\frac{n'}{n} = \sqrt{\frac{H'}{H}},$$

from which we obtain the new speed

$$n' = n \sqrt{\frac{H'}{H}} = 600 \sqrt{\frac{1}{3}} = 347 \text{ r. p. m.}$$

To determine the flow rate we use the relation

$$\frac{Q'}{Q} = \sqrt{\frac{H'}{H}},$$

from which it follows

$$Q' = 2 \sqrt{\frac{1}{3}} = 1.16 \text{ m}^3/\text{sec}.$$

2. Influence of Size

Geometrically similar turbines of different sizes (different diameters D), working under the same head, will have the same peripheral and flow velocities, as can be easily deduced from the following equation:

$$U_1 C_{u1} - U_2 C_{u2} = g H \eta_h,$$

as head H is the same, and the peripheral velocities U_1 to velocity U_2 must be in the same relation as components C_{u1} to C_{u2} if the flow has to be hydraulically similar, as already previously explained. The velocity triangles are not only similar but congruent. Only owing to the fact that the dimensions are different, will the Reynolds numbers also be different, and so, therefore, the efficiencies will be somewhat different. This last difference, however, will not be taken into account at present, so we may assume the efficiencies to be the same.

Both turbines will have the same peripheral velocities, e. g. at the leading edges of the blades, and the corresponding diameters will be denoted by D_1 and D'_1 . This velocity will be

$$U_1 = \frac{\pi n}{60} D_1 = \frac{\pi n'}{60} D'_1,$$

so it applies that

$$\frac{n}{n'} = \frac{D'_1}{D_1}.$$

The flow rate Q at the same flow velocity will vary with the through-flow area and hence it holds good:

$$Q = \frac{\pi D_1^2}{4} C_m \quad \text{and} \quad Q' = \frac{\pi D_1'^2}{4} C_m,$$

where C_m denotes the meridional component of the velocity. Therefore applies:

$$\frac{D'}{D_1} = \sqrt{\frac{Q}{Q'}} = \frac{n'}{n}.$$

In order to obtain the relation for the output, and assuming the head to be the same for both turbines we write:

$$\frac{D_1}{D'_1} = \sqrt{\frac{Q H}{Q' H}} = \frac{n'}{n},$$

Finally, subscript 1, can be omitted in all these relations, because for the geometrical similarity of both machines we can select an arbitrary diameter D as characteristic. Hence, we can write e. g.:

$$\frac{D}{D'} = \sqrt{\frac{N}{N'}} = \frac{n'}{n}. \quad (34)$$

3. Unit Values

If we recalculate step by step the characteristic values of the turbine for a head of 1 m and a diameter of 1 m, we obtain the so-called unit values. These unit values are to a certain degree characteristic for a given type of turbine and, therefore, are suitable for a graphical representation of the properties of the various kinds of turbines, as will be seen in Chapter XI.

Speed n , flow rate Q , and the torque M of the turbine with a characteristic diameter D , working under the head H , we convert to unit values in the following way.

To convert the speed to the characteristic diameter of 1 m we use the expression (34)

$$\frac{D'}{D} = \frac{n}{n'},$$

and when $D' = 1$ m, we obtain

$$n' = n D.$$

Furthermore, we reduce the speed to the head of 1 m, by applying the relation (31)

$$n_1 = \frac{n}{\sqrt{H}},$$

into which we substitute $n = n'$ and obtain

$$n'_1 = \frac{n'}{\sqrt{H}}.$$

$$n'_1 = \frac{n D}{\sqrt{H}}, \quad (35)$$

which is the expression for unit speed.

In a similar way we calculate the flow rate of the turbine first for a diameter of 1 m according to the previously derived relation $\frac{D}{D'} = \sqrt{\frac{Q}{Q'}}$, where we again substitute $D' = 1$, and obtain $Q' = \frac{Q}{D^2}$, and then by means of Equation (32), we calculate the unit flow rate:

$$Q'_1 = \frac{Q}{D^2 \sqrt{H}}. \quad (36)$$

By the same method we obtain the unit output

$$N'_1 = \frac{N}{D^2 \sqrt{H^3}}. \quad (37)$$

The expression for the moment we derive from the relation

$$M'_1 = 71620 \frac{N'_1}{n'_1} = 71620 \frac{N}{D^2 \sqrt{H^3}} \frac{\sqrt{H}}{n D} = 71620 \frac{N}{n} \frac{\sqrt{H}}{D^3 \sqrt{H^3}},$$

and thus the result is

$$M'_1 = M \frac{1}{D^3 H}. \quad (38)$$

Here we must again emphasize our assumption that the efficiency of a turbine with a diameter of 1 m, working under a head of 1 m, is the same as the efficiency of the original machine.

VIII. SPECIFIC SPEED OF THE TURBINE AND SPECIFIC VELOCITIES

1. Specific Speed from Reference Values

We have seen that the values (n , Q , etc.) of geometrically similar turbines are linked together by exact relations. Geometrically similar turbines must therefore have a common characteristic, which we obtain if we recalculate the turbines for the same conditions.

Such a generally adopted characteristic is given by the so-called specific speed, which we obtain if we reduce the dimensions of the turbine in such a way so that its output under the head of 1 m is 1 metric horse-power (0.987 h. p.). The specific speed n_s of any turbine hence equals the speed of a geometrically similar turbine working under the head of 1 m, when the latter turbine has such dimensions that it delivers under the head of 1 m an output of 1 metric horse-power.

We have denoted the speed for the head of 1 m by n_1 , and the output for this head by N_1 . Between the speed n_1 and the specific speed relation (34) holds good, the output at the specific speed being 1 metric h. p., so that we can write

$$\frac{n_s}{n_1} = \sqrt{\frac{N_1}{1}},$$

and hence

$$n_s = n_1 \sqrt{N_1}. \quad (39)$$

When we further substitute for n_1 and N_1 Equations (31) and (33) respectively, there will be

$$n_s = \frac{n}{\sqrt{H}} \sqrt{\frac{N}{\sqrt{H^3}}} = \frac{n}{H} \sqrt{\frac{N}{H}}. \quad (40)$$

Note: Equation (40) is not dimensionally homogeneous. The reason for this is that in our derivation we have substituted number one, for the output at specific speed, and thereby the dimension $\frac{\text{kgm}}{\text{sec.}}$ has disappeared. The physical dimension of n_s is 1/sec., for this is an actually possible speed.

It is evident from expression (40), that the specific speed (i. e. the speed of a turbine of a given shape and a diameter that under the head of 1 m output equals 1 metric horsepower) characterizes the ability of the machine to deliver at the highest possible speed the largest possible output.

According to Equation (40), the specific speed results from the values n , H , N , and the equation thus indicates which specific speed is required under given conditions. In order to determine the shape of the turbine (the type which meets this requirement), we must derive the expression for the specific speed from the design data of the turbine.

For this purpose, however, we must have an idea of specific velocities and, therefore, we now insert a chapter dealing with this subject.

2. Specific Velocities

As previously shown, we may encounter various through-flow and peripheral velocities according to the head under which the turbine works.

The energy equation

$$\frac{1}{g} (U_1 C_{u1} - U_2 C_{u2}) = H \eta_h$$

or the flow rate equation

$$\frac{C_1^2 - C_2^2}{2g} + \frac{W_2^2 - W_1^2}{2g} + \frac{U_1^2 - U_2^2}{2g} = H \eta_h$$

will again be satisfied if we multiply the head by a certain number a and at the same

time all velocities by the number \sqrt{a} . We have just used this property of the energy equation to derive the laws of hydraulic similarity. The actual velocities (through-flow and peripheral velocities) are, therefore, by no means characteristic for a given turbine, unless the head is also given. On the other hand, if we want to compare the velocities of different turbines we can only do so by recalculating their data and relating them all to the same head. Similarly, as we have already selected the reference head of 1 m for defining specific speed, we can now also take the same reference head. The velocities thus defined, however, would have the physical dimension $l^{\frac{1}{2}} t^{-1} \left(\frac{C}{\sqrt{H}} \right)$, and hence they would still be dependent on the acceleration of gravity. Therefore, in order to obtain dimensionless values and to attain the advantages dealt with in the following paragraphs, we select the reference head $\frac{1}{2g}$.

The specific speed will then be given by the following expressions and either denoted by small letters, to distinguish them from the actual velocities denoted by capital letters (as it is general), or marked with the subscript σ .

$$\frac{C_0}{\sqrt{2gH}} = c_0 = C_{0\sigma} = c_{0\sigma},$$

$$\frac{W_2}{\sqrt{2gH}} = w_2 = W_{2\sigma},$$

$$\frac{U_1}{\sqrt{2gH}} = u_1 = U_{1\sigma} = u_{1\sigma}.$$

Note: The previously introduced value $\alpha = \frac{C_0^2}{2gH}$ is, therefore, the square of the specific velocity c_0 ; $\alpha = c_0^2$.

These specific velocities are dimensionless expressions but indicate at the same time the values of the actual velocities, provided that the head $H = \frac{1}{2g}$; because

$$C = c\sqrt{2gH}, \text{ and when numerically } H = \frac{1}{2g}, \text{ then } C = c\sqrt{2g \frac{1}{2g}} = c.$$

Another advantage of specific velocities defined in this way is the fact that their squares indicate the proportion of the total head consumed to create these velocities; to create velocity C a head equalling the velocity head $\frac{C^2}{2g}$, is required and its ratio to the total head is given by

$$\frac{\frac{C^2}{2g}}{H} = \frac{C^2}{2gH} = c^2.$$

When e. g. the discharge velocity from the runner $c_2 = 0.65$ (as would be the case with a high-speed Kaplan turbine), it means that this velocity represents in p. c. $c_2^2 = 0.42 = 42\%$ of the total head and must, therefore, be unconditionally utilized and converted into pressure in the draft tube.

The specific velocities are not dependent on the head, nor on the dimensions of the turbine, but are characteristic for a certain type of turbine.

For all their advantages, the specific velocities are very often employed for design calculations of hydraulic turbines, and, therefore, we are going to express the energy and flow rate equations by means of these velocities. For this purpose we divide the original energy equation by the value $2H$ and obtain

$$\frac{U_1 C_{u1}}{2gH} - \frac{U_2 C_{u2}}{2gH} = \frac{\eta_h}{2},$$

and hence

$$u_1 c_{u1} - u_2 c_{u2} = \frac{\eta_h}{2}, \quad (41)$$

it also applies for a flow approach with shock

$$u_1 c_{u0} - u_2 c_{u2} = \frac{\eta_h}{2}. \quad (41a)$$

In a similar way, by dividing the original flow rate equation by the head H and calculate

$$\frac{C_1^2 - C_2^2}{2gH} + \frac{W_2^2 - W_1^2}{2gH} + \frac{U_1^2 - U_2^2}{2gH} = \eta_h$$

or

$$c_1^2 - c_2^2 + w_2^2 - w_1^2 + u_1^2 - u_2^2 = \eta_h = 1 - \rho - \alpha + \nu = 1 - \rho - c_2^2 + \nu,$$

$$c_1^2 + w_2^2 - w_1^2 + u^2 - u_2^2 = 1 - \rho + \nu.$$

The expression $H(1 - \rho + \nu)$ is also called the indicated head H_i , and the expression $\frac{H(1 - \rho + \nu)}{H} = 1 - \rho + \nu = c_i^2$, is likewise a dimensionless value the same as the specific velocities; c_i is called the indicated specific velocity.

For this value we finally obtain

$$c_1^2 + w_2^2 - w_1^2 + u_1^2 - u_2^2 = c_i^2. \quad (42)$$

Entry with shock similarly applies

$$c_0^2 - c_2^2 + w_2^2 - w_0^2 + u_1^2 - u_2^2 = \eta_h = 1 - \rho - \alpha - \zeta + \nu =$$

$$= 1 - \rho - c_2^2 - w_2^2 + \nu; \quad (42')$$

here we have substituted $\zeta = w_z^2$, where by w_z we can denote the specific shock velocity, for there has been

$$\frac{W_z^2}{2g} = \zeta H, \text{ hence } \zeta = \frac{W_z^2}{2gH} = w_z^2,$$

and therefore

$$c_0^2 + w_z^2 - w_0^2 + u_1^2 - u_2^2 + w_z^2 = c_t^2. \quad (42a)$$

3. Specific Speed Determined by Design Data

Now we are going to express the specific speed by design data in order to obtain the relationship between the dimensions of the machine and the specific velocities.

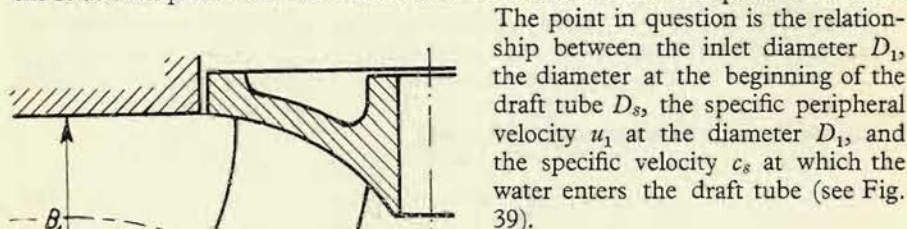


Fig. 39

The point in question is the relationship between the inlet diameter D_1 , the diameter at the beginning of the draft tube D_s , the specific peripheral velocity u_1 at the diameter D_1 , and the specific velocity c_s at which the water enters the draft tube (see Fig. 39). We shall assume that the inlet diameter D_1 , to which the specific peripheral velocity u_1 corresponds, is valid (in this case of specific speed) for the central stream line; the total flow rate we can replace by the quantity of water flowing per second along the central stream line, and thus we can calculate the mean peripheral specific velocity valid for the total through-flow.

We return to Equation (39):

$$n_s = n_1 \sqrt{N_1},$$

in which we replace the values n_1 and N_1 according to the following relations

$$U_1 = \frac{\pi D_1 n_1}{60} \quad \text{and} \quad U_1 = u_1 \sqrt{2gH}$$

and since $H = 1$, there will be $U_1 = u_1 \sqrt{2g}$, so that

$$n_1 = \frac{u_1 \sqrt{2g} \cdot 60}{\pi D_1}.$$

Further

$$N_1 = \frac{Q_1 \cdot 1 \cdot \gamma \cdot \eta}{75} \quad \text{and} \quad Q_1 = \frac{\pi D_s^2}{4} c_s \sqrt{2g},$$

and hence

$$N_1 = \frac{\gamma \eta}{75} \frac{\pi D_s^2}{4} c_s \sqrt{2g}.$$

By substituting the values n_1 and N_1 , expressed in this way, into Equation (39)

$$n_s = \frac{u_1 \sqrt{2g} \cdot 60}{\pi} \frac{D_s}{D_1} \sqrt{\frac{\pi}{4} c_s \frac{\gamma}{75} \eta \sqrt{2g}}$$

and by numerical expression of the constants we finally obtain

$$n_s = 576 u_1 \frac{D_s}{D_1} \sqrt{c_s \eta}. \quad (43)$$

Should the outlet cross section be restricted by the hub of the runner (as in propeller and Kaplan turbines, see Fig. 41e), the quantity of the through-flowing water will be smaller and hence the output, too. Therefore the following holds good:

$$n_s = 576 u_1 \frac{D_s}{D_1} \sqrt{c_s \eta \varphi}, \quad (43a)$$

where φ is the restriction of the cross section ($F_s = \varphi \frac{\pi}{4} D_s^2$, F_s is the through-flow cross section at the beginning of the draft tube).

These formulas relate to Francis, propeller and Kaplan turbines. They are not applicable to Pelton turbines, for which we must derive a separate formula.

But before doing so we must investigate the principles to achieve the required specific speed of these turbines from the formula (43, 43a).

It is evident that the specific speed increases with a rising peripheral velocity u_1 , with an increasing ratio $\frac{D_s}{D_1}$ and to a smaller degree with the inlet specific velocity (since the value of this specific velocity is under the radical sign) at which the water enters the draft tube, i. e. c_s .

What influence do these individual values exert on the shape of runner and blades?

1. With increasing specific speed u_1 increases according to Equation (43); at the same time the blade angles β_1 and β_2 decrease, and, thereby, the deviation angle of the blades. E. g., when for certain specific speeds the velocity triangles are represented by Fig. 40a, then with increasing u_1 also u_2 increases because these velocities are linked together by the shape of the runner. Hence, at the same flow rate and thus at the same value c_2 the angle β_2 decreases (see Fig. 40b). The inlet

angle β_1 decreases at the same time still more intensely, because in both cases the energy equation holds good, which, expressed in terms of specific velocities, reads:

$$u_1 c_{u1} - u_2 c_{u2} = \frac{\eta h}{2},$$

and for $c_{u2} = 0$ it assumes a simpler form

$$u_1 c_{u1} = \frac{\eta h}{2}.$$

If we increase u_1 , we must appropriately decrease c_{u1} in order to satisfy the equation. The angle β_1 , therefore, decreases very intensely when u_1 increases. The deviation angle also decreases and the blades assume a flatter shape.

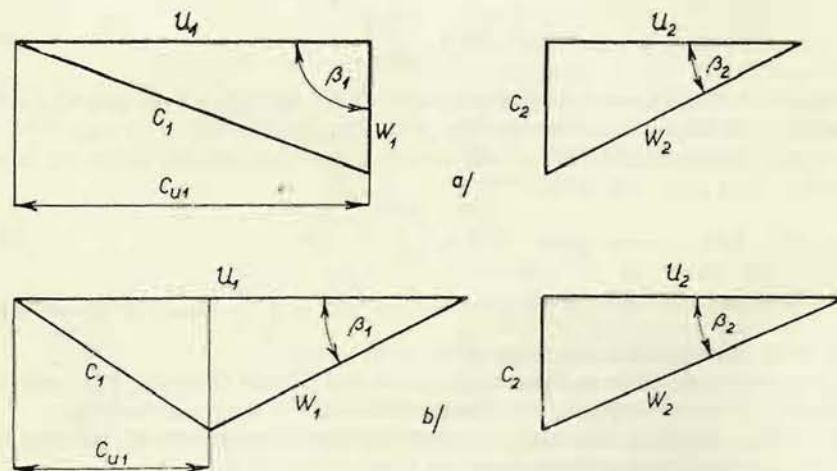


Fig. 40

2. With increasing specific speed the ratio $\frac{D_s}{D_1}$ must increase. At a low specific speed this ratio will be less than unity, the an runner will have a prevailingly radial shape; at higher specific speeds the value of this ratio will approach unity, and the runner will assume a radiaxial shape. At still higher speeds this ratio will exceed unity, and the runner will assume an axial shape; the highest value of this ratio, i. e. equaling approximately two, is encountered in propeller turbines which are operated at the highest specific speed. The effect of both these influences on the shape of the runner is indicated in Fig. 41.¹⁾

¹⁾ According to Kieswetter.

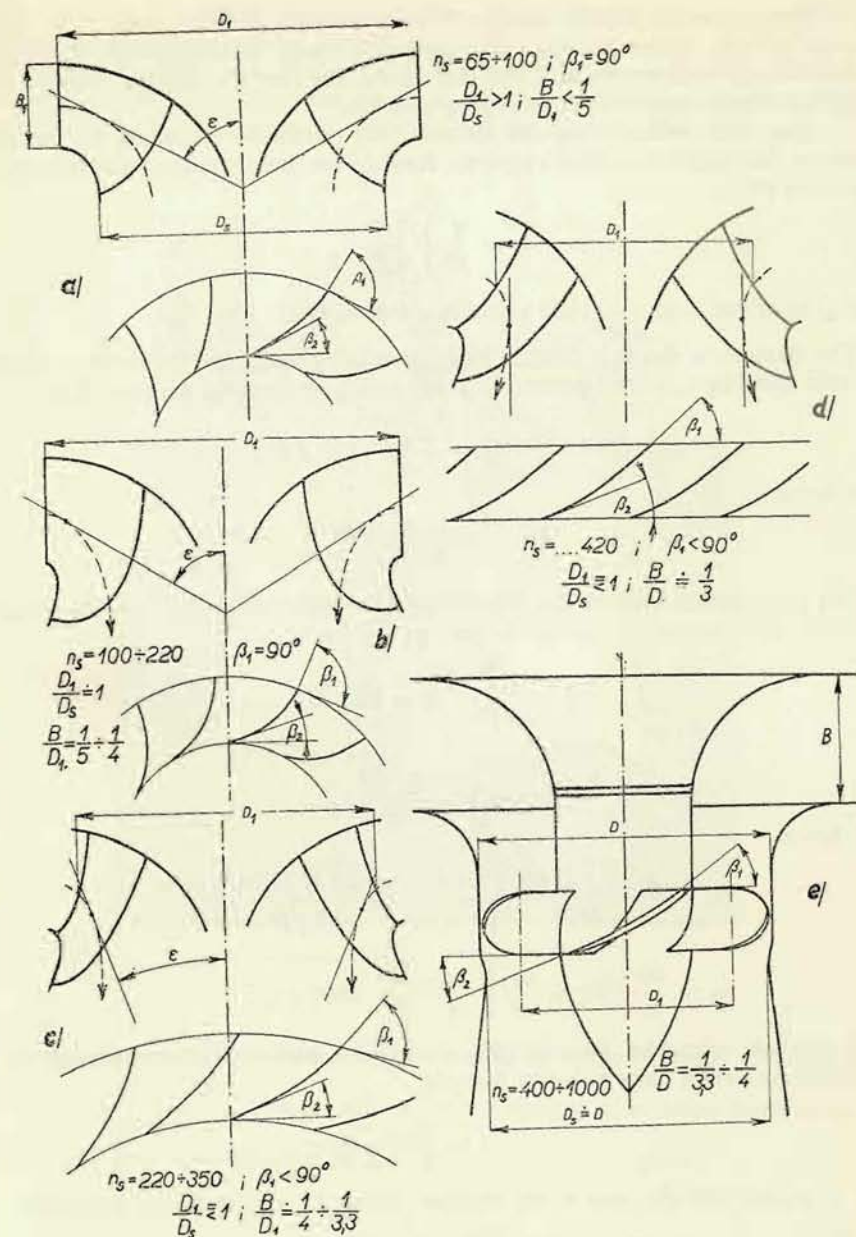


Fig. 41

3. With increasing specific speed the inlet velocity into the draft tube also increases. This means that more non-converted energy steadily enters the draft tube, where it must be utilized. For this reason, the function of the draft tube of high-speed turbines must be as perfect as possible.

As previously pointed out, the formula (43) cannot be employed for Pelton turbines. We therefore derive a separate formula for these turbines; we start with Equation (40):

$$n = \frac{n}{H} \sqrt{\frac{N}{H}}.$$

For Q in m^3/sec . and $\gamma = 1000 \text{ kg/m}^3$ holds $N = Q H \cdot 1000 \frac{\eta}{75}$.

The diameter of the jet is denoted by d_0 , its velocity by C_0 , and the corresponding specific speed by c_0 , so the quantity of water emerging from the nozzle will be

$$Q = \frac{\pi d_0^2}{4} C_0 = \frac{\pi d_0^2}{4} c_0 \sqrt{2gH},$$

and hence

$$N = \frac{\pi d_0^2}{4} c_0 \sqrt{2gH} \frac{1000 H \eta}{75}.$$

The peripheral velocity of the runner along the circle contacting the axis of the water jet, the diameter of this circle being D , will be

$$U_1 = \frac{\pi D n}{60} = u_1 \sqrt{2gH}.$$

so that

$$n = u_1 \sqrt{2gH} \frac{60}{\pi D},$$

and hence

$$n_s = \frac{u_1 \sqrt{2gH} 60}{\pi D H} \sqrt{\frac{\pi d_0^2}{4} c_0 \sqrt{2gH} \frac{1000 H \eta}{75}},$$

$$n_s = \frac{60}{\pi} \sqrt{2g} u_1 \frac{d_0}{D} \sqrt{\frac{\pi}{4} \frac{\sqrt{2g}}{75} 1000 \eta c_0}.$$

This formula resembles formula (43), so that by numerical expression of the constants we obtain quite a similar formula:

$$n_s = 576 u_1 \frac{d_0}{D} \sqrt{c_0 \eta}. \quad (44)$$

It is evident that the ratio of the diameter of the jet to diameter of the runner, i. e. the ratio $\frac{d_0}{D}$, is here of major importance.

In all types of turbine installations we can increase the specific speed still further by employing several parallel flows; this can be carried out either by equipping the turbine with a runner with a double-sided discharge (Fig. 42), or by arranging several single-flow runners on a common shaft (Fig. 11), or, as far as Pelton turbines are concerned, by employing several nozzles (injections).

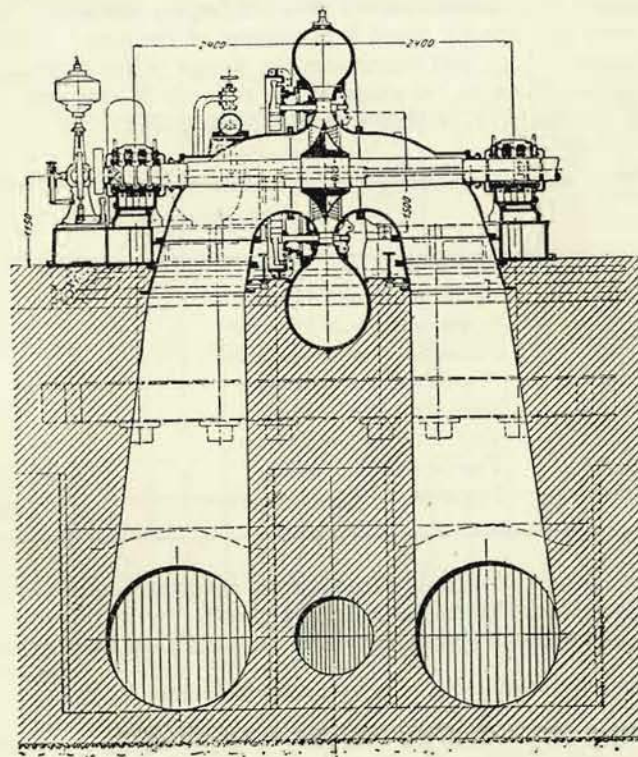


Fig. 42

If one runner or a Pelton wheel with one nozzle has at the output N' the specific speed $n'_s = \frac{n}{H} \sqrt{\frac{N'}{H}}$, then a machine with z runners or a Pelton wheel with z nozzles will deliver the output $z N'$ and develop the specific speed

$$n_s = \frac{n}{H} \sqrt{\frac{z N'}{H}} = n'_s \sqrt{z}. \quad (45)$$

The specific speed, therefore, increases with the square root of the number of flows.

In practical operation we encounter a maximum of 2 runners on one shaft or one runner with a double-sided discharge, and with Pelton turbines at the most two injections for one wheel on a horizontal shaft or 4 (up to 6) nozzles for a wheel on a vertical shaft. If 4 injections are to be employed in a Pelton turbine with a horizontal shaft, two wheels, each with two nozzles, are selected.

We have seen that specific speed is a measure of the speed of turbine under certain conditions (H , Q) and determines the design of the turbine, and consequently its shape (above all the shape of the runner). In this way, turbines are classified into certain types, according to the following table:

n_s	Turbine type
4 to 35	Pelton wheel with 1 nozzle
17 to 50	Pelton wheel with 2 nozzles
24 to 70	Pelton wheel with 4 nozzles
80 to 120	Francis turbine, low-speed
120 to 220	Francis turbine, normal
220 to 350	Francis turbine, high-speed
350 to 430	Francis turbine, express
300 to 1000	Propeller and Kaplan turbines

For certain heads, with regard to strength and cavitation, certain specific speeds are suitable, as indicated by the diagrams in Fig. 43.¹⁾

The dependence of the specific speed on the head²⁾ has been expressed in an analytical form by Morozov: $n_s \leq \frac{2200}{H^{0.57}}$ and by Zhapov: $n_s \leq \frac{2420}{\sqrt{H}} - 80$.

Example: We have to construct a turbine for $H = 240$ m, $Q = 2$ m³/sec., and hence for the output $N = \frac{240 \cdot 2000 \cdot 0.88}{75} = 5600$ metric horse power, the assumed efficiency being 0.88. With regard to a direct connection with the alternator we can select a specific speed of $n = 750$ r. p. m., or $n = 1000$ r. p. m. For $n = 750$ r. p. m. there will be

$$n_s = \frac{750}{240} \sqrt{\frac{5600}{240}} = 60 \text{ r. p. m.}$$

¹⁾ Armanet: Quelques applications des lois de similitudes... Informations techniques Charmilles, No. 3, p. 51.

²⁾ Sokolov: Gidravlicheskiye turbiny dlya malych GES, Moscow 1951.

For $n = 1000$ r. p. m. there will be similarly

$$n_s = \frac{1000}{240} \sqrt{\frac{5600}{240}} = 80 \text{ r. p. m.}$$

It is evident that in the first case a Pelton turbine with 4 nozzles will be satisfactory and in the second case a low-speed Francis turbine.

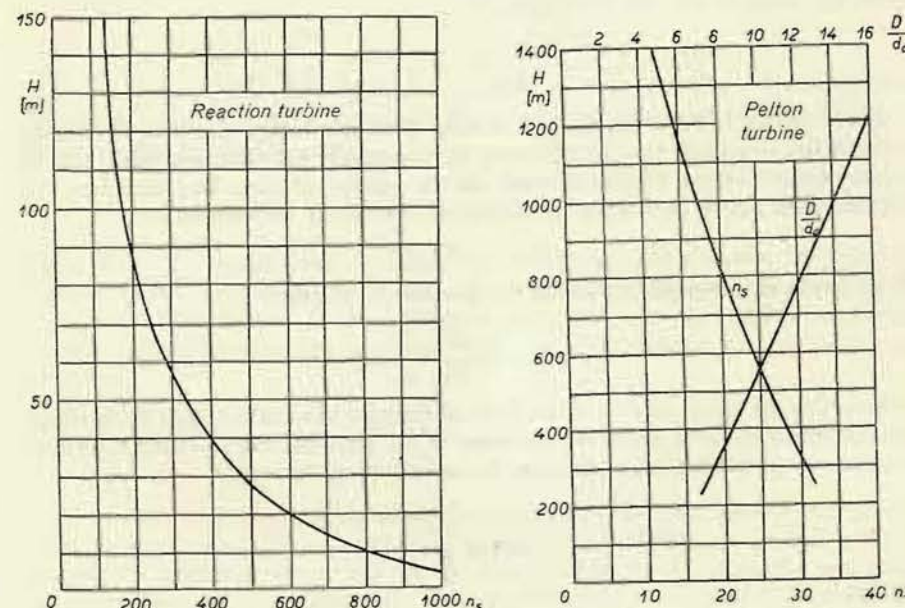


Fig. 43

IX. EFFICIENCY VARIATIONS IN DEPENDENCE ON THE DIMENSIONS OF THE MACHINE.

So far we have assumed in our calculations that the efficiency will not vary with a variation of the head and the dimensions of the turbine. At the same time, however, we have pointed out that this assumption will not be completely accurate. We can employ the derived formulas of hydraulic similarity with sufficient accuracy, as the efficiency variations are of a minor degree and can only in extraordinary cases assume higher values, nevertheless we shall subject these variations to a closer investigation, in order to determine the change in the efficiency under changed conditions.

We can express the hydraulic efficiency of a turbine on the basis of the work done by one kilogram of water, denoting the utilized head by H and the losses by H_z :

$$\eta_h H = H - H_z, \text{ hence } \eta_h = 1 - \frac{H_z}{H}. \quad (46)$$

Between two turbines, the data of one we mark with subscripts m , and the other which is similar to the first, with the subscripts s , but working under another head and having other dimensions, the following relationships must hold good to preserve the shape of the velocity triangles:

$$\frac{C_m}{C_s} = \frac{U_m}{U_s} = \frac{(R\omega)_m}{(R\omega)_s} = \frac{(Dn)_m}{(Dn)_s} = \sqrt{\frac{H_m}{H_s}}.$$

If the turbine is well designed, i. e. if it has good efficiency, the losses H_z (during a shock-free operation with an efficiency approximately the optimum value) will be mainly caused by the friction of water on the wetted surfaces. We, therefore, can express these losses, indicating the Reynolds number by the symbol Re :

$$H_z = f(Re) C^2.$$

E. g., in the pipe line holds good in the formula for the loss

$$h_z = \lambda \frac{C^2}{2g} \frac{l}{d}$$

(where C is the mean velocity of the flow in the pipe line, l the length along which we determine the loss, and d the diameter of the pipe) for the coefficient λ within a certain range the Blasius expression (accurately up to $Re = 10^5$)

$$\lambda = 0.316 \sqrt[4]{\frac{1}{Re}},$$

so that

$$h_z = 0.316 \frac{l}{d} \frac{1}{2g} \sqrt[4]{\frac{1}{Re}} C^2 = k \frac{C^2}{\sqrt[4]{Re}} = f(Re) C^2.$$

We see that the loss is actually a function of the number Re .

Hence, the following relation between the losses will apply in both cases:

$$\frac{H_{zm}}{H_{zs}} = \frac{f(Re)_m \cdot C_m^2}{f(Re)_s \cdot C_s^2} = \frac{f(Re)_m \cdot (nD)_m^2}{f(Re)_s \cdot (nD)_s^2}.$$

and, therefore, we can write

$$\eta_{hs} = 1 - \frac{H_{zs}}{H_s} = 1 - H_{zm} \frac{f(Re)_s \cdot (nD)_s^2}{f(Re)_m \cdot (nD)_m^2} \frac{1}{H_m \frac{(nD)_s^2}{(nD)_m^2}},$$

because

$$H_s = H_m \frac{(nD)_s^2}{(nD)_m^2}.$$

Since

$$\frac{H_{zm}}{H_m} = 1 - \eta_{hm},$$

there is

$$\eta_{hs} = 1 - (1 - \eta_{hm}) \cdot \frac{f(Re)_s}{f(Re)_m}.$$

In the expression for the Reynolds number we may select any characteristic dimension, provided that it is in fixed dependence on the dimension of the duct. For turbines one usually selects

$$Re = \frac{D\sqrt{H}}{\nu}, \quad (47)$$

where D is the largest inlet diameter of the runner, \sqrt{H} indicates the velocity of the flow, and ν is the kinematic viscosity of the flowing medium. For simplicity we select for the function $f(Re)$ the Blasius expression, and since in both turbines the same liquid flows at approximately the same temperature, so that $\nu_s \doteq \nu_m$, we obtain

$$\eta_{hs} = 1 - (1 - \eta_{hm}) \sqrt[4]{\frac{D_m \sqrt{H_m}}{D_s \sqrt{H_s}}} = 1 - (1 - \eta_{hm}) \sqrt[4]{\frac{D_m}{D_s}} \sqrt[8]{\frac{H_m}{H_s}}. \quad (48)$$

Thus we have determined the relation according to which the hydraulic efficiency of the turbine varies with a variation in size and with a variation of the head. Since in practical operation we usually do not know the hydraulic efficiency but only the total efficiency, we replace η_h by the total efficiency η and instead of the eighth root of the head ratio we substitute the tenth, whereby we obtain somewhat safer results in recalculations from a smaller to a larger head. The correspondingly modified formula, which is ascribed to Moody,¹⁾ then reads:

$$\eta_s = 1 - (1 - \eta_m) \sqrt[4]{\frac{D_m}{D_s}} \sqrt[10]{\frac{H_m}{H_s}}. \quad (49)$$

It is evident that this formula is derived on the basis of the fact that the hydraulic losses are in exact proportion to the square of velocity only when the same Reynolds number of the flow is also encountered. As this number is expressed in dependence on the size of the machine, the other dimensions, too, and hence also the roughness of the blades must be increased or decreased in the same proportion as the dia-

¹⁾ See e. g. Mühlemann E.: Zur Aufwertung des Wirkungsgrades. Schweizerische Bauzeitung (1948), p. 331.

meters of the machines (runners). This formula, therefore, involves the assumption that the roughness of the wetted surfaces of a smaller turbine is proportionally smaller than that of a larger machine.

In this country, frequent use is made of the Camerer formula which disregards the head variations and only takes into account the variations in the size of the machine. For expressing the losses, Camerer has applied the Mises formula or eventually Biel's for the losses in the pipe line:

$$H_z = l \frac{C^2}{R_h} \frac{\psi}{1000},$$

where R_h is the hydraulic radius, in our case that of the blade duct, i. e. $R_h = \frac{f}{u}$,

where f is the cross section area and u the circumference of the duct. Provided that:

$$\frac{F}{\sqrt{R_h}} = \sqrt{\frac{s}{R_h}},$$

where s represents the unevenness of the surface. The value ψ is given by Mises as:

$$\psi = 0.12 + \frac{F}{\sqrt{R_h}} + \frac{0.012}{\sqrt{C R_h}},$$

and by Biel as:

$$\psi = 0.12 + \frac{F}{\sqrt{R_h}} + \frac{0.0003}{(F + 0.02) C \sqrt{R_h}}.$$

Therefore, we now express the loss ratio

$$\frac{H_{zm}}{H_{zs}} = \frac{l_m \frac{C_m^2}{R_{hm}} \psi_m}{l_s \frac{C_s^2}{R_{hs}} \psi_s}.$$

Since in the case of geometrical similarity it holds good that $\frac{l_m}{R_{hm}} = \frac{l_s}{R_{hs}}$, we can replace the ratio of the squares of the velocities by the ratio of the heads, it follows

$$\frac{H_{zm}}{H_{zs}} = \frac{H_m \psi_m}{H_s \psi_s}$$

and hence

$$\eta_{hs} = 1 - \frac{H_{zs}}{H_s} = 1 - \frac{H_{zm} \psi_s}{H_m \psi_m} = 1 - (1 - \eta_{hm}) \frac{\psi_s}{\psi_m}.$$

Camerer, too, replaces the hydraulic efficiency by the total efficiency and puts

for ψ the above-mentioned function, in which he disregards the third term – thus neglecting the influence of the head – and in this way he obtains

$$\eta_s = 1 - (1 - \eta_m) \frac{0.12 + \frac{F_s}{\sqrt{f_s u_s}}}{0.12 + \frac{F_m}{\sqrt{f_m u_m}}}.$$

The hydraulic radius can with regard to geometrical similarity be replaced as follows:

$$\frac{f_s}{u_s} = R_{hs} = R_{hm} \frac{D_s}{D_m} = \frac{f_m}{u_m} \frac{D_s}{D_m},$$

so that

$$\eta_s = 1 - (1 - \eta_m) \frac{0.12 + \frac{F_s}{\sqrt{\frac{f_m}{u_m} \frac{D_s}{D_m}}}}{0.12 + \frac{F_m}{\sqrt{\frac{f_m}{u_m} \frac{D_s}{D_m}}}}.$$

If we now, according to Camerer, assume that the value F which characterizes the roughness of the wetted surfaces is in both cases the same and equal to

$$F_s = F_m = 0.015,$$

and hence

$$\sqrt{s} = 0.015, \text{ i. e. } s = 0.00025 \text{ m} = 0.25 \text{ mm},$$

and if further we take for a smaller machine

$$\frac{f_m}{u_m D_m} = 0.0275,$$

we obtain the approximate numerical expression

$$\eta_s = 1 - (1 - \eta_m) \frac{1.35 + \frac{1}{\sqrt{D_s}}}{1.35 + \frac{1}{\sqrt{D_m}}}.$$

In literature, this formula is usually quoted with the coefficients rounded off:

$$\eta_s = 1 - (1 - \eta_m) \frac{1.4 + \frac{1}{\sqrt{D_s}}}{1.4 + \frac{1}{\sqrt{D_m}}}. \quad (50)$$

In this formula we do not take into account the influence of the head and we assume that both turbines compared have the same roughness.

There are still other conversion formulas but we shall not quote them as, in general, they resemble the both above-mentioned formulas.

Both conversion formulas have been derived for shock-free approach of the water flow to the blade. As far as reaction (or pressure) turbines are concerned, when recalculating the efficiency for fillings accompanied by shocks we must use these formulas with a certain reservation.¹⁾

The efficiency of Pelton turbines increases more slowly with increasing dimensions. The reason for this is that with an increasing size of the machine the path along which the jet passes through the air before it reaches the bucket also extends; this also increases the rippling of the jet surface by the air and the losses which result of this phenomenon.²⁾

X. TURBINE PERFORMANCE AT OPERATION VARIATIONS

1. Turbine Performance at Constant Head and Speed and Varying Flow Rate

So far we have investigated cases of hydraulic similarity; we have determined how the speed of the turbine and the maximum flow rate, and thus the output also will vary with a varying head or size of the machine in order to maintain similar flow conditions. For these results we have compared two machines at the same relative filling.

Now let us consider how the operating conditions of the machine vary when the speed of the turbine has to be constant under a constant head which is most important in practical operation. In this case, the operation of the turbine must be adjusted to the required output (or to the available through-flow). This can be achieved, as has already been explained by turning the guide blades of Francis and propeller turbines, i. e. by varying their through-flow cross section, with Kaplan turbines by turning both the guide and the runner blades, and with Pelton turbines by varying the opening of the nozzle. Therefore the flow through the turbine also varies (we also say that the filling varies), which exercises an influence on the output, and, at the same time, on the efficiency.

¹⁾ In a treatise by S. P. Hutton, which deals with Kaplan turbines, it is pointed out that even during an operation corresponding to optimum efficiency only 7/10 of the losses are caused by friction. The remaining 3/10 are kinetic losses which do not vary with the size of the machine and with the head. The author has therefore derived formula which corresponds most correctly to actual conditions:

$$\eta_s = 1 - (1 - \eta_m) \left[0.3 + 0.7 \sqrt[5]{\frac{Re_m}{Re_s}} \right]$$

(S. P. Hutton: Component losses in Kaplan turbines and the prediction of efficiency from model tests. Proceedings of the Inst. of Mech. Eng. 168 — 1954 — p. 743.)

²⁾ Ogüey, Mamin: Étude théorique et expérimentale de la dispersion du jet... Lausanne 1944.

α. Progress of Efficiency with regard to the Filling of the Turbine

Efficiency is not the same at various fillings, but varies considerably. For a certain filling, as well as for a certain load, it is high and for all other fillings — larger or smaller — it is lower.

The flow rate belonging to the best efficiency η_{\max} we shall term Q_η . The efficiency value as a function of the flow rate plotted on the axis of abscissas diminishes towards both sides from Q_η and proceeds approximately as indicated in Fig. 44. The shape of the curve can be explained about in such a way that we consider the losses which here arise and are in principle of three kinds: losses due to friction and curvature of the flow, shock losses, and losses at the discharge from the runner.

We can express these losses for each kilogram of water as relative losses $\frac{H_z}{H}$ related to the head, and they are indicated in Fig. 44 by curves I and II.

1. Losses due to friction and curvature of the flow are proportional to the square of the through-flow velocity and thus also to the square of the flow rate according to the equation for losses due to the flow through the duct:

$$H_{z1} = \lambda \frac{l}{d} \frac{C^2}{2g} = \lambda \frac{l}{d} \frac{Q^2}{F^2} \frac{1}{2g},$$

if $d = \frac{4f}{u}$ it means, it is four times the value of the hydraulic radius $\frac{f}{u}$.

This equation represents a parabola with its vertex in the origin. In Fig. 44 these losses are shown at a relative value $\frac{H_{z1}}{H}$ together with the losses 3 — which, as will be seen later, are also dependent on Q — illustrated by the parabola I.

2. Losses due to shock are dependent on the magnitude of the shock (see p. 44), which is given by the expression $\frac{W_z^2}{2g}$, as previously determined. Losses are dependent on the deviation of the flow from the direction of the regular stream, where $W_z = 0$. This deviation is exclusively determined (see Fig. 45) by the reduction of the meridional velocity C_{m0} (component of the inlet velocity, lying in the

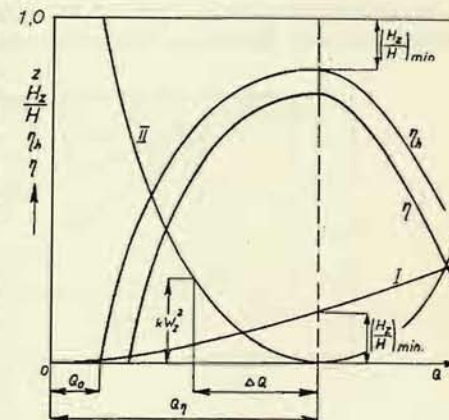


Fig. 44

plane of the meridional section and perpendicular to the inlet surface of the runner, given e. g. for a radial-flow runner by the cylinder created by turning the leading edge of the blade around the axis of rotation of the runner; its magnitude, therefore, is directly proportional to the flow rate) to C_{max} at the reduced flow rate Q_x . When the flow rate is reduced, the opening of the guide blades diminishes from the angle α' to α_x ; in this way both flow rate and meridional velocity decrease. At the same time, however, the discharge velocity from the guide wheel increases and thereby also the velocity immediately in front of the runner C_0 rises to the value C_{0x} , because in front of the runner which is now not entirely filled (but whose flow cross sections have not changed) pressure decreases. The water from the guide apparatus will now flow into a space with a lower pressure, and hence $C_{0x} > C_0$. In

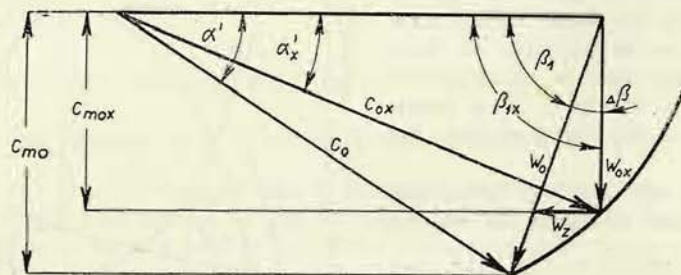


Fig. 45

figure 44 the line is indicated along which the vertex of the triangle will travel at a variation of the filling. It is to be seen that different fillings result in different magnitudes of shock velocity W_z . Plotting the relative losses

$$\frac{H_{z2}}{H} = \frac{W_z^2}{2gH} = w_z^2$$

in our diagram, we obtain the parabola II with zero ordinate at the optimum filling Q_η , when the water enters without shock.

3. Losses at the discharge are directly proportional to the square of the discharge velocity at which the water leaves the runner (or, when a draft tube is employed, they are proportional to the square of the velocity at which the water leaves the draft tube), and this velocity is proportional to the flow rate Q . These losses, therefore, are of the same character as those according to point 1 and can be represented together with them by parabola I.

By deducting the relative losses $\sum \frac{H_z}{H}$ from unity we obtain the progress of hydraulic efficiency η_h , which at a certain flow rate Q_0 assumes a value equalling zero. From this we see that the progress of the curve of hydraulic efficiency is materially influenced by shock losses and that the flow rate Q_0 also depends on

shock losses. If we further deduct mechanical losses, we obtain the progress of total efficiency η , which is also indicated in Fig. 44. In turbines with a higher specific speed the relative velocities are comparatively higher (see Fig. 40 and the respective text), and, therefore, shock losses are also more noticeable, which is manifested by a higher value of Q_0 in relation to Q_η (see Fig. 46). High-speed turbines, therefore, have a steeper progress of efficiency.

If we put Q_η into the value of the maximum through-flow (or flow rate) of turbine, i. e. Q_{max} , efficiencies at partial loads are lower than when we select $Q_\eta = k \cdot Q_{max}$, where k is less than unity (compare in Fig. 46 the line A with the lines drawn in full).

Therefore, we usually select k in the range between 0.75 and 0.9, according to the steepness of the efficiency curves, as follows:

$$n_s = 80, \quad k = 0.75, \\ \text{and } n_s = 450, \quad k = 0.9,$$

for Francis and propeller turbines, whilst for Pelton and Kaplan turbines we select $k = 0.75$ as here the efficiency curves have a flatter shape.

The flat efficiency curve of the Pelton turbine is due to a feature common to all impulse turbines, i. e. that at filling variations the angle of the entering water flow to the leading edge of the blade does not change (see the description of the Pelton turbine) and for this reason no shock losses are encountered.

In Kaplan turbines, this can be achieved by turning the runner blades. If we consider that the runner blades of the Kaplan turbine are fixed, then this turbine represents propeller turbine with a very steep (high n_s) progress of its efficiency, indicated as a function of the flow rate in dependence of the setting of the guide blades. Various setting of the runner blades results in various efficiency curves with various values of the optimum flow rate Q_η , such as indicated by the dashed lines in Fig. 47. When both the guide and runner blades are simultaneously turned, and when the setting of the runner blades in relation to that of the guide blades is correct, we obtain an efficiency curve as envelope of the mentioned dashed lines, and its shape is indeed very flat.

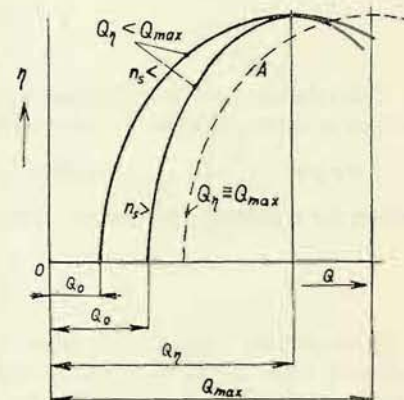


Fig. 46

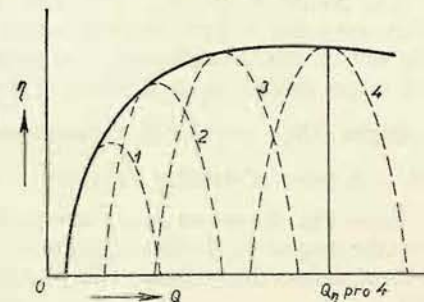


Fig. 47

β . Relation between Efficiency Curve and Output

If we know the efficiency curve of a turbine, represented as a function of the flow rate (e. g. determined by measurements), then for each flow rate Q the output N of the turbine is given in metric horse power (or in kw if we divide by 102 instead of by 75)

$$N = \frac{\gamma H Q \eta}{75} = \frac{\gamma H}{75} Q \eta. \quad (51)$$

This relation can also be used for a graphical determination of the progress of the output in dependence on the flow rate.¹⁾

If we put $\frac{\gamma H}{75} = \frac{1}{k}$, Equation (51) goes over into the relation $N = \frac{Q\eta}{k}$, which for graphical solution we transform into

$$\frac{k}{O} = \frac{\eta}{N}. \quad (52)$$

If we plot the output curve from the efficiency curve, k may be selected in an arbitrary scale. When selecting the scale for k it is advantageous to take the intersection of the lines η and N . For this point S (see Fig. 48) holds $\eta_s = N_s$, and hence $k = O_s$.

The points A' of the output curve we then determine in the following way: Through point A of the efficiency curve we draw a horizontal line until it intersects the vertical put through point S in point B . The connection between point B and the origin defines on the ordinate of point A point A' , from the similarity of the triangles OBQ_s and $OA'Q_A$ follows that $\frac{\eta_A}{Q_s} = \frac{N_A}{Q_A}$, and since at the same time $Q_s = k$, point A' satisfies Equation (52).

From Fig. 48 we can derive two particularly important relations. First, we find that the tangent T_N to the output curve, drawn through the origin of the coordinate system, defines the optimum filling (or flow rate) Q_η , because for η_{\max} the condition $\frac{d\eta}{dQ} = 0$ holds good; from Equation (52), however, it is seen that

$$\eta = \frac{N}{O} k,$$

and hence

$$\frac{d\eta}{dQ} = k \frac{Q \frac{dN}{dQ} - N}{Q^2} = 0,$$

¹⁾ Schauta: Der geometrische Zusammenhang der Betriebskurven. Wasserkraft und Wasserwirtschaft (1935), p. 222.

so that for the maximum efficiency the following holds good:

$$\frac{dN}{dQ} = \frac{N}{Q}.$$

Secondly, we can find – without having plotted curve N – the point on the effi-

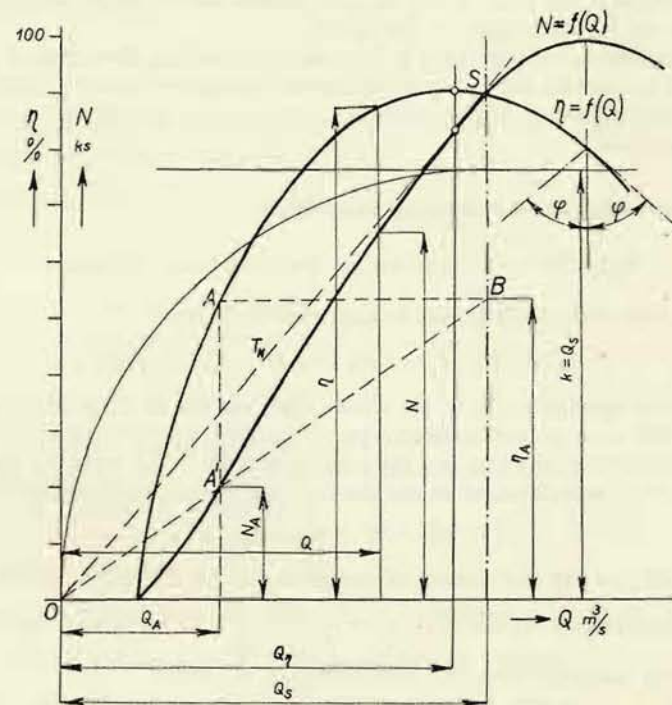


Fig. 48

ciency curve which corresponds to the maximum output. We write the condition for the maximum output as:

$$\frac{dN}{dO} = 0.$$

From Equation (52) in the form of $N = \frac{1}{k} Q \eta$ results

$$\frac{dN}{dO} = \frac{1}{k} \left(Q \frac{d\eta}{dO} + \eta \right) = 0,$$

and hence

$$\frac{d\eta}{dQ} = -\frac{\eta}{Q}.$$

This condition is fulfilled at that point of the efficiency curve where abscissa Q equals the negative subtangent of the curve, i. e. the point in which the angle φ from the vertical is the same as for the straight line drawn from the origin of the coordinates and for the tangent to the curve.

The determination of this point is important in practical designing as it would be of no use to increase the filling of the turbine beyond the value Q found in this way, because the output of the machine would not rise any further but, on the contrary, decrease.

2. Behavior of the Turbine at Speed Variations

α. Flow Rate Variation in Dependence on Speed

The flow rate of the turbine may be expressed as follows:

$$Q = f' c' \sqrt{2gH} = f_1 w_1 \sqrt{2gH} = f_2 w_2 \sqrt{2gH},$$

where c' is the specific speed in the outlet cross section of the guide wheel, f' is the area of this cross section measured perpendicularly to the velocity c' ; the subscripts 1 indicate the inlet into and the subscripts 2 the outlet from the runner.

In our further consideration we use the flow rate equation according to (42)

$$c_1^2 + w_2^2 - w_1^2 + u_1^2 - u_2^2 = c_i^2.$$

For a shock-free entry (for reasons of simplification we disregard the influence of shocks) approximately applies $c_1 = c' = \frac{Q}{f' \sqrt{2gH}}$. If we express similarly also w_1 and w_2 and substitute then into Equation (42), we obtain

$$\frac{Q^2}{f'^2} + \frac{Q^2}{f_2^2} - \frac{Q^2}{f_1^2} = (c_i^2 - u_1^2 + u_2^2) 2gH,$$

it therefore applies

$$u_2 = u_1 \frac{D_2}{D_1}, \text{ hence } n^2 - u_1^2 = -u_1^2 \left[1 - \left(\frac{D_2}{D_1} \right)^2 \right],$$

and we obtain

$$Q^2 \left(\frac{1}{f'^2} + \frac{1}{f_2^2} - \frac{1}{f_1^2} \right) = \left\{ c_i^2 - u_1^2 \left(1 - \frac{D_2^2}{D_1^2} \right) \right\} 2gH.$$

However, the expression in brackets on the left side of the equation is a function of the through-flow areas of the turbine, i. e. a constant, which we denote by k .

It then holds good

$$Q^2 k = 2gH_i - U_1^2 \left[1 - \left(\frac{D_2}{D_1} \right)^2 \right],$$

and since $U_1 = R_1 \omega = R_1 \frac{n}{9.55}$, where ω indicates the angular velocity and R_1 the inlet radius of the runner, there is

$$Q^2 k = 2gH_i - n^2 \frac{R_1^2}{9.55^2} \left[1 - \left(\frac{D_2}{D_1} \right)^2 \right], \quad (53)$$

Since the value of k is always positive, it is evident that the dependence of the flow rate on the speed will vary according to the ratio $\frac{D_2}{D_1}$. In low-speed

turbines the ratio $\frac{D_2}{D_1}$ is less than unity, and hence the end term on the right side of the equation is negative. The flow rate therefore decreases with a rising speed approximately according to the ellipse quadrant illustrated in Fig. 49 (in this diagram the correction has already been written in full with regard to the fact that so far we have neglected the entry shock, which will have its highest value at $n = 0$).

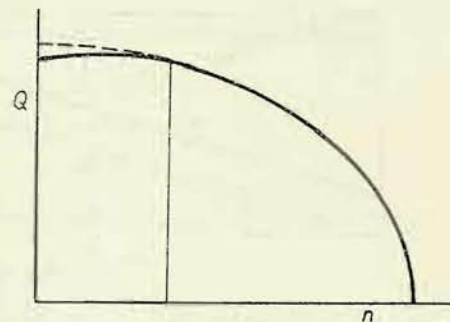


Fig. 49

In axial-flow turbines holds good $\frac{D_2}{D_1} = 1$, hence the last term in Equation (53) falls off and the flow-rate will be approximately constant.

In high-speed Francis turbines $\frac{D_2}{D_1}$ may be greater than unity at least for the outer layers of the flow, and the flow-rate then will moderately increase with rising speed.

In centrifugal turbines, which are no longer built,¹⁾ $\frac{D_2}{D_1}$ would be greater than unity, and the flow-rate would be increased by the speed of the machine.

In our analysis we have not taken into account the influence of shocks. It can be shown²⁾ that the influence of shocks is not manifested when the inlet blade angle equals 90° ; on the other hand, when the inlet angle β_1 is less than 90° , the shock

¹⁾ An example is the well-known Segner wheel.

²⁾ Thomann: Wasserturbinen und Turbinenpumpen, Part I, p. 93. Stuttgart, K. Wittwer 1924.

increases the flow-rate with a rising speed of the machine. This is, therefore, encountered in high-speed Francis and in Kaplan turbines.

The indicated head $H_i = H(1 - \rho + \nu)$ is not constant, as with an increasing flow-rate the through-flow losses $H\rho$ increase as well. With rising speed the shock losses, too, increase (see the following chapter). For this reason a fully relieved but open turbine will increase its speed only to the value at which the entire head is consumed for overcoming these losses. This speed is termed runaway or racing speed. If, by means of an external drive, we increase the speed beyond the runaway speed, then in a turbine in which $\frac{D_2}{D_1}$ is greater than unity the flow-rate would further increase, and the turbine would act as a pump in the direction of the head.

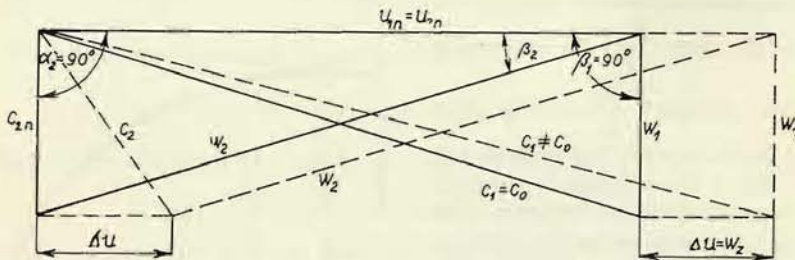


Fig. 50

On the other hand, in turbines in which $\frac{D_2}{D_1}$ is less than unity the flow-rate would diminish and finally completely cease at a speed of

$$n = \frac{9.55}{R_1} \sqrt{\frac{2gH_i}{1 - \left(\frac{D_2}{D_1}\right)^2}},$$

which follows from Equation (53) by substituting $Q = 0$; at a further increase of the speed the turbine would work as a centrifugal pump acting against the head.

Finally it must be emphasized that all these considerations only hold good for pressure (reaction) turbines. In impulse (action) turbines, e. g. in a Pelton turbine, the discharge from the nozzle is constant and independent of the speed of the wheel.

β . Dependence of Efficiency and Torque on Speed

In order to obtain a conception of this relationship, let us consider an axial-flow turbine in which the flow-rate does not change with the speed. Further let us assume an inlet triangle with angle $\beta_1 = 90^\circ$, and a perpendicular discharge from the runner, i. e. $\alpha_2 = 90^\circ$, as indicated in Fig. 50.

We again employ the flow-rate equation in the form given in Equation (42a):

$$c_0^2 + w_2^2 - w_0^2 + u_1^2 - u_2^2 + w_z^2 = c_1^2.$$

Since the flow-rate does not vary with the speed, the shock component w_z must be parallel to the peripheral velocity, and since the blade angle β_1 does not change, there must be $w_z = \Delta u$, where Δu denotes the change (increment) of the peripheral velocity.

Since the outlet angle β_2 is invariable as well, with increasing speed the vertex of the outlet triangle, too, must shift by the same value, so that for the outlet velocity c_2 holds good

$$c_2^2 = c_{2n}^2 + (\Delta u)^2,$$

where subscript n marks the value of the specific outlet velocity under normal conditions.

For hydraulic efficiency we have previously defined Equation (42')

$$\eta_h = 1 - \rho + \nu - c_2^2 - w_z^2,$$

from which it follows after substitution for c_2 and w_z

$$\eta_h = 1 - \rho + \nu - c_{2n}^2 - 2(\Delta u)^2.$$

However, $1 - \rho + \nu - c_{2n}^2$ is the maximum efficiency $\eta_{h\max}$ with a shock-free flow approach, so that

$$\eta_h = \eta_{h\max} - 2(\Delta u)^2.$$

For the assumed turbine in which $\beta_1 = 90^\circ$ and $\alpha_2 = 90^\circ$ (in normal operation), the energy equation holds good since $c_{u1,n} = u_{1,n}$ and $c_{u2,n} = 0$ (we have again used subscript n to indicate normal operating conditions with shock-free entrance)

$$u_{1,n}^2 = \frac{\eta_{h\max}}{2} \quad \text{or} \quad \eta_{h\max} = 2 \cdot u_{1,n}^2,$$

so that

$$\eta_h = 2[u_{1,n}^2 - (\Delta u)^2].$$

Since further $\Delta u = u - u_n$, there is

$$(\Delta u)^2 = (u - u_n)^2 = u^2 - 2u_n \cdot u + u_n^2,$$

and hence

$$\eta_h = 2(u_n^2 - u_n^2 + 2u_n \cdot u - u^2),$$

so that

$$\eta_h = 2u(2u_n - u). \quad (54)$$

Hydraulic efficiency depending on speed is, therefore, given by the parabola (Fig. 51) and has the value $\eta_h = 0$ for $u = 0$, and for $u = 2u_n$, i. e. for zero velocity and for a velocity equalling twice the normal velocity.

The considered turbine, therefore, cannot run faster than twice the normal

speed. This highest speed which a turbine can attain is termed runaway or racing speed.

Through the influence of mechanical losses the total efficiency η shifts to a lower value and the runaway speed still decreases. Here it must be taken into account that with decreasing speed the mechanical losses, which appear as the difference between hydraulic and total efficiency, also diminish.

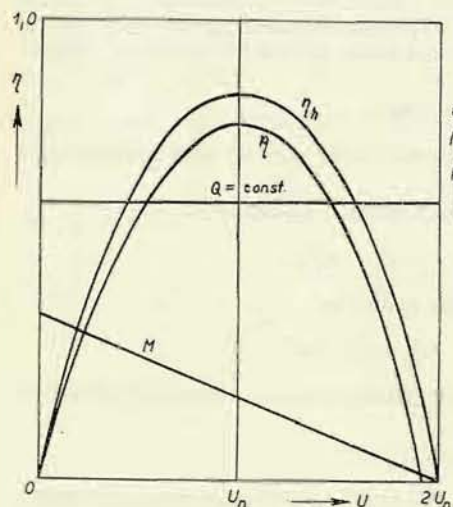


Fig. 51

The progress of the moment is therefore linear (Fig. 51), and the moment assumes zero value at runaway speed; at zero speed this so-called starting moment has double the value of the normal.

The output of the turbine is defined by the expression $N = \frac{1000 \cdot Q H \eta}{75}$, when given in metric horse-powers. So far we have considered Q and H invariable, therefore the progress of the output is defined by the progress of the total efficiency and is likewise approximately parabolical, the vertex of the parabola being situated at the normal speed.

These considerations apply to a turbine the flow-rate of which does not vary with speed. With regard to the fact that in low-speed turbines the flow-rate diminishes with a rising speed, and inversely, the runaway speed in this case will be somewhat lower than double the normal speed, and inversely, the starting moment will be somewhat higher than double the normal moment. In high-speed turbines, where the flow-rate rises with the speed of the machine, the contrary occurs, and the runaway speed will be somewhat higher and the starting moment somewhat lower than double the respective normal values.

If we denote the hydraulic output, i. e. the output transmitted to the blades, by N_h , the torque of the runner is defined by the relation:

$$N_h = M \omega = \frac{M u \sqrt{2 g H}}{r} =$$

$$= \gamma Q H \eta_h,$$

whence

$$M = \frac{\gamma Q H \eta_h r}{u \sqrt{2 g H}}$$

and after substitution η_h from Equation (54)

$$M = 2 \frac{\gamma Q H r}{\sqrt{2 g H}} (2 u_n - u) - 2 \frac{\gamma Q H r}{\sqrt{2 g H}} \frac{1}{\sqrt{2 g H}} (2 U_n - U)$$

$$M = \frac{\gamma}{g} Q r (2 U_n - U). \quad (55)$$

These values, which may be of importance when the strength calculation of the turbine can (according to the specific speed) be arranged approximately as per the following table:

$n_s =$	50	100	200	300	400	800	1000
$M_{\max} = k M_n : k$	2.2	2.05	1.88	1.8	1.75	1.7	1.6
$n_{\max} = K n_n : K$	1.6		1.8		1.9	2.4	2.6

XI. CHARACTERISTIC OF A TURBINE

1. Normal Characteristic

In order to ensure that a turbine to be constructed will be satisfactory as to maximum flow-rate and efficiency, the turbine-manufacturing works determine beforehand the properties of the turbine in question by means of a model test, utilizing the laws of hydraulic similarity.

Therefore, they construct a geometrically entirely similar turbine of smaller dimensions (diameter of the runner 200 to 400 mm), a so-called model turbine, which is then investigated in the testing station. In the testing station a pump transports the water to a higher tank from where piping leads to the model turbine. The station is equipped with instruments which permit exact measurements of the head, flow-rate and speed of the turbine. Breaking is used to determine flow-rates, efficiencies, runaway speeds and starting moments at various speeds and fillings, and by means of the previously derived formulas the values obtained are recalculated for the actual diameter and head of the ordered turbine.

The results achieved in this way may be also used for many other turbines ordered; they may be applied in all cases concerning turbines of the same geometrical shape, or as we say of the same type, i. e. in all cases where approximately the same specific speed is encountered.

For this reason the results of these tests are plotted into a clearly arranged diagram, the so-called characteristic of the turbine.

Therefore, the measured speed, flow-rates, and sometimes the efficiencies, too, are recalculated to unit values, i. e. corresponding to a runner diameter of 1 m and a head of 1 m. When the efficiency has also to be recalculated, one of the previously derived formulas is used.

The unit values have been derived in the forms

$$n'_1 = \frac{n D}{\sqrt{H}}, \quad Q'_1 = \frac{Q}{D^2 \sqrt{H}}.$$

As diameter we may select an arbitrary characteristic diameter of the runner. Manufacturing in this respect is not uniform. Most frequently, the largest diameter of the leading or inlet edge of the blade is selected in the case of Francis turbines, and the largest diameter of the runner for propeller and Kaplan turbines (see Fig. 54b). In the diagram we then draw these values in such a way to indicate on one axis n'_1 in a convenient scale, and on the other axis the value Q'_1 , whereupon we draw the curves of the same efficiencies η or of the same unit efficiencies η'_1 .

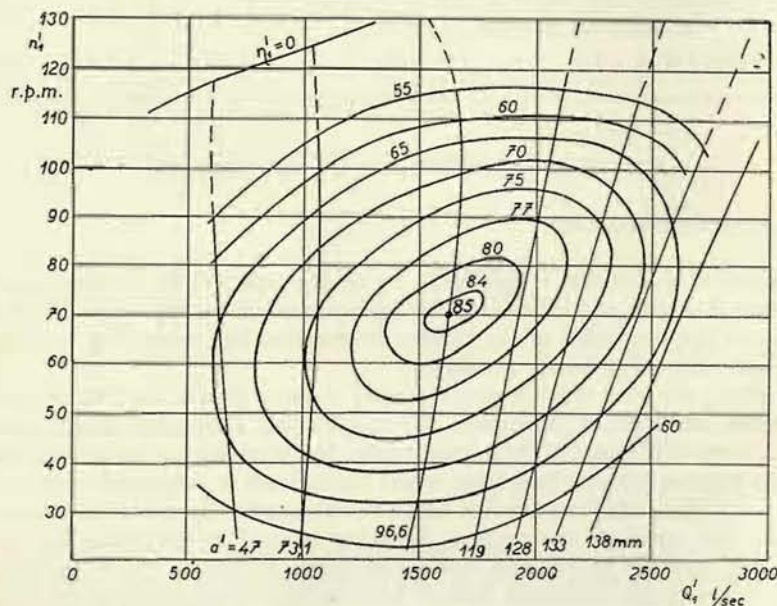


Fig. 52

Thus we obtain approximately the characteristic as indicated in Fig. 52. Into this we still draw the curves of the same opening of the guide apparatus (in the case of Kaplan turbines the curves of the same angles of the blades of the runner and of the opening of the guide apparatus). Since we measure stepwise at the same opening and stepwise varied speed, we obtain in our measurement directly these points. The opening of the guide apparatus is e. g. dimensioned according to the inner diameter at the trailing or outlet edge (see Fig. 53), which we denote by a' , recalculated for the diameter of 1 m. Usually we draw the curve indicating the dependence of the starting moments on the flow-rate, and the curves showing the dependence of the same cavitation coefficients σ on n'_1 and Q'_1 according to the results obtained in the cavitation test room (see Part II).

By the characteristic thus obtained the properties of the runner are therefore fully defined. The runner may then be used for a certain range of specific speeds.

For an easy determination of the specific speed from the unit values we further transform the corresponding formula as follows:

$$n_s = \frac{n}{H} \sqrt{\frac{N_1}{H}} = \frac{n}{H} \sqrt{\frac{1000 Q H \eta}{75 \sqrt{H}}} = \frac{n D}{\sqrt{H}} \sqrt{\frac{1000 Q \eta}{D^2 \sqrt{H} \cdot 75}},$$

so that

$$n_s = n'_1 \sqrt{1000 \frac{Q'_1 \eta}{75}}.$$

For instance, from the characteristic given in Fig. 52 we would more or less get this range of specific speeds for the runner in question. If we do not want for the maximum filling the efficiency η'_1 to be lower than 79 %, we may take into account

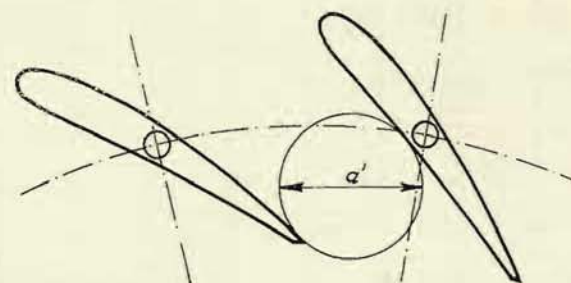


Fig. 53

a maximum opening $a'_{\max} = 119$ mm. The value of n'_1 we can select within the range of about 80 to 65 r. p. m. if we do not want the optimum unit efficiency $\eta'_{1, \max}$ to be lower than 80 %. We, therefore, can use the runner within the range of specific speeds from

$$n_s = 65 \sqrt{1000 \frac{1.8 \cdot 0.79}{75}} = 295 \div 300 \quad \text{to}$$

$$n_s = 80 \sqrt{1000 \frac{1.9 \cdot 0.79}{75}} = 358 \div 350.$$

From these characteristics it is evident how sensitive the turbine is to head variations, and, therefore, we must take into account this circumstance if the runner has to be employed in a hydraulic power station where the head varies to a greater extent.

The unit speed, according to which the characteristic has been plotted, is given by the relation $n'_1 = \frac{n D}{\sqrt{H}}$ and varies, and the operating point in the characteristic shifts (at a constant opening and at the same time varying flow-rate Q'_1) when

the speed varies under a constant head – which is the case of measurements in the testing station. The same variations, however, are encountered when the speed remains constant and the head varies – the case of the hydraulic power station. It is thus possible to predetermine from the characteristic how the flow-rate and efficiency of the turbine will vary at certain head fluctuations.

In general it can be stated that Pelton turbines are very sensitive to head variations; since they are only employed for large heads, i. e. where the relative head variations are not considerable, this point is of no account. Low-speed and normal

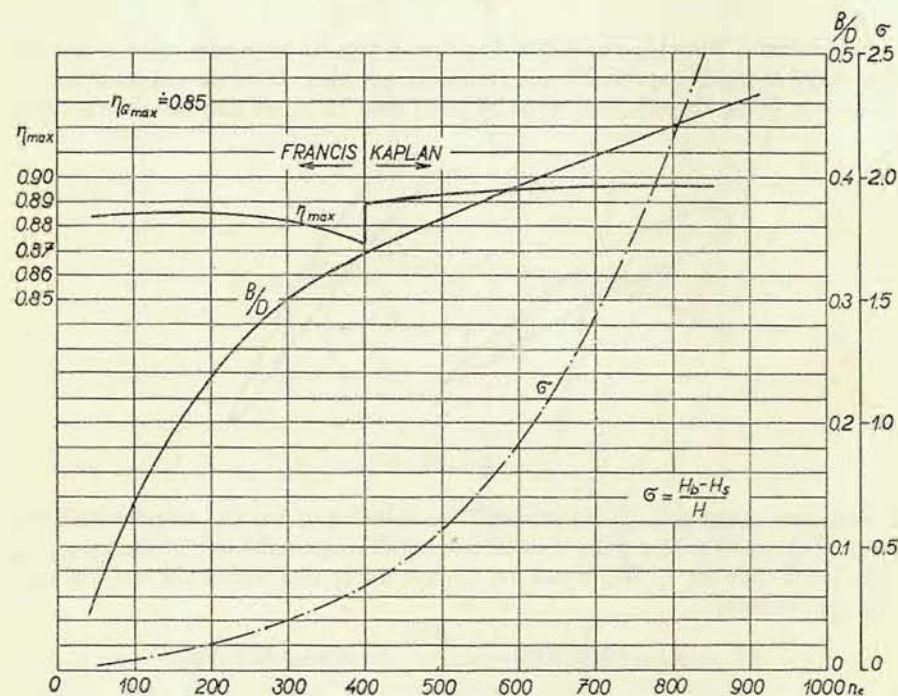


Fig. 54a

Francis turbines are less sensitive to head variations. Very sensitive to head variations are high-speed Francis turbines and propeller turbines. The least sensitive are Kaplan turbines.

To conclude our investigations on the similarity of turbines let us discuss similar problems with regards to stress. The parts of two turbines of different size, working under the same head, are subjected to the same stress when also the dimensions of the parts (e. g. wall thickness) are proportionally increased, for the bending moment (e. g. the load on the blade) as well as the torque (stress on the shaft) augment proportionally to the increase of the perpendicular distance of the force from the

axis, i. e. as the first power of the turbine diameter D . The force itself increases proportionally to the area on which the water pressure acts, i. e. proportionally to D^2 . The moment therefore increases proportionally to D^3 . The moduli of the cross section (resistance moment) of the part increases proportionally to the same power of D . The stress is therefore the same. For the same reason it holds good that with different heads the stress varies linearly with the head.

Figs. 54a and 54b illustrate the diagrams of the values n'_1 , $Q'_{1\max}$ (relative flow-rate), $Q'_{1\eta}$ (corresponding to the best efficiency), η_{\max} , and the dependence of the

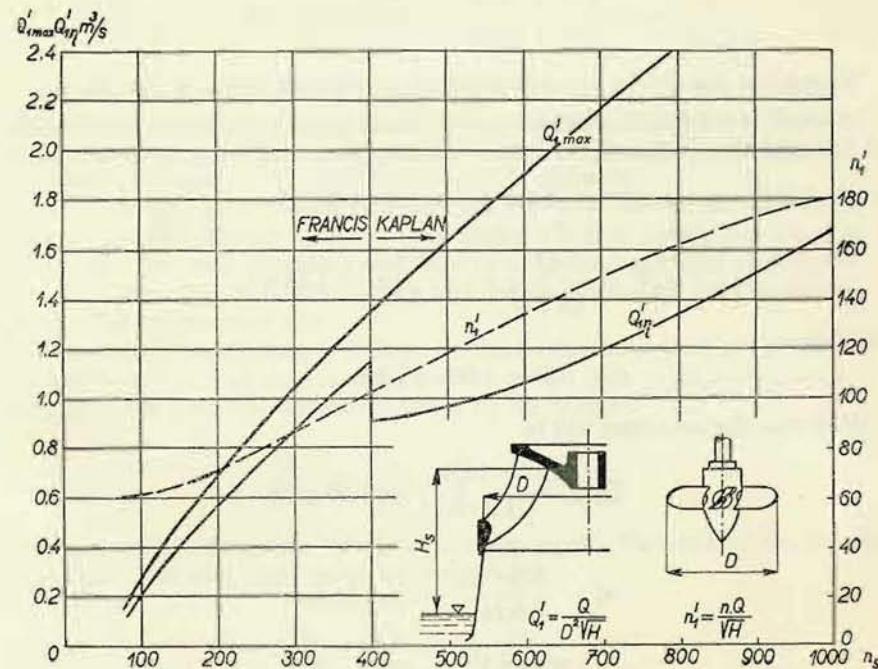


Fig. 54b

cavitation coefficient σ on the specific speed. The diagram is further supplemented by an indication of the ratio $\frac{B}{D}$ (the ratio of the face of the guide-wheel to the diameter of the runner). These are mean directive values as approximately employed for various specific speeds.

Example of applying the characteristic to determine the design details of a turbine for given conditions.

The principal dimensions and the speed of the turbine are to be determined for the following conditions: $H = 40$ to 35 m, $Q_{\max} = 13$ m³/sec.; the head most

frequently encountered during the year amounts to 38 m, and, therefore, we term it the rated or design head and construct the turbine so as to attain the best efficiency under this head.

We assume the total efficiency at maximum flow-rate to be $\eta = 0.8$, and hence the output will be $N_{ef} = \frac{38 \cdot 13,000 \cdot 0.8}{75} = 5300$ metric horsepower. We select the synchronous speed $n = 375$ r. p. m., so that

$$n_s = \frac{375}{38} \sqrt{\frac{5300}{\sqrt{38}}} = 9.9 \sqrt{860} \doteq 300.$$

We see that the specific speed corresponds to the type shown in Fig. 52.

In order to safeguard ourselves against inaccuracies, we calculate the flow-rate 10 % higher than required, i. e. $Q_{max} = 14.5$ m³/sec. The diameter of the runner is calculated from the expression for the unit flow-rate $Q'_1 = \frac{Q}{D^2 \sqrt{H}}$:

$$D^2 = \frac{Q}{Q'_1 \sqrt{H}} = \frac{14.5}{2 \cdot 6.16} = 1.18 \text{ m}^2,$$

and hence

$$D = 1.08 \doteq 1.1 \text{ m}.$$

With this diameter there will be

$$Q'_{1max} = \frac{14.5}{1.2 \cdot 6.16} = 1.95 \text{ m}^3/\text{s}$$

and

$$n'_1 = \frac{375 \cdot 1.1}{6.16} = 66.5 \text{ 1/min}.$$

For the highest head $n'_1 = \frac{375 \cdot 1.1}{6.3} = 65$, and for the lowest head $n'_1 = 70$.

In order to locate the operating point for the rated head in a more favourable position of n'_1 , we slightly increase the diameter of the runner, namely to $D = 1150$ mm.

Thus we obtain for a head of 38 m, $n'_1 = 70$, $Q'_1 = 1.81$,

a head of 40 m, $n'_1 = 68.5$, $Q'_1 = 1.76$,

a head of 35 m, $n'_1 = 73$, $Q'_1 = 1.9$.

The operating point is now very conveniently located in the characteristic, and the opening of the turbine is restricted to $a' = 122$ mm for a diameter of 1 m, and

to the value $a' = 140$ on the actual turbine. From the characteristic we can now exactly determine the efficiencies for various fillings and heads and recalculate them for the given diameter of the actual turbine $D = 1150$ mm.

2. Influence of Efficiency Variations upon the Unit Values

As already mentioned, we work out our recalculations from the model turbine to the ordered machine, or inversely, with unit values of the forms

$$Q'_1 = \frac{Q}{D^2 \sqrt{H}}, \quad n'_1 = \frac{n D}{\sqrt{H}}, \quad M'_1 = \frac{M}{D^3 \sqrt{H}}, \quad N'_1 = \frac{N}{D^3 H \sqrt{H}}. \quad (35 \text{ to } 38)$$

These conversions would be quite correct if the efficiencies of both compared turbines — η_m total efficiency of the smaller (model) turbine and η_s total efficiency of the large (actual) turbine), $\eta_{h,m}$ hydraulic efficiency of the smaller turbine and $\eta_{h,s}$ hydraulic efficiency of the larger turbine — were the same.

We have, however, shown that the efficiency of hydraulic turbines depends upon the size of the machine and upon the head under which it works, and that the efficiency improves with increasing size. The recalculation according to formulas (35 to 38) is, therefore, not quite correct and the deviations will be the greater, the greater the differences in size.

For this reason, in designing very large machines, the unit values of the actual turbine (subscripts s) and the unit values of the model (subscripts m) are not in accordance and (as given by Smirnov¹), linked by the relation

$$\frac{Q'_{1,s}}{Q'_{1,m}} = \frac{n'_{1,s}}{n'_{1,m}} = \sqrt{\frac{\eta_{h,s}}{\eta_{h,m}}},$$

Since the ratio of hydraulic efficiency roughly equals the ratio of the total efficiencies, we can write with sufficient accuracy:

$$\frac{Q'_{1,s}}{Q'_{1,m}} = \frac{n'_{1,s}}{n'_{1,m}} = \sqrt{\frac{\eta_s}{\eta_m}},$$

so that for the unit values which correspond on the model turbine to the operation of the large machine, we have to write

$$Q'_{1,m} = \frac{Q}{D^2 \sqrt{H}} \sqrt{\frac{\eta_m}{\eta_s}} \quad (36a)$$

$$n'_{1,m} = \frac{n D}{\sqrt{H}} \sqrt{\frac{\eta_m}{\eta_s}}, \quad (35a)$$

¹) Smirnov: Zakon podobiya i modelirovanie gidroturbin, Kotloturbostroyenie (1947), No. 3.

In deriving these expressions, Smirnov commences with the relations for the inlet angular velocities of both compared turbines:²⁾

$$U_{1,m} = \text{const} \cdot \sqrt{\eta_{h,m} H_m} = \frac{\pi D_m n_m}{60}$$

$$U_{1,s} = \text{const} \cdot \sqrt{\eta_{h,s} H_s} = \frac{\pi D_s n_s}{60},$$

Substituting into both these expressions $D = 1$ and $H = 1$, we obtain the unit speeds for the model and the full-size turbine

$$n'_{1,m} = \frac{60 \cdot \text{const} \sqrt{\eta_{h,m}}}{\pi}, \quad n'_{1,s} = \frac{60 \cdot \text{const} \sqrt{\eta_{h,s}}}{\pi}$$

hence one of the relations mentioned immediately follows

$$\frac{n'_{1,s}}{n'_{1,m}} = \sqrt{\frac{\eta_{h,s}}{\eta_{h,m}}},$$

The other relation

$$\frac{Q'_{1,s}}{Q'_{1,m}} = \frac{n'_{1,s}}{n'_{1,m}}$$

follows from the hydraulic similarity which requires for both compared turbines the same ratio of the meridional velocity to the angular velocity.

The actual turbine always has a certain prescribed flow-rate Q . Therefore, we shall have to restrict it (deviating from the conversion formulas 35 to 38) to the model value $Q'_{1,m}$ according to Equation (36a). Similarly, the speed of the actual turbine is also prescribed; in order to fulfil this requirement, we must select the model value $n'_{1,m}$ according to Equation (35a).

The efficiency of large machines may vary considerably, up to e. g. by 10 %. For this reason we must calculate with another point in the model characteristic of the turbine, which will correspond to lower values of Q'_1 and n'_1 than would be the case if we disregarded this influence. According to the point shifted in this way we must also determine the opening of the guide wheel (α') and that of the runner (β).

To this new point in the characteristic also corresponds a certain cavitation coefficient σ . For the actual turbine, however, we must multiply this value by the efficiency ratio $\frac{\eta_s}{\eta_m}$.²⁾

¹⁾ We have derived this relation in Chapter VII/1.

²⁾ Nechleba: K zákonu hydraulické podobnosti vodných turbin (On the Law of Hydraulic Similarity of Hydraulic Turbines). Technický sborník pre odbor strojno-elektrotechnický, Slov. akademie vied a umění (Technical Review of Mechanical and Electrical Engineering, Slovak Academy of Sciences and Arts). Bratislava (1953), No. 3, p. 33.

For the derivation we shall need such an equation for the torque in which the efficiency variations are taken into account. This equation is derived as follows:

If there were no efficiency variations, the output of the actual machine would be

$$N_s = \frac{Q_s H \eta_m}{75} = \frac{Q'_{1,m} D^2 \sqrt{H} \cdot H \eta_m}{75} = N'_{1,m} D^2 H \sqrt{H} \quad (37)$$

and, similarly, the moment would be according to Equation (38)

$$M_s = M'_{1,m} D^3 H. \quad (38)$$

Since, however, efficiency varies, we obtain at the same opening of both turbines

$$N_s = \frac{Q_s H \eta_s}{75} = \frac{Q'_{1,m} \sqrt{\frac{\eta_s}{\eta_m}} D^2 \sqrt{H} \cdot H \eta_s}{75}$$

and the moment

$$M_s = \frac{71,620}{75} \frac{Q'_{1,m} \sqrt{\frac{\eta_s}{\eta_m}} \cdot D^2 \sqrt{H} \cdot H \eta_s}{n'_{1,m} \sqrt{\frac{\eta_s}{\eta_m}} \frac{\sqrt{H}}{D}} \frac{\eta_m}{\eta_m} = M'_{1,m} \cdot D^3 \cdot H \frac{\eta_s}{\eta_m}. \quad (38a)$$

It is evident that not only the flow-rate and speed have increased but also the driving moment; the moment has increased in direct proportion to the efficiency ratio. For this reason, the Thoma cavitation parameter σ will assume a higher value than that corresponding to the point $Q'_{1,m}, n'_{1,m}$ in the model characteristic. If the efficiency of the large machine were the same as that of the model (we could attain this condition by roughening the blades), the moment according to Equation (38) would be increased in comparison with the unit moment as D^3 – which means increasing the area of the blade and the arm of the moment – and further as the rise of the pressure on the blade, i. e. as H . The influence of the head, however, has already been taken into account in the cavitation formula (28): $H_s = H_b - \sigma H$. For this reason the same cavitation coefficient would apply. Let us imagine that efficiency improves, then the moment would increase according to Equation (38a) as the ratio of the efficiencies; i. e. the forces acting upon the blade will rise, and thus also the specific pressures and underpressures will increase as the ratio of the efficiencies.

These underpressures are involved in the product σH in Equation (28). It also includes the regain of the draft tube, because according to Chapter V the following holds good:

$$\sigma H = \eta_s \frac{C_2^2 - C_4^2}{2g} + \Delta h',$$

But we have found out that $\Delta h'$ varies proportionally to the efficiency. In the

same ratio the squares of the velocities C_2 and C_4 , also vary. The total value of σ therefore varies in the ratio of the efficiencies.

We, therefore, can determine the correct permissible suction head if we multiply the value σ , which otherwise we would introduce as corresponding to the point Q'_{1m}, n'_{1m} , by the efficiency ratio $\frac{\eta_s}{\eta_m}$.

The recalculations given in this section are suitable in those cases concerning great differences in efficiencies, i. e. a great difference between the sizes of the model and the actual machine. In other cases we disregard the influence of efficiency variations upon the unit values and the cavitation coefficient.

XII. BRAUN'S DIAGRAMS

1. Derivation of the Diagram

We have already previously shown that the inlet and outlet triangles of the turbine are linked together by the energy equation or by the flow-rate equation. When we e. g. freely select the outlet triangle, we can no longer entirely freely select the inlet triangle, but we must e. g. determine c_{u1} , from the energy equation (41)

$$u_1 c_{u1} - u_2 c_{u2} = \frac{\eta_h}{2}$$

and this value must be maintained in the inlet triangle.

In runner designing this calculating procedure is often replaced by a graphical method which is clearer and more suited for following the variations of the triangles under various operating conditions.

There are several graphical designing methods (Prášil, Camerer, Thomann)¹⁾, the most universal, however, is the method given by Braun,²⁾ which we will now explain.

Hydraulic efficiency when a draft tube is employed is generally given by the expression

$$\eta_h = 1 - \rho - \zeta - \alpha + \nu. \quad (56)$$

If we use the notion of indicated speed according to Chapter VIII, it will hold good:

$$c_i^2 = 1 - \rho + \nu \quad (57)$$

$$\eta_h = c_i^2 - \alpha - \zeta = c_i^2 - c_2^2 - w_2^2. \quad (58)$$

¹⁾ See e. g. Thomann: Wasserturbinen und Turbinenpumpen, Part I, Stuttgart, K. Wittwer 1921.

²⁾ E. Braun: Über Turbinendiagramme, Zeitschrift für d. ges. Turbinenwesen 1909, and also Thomann, as cited above.

With these symbols the energy equation now generally reads (Chapter VIII):

$$c_0^2 - c_2^2 + w_2^2 - w_0^2 + u_1^2 - u_2^2 = \eta_h = 1 - \rho - \alpha - \zeta + \nu \quad (59)$$

or

$$c_0^2 + w_2^2 - w_0^2 + u_1^2 - u_2^2 + w_z^2 = c_i^2. \quad (60)$$

Following this repetition of fundamental relations we shall first, in Part α , give the derivation for the case of a shock-free entry, when $w_z = \zeta = 0$, and then in Part β the derivation for a general case.

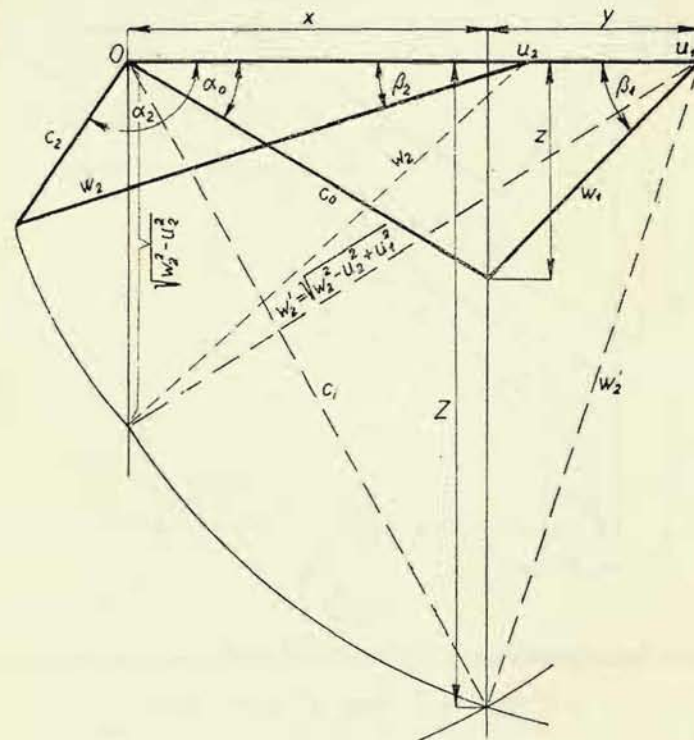


Fig. 55

α . Shock-Free Entry

In this case, the energy equation (60) assumes a simpler form

$$c_i^2 = w_2^2 - w_1^2 + c_0^2 + u_1^2 - u_2^2.$$

We introduce the auxiliary value w_2' according to the relation

$$w_2'^2 = w_2^2 - u_2^2 + u_1^2 \quad (61)$$

and obtain

$$c_i^2 - w_2'^2 = c_0^2 - w_1^2, \quad (62)$$

which can be expressed graphically as indicated in Fig. 55.

According to this figure it applies that

$$z^2 + x^2 = c_0^2 \quad \text{and} \quad z^2 + y^2 = w_1^2,$$

and hence

$$c_0^2 - w_1^2 = x^2 - y^2.$$

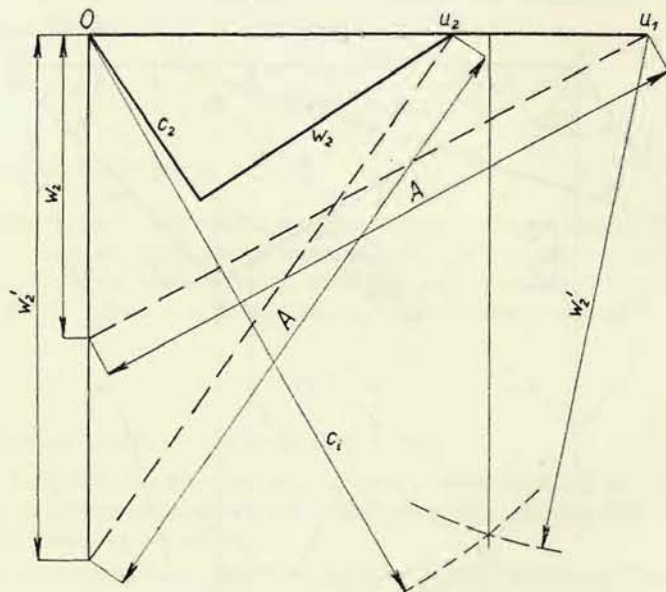


Fig. 56

It similarly holds good that

$$Z^2 + x^2 = c_i^2 \quad \text{and} \quad Z^2 + y^2 = w'_{\frac{3}{2}}^2,$$

and hence

$$c_1^2 - w_2'^2 = x^2 - y^2,$$

Combining the equations now derived, we obtain

$$c_i^2 - w_2'^2 = c_0^2 - w_1^2,$$

which is in accordance with Equation (62), and so we see that this construction satisfies the flow-rate equation.

The construction is as follows (Fig. 55): The circle of the radius w_0 , drawn from the end point of the velocity u_0 as centre, we intersect by the perpendicular from

the origin O of the diagram. Through this intersection we then draw a circle with its centre in the end-point of the velocity u_1 . Its intersection with the circle of the radius c_i and its centre in the origin O of the diagram then determine the position of the vertical on which the vertex of the inlet triangle must be located.

When $w_0 < u_0$, we rewrite Equation (61) as follows:

$$w_2'^2 + u_2^2 = w_2^2 + u_1^2 = A^2,$$

whereupon the length w'_2 by which the circle c_i in Fig. 55 must be intersected from the end point of the velocity u_1 , in order to find the position of the inlet vertical, is obtained by means of the construction shown in Fig. 56.

β . Entry with Shock

From the general energy equation (41a)

$$u_1 c_{u0} - u_2 c_{u2} = \frac{\eta_h}{2}$$

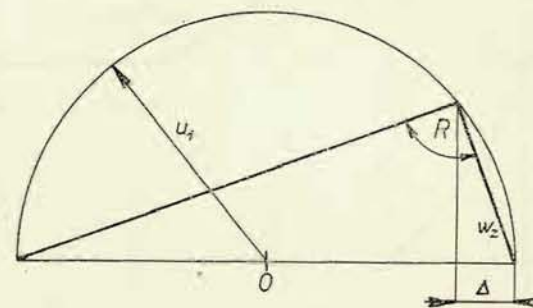


Fig. 57

follows when we substitute from Equation (58): $\eta_h = c_i^2 - c_2^2 - w_z^2$

$$c_{u0} = \frac{\eta_h}{2u_1} + \frac{u_2}{u_1} c_{u2} = \frac{c_i^2 - c_2^2 - w_z^2}{2u_1} + \frac{u_2}{u_1} c_2 =$$

$$= \frac{c_i^2 - c_2^2}{2u_1} + \frac{u_2}{u_1} c_{u2} - \frac{w_z^2}{2u_1}$$

or

$$c_{u0} = c_{u0(n)} - \frac{w_z^2}{2u_1}, \quad (63)$$

where $c_{u,0}(n)$ is the peripheral component of the velocity c_{u0} in the case of a shockless entry, when $w_z = 0$, as follows from the foregoing construction.

In the case of entry with shock, the position of the inlet vertical therefore remains

unchanged, but the end point of the velocity c_0 is shifted from it in a direction opposite to the velocity u_1 by the value $\frac{w_z^2}{2u_1} = \Delta$.

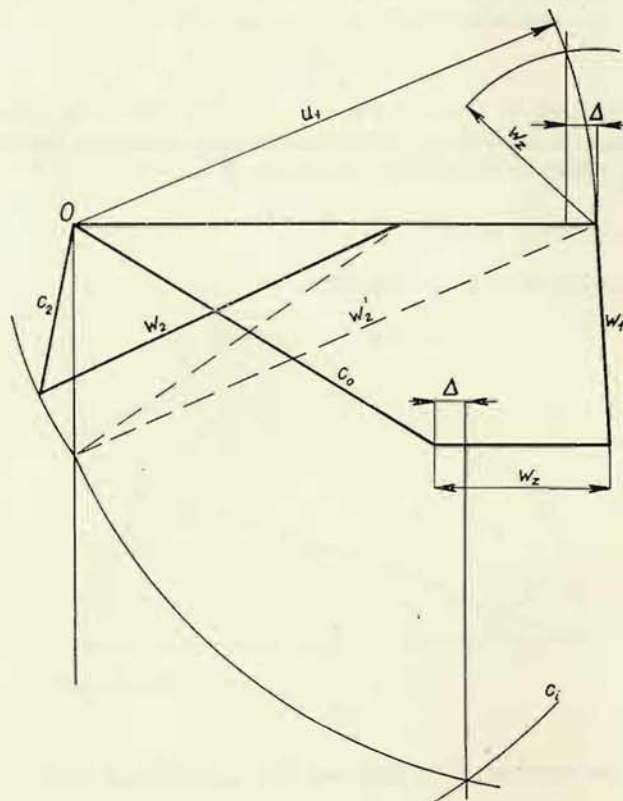


Fig. 58

This value we construct according to Fig. 57 on the base of the relation (w_z is the mean geometric proportional of Δ and $2u_1$)

$$\frac{\Delta}{w_z} = \frac{w_z}{2u_1},$$

so that the entire diagram for the case of entry with shock then appears as indicated in Fig. 58.

These diagrams are suitable for runner design, and in particular, for investigating a turbine which works under variable operating conditions. The use of the diagrams will now be explained by several examples.

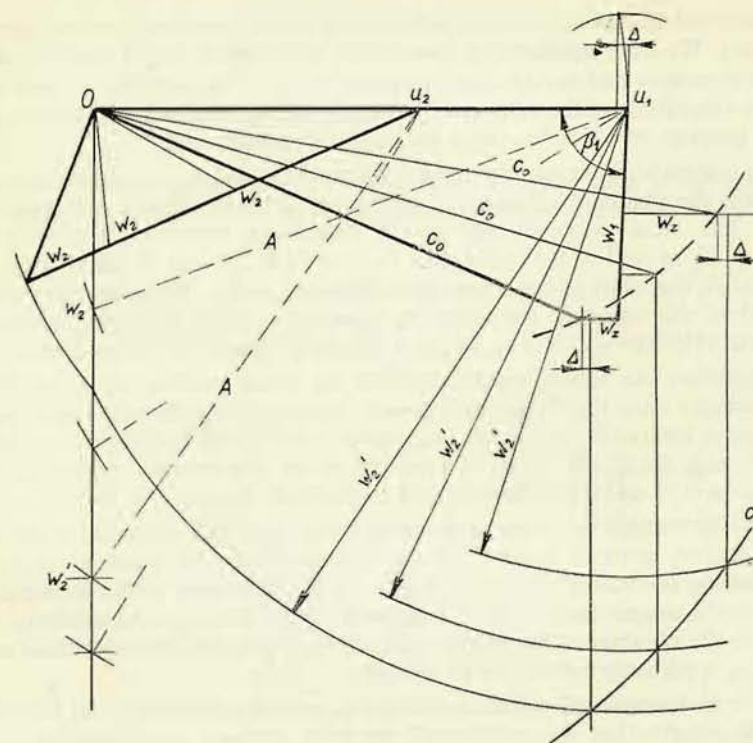


Fig. 59

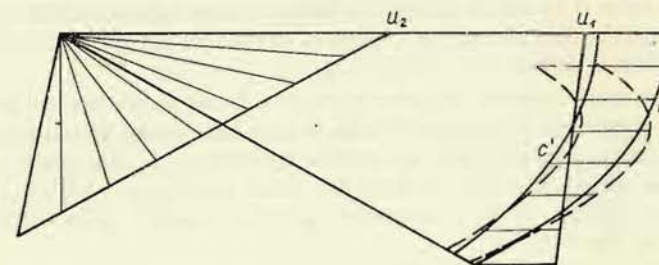


Fig. 60

2. Influence of Filling Variations in the Francis Turbine

We have already mentioned the influence of filling variations in the operation of turbines. We have assumed that the turbine is equipped with a Fink regulation which is at present exclusively used. By means of the Braun diagram we can determine the magnitude of the velocity c_0 at various fillings and also the shock component w_z progress of which has previously only been indicated.

In our design work we start from the flow-rate variation, i. e. we shall investigate what form the diagram will assume for various flow-rates, when the solution is simple. The areas perpendicular to the meridional velocities, the inlet area $F_0 = \pi D_1 B_1$ as well as the outlet area $F_2 = \pi D_2 B_2$ (where D_1 denotes the diameter and B_1 the width of the runner at the inlet, D_2 and B_2 the mean diameter and the width of the runner at the outlet) do not vary with the flow-rate, so that the meridional velocities $c_{m,0}$ and $c_{m,2}$ will be directly proportional to the flow-rate.

We therefore can immediately determine the corresponding variations in the outlet triangles since the direction of velocity w_2 is given by the outlet blade angle, and hence is invariable, whilst the meridional velocity will be proportional to the flow-rate; e. g. for fillings up to 0.75 and 0.5 of the flow-rate the meridional velocities will be 0.75 and 0.5 respectively, of the original velocity (see Fig. 59).

In the inlet triangle we know the horizontal lines on which the peaks of the velocities c_0 and w_1 must be located. These horizontal lines are again given by the corresponding meridional velocities, which for the flow-rates of our example will again have the magnitudes 0.75 and 0.5 respectively, of the original meridional velocity. Since the direction of the relative velocity w_1 is given by the inlet blade angle, velocity w_1 is perfectly defined for all fillings.

In order to determine the absolute velocity c_0 , we first ascertain by the previously described construction the positions of the inlet verticals corresponding to the individual fillings. Their intersections with the previously mentioned horizontal lines define, with the exception of the value Δ , the position of the peaks of the velocities c_0 and the magnitude of the shock velocities w_z . Now we determine experimentally the value Δ by which the peak of the velocities c_0 is shifted from the inlet verticals against the direction of the rotation of the runner, carry out this correction, and the problem is solved.

Now we can read from the diagram the values c_2 and w_z for various flow-rates, so substitute them into Equation (58) and hence define more accurately the progress of efficiency, provided that c_t remains constant, i. e. that ϱ and ν remain constant. This assumption approximates the actual conditions with the exception of the smallest fillings, when ϱ increases, c_0 is then smaller, as indicated by the dashed lines in Fig. 60.

The velocity c_0 is the velocity at the diameter D_1 immediately in front of the inlet into the runner. At the outlet from the guide apparatus (at the diameter D' of the ends of the guide blades) the velocity will be somewhat different and amount to c' .

When we resolve these velocities into meridional and peripheral components,

then the meridional component must hold good according to the continuity equation

$$c_{m,0} \pi D_1 B_1 = c'_m \pi D' B',$$

and in so far the width of the wheels are the same, it will apply

$$\frac{c'_m}{c_{m,0}} = \frac{D_1}{D'},$$

that means that the meridional velocities are in the inverse ratio of the diameters. In the space between the guide wheel and the runner there are no blades and, there-

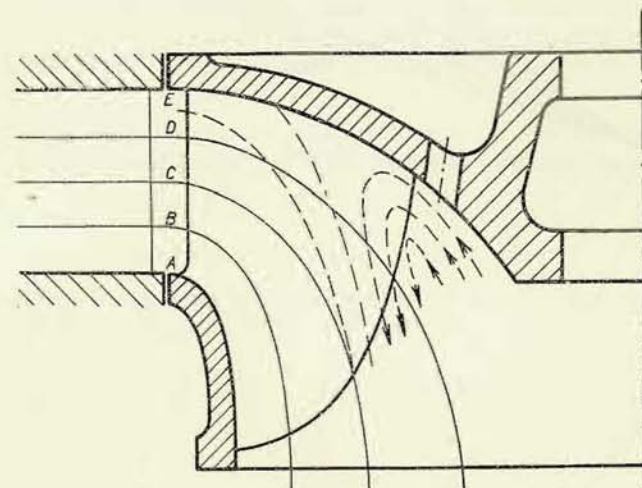


Fig. 61

fore, there is no action of any moment. Hence for this space there applies the theorem of the moment of momentum Equation (13a):

$$M = \frac{1}{g} (D' C'_u - D_1 C_{u,0}) = 0;$$

In this equation we have replaced the radii by the diameters, which is permissible. If we divide the equation by the value $\sqrt{2gH}$, we arrive at the same relationship for the specific velocities, so that

$$\frac{c'_u}{c_{u,0}} = \frac{D_1}{D'}.$$

These two relations, however, only show that the angle α' equals the angle α_0 , where the angles α are the angles enclosed by the absolute velocities and the

peripheral velocities. Flowing, therefore, takes place on lines of those tangents which have always the same inclination to the directrix drawn from the centre of the runner (logarithmic spiral). Composing the velocities c_u' and c_m' at diameter D' , we determine velocity c' at which the water leaves the guide blades. It is clear that

$$c' = c_0' \frac{D_1}{D'}.$$

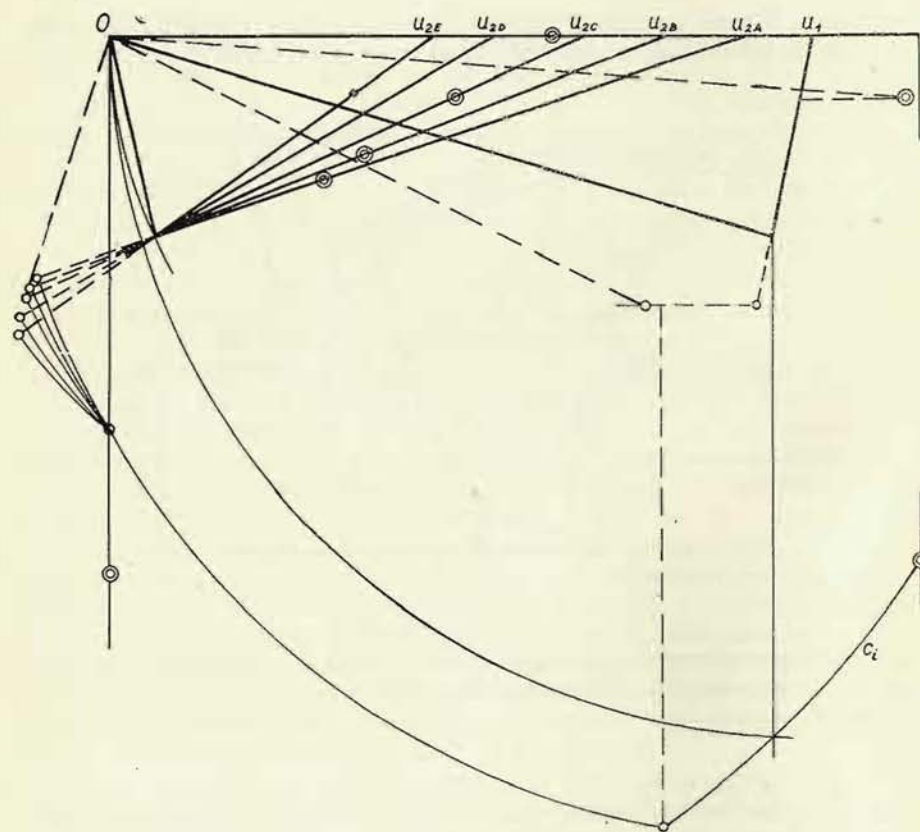


Fig. 62

The progress of this velocity is also shown in Fig. 60, and we see that this velocity varies much less with filling variations.

When a turbine with a larger inlet width of the runner is concerned – as is the case with most turbines – we cannot solve the diagram only on one stream line since the peripheral velocities at the outlet from the wheel are too differ-

ent (see Fig. 61). In such a case we divide the flow by flow areas into several individual flows – we then speak of so-called partial or elementary turbines – through which pass the same parts of the through-flow (for a determination of these areas see further). On these flow areas we then solve the inlet and outlet triangles (see Fig. 62).

In so far the inlet edge of the blade is parallel to the axis of rotation, the peripheral velocity of all the elementary turbines is the same on this inlet edge of the blade, and in so far as the individual flow areas are subject to the same conditions on the inlet edge (e. g. when they proceed under the same angle to the inlet edge), the inlet triangle is the same for all elementary turbines. For this reason, all elementary turbines also have a common inlet vertical and according to the described construction by Braun the magnitudes of the relative outlet velocities w_2 are therefore always defined for a certain filling by a common point on the vertical in the origin of the diagram.

Note: This circumstance can also be derived from the flow-rate equation if we write it for the elementary turbine a and the elementary turbine b as follows:

$$c_{i,a}^2 = w_{2,a}^2 - w_{1,a}^2 + c_{0,a}^2 + u_{1,a}^2 - u_{2,a}^2$$

$$c_{i,b}^2 = w_{2,b}^2 - w_{1,b}^2 + c_{0,b}^2 + u_{1,b}^2 - u_{2,b}^2,$$

and if we assume for all flows the same indicated velocity c_i and the same over-pressure according to Equation (25)

$$\frac{h_p}{H} = 1 - \varrho - c_0^2 \div c_i^2 - c_0^2,$$

there also is

$$c_{0,a} = c_{0,b};$$

it further applies

$$u_{1,a} = u_{1,b}; \quad \alpha_{0,a} = \alpha_{0,b},$$

and hence also

$$w_{1,a} = w_{1,b},$$

so that

$$w_{2,a}^2 = w_{2,b}^2 + u_{2,a}^2 - u_{2,b}^2,$$

which is in accordance with the consideration mentioned above.

From this the important fact follows, that at filling variations the relative outlet velocities do not vary to the same extent. This circumstance is indicated in Fig. 62. For instance, if for a shockless entry we construct such an outlet triangle that the relative outlet velocity equals in magnitude the peripheral velocity (isocles triangle), we see that at a greater filling the relative outlet velocity w_2 increases for the inside elementary turbines relatively more than for the outside turbines (points marked by a single circle \circ). Similarly, at smaller fillings the relative outlet velocities decrease for the inside elementary turbines far more rapidly than for the

outside elementary turbines, so that e. g. at a quarter of the maximum filling (points marked by a double circle \odot) there is already no through-flow on the flow areas *D* and *E*. On the contrary, here the water flows back, as indicated by the dashed lines in Fig. 61, and at the beginning of the draft tube, in the axis of rotation, there is an empty space.

This space is alternately filled with water and emptied again; thereby shocks arise in the draft tube (at small fillings, they may, however, occur also at an excessive opening, due to a high value of the component c_u). This objectionable consequence of flow variations, (in principle brought about by the shifting of the flow areas, as indicated by the dashed lines in Fig. 61) is eliminated by supplying air at small fillings to the centre of the draft tube through valves which at a greater filling close again, as will be explained later (Part II).

3. Influence of Filling Variations in the Kaplan Turbine

In Chapter X we have shown that the Kaplan turbine has a very flat progress of the curve representing the dependence of the efficiency on a variable filling. We have demonstrated this by plotting the efficiency curves for certain positions of the runner blades.

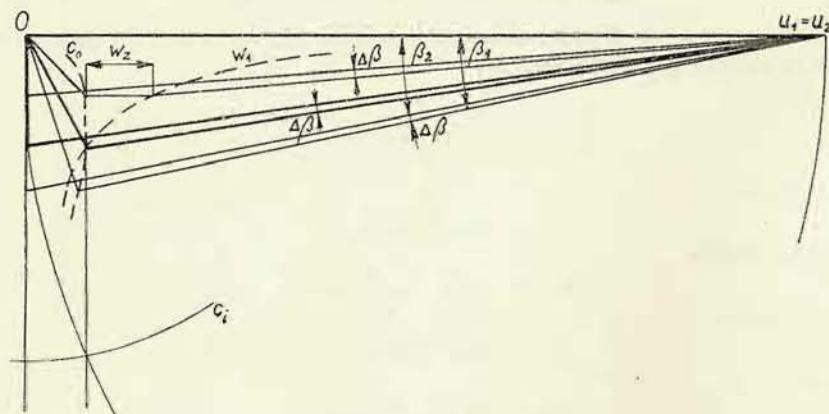


Fig. 63

Now we shall investigate how a simultaneous turning of the guide blades and the runner blades manifests itself in the Braun diagram.

In Fig. 63 are (drawn in thick lines) the velocity triangles for a shockless entry. As here an axial-flow turbine is concerned, the peripheral velocity at the inlet equals the peripheral velocity at the outlet; the meridional component of the velocity is also the same for both triangles. In the outlet triangles we assume a perpendicular outlet, i. e. $c_{u2} = 0$, and by means of the construction known we draw the inlet vertical on which the vertex of the inlet triangles must be located. As already

stated, the meridional velocity in both triangles is the same, and thus the inlet triangle, too, is fully defined.

When following the filling variations, we must remember that the meridional velocities in both triangles are always the same. When, for instance, the filling amounts to half the original magnitude, the meridional velocities, too, are half the former value. In the outlet triangle, the angle $\alpha_2 = 90^\circ$ will be maintained (minimum losses), so that the outlet triangle is defined. We must further remember that the angle $\Delta\beta = \beta_1 - \beta_2$ is the angle of deviation of the blade, which remains the same. Thus we know for the new flow-rate the direction of the velocity w_1 , we know the meridional velocity, and therefore we also know the magnitude of w_1 . By constructing the inlet vertical we also determine the velocity c_0 (we must again

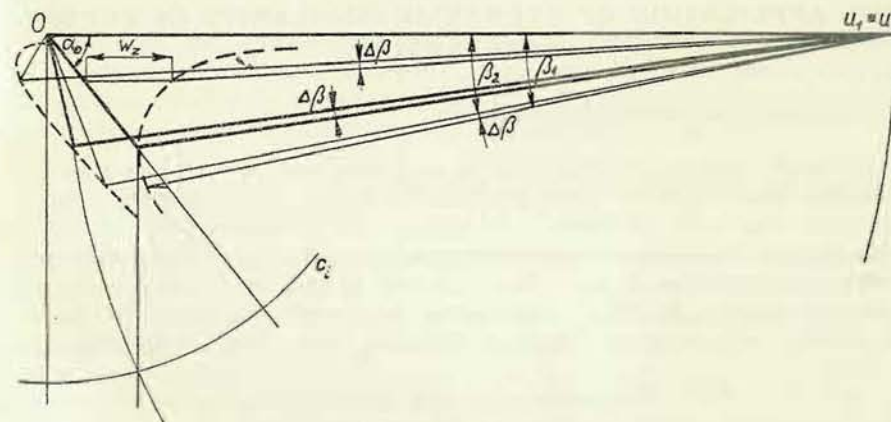


Fig. 64

find experimentally the value of the correction and also w_2). In the figure are indicated the loci of the peaks of the velocities w_1 and c_0 . It is evident that the favourable conditions at the outlet are maintained at any filling, and that the shock velocity w_2 at the outlet assumes higher values only at a very small filling. Thus we have explained, in accordance with our previous considerations, the flat progress of the efficiency curve.

4. Axial-Flow Propeller Turbine with Adjustable Runner Blades and Stationary Guide Wheel Blades

This arrangement, although having a less favourable progress of the efficiency curve than the Kaplan turbine, has a considerably more advantageous efficiency progress than a propeller turbine with fixed runner blades and adjustable guide blades. Since such a turbine is cheaper than the Kaplan turbine, this arrangement is also sometimes employed.

In Fig. 64 again, the triangles for a shock-free entry are drawn in thick lines. At varying fillings the meridional velocities are again proportional to the through-flow, and owing to the fact that the direction of velocity c_0 is invariable (stationary guide blades), we can always immediately know the direction and magnitude of velocity c_0 . Then we must experimentally determine the position of the vertex of the outlet triangle in such a way so that, on the one hand, always the same angle of deviation $\Delta\beta$ is maintained and, on the other hand, the Braun construction is satisfied.

It is evident that the direction of the velocity c_2 is not invariable, but the change of the angle α_2 is only small and also the shock velocity w_2 has within a considerably wide range of filling variations only a small magnitude.

XIII. APPLICATION OF HYDRAULIC SIMILARITY IN TURBINE MANUFACTURE

1. General Requirement of Manufacture

Hydraulic turbines are constructed in such sizes and for such flow-rates and heads that it is impossible to test them prior to delivery at the factories, although manufacturers would be interested in making sure beforehand that the turbine ordered meets the required conditions as to maximum flow-rate, efficiency, output, and cavitation resistance. Apart from this, even if such tests were possible, the results would be at disposal too late, because the expensive machine would already be finished and necessary alterations would be very costly, if altogether still feasible.

On the other hand, the previously described laws of hydraulic similarity provide the possibility of checking in advance the properties of the turbine in question on a small and inexpensive so-called model turbine in a testing station specially installed for this purpose, and of making sure by recalculation that the machine will satisfy the prescribed specifications. We have already seen that each turbine type with a certain specific speed meets several different specifications (Chapter XI). Regarding to hydraulic considerations it is common practice that turbines are not designed separately for each individual order, but that a series of in advance designed (hydraulically) types with a convenient sequence of specific speeds is utilized. These types are subjected to detailed measurements in the testing station and, if necessary, further improved upon on the basis of the measuring results obtained. When a turbine is ordered a suitable type is selected from this series, and by means of recalculation from the characteristic obtained by the mentioned measurements, a manufacturer can then guarantee the required hydraulic properties of the ordered turbine.

When a manufacturer is equipped with a series, his further work in the field of hydraulic design is concerned with the experimental determination of the influence of modifications necessary for certain orders, as well as with the further development of better efficiency, better cavitation resistance of the present runner types,

and with an enlargement of the series so as to achieve higher specific speeds and the utilization of the highest possible heads by the fastest possible runners.

The first part of this development work deals mainly with modifications of the shape of the draft tube. Such an alteration may be desirable e. g. in order to restrict excavation work on an unfavourable site or to provide a better location of the power station. For the same reason, changes in the supply section to the turbine pit, or on the pit or spiral casing itself, may be desirable.

In such an event new measurements are taken and a new characteristic is determined, on the basis of which the hydraulic properties are guaranteed; it may also be found that these changes have no unfavourable influence and that the original characteristic may be further applied. If possible, an original model turbine is used for this work and corrected according to requirements, care being taken to maintain geometrical similarity to the actual turbine.

The second part of these activities is in principle concerned with the designing of new runners. Checking of newly designed runners by measurements does not only reveals whether the runner is satisfactory, but, if necessary we can also determine where to apply corrections in order to achieve perfect operation.

2. Selection of the Type Series according to Specific Speeds and the Diameter Series according to Flow-Rates

As we shall see later, the manufacture of runners requires certain implements. These are patterns for runner casting and gauges for checking the machining of the blades. In order to keep the number of these implements within reasonable limits, the type series should contain the least possible number of individual types. On the other hand, the series must be sufficiently close to provide for the necessary values of Q , H , and n at convenient gradations of diameters.

For each type with a certain specific speed (the specific speed is that which corresponds to the maximum flow-rate of the type at optimum n'_1) we must build up a suitable series of diameters.

In determining the diameter series, we have as a guide the circumstance that for a turbine with a certain diameter we can reduce the maximum flow-rate by merely restricting the opening of the guide apparatus. In this way the flow-rate can be reduced by up to 10 % in comparison to the original value without any danger of getting into an unfavourable section of the efficiency curve when the optimum efficiency would be too near the maximum flow-rate, which is undesirable (Chapter X).

If we, therefore, select a flow-rate gradation by 10 %, we must graduate the diameters by 5 % as the flow-rate is proportional to the square of the diameter.

Whether the selected number of types (specific speeds) and diameters are satisfactory and whether they cover the entire range of $Q - H - n$, can be checked in two ways.

First for each turbine type we can draw a separate diagram, in which on one axis we put the head H and on the other the output N , using logarithmic scales. For the selected number of runner diameters and for the selected speeds (above all the synchronous speeds which are of importance for a direct drive of electric

three-phase alternators) we obtain a total of characteristics¹⁾ (Fig. 65) which must cover the entire range of the diagram corresponding to the specific speeds of the type in question in such a way that the efficiencies at the extreme parts of the characteristics are still within acceptable limits.

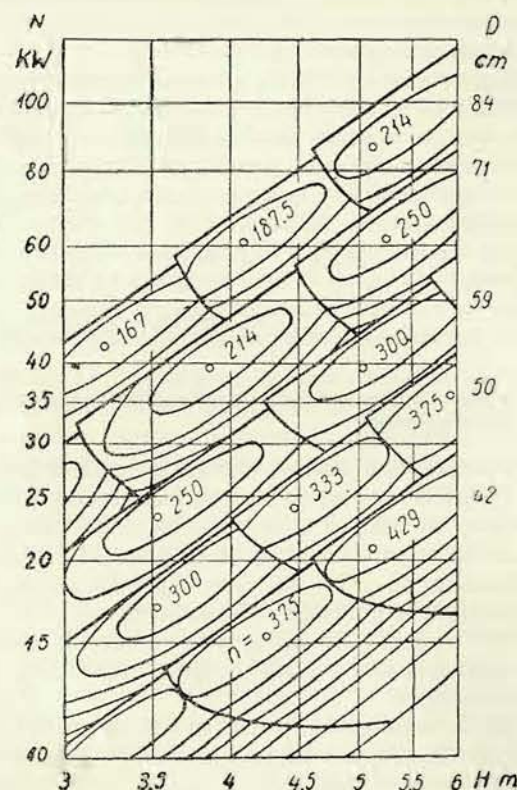


Fig. 65

These diagrams can then also be used for a rapid determination of the type and diameter of the turbine, suitable for the given values Q , H and n , by determining the output N as well as its most advantageous location in the diagrams.

Another arrangement of a suitable diagram is indicated in Fig. 66. This diagram is again plotted by means of the double logarithmic scale, the gradation of the head being indicated on both axes. The scale on the horizontal axis serves for reading on the lines $Q = \text{const.}$, and the scale on the vertical axis for reading on the lines

¹⁾ Koyatkovski: Maliye gidroturbiny, Moskva 1950.

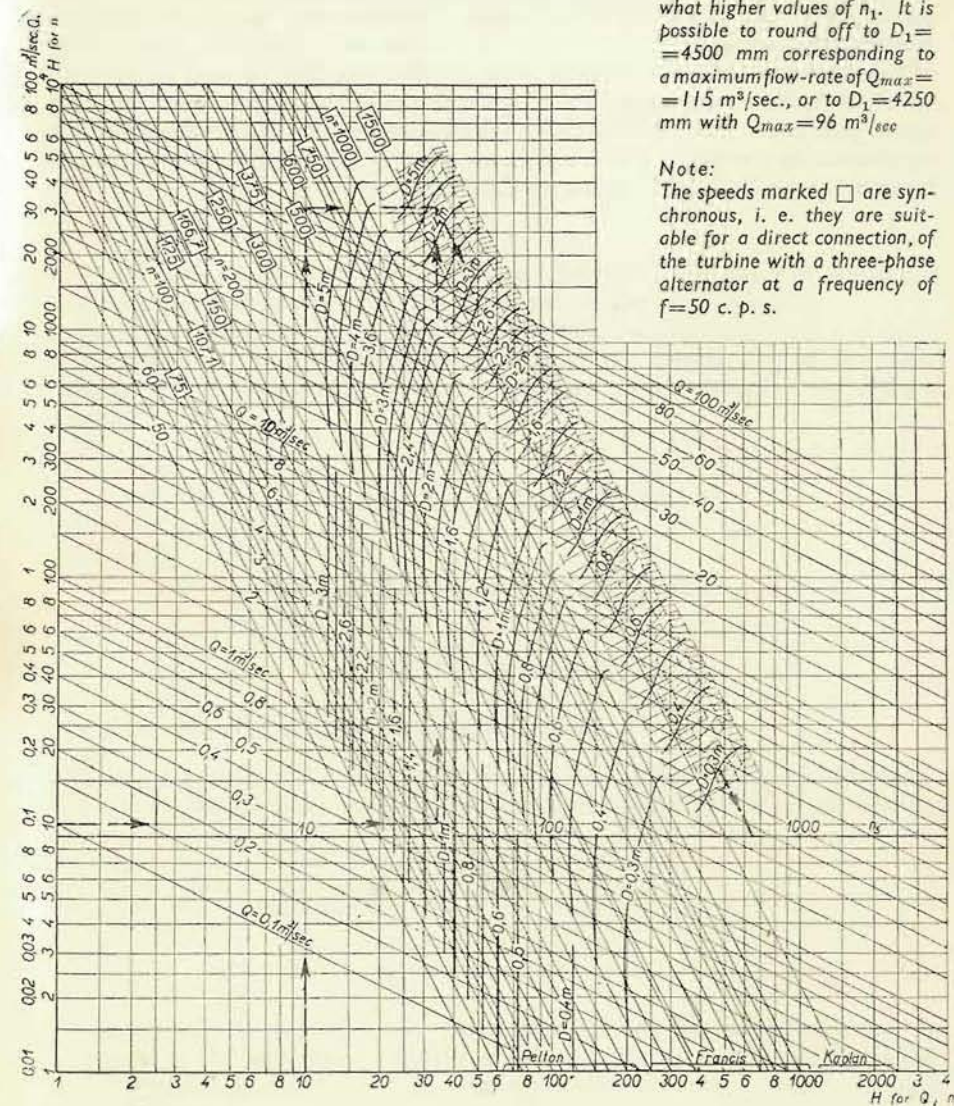


Fig. 66

Example:
For $H=10$ m, $Q=100$ m³/sec.,
 $n=107.1$ r. p. m., we obtain
a runner diameter $D_1=4300$
mm, type $n_s=600$, with some-
what higher values of n_1 . It is
possible to round off to $D_1=$
 $=4500$ mm corresponding to
a maximum flow-rate of $Q_{max}=$
 $=115$ m³/sec., or to $D_1=4250$
mm with $Q_{max}=96$ m³/sec

Note:
The speeds marked \square are syn-
chronous, i. e. they are suit-
able for a direct connection of
the turbine with a three-phase
alternator at a frequency of
 $f=50$ c. p. s.

$n = \text{const.}$, which on logarithmic paper are straight lines. The lines $n_s = \text{const.}$ are likewise straight lines, as seen in the figure. The points of equal diameters of the individual types are connected for clarity, although actually there is no uninterrupted continuity. If we hatch the range where there is still an acceptable efficiency (as has been done in Fig. 66 in the region of Kaplan turbines), we can again see whether the selected series meets our requirements and whether the entire range of the diagram is correctly covered. This diagram, too, may be used for approximately a rapid determination of the type and size of the turbine from the given values Q , H and n . The procedure of this determination is evident from the example supplementing the figure, which represents a survey of older turbine types manufactured by the National Corporation ČKD-Blansko.

TURBINE DESIGN

The Francis, Kaplan, and Pelton turbines differ so considerably in design that it will be necessary to deal with each individual turbine type separately.

In the first place, we shall deal with the hydraulic investigation which is of major importance and provides the reference data for the construction of the model turbine. In the second place, with the directions for the design of the full-size machine.

1. FRANCIS TURBINES

A) HYDRAULIC INVESTIGATION

I. RUNNER DESIGN

1. Elementary Turbines, Meridional Flow Field

The runner ducts of the turbine, between the inlet and outlet edges of the blades, must, as we know, satisfy the energy equation, which in terms of actual velocities reads:

$$U_1 C_{u1} - U_2 C_{u2} = g H \eta_h,$$

or in terms of specific velocities

$$u_1 c_{u1} - u_2 c_{u2} = \frac{\eta_h}{2}.$$

The peripheral velocities, and hence also the specific velocities along the outlet edge (in high-speed turbines along the inlet edge, too) are not equal, and therefore the outlet – and in some cases also the inlet – velocity triangles must differ from each other. This, of course, results in the need for runner blades to be of different shape along the outlet and inlet edges. From this circumstance

it follows that the shape of the runner blade must be investigated stepwise, in section, according to the inlet and outlet conditions in the appropriate places of the inlet and outlet edges.

This is done by subdividing the space of the turbine by a system of rotating flow surfaces into a system of elementary (partial) flows, as indicated in Fig. 67.

We assume that the water particles in each spot of the through-flow cross section passes through the runner along a stream line which helically extends on the flow surface and does not change its position. For this reason we also assume that the water particles of a certain elementary flow stream steadily flow and do not deviate into the adjacent elementary flows. If we divide the space of the turbine into a sufficiently large number of elementary flows, the through-flow conditions of the individual elementary flows will only slightly differ from one another so

that the passage of any elementary flow can be determined according to the mean values corresponding to its cross sections. In this way we can build up the shape of a blade that will meet the conditions of the individual flows; by constructing them with appropriate transitions we obtain the shape of the complete blade.

The designing of the blade thus consists of designing the blade surfaces of the so-called elementary (partial) turbines.

The flow surfaces which divide the space of the turbine into elementary flows may be according to various assumptions. In principle there are two assumptions.

α. In low-speed turbines, where the transition of the flow from the radial into the axial direction takes place at large radii (from Chapter VIII/3 we know that this is the case in specifically low-speed turbines), we assume that the centrifugal force O created by this deflection of the flow (Fig. 67) is so small that it has no influence on the distribution of the pressure in the streaming liquid. On this assumption we apply to the flows the continuity equation.

If we draw the progress of the flow surfaces (actually the intersecting lines of these rotating surfaces and the picture plane) and the trajectories orthogonal to them, there must apply at any place

$$\frac{Q}{x} = F C_m,$$

where x is the number of flows with equal flow-rates, into which we have divided the space of the turbine, C_m the meridional velocity (i. e. the component of the actual velocity of the flow in the meridional plane, that is to say the plane extending through the axis of the rotating turbine surfaces; a meridional plane is e. g. also

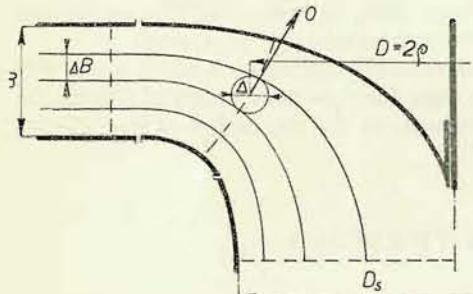


Fig. 67

the picture plane), and F is the through-flow area perpendicular to the direction of velocity C_m . Since this area, according to Fig. 67, equals

$$F = \pi D \Delta,$$

this must hold good for all places in the space of the turbine

$$\frac{Q}{x} = \pi D \Delta C_m, \quad (64)$$

and here, according to the previous assumption, also the value of C_m on one and the same orthogonal trajectory must be the same, because along the trajectory the Bernoulli equation

$$\frac{p}{\gamma} + \frac{C_m^2}{2g} + z = \text{const.},$$

must hold. If we disregard the height dimension of the space of the turbine, which is small in relation to the head, i. e. if we neglect the differences in the value of z for the individual places, velocity C_m must be the same along the entire orthogonal trajectory, for we also assume that pressure p is invariable, that it is not subjected to centrifugal force at the deflection of the flow in the meridional plane.

In our investigation of the flow field in low-speed turbines we go still further and select a contour of the turbine space so as to obtain the same meridional velocity C_m in the entire space. For two arbitrarily selected places of the turbine space it evidently holds good according to Equation (64)

$$\frac{Q}{x} = \pi D \Delta C_m = \pi D' \Delta' C_m = \text{const.},$$

and since C_m is invariable, applies

$$D \Delta = \text{const.},$$

or if we replace the diameter by the radius

$$\rho \Delta = \text{const.} \quad (65)$$

Actually we, therefore, build up the flow field on the assumptions described in the following paragraphs.

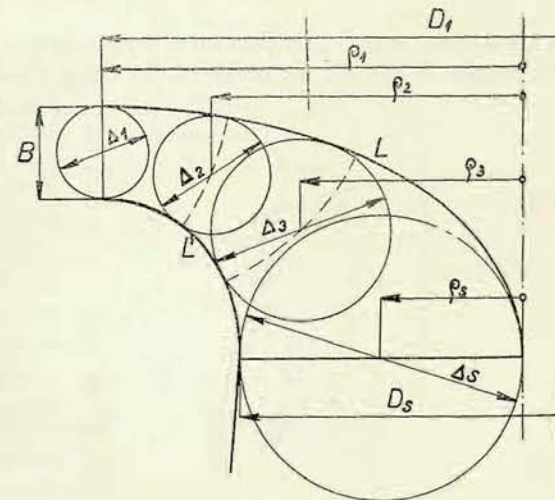


Fig. 68

We start with a suitably selected value of the meridional velocity C_m and the given flow-rate Q and determine the diameter D_s at the beginning of the draft tube (Fig. 68) from the continuity equation

$$\frac{\pi D_s^2}{4} C_m = Q.$$

Then we draw by a continuous line the inner contour L of the turbine space from the axis of this area up to a suitably selected external diameter D_1 . There, in turn, we determine from the continuity equation the axial height of the turbine space,

$$B \equiv \Delta_1, \pi D_1 B C_m = Q.$$

We now draw the outer contour L' by a continuous line in such a way that the dimensions B and D_s are observed. In doing this, we take care from the very beginning to obtain within the turbine space the same velocities C_m and hence also the same through-flow areas, which we check by inscribing circles, whereupon we appropriately adjust the progress of the contour L' . There must be

$$\begin{aligned} \varrho_1 \Delta_1 &= \varrho_2 \Delta_2 = \\ &= \varrho_3 \Delta_3 = \dots = \varrho_s \Delta_s. \end{aligned}$$

Then we divide the height B of the turbine space into the selected number of equal parts $\frac{B}{x}$; the circular area of the diameter D_s we divide similarly into annuli of equal areas. Then we draw in full lines

the flow surfaces. If we inscribe circles between them, in such a way that they always contact two adjacent flow surfaces (Fig. 69), it holds good according to Equation (65):

$$\varrho \Delta = \varrho' \Delta' = \varrho'' \Delta'' = \dots = \text{const.}$$

Should this condition not be satisfied, we must suitably adjust the progress of the flow surfaces so as to fulfil this condition rather exactly. Thus the meridional flow field is defined.

In this approach to the problem we have assumed that there is an equal velocity on the trajectories normal to the traces of the flow surfaces. We here admit the possibility of a velocity change only along the traces of the flow surfaces, i. e. only in one direction. For this reason is the theory of blade design based on these conditions termed the one-dimensional theory.

β . In turbines of higher speed, where the curvature of the flow in the meridional

plane is greater - i. e. the radii of curvature are smaller - the assumption stipulated in the foregoing paragraph no longer holds good.

Here we must admit that the water particles streaming on the meridionally curved paths generate centrifugal forces with which they act upon adjacent particles, so that the flow along the inner contour (L in Fig. 68) proceeds under a higher pressure than the flow along the outer contour (L' in Fig. 68). The Bernoulli equation, in which we again disregard the changes of position energy as it is negligible in relation to the total energy, will therefore read

$$\frac{p}{\gamma} + \frac{C_m^2}{2g} = \text{const.},$$

it then follows that the meridional velocity in flows nearer to the inner contour must be lower and in flows nearer to the outer contour higher. For this reason the flow surfaces are closer spaced towards the outer contour, as indicated in Fig. 70.

In order to derive a satisfactory method of determining the flow field under these circumstances, we must bear in mind that the water always passes through the turbine under turbulent flow conditions. This turbulent flow, however, generally proceeds as if the liquid had no internal friction, i. e. if it were non-viscous.

This fact can be easily realized by comparing laminar and turbulent flow in a pipe (Fig. 71). In laminar flow (Fig. 71a) the influence of the viscosity of the liquid manifests itself by tangential forces between the individual concentric layers of the flow, which tend to reduce the velocity of the liquid within the considered cylindrical layer and, inversely, to accelerate the liquid which is outside this layer. The result of this action appears in the velocity profile (in the velocity distribution across the cross section), which has the shape of parabola (Poiseuille flow). On the other hand, in turbulent flow the velocity of the individual layers is equalized by a secondary transverse flow - turbulent mixing, and the velocity is, therefore, equal over the entire cross section (Fig. 71b), with the exception of a very thin so-called boundary layer, in which the influence of viscosity becomes manifest and the velocity rapidly drops to zero on the wall of the pipe. If we disregard this boundary layer the thickness of which is negligible, of the order of 10^{-1} mm, in comparison with the dimension of the total diameter, we see that the velocity is equal over the entire cross section. But such a shape of the velocity profile is, as is well-known, characteristic for a liquid without

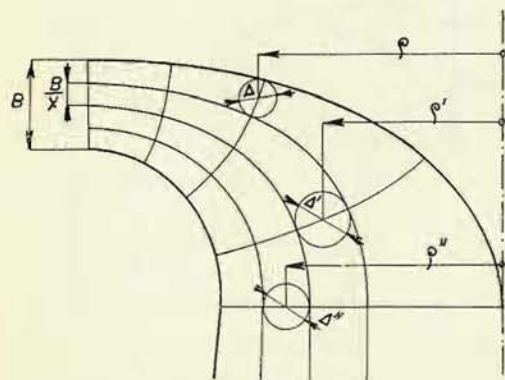


Fig. 69

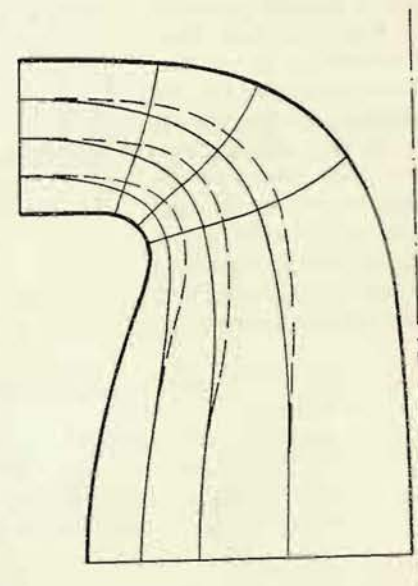


Fig. 70

internal friction. For this reason we may (in so far as we consider the entire flow) neglect the internal friction of the liquid passing through the turbine.

If, however, we neglect the internal friction of the liquid, then we can apply to the flow the laws of potential flow.

Potential flow exists in a non-viscous liquid when streaming is brought about from the rest position by the action of gravitation — which is our case — and is characterized by the fact that it involves the so-called velocity potential. This is a function whose derivative by an arbitrary direction denotes with the opposite sign the velocity of the flow in this direction (the change of the sign is due to the fact that the velocity arises in the sense of the falling potential). When we have selected a co-ordinate sys-

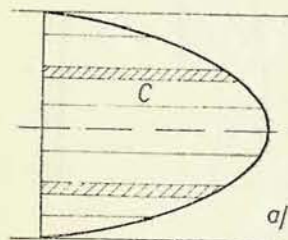


Fig. 71

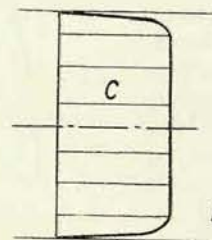
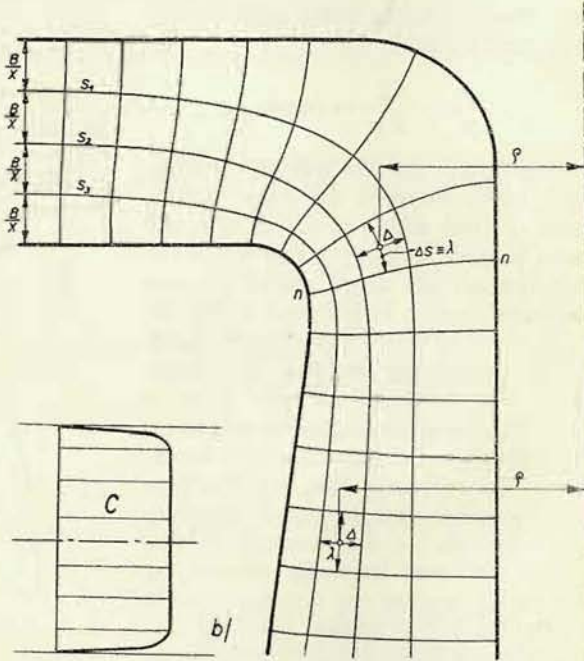


Fig. 72



tem in the space passed by the liquid and want to determine e. g. the velocity in the direction of the X-axis, it will suffice to differentiate the velocity potential by x to obtain, apart from the sign, the value sought.

We make use of this now and derive the distribution of the meridional velocities in the investigated case. For this purpose let us first assume that we already know the correct progress of the flow surfaces s_1, s_2, \dots in the rotating space of the turbine (see Fig. 72). Normally we erect surfaces of equal potential (equipotential surfaces); these must be perpendicular to the flow surfaces, because only perpendicularly to the flow surfaces does velocity equals zero, so that in this direction there cannot exist any difference of potential. We locate these equipotential surfaces so as to establish between two subsequent surfaces the same potential difference.

Since each elementary flow carries the same quantity $\frac{Q}{x}$, we can write on the surface $n - n$ according to the continuity equation

$$\frac{Q}{x} = 2\pi \rho \Delta C_m,$$

but the magnitude of velocity C_m is given by the derivative of the velocity potential Φ by the direction of the trace of the flow surface

$$C_m = \frac{d\Phi}{ds},$$

and when, for the purpose of a graphical solution, we pass over from the differentials to values, though small but of a finite magnitude, we can write

$$C_m = \frac{\Delta\Phi}{\Delta s},$$

and hence

$$\frac{Q}{x} = 2\pi \rho \Delta \frac{\Delta\Phi}{\Delta s} = \text{const.}$$

$\Delta\Phi$ is here the potential difference appertaining to two subsequent equipotential surfaces, Δs being their interval in the considered place, as indicated in Fig. 72. For the purpose of a better discrimination let us further replace Δs by the letter λ : $\Delta s = \lambda$; the potential difference $\Delta\Phi$ between two subsequent potential surfaces is always the same, so that we can take $\Delta\Phi$ for a constant. Combining therefore this value with the factor 2π into the constant on the right side of the equation, we obtain the dependence sought

$$\begin{aligned} \rho \frac{\Delta}{\lambda} &= \frac{\text{const.}}{2\pi \Delta\Phi} = \text{const.}, \\ \rho \frac{\Delta}{\lambda} &= \text{const.} \end{aligned} \quad (66)$$

The flow surfaces are correctly drawn when in the entire flow field the condition of Equation (66) is satisfied. The value of the meridional velocity C_m is then readily determined in any place of the field by dividing the flow-rate of the elementary flow by the through-flow area.

$$C_m = \frac{Q}{2\pi \rho \Delta x}. \quad (66a)$$

In determining the meridional flow field in this case we proceed as follows (see Fig. 73): We design in a suitable way (according to directions given later) the

inner and outer contours of the space of the turbine. At a sufficient distance behind the bend, in the plane $A - A$ normal to the axis of rotation, we divide the cross section into annuli of equal areas; thus we obtain points through which the traces of the flow surfaces must pass. At a sufficient distance in front of the bend of the flow, in the cylindrical section $B - B$, we divide the height of the space B into the same number of equal parts; in this way we determine the position of the traces of the flow surfaces in this place.

By connecting the corresponding points in the sections $B - B$ and $A - A$, we draw the traces of the flow surfaces. In the place where they begin to bend we then draw perpendicularly to these traces (which are also termed meridional stream

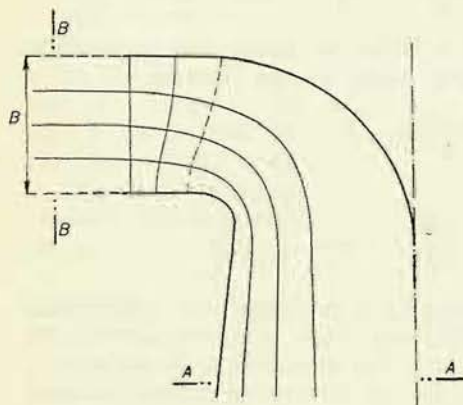


Fig. 73

lines) two trajectories, which are the traces of two subsequent equipotential surfaces, and in this place we adjust the progress of the flow surfaces (with a simultaneous adjustment of the equipotential surfaces, which must be kept perpendicular to the flow surfaces) until for this first vertical band the condition of Equation (66) is satisfied. Then we insert another equipotential surface (indicated in the figure by a dashed line) at such a distance to satisfy some of the following pictures (following in the direction of the flow) of the same elementary flow again the condition of Equation (66). Thus we have made sure that the potential difference between these surfaces is the

same as between the first two. Then we check again the fulfilment of the condition of Equation (66) for the second vertical column and if necessary likewise suitably correct the progress of the traces. In this way we proceed further, until the entire flow field is set up.

It is clear that this method is more laborious than that which neglects the centrifugal forces due to the meridional curvature, but, having acquired sufficient practice, we can obtain the progress of the flow surfaces rather quickly. Here we notice that the influence of the curvature manifests itself considerably at a distance from the beginning and the end of the curvature, which we must bear in mind already at the first draft of the flow surfaces.

In this procedure we have taken into consideration changes of the meridional velocity in two directions, i. e. on the one hand, along the traces of the flow surfaces and, on the other hand, in the direction perpendicular to it. For this is the theory of blade design based on the method just described termed the two-dimensional theory.

In the designing of blades we may further investigate the influence of the velo-

cities in the peripheral direction as well as changes of these velocities. These considerations are dealt with by the three-dimensional theory (e. g. that of Bauersfeld); but it leads to blade shapes which materially differ from these generally manufactured, and is usually not employed.¹⁾

The three-dimensional theory is also involved in designing blades of propeller and Kaplan turbines on the basis of using aircraft wing profiles, as will be explained later.

Note: The meridional flow field may be determined to a certain extent by the shape of the blade. If we establish the flow field one-dimensionally in spite of the fact that there is a considerable meridional curvature of the flow, we obtain a blade shape (blade angles) with which it is no longer possible to develop a flow field, satisfying the two-dimensional theory during the operation of the machine.

2. Shape of the Turbine Space

The shape of the turbine space at a certain specific speed is to some extent already given by the expression (43)

$$n_s = 576 u_1 \frac{D_s}{D_1} \sqrt{c_s \eta}. \quad (43)$$

For the maintenance of the required specific speed the product on the right side of the equation must, therefore, have a certain magnitude. This expression, however, gives us no information as to the mutual relation between these values, and, therefore, let us once again consider their influence.

It is clear that we shall not influence the specific speed by altering the value of the efficiency. Certainly, we shall not forcibly decrease the efficiency of the machine just for the sake of achieving a low specific speed. On the contrary, we shall endeavour to attain the maximum efficiency feasible at the given specific speed. The efficiency decreases somewhat with rising speed (this relates only to Francis turbines), the differences, however, are not considerable; certain directions are shown in Fig. 54a.

The specific inlet speed into the draft tube changes far more perceptibly, its influence, however, is restricted by the fact that c_s appears in Equation (43) under the radical sign. Although in high-speed propeller turbines c_s may attain a value of up to 0.65, in Francis turbines we do not surpass a value of 0.35 to 0.4. We must again emphasize that the selection of higher values of c_s requires an efficient draft tube in order not to lose the great outlet energy of the runner.

The tapering coefficient of the inlet cross section of the draft tube, φ , equals 1 in Francis turbines (see Equation 43a); even in case that shaft the of the turbine extends through the draft tube (see e. g. Fig. 8), the value of φ is so near unity that we can always employ Equation (43). Only in propeller turbines due to the hub of the runner does φ vary in the range from 0.9 to 0.7.

¹⁾ For details, see Hýbl J.: Vodní motory, 3. díl (Hydraulic Motors, Part 3), Prague, Česká matice technická, 1928.

The ratio $\frac{D_s}{D_1}$ may be varied within a very wide range and exerts a great influence upon the specific speed. Its magnitude may be varied approximately from 0.5 (in low-speed turbines) up to 1.5 (in high-speed turbines). The principal influence of this ratio upon the shape of the turbine space has already been explained in Part I, Chapter VIII.

Similarly, the specific peripheral velocity u_1 may be selected within a wide range. Its influence upon the angle of the deviation of the blade we have already explained in the above-mentioned chapter. This influence results from the fact that — if, for the sake of simplification, we consider a perpendicular discharge from the runner ($c_{u2} = 0$) — the energy equation $u_1 c_{u1} = \frac{\eta_h}{2}$ must be satisfied. Therefore, if we increase u_1 , we must at the same time select a lower value of c_{u1} , so that the inlet blade angle β_1 rapidly decreases with rising value of u_1 . Figure 74 illustrates this circumstance. Each of the sketches represents the diagram and shape of the blade, and this for a gradually increasing value of u_1 . It can be seen that at a low peripheral velocity u_1 not only the component c_{u1} is large, but also the absolute velocity c_0 at which the water approaches the blade.

According to Equation (25) the overpressure of the runner for a shock-free entry and a turbine without draft tube is

$$h_p = H(1 - \varrho) - \frac{C_1^2}{2g}.$$

For the general case of a turbine with a draft tube and an operation with inlet shock follows from the general flow-rate Equation (42a) — since also for the creation of the shock velocity w_z a certain part of the overpressure is consumed —

$$\frac{h_p}{H} = w_z^2 - w_0^2 + u_1^2 - u_2^2 + w_z^2 = c_1^2 - c_0^2. \quad (67)$$

As we see from Fig. 74, c_0 increases in particular, when there is $\beta_1 > 90^\circ$. The overpressure of the runner then approaches zero and thus also the pressure in front of the runner approaches the pressure at the beginning of the draft tube.

At the same time also the blades become very strongly curved, whereby, on the one hand, the losses due to the curvature of the duct increase and, on the other hand, separating of the current from the suction side of the blade is enhanced, which together with a low pressure across the entire blade supports the formation of cavitation.

For this reason, nowadays the value of the specific peripheral velocity u_1 is not selected lower than 0.65, and Francis turbines are not manufactured with a lower specific speed than 80 r. p. m.

In selecting these values according to the required number of specific speeds, we do not alter the values one after the other, but simultaneously and take care to keep their mutual relationship as favourable as possible for obtaining a high efficiency.

For this selection we may use Fig. 75, in which the characteristic values are

given in terms of the specific values according to Thomann¹⁾. Fig. 76 presents these values according to Prof. Kieswetter²⁾; Prof. Hýbl³⁾ has published directions for the selection of these values.

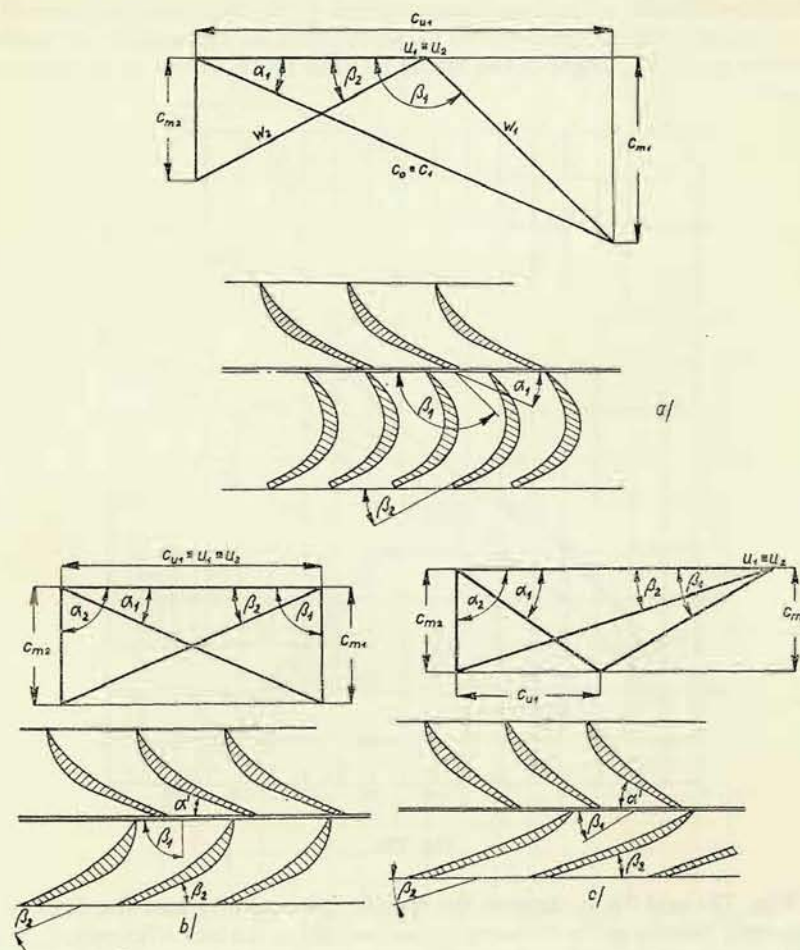


Fig. 74

¹⁾ Thomann R.: Die Wasserturbinen und Turbinenpumpen, 2nd Part, Stuttgart, K. Wittwer 1931, pp. 20, 21.

²⁾ Kieswetter J.: Vodní stroje lopátkové, přednášky (Hydraulic Turbomachinery, Lectures), 1st Part, Brno, Donátův fond 1939.

³⁾ Hýbl J.: Vodní motory (Hydraulic Motors), 3rd Part, Prague, Česká matice technická 1928.

The values recommended by various authors show rather great differences, and we can see that the given diagrams are actually only approximate directions from which the designer may depart should he consider it necessary.

The values relating to the meridional shape of the turbine space are to be found e. g. in Fig. 75a. Fig. 75b presents the values required for determining the position of the inlet and outlet edges of the blade; we shall revert to this in the respective chapter.

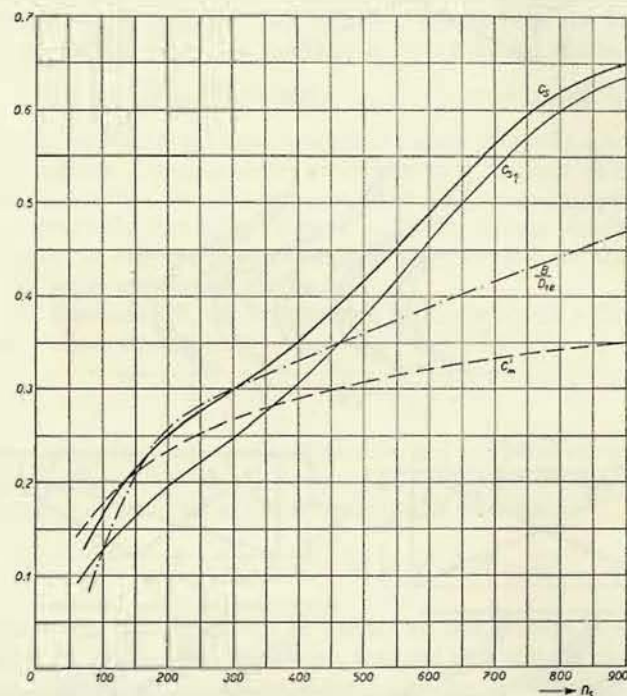


Fig. 75a

In Figs. 75a and 76, c_s denotes the specific inlet velocity into the draft tube, $c_{s,\eta}$ the same velocity at the flow-rate corresponding to the best efficiency, c'_m is the specific meridional velocity at the outlet from the guide blades; by means of this velocity we can check the height B of the guide apparatus. In addition to that, this height is further determined by the ratio $\frac{B}{D_{1e}}$.

From the foregoing chapter we know that in turbines of higher speed, which have a greater meridional curvature, the flow surfaces condense towards the outer contour and that the meridional velocities increase at the outer contour. In order to keep this increase within acceptable limits, the radius of the meridional curvature

of the outer contour should not be smaller than about $1/10$ of the diameter (D_{1e}), on which the outer inlet point of the blade is located: $r \geq \frac{1}{10} D_{1e}$.¹⁾ For the same

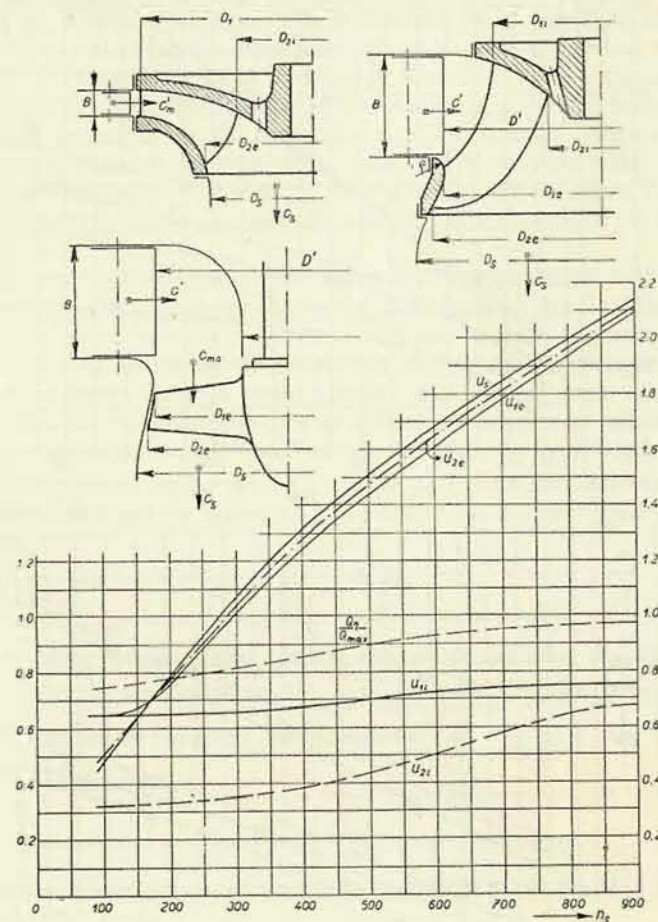


Fig. 75b

reason, also the outlet meridional velocity from the guide apparatus should not be too high; according to the specific speed one selects $c'_m = 0.2 - 0.25 - 0.35$. Here it is advantageous to build up the greater part of the curvature in front of the space

¹⁾ E. g. Dahl: Die Strömungs- und Druckverhältnisse in schnelllaufenden Wasserturbinen, Wasserkraft u. Wasserwirtschaft 1940, p. 1.

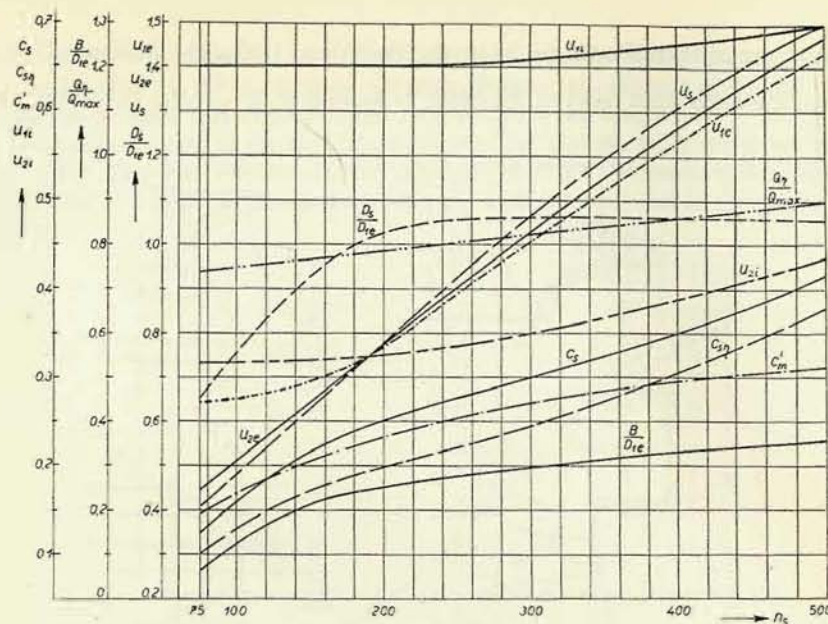


Fig. 76a

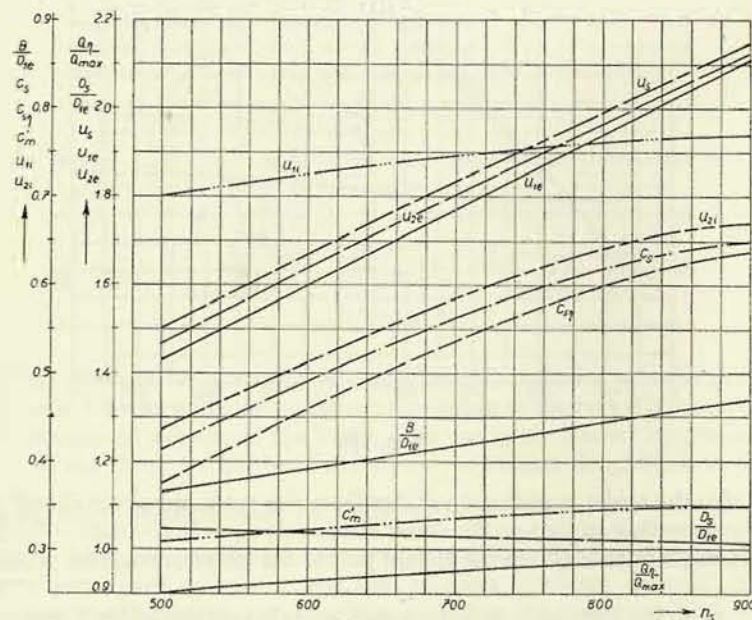


Fig. 76b

of the runner blades so that even in this space it is as moderate as possible. The reason for these rules is to restrict the danger of cavitation at the rim and at the blades near the rim because here is the greatest danger of cavitation, as in this region the highest relative velocities are encountered.

The space of high-speed runner usually widens towards the draft tube. This reduces the velocity at which the water enters the draft tube. Otherwise, we should be compelled to reduce the velocity in the draft tube itself, which would result in greater losses there. This enlargement of the runner space is performed under an angle (of the generatrix to the axis of rotation) of 10 to 20°. Such an intense enlargement is restricted to the space of the blades only, where the water is pressed by the action of the runner blades to the outer rim and not separated from it. In back of the runner blades, we immediately pass over to the shape of the draft tube by curved contours.

An enlargement in the region of the runner blades towards the draft tube has also the advantage that it also reduces outer inlet diameter (D_{1e}) of the runner, whereby the peripheral velocity is decreased and consequently the component c_{u1} is increased, and this results also in an increase of the inlet blade angle β_1 , which usually is advantageous for high-speed turbines with a small angle of deviation.

In general practice we design the contour of the turbine space as follows:

According to the given specific speed we select the specific inlet velocity into the draft tube. Multiplying it by the value $\sqrt{2gH}$ we determine the actual velocity C_{8s} , and by means of this and the flow-rate Q we determine the inlet cross section of the draft tube.

$$F_s = \frac{Q}{C_{8s}} = \frac{\pi D_s^2}{4}$$

Similarly, we select the peripheral specific velocity at the inlet into the runner, u_{1e} , and determine the actual velocity $U_{1e} = u_{1e} \sqrt{2gH}$. Dividing it by the angular velocity ω , defined by the given service speed n ($\omega = \frac{n}{9.55}$), we determine the inlet radius of the runner

$$R_{1e} = \frac{U_{1e}}{\omega}$$

a) For low-speed turbines we determine the height B of the space at this radius $D_{1e} = D_{1t} = D_1$:

$$B = \frac{Q}{\pi D_1 C'_m}$$

For this purpose we have selected the specific velocity c'_m and from it the actual velocity C'_m . Thus the space of the turbine is determined.

b) For high-speed turbines, the diameter D_{1e} approximately defines the minimum cross section of the respective space. By the radius $R \doteq \frac{1}{10} D_{1e}$ we pass

to the lower contour of the guide blade space and to the transition to the draft tube; here we take care to keep the inclination of the generatrix below 10 to 20°. The height of the space in the guide apparatus is determined at the diameter of the outlet edges of the fully opened guide blades, D' , which usually is $D' = D_{1e}$ (Fig. 75b). Therefore we determine again $C'_m = c'_m \sqrt{2gH}$, whereupon

$$B = \frac{Q}{\pi D' C'_m}.$$

Thus the space of the turbine is defined.

Note: So that we are not compelled to determine the actual velocities from the specific velocities, we may calculate directly from the specific velocity if we ascertain the flow-rate in terms of the specific value $Q_\sigma = \frac{Q}{\sqrt{2gH}}$ and the operating speed in terms of the specific value $n_\sigma = \frac{n}{\sqrt{2gH}}$ (not to be confused with the specific speed!), whereupon e. g. for the inlet cross section of the draft tube and for the

given radius $R_{1e} = \frac{D_{1e}}{2}$ the following holds good

$$F_\sigma = \frac{Q_\sigma}{c_m}$$

$$\text{and } R_{1e} = \frac{u_{1e}}{\frac{n_\sigma}{9.55}}.$$

In concluding this chapter we must call the reader's attention to the shapes of high-speed turbines of Soviet manufacture. In Fig. 77 we see

that the continuous shape of the inner contour is replaced by two straight lines, which results in an advantageous shape from the point of view of manufacture.¹⁾

3. Flow without Extraction of Energy

In the space of the turbine there are parts without blades, in which therefore no energy is extracted from the water. This relates mainly to the space between the guide wheel and the runner.

We shall now derive the law governing such a circular flow in which no energy is extracted. For this purpose we consider the flow to proceed as approximately

¹⁾ Morozov: Ispolzovaniye vodnoy energii, Leningrad-Moskva 1948.

indicated in Fig. 78. We have here the case of a plane flow which we can imagine as taking place between two parallel plates, flowing from all directions from the infinite into an opening – a discharge – in one of the plates, the progress of the flow being not rectilinear but in spirals the shape of which is unknown to us.

The space between the walls is entirely free for the flow; there are no blades which could be acted upon by a moment under the influence of the flow. Therefore, this moment must equal zero; applying Equation (13), we can for a certain partial flow between points 1 and 2 write

$$M_{1,2} = \frac{Q\gamma}{g} (r_1 C_{u1} - r_2 C_{u2}) = 0;$$

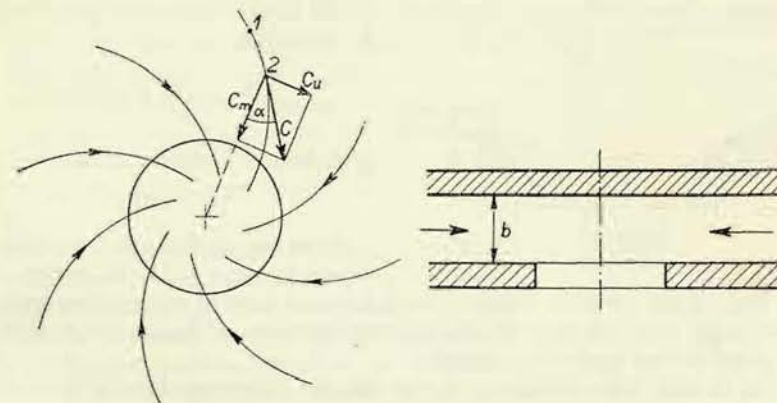


Fig. 78

since the first factor is not equal to zero, there must be

$$r_1 C_{u1} - r_2 C_{u2} = 0,$$

or

$$r_1 C_{u1} = r_2 C_{u2}.$$

As we have selected points 1 and 2 quite arbitrarily, this relationship must hold good between any points in any partial flows, and consequently for the entire flow field the so-called law of constant circulation must hold good

$$r C_u = \text{const.} \quad (68)$$

This law relates to the peripheral component C_u of the velocity C of the flow (Fig. 78). The meridional (here radial) velocity C_m must satisfy the continuity equation, e. g. for cylindrical surfaces passing through points 1 and 2. If we denote the height of the flow by b , there must apply

$$2\pi r_1 b C_{m1} = 2\pi r_2 b C_{m2},$$

i. e.

$$r_1 C_{m1} = r_2 C_{m2}.$$

Thus, we arrive by the same consideration at the conclusion that for the entire flow field it must hold good that

$$r C_m = \text{const.} \quad (69)$$

Dividing Equation (68) by Equation (69) results in

$$\frac{C_u}{C_m} = \text{const.}, \quad (70)$$

which evidently also holds good for the specific velocities.

This ratio, however, represents the tangential function of the angle which is enclosed by the tangent to the spiral – to the stream line – and the direction of the radius.

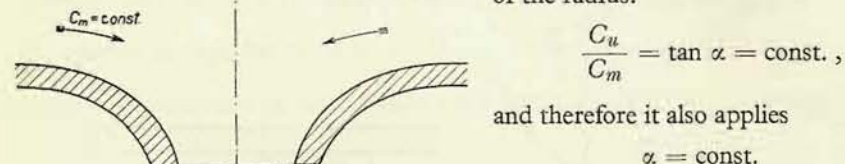


Fig. 79

Thus we see that the line which the liquid particles follow in its flow – the stream line – must have the shape of a spiral whose tangent at any point encloses the same angle with the directrix drawn from the centre of the discharge opening; such a spiral we call logarithmic spiral.

Now let us deal with a similar case, but with the difference that the liquid flows through the gap – Fig. 79 – in such a shape that the meridional velocity C_m is the same in the entire flow.

In this case, Equation (68) still holds good for the peripheral component C_u , but for the meridional velocity, however, applies $C_m = \text{const.}$, so that by division we obtain

$$r \frac{C_u}{C_m} = \text{const.}, \quad (71)$$

and hence, since $\frac{C_u}{C_m} = \tan \alpha$,

$$r \cdot \tan \alpha = \text{const.},$$

which condition characterizes the Archimedean spiral.

4. Position of the Inlet and Outlet Edges of the Blade; Increase in Meridional Velocities due to the Thickness of the Blade

When the shape of the turbine space is established, we must determine the position of the inlet edge of the blade in the elevation and in the plan.

In the elevation we draw the inlet edge of the blade and also the meridional

sections of the blade created in a pencil of planes 1, 2, ... – see Fig. 80 – which pass through the axis of rotation, employing the so-called circular projection. By this method we represent all points of the blade on the picture plane – as indicated in Fig. 80 for the points of the inlet and outlet edges – by rotating these points into the picture plane along circular arcs with their centres in the axis of rotation. When the inlet or outlet edge lies in the meridional plane (Fig. 80a), it appears in the projection in its actual shape and size, similarly as the mentioned sections in the meridional planes 1, 2, ...

The outlet edge usually lies in the meridional plane, so that it appears in the plan as a radial straight line (Fig. 80a). It may also lie in a plane parallel to the turbine axis (Fig. 80b) or have a spatial shape. These two last methods, however, are not so frequently used, because in both cases it is not so easy to achieve the same discharge conditions along the entire outlet edge as it is the case when this outlet edge lies in the meridional plane.

The outlet edge should not be at too great distant from the axis of the turbine or, on the other hand, at too small a radius. If it is too far from the axis (Fig. 81-I), the blade is too short, has a small surface, and is, therefore, subject to the danger of cavitation. In addition to this, it leads to another drawback at an operation where the discharge from the runner is not exactly perpendicular. In this case, the peripheral component of the outlet velocity C_{u2} enters the space at the back of the runner at a large radius and, proceeding into the draft tube, arrives at smaller radii, and according to Equation (68), $r C_u = \text{const.}$, increases its magnitude. The consequence is that the peripheral component entering the draft tube is too large and cannot be converted there into pressure and utilized (in the draft tube only the meridional component is efficiently converted into pressure – Chapter IV.) For this reason, another discharge from the runner, other than perpendicular results in losses, which rapidly augment when the deviation of the outlet direction from the perpendicular increases. Then the efficiency curve of the turbine drops very rapidly towards both sides from the optimum point.

If, on the other hand, the outlet edge is too near the turbine axis (Fig. 81-III), and if we want to maintain at the outlet a sufficiently wide spacing of the blades,

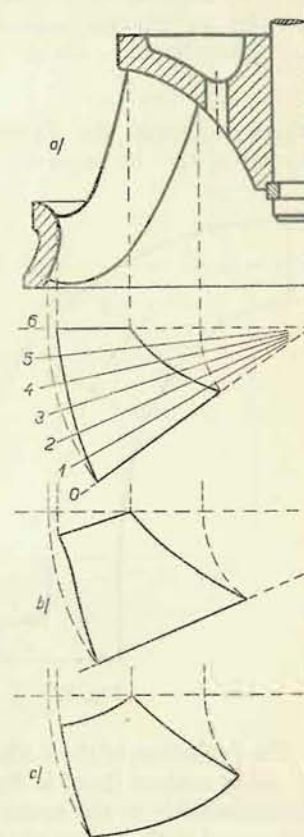


Fig. 80

in order to prevent their clogging, their spacing at the inlet diameter would have to be unsuitably wide.

For these reasons we select a mean distance (Fig. 81-II), as also follows from diagrams (Figs. 75b, 76) given previously. The position of the outlet edge is here given by the peripheral velocities at the outer and inner contours. For checking we can also use the meridional length of the blade at the outer contour (at the rim), l_m , which should be about

$$l_m = \lambda \sqrt{D_{1e}},$$

where we express the diameter D_{1e} in mm, and λ should have a magnitude from 6.5 to 8 at $n_s = 80$ down to 4.5 to 5 at $n_s = 400$.

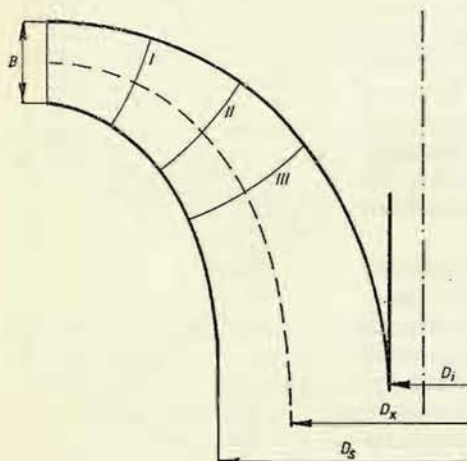


Fig. 81

The projection of the outlet edge from the outer contour (rim of the wheel) to the inner contour (hub) is drawn in such a way that it proceeds as far as possible perpendicularly to the traces of the flow surfaces. This principle can readily be maintained with low-speed runners. With high-speed runners we endeavour to maintain it at least at the rim; towards the hub we must (the farther the more) depart from it (Fig. 82) as otherwise at the hub the blade would become meridionally too long.

The inlet edge in low-speed turbines is usually either parallel to the turbine axis or proceeds on the surface of the cylinder of the diameter D_1 obliquely in the direction of rotation. In high-speed turbines with an inclined inlet edge ($D_{1e} > D_{1i}$) it may lie in the meridional plane (Fig. 80a), as a rule, however, it proceeds obliquely along the circumference, and its projection into the plan then appears either as a straight line (Fig. 80b) or as an arc (Fig. 80c).

By inclining the inlet edge we attain a reduction of the peripheral length of the

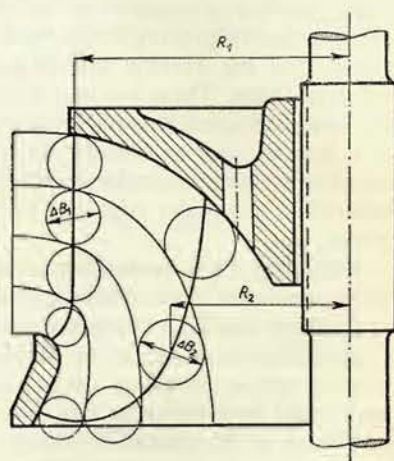


Fig. 82

blade at the rim, where otherwise the blade would be too long in the peripheral direction. Since the relative velocities, which in high-speed turbines are already inherently high, are highest at the rim, great losses arise here by friction of the water on the blade; we must endeavour to keep these losses within acceptable limits; therefore, we shorten the blade. Apart from this, by inclining the inlet edge in the peripheral direction we establish a better transition of the inlet surface into the further surface of the blade at the rim.

The inlet edge (in high-speed turbines), too, should proceed at the rim as far as possible perpendicularly to the meridional stream lines and then be more or less parallel to the outlet edge (see Fig. 83 – runner with $n_s = 400$).

In the space of the blades the velocities increase in comparison with the other space of the turbine, because the space is here partly occupied by the blades. Behind the blades – both guide and runner blades – the velocity decreases again, and this is connected with a small loss (Carnot-Bord loss). This velocity increase we take into account in the velocity triangles mainly at the outlet edges (of both the guide and the runner blades). We must namely determine the outlet angle for the velocities at which the water leaves the end of the blade, i. e. for the velocities which are encountered at the blade end, but still within the space of the blades. At the inlet into the runner we disregard as a rule the velocity increase, because the inlet blade angle has to determine the direction in which the water approaches the runner blade and is therefore given by the velocities prevailing immediately in front of the space of the blades.

All that has been said of velocity increase holds good also for the meridional

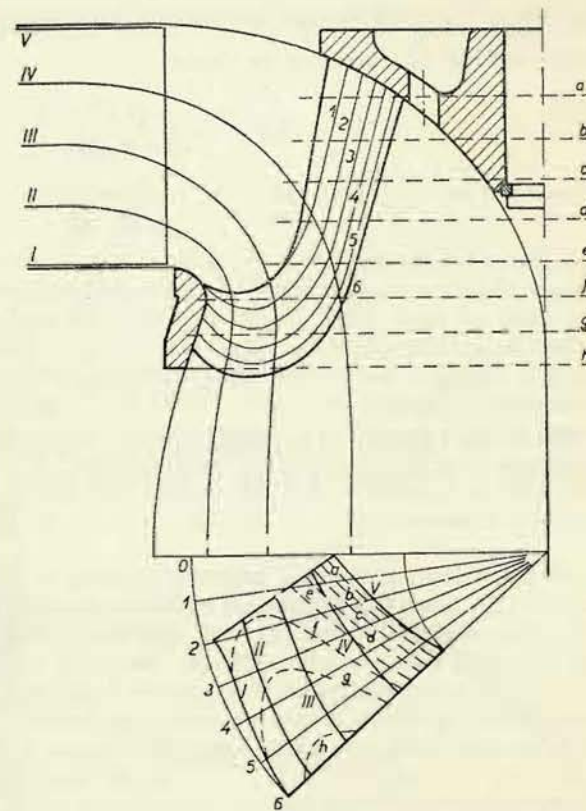


Fig. 83

velocities C_m . The magnitude of the meridional velocities at the blade edges, without regard to the influence of the blade thickness (which increases the velocity), we can readily determine when we have already established the meridional flow field. The velocity is then given as the ratio of the flow-rate of the elementary turbine, $\frac{Q}{x}$, to the through-flow area of the elementary turbine on the respective edge – see Fig. 82 – and thus we obtain

$$\left. \begin{aligned} C_{m1} &= \frac{Q}{x \cdot 2 \pi R_1 \Delta B_1}, \\ C_{m2} &= \frac{Q}{x \cdot 2 \pi R_2 \Delta B_2}, \\ c_{m1} &= \frac{Q}{x \cdot 2 \pi R_1 \Delta B_1 \sqrt{2gH}}, \\ c_{m2} &= \frac{Q}{x \cdot 2 \pi R_2 \Delta B_2 \sqrt{2gH}}. \end{aligned} \right\} \quad (72)$$

Due to the influence of the blade thickness the meridional outlet velocity will be higher, as indicated in Fig. 84. If the blades had no thickness at all, the water would discharge from the runner duct at the relative velocity W_2 , whose meridional component is C_{m2} . Since, however, the blades have a thickness s , the outlet cross section perpendicular to the velocity C_{m2} , of a width equalling the spacing t , is restricted for each duct by the blade thickness measured in the direction of this width, i. e. by the peripheral blade thickness s_0 . Consequently, in each duct the width of the outlet cross-section – measured perpendicularly to

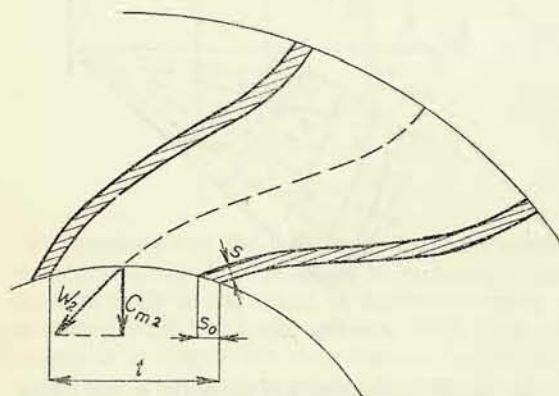


Fig. 84

the velocity C_{m2} – is reduced from the value t to the value $t - s_0$. Hence, according to the continuity equation, for one duct must hold good, when the total number of the ducts is z_2 :

$$\frac{Q}{z_2 x} = C_{m2} t \Delta B_2 = C_{m2}^x (t - s_0) \Delta B_2.$$

The augmented velocity C_{m2}^x will thus be given by the expression

$$C_{m2}^x = C_{m2} \frac{t}{t - s_0} = \frac{C_{m2}}{\varphi_2}. \quad (73)$$

Similarly, also for the meridional outlet velocity from the guide blades the following will apply

$$C_m'^x = C_m' \frac{t}{t - s_0} = \frac{C_m'}{\varphi'}. \quad (73a)$$

5. Representation of the Blade Cross Sections on the Flow Surfaces and Representation of the Blade

After having stepwise designed the contour of the turbine space, investigated the meridional flow field and drawn the inlet and outlet edges of the blade, we can on each flow surface determine the velocity triangles. From them we know the peripheral velocity on the inlet edge as well as on the outlet edge and the respective meridional velocities. If we further select the shape of the outlet triangle – e. g. we select a perpendicular discharge, i. e. $\alpha = 90^\circ$ – the outlet triangle is completely defined, and then we also determine the inlet triangle, e. g. by means of the Braun construction. Thus the inlet (β_1) and the outlet (β_2) angles of the blade are determined on each flow surface, and our further task now consists in drawing the progress of the section of the blade surface with the flow surface so as to maintain these angles.

The flow surface, however, is generally a surface of revolution which cannot be developed into the picture plane, as would be necessary for drawing the progress of its intersection by the blade. Therefore, we must replace the flow surface by another surface which can be developed, or employ the so-called conformal representation in which we effect the development in subsequent parts.

In the first case we use as a substitute surface the conical surface K , which lends itself to development. This is co-axial with the flow surface P and contacts it in circle k , as perspectively shown in Fig. 85.

The meridional planes, which pass through the axis common to the cone and the flow surface, intersect the latter in the meridians M_1, M_2, \dots , and the conical surface in the co-ordinate rectilinear sections M_1^x, M_2^x, \dots . The individual points on the flow surface, e. g. A_1 , we transfer to the conical surface in such a way that we mark them in the meridional section on the cone so as to obtain the same distance from the circle of contact on both surfaces (indicated by thick lines in Fig. 85). When in this way we have marked out all necessary points, we obtain a picture on the cone, which we can develop into a plane.

The angles enclosed by the line drawn on the flow surface and by the peripheral circles of the flow surface will here equal the angles enclosed by the line drawn on the cone and by the circles of the cone only in the proximity of the circle of contact k . The farther we depart from this circle, the greater will be the difference between the angles mentioned. Only the right angle appears undistorted, because the meri-

dians on both surfaces are perpendicular to the peripheral circles. From this it follows that the deviation mentioned will be the greater, the more the respective angle differs from the right angle. Since the inlet angle approaches the right angle closer than the outlet angle does, the distortion of the former will be smaller, and, therefore, we select the substitute cone so that it contacts the flow surface on the outlet edge of the blade – see Fig. 86.

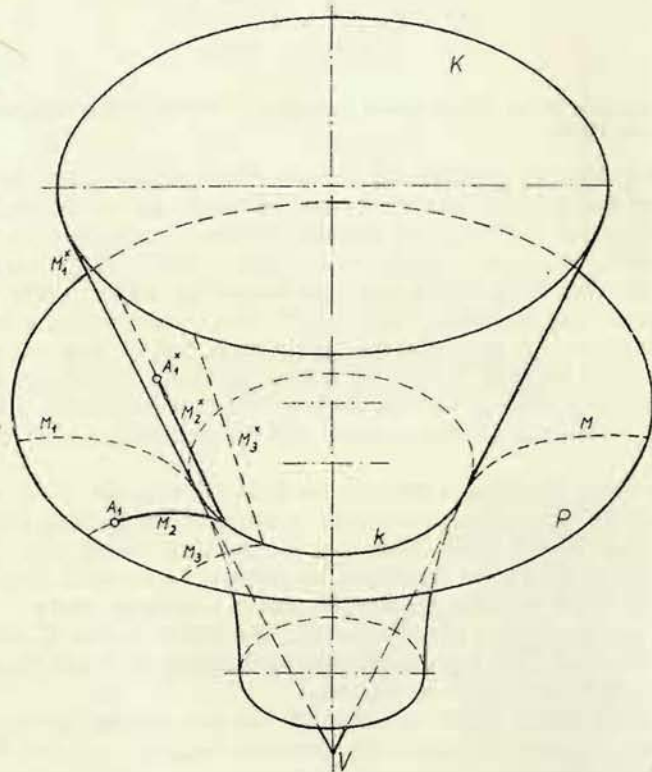


Fig. 85

In this case we obtain a true representation of the outlet end of the blade on the substitute surface. But the closer we approach the inlet, the greater is the deviation of the flow surface from the conical surface; therefore, also the angles drawn on the cone differ from the angles on the flow surface.

The magnitude of their difference can be determined. In Fig. 86 arbitrary line C is represented lying on the flow surface P . Its representation on the cone K , obtained by the previously described method, is C^* . Through point a of this line and its picture a^* we draw the peripheral circle. Now we want to find the relationship

between the angle β , enclosed by the original line C and the peripheral circle on the surface P , and the angle β^* which corresponds to it on the conical surface.

For this purpose we lay a meridional plane through point b and its picture b^* on the cone. This plane intersects the mentioned peripheral circle at points c and c^* . Now we can write

$$\tan \beta = \frac{m}{r \varphi}$$

$$\text{and } \tan \beta^* = \frac{m^*}{r^* \varphi} \quad (74)$$

The points a and a^* , too, lie in a common meridional plane – according to the principle of the representation – so that the angle φ is the same for the original and for the picture on the cone.

Similarly, the meridional lengths are likewise the same $m = m^*$. The radii of the peripheral circles, however, differ from each other: $r \neq r^*$. Consequently we can derive from the expressions (74)

$$m = r \varphi \tan \beta = r^* \varphi \tan \beta^*,$$

whence follows

$$\tan \beta^* = \frac{r}{r^*} \tan \beta \quad (75)$$

Since only the maintenance of the inlet and outlet blade angles is of importance, whilst the other progress of the blade may be arbitrary –

in so far it is not accompanied by excessive losses (Part I, Chapter III/2) – it will suffice to correct only the inlet blade angle. On the developed conical plane we design the blade for the inlet angle β_1^* , and when we then transfer the section back to flow surface (see further), the blade will have the correct angle β_1 .

At the same time we see that only on circle k , which passes through the discharge ends of the blades, will a true picture of the spacing of the blades appear on the conical surface. On the inlet side the spacing of the blades will be smaller than the actual distance.

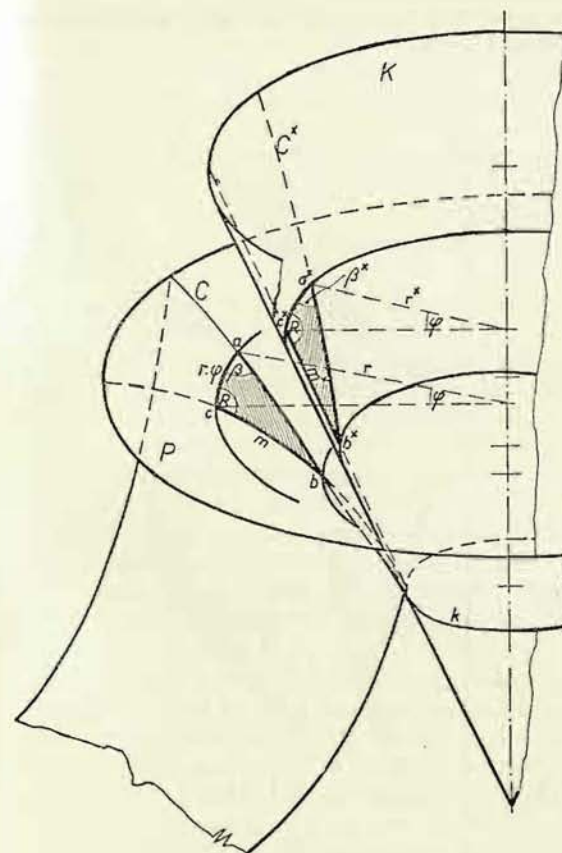


Fig. 86

Thus we see that we can design the shape of the blades not on the flow surfaces but on the conical surfaces which lend themselves to development; here we must take care to design the sections on the individual cones – which replace the individual flow surfaces – in their correct mutual relationship, in order to obtain (on transferring the sections from the cones back to the flow surfaces), a continuous blade surface, without irregularities and breaks.

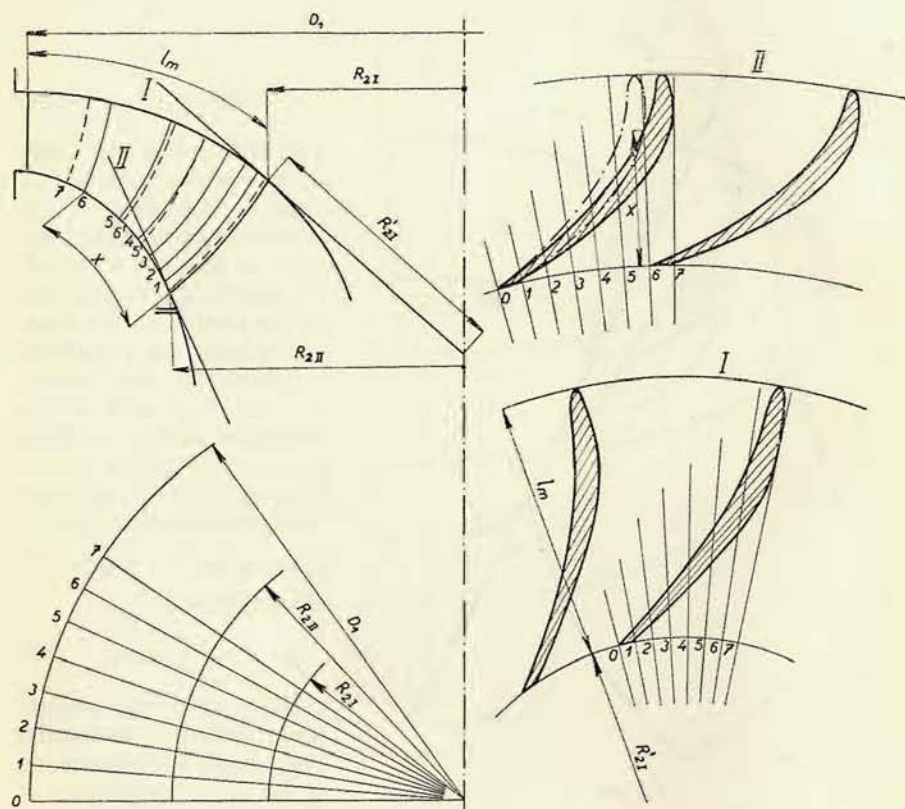


Fig. 87

The procedure is explained in Fig. 87. As flow surfaces, on which the blade sections are to be designed, we have here selected directly the contour surfaces which are replaced by the conical surfaces *I* and *II*; these contact the flow surfaces in the circles on which the outlet edges of the blades are located.

We develop the cone *I*; the circle on which the outlet edges lie we draw as a circle with the radius R_{2I} , and the circle on which the inlet edges are located we obtain

on extending this radius by the rectified meridional length of the blade on the flow surface l_m . Between these two circles we design the shape of the blade in such a way that the inlet and outlet angles are in agreement with the velocity diagram (see further). Similarly, we develop the cone *II*. On this cone, however, we can no longer design the blade independently, but must pay attention to the connection with the section on cone *I*. For this reason we divide the section on cone *I* by a pencil of rays, e. g. 0 to 7. On the cone these rays represent sections by meridional planes, which we also indicate in the plan of the runner. Therefore, we draw on the plan a circle of the radius R_{2I} . This is the circle in which the cone contacts the flow surface, and hence the lengths on the latter are the same in the plan and in the conical section. Therefore, we transfer the distances between the rays 0 — 1, 1 — 2, 2 — 3, etc. from the circle R_{2I} to the circle R_{2II} in the plan and obtain in this way a pencil of rays which represents the traces of the selected meridional planes.

Now we draw in the plan a circle with the radius R_{2II} , which is the circle of contact between the outer contour (of the flow surface) and cone *II*. The division of this circle by the traces of the meridional planes therefore coincides with the division on the circle of the developed cone and so we transfer it to this circle. Thus we have obtained rays on cone *II* which are the sections of the same meridional planes as on cone *I*. When the outlet edge itself lies in the meridional plane, the outlet end of the blade must line on both cones on the same ray. This also applies to the inlet edge when it is parallel with the axis of the turbine.

We therefore draw the shape of the blade on cone *II* into the obtained pencil of rays as indicated in the figure. The dot and dash line represents here the alternative progress of the blade contour for a peripherally oblique inlet edge and shows how this obliquity shortens the peripheral length of the blade and leads to a more advantageous shape.

We are further concerned with transferring the shape of the blade, designed on the conical surfaces, back into the circular projection. For this purpose we advantageously employ the already selected pencil of meridional planes 0 — 7. Since here we have to deal with a circular projection (see also Fig. 80), our procedure consists in transferring the distance of the sought point on the meridional plane in the conical section (e. g. x on cone *II*) to the corresponding flow surface. When we effect this for one and the same meridional plane on all cones and flow surfaces, the connecting line of the points so obtained will appear in the circular projection as the intersection of the blade with this meridional plane. We number the section in accordance with the meridional planes and draw the sections of the pressure side of the blade in full lines, whilst those of the suction side are indicated by dashed lines and their numbers are marked with dashes. These meridional sections are continuous lines when the blade has the required smooth shape.

By these meridional sections the blade is already fully defined, but this method of representation is not suitable for manufacturing purposes. Here we need the so-called contour line sections. These are sections of the blade surface with a system of parallel planes perpendicular to the axis of the runner. For production

it is more advantageous to select these planes at equal distances to each other. The contour line sections, or also briefly contours lines, appear in the plan, where we derive them from the meridional sections, as illustrated in Fig. 88. For instance, plane *I* intersects meridional section 1 at the radius denoted by r_1 ; we intersect in

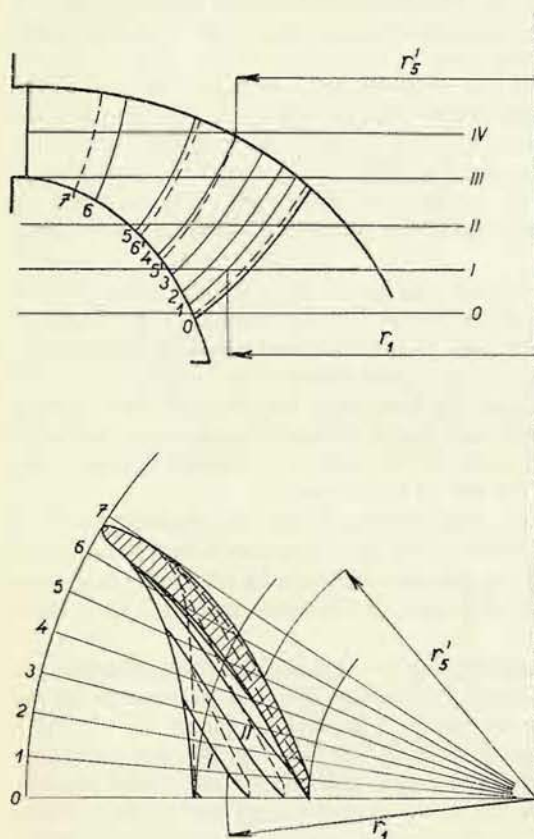


Fig. 88

the plan the trace of the meridional plane *I* by this radius and thus obtain one point of contour line *I*. Similarly, by the radius at which the plane *I* intersects meridional section 2 we intersect the trace of meridional plane 2, etc.; by connecting all these points lying in plane *I*, we obtain the complete contour line *I*. We proceed in the same way with the other planes and also with the meridional sections of the suction side. Finally, we draw in the plan the penetration of the blade with the contour surfaces of the turbine space. The construction is analogous and indicated in Fig. 88 for the inner contour and for meridional section 5'.

The contour line must again show continuous progress, and this condition provides further control as to whether the blade surface is smooth and without irregularities.

In Figs. 87 and 88 the inlet blade angle was 90° , so that no correction was required. When the inlet angle differs

materially from the right angle and when at the inlet the substitute cone surface considerably deviates from the flow surface, we must draw on the cone the corrected β_1^c – according to Equation (75) – in order to obtain in the transformation to the flow surface the section of the blade with the correct angle.

This correction can be avoided if we replace the flow surface by two cones, one of which contacts the flow surface in the circle of the outlet edges and the other one in the circle of the inlet edges – see Fig. 89. About half the meridional stream line from the outlet we rectify on the first cone and half from the inlet on the second

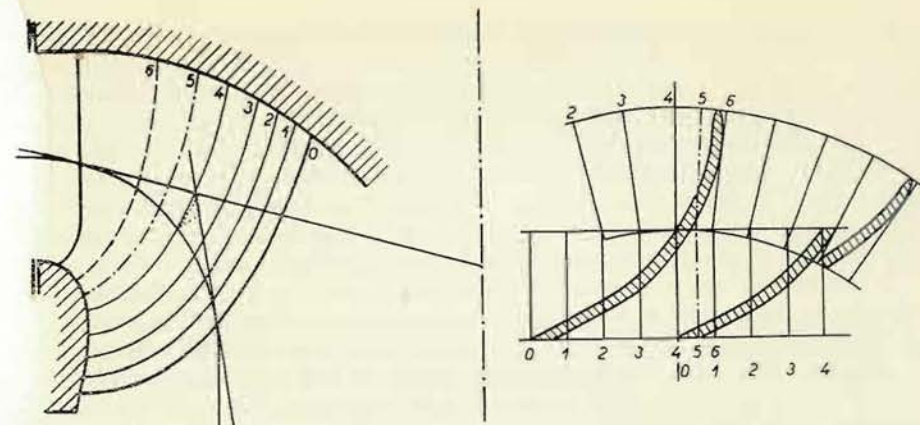


Fig. 89

cone; then we put the developed cones together so as to obtain a continuous progress of the blade section. In this case the inlet as well as the outlet angle is represented correctly, but no continuous picture of the duct is obtained.

We obtain a true picture of the intersection of the blade with the flow surface if we use the so-called conformal representation. In this procedure we develop the

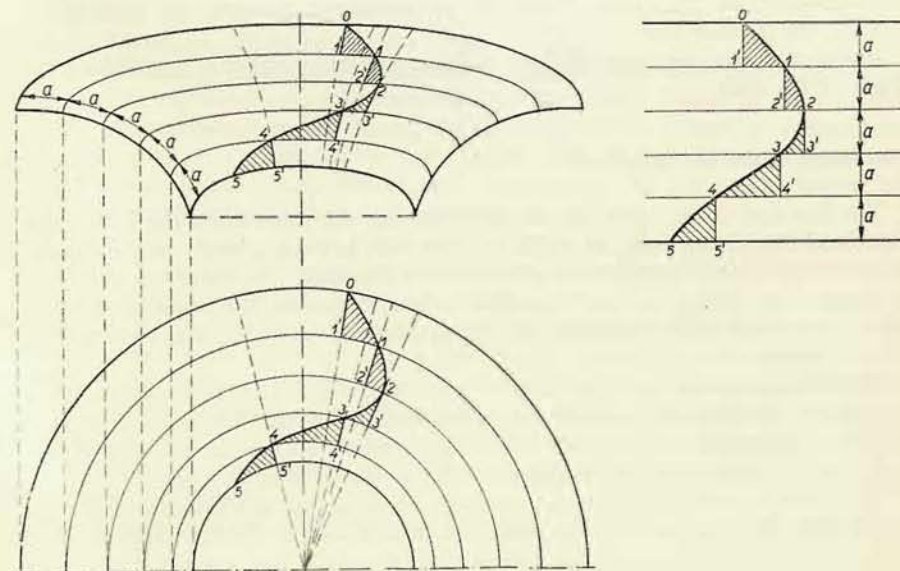


Fig. 90

line on the flow surface stepwise. Fig. 90 shows a half of the flow surface with the line $0-1-\dots-5$, which has to be represented conformally. On the flow surface we draw a system of peripheral circles at equal meridional distances a . These circles intersect the line to be investigated at points $0-1-2-3-4-5$. Through these points we lay meridional lines. The triangles – the hatched areas in the figure – are rectangular, and in our representation we put them together in such a way (Fig. 90, on the right) that the bases of the triangles, formed by parts of the peripheral circles, are parallel to one another, as they were on the flow surface, and the vertices are again connected in the appropriate sequence.

In this way we have an exact picture of the line in its entire progress, because the triangles in the original as well as in the picture are congruent, and consequently also the inclination of the line to the peripheral circles has been exactly reproduced in all points. The figure also indicates the connection with the plan, from which it is evident how we proceed with the layout in the conformal picture. We divide the meridian of the flow surface into the same number of parts of meridional length a . Then we draw the corresponding system of parallels, likewise at intervals of the magnitude a . Into this system we design the progress of the blade section, and the perpendiculars from its intersections with the parallels define the hatched triangles. In the plan we draw circles corresponding to the division of the meridian of the flow surface; then we transfer the hatched triangles into the plan by marking off the distances $1-1'$, $2-2'$, etc. in their correct sequence on the circles. By connecting the vertices $0-1-\dots-5$ we obtain a plan of the line in agreement with the layout.

From these we must again construct the meridional sections, and from these, in turn, the contour lines.

In the conformal representation we have no possibility either of establishing the shape of the duct.

6. Shape of the Blade Duct

The function of the blade consists in conveying the water from the inlet cross section of the runner into the outlet cross section in such a way that the change of the water velocity corresponds to the velocity diagram. The water has to deliver as much of its energy as possible to the runner; therefore, the losses must be as small as possible and, moreover, all water particles must be subjected to this velocity change.

The losses due to the bending of the flow and whirling will be at a minimum when the shape of the blade is continuous and its curvature gradual. The losses due to the friction of the water on the blade will be the smaller, the smaller the wetted surfaces are, i. e. the shorter the blades are and the smaller their number.

The other demand that all water particles are subjected to the required change of the flow, is identical with the condition to establish at the inlet into and the outlet from the runner on the peripheral circle along the flow surface at all points the same velocities as to direction and magnitude; this condition can only be

satisfied with a very great number of blades (an infinite number of infinitely thin blades).

These facts we must bear in mind when selecting the number of blades. As a rule, we already have an idea of the appropriate number of blades when drawing the blade duct on the developed conical surface. From this it follows that we shall select a smaller number of blades for specifically high-speed turbines, where the specific relative velocities are higher; the losses due to the friction of the water on the blades increase proportionally to the squares of the velocity, and we must counteract this circumstance by a smaller wetted blade surface, i. e. by fewer and shorter blades.¹⁾

Some manufacturers vary the number of the blades of the runner according to the diameter. This, however, is not quite correct; the runner for the ordered turbine should be geometrically similar to the model runner on which tests were carried out and the outputs determined by braking; consequently a full-size runner should also have the same number of blades, regardless of diameter. Only for runners of very small diameters, sometimes manufactured to special order, are the number of blades reduced in order to avoid too narrow outlet cross sections of the ducts, which are subject to clogging, or to eliminate the necessity of an excessively dense grid as protection against clogging of the runner.

Therefore, we can only select the number of blades according to speed, using as a guide the following formula:

$$z_2 = \frac{10 \text{ to } 12}{u_1}, \quad (76)$$

where u_1 is specific peripheral velocity of the inlet edge.

Note: Increasing the number of blades with the diameter of the runner results in a somewhat improved cavitation resistance of the runner owing to the reduced specific underpressure on the blade; the flow-rate, too, is somewhat reduced as the cross section is restricted by more blades. The runner, however, does not remain exactly geometrically similar, and consequently the test results cannot be in perfect agreement with the actual conditions.

It is a matter of course that in propeller turbines the same number of blades is used even for various diameters; on the contrary, – as we shall see – with a change in the number of blades their speed also changes.

In order to obtain a runner duct of an appropriate length at the inner and outer contour, it is usually necessary to provide turbines showing a greater height B of the inlet cross section – i. e. turbines of higher speed – with a peripherally inclined edge. Thereby the blade length at the outer rim is reduced, as e. g. indicated by the dashed line in Fig. 87 (the effect here is not so marked as the runner in question is comparatively narrow); moreover, it is advantageous to increase the radius of the curvature of the blade.

The curvature of the blade may also be reduced, if necessary, by changing the

¹⁾ See also Kaplan-Lechner: *Theorie und Bau von Turbinen-Schnellläufern*, München u. Berlin, Oldenburg, 1931, p. 145.

inclination of the inlet edge in the meridional plane. This is evident from Fig. 91. The fully drawn shape of the runner duct at the outer contour agrees with the progress of the inlet edge according to a and with the fully drawn inlet triangle. In order to eliminate too intense a curvature of the blades, it will suffice to correct the progress of the circular projection of the inlet edge according to k . Thereby the peripheral velocity increases from u_{1a} to u_{1k} , to which, according to the energy equation, corresponds a reduction of the component c_u . The inlet angle, therefore, rapidly decreases, and we obtain a materially more suitable shape of the duct, as indicated by dashed lines.

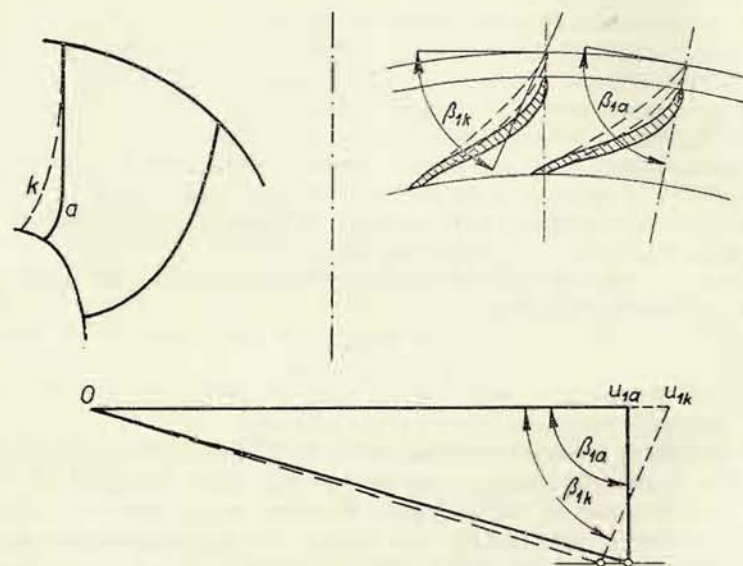


Fig. 91

The inlet end of the blade must show an inclination which agrees with the inclination of the relative velocity at which the water at a shockless entry – i. e. at a filling and speed corresponding to the optimum efficiency – approaches the runner.

The outlet end of the blade must be so inclined that the water discharges from the runner ducts at a relative velocity and under an angle as required by the velocity diagram. This angle under which the water discharges from the runner ducts must here not always agree with the outlet angle of the blade. To explain this circumstance, we have indicated the blade ducts in Fig. 92, and for the sake of simplification we assume that the turbine in question is of the axial-flow type and that the blades are drawn in their developed cylindrical section. We see that the duct is delimited by the blades only up to the profile passing through the point A ; in this part of the duct the water is perfectly guided. Further on, the duct has only one side of the

blade – the suction side – and is therefore incomplete. When this suction side of the blade deviates from the direction of the discharging water, it may happen that the flow separates from the suction side of the blade; this case is expressively indicated in the right half of Fig. 92; the discharging water is then less deflected from the original direction than we have assumed. But even if the flow does not separate from the suction side of the blade, the particles streaming in the centre of the duct are still less deflected than those streaming along the surfaces of the blades (see the left half of the figure), so that the average discharge angle will not agree with the angle of the blade.

This disagreement can be avoided by effecting the complete required deflection of the flow still within the enclosed duct and by directing the further part of the blade so that it exerts no longer influence upon the water flow, i. e. that behind

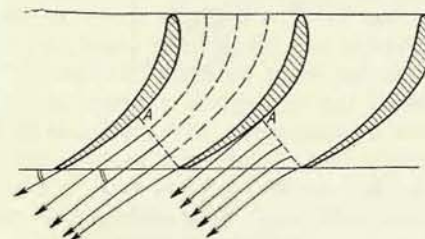


Fig. 92

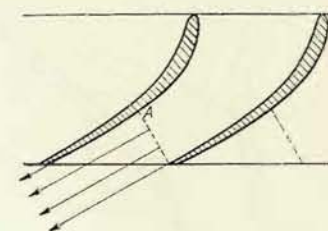


Fig. 93

point A the blade extracts no longer energy from the water. In the case of the mentioned axial-flow runner this requirement is fulfilled by a straight continuing blade according to Fig. 93. For a runner with a fully radial through-flow a suitable shape, according to Chapter I/3, is given by the logarithmic spiral, provided that the contours of the turbine are parallel (Fig. 78), or by the Archimedean spiral when the chamber of the turbine is of such a shape that meridional velocity is constant.

Both these curves may, within the range applied for turbine blades, be replaced with sufficient accuracy by a circle. Deviations from the correct shape are of minor importance as they appear in the substitutive conical sections, where a certain inaccuracy is already involved in the replacement of the flow surface by the cone. The centre of the circle which with sufficient accuracy defines the shape of the ineffective end of the blade, is the intersection of the perpendiculars to the sides of the outlet angles of two adjacent blades, as indicated in Fig. 94.

Until quite recently, this method of determining the blade ends was exclusively used for the reasons mentioned. For low-speed and even for normal turbines an inlet angle $\beta_1 = 90^\circ$ and in the outlet triangle the angle of the absolute velocity $\alpha_2 = 90^\circ$ were selected. It is understandable that the inlet and outlet triangles could not be selected arbitrarily, without regard to the energy equation. For the selection mentioned a certain specific peripheral speed at the inlet had to be

assumed, and we obtain it by substituting the values $c_{u2} = 0$ and $c_{u1} = u_1$, which result from the selected triangles, into the energy equation

$$u_1 c_{u1} - u_2 c_{u2} = \frac{\eta h}{2}.$$

Thus we obtain

$$u_1^2 = \frac{\eta h}{2},$$

and if we further substitute $\eta h \doteq 90\%$, we see that the following must hold good

$$u_1 \doteq \sqrt{0.45} = 0.67.$$

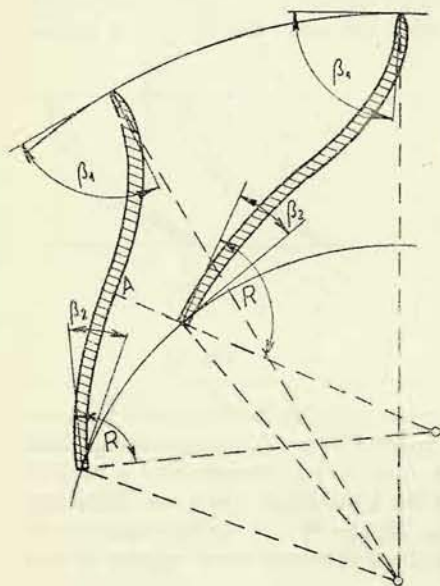


Fig. 94

blade) smaller by about 2 to 5° (more for a wider spacing of the blades), which is called exaggeration of the outlet angle. Here it is also advantageous to select a higher peripheral velocity at the inlet diameter (in other words, a somewhat larger inlet diameter is selected); this results in a smaller inlet angle (see Fig. 91), so that the blade is nearly straight, with smaller losses. Such blade designs will be described later and illustrated by examples.

The end of the suction side of the blade, where the duct is no longer enclosed on both sides, is subjected to underpressure. When the blade end is designed as effective, the driving underpressure also becomes manifest, enhancing the conditions for cavitation. An ineffective blade end will naturally be more resistant against cavitation. On the other hand, an effective blade end lengthens the effective part

The section on the developed cone had then approximately the shape indicated in Fig. 94. The blade in this case was curved in two places. The curvature, in particular when doubled, of course, increases the through-flow losses of the duct in comparison with the losses in a straight duct. Apart from this, by designing such an outlet blade end, we have indeed knowingly lengthened the blade in a way ineffective for energy transfer; this lengthening, however, results in an increase of the wetted blade surface and, therefore, of losses also.

For that reason, this method of designing the blade end is no longer employed. The blade is designed as effective up to the outlet end, and the disagreement between the mean discharge angle of the water and the blade angle is cancelled out by making the outlet angle of the blade β_2 (of the centre line of the

of the blade and so reduces the driving underpressures, which in turn is advantageous and cancels the afore-mentioned drawback.

The thickness of the blade itself is either varying or constant. Blades of a variable thickness are manufactured when they are cast as one unit with the hub and the rim. In this case we give them the cross section of a body of minimum hydraulic

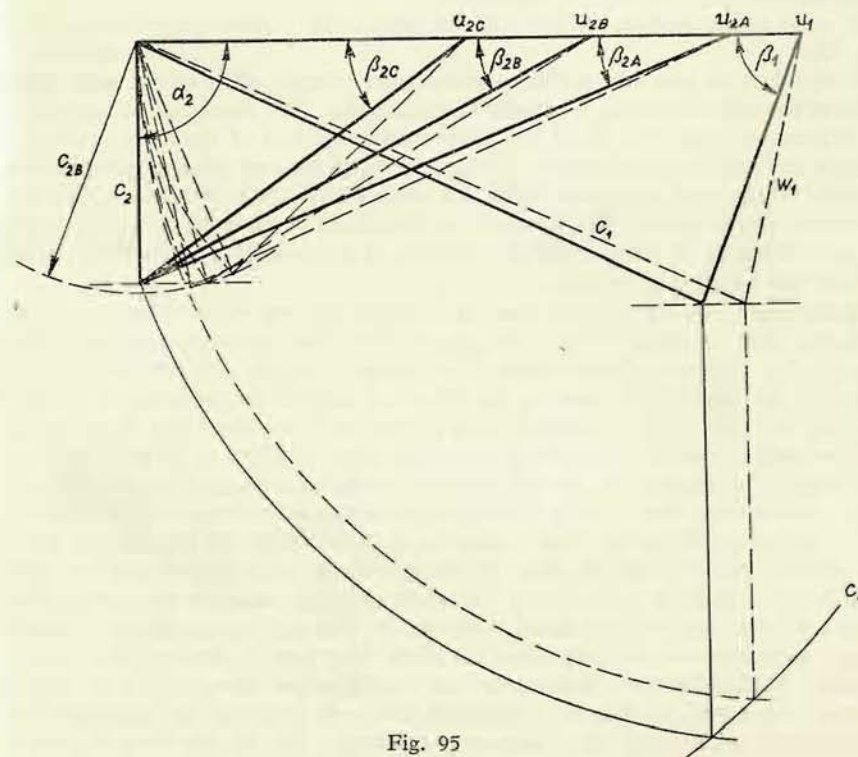


Fig. 95

resistance (drop-shaped). When the blades are pressed from sheet metal and then cast into hub and rim (Chapter B, II), they are of constant thickness and only sharpened at the inlet and outlet (Fig. 94). This design is not much used at present and only employed for turbines of smaller diameters and for lower heads.

7. Interrelation of the Velocity Diagrams on the Flow Surfaces; Oblique Discharge from the Guide Apparatus

Already in Part I, Chapter XII/2, we saw how the outlet triangles on the various flow surfaces of the same turbine are linked together, when the peripheral as well as the inlet velocities at the inlet edge are the same on all flow surfaces, and when

all these surfaces are perpendicular to the outlet edges of the guide blades. All meridional stream lines have then a common inlet triangle, so that the auxiliary velocity w_2 in the Braun diagram is the same in all outlet triangles.

We first draw the velocity diagram for the conditions at which the efficiency has to be the best. For these conditions we then select a shock-free entry and the most advantageous shape of the outlet triangle.

As most advantageous, we consider an isosceles or a rectangular triangle (see Fig. 95).

If we select on one flow surface a rectangular triangle, then on the other flow surfaces the outlet triangles must also be rectangular. The discharge velocity c_2 in all elementary flows will be of the same magnitude and of the same direction, without any rotational component. These conditions are very advantageous for the function of the draft tube into which the water enters from the runner, because there is no component c_u (which would not be utilized in the draft tube), and there are no differences in the meridional velocities, which would increase the internal friction and whirling of the liquid.

At the inner, smaller diameter there is a smaller spacing of the blades, and consequently also a smaller width of the outlet ducts than the outlet spacing at the outer, larger diameter of the runner. If we want to reduce this difference in the width of the outlet cross section, we select an isosceles outlet triangle, so that $w_2 = u_2$, as indicated by the dashed lines in Fig. 95. If we select this condition on one flow surface, we must observe it also on the other surfaces, as follows from the construction of the diagram. In this case we select the vertices of the triangles in such a way so that they lie on a circle with its centre in the origin of the diagram and its radius equalling the outlet velocity c_2 , as follows from the required meridional velocity on the stream line near the outer contour, or so that all relative velocities pass through the end point of the relative velocity valid for the central flow surface. In this case the meridional components of all outlet velocities $c_{m,2}$ are not equal – as assumed in the determination of the flow field by the one-dimensional method – but the difference is not great, and the higher meridional velocities appear at larger diameters, so that this procedure means in principle an approximation to the actual conditions (two-dimensional approach). We see that here the outlet angles increase on all flow surfaces, so that the width of the outlet cross section of the duct advantageously increases, but it increases more at smaller diameters, whereby at the same time the widths are partly equalized.

We now introduce into the draft tube the peripheral component of the outlet velocity, $c_{u,2}$, which is not utilized in the draft tube and consequently represents a loss; but these components are small and also the relative velocities w_2 are smaller; and losses due to the friction of the water on the runner blades have decreased proportionally to their squares. In particular at a higher specific speed, when the specific relative velocities assume higher values, this gain prevails and the isosceles outlet triangle is advantageous also as far as efficiency is concerned. A rectangular outlet triangle is therefore only used for low-speed turbines.

The mentioned interconnections of the outlet triangles are no longer valid if we

must resort to a two-dimensional determination of the flow field. In this case the meridional velocities $c_{m,1}$ along the inlet edge of the blade differ, and for this reason the inlet triangles on the various flow surfaces cannot be congruent. In addition to this, the contraction of the stream lines towards the outer contour reaches far in front of the runner, even into the space of the guide blades, and the outlet edge

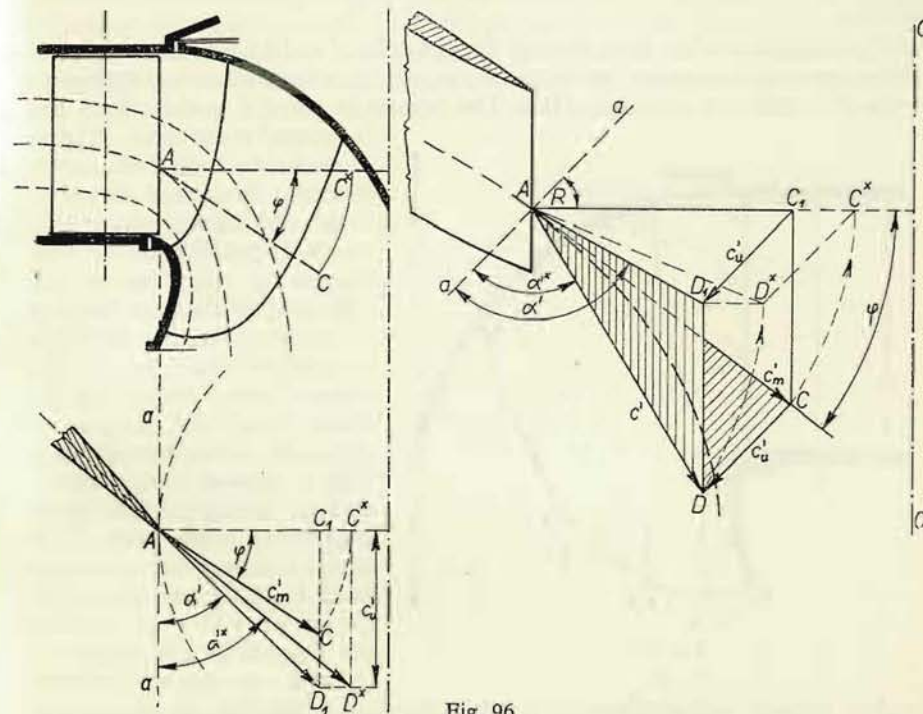


Fig. 96

of the guide blades is no longer intersected by the meridional stream lines under a right angle, but under the oblique angle φ (Fig. 96), which is not the same on all flow surfaces.

Consequently, however, the angle enclosed by the discharge velocity from the guide apparatus and the tangent to the peripheral circle is no longer identical with the angle α' of the blade end, measured in the plane normal to the axis of rotation (as appears in the section of the guide blade normal to the axis of rotation).

Since the angle of inclination φ (Fig. 96) of the meridional stream line to the outlet edge is different for each flow surface, the angle of discharge velocity to the tangent of the peripheral circle will also vary, and we must determine it separately on each flow surface, for this angle is the starting point for the construction of the inlet triangles, as will be seen later.

The determination of this actual angle α'^x (enclosed by the direction of the discharge velocity from the guide apparatus and the tangent to the peripheral circle) from the angle of the guide blade α' (measured in the plane normal to the turbine axis) is carried out by means of the construction indicated in the lower part of Fig. 96. In the right side of the figure we have endeavoured to provide a simpler explanation of the construction by illustrating the discharge conditions perspective.

The outlet edge of the blade passing through point A and the turbine axis $O - O$ define the meridional plane. On this plane the meridional stream line passing through point A is indicated by a dashed line. The tangent in point A to this stream line

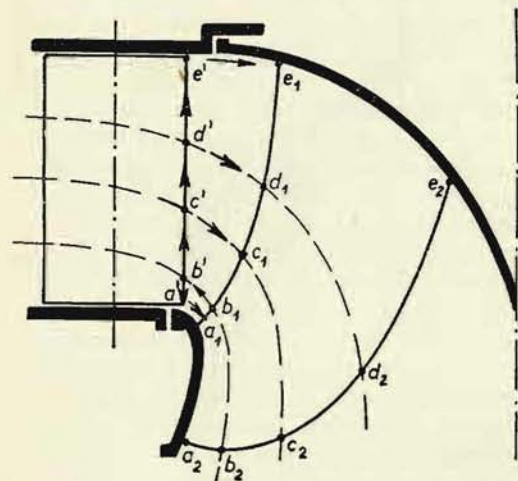


Fig. 97

is inclined to the radius of point A under the angle φ and represents the direction of the meridional discharge velocity c'_m , which is marked off on this tangent by the distance AC . The actual discharge velocity c' , however, does not lie in this meridional plane but in the plane of the extension of the blade. The both mentioned planes form together a wedge with a common line of intersection, which is the outlet edge of the guide blade. This wedge is intersected on the one hand by the plane normal to the axis $O - O$, which contains the tangent to the peripheral circle $a - a$, on which blade

angle α' appears, and on the other hand by the plane which likewise contains the tangent $a - a$, but is inclined to the first plane under the angle φ ; this inclined plane contains the actual velocity c' and here also the actual angle α'^x appears which this velocity encloses with the tangent $a - a$.

In order to determine this angle in the plane normal to the axis of rotation — which as a rule is the picture plane of the plan — it will suffice to rotate the triangle ACD about the tangent $a - a$ into this plane (normal to the axis), as indicated by the arrows. Thus we obtain the triangle $AC^x D^x$. The distance AD^x , which represents the actual rotated velocity, encloses with the tangent $a - a$ the actual angle α'^x .

In the left part of the figure this construction is drawn in the plan, into which the meridional plane with the angle φ and the meridional velocity c'_m has also been rotated. The notation by letters corresponds to the perspective picture and no further explanation is required.

In this construction the inlet triangles on the various flow surfaces are linked together by the fact that for all surfaces the blade angle α' is the same in the plane normal to the turbine axis. (This was also formerly the case, and since throughout $\varphi = 0$, all inlet triangles were equal.)

We utilize this construction in the following way: On one of the flow surfaces we select a suitable outlet triangle at optimum efficiency conditions and determine the corresponding inlet triangle (from the picture of the flow field we already know the meridional velocities in both triangles). This flow surface is selected near the outer contour, where the flow is not yet acted upon by friction against the contour, but where there are already high velocities, so that it is of primary importance to satisfy the conditions of good efficiency; this surface is indicated in Fig. 97 by the dashed line $b' - b_1 - b_2$. Now we proceed along the stream line against the flow up to the outlet edge of the guide blade (see the arrows in Fig. 97) and determine the components of the velocity at point b' . We already know the meridional component or we determine it from the meridional flow field; the peripheral component we recalculate according to the law (68) $r_1 c_{u1} = r' c'_u$.

Thus we know both components, and in the construction in Fig. 96 the triangle $AC^x D^x$ is defined in this way. ($AC^x = c'_m$, $C^x D^x = c'_u$.) As we also know the inclination of the meridional stream line φ , we can by the described construction define the triangle $AC_1 D_1$, whereby we determine the blade angle α' , equal for all flow surfaces.

Now we proceed along the outlet edge of the guide blade to the further individual meridional stream lines. At the intersections of each stream line with the outlet edge, a', c', d', e' , we know: the angle of inclination φ , the meridional velocity c'_m , and the blade angle α' , which is the same at all points of the outlet edge. Hence, we have for each point the triangle $AC_1 D_1$ and can determine the peripheral component c'_u (eventually we can also determine the triangle $AC^x D^x$ and from this the angle α'^x , however, it will suffice to determine the component c'_u). We now proceed along the stream line to the inlet edge of the runner blade. Here there is no need to recalculate the meridional velocity as we already know it from the flow field; the

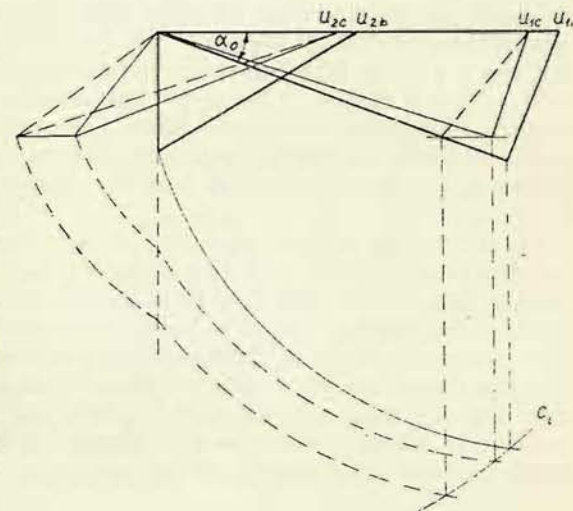


Fig. 98

peripheral component we recalculate again according to (68), $r'c_u' = r_1 c_{u1}$. Thus we know both components at the inlet edge, and since we also know the peripheral velocity, the inlet triangle is defined. Then we determine the corresponding outlet triangle, e. g. by means of the Braun construction.

We now see that, when starting from the main stream line and selecting on it a suitable outlet triangle, we do not obtain equally suitable outlet triangles on the other stream lines. Hence conditions for entry into the draft tube will not be equally advantageous on all stream lines. This procedure is nevertheless indispensable for obtaining on all stream lines simultaneously a shockless entry into the runner, which is a necessary condition for attaining good efficiency with regard to the comparatively narrow bladeless space between the guide wheel and the runner.

An oblique discharge from the guide wheel reduces this disadvantage. This is evident from the velocity diagram in Fig. 98. The diagram for the initial stream line, as e. g. b in Fig. 97, is here drawn in full lines. On the stream line c the meridional velocity is smaller. If the outlet angle from the guide wheel, and hence also the angle of approach to the runner blade α_0 , were the same as on the stream line b , we should obtain the diagram as indicated by the dashed lines, with a discharge velocity c_2 considerably diverted from the same velocity on the initial stream line b .

The fact that the angle of approach decreases (because on the stream line c the discharge is less oblique) leads to a favourable result, i. e. the vertex of the inlet triangle (drawn in thin, full lines) shifts in such a direction as to diminish the deviation of the discharge velocity c_2 , as can be seen in the diagram.

An oblique discharge is, therefore, amply utilized in high-speed turbines by arranging the outlet edges of the guide blades at the least possible diameter. At the same time, it is cheaper as the guide apparatus and also the spiral is of smaller diameter. In this respect we have even constructed the guide wheel with approximately the same outlet diameter as the outside inlet diameter D_{1e} of the runner.

8. Measurable Widths at the Outlet Edge

The through-flow of the turbine and the flow-rate are given by the relative discharge velocity W_2 and the discharge area of the duct, perpendicular to this velocity. The through-flow and the flow-rate for any elementary turbine are hence given by the width of the blade duct at the outlet. It is therefore necessary to control these internal diameters during manufacture. If the internal diameters as well as the spacing of the blades are observed, the outlet angle β_2 , important for satisfying the energy equation, is maintained.

The width of the duct, which appears in the developed conical sections, is identical with the so-called measurable width, i. e. with the least distance between the outlet of one blade and the following blade (which we can measure by means of calipers), when the flow surfaces are perpendicular to the outlet edge.

In cases where the outlet does not enclose a right angle with the flow surfaces, the net width a_2 appears as identical with the width on the cone surface in the

tangential plane to the substitutive cone. In fig. 99, the line $B - B$ represents the part of the outlet edge which is not perpendicular to the trace of the flow surface $b - b$, replaced by the cone $k - k$. The net width appears here in the plane defined by the generatrix of the cone $K - K$ and perpendicular to the picture plane.

By rotating this plane into the picture plane, which is represented by the rotated picture of the tangent to the cone in point II , drawn by the straight line $n - n$, and by marking off the spacing t_2 and the angle β_2 , we obtain the triangle $IIxy$, whose hypotenuse is the rotated section of the blade end.

In it the width a_2^x appears. The measurable width a_2^x we obtain by projecting the triangle $IIxy$ from the plane $K - K$ into the plane $N - N$ perpendicular to the outlet edge. This is done by projecting the length IIy into IIy' , whereby we obtain the triangle $IIxy'$. This picture also presents the actual blade thickness s_2 , whilst s_2^x is the distorted thickness. For this reason we better determine the correct coefficient of restriction φ_2 in our final control from the relation

$$\varphi_2 = \frac{a_2^x}{a_2^x + s_2}.$$

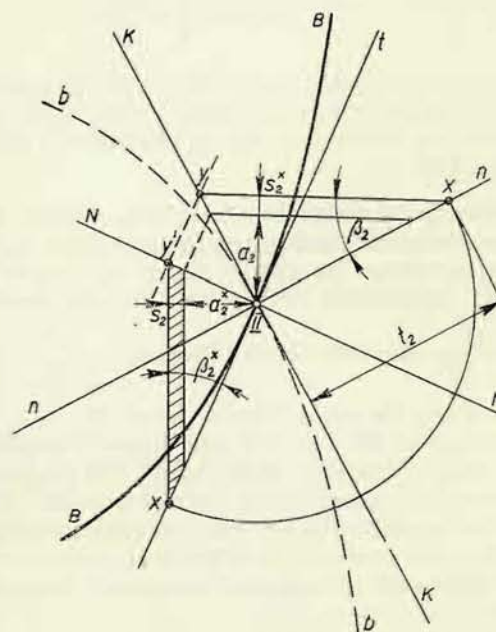


Fig. 99

The measurable widths are marked off on the drawing of the runner above the rectified length of the outlet edge for the purpose of checking in the workshop.

9. General Hydraulic Design of the Runner of the Francis Turbine

Now, that we understand the individual partial problems arising in the hydraulic design of the runner, we can collate them into a general procedure in order to reach the desired result – the blade lay out. This procedure will be explained for low-speed turbines, where the establishment of the flow fields is effected by the one-dimensional method, for normal turbines, where it is possible to adjust the flow field by mere intuition, and for high-speed turbines, where a two-dimensional approach is necessary. Each procedure will be illustrated by examples.

α. Low-Speed Turbines

Following to the considerations dealt with in Part I, Chapter XIII, let us start investigating the runner of a low-speed Francis turbine with a certain required specific speed n_s (at its maximum flow-rate).

For the specific speed we employ the relation

$$n_s = n'_1 \sqrt[3]{\frac{1000 \eta}{75} Q'_1}.$$

We estimate the efficiency and select n'_1 and Q'_1 so as to obtain with these values the required specific speed. As a guide for the selection of the unit speed and the unit flow-rate we can use Fig. 54b; as efficiency for the maximum flow-rate let us select about 0.85.

Note: If we had to design the runner for a certain turbine on order, the following values would be given: the flow-rate Q_{\max} , the head H , and the speed n . From these values we determine the specific speed n_s ; further we select e. g. the unit flow-rate Q'_1 , from which we determine the inlet diameter of the runner

$$D = \sqrt{\frac{Q}{Q'_1 \sqrt{H}}} \text{ and then the unit speed } n'_1 = \frac{n D}{\sqrt{H}}.$$

Now we select the head; either we select $H = 1$ m or the maximum head for which a runner of this type will still be used (directions are given in Fig. 43); thus we obtain a group of values which will be applicable in the subsequent strength test of the runner blades. Further we select a suitable diameter (inlet diameter) of the runner; we do not select this diameter according to the model runner as it would be too small for the accuracy requirements of the design, but we take such a diameter as to accommodate the complete construction.

Now we proceed as follows:

1. We design the shape of the turbine space.
2. We establish the meridional flow field. We employ the one-dimensional method, here it will suffice to select two elementary flows. Hence we obtain three flow surfaces, two of which will be border surfaces of the turbine space.
3. We design the meridional shape of the inlet and outlet edges. The inlet is in the circular projection parallel to the axis of the runner.
4. We draw the velocity diagrams. As the scale for specific velocities we usually select $1 = 1$ dm.
5. We trace the substitutive conical surfaces, develop them and design on them the blade sections.
6. We select the pencil of meridional planes and draw the corresponding meridional sections in circular projection.

7. In the circular projection we select a system of planes perpendicular to the axis of the runner and draw the layout plan of the blade.

8. We mark off the widths of the ducts at the outlet above the rectified outlet edge.

Example: We have to design a runner with a specific speed of about $n_s = 80$ r. p. m. We select the values (see Fig. 54): $n'_1 = 62$; $Q'_{1\eta} = 0.125 \text{ m}^3/\text{sec.} = \frac{3}{4} \cdot Q'_{1\max}$; so that $Q'_1 = 0.167 \text{ m}^3/\text{sec.} \doteq 0.160 \text{ m}^3/\text{sec.}$ With these values we check the specific speed

$$n_s = n'_1 \sqrt[3]{\frac{1000 \cdot \eta}{75} Q'_1} = 62 \sqrt[3]{\frac{1000 \cdot 0.85}{75} \cdot 0.160} = 62 \cdot 1.34 = 83 \text{ r. p. m.}$$

and find it satisfactory.

For construction we take into account a head $H = 300$ m and an inlet diameter of the runner $D_1 = 600$ mm. The face of the runner at the inlet let us select with $B_1 = 45$ mm, hence a ratio $\frac{B_1}{D_1} = 0.075$, which roughly agrees with Fig. 54a.

For this diameter and head we determine the actual speed, the angular velocity and the flow-rate at optimum efficiency

$$n = \frac{n'_1 \sqrt{H}}{D_1} = 62 \frac{\sqrt{300}}{0.6} = 1790 \text{ r. p. m.}, \quad \omega = \frac{n}{9.55} = 187 \text{ 1/sec.}$$

$$Q_\eta = Q'_{1,\eta} D_1^2 \sqrt{H} = 0.125 \cdot 0.36 \cdot 17.3 = 0.779 \text{ m}^3/\text{sec} \doteq 780 \text{ litres/sec.}$$

The layout of the contour of the turbine space further requires that the inlet diameter of the draft tube, D_s is determined. For this reason let us determine the meridional velocity at the inlet into the runner

$$C_{m,\eta} = \frac{Q_\eta}{\pi D_1 B} = \frac{0.78}{\pi \cdot 0.6 \cdot 0.045} = 9.2 \text{ m/sec.}$$

If we want to obtain the same meridional velocity in the inlet cross section of the draft tube, we must determine the diameter of this cross section from the equation

$$\frac{\pi D_s^2}{4} C_{m,s,\eta} = Q_\eta \quad C_{m,s,\eta} \doteq C_{m,1,\eta},$$

so that

$$D_s = 2 \sqrt{\frac{Q_\eta}{\pi C_{m,s,\eta}}}.$$

In our case we obtain

$$(C_{m,s,\eta} = C_{m1\eta} = 9 \text{ m/sec.}).$$

$$D_s = 2 \sqrt{\frac{0.78}{\pi \cdot 9}} = 0.33 \text{ m.}$$

With these dimensions (D_1, B_1, D_s) we start to design the contour of the runner space. Here it appears that the end of the runner hub protrudes into the inlet cross section of the draft tube (see Appendix II), and consequently we must increase the diameter D_s . In the final arrangement the contour of the rim is formed by a part of one circle and the contour of the hub as well as by a part of one circle to which the top of the hub is connected in the direction of the tangent.

On checking the velocity of the entry into the draft tube we find that

$$C_{m,s,\eta} = \frac{Q_\eta}{2\pi \varrho_s \Delta_s} = \frac{0.78}{2\pi \cdot 0.127 \cdot 0.115} = 8.5 \text{ m/sec.}$$

The meridional component of the inlet velocity into the draft tube is, therefore, only slightly smaller than the meridional velocity at the inlet into the runner, which is satisfactory.

Now we divide the runner space into two flows, which is quite sufficient for the design of such a narrow wheel. We lay the dividing flow surface at the inlet through the centre of the height of the runner duct, and within the duct we determine its progress on the orthogonal trajectory by means of circles inscribed between the trace of the dividing surface and the contour, as indicated in the figure by dot and dash lines. The product of the diameter of these circles and the distance of their centres from the turbine axis must be approximately the same in all cases. In our case this amounts to $14.1 \cdot 5.1 = 71.8 \text{ cm}^2$ for the circle at the hub and to $17.9 \cdot 3.95 = 70.8 \text{ cm}^2$ for the circle at the rim, which is satisfactory.

We design the inlet and outlet edges of the blade in circular projection. The projection of the inlet edge for low-speed turbines is always parallel with the axis of the runner, whereby the inlet is defined, because we have previously selected the inlet diameter D_1 . For the outlet edge we use as a rough guide the specific peripheral velocities at the hub, $u_{2,i}$, and at the rim, $u_{2,e}$, according to Fig. 75 or 76.

For the shape designed we obtain

$$u_{2,i} = R_{2,i} \frac{\omega}{\sqrt{2gH}} = 0.1196 \frac{187}{76.6} = 0.292$$

$$u_{2,e} = R_{2,e} \frac{\omega}{\sqrt{2gH}} = 0.191 \frac{187}{76.6} = 0.466$$

which roughly agrees with the values given in Figs. 75 or 76.

Now we draw the velocity diagram. For this purpose we determine the following specific velocities: the peripheral velocities at the inlet and at the outlet edge on all

three flow surfaces, and for the same points also the meridional velocities. We then obtain

$$u_1 = \frac{R_1 \omega}{\sqrt{2gH}} = \frac{0.3 \cdot 187}{76.6} = 0.732$$

$$u_2^C = u_{2,i} = 0.292$$

$$u_2^B = \frac{0.154 \cdot 187}{76.6} = 0.376$$

$$u_2^A = u_{2,e} = 0.466$$

$$c_{m,1,\eta} = \frac{C_{m,1,\eta}}{\sqrt{2gH}} = \frac{9.2}{76.6} = 0.12.$$

As far as the meridional velocities at the outlet edge are concerned, we have to take into account the restriction of the through-flow areas by the outlet end of the blades, which we will estimate by giving the coefficient φ_2 the value 0.8, with a reservation of subsequent verification. Thus we obtain by means of the circles inscribed between the flow surfaces, with their centres on the outlet edge (drawn in full lines):

For the flow between $A_1 - A_2$ and $B_1 - B_2$

$$c_{m,2,\eta}^{A,B} = \frac{Q/2}{2\pi \varrho \Delta \varphi \sqrt{2gH}} = \frac{0.39}{2\pi \cdot 0.171 \cdot 0.0407 \cdot 0.8 \cdot 76.6} = 0.146$$

and for the flow between $B_1 - B_2$ and $C_1 - C_2$

$$c_{m,2,\eta}^{B,C} = \frac{0.39}{2\pi \cdot 0.135 \cdot 0.052 \cdot 0.8 \cdot 76.6} = 0.144.$$

Along the entire outlet edge we shall use the same specific meridional velocity $c_{m,2,\eta} = 0.145$.

With these values we now draw the velocity diagram (Appendix II). We start with the outlet triangles, for which we know the peripheral velocities and the meridional velocity. If we decide e. g. on isosceles triangles and draw the outlet triangle for the central flow surface with the values $u_2^B = 0.376$, $c_{m,2} = 0.145$, $w_2^B = u_2^B$. We draw on the scale $1 = 1 \text{ dm}$. In the triangles on the two remaining flow surfaces (the border surfaces) the peripheral velocities are again defined, and for the direction of the relative velocities let us select the end point of the velocity w_2^B . The triangles will again be isosceles. The meridional velocities will here, it is true, differ from the values previously determined, however, as can be seen, the difference is only slight; we have satisfied the condition of mutual relations between the triangles on different flow surfaces.

By means of the Braun construction we draw the inlet triangle, which will be common to all three flow surfaces. In it we know the peripheral velocity $u_1 = 0.732$,

and the magnitude of the meridional velocity $c_{m,1} = 0.12$. For determining the inlet vertical, on which the vertex will be located, we must still find the magnitude of the indicated velocity. For this purpose we can employ e. g. Equation (58): $\eta_h = c_i^2 - c_2^2 - w_2^2$, so that we can write $c_i^2 = \eta_{h,\eta} + c_2^2$, as for the optimum hydraulic efficiency $\eta_{h,\eta}$ we have the shock component $w_2 = 0$.

If we select for the optimum hydraulic efficiency the rather high value 0.96, assuming perfect manufacture (shaped blades, ground and polished), and if we substitute for $c_2 = 0.15$, as we read in the diagram, $c_i^2 = 0.96 + 0.02 = 0.98$, and hence $c_i = 0.99$.

With this value as radius we draw a circle with the centre in the origin of the diagram and intersect it with another circle of the radius equalling the value of the velocity u_1 and its centre in the end point of this velocity u_1 . In this way we obtain the position of the inlet vertical, and the inlet triangle is defined. The diagram defines the blade angles on the three selected flow surfaces: the inlet angle β_1 (which is the same for all surfaces) and the outlet angles β_2^A, β_2^B and β_2^C .

Whether the inlet angle meets the requirement of the suitable shape will only be shown by the construction of the blade sections on the flow surfaces. In the case of an unsuitable curvature of the blade we should have to alter the inlet diameter of the runner, D_1 , and also the peripheral velocity u_1 , in order to obtain another, more suitable inlet angle β_1 . In the velocity diagram in Appendix II conditions are also indicated for the flow-rate $Q_{\max} = \frac{4}{3} Q_\eta$.

Now we can begin to draw the blade sections on the developed substitutive flow surfaces. The flow surface $C_1 - C_2$ we replace by a cone which contacts it in the peripheral circle passing through the outlet edge and which is co-axial with the runner, and by a plane normal to the runner axis and contacting the flow surface in the peripheral circle passing through the inlet edge, with its centre O'_1 in the axis of the runner. On the appropriate generatrices in the circular projection we rectify the contour of the flow surface so as to obtain approximately one half of it on the cone with its centre in O_1 and the other half on the trace of the plane passing through point O'_1 , as indicated by arrows in Appendix II. The truncated cone, delimited in this way, we develop (the vertex of the developed conical surface in Appendix II is identical with the original vertex of the cone O_1) and add to it the annulus of the plane (the transferred vertex of the peripheral circles of O'_1). Into the developed surface, created in this way, we now design the shape of the blade sections so that it passes through the place of contact of both developed substitutive surfaces, and that the extension of the pressure side of the blade encloses with the tangent to the peripheral circle at the inlet the angle β_1 , and that the extension of the pressure side at the outlet encloses with the tangent to the circle of the developed cone the angle β_2 , as is to be seen in Appendix II. Here we emphasize once again that if the resulting blade was unsuitably curved, we should have to alter the inlet diameter of the runner.

Since the runner has to be employed for large heads, the blades will have to be cast with hub and rims as one unit. For this reason we design a cross section in the

form of a body of small hydraulic resistance, similar to the cross section of an airfoil. We select a sufficient thickness of the cross section, not only with regard to strength considerations (strength control see later), but also to foundry requirements. The fact that we relate the angles β_1 and β_2 to the pressure side of the blade and not to the centre line results in a suitable exaggeration of the outlet angle.

For a better judging of the shape of the duct we add to our drawing the cross section of the adjacent blade. The number of blades according to Formula (76) is approximately

$$z_2 = \frac{10 \text{ to } 12}{u_1} = \frac{10 \text{ to } 12}{0.732} \doteq 13-17.$$

In the case in point 15, blades were selected. By dividing the periphery of the contact circles of the flow surface by the number of blades we obtain the spacing on the outlet and on the inlet circles, which appears in the plan in the true dimension. Therefore, we mark it off and, maintaining the inlet and the outlet angle, we draw the parts of the cross section, shifted by the spacing, on the first and on the second substitutive surface. Here we see that the parts of the cross section pass no more from one into the other, nevertheless, we can still form a sufficiently distinct picture of the shape of the runner duct.

The central angle of the cross section we divide by a pencil of rays drawn from the centres O_1 and O'_1 into a convenient number of parts. These rays represent the sections of a pencil of meridional planes with the substitutive flow surfaces. The pencil of meridional planes is thus already defined and must also be transferred into the pictures of the cross sections on the other flow surfaces. For this reason, we first determine the traces of these planes in the plan of the runner. We take into account that the circles of contact of the substitutive surfaces and the actual flow surface (circles passing through the outlet edge) are common to the substitutive and the actual surface, and that consequently the parts cut out on them by the meridional planes are in the development as well as in the plan of the same magnitude. We, therefore, draw into the plan the circles appertaining to the intersections of the inlet and outlet edges with the flow surface $C_1 - C_2$ and transfer to them the division from the developed cone, e. g. $0-1-2 \dots$ on the circle belonging to the outlet edge of the blade. In this way we obtain in the plan a pencil of the traces of these meridional surfaces.

Now we shall design the shape of the blade on the other border surface $A_1 - A_2$. The layout is represented conformally, with regard to the considerable curvature of this surface. For this purpose we rectify the meridional length of the blade, in order to obtain the height of the band into which we must draw the cross section. First we estimate the peripheral length as equalling the arc enclosed in the plan between the meridional planes 0 to 6 at the mean diameter. Observing the already known directions we design the cross section and transfer it into the circular projection and into the plan. Therefore, we transfer the part between the rays 0 and 1 on the plan of the circle of the outlet edge into the conformal picture (see the indication in the Appendix), and the distance of the cross section, measured on the

perpendicular drawn through this point, we transfer into the circular projection (see the notation $0 - 1$). The radius of point 1 thus obtained we transfer into the plan of ray 1, whereby we obtain the plan of this point; and at the same time we transfer the part created on the circle in the plan between the rays 1 and 2 into the conformal picture, and in this way proceed further until the complete cross section is represented. We may find that the selected peripheral length of the cross

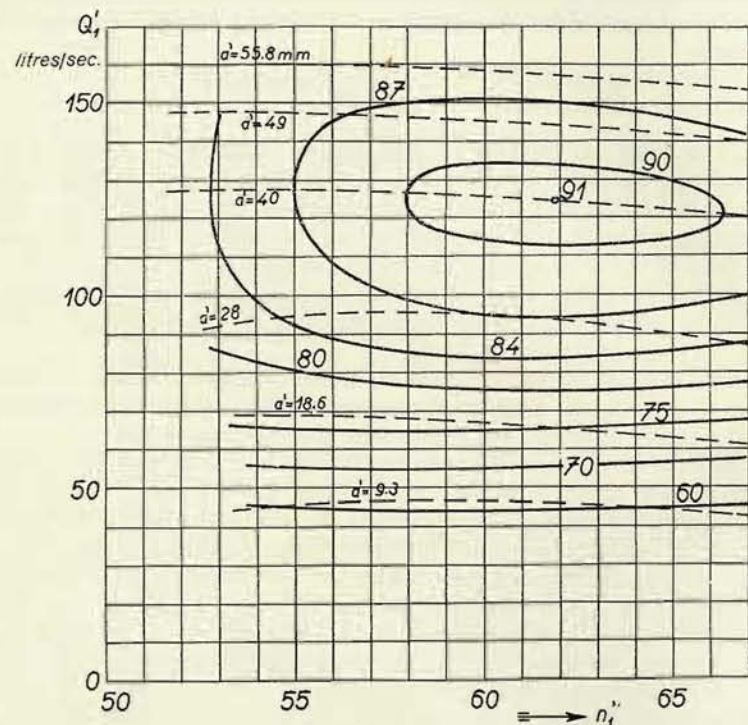


Fig. 100

section is not satisfactory and we shall have to correct it. In our case, the cross section is selected peripherally somewhat shorter than the cross section on the surface $C_1 - C_2$ in order to avoid a too intense curvature at the inlet. The inlet edge will therefore be peripherally inclined by the distance which appears in the conformal representation between the inlet end of the cross section and the meridional plane 6.

According to this procedure we design the progress of the inclination of the inlet edge (in Appendix II the progress of the inlet edge is indicated by the dash and dot line on the left side of the inlet of the circular projection), whereby we already determine the shift of the inlet end of the cross section on the flow surface $B_1 - B_2$,

which we develop in the same way as the flow surface $A_1 - A_2$, and on which we design in the same way the cross section of the blade.

Then we draw the meridional sections by the planes $0 - 6$ in the circular projection by winding up the meridional distances of the points of the cross section from the outlet circle onto the flow surfaces, and by connecting the corresponding points. The section of the pressure side of the blade are drawn in full, the sections of the suction side by dash lines. The machining allowance, too, - indicated in the developed section of the cone O_1 by the cross-hatched area - we transfer into the circular projection.

Now we verify the value of the coefficient of restriction φ_2 and find that it varies in the range from 0.8 to 0.83, so that the original estimate is satisfactory. If a greater disagreement would become manifest, we must correct the meridional velocity and the velocity diagram, whereby we obtain the corrected angles β_2 and β_1 , and according to them we also correct the shapes of the individual sections.

We select a convenient number of planes normal to the runner axis, $0 - 6$, and draw in the plan the contour lines (for greater clarity only the contour lines 1, 3, 5 are indicated) and the penetration of the blades with the hub and the rim.

The widths of the ducts, which here are identical with the measurable widths (as the circular projection of the outlet proceeds approximately perpendicularly to the meridional stream lines), we mark off above the rectified length of the outlet edge in order to make sure that there is not too great a difference, and to obtain at the same time reference data for the control of the manufactured runner.

Thus the blade layout is finished.

Fig. 100 shows (in a somewhat simplified form) the characteristic of this runner, recalculated for the diameter $D = 1$ m (the drawing of the runner has been taken from the archives of the engineering works ČKD-Blansko). As we see, the values n'_1 and Q'_1 for the optimum efficiency agree very well with the values employed in the calculation.

β. Normal Turbines

1. The procedure is exactly the same until including the design of the turbine space. Then follows:

2. Establishment of the meridional flow field. We must select more flows; we determine the progress of the meridional stream lines either by the one-dimensional method, but in the bend of the flow we contract the stream lines, according to what we assume, more towards the outer rim, or we employ the two-dimensional method.

3. We design the shape of the inlet and outlet edges in circular projection. Only in units of lower specific speed will the inlet edge be in circular projection parallel with the runner axis. The outlet edge will no longer be perpendicular to the meridional stream lines.

4. We draw the velocity diagrams; at higher speeds we must here pay attention to an oblique discharge from the guide blades.

5. We lay the substitutive surfaces, on whose development we design the sections of the blade.

6. We select the pencil of meridional planes, and in the circular projection we draw the appropriate meridional sections.

7. We select a system of planes normal to the axis and draw the plan of the blade layout.

8. We determine the measurable widths and mark them off on the drawing of the blade.

Example: We have to design a runner with a specific speed of about 180 r. p. m. The procedure of the design is illustrated in Appendices III, IV and V. (The drawing of the runner is from the archives of the engineering works ČKD-Blansko. The author of the original design is Ing. J. Karásek, but the author of this book has altered the method of calculation and of constructing the velocity diagrams. The Appendices also contain the constructions necessary for the subsequent strength calculation.)

We select the values $n'_1 = 65.5$ r. p. m.; $Q'_{1,\eta} = 0.6$ m³/sec. $Q'_{1\max} \doteq 0.7$ m³/sec. (see Fig. 54b).

With these values we obtain

$$n_s = n'_1 \sqrt{\frac{1000 \eta}{75} Q'_1} = 65.5 \sqrt{\frac{1000 \cdot 0.85}{75} 0.7} = 184 \text{ r. p. m.}$$

A runner with this specific speed is, according to Fig. 43, suited for a maximum head $H = 100$ m. With regard to the subsequent calculation we select this head for the design of the runner. As diameter of the runner let us select $D_1 = 1250$ mm. Under these conditions the speed is

$$n = \frac{n'_1 \sqrt{H}}{D_1} = \frac{65.5 \cdot 10}{1.25} = 524 \text{ r. p. m.},$$

whence follows the angular velocity

$$\omega = \frac{524}{9.55} = 54.8 \text{ 1/sec.};$$

and further, the flow-rate at optimum efficiency will be

$$Q_\eta = Q'_{1,\eta} \sqrt{H} D^2 = 0.6 \cdot 10 \cdot 1.56 = 9.4 \text{ m}^3/\text{sec.}$$

From this flow-rate we determine the diameter at the entrance into the draft tube according to

$$\frac{\pi D_s^2}{4} C_{s,\eta} = Q_\eta.$$

From this relation it follows

$$D_s^2 = \frac{4}{\pi} \frac{Q_\eta}{c_{s,\eta} \sqrt{2gH}}.$$

If we roughly select, according to Fig. 75a, $c_{s,\eta} = 0.15$, there will be $D_s = 1300$ mm.

We divide the turbine space into four elementary flows, each with an elementary flow-rate of $Q/4 = 2.35$ m³/sec. (In comparison with the one-dimensional approach, the meridional stream lines have been contracted in the bend closer to the outer contour, but by far not so much as it would be the case in a two-dimensional approach).

For the layout of the inlet and outlet edges in circular projection (compare the values marked* in the following table with Figs. 75 and 76) we can determine the peripheral velocities on the individual flow surfaces, which we arrange with regard to the greater number of elementary flows in the following table:

Stream line	R_1 mm	R_2 mm	U_1 m/s	U_2 m/s	u_1	u_2
A	625	645	34.2	35.3	0.772*	0.797*
B	588	564	32.2	30.9	0.726	0.697
C	576	465	31.6	25.5	0.713	0.575
D	564	385	30.9	21.1	0.697	0.477
E	551	366	30.2	20.05	0.682*	0.454*

In a similar way, we also determine the meridional velocities; here we estimate the coefficient of restriction of the through-flow cross section at about $\varphi_2 = 0.80$ —0.85 for the runner blades, and $\varphi' = 0.85$ —0.9 for the guide blades, again with a reservation of subsequent verification. The following table contains these coefficients together with other necessary values, already corrected, as determined from the individual sections

Flow	Inlet into the runner					Outlet from the runner					Outlet from the guide wheel				
	Δ mm	R mm	F m ²	$C_{m,1}$ m/s		Δ mm	R mm	F m ²	φ_2	$C_{m,2}$ m/s	Δ mm	R mm	F m ²	φ'	C'_m m/s
I	64.5	601	0.243	9.67		81	604	0.307	0.865	8.85	64	650	0.26	0.915	9.84
II	70.8	582	0.258	9.1		98.5	514	0.317	0.84	8.83	69.5	650	0.28	0.915	9.05
III	77.8	570	0.279	8.44		126	410	0.324	0.8	9.06	70.6	650	0.29	0.915	8.9
IV	81.6	557	0.286	8.32		133	365	0.304	0.85	9.1	73	650	0.298	0.915	8.61

The meridional velocities determined in this way hold good for the central part of each elementary flow, however, we must also know them on the flow surfaces. We determine them by graphical interpolation. For this purpose we rectify the

inlet and outlet edges of the runner, and perpendicular to them, as well as to the outlet edge of the guide blade, we mark off the found velocities in the appropriate places. We connect the points obtained by continuous lines and on them, in the places appertaining to the intersections of the flow surfaces with the inlet and with the outlet edges, we determine the meridional velocities on the flow surfaces.

The meridional velocities on the flow surfaces we further convert into specific values and arrange them together with the previously determined peripheral velocities into a table, the last two columns of which (c_u^x , $c_{u,1}$) we supplement subsequently from the velocity diagrams.

Stream line	u_1	u_2	c_m	$c_{m,1}$	$c_{m,2}$	c_t	c_u^x	$c_{u,1}$
A	0.772	0.797	0.234	0.221	0.199	0.98	0.632	0.657
B	0.726	0.697	0.212	0.212	0.199	0.98	0.557	0.615
C	0.713	0.575	0.202	0.196	0.201	0.98	0.54	0.609
D	0.697	0.477	0.198	0.1875	0.205	0.98	0.54	0.622
E	0.682	0.454	0.192	0.1855	0.2055	0.98	0.525	0.619

The indicated velocity we have determined after assessing the hydraulic efficiency at the value of 0.93 from the relation $c_t^2 = \eta_{h,\eta} c_2^2 + c_2^2$ for the flow surface $B_1 - B_2$, where we select $c_2 = 0.2$, $c_t^2 = 0.93 + 0.04 = 0.97$, whence $c_t = 0.98$; with this value we shall calculate on all flow surfaces.

Note: For the border surfaces often a somewhat lower value of the indicated velocity is taken; this is done with regard to the losses due to friction on the wall of the turbine space in these extreme elementary flows.¹⁾

First we establish the velocity diagram (see Appendix V) on the flow surface $B_1 - B_2$, which is of major importance; we select a perpendicular discharge, and to the outlet triangle we determine the inlet triangle. In it we read $c_{u,1} = 0.615$, which is the component of the velocity at the inlet into the runner; we recalculate this value according to the law of constant circulation, $Rc_u = \text{const.}$, for the outlet edge of the guide blade. We obtain

$$c_u^x = \frac{R_1}{R'} c_{u,1} = \frac{588}{650} 0.615 = 0.557$$

(we enter both values into the table).

By means of the previously described construction we determine the blade angle $\alpha' = 19^\circ$ for an oblique discharge under the angle φ . With this angle $\alpha' = 19^\circ$ we then calculate in all further diagrams, and we proceed inversely; to the blade angle we determine the component c_u^x , recalculate it for the inlet into the runner,

¹⁾ E. g., Ténor A.: Turbines hydrauliques et régulateurs de vitesse, Part III, Paris, Eyrolles, 1935.

and, knowing u_1 as well as $c_{m,1}$, we draw the inlet triangle, and only to this, do we establish the outlet triangle. The construction is evident from the enclosure.

Further procedure is the same as in the foregoing example and will therefore not be repeated. Appendix IV shows only the reproductions of two developed sections, i. e. the section on the border surface $E_1 - E_2$, which has been designed on the developed substitutive cone, and the section on the flow surface $A_1 - A_2$, on the substitutive cylindrical surface, which passes through point A_2 . No correction of the inlet angle has been performed as the difference in the radii of the inlet edge on the original surface and on the substitutive surface is small. In contradistinction to the first example, the outlet end of the blade is here designed as ineffective.

Appendix III further contains the meridional sections and the layout of the blade in the plan.

The only thing which still remains to be done, is to determine the measurable widths and mark them off above the rectified outlet edge for control of the manufactured runner.

Figure 101 presents a reproduction of the simplified characteristic of this runner obtained by measurements on the model runner.

It is evident that although speeds n'_1 at optimum efficiency agree rather well, the flow-rate at optimum efficiency is greater. Hence the specific speed of the runner will actually be higher, about $n_s = 200$.

Note. The author had the opportunity to design a runner with the specific speed $n_s = 300$ r. p. m. for the following values at optimum efficiency: $n'_1 = 71.7$, $Q'_{1,\eta} = 1.05$ m³/sec.; the meridional field was established two-dimensionally. Further procedure while solving this problem was the same as just described. Measurements resulted in the following values at optimum efficiency: $n'_1 = 76-79$, $Q'_{1,\eta} = 1-1.025$, $\eta_\eta = 88.5\%$ (at the diameter of 1 m); the agreement in general is satisfactory.

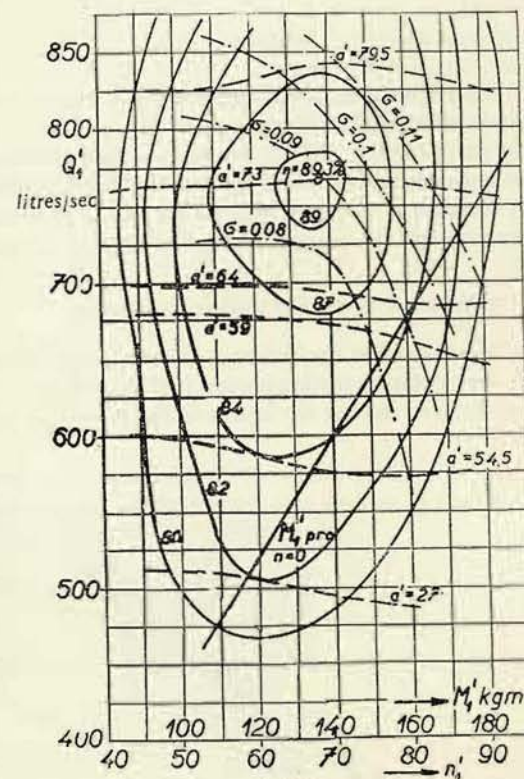


Fig. 101

γ. High-Speed Turbines

For these turbines it is always recommendable to establish the flow field two-dimensionally. Further procedure is the same as for a normal turbine. The wheel described in the foregoing note belongs to this group.

δ. Express Turbines

These fast Francis turbines have a considerable bladeless space between the guide wheel and the runner. For this reason it is more advantageous when linking the velocity triangles on the various flow surfaces to employ the rule, which will be explained and proved later, in the part dealing with Kaplan turbines – the rule of constant circulation in the back of the runner. Apart from this, the solution of the problem is the same as for the turbines already mentioned.

10. Control of the Cavitation Coefficient

The cavitation coefficient is determined by measurements on the model turbine in the cavitation testing station (see Section B, of this part). The designer wants to ensure even during the layout of the runner, i. e., prior to the manufacture of the

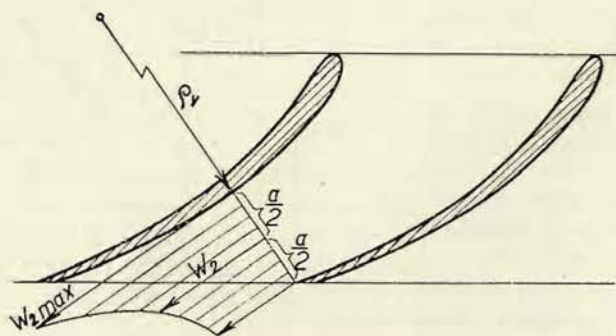


Fig. 102

model turbine, whether the runner will have approximately the required cavitation properties. This relates mainly to high-speed and normal runners, where for the sake of a higher specific speed we select a smaller number of short blades. For this type of runner we have at our disposal a convenient, simple and sufficiently exact method of predetermining the cavitation coefficient¹⁾, which we are now going to explain.

¹⁾ Dahl: Die Strömungs- und Druckverhältnisse in schnelllaufenden Wasserturbinen, Wasserkraft u. Wasserwirtschaft 1940, p. 1.

As already pointed out, the greatest danger of cavitation arises in the flow surfaces near the rim, where the highest peripheral velocities are encountered, and consequently also the highest relative velocities of the water flow along the blade. We restrict, therefore, our control to these sections, in which the water flows approximately axially (see e. g. Appendix III).

Such a developed section is shown in Fig. 102. If we assume a flow between two cylindrical surfaces very close to each other, we may after developing the cylindrical section consider the flow to be plane; the water streams through a curved duct, and to this flow we can apply the law of constant circulation. The velocity on the central stream line of the duct in its outlet cross section is W_2 , which also appears in the velocity diagram. The maximum velocity $W_{2,max}$ will be on the suction side of the blade, which is curved at the radius ρ_v , and between these velocities the following relation will hold good:

$$W_{2,max} \rho_v = W_2 \left(\rho_v + \frac{a}{2} \right), \quad (110)$$

Further the Bernoulli equation will apply

$$\frac{W_{2,max}^2}{2g} + \frac{p_{min}}{\gamma} = \frac{W_2^2}{2g} + \frac{p_{mean}}{\gamma},$$

whence we can determine the pressure reduction Δp on the suction side of the blade as compared with the mean pressure p_{mean} in the outlet cross section of the blade, i. e. the so-called maximum driving underpressure of the blade.

$$\Delta h' = \frac{\Delta p}{\gamma} = \frac{p_{mean} - p_{min}}{\gamma} = \frac{W_{2,max}^2 - W_2^2}{2g}.$$

Substituting the appropriate value for $W_{2,max}$ - from Equation (110), we further obtain

$$\frac{\Delta p}{\gamma} = \frac{W_2^2}{2g} \left[\left(\frac{\rho_v + \frac{a}{2}}{\rho_v} \right)^2 - 1 \right] \quad (111)$$

and if we consider half the width of the duct $\frac{a}{2}$ to be small in relation to the radius of the curvature of the suction side of the blade, ρ_v , and, therefore, neglect the square of $\frac{a}{2}$, we obtain

$$\frac{\Delta p}{\gamma} = \frac{W_2^2}{2g} \frac{a}{\rho_v}. \quad (112)$$

Since in the cylindrical section we can readily determine the width of the outlet cross section of the duct and also the radius of curvature ρ_v of the suction side of

the blade, we can, according to Equation (112), establish by which value the lowest pressure on the blade is lower than the mean pressure at the beginning of the draft tube. This is exactly the value $\Delta h'$ in Equation (27a) in Chapter V/2 of Part I. It is consequently the permissible suction head

$$H_s = H_B - H_t - \eta_s \frac{C_2^2 - C_4^2}{2g} - \frac{W_2^2}{2g} \frac{a}{\varrho_v},$$

and the cavitation coefficient is

$$\sigma = \frac{H_B - H_t - H_s}{H} = \eta_s (c_2^2 - c_4^2) + w_2^2 \frac{a}{\varrho_v}.$$

We are now interested in the highest value of the cavitation coefficient, i. e. as encountered at the maximum flow-rate. We must then calculate with the velocities c_2 , c_4 and w_2 , which correspond to this maximum flow-rate.

Example: We have to determine the cavitation coefficient for the runner of normal speed which was designed in the last example. We solve the problem on the developed section $A_1 - A_2$, on which the highest velocities are encountered as well as an approximate axial discharge.

In this section we measure the width of the duct at the outlet, $a = 55$ mm, and the radius of curvature of the suction side of the blade in the same place, $\varrho_v = 1000$ mm. For the conditions of optimum efficiency $c_2 = 0.22$, $w_2 = 0.74$, and if we select the velocity at the end of the draft tube, $C_4 = 1.5$ m/sec., its specific value will be $c_4 = \frac{1.5}{44.3} = 0.034$, and if we further assess the efficiency of the draft tube at the value $\eta_s = 0.88$, we find:

$$\sigma = 0.88 (0.0485 - 0.0009) + 0.55 \frac{55}{1000} = 0.072.$$

For the maximum flow-rate $Q'_{1,\max} = 0.7$ m³/sec. we may assume the velocities to be approximately higher in the ratio $\frac{0.7}{0.6} = 1.17$, and their squares higher in the ratio $1.17^2 = 1.36$. Thus we obtain

$$c_2^2 = 1.36 \cdot 0.0485 = 0.066, \quad c_4^2 = 1.36 \cdot 0.0009 = 0.0012.$$

$$w_2^2 = 1.36 \cdot 0.55 = 0.75,$$

and hence

$$\sigma = 0.88 \cdot 0.065 + 0.75 \frac{55}{1000} = 0.098.$$

Fig. 101 also shows the cavitation coefficients obtained by measurement (critical value – see further); it can be seen that they satisfactorily agree with the calculated values.

11. Strength Control of the Runner Blades

As a guide for the selection of the blade thickness when designing the runner the following expression¹⁾ may serve:

$$s_2 = 20 B \sqrt{\frac{H}{z_2}},$$

where s_2 (mm) is the blade thickness, B (m) is the face of the guide wheel, z_2 the number of the runner blades and H the utilized head (m).

Camerer²⁾ gives the expressions

$$s_2 = 0.005 D \sqrt{\frac{H}{z_2}} + 0.002 \text{ m for low-speed turbines,}$$

$$s_2 = 0.01 D \sqrt{\frac{H}{z_2}} + 0.002 \text{ m for high-speed turbines.}$$

The expressions by Camerer resulted from tests carried out on the finished runner by a torque acting on the hub and the rim up to permanent distortion. In his recalculation of the conditions of the torque acting upon the rim to the conditions under which the torque rose by the pressure of the water on the blades, he assumed that the load on the blade per unit area, was uniform. The test was carried out with a runner equipped with blades of a certain shape and this shape is not in the given expressions. For this reason even these formulas can only serve as an approximate guide.

For the final construction of the runner, however, we often need a more exact determination of the stress to which the blades are subjected.

The following method of strength calculation³⁾ is from the hydraulic point of view based upon the assumption that the blade guides the water perfectly. This assumption is correct with Francis turbines; if in the layout the angles are exaggerated, this fact must be taken into consideration.

The moment when the water, passing through the rotating runner duct, acts between points 1 and 2 upon the blade is on the assumption mentioned and given according to Equation (18) by the expression

$$M_{1-2} = \frac{q\gamma}{g} (R_1 C_{u1} - R_2 C_{u2}), \quad (113)$$

¹⁾ Kieswetter: Přednášky o vodních strojích lopatkových (Lectures on Hydraulic Turbo-machinery), 1939.

²⁾ Camerer: Vorlesungen über Wasserkraftmaschinen, Leipzig, 1924, p. 375.

³⁾ Thomann (Die Wasserturbinen und Turbinenpumpen, Part 2, Stuttgart 1931, p. 123) presents a calculation method based upon the assumption that the specific load is uniform across the entire blade, which is not in agreement with the actual conditions; moreover, he divides the fix-end moment into equal parts for the rim and the hub, which likewise is not in agreement with the actual conditions. For this reason, the author presents his own method which complies far more with the actual conditions. See also Nechleba: Výpočet pevnosti oběžného kola Francisovy turbíny, Strojirenstvi (Strength Calculation of the Francis Turbine Runner, Mechanical Engineering) 2, 1952, No. 7, p. 292.

where q is the volume of water flowing through a runner duct per second, γ is the specific gravity of the liquid, and g is the gravitational acceleration; R is the radius of the point in question in relation to the axis of rotation, C_u the peripheral component of the absolute velocity expressed by its actual value.

In designing the blade we have divided the turbine space into a series of elementary flows. Regardless of the method of establishing the flow field, the distribution is such that the flow rate is equal for each elementary flow. Expressed by the previously used symbols, the flow-rate for each flow amounts to $\frac{Q}{x}$ (see Fig. 103).

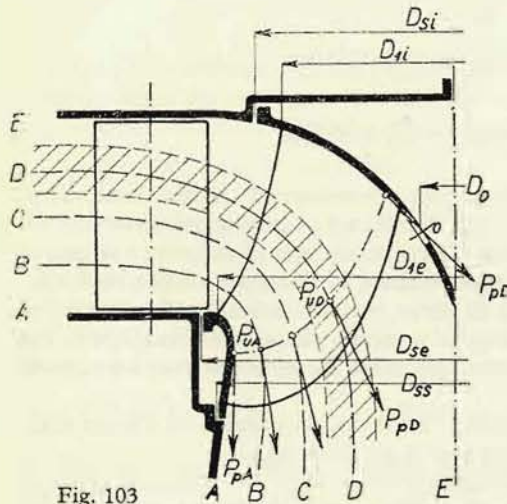


Fig. 103

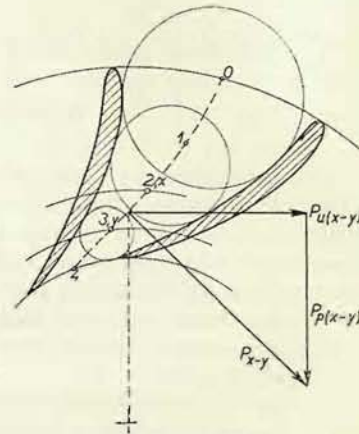


Fig. 104

Fig. 104 indicates a section on the developed cone, containing one blade duct. When z_2 is the number of blades, the duct of each elementary flow has the flow-rate

$$q = \frac{Q}{x z_2}.$$

Since the blade sections belong to a certain flow surface, e. g. $D - D$ (Fig. 103), we shall consider as the appropriate elementary flow that one which has the central flow surface $D - D$, i. e. the lightly hatched flow in Fig. 103. In this flow, too, one blade duct is passed by given quantity q , which applies also to the other flow surfaces ($C - C$, $B - B$), with the exception of the border surfaces ($A - A$, $E - E$) where we must take half the quantity passing per second, i. e. $\frac{q}{2}$.

To such a runner duct of one elementary flow we shall apply the relation (113). Therefore, we determine the central stream line (e. g. by inscribing the circles of contact, Fig. 104), and the relation holds good not only between the initial point

and the end point of this stream line of the duct, but for any arbitrary pair of points within the duct. Therefore, we divide the length of the stream line into a certain number of parts, 0 — 1, 1 — 2, etc., whose density will depend on the required accuracy. Then we shall apply the above-mentioned relation to all pairs of subsequent points, which we denote generally by $x - y$. Since in the layout of the blade we calculate as a rule with the specific velocities, we transform the expression as follows:

$$M_{x-y} = \frac{Q\gamma}{x z_2 g} \sqrt{2gH} (R_x c_{ux} - R_y c_{uy}). \quad (114)$$

Thus, we can determine the moment when the water passing through the part $x - y$ develops, because for each point of the stream line we can readily determine the peripheral as well as the meridional velocity; knowing the inclination of the relative velocity, given by the inclination of the tangent to the stream line in the respective point, we can for each point of the stream line draw the complete velocity triangle and thus determine the component c_u .

On the assumption of sufficiently small parts $x - y \dots$ we may divide the value thus obtained by the mean radius of the part

$$R_{x-y} = \frac{R_x + R_y}{2}$$

and obtain the peripheral force P_u , which the water in this part — with the point of application at the radius R_{x-y} — develops

$$P_{u\ x-y} = \frac{M_{x-y}}{R_{x-y}} = 2 \frac{Q}{x z_2} \frac{\gamma}{g} \sqrt{2gH} \frac{R_x c_{ux} - R_y c_{uy}}{R_x + R_y} \quad (115)$$

This peripheral force is a component of the force with which in the part $x - y$ the pressure of the water acts upon the blade. Since the pressure of the liquid (if we neglect the friction in streaming) acts perpendicularly to the wall, the total force P_{x-y} must be perpendicular to the blade, and consequently also to the stream line in the part $x - y$. Based on this circumstance, we determine this force graphically, see Fig. 104.

In this way we proceed in all parts and by graphical composition of these forces we obtain the magnitude, direction and position of the resultant force P on the entire blade in the investigated elementary flow, and then we also know its point of application on the stream line.

In this procedure the velocity triangles in the initial and end points of the duct will be congruent with the triangles of the velocity diagrams of the corresponding elementary turbine. If, however, we have employed an exaggeration of the angles for the layout of the blades, we can now eliminate exaggeration and adjust the triangles to the theoretical diagram without angle exaggeration, which in fact holds good for the motion of the water as a whole.

The obtained resultant P we now resolve again into the peripheral direction — the component P_u , and into the radial direction — the component P_p , which is the component in the meridional plane.

The components determined in this way on the individual flow surfaces we draw into the circular projection of the blade. The components P_u will act perpendicularly to the picture plane, whilst the components P_p will lie in the picture plane and act in the direction of the tangents to the traces of the flow surfaces (see Fig. 103). Thus we have obtained rather a true picture of the load acting upon the blade.

Now we can set about calculating actual strength conditions. We must take into account that the blade is fixed into the hub as well as into the rim. But the blade is not generally supported in the rim, for under the influence of the peripheral forces the rim may be shifted in the peripheral direction, under the influence of the forces

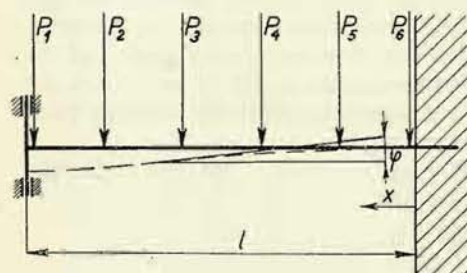


Fig. 105

in the meridional planes it may be shifted axially (low-speed runners, where this is not the case, will be mentioned later), the angle of fixing, however, does not change. Consequently we have a case of stress conditions as diagrammatically indicated in Fig. 105.

For the solution of this case we use the relation for the angle of the deflection line¹⁾

$$d\varphi = dx \frac{M}{E\mathcal{J}},$$

from which results by integrating, on the assumption that the moment of inertia \mathcal{J} is constant across the entire length of the beam,

$$\varphi = \frac{\int M dx}{E\mathcal{J}} = \frac{\text{moment area}}{E\mathcal{J}}, \quad (116)$$

because the integral represents the area of the moment when we draw the progress of the moment above the length of the beam (see Fig. 106). This area is here represented by a cantilever, acted upon by individual loads.

Since in the case of the rim the angle does not change, for $x = l$, there must be $\varphi = 0$, and consequently the sum of the moment areas, above the entire length of the beam, must equal zero.

The procedure will therefore be as follows: We determine the moment curve of the considered beam without regard to the fixing on its outer end, i. e. as if it were a cantilever. Then we divide the moment area by a line parallel to the axis of the beam so as to obtain the hatched areas of equal size in Fig. 107. The ordinates in the hatched areas then define the moments in the individual points of the beam for fixing on both ends; the extreme values M_V and M_N are the fix-end moments in the rim and in the hub respectively, because the sum of the moment areas for $x = 0$ and $x = l$ equals zero, and consequently the condition is satisfied that the

¹⁾ Technický průvodce – pružnost (Technical Guide – Strength of Materials, Prague ČMT 1944, p. 46.

deflection line does not change its inclination at these points subsequent to distortion.

In these considerations we have assumed a straight beam. In our case, however, concerning the runner blade, the centre line of the beam – given as the locus of the centres of gravity of the blade cross sections in the individual flow sections – is curved. The curvature is spatial; in the peripheral direction it is on the whole small, because the outlet edge of the blade is usually in the meridional plane, and, therefore, also the locus of the centres of gravity and of the points of application of the forces will not depart too much from the meridional plane. The curvature

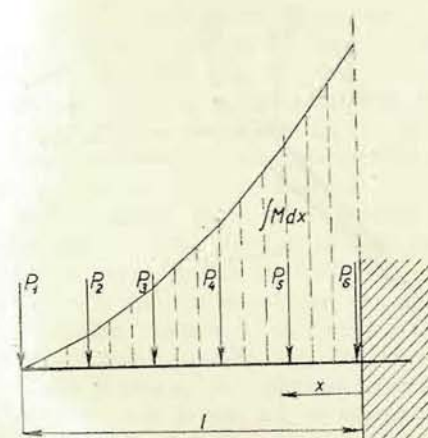


Fig. 106

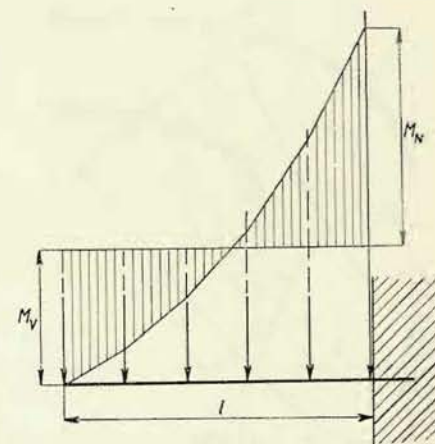


Fig. 107

in the meridional plane, however, must be taken into account when determining the bending moments of the individual forces. We must establish their progress along the line of the centres of gravity of the beam.

For this purpose – see Fig. 108 – we determine the progress of the locus of the centres of gravity $T-T$, and the length of this curve we divide into a convenient number of parts, $0-1$, $1-2$, etc., according to the accuracy required. To each individual point we determine the moments of all forces which must be taken into account for the respective point, the arm p_p of the force P_p being measured normally to the direction of this force, and the arm p_u of the force P_u normally to the axis of the cross section passing through the given point. Then we rectify the curve $T-T$, and by tracing out the moments obtained in this way from the corresponding points of the rectified line, separately for the forces P_u and separately for the forces P_p , we arrive at moment pictures resembling those in Fig. 106, in which in the same way as in Fig. 107, we determine the fix-end moments in the hub and in the rim. (This procedure involves a certain inaccuracy as the moment of inertia is not constant across the entire length of the blade.)

If we know the fix-end moments, we thus also know the moments in any arbitrary point of the blade and consequently we can determine for any point the stress in the blade; our greatest interest will be directed to the extreme values, i. e., those appertaining to the places of the fixing of the blade into the hub and into the rim. Since the procedure is the same for the cross section at the hub as for the cross section at the rim, we shall in our further considerations deal only with the cross section at the hub.

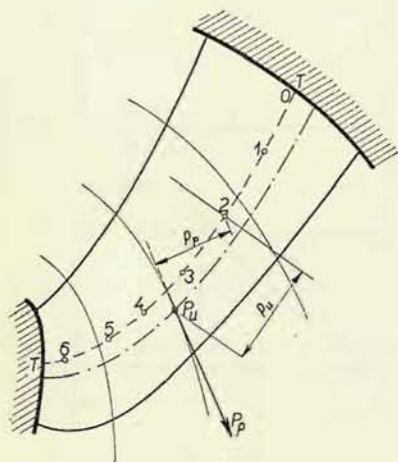


Fig. 108

The bending moments of the forces P_p act in the meridional plane, so that the fix-end moment, too, resulting from these forces, will be in the meridional plane. The vector by which we represent it in the developed conical section of the blade will, therefore, be perpendicular to the radius (to the trace of the meridional plane).

The bending moments of the forces P_u act in the plane normal to the meridional plane (the forces act in the peripheral direction), and the vector expressing the fix-end moment of these forces will be in the direction of the radius. By geometrical addition of these vectors we obtain the resultant vector M_N . We project it into the neutral axis $N-N$ of the minimum resistance moment of the blade and obtain the vector M'_N (see Fig. 109) of the moment by which the blade is deflected in the plane normal to the axis of the minimum resistance moment W_{min} . Bending stress, therefore, is

$$\sigma_0 = \frac{M'_N}{W_{min}}. \quad (117)$$

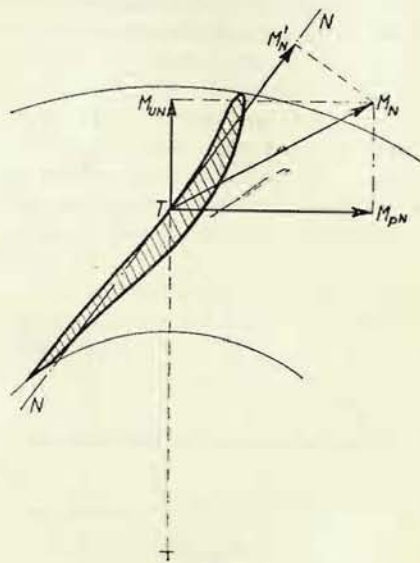


Fig. 109

The bending stress resulting from the deflection in the plane normal to the axis of the maximum resistance moment need not be determined as it will obviously be negligible.

It will be, however, more useful, to determine the tensile stress from the total of the components of the forces P_p normal to the plane of intersection of the blade with the hub; this stress is added to the stress σ_0 . Similarly, we may also determine the shearing stress from the total of the forces P_u and the total of the components of the forces P_p parallel to the plane of intersection of the blade with the hub. These two shearing stresses are normal to each other and added geometrically.

These three mentioned stresses, i. e. the tensile stress and both shearing stresses, do not come into consideration in the cross section of fixing into the rim, as in the rim no reactions are encountered. In this cross section there will only be the bending stress, which we determine by the same procedure as for the cross section of the fixing into the hub.

Here it must be noted that in narrow radial-flow runners, as employed at low specific speeds (see Fig. 110), the rim will be able to take up the reactions upon the forces P_p , which here act for the greater part in the radial direction, so that by acting upon the rim they counterbalance one another. For the determination of the fix-end moment resulting from these forces the diagram in Fig. 110 will apply, the solution of which is not difficult¹⁾. The determination of the fix-end moment from the forces P_u will be the same as before.

Example: We are going to demonstrate the procedure on a runner of normal speed, as designed previously. Appendix III shows the drawing of the runner. Appendix V contains the corresponding velocity diagrams for the optimum design efficiencies (i. e. those considered in the layout), i. e. for $n_1 = 65.5$ r. p. m. and for $Q'_1 = 0.6$ m³/sec.

The procedure, which, of course, must be carried out on all flow surfaces, will be described on two of them which are shown in Appendix IV. Into the ducts which appear here the central stream lines are drawn. Their lengths are divided by a few points, to which, according to the previously given principles, the velocity triangles are drawn (the value c_m and the direction of the velocity w are known);

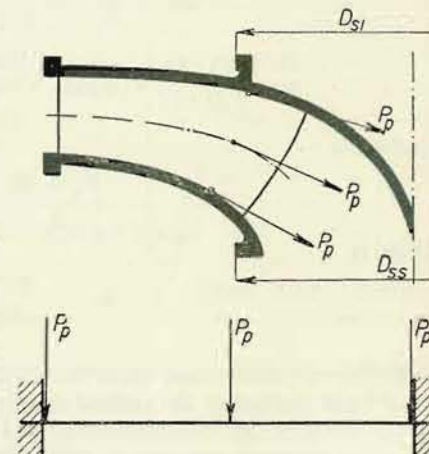


Fig. 110

¹⁾ The fix-end moment (for 1 load P_p in the centre) is $\dots M_N = \frac{1}{8} P_p l \dots$, see: Techn. průvodce - pružnost (Technical Guide - Strength of Materials), Prague, ČMT 1944, p. 87.

here we assume that the meridional velocity changes linearly from the inlet value to the outlet value, i. e. we neglect the influence of the varying thickness of the blades.

From the velocity triangles we then determine the peripheral components of the forces; e. g. between the inlet and the adjacent dividing point it holds good (we substitute $Q/8$ as a border surface is concerned)

$$M = \frac{Q}{8} \frac{\gamma \sqrt{2gH}}{g z_2} (R_1 c_{u2} - R c_u) =$$

$$= \frac{1175 \cdot 44.3}{9.81 \cdot 17} (0.551 \cdot 0.619 - 0.451 \cdot 0.35) = 57.2 \text{ kgm},$$

and since

$$\frac{R_1 + R_2}{2} = 501 \text{ mm},$$

there is

$$P_u = \frac{57.2}{0.501} = 114 \text{ kg}.$$

This force is marked out in the central point of the part, and the magnitude of the total force normal to the central stream line is determined graphically. Similarly we proceed in the following parts, and the forces are then graphically composed into the resultant, as shown in Appendix IV.

The resultant $P_x = 430 \text{ kg}$ is again resolved into the peripheral component $P_{u,x} = 280 \text{ kg}$ and the component in the flow surface $P_{p,x} = 320 \text{ kg}$. In this way we have proceeded in all flow sections and the components of the resultant forces have then been transferred into the circular projection (see Appendix III.) The points of application of the forces can be connected by a continuous line P . In this projection also the centre of gravity line T is drawn as the connecting line of the centres of gravity of the blade cross sections in the developed sections of the individual flow surfaces.

The centre of gravity curve is further divided by a number of points a, b, c, d , to which the moments are determined according to the following table.

The moments of the peripheral components of the forces were then separately marked out above the rectified centre of gravity curve T . Similarly, also the moments of the meridional components and the fix-end moments in the hub and in the rim were then determined by the previously described method, as evident in Appendix III.

We compose the fix-end moments and project the resultant moment into the neutral axis of the smaller moment of inertia, as indicated in Fig. 111a for the fix-end moment in the hub, and in Fig. 111b for the fix-end moment in the rim. The component of the fix-end moment in the hub which deflects the blade is $M_0 = 26,750 \text{ kgcm}$ for the smaller moment of inertia.

Stream line	P_u kg	R_u cm	P_p kg	R_p cm	Moments in the hub		Moments of the forces P_u at the points				Moments of the forces P_p to the points			
					M_u kg cm	M_p kg cm	a	b	c	d	a	b	c	d
A	172.—	43.2	325.—	16.1	7440	5240	5160	3970	2890	1340	5550	5400	4230	2080
B	390.—	40.7	710.—	12.2	15850	8660	11500	8270	4760	546	8680	7800	4620	—
C	480.—	31.5	630.—	7.8	15120	4920	10800	6050	672	—	4220	2390	—	—
D	520.—	12.4	600.—	9.5	6450	5700	1660	—	—	—	1560	—	—	—
E	280.—	0.—	320.—	0.—	0	0	—	—	—	—	—	—	—	—
					$\Sigma M_u = 44860$		29120	18290	8322	1886	—	—	—	—
						$\Sigma M_p = 24520$					20010	15590	8850	2080

The appropriate moment of the resistance of the blade cross section in the place of the fixing into the hub was graphically determined as equalling the value $W = 11.22 \text{ cm}^3$, and the area of the cross section as being $f = 51 \text{ cm}^2$.

The bending stress in the blade in the place of its fixing into the hub, acting in the fibre subjected to tension, therefore is $\sigma_0 = \frac{26,750}{11.22} = 2190 \text{ kg/cm}^2$.

We further can determine the shearing stress from the forces P_u , all of which act parallel to the plane of shearing

$$\tau_u = \frac{\Sigma P}{f} = \frac{1842}{51} = 360 \text{ kg/cm}^2.$$

Similarly we can also find the shearing stress from the forces P_p parallel to the plane of shearing

$$\tau_p = \frac{920}{51} = 18 \text{ kg/cm}^2,$$

which evidently may be neglected, and further the tensile stress in the blade from the forces P_p acting perpendicularly to the stressed cross section

$$\sigma_t = \frac{1665}{51} = 32.6 \text{ kg/cm}^2.$$

The maximum total of the tensile stresses therefore is

$$\Sigma \sigma_t = 2190 + 32.6 = 2222.6 \text{ kg/cm}^2.$$

At the place of its fixing into the rim, the blade is only subjected to bending stress. As follows from Fig. 111b, the appropriate bending moment is $M_0 = 18,000 \text{ kgcm}$, and the resistance moment has again been graphically determined as $W = 15.3 \text{ cm}^3$. The maximum bending stress therefore is

$$\sigma_0 = \frac{18\,000}{15.3} = 1176 \text{ kg/cm}^2.$$

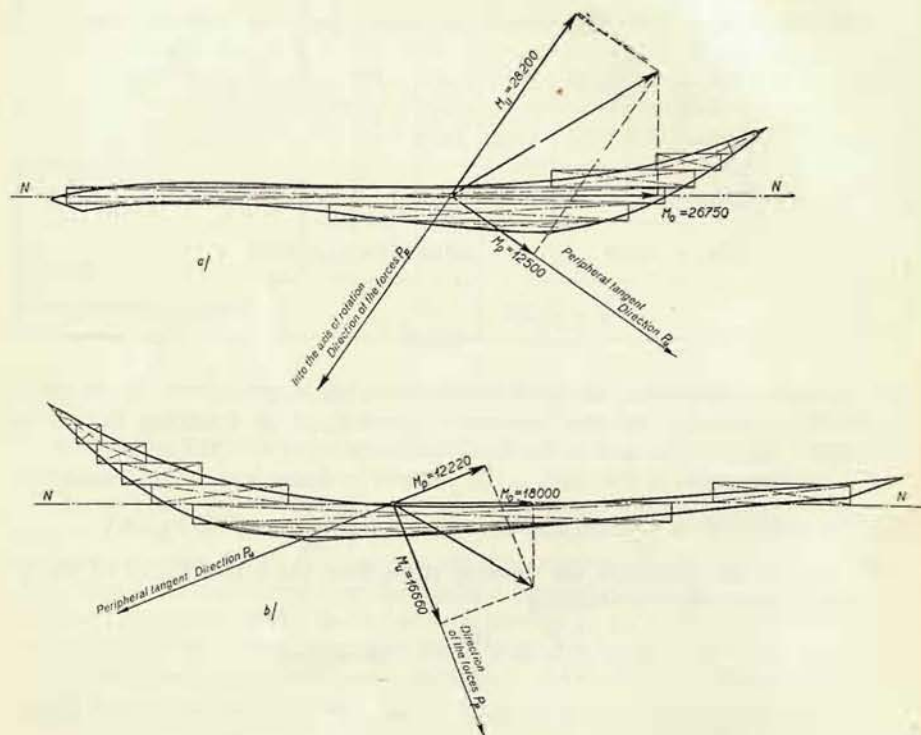


Fig. 111

These values have been determined for a head $H = 100 \text{ m}$ and for a unit flow-rate $Q'_1 = 0.6 \text{ m}^3/\text{sec}$. For the maximum flow-rate we may calculate with a stress increased proportionally to the augmentation of the flow-rate (the driving moment varies proportionally to the flow-rate variation). Consequently, at the maximum unit flow-rate $Q'_{1,\text{max}} = 0.7 \text{ m}^3/\text{sec}$, will hold good:

$$\Sigma \sigma_t = \frac{0.7}{0.6} 2616 = 2930 \text{ kg/cm}^2.$$

Permissible stress may be selected up to 3000 kg/cm^2 for stainless steel,¹⁾ as employed with regard to cavitation (static tensile strength 7000 to 8000 kg/cm^2), and between 1600 and 1800 kg/cm^2 for ordinary cast steel. These are the approximate values of permanent strength under alternating stress; this does not mean that the blade is actually subjected to alternating forces, but, nevertheless, we must reckon with certain variations of the stresses (turbulence of the flow, cavitation, irregularities in the supply line), and we must also bear in mind that on stopping the open turbine, or on suddenly opening the guide apparatus on the resting runner, the moment and, thus, also the stress acting upon the blade would rise to about double the normal value.

12. Hydraulic Load of the Runner

By the hydraulic load or hydraulic tension of the runner we mean the axial force with which the water pressure acts upon the runner, i. e. upon the runner blades and the hub and rim of the runner.

This hydraulic load represents the main part of the axial force on the shaft of the set, which the thrust bearing must hold up (see Part 3, B, where also the other components of the axial force are enumerated). This load must therefore be determined in the design.

If we know from the strength calculation of the runner the meridional components of the forces P_p on the individual flow surfaces (see Fig. 103), the total of their axial components multiplied by the number of blades immediately gives the axial force S_1 which the water develops upon the blades.

To this force we must add the further forces with which the water acts upon the hub and rim of the runner. The hub is acted upon, on one hand, by the water pressure from the side of the space of the blades on the annulus (see Fig. 103)

$\frac{\pi}{4} (D_{s,i}^2 - D_{1,i}^2)$ — in the direction against the axial components of the forces

P_p — and, on the other hand, by the water pressure between the hub and the lid

on the annulus $\dots \frac{\pi}{4} (D_{s,i}^2 - d^2)$, where $d = 2 R_d$ is the shaft diameter in the

stuffing box. The rim is similarly acted upon by the water pressure from the side

of the space of the blades on the annulus $\frac{\pi}{4} (D_{s,e}^2 - D_{1,e}^2)$ and by the water pressure

in the space between the rim and the bottom lid on the annulus $\frac{\pi}{4} D_{s,e}^2 - D_{s,s}^2$.

Apart from this, there is an action against the axial components of the forces P_p , developed by the force resulting from the meridional deflection of the water (from the radial to the axial direction, according to the equation defining the variation of

¹⁾ The calculation relates to the machine in Appendix X. The relative high stress is permitted, because the centrifugal forces acting against the radial components of the forces P_p and partially relieving the blades, have not been considered in the calculation.

the momentum), and the surface of the shaft in the stuffing box is acted upon by the overpressure of the atmosphere above the pressure in the draft tube.

The water pressure in the spaces mentioned, i. e., in front of the inlet into the runner (between the guide apparatus and the runner), between the hub and the top lid, and between the rim of the runner and the bottom lid, is not the same (this pressure is a function of the distance from the axis of rotation), and therefore we first determine the distribution of the pressure across the individual spaces.

In the spaces in front of the runner, the water flows between parallel walls without releasing any energy, and, therefore, Equations (68) and (69) apply here

$$r C_u = \text{const.} \quad r C_m = \text{const.}$$

By squaring and adding both equations we obtain

$$r^2 (C_u^2 + C_m^2) = r^2 C^2 = \text{const.},$$

and after extracting the square root the following holds good:

$$r C = \text{const.} \quad (118)$$

Immediately in front of the inlet edge of the runner, at the radius R_1 , the absolute velocity of the water has the value C_0 ; the velocity in the space in front of the runner in a point at an arbitrary radius $R > R_1$ will be

$$C = C_0 \frac{R_1}{R}. \quad (119)$$

If we use for this space the Bernoulli equation and if we designate the pressure closely in front of the inlet into the runner by H_p , pressure $H_{p,R}$ at the radius R will be

$$H_{p,R} + \frac{C^2}{2g} = H_p + \frac{C_0^2}{2g},$$

and hence

$$H_{p,R} = H_p + \frac{1}{2g} (C_0^2 - C^2) = H_p + \frac{C_0^2}{2g} \left[1 - \left(\frac{R_1}{R} \right)^2 \right]. \quad (120)$$

We know the difference between the pressure H_p immediately in front of the runner and the pressure $\frac{p_3}{\gamma}$ at the back of the runner blades, at the beginning of the draft tube; this is the so-called overpressure of the runner, which according to Equation (67), equals

$$H_p - \frac{p_3}{\gamma} = h_p = H c_i^2 - \frac{C_0^2}{2g}. \quad (121)$$

The pressure at the beginning of the draft tube, $\frac{p_3}{\gamma}$ we take as the reference zero pressure. Then the following holds good:

$$H_p = h_p = H c_i^2 - \frac{C_0^2}{2g};$$

and by substitution into Equation (120), we consequently obtain the pressure in the space in front of the runner, at an arbitrary radius R

$$\begin{aligned} H_{p,R} &= H c_i^2 - \frac{C_0^2}{2g} + \frac{C_0^2}{2g} - \frac{C_0^2}{2g} \left(\frac{R_1}{R} \right)^2 \\ &= H c_i^2 - H c_0^2 \left(\frac{R_1}{R} \right)^2 \\ H_{p,R} &= H \left[c_i^2 - c_0^2 \left(\frac{R_1}{R} \right)^2 \right]. \end{aligned} \quad (122)$$

Equation (122) is the equation of a paraboloid of revolution with its axis in the axis of the runner. The pressure in the space in front of the runner, resolved according to the law just derived, acts on the annulus $\frac{\pi}{4} (D_{s,i}^2 - D_{1,i}^2)$, maybe on the annulus $\frac{\pi}{4} (D_{s,e}^2 - D_{1,e}^2)$. With regard to the small difference between diameters $D_{s,i}$ and $D_{1,i}$, as well as between $D_{s,e}$ and $D_{1,e}$ respectively, as employed in the practical design, we make no serious error if we assume the pressure to be constant on the entire annulus and equal to the pressure at the mean radius $\frac{R_{s,i} + R_{1,i}}{2}$, or maybe $\frac{R_{s,e} + R_{1,e}}{2}$.

The corresponding mean pressures we designate by $H_{p,i}$ and $H_{p,e}$ respectively, and obtain

$$H_{p,i} = H \left[c_i^2 - c_{0,i}^2 \frac{4 R_{1,i}^2}{(R_{s,i} + R_{1,i})^2} \right]$$

and

$$H_{p,e} = H \left[c_i^2 - c_{0,e}^2 \frac{4 R_{1,e}^2}{(R_{s,e} + R_{1,e})^2} \right].$$

By multiplying the pressures we thus get the force acting upon the annulus of the disc (hub)

$$S_{p,i} = \frac{\pi}{4} (D_{s,i}^2 - D_{1,i}^2) \gamma H \left[c_i^2 - c_{0,i}^2 \frac{4 R_{1,i}^2}{(R_{s,i} + R_{1,i})^2} \right] \quad (123)$$

and upon the annulus of the rim

$$S_{p,e} = \frac{\pi}{4} (D_{s,e}^2 - D_{1,e}^2) \gamma H \left[c_i^2 - c_{0,e}^2 \frac{4 R_{1,e}^2}{(R_{s,e} + R_{1,e})^2} \right].$$

In the space between the hub of the runner and the top lid, or between the rim of the runner and the bottom lid, the water is in rotary motion. Firstly, the water entering these spaces through the sealing gap has a certain rotational component

from the guide apparatus, but the main rotation results from the friction against the rotating disc or rim. However, its motion is retarded by the friction against the lid. For this reason, the water rotates, as has also been shown by experiments¹⁾, at half the angular velocity of the runner. Since the radial velocity is insignificant in comparison with the peripheral velocity, we may neglect it and consider only the purely rotatory motion. The pressure difference (in metres of water column) between two places at radii R_1 and R_2 , or the peripheral velocities U_1 and U_2 , is then defined by the expression (see Fig. 29):

$$h_1 - h_2 = \frac{U_1^2 - U_2^2}{2g} = \frac{\omega^2}{2g} (R_1^2 - R_2^2).$$

Hence the pressure difference between the places at the diameter $D_{s,i}$, where the water enters the space under the top lid, and the places at the diameter D_0 (radius R_0), where the water discharges from it through the relief openings o into the draft tube (ω' of the water = $\frac{1}{2}$ ω of the runner), equals

$$h_1 - h_2 = \frac{\omega^2}{8g} (R_{s,i}^2 - R_0^2).$$

From the side of the space of the blades, there is a pressure difference equaling the overpressure of the runner between the same places, increased by the pressure difference Δh_p that exists between the gap and the inlet edge of the blade (whilst as to the openings o we assume that they are close to the back of the outlet edge), according to Equation (122):

$$h_p + \Delta h_p = H \left[c_i^2 - c_{0,i}^2 \left(\frac{R_1}{R_{s,i}} \right)^2 \right].$$

These differences on both sides of the disc cannot be the same, because between them there must be a pressure difference for pressing the water through the gap at the diameter $D_{s,i}$ and the openings o , and here the continuity equation must be satisfied for the quantity Q_s flowing through these cross sections:

$$Q_s = \mu_s f_s \sqrt{2g h_s} = \mu_0 f_0 \sqrt{2g h_0}, \quad (124)$$

where μ_s and μ_0 denote the discharge coefficients of the gap and of the relief openings respectively, and these can be taken according to Oesterlen²⁾ as $\mu_s = 0.5$ to 0.6 for the gap, and $\mu_0 = 0.45$ for the circular openings; f_s denotes the through-flow cross section of the gap, $f_s = \pi D_s s$ (where s is the width of the gap), and f_0 is the through-flow cross section of all relief openings, h_s the head in the gap,

¹⁾ Oesterlen in Dubbel's Handbook: Taschenbuch für den Maschinenbau, Part II, Berlin 1943, p. 253.

²⁾ See the foregoing reference and also Hýbl: Vodní motory (Hydraulic Motors), Part 2, Prague, ČMT, 1924, p. 141; when using labyrinths, see p. 241.

and h_0 the head in the openings o required for forcing the quantity (flow-rate) Q_s through them. Further it holds good that:

$$h_p + \Delta h_p = h_1 - h_2 + h_s + h_0 = \frac{\omega^2}{8g} (R_{s,i}^2 - R_0^2) + h_s + h_0 = H \left[c_i^2 - c_{0,i}^2 \left(\frac{R_1}{R_{s,i}} \right)^2 \right], \quad (125)$$

From Equations (124) and (125) we eliminate h_s ; from Equation (124) results that

$$h_s = \left(\frac{\mu_0 f_0}{\mu_s f_s} \right)^2 h_0,$$

which, when substituted into Equation (125), leads to

$$\frac{\omega^2}{8g} (R_{s,i}^2 - R_0^2) + h_0 \left[1 + \left(\frac{\mu_0 f_0}{\mu_s f_s} \right)^2 \right] = H \left[c_i^2 - c_{0,i}^2 \left(\frac{R_1}{R_{s,i}} \right)^2 \right],$$

whence

$$h_0 = \frac{H \left[c_i^2 - c_{0,i}^2 \left(\frac{R_1}{R_{s,i}} \right)^2 \right] - \frac{\omega^2}{8g} (R_{s,i}^2 - R_0^2)}{1 + \left(\frac{\mu_0 f_0}{\mu_s f_s} \right)^2}.$$

If we substitute for $\frac{\omega^2 R_{s,i}^2}{2gH}$ and $\frac{\omega^2 R_0^2}{2gH}$ the specific peripheral velocities, we can write

$$h_0 = H \frac{\left[(c_i^2 - c_{0,i}^2) \left(\frac{R_1}{R_{s,i}} \right)^2 \right] - \frac{u_{s,i}^2 - u_0^2}{4}}{1 + \left(\frac{\mu_0 f_0}{\mu_s f_s} \right)^2}.$$

The pressure in any place (at any radius) in the space above the runner disc is, therefore,

$$h_R = h_0 + \frac{\omega^2}{8g} (R^2 - R_0^2) = \frac{p_R}{\gamma},$$

and hence the differential of the axial force acting upon the disc of the runner on the annulus of the very small width dR with the general radius R , may be expressed as

$$dS_i = 2\pi R \cdot dR \cdot p = 2\pi R \cdot dR \cdot h_R \gamma = 2\pi \gamma R dR \left[h_0 + \frac{\omega^2}{8g} (R^2 - R_0^2) \right].$$

Hence we obtain for the force S_i acting upon the entire disc with the outer radius R_s and the inner radius R_d , where R_d is the radius of the shaft in the stuffing box,

up to which the pressure acts upon the disc and which in general differs from the radius of the relief openings R_0 :

$$S_i = 2\pi\gamma \left[\int_{R_d}^{R_{s,i}} h_0 R \cdot dR + \frac{\omega^2}{8g} \int_{R_d}^{R_{s,i}} R^3 \cdot dR - \frac{\omega^2}{8g} R_0^2 \int_{R_d}^{R_{s,i}} R dR \right],$$

which after integration and a small adjustment leads to

$$S_i = \pi\gamma \left(h_0 - \frac{\omega^2 R_0^2}{8g} \right) (R_{s,i}^2 - R_d^2) + \pi\gamma \frac{\omega^2}{16g} (R_{s,i}^4 - R_d^4),$$

and hence

$$S_i = \pi\gamma (R_{s,i}^2 - R_d^2) \left[h_0 - \frac{\omega^2 R_0^2}{8g} + \frac{\omega^2}{16g} (R_{s,i}^2 + R_d^2) \right]. \quad (126)$$

If we introduce again the specific velocities and substitute them for h_0 , we finally obtain

$$S_i = \gamma H \pi (R_{s,i}^2 - R_d^2) \left[\frac{c_i^2 - c_{0,i}^2 \left(\frac{R_{1,i}}{R_{s,i}} \right)^2 - \frac{u_{s,i}^2 - u_0^2}{4}}{1 + \left(\frac{\mu_0 f_0}{\mu_s f_s} \right)^2} + \frac{u_{s,i}^2 - 2u_0^2 + u_d^2}{8} \right]. \quad (126a)$$

The same expression also applies for the force acting upon the rim. Since, however, instead of the relief openings there is a second gap, so that the pitch diameter R_0 of the relief openings is identical with inner diameter of the loaded surface, we may put

$$R_0 = R_d = \frac{D_{s,s}}{2} = R_{s,s}$$

(Fig. 103), so that

$$S_s = \gamma H \pi (R_{s,e}^2 - R_{s,s}^2) \left[\frac{c_i^2 - c_{0,e}^2 \left(\frac{R_{t,e}}{R_{s,e}} \right)^2 - \frac{u_{s,e}^2 - u_{s,s}^2}{4}}{1 + \left(\frac{\mu_{s,s} f_{s,s}}{\mu_s f_s} \right)^2} + \frac{u_{s,e}^2 - u_{s,s}^2}{8} \right]. \quad (127)$$

This force may act in a direction from the draft tube (when $R_{s,e} > R_{s,s}$) or in a direction to the draft tube (when the relation is inverse).

A further component of hydraulic load is - as has been mentioned - the force from the meridional change of the flow direction, S_m , which we readily determine from the theorem of momentum by means of Equation (11), which in our notation reads

$$S_m = \frac{Q\gamma}{g} (0 - C_s),$$

hence

$$S_m = -\frac{Q\gamma}{g} C_s, \quad (128)$$

where C_s is the axial component of the velocity at the inlet into the draft tube and Q the flow-rate of the turbine. As it is evident from the sign, this force is always directed from the draft tube and relieves the runner. It is not effective in its full magnitude when the meridional deflection of the water flow is partly enforced by the fixed parts of the turbine (e. g. the top lid, see Fig. 103).

The last component, which, however may be neglected, results from overpressure of the atmosphere against the pressure in the draft tube $\frac{p_3}{\gamma}$ and acts upon the cross section of the shaft in the stuffing box. Since according to Equation (26) it holds good that

$$\frac{p_3}{\gamma} = H_B - H_s - \eta_s, \quad \frac{C_2^2 - C_4^2}{2g} = H_B - H_s - \nu H,$$

the overpressure acting upon the cross section of the shaft $\frac{\pi d^2}{4}$ is

$$H_B - \frac{p_3}{\gamma} = H_s + \nu H,$$

and hence the force acts upon the shaft in the direction into the draft tube and equals

$$S_h = \frac{\pi}{4} d^2 \gamma (H_s + \nu H). \quad (129)$$

The total hydraulic tension, if we retain the validity of the signs in the formular of the components, is then:

$$S = S_1 - S_{p,i} + S_{p,e} + S_i - S_s + S_m + S_h. \quad (130)$$

In this case we have made use of reference data from the hydraulic layout of the runner (the velocity in front of the inlet to the blade C_0 , or c_0) and from the strength calculation (determination of the axial force acting upon the blades) for the determination of the axial force acting upon the runner blades. These data are not always at the designer's disposal.

In such a case, the designer determines velocity c_0 , or maybe C_0 , from the discharge velocity from the guide apparatus, C' . This velocity C' we determine most conveniently by projecting the meridional velocities at the outlet edge of the guide apparatus into the direction of the outlet edge of the guide blade, $C' = \frac{C'_m}{\sin \alpha}$, whereupon from velocity C' we can determine velocity C_0 with sufficient accuracy by applying the relation (118), $C_0 R_0 = C' R'$.

The axial component of the force acting upon the blades, we may then approximately replace by the force with which the overpressure of the water acts on the annulus defined by the projection of the inlet edge, because this overpressure (directed against the pressure in the draft tube) is brought about by the components of the hydraulic forces P_p which act upon the blades, as is clearly evident from the calculation of the forces acting upon the blade of a propeller turbine (2/A, Chap. I/1). Hence we may approximately write

$$S_1 = \frac{\pi}{4} (D_{1,e}^2 - D_{1,i}^2) \gamma h_p = \frac{\pi}{4} (D_{1,e}^2 - D_{1,i}^2) \gamma H (c_i^2 - c_0^2).$$

We see that we may also write with sufficient accuracy

$$S_1 - S_{p,i} + S_{p,e} = \frac{\pi}{4} (D_{s,e}^2 - D_{s,i}^2) \gamma H (c_i^2 - c_0^2), \quad (131)$$

and determine the other components the same way as before.

The result will not be entirely the same as that of the first method, as may be readily shown by means of the example of the low-speed runner in Fig. 110. If this runner has the sealing gaps at the same diameters $D_{s,i} = D_{s,s}$, as indicated, the load resulting from the forces acting upon the blade will equal zero, when calculated by the second method; and hydraulic load will show only the components S_i , S_m , S_h , because S_s is in this case counterbalanced. The first method, however, leads to a certain, though small, force from the pressures upon the blades.

Since all components of hydraulic load are proportional to the head H (with the exception of the force with which the atmospheric pressure acts upon the shaft and to the squares of the diameters, we can write

$$S = k H D^2, \quad (132)$$

which consequently is the law of model similarity of geometrically similar machines. This, however, assumes an exact geometrical similarity also of the labyrinths and the relief openings, because their arrangement exerts a great influence upon the hydraulic load.

For an approximate determination of hydraulic tension (provisionally), the expression (132) may be employed, k having the approximate value¹⁾ $k = n_s \cdot H$ as well as D are expressed in metres, D being the maximum diameter of the inlet edge.

Soviet literature²⁾ in expression (132) gives k the following values:

n_s	100	130	160	200	300	400
k	60	85	115	150	300	500

To determine the runner weight, a guide is given for $n_s = 150$ to 400 by the expression $G = 110 \cdot D_1$ (kg).

¹⁾ According to Braun in Hütte II, 1936, p. 605.

²⁾ Mashinostroyeniye, tom 12, Gosudarstvennoye nauchnotekhnicheskoye izdatelstvo, Moskva 1948, p. 299 =

According to other sources¹⁾ it applies

$$S = K \frac{\pi D_s^2}{4} H, \quad (133)$$

where

$$K = n_s + 50,$$

H and D_s are again expressed in metres, but D_s is the outlet diameter of the runner. This information is based on measurements carried out up to $n_s = 400$.

The last fraction in brackets in Equation (126a) and (127) expresses the influence of the rotation of the water in the space outside the runner. From its positive value in the expression (126a) it can be seen that the rotation of the water increases the hydraulic load. If this rotation were prevented, these terms would disappear (the peripheral velocities denote, it is true, the velocities of the runner, but they are in the expression due to our assumption that the angular velocity of the rotation of the water is half the angular velocity of the runner; if the water did not rotate, the numerator would assume an infinite value).

For this reason, the top lid in the past was equipped with ribs to prevent the rotation of the water. In order to actually achieve this purpose, the ribs had to be extended until very near the disc of the runner, which was rather difficult from the constructional point of view. In addition, the water whirls behind the ribs represent losses. These ribs are therefore no longer used.

In order to increase the last term in the fraction mentioned $-2u_0$, the relief openings must be made at the largest possible radius, i. e. closely behind the runner blades. They should be in the axial direction because if they were inclined to the axis of rotation, they would act as a pump (the water in them has the full velocity of the disc!) and thus increase the pressure between the runner and the lid. For this reason, particularly in low-speed runners, the relief openings in the runner are replaced by a by-pass relief piping into the draft tube (see Fig. 36) and the mouth in the space under the lid is then arranged at the largest possible radius.

Example: We want to determine the hydraulic load of the runner in Appendix III for the values as will be given in the course of calculation.

1. S_1 : The axial load of one blade equals the total of the axial components of the forces P_s and P_p , which amounts to

$$\Sigma P_s = 115 + 420 + 625 + 710 + 315 = 2185 \text{ kg}$$

and hence for the blade number $z_2 = 17$, there is

$$S_1 = 17 \cdot 2185 = 37,100 \text{ kg.}$$

$$2. \quad S_{p,i} = \frac{\pi}{4} (D_{s,i}^2 - D_{1,i}^2) \gamma H \left[c_i^2 - c_{0,i}^2 \frac{4 R_{1,i}^2}{(R_{s,i} + R_{1,i})^2} \right]$$

¹⁾ Casacci & Jarriaud: Mesure des poussées hydrauliques des turbines Francis à axe vertical, La Houille Blanche 1950, p. 326.

here is

$$D_{s,i} = 960 \text{ mm}, D_{1,i} = 940 \text{ mm}, R_{s,i} = 480 \text{ mm}, R_{1,i} = 470 \text{ mm};$$

$$c_i = 0.98, c_i^2 = 0.96, c_{0,i} = 0.65 \text{ (according to Enclosure V), } c_{0,i}^2 = 0.42,$$

so that

$$H \left[c_i^2 - c_{0,i}^2 \frac{4 R_{1,i}^2}{(R_{s,i} + R_{1,i})^2} \right] = 100 \left[0.96 - 0.42 \frac{4 \cdot 0.22}{0.9} \right] = 55 \text{ m}$$

and

$$S_{p,i} = \frac{\pi}{4} (0.92 - 0.89) \cdot 1000 \cdot 55 = 1300 \text{ kg.}$$

$$3. \quad S_{p,e} = \frac{\pi}{4} (D_{s,e}^2 - D_{1,e}^2) \gamma H \left[c_i^2 - c_{0,e}^2 \frac{4 R_{1,e}^2}{(R_{s,e} + R_{1,e})^2} \right],$$

$$D_{s,e} = 1330 \text{ mm}, D_{1,e} = 1250 \text{ mm}, R_{s,e} = 665 \text{ mm}, R_{1,e} = 625 \text{ mm};$$

$$c_i^2 = 0.96, c_{0,e} = 0.7, c_{0,e}^2 = 0.49,$$

$$H \cdot [\dots] = 100 \cdot \left(0.96 - 0.49 \frac{4 \cdot 0.39}{1.56} \right) = 47 \text{ m},$$

and hence

$$S_{p,e} = \frac{\pi}{4} (1.77 - 1.57) \cdot 1000 \cdot 47 = 7380 \text{ kg.}$$

$$4. \quad S_t = \gamma H \pi (R_{s,i}^2 - R_{0,i}^2) \left[\frac{c_i^2 - c_{0,i}^2 \left(\frac{R_{1,i}}{R_{s,i}} \right)^2 - \frac{u_{s,i}^2 - u_0^2}{4}}{1 + \left(\frac{\mu_0 f_0}{\mu_s f_s} \right)^2} + \frac{u_{s,i}^2 - 2 u_0^2 + u_d^2}{8} \right].$$

The disc of the runner is sealed with an axial gap of a radius $R_{s,i} = 480 \text{ mm}$ and a width $s = 0.5 \text{ mm}$. Hence there is

$$f_s = 2 \pi R_{s,i} s = 2 \pi \cdot 48 \cdot 0.05 = 15.1 \text{ cm}, \mu_s = 0.5.$$

There are 6 relief openings of 60 mm diameter at a pitch radius of 225 mm. Therefore,

$$f_0 = 6 \cdot 28.4 = 170 \text{ cm}^2, \mu_0 = 0.45,$$

and hence

$$1 + \left(\frac{\mu_0 f_0}{\mu_s f_s} \right)^2 = 1 + 10.2^2 = 141.$$

We further determine $u_{s,i} = 0.594; u_0 = 0.278$

$$c_i^2 - c_{0,i}^2 \left(\frac{R_{1,i}}{R_{s,i}} \right)^2 - \frac{u_{s,i}^2 - u_0^2}{4} = 0.96 - 0.42 \left(\frac{0.47}{0.48} \right)^2 - \frac{0.35 - 0.078}{4} = 0.49,$$

and hence the first term in the brackets has the value of $\frac{0.49}{141} = 0.00347$.

The second fraction in the brackets has the value (the diameter of the shaft in the stuffing box is $d = 300 \text{ mm}$, hence $u_d = 0.186$)

$$\frac{u_{s,i}^2 - 2 u_0^2 + u_d^2}{8} = \frac{0.35 - 2 \cdot 0.08 + 0.034}{8} = 0.0275.$$

The total expression in the brackets therefore equals $0.0035 + 0.028 = 0.032$.

The expression in front of the brackets is

$$\pi (R_{s,i}^2 - R_d^2) \gamma H = \pi (0.48^2 - 0.15^2) \cdot 1000 \cdot 100 = 60,000 \text{ kg},$$

and hence

$$S_t = 60\,000 \cdot 0.032 = 1920 \text{ kg.}$$

5.

$$S_s = (127)$$

The first scaling slot is at the radius $R_{s,e} = 665 \text{ mm}$, its width 1 mm; the second is at the radius $R_{ss} = 685 \text{ mm}$, its width 1.5 mm. There will be

$$f_{ss} = 2 \pi R_{ss} s = 2 \pi \cdot 68.5 \cdot 0.15 = 64.6 \text{ cm}^2, \mu_{ss} = \mu_s = 0.5.$$

$$f_s = 2 \pi R_{s,e} \cdot s = 2 \pi \cdot 66.5 \cdot 0.1 = 41.7 \text{ cm}^2.$$

The denominator in brackets in Equation (127) has therefore the value

$$1 + \left(\frac{64.6}{41.7} \right)^2 = 3.42.$$

Again we find

$$u_{s,e} = 0.823; u_{ss} = 0.847$$

and the numerator of the first fraction in brackets is

$$0.96 - 0.49 \left(\frac{0.625}{0.665} \right)^2 - \frac{0.68 - 0.72}{4} = 0.96 - 0.434 + 0.01 = 0.54$$

and hence the first fraction in brackets has the value

$$\frac{0.54}{3.42} = 0.158.$$

The second fraction is

$$\frac{0.68 - 0.72}{8} = -0.005,$$

and hence the total expression in brackets $0.158 - 0.005 = 0.153$. The expression in front of the brackets is $\pi (0.665^2 - 0.685^2) \cdot 1000 \cdot 100 = -8800$ kg, and hence

$$S_s = -8800 \cdot 0.153 = -1350 \text{ kg.}$$

$$6. \quad S_m = -\frac{Q}{g} C_s = -\frac{9.4 \cdot 1000}{9.81} \cdot 0.72 = -690 \text{ kg,}$$

because

$$C_s = \frac{Q}{F} = \frac{9.4}{130} = 0.72 \text{ m/sec.}$$

So that

$$S = 37,100 - 1300 + 7380 + 1920 + 1350 - 690 = 45,760 \text{ kg.}$$

For comparison with the second calculating method let us replace

$$S_1 - S_{pi} + S_{pe} = \frac{\pi}{4} (D_{se}^2 - D_{el}^2) \gamma H (c_i^2 - c_0^2),$$

and substitute here

$$c_0 = \frac{c_{ot} + c_{oe}}{2} = \frac{0.65 + 0.7}{2} = 0.675,$$

so that the previously given expression equals

$$\frac{\pi}{4} (1.33^2 - 0.96^2) \cdot 1000 \cdot 100 \cdot (0.96 - 0.46) = 33,400 \text{ kg,}$$

hence

$$S = 33,400 + 1920 + 1350 - 690 = 36,000 \text{ kg.}$$

This agreement is apparently not quite satisfactory.

The load has been calculated for the flow-rate of optimum efficiency, for which the velocity diagrams and the forces acting upon the blades were known. For the full flow-rate we may calculate with a load increased proportionally to the augmentation of the unit through-flow. (See also example p. 245.)

II. DESIGN OF THE GUIDE WHEEL

1. Hydraulic Design of the Guide Wheel

As already pointed out in the first chapter, adjustable guide blades of the Fink type are almost exclusively used at present for the regulation of the through-flow.

The purpose of the guide blades is to supply the water to the runner at a certain velocity and in a certain direction in such a way that these values are the same for the entire circumference. It follows from this that only the discharge part of the guide blade is of importance, whilst from its other parts only the prevention of

superfluous losses is required. For this reason it is not necessary in turbines of different sizes to have the same number of blades as in the model. On the contrary, it is advantageous to select for larger turbines a greater number of guide blades, which are then shorter (their length is given by the requirement of mutual overlapping and thus cutting off the through-flow in their closed position), and also the pitch diameter of the pivots and hence the outer diameter of the turbine will be smaller. For selecting the number of the guide blades, the following approximate formula may be used

$$z_1 = \frac{1}{4} \sqrt{D'} + 4 \text{ to } 6, \quad (134)$$

where D' is the diameter of the outlet edges of the guide blades at full opening in mm.

The magnitude of this diameter has already been dealt with before. For low-speed turbines it is somewhat larger, by 40 to 100 mm, than the inlet diameter of the runner; in turbines of normal speed, the outlet edge is laid (measured radially) about into the places where the meridional curvature of the outer contour begins; for high-speed turbines we select the diameter D' as approximately equal to the outer diameter of the inlet edge of the runner, and in this case we locate the pivots of the blades at the beginning of the meridional curvature of the outer contour of the turbine space. The number of guide blades is always selected so as to differ from the number of the runner blades in order to prevent periodical flow-rate variations when the runner blades pass over the guide blades.

When we change the number of guide blades with the turbine diameter changes, we observe the rule, that at the opening corresponding to the optimum efficiency the diameter of the outlet edges of the guide wheel should agree with the geometric enlargement of the model turbine, and at the same time the outlet angle of the guide blades should also be maintained. In this case, the discharge conditions of the guide apparatus at this opening will be in full agreement with those of the model turbine, and hence also the efficiencies will be in agreement. At other openings this agreement will not be encountered, but the efficiency differences will not be considerable.

We have shown that, as far as the guide blades are concerned, the main importance is the correct design of the outlet blade angle, which must correspond to the velocity diagram. We design this angle for the flow-rate appertaining to the optimum efficiency, and for practical reasons for the maximum flow-rate, too. The angle of the outlet part - of the centre line of the blade - in the one-dimensional solution is given by the meridional velocity at the outlet edge of the guide blade

$$c'_m = \frac{Q}{\pi D' B' \sqrt{2 g H}}$$

and by the peripheral component

$$c'_u = c_{u,0} \frac{D_1}{D'},$$

so that

$$\tan \alpha' = \frac{c'_m}{c'_u}.$$

As to the meridional velocity, we must here take into account the restriction of the outlet cross section due to the thickness of the blade ends by introducing the restriction coefficient

$$\varphi' = \frac{t - s_0}{t},$$

so that

$$c'_m = \frac{Q}{\pi D' B \varphi' \sqrt{2 g H}}.$$

This correction, by the way, is of minor importance since the blades are turnable in any case, and by a slight adjustment the error is adjusted.

In turbines in which we have taken into account an oblique discharge from the guide apparatus, the angle of the outlet end of the guide blade is already determined by the runner design.

In both cases, however, we must bear in mind that the blades must be capable of being opened to a greater angle, α'_{\max} , corresponding to the full flow-rate. We determine this maximum angle either by laying out the velocity diagram for the main flow surface and for the maximum flow-rate (see e. g. Appendix I), or by taking $\alpha'_{\max} = 1.25 \cdot \alpha'_{\eta}$, where α'_{η} is the angle for the maximum efficiency.

As far as the remaining part of the blade is concerned, we endeavour to design it in such a way that no excessive losses are involved.

The main rule is to have a constant contraction of the guide duct from the inlet to the outlet, and consequently a steady rise of the water velocity, and this at any opening. Further, we select a cross section of the guide blade so as to have the least possible losses in the water flow. Here, we may advantageously employ air-foil profiles.¹⁾

These profiles, in fact, are linked to the assumption of the approach and discharge with parallel stream lines, while our case relates to an axially symmetrical flow. We can, however, easily alter the shape of the air-foil profile for this flow by conformal representation by means of a rectangular network, which in the original picture is parallel, whilst in the new picture it is axially symmetrical, as indicated in Fig. 112. The axially symmetrical network must have the same ratio of height to width of the small "rectangles" formed by the circles and radii as in the original network.

As illustrated in Fig. 112, the blades may have various curvatures according to the way in which the water approaches the guide apparatus.

If a turbine is in an ordinary pit, the water approaches approximately radially; the guide blades will then have the shape as in Fig. 112a; through the influence of

¹⁾ See e. g. Letecký průvodce (Aeronautical Guide), Part 2, Prague, ČMT, 1939.

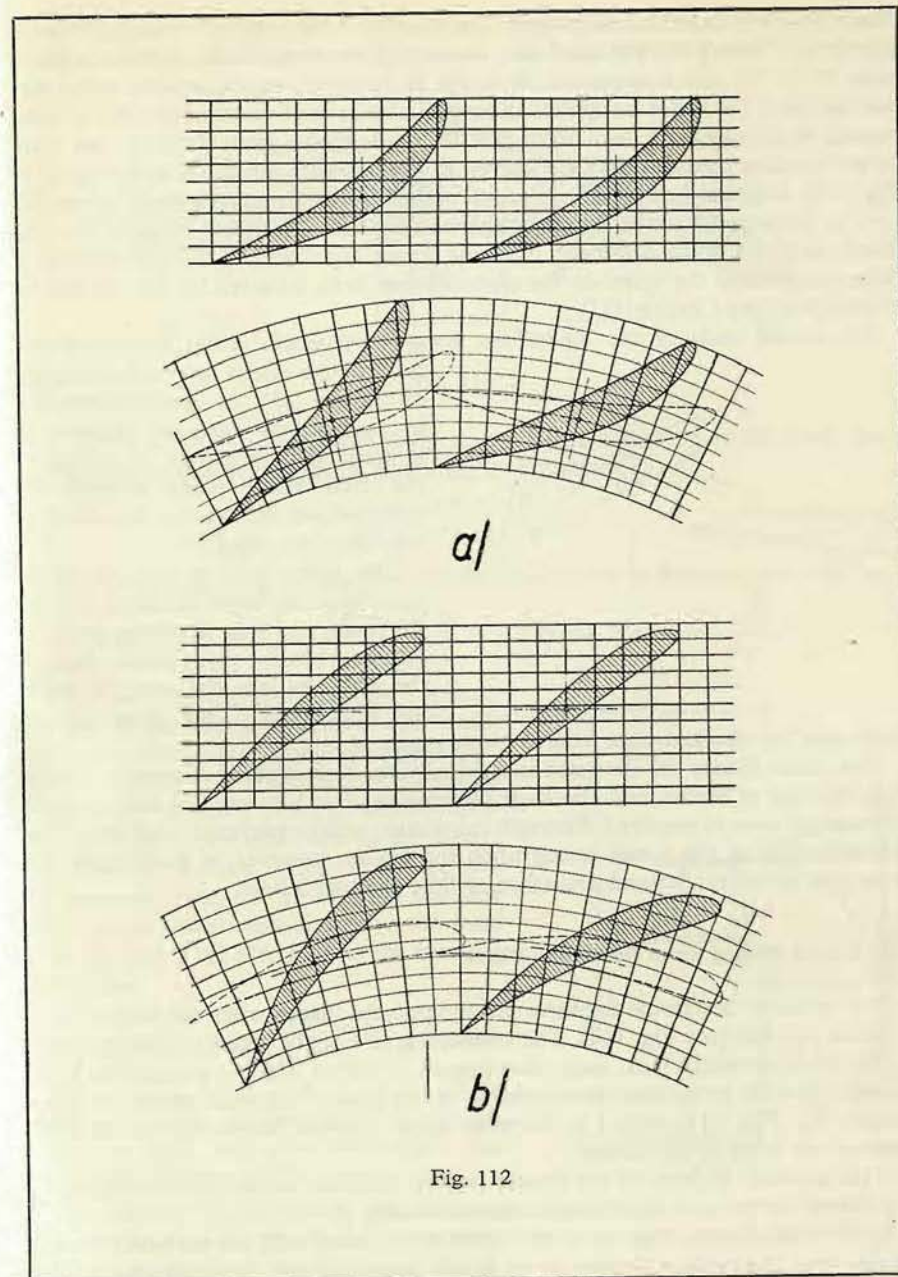


Fig. 112

this shape of blade the peripheral component of velocity is created, or even increased. The inlet end of the blade lies, in this case, as a rule under an angle of from 60° to 70° to the tangent of the circle. If, however, we are dealing with a turbine to which the water is supplied in a spiral, this in itself creates a peripheral component of velocity, so it may occur that the guide blades must decrease this component, and in this case they are curved in the opposite direction, as indicated in Fig. 112b. In spiral turbines the inlet end of the blade is arranged in such a direction so as to correspond (at the opening appertaining to the maximum efficiency) to the direction of the water approach from the spiral, regardless of the fact whether it flows freely from the spiral or the direction has been adjusted by the stay blades of the spiral (see Chapter III).

The outlet ends of the blades are always sharpened, either symmetrically, towards the centre line under an angle of 12° to 20° , or unsymmetrically, in such a way that the sharpening is made approximately according to the circle which passes through the outlet edge at the opening for optimum efficiency (see Fig. 113).

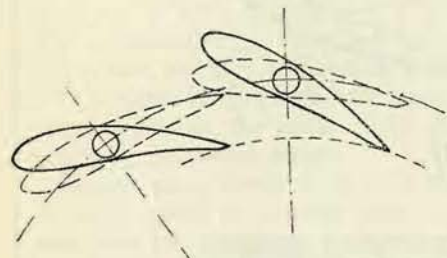


Fig. 113

The cross section of the blade must be of sufficient thickness around the pivot, and this thickness must be greater when the pivot passes through the blade, as it is the case for internal regulation. This cross section must also be checked with regard to strength.

The guide blades are designed individually for each turbine diameter, at least as to number of blades, and also their dimensions; that is to say that new strength controls are always required. Strength calculation will be presented in Part b. The determination of the forces acting upon the blades, however, is based upon the principles of hydraulics and, therefore, will be dealt with here.

2. Forces Acting upon the Guide Blade

It is easier to determine the force acting upon the blades when the blades are in a closed position (see Fig. 114). The connecting line of the contact (sealing) points of the blade separates from each other spaces, in one of which – outside the guide blades – there is a pressure corresponding to the head of the water above the guide blades, H_n (Fig. 115), whilst in the other space – inside the blades – there is the pressure in front of the runner.

This pressure in front of the runner may be different under different operating conditions; let us investigate three important cases.

a) We shall assume that the guide blades were closed with the turbine running; in this case, the turbine slowing down is still in motion and the draft tube is filled

with water. The water in the draft tube develops on the inner side of the guide blades a sucking effect by an underpressure which equals the water column H_d

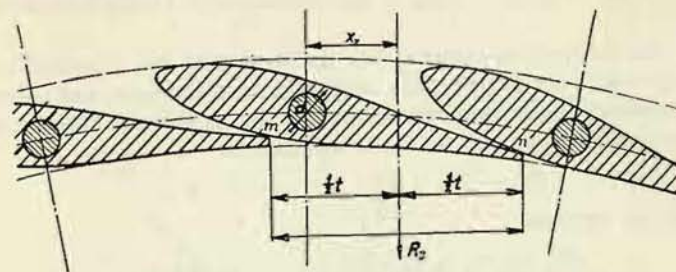


Fig. 114

(Fig. 115) minus the overpressure of the runner. The relative velocities equal zero, and, therefore, this overpressure, according to Equation (25) is

$$h_p = \frac{U_1^2 - U_2^2}{2g}$$

The pressure difference between both considered spaces is therefore given by

$$\gamma H_n - \gamma \left(-H_d + \frac{U_1^2 - U_2^2}{2g} \right) = \gamma \left(H_n + H_d - \frac{U_1^2 - U_2^2}{2g} \right)$$

This overpressure acts upon the connecting line of the contact points of the blade, the length of this line equals the spacing of the blades, t ; the resultant force passes through the bisecting point of this connecting line and is perpendicular to the latter. The effective surface, acted upon by the overpressure, equals $t \cdot B$, B being the face of the guide wheel; consequently, the total force R_z (Fig. 114) acting upon the blade is in this case

$$R_z = \left(H_n + H_d - \frac{U_1^2 - U_2^2}{2g} \right) t B \gamma \quad (135)$$

(when all values are expressed in metres, m/sec., m/sec.², and $\gamma = 1000 \text{ kg/m}^3$, the value of R_z will be given in kg).

The resultant R_z in general will not pass through the pivot of the blade. Its perpendicular distance from it will be x_z . In this

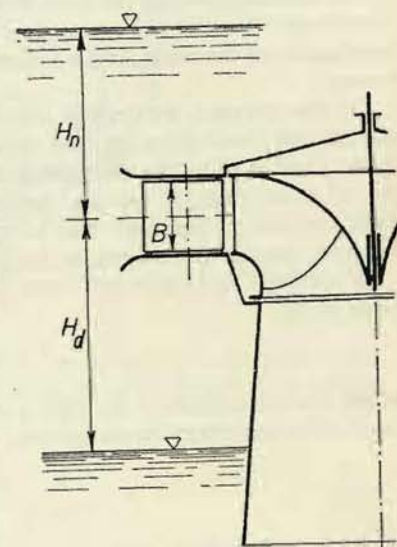


Fig. 115

case, the force R_z endeavours to rotate the blade with the moment

$$M_z = R_z x_z = \left(H_n + H_d - \frac{U_1^2 - U_2^2}{2g} \right) t B \gamma x_z. \quad (136)$$

b) When the turbine has stopped, but the draft tube has remained until then filled up with water, the overpressure of the runner disappears, and consequently the corresponding term in the expression (135), or, as the case may be, in (136), falls off. The force acting upon the blade will then be

$$R_z = (H_n + H_d) \cdot t B \gamma = H t B \gamma \quad (137)$$

and act with the moment

$$M_z = (H_n + H_d) t B \gamma x_z = H t B \gamma x_z. \quad (138)$$

c) When, after the turbine has been stopped, air penetrates into the draft tube through leaks, the underpressure created by the draft tube and given by the water column H_d disappears, and the force acting upon the blade will be

$$R_z = H_n t B \gamma, \quad (139)$$

and the moment will equal

$$M_z = H_n t B \gamma x_z. \quad (140)$$

It is evident that the greatest force and moment will act upon the blade in case b), and we must reckon with these values from Equations (137) and (138) as maximum magnitudes in our strength calculation.

The determination of the force acting upon the blade in an open position is more complicated because the pressure of the water varies continuously along the circumference of the blade, and we must find its value in certain points of the circumference.

For this purpose, we draw at least 3 guide blades in their appropriate positions, and into the blade ducts we draw the stream lines and the trajectories orthogonal to them. Thus, we find the through-flow areas of the duct, and as we know the quantity of water passing, we can determine the through-flow velocities in various cross sections of the duct and according to them, by means of the Bernoulli equation, we can also determine the pressure upon the blade surface.

At velocity C in an arbitrary cross section of the guide duct the following relation holds good

$$h = H_n - \frac{C^2}{2g}. \quad (141)$$

where h is the column of the liquid, expressing the pressure upon the blade in the place of the considered cross section; the pressure upon 1 cm² will be

$$p = \frac{h}{10} = \frac{1}{10} \left(H_n - \frac{C^2}{2g} \right). \quad (142)$$

H_n is again the height of the water level above the centre of the guide wheel as it was in Fig. 115.

Velocity C is determined from the continuity equation for the known flow-rate Q corresponding to the setting of the guide blades (which we know from the velocity diagram, or rather from the characteristic):

$$C = \frac{Q}{z_1 a' B} = \frac{Q}{z_1 F}, \quad (143)$$

$F = a' B$ is the through-flow area of the duct in the appropriate place.

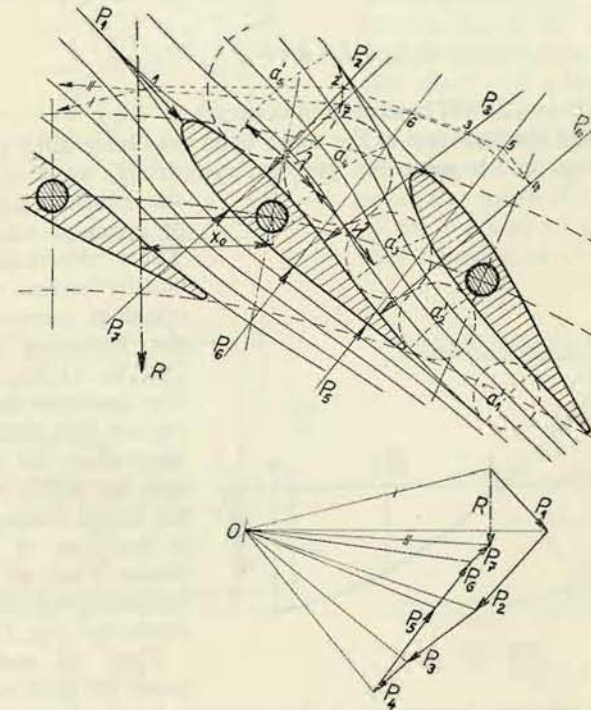


Fig. 116

We then proceed in such a way that we divide the entire circumference of the blade into a number of parts, most conveniently of the same length λ , so that to each part then corresponds the total pressure

$$P = \lambda B p = B \lambda \frac{H_n - \frac{C^2}{2g}}{10}, \quad (144)$$

in which we express λ and B in cm, H_n in m, and C in m/sec., in order to obtain P in kg.

Thus we obtain the individual forces acting in the bisecting points of the lengths λ perpendicularly upon the surface of the blade. These forces we compose graphically into the resultant R , and thus we determine its magnitude, direction and location (see Fig. 116).

The resultant R will not generally pass through the axis of rotation of the blade. Its perpendicular distance from this axis will be x_0 . Therefore, it will act upon the blade with the moment about the axis of rotation

$$M = R x_0 = \Sigma \lambda B \frac{H_n - \frac{C^2}{2g}}{10} x \quad (145)$$

(when x is given in cm, M will be expressed in kgcm).

The moments of the pressures of the water upon the blades differ according to the blade opening, and to solve the problem completely, we must determine the moments for a number of openings of the blades. These determinations are usually carried out for the openings corresponding to the flow-rates 0, $Q_{\max}/4$, $Q_{\max}/2$, $3/4 Q_{\max}$ and Q_{\max} . The moments found in this way are then plotted as ordinates above the co-ordinate axis, on which we indicate the corresponding flow-rates or openings of the guide blades. Thus we obtain the complete progress of the moments (see Fig. 117).

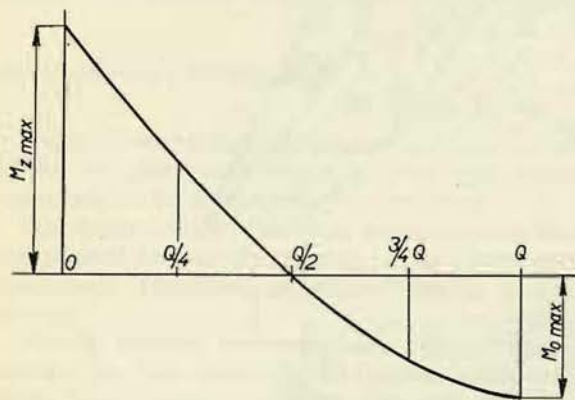


Fig. 117

so as to have the extreme moments, i. e. the moments in the closed as well as in the opened position, of approximately equal magnitudes.

Note: The moments created by the water pressure upon the guide blades may also be measured on the model turbine and recalculated for the actual turbine according to Equation (38). This recalculation, however, holds good only when the number of guide blades on the model and the actual turbine is the same (the assumption of geometrical similarity of the blades, including the pitch circles, too, we already consider as being understood).

III. HYDRAULIC DESIGN OF THE SPIRAL

At small heads (maximum 10 m) and small dimensions of the machine, the turbines are placed into a concrete pit, the shaft being either horizontal or vertical. The approach of the water is disadvantageous, particularly in that part of the

pit into which the water flows at a velocity directed against the rotation of the turbine (Fig. 118), and where for this reason the velocity violently changes its direction; we must therefore select only a low velocity of the water. We select a velocity of 0.8 to 1 m/sec. and specific velocity within the range of 0.05 up to 0.1. Here we select the width B of the pit as $B = D_1 + 1.3$ to 1.5 m, D_1 being the inlet diameter of the runner.

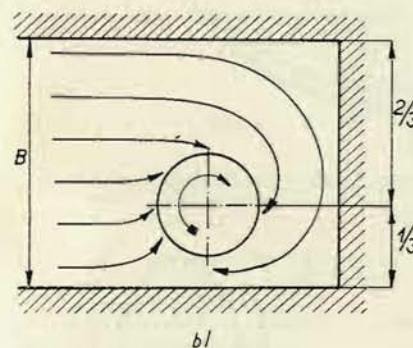
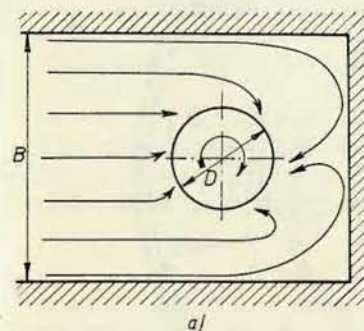


Fig. 118

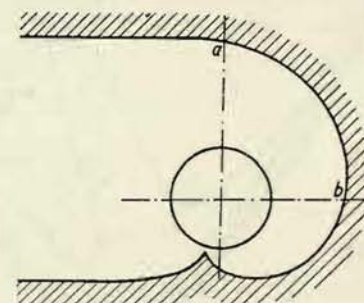


Fig. 119

In order to obtain a more advantageous approach of the water to the guide wheel, it is preferable to place the turbine eccentrically in the pit, as shown in Fig. 118b.

Turbines of larger sizes are placed into a spiral-shaped pit (according to Fig. 119), where approximately $2/3$ of the through-flow are supplied by the spiral with cross sections selected so as to attain always the same mean velocities in them (e. g. the profiles "a" and "b"). The velocity of the inflow is selected somewhat higher than given for the pit, in the specific value of about 0.1 to 0.12.

For heads of about 20 m upwards the spirals are made of sheet metal or cast iron; such spirals then form a constructional part of the turbine. In this case, the spiral completely surrounds the guide wheel and its function is to supply it with

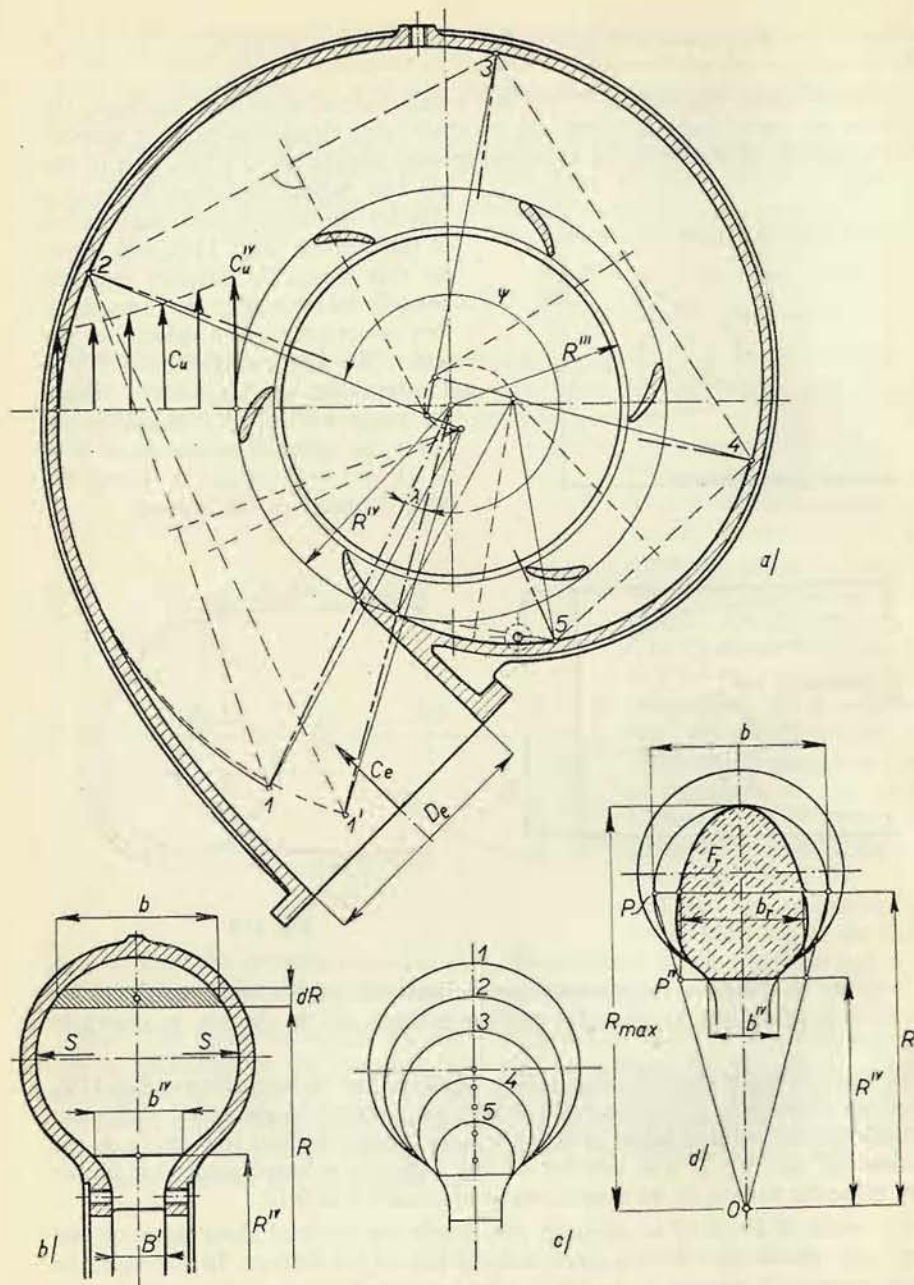


Fig. 120

water uniformly along the circumference (Fig. 120). In order to prevent excessive stress of the spiral due to the water pressure which tends to open it up (the forces S in Fig. 120b), we strengthen it around the inner opening by stay blades. Their strength calculation will be presented in Part *b*, whilst their hydraulic design will be given in this chapter.

Since the water in its flow through such a spiral moves along curved paths, it seems that the peripheral velocity of the particles nearer the spiral axis will be greater and that of the more distant particles smaller according to the law of constant circulation (Chapter I/3), as also indicated for the profile in Fig. 120a: $RC_u = \text{const.}$

If we denote by C_u^{IV} the peripheral component of the flow velocity at the radius R^{IV} of the circle circumscribed about the reinforcing blades, which from the inner side delimit the through-flow profiles of the spiral, the peripheral component of the velocity C_u at the arbitrary radius R is defined by the relation

$$C_u = C_u^{IV} \frac{R^{IV}}{R}. \quad (146)$$

According to Fig. 120b, the elementary quantity dQ , passing through the strip of the width b and the radial dimension dR at the radius R in the cross section deflected from the end of the spiral, (1') by the angle ψ , is then given by the expression

$$dQ_\psi = b \cdot dR \cdot C_u = C_u^{IV} \cdot b \frac{R^{IV}}{R} dR,$$

and the through-flow for the entire cross section equals

$$Q_\psi = C_u^{IV} \int_{R^{IV}}^{R_{\max}} b \frac{R^{IV}}{R} dR. \quad (147)$$

If we determine the so-called reduced width b_{red} according to the proportion

$$b_{\text{red}} : R^{IV} = b : R$$

by means of the geometrical construction indicated in Fig. 120d (similarity of the triangles under the hypotenuses $P^{IV}O$ and PO), the integral

$$\int_{R^{IV}}^{R_{\max}} b \frac{R^{IV}}{R} dR = \int_{R^{IV}}^{R_{\max}} b_{\text{red}} dR$$

is represented by the hatched area in the figure mentioned, and the through-flow is obtained by multiplying the found area F_{red} by the velocity C_u^{IV}

$$Q_\psi = C_u^{IV} F_{\text{red}, \psi}. \quad (148)$$

The place where we must locate this cross section is defined by the angle ψ , measured from the extreme cross section I' of the spiral, which is no longer passed by the water. Since the total flow-rate of the turbine Q , discharges from the spiral along its inner circumference at an angle of 360° (or an angle of $360^\circ - \lambda^\circ$ if we take into account the "tongue" of the spiral – the "splitter" – which occupies a part of the circumference with the central λ), the proportion is

$$\frac{\psi_0}{360^\circ - \lambda^\circ} = \frac{Q_\psi}{Q},$$

so that

$$\frac{\psi^\circ}{360^\circ - \lambda^\circ} = \frac{C_u^{IV} \cdot F_{red,\psi}}{C_u^{IV} \cdot F_{red,1}} = \frac{F_{red,\psi}}{F_{red,1}}. \quad (149)$$

$F_{red,1}$ is here the reduced through-flow area of the cross section I , which is the last through which passes the full flow-rate Q of the turbine. Velocity C_u^{IV} is again linked by the law of constant circulation to the velocity $C_{u,1}$ on the fibre farthest from the axis of the spiral in this cross section, so it applies

$$C_u^{IV} = C_{u,1} \frac{R_1}{R^{IV}}. \quad (150)$$

We select velocity $C_{u,1}$ as equalling the inlet velocity into the throat of the spiral, C_e , which is linked to the flow-rate by the relation]

$$\frac{\pi D_e^2}{4} C_e = Q.$$

One reason for this selection is that all water particles passing from the throat into the spiral itself are accelerated, which means smaller losses than there would arise if some of the particles had to reduce their velocity.

Velocity C_e , which defines the internal diameter of the throat, is selected so as to have its specific value within the range

$$c_e = (0.12) \text{ to } 0.15 \text{ to } 0.20 \text{ to } (0.25). \quad (151)$$

To avoid erosion due to sand entrained by the water, the actual velocity should, however, not exceed 10 m/sec.

Fig. 121 presents the values of the specific inlet velocities c_e of some machines actually manufactured¹⁾ and indicates the approximate dependence of this value on the head; the higher specific inlet velocities c_e at lower heads result mainly from economic considerations, in order to keep the size of the spiral within certain dimensions.

The procedure of the design is as follows:

According to the head we select (using Fig. 121 as a guide) the specific inlet

¹⁾ Kohn, Fr.: Uzavírací orgány vodních turbin (The Closing Organs of Hydraulic Turbines), Strojírenství (Mechanical Engineering) 1952.

velocity into the spiral, c_e , and determine its actual value $C_e = c_e \sqrt{2gH}$. We select the inner radius R'' of the stay blades so as to obtain a small clearance between the end of the stay blade and the beginning of the guide blade at the radius R'' . We assess the radial width of the stay blades, whereby we find the radius R^{IV} .

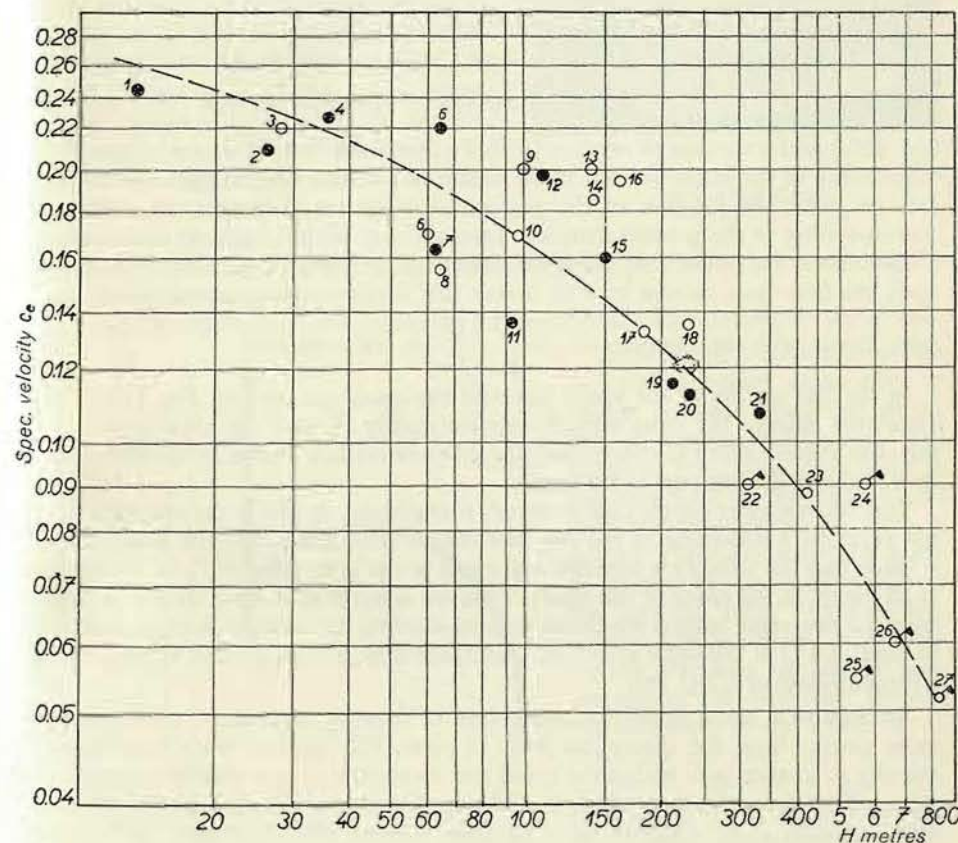


Fig. 121

Erected in Czechoslovakia ●

Pelton turbines ○

- 3 Shannon, Wasserkraft und Wasserwirtschaft 1930.
- 6 Sungari, Wasserkraft und Wasserwirtschaft 1942.
- 8 Génissiat, Schweizerische Bauzeitung 1948
- 9 Grand Coulee Dam, Wasserkraft und Wasserwirtschaft 1943.

- 10 Castelo do Bode, Schweizerische Bauzeitung 1951.
- 13 Niederwartha, Wasserkraft und Wasserwirtschaft 1930.
- 14 Boulderdam, Wasserkraft und Wasserwirtschaft 1941.
- 16 Herdecke, Wasserkraft und Wasserwirtschaft 1930.
- 17 Seibnen, Das Kraftwerk Waggital.
- 18 Rempfen, Das Kraftwerk Waggital.
- 23 Andeer, Wasserkraft und Wasserwirtschaft 1943.

Now we determine the peripheral component of the flow velocity $C_{u'}^{IV}$ at this radius, putting $C_{u,1} = C_e$; according to Equation (150) therefore $C_{u'}^{IV} = C_e \frac{R_1}{R^{IV}}$.

We substitute this value into the expression (148) and apply the relation to the first cross section of the spiral which is still passed by the full flow-rate: hence $Q = C_{u'}^{IV} F_{red,1}$.

By a trial and error procedure we find the shape and size of the first cross section 1 (Fig. 120c) in such a way that its reduced area $F_{red,1}$ satisfies the just mentioned condition $F_{red,1} = \frac{Q}{C_{u'}^{IV}}$. Then we lay out the further cross sections (2, 3, 4, 5, in

Fig. 120c) and according to relation (149) we determine their locations on the circumference of the outer contour circle of the stay blades, and in agreement with this we mark the location of the profiles. The points of these cross sections, corresponding to the greatest distances from the axis of the spiral, we connect by a continuous line, which we compose from circular parts (Fig. 120a). Then we open the first cross section in such a way that a convenient construction of the

inlet throat with the diameter $D_e = \sqrt{\frac{4Q}{\pi C_e}}$ is made possible.

In the last section of the spiral (around the cross section 5 in Fig. 120a) we somewhat enlarge the cross sections (approximately by 10 % of their areas); in this way we endeavour to compensate for the pressure loss caused by the through-flow in the preceding part of the spiral.

Very often a more simple construction¹⁾ is employed, in which the calculation is not performed according to the law of constant circulation, but the assumption is made that the velocity is constant and equal to the inlet velocity C_e in the spiral at all places in the space of the spiral. Thus we select e. g. a cross section at 90° from the first cross section which has an area allowing the through-flow per second to equal $3/4 Q$ at the same velocity C_e , and similarly, a cross section at 180° with a through-flow of $1/2 Q$, etc.

An approach based upon the assumption of constant circulation seems to be more correct from the theoretical point of view. This method leads to a higher velocity at smaller radii within the spiral and consequently to a smaller size of the spiral. Therefore, this procedure is often employed, mainly with lower specific inlet velocities C_e , as encountered in turbines of lower specific speeds. At higher values of C_e (appertaining to turbines with higher unit flow-rates and consequently with higher specific speeds) we find that turbines equipped with such a spiral have a lower unit flow-rate, and maybe also a lower efficiency, than turbines with a spiral designed for constant velocity or even for a velocity decreasing from the inlet to the end of the spiral. These values (unit flow-rate, efficiency) also depend upon the magnitude of the specific inlet velocity in the spiral.

¹⁾ Ténor, A.: Turbines hydrauliques et régulateurs automatiques de vitesse, Part I, Paris, 1935, p. 334.

With a decreasing unit flow-rate, the dimensions of the runner and of the whole turbine increase and also the costs; therefore it is, not advisable to select too high a specific inlet velocity C_e . For high-speed turbines (high-speed Francis and Kaplan turbines) it is preferable that the spiral is designed so that we calculate with a decreasing¹⁾ through-flow velocity from the inlet to the end of the spiral (to the tongue), according to an ellipse quadrant to nearly zero.

As far as high-speed turbines are concerned, it is, therefore, also advisable to use for the ordered turbine spirals of the same hydraulic shape as tested on the model turbine or, at least, to preserve the same velocity progress.

The discrepancy can be explained by a secondary flow arising in the spirals.

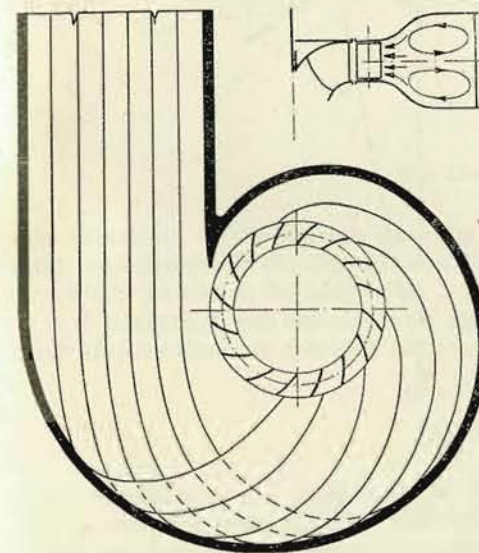


Fig. 122b



Fig. 122a. Picture of a stream line at the wall of the spiral

Experiments²⁾ have shown that no axial symmetry exists even in spirals designed according to the law of constant circulation. The pressure rises from both sides in the direction of the tongue and here the velocity of the flow is lowest. These variations are mainly caused by the transition from the straight inlet. Thus a secondary flow is set up, which materially increases the radial components of the velocities towards the side walls of the spiral. If we construct the inlet with a flatter curvature, and of a more flat shape, the axial asymmetry will be considerably increased; on the other hand, a more intense curvature of the inlet only results in a slight decrease of asymmetry.

If we eliminate the tongue (split-

¹⁾ See also Ténor A.: Turbines hydrauliques et régulateurs de vitesse, Part I, Paris, 1935, p. 338.

²⁾ Kraus H.: Strömung in Spiralgehäusen, Zeitschrift des Vereines deutscher Ingenieure (1935). Vol. 79, No. 44, p. 1345.

ter) from the spiral, the friction losses will be smaller, but, the deviations due to secondary flow will increase.

The guide blades equalize the flow considerably, and even more so, if they are closely spaced and set more in the direction of the wall of the spiral. Fig. 122a (see also Fig. 147, p. 236.) shows a photograph of the stream lines at the wall of the spiral; Fig. 122b indicates the creation of the secondary flow. It is obvious that a design according to constant circulation, although apparently justified from the theoretical

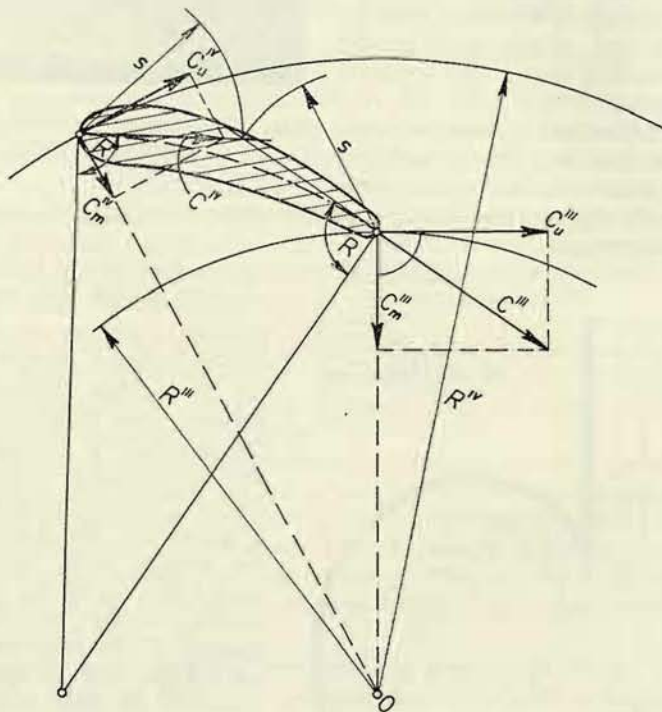


Fig. 123

point of view is not justified in fact. On the other hand, it is clear that the stay blades of the spiral are advantageous, and also, exert the same influence as the guide blades, which improve the flow within the spiral and the efficiency of the turbine. Let us now deal with stay blades.

The cross section area of the stay blades of the spiral is given by strength considerations. The hydraulic design of these blades is directed to the selection of such a shape of their cross section and to such a position in front of the guide blades so that they offer the least possible resistance to the flow of the water. For this reason, we have selected, the shape of the cross section of the stay blades similar to that

of an airfoil; the deflection must be of such a shape as to secure a shockless approach of the water from the spiral. The end must have the same inclination as that at the beginning of the guide blades, particularly when in position according to optimum efficiency.

The angle under which the water must approach from the spiral is easily determined, because we know the peripheral component C_u^{IV} , so we can also find the meridional component $C_m^{IV} = \frac{Q}{2\pi R^{IV} b^{IV}}$, (where b^{IV} is the width of the spiral at the radius R^{IV} at the inlet ends of the blades). By composing them we find both the magnitude of the total velocity C^{IV} and its direction (see Fig. 123). Since both the peripheral component and the meridional component of velocity C^{IV}

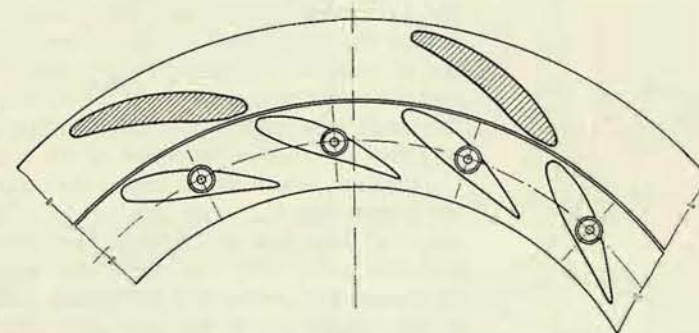


Fig. 124

are in proportion to the through-flow, the direction of this velocity does not change with changes in the through-flow. It is, therefore, of no account which through-flow we take as the basic value.

If it is compatible with the design of the guide blades, we shall endeavour to arrange the stay blades so that they exert no influence upon the flow, i. e. to have

$$C_u^{III} = C_u^{IV} \frac{R^{IV}}{R^{III}}$$

and

$$C_m^{III} = \frac{Q}{2\pi R^{III} B},$$

Then we draw the initial and final directions with regard to the contour circles in such a mutual position that the intersection cuts off on both directions the equal segments S (see Fig. 123). Then we inscribe between them a part of a circle along which as a centre line we lay out the cross section.

The profile of the stay blades is very often made inversely, with the narrower end directed against the flow, as indicated in Fig. 124. In this case, there is more material in the places subjected to the greatest stress (Part B, Chapter V).

IV. HYDRAULIC DESIGN OF A DRAFT TUBE

The function of the draft tube has already been explained in Chapter V, Part I. There, the two purposes of the draft tube have been pointed out: First, a draft tube permits to locate the turbine within certain limits (defined by cavitation considerations) independent of the tail water level, and, second it permits, at least partially, to utilize the discharge velocity from the runner. With increasing specific speeds this second purpose assumes greater importance, so that for high-speed runners we must employ a draft tube even if for cavitation reasons the runner must be located below the tail water level.

The draft tubes only utilize the meridional component of velocity, because they reduce this component, and so convert it into pressure. If they had to utilize also the peripheral component, they would have to reduce this component as well. Considering the law of constant circulation $r C_u = \text{const.}$, we see that this could be carried out if the discharge from the draft tube passed to a large radius, in such way that no sudden reduction of the component C_m resulted (which would impair the utilization of the component C_m - see further). The simplest shape of draft tube which meets this requirement is shown in Fig. 125. The meridional section can be designed to reduce the meridional component of the velocity in the required way¹. Draft tubes based upon this principle are mainly made in America and known under the name of hydraucone. Fig. 126 shows the hydraucone of White and of Moody. Nevertheless, they did not come up

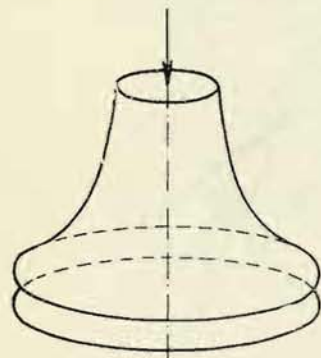


Fig. 125

to the designers' expectations and are now not used so much in America. Their failure has been obviously caused firstly by the enlargement of the wetted surface resulting in greater losses due to the friction of the water, and secondly by the circumstance that the circulating component sets up a secondary flow in the form of a whirling ring within the draft tube, which cannot be prevented even by these designs.²

If we divide the regain from the draft tube into a component expressing the regain from the meridional velocity and a component expressing the regain from the peripheral velocity we get

$$v = \eta_s (c_2^2 - c_1^2) = k_m \cdot c_{m,2}^2 + k_u \cdot c_{u,2}^2 \quad (152)$$

then the coefficient k_u has a small value, which, according to Thomann,³) is about

¹) Kaplan-Lechner: Theorie und Bau von Turbinen-Schnellläufern, Berlin, Oldenbourg, 1931, p. 226.

²) For details see Thomann R.: Die Wasserturbinen u. Turbinenpumpen, Part 2, Stuttgart, Wittwer, 1931, p. 158.

³) Loc. cit., p. 160.

$k_u = 0$ to 0.1 to 0.4. The coefficient k_m , on the other hand, is approximately the value:

$k_m = 0.7$ to 0.85 to 0.9 for straight draft tubes,

$k_m = 0.6$ to 0.85 for draft tubes with an elbow,

according to the perfectness of the construction.

The most perfect conversion of the component C_m is offered by a draft tube in the shape of cone of revolution, the angle of taper, however, must not be too great

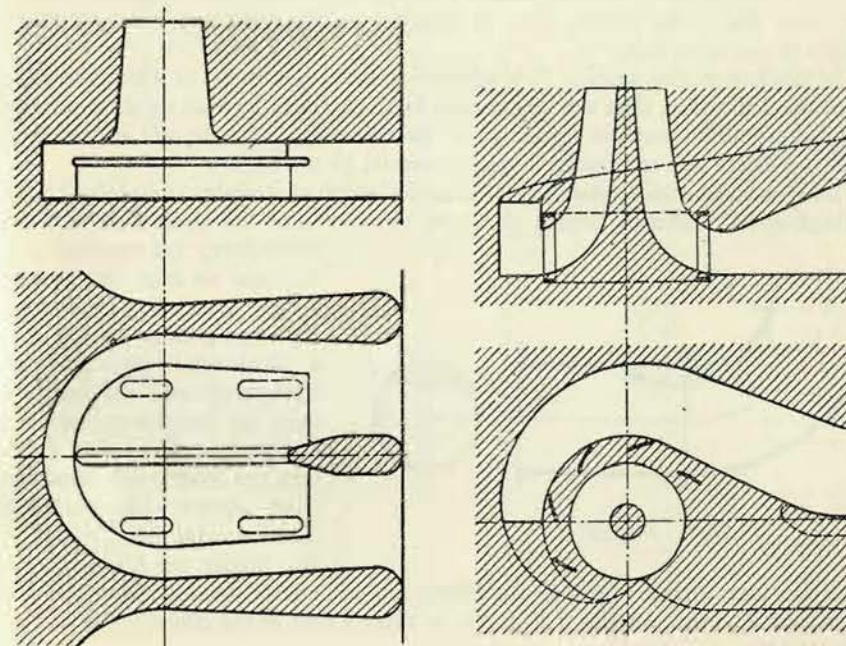


Fig. 126

as otherwise the flow from the walls of the draft tube would depart. A properly regulated flow is in this case confined to a cone with a vertical angle of about 10° .¹) Otherwise, whirls would be created, between the cone and the wall of the draft tube causing great losses and impairing the efficiency of conversion. If, on the other hand, the vertical angle of the tube is too small, the cone would be too long for given discharge velocity (discharge area), and losses due to friction on the extended wall would again reduce the efficiency of the conversion. Apart from this,

¹) Kaplan-Lechner: Theorie und Bau von Turbinen-Schnellläufern, Berlin, Oldenbourg, 1931, p. 225.

it is also desirable from the constructional point of view that the draft tube is as short as possible. For this reason, we select the vertical angle within the range of 8° to 13° . This is also expressed by the formula

$$\frac{\sqrt{F_4} - \sqrt{F_3}}{L} = \frac{1}{5} \text{ to } \frac{1}{8}, \quad (153)$$

where F_4 is the area of the end cross section of the draft tube, F_3 the area of the inlet cross section, and L the distance (length of the draft tube). This formula is suited also for shapes other than that of a cone of revolution, but assumes a uniform taper over the entire length, i. e., it must be satisfied for any two subsequent profiles of the draft tube.

The discharge cross section F_4 is selected so that velocity C_4 , at which the water leaves the draft tube, does not drop below 1 m/sec. (in order that no air is retained in the draft tube), but the square of its specific value, c_4^2 must not exceed 0.04, otherwise losses due to unutilized velocity would be too high.¹⁾

This condition would result in an excessive length of straight conical draft tubes for high-speed turbines, where the inlet velocity into the draft tube is high.

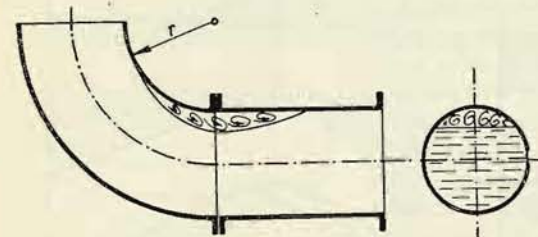


Fig. 127

Therefore, for vertical-shaft turbines we must also employ a bent draft tube, in order to have the greater part of it in a horizontal position. For horizontal-shaft turbines, always an elbow must be used.

The insertion of an elbow into the draft tube manifests itself always unfavourably.²⁾

The harmful effect is greater, the higher the velocity is at

which the water streams through the elbow, i. e. the nearer the bend of the draft to the runner. For this reason, it is better to place a part of the conical tube in front of the elbow.

In order to clearly understand the influence of an elbow upon a draft tube and of the rules for its design, let us consider Kaplan's experiments concerned with this problem.³⁾ On a model turbine Kaplan studied the effect of a combination of a straight tube (without taper), a rectangular elbow (a constant cross section), and a cone of revolution, and arrived at the following results:

When using only an elbow at the back of a runner, he found an efficiency of 54

¹⁾ Czechoslovak Standard "Vodní turbíny, předpisy pro zkoušení a záruky hydraulických a regulačních vlastností" ("Hydraulic turbines, directions for testing and guarantee of hydraulic and regulating properties"), ČSN 085010-1951, Part 5.

²⁾ Dubs: Die Bedeutung des Saugrohres, Wasserkraftjahrbuch, 1924, p. 437.

³⁾ Kaplan-Lechner: Konstruktion und Bau von Turbinen-Schnellläufern, München, Berlin, Oldenbourg, 1931, p. 219.

to 55 %; with only a straight tube, efficiency was 62 to 63 %; the combination of an elbow with a cone immediately behind, resulted in efficiency of 59 to 60 %; the arrangement of a straight tube behind the elbow led to efficiency of 61 to 63 %; and, finally, the combination elbow – straight tube – cone showed an efficiency of 66 to 67 %.

Thus, it is obvious that with the cone connected directly behind the elbow the efficiency was lower than if behind the elbow only a straight tube was used. This is

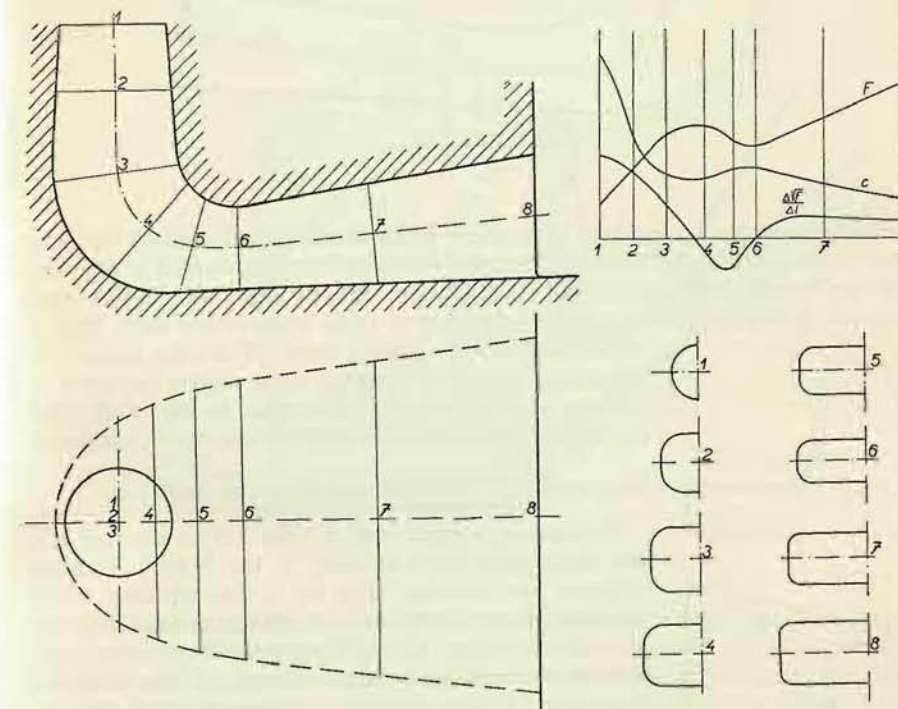


Fig. 128

evident from Fig. 127. In the end part of the elbow, on the side of the greater curvature, a space was created, filled with whirls, which restrict the through-flow area, and, in addition, the whirls absorb energy. When the cone was directly connected behind the elbow, this „dead space“ was extending into the cone, and the flow was no longer adhered to the wall of the cone, and the latter could not fulfil its function. When a straight tube was connected to the elbow, the flow returned to the wall – as indicated in the figure – and this improved efficiency. The cone connected to the straight tube could develop its full effect.

These results offer us a rule which must be observed in the design of an elbow-

fitted draft tube, as far as higher through-flow velocities, (i. e. draft tubes for high-speed turbines), are concerned. We must prevent the departure of the flow from the wall in the elbow. We achieve this by reducing the through-flow cross sections

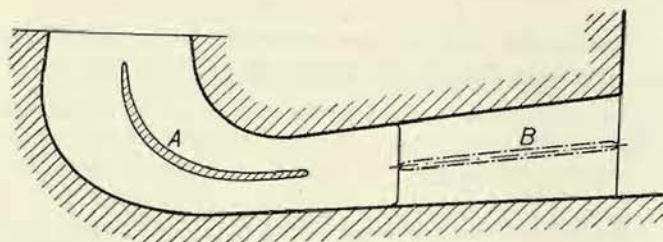


Fig. 129

of the elbow in the second half, in the same way as if in Fig. 127, we lead the inner wall of the elbow along the discontinuous surface between the regions of the flow and the whirls. Only further on we can again increase the through-flow cross sections. Formula (153) is applied here only to those parts of the draft tube in which the flow is slowing down. The part behind the elbow has then a rectangular cross section in order to achieve a small height, (illustrated in Fig. 128). This figure also indicates the progress of velocity C , surfaces F and ratio $\frac{1/F}{L}$ over the length of the draft tube.

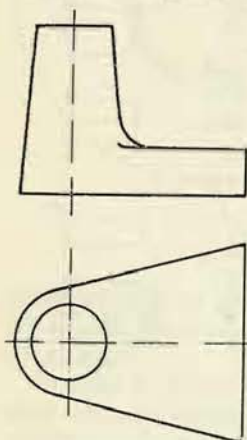


Fig. 130

Sometimes, a guide wall A (Fig. 129) is inserted into the elbow to guide the water in the bend.¹⁾ This can improve the function only at a through-flow which corresponds to a perpendicular discharge from the runner. At all other throughflows, on the contrary, the function is impaired by the influence of the shockwise destruction of the rotational component, and for this reason the described partition is no longer employed. If the width of the last cross sections of the draft tube is very large, a vertical wall B is inserted to support the ceiling. This wall somewhat reduces the efficiency, and therefore we endeavour to eliminate it.

The peripheral component of the velocity behind the elbow causes an irregular discharge from the draft tube. In that half of the draft tube in which in the horizontal part the component C_u is added to the mean through-flow velocity a higher discharge velocity appears, often accompanied by violent discharge. But in spite

¹⁾ Dubs: Die Beeinflussung des Wirkungsgrades durch das Saugrohr, Wasserkraftjahrbuch 1925/26, p. 338.

of this, better efficiency is obtained by this draft tube than by one where the regular discharge has been achieved by forcibly suppressing the peripheral component within the draft tube.

As we have shown, the main source of losses in the elbow of the draft tube is the inner wall with the sharper curvature. The curvature of the outer wall is of minor importance, which is proved by the Kaplan draft tube where the outer wall changes its direction under a right angle.

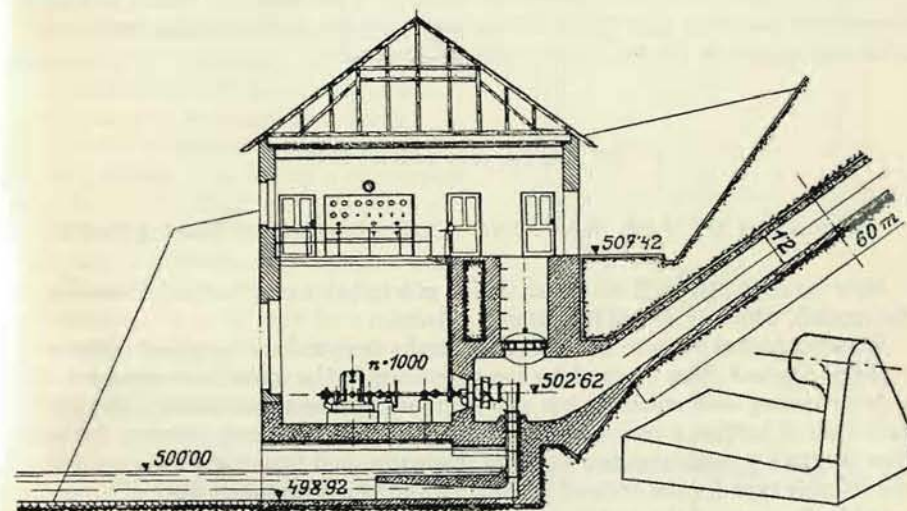


Fig. 131

Fig. 130 shows the shape of such a draft tube with one bend, Fig. 131 a design with two bends. The abrupt bend is filled with a water cushion, which, however, is not stationary; its motion absorbs work, and therefore, the efficiency of this draft tube is somewhat lower than that of a properly constructed draft tube with a rounded transition.

For completeness we must mention that draft tubes were also suggested with a shape of a body of revolution, but with the generatrix departing from a straight line. Thus, e. g., if in a vertical draft tube we denote the vertical distance from the basic plane under the last profile by z and the radius of the profile by r , the generatrix of the draft tube designed by Prášil¹⁾ was defined by the relation $zr^2 = \text{const.}$; we can derive that, in this shape, the retardation of the flow is proportional to the (meridional) velocity, $\frac{dC_m}{dt} = \frac{Q}{\pi \text{ const.}} C_m$. The generatrix of the draft tube

¹⁾ Prášil: Über die Flüssigkeitsströmungen in Rotationshöhlräumen, Schweiz. Bauzeitung, fol. 41 (1903).

suggested by Grimm was defined by the relation $zr^3 = \text{const.}$ The improved efficiency of these draft tubes, however, did not counterbalance the increased costs of manufacturing, and, therefore, they are no longer used.

From these considerations it follows that the efficiency of the draft tube depends to a considerable extent upon the conditions under which the water enters (distribution of the velocities, the component C_u , etc.). A draft which has proved satisfactory with one runner may, therefore, be a failure in connection with another runner. For this reason when designing high-speed turbines, the model turbine is tested with that draft tube which will be used with the actual turbine, and it is not advisable to change the shape of the proved draft tube.

B) ACTUAL DESIGN

I. DESIGN OF THE MACHINE AND CONSTRUCTION UNITS

Now we shall deal with the actual design of a full-size machine (in distinction to the model), which relates to the turbine ordered.

We assume that we have already hydraulically designed the necessary number of types and tested them on models; measurements in the model rest room are not only concerned with efficiency but also with the cavitation coefficients¹⁾, so that for each type of turbine a complete characteristic is at our disposal. Further, for each type we have a predetermined series of diameters, and from these data we select, the suitable type for the ordered turbine (with the appropriate values of n_s) and a suitable diameter of the turbine, given by the inlet diameter of the runner (see Part I, Chapter XI).

After having determined these values, we can start designing the machine. First, we lay out the complete installation of the machine, whereupon we direct our attention to the design of the individual constructional units and their details. In this work we shall sometimes be compelled to depart somewhat from the initial layout and make certain changes. From the drawings of the details we finally compose the drawing of the definite arrangement of the machine. This drawing is not only indispensable for the manufacture and assembly of the machine, but also provides a control of the mutual conformity of the individual constructional units.

For Francis and Kaplan turbines we may count with the following principal constructional details, e. g. according to the arrangement shown in Appendix VI:

1. Runner with labyrinths and connections to the shaft, and the shaft itself.
2. Guide apparatus, i. e. guide blades with their seat and regulating mechanism consisting of the regulating cranks, pull rods and regulating ring.
3. Extension of the regulation, i. e. regulating pull rods, regulating heart, regulat-

¹⁾ For a description of a cavitation test room see e. g.: V. Foltýn, Kavitační zkoušky na modelech vodních turbin (Cavitation tests on models of hydraulic turbines), Strojnický obzor (Mechanical Engineering Review) 1950, No. 12.

ing shaft and seat, or, for large turbines, servomotors to be mounted in the turbine shaft, with pull rods.

4. Spiral casing with a ring of stay blades.

5. Top (front) lid of the turbine with labyrinths, stuffing box, and bearing with accessories.

6. Bottom (rear) lid of the turbine with extension for connecting the draft tube.

7. Draft tube with air supply valves.

8. Gear case with auxiliary drives.

9. Other accessories, such as operating floors, piping, if necessary a supporting ring between turbine and generator, etc.

According to this list we shall now stepwise deal with the design of the individual details, taking into account the strength calculations (in so far they have not been dealt with in Part A), as well as manufacturing considerations and the selection of the materials for construction.

II. RUNNER AND SHAFT

1. Runner

a) *Runners with steel plate blades cast in to the disc and rim of the runner.* With regard to the progress in foundry technology no difficulties are encountered when casting the runner with the blades as one unit, and, therefore, blades pressed from steel plate and cast into the disc and rim of the runner of gray cast iron or cast steel are nowadays very rarely used. It is not advisable to employ them for heads exceeding 30 to 60 m as runner manufactured in this way show inferior strength properties.¹⁾

The blades in this case are pressed by means of press dies (see Fig. 132), which are made of gray cast iron as will be described later. In these, the blades are hot-pressed. Large blades are also pressed in power presses. After pressing, the blades are trimmed precisely to the correct shape.

¹⁾ Thomann R.: Die Wasserturbinen und Turbinenpumpen, Part 2, Stuttgart, K. Wittwer, 1931, p. 137.

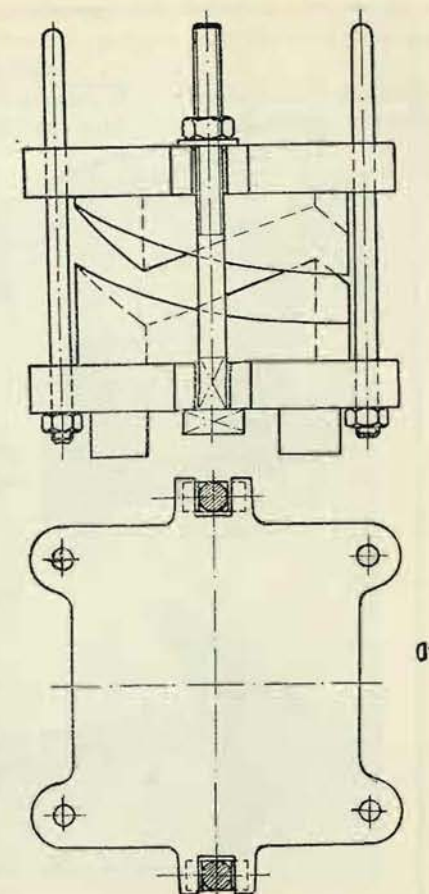


Fig. 132

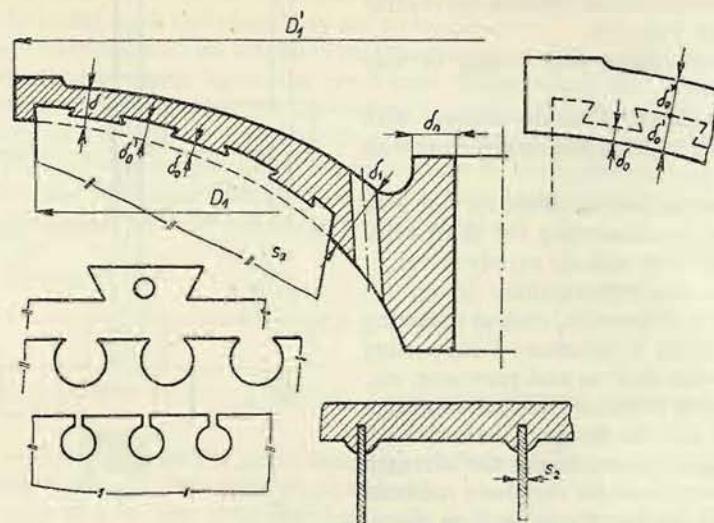


Fig. 133

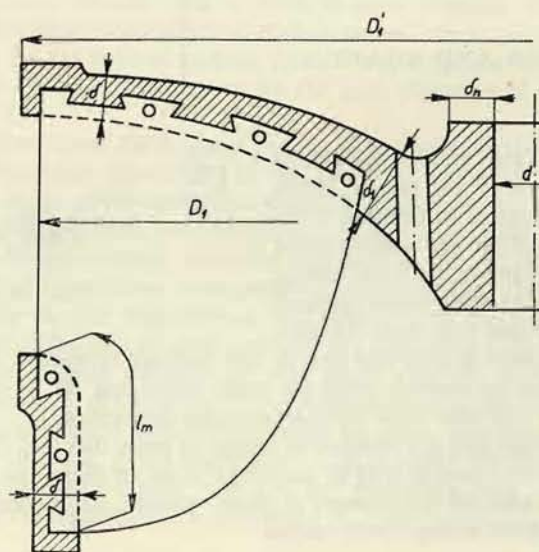


Fig. 134

Here, the blades are of a uniform thickness throughout; they cannot be profiled. If they are to be profiled, forging dies of special material must be employed and the blades must be forged under a forging press.

The pressed blades are then inserted into a mould if the runner is to be moulded. In order to secure the correct position, they are held by a so-called cage which is

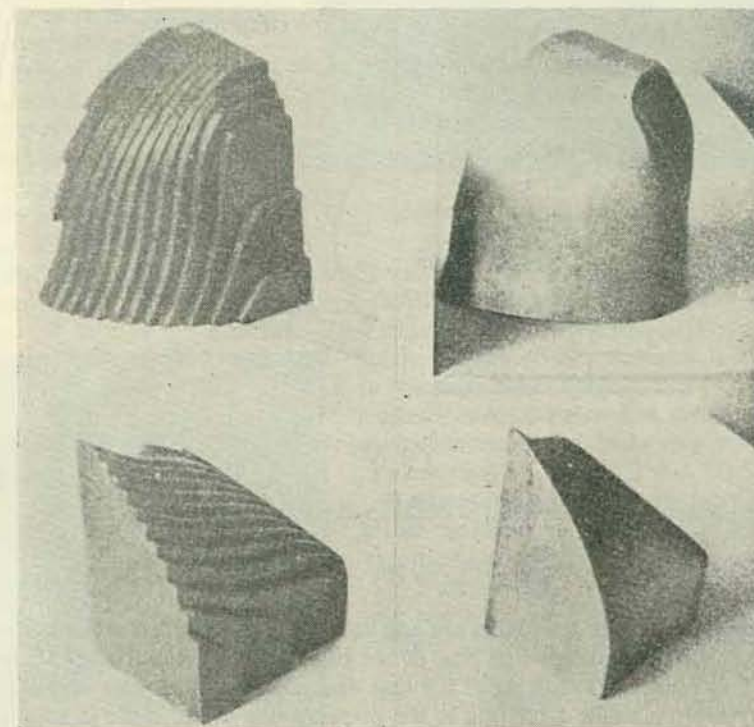


Fig. 135

only taken asunder after the moulding sand has been stamped into the space between the blades. The part of the edge of the blade which is to be cast-in must be carefully cleaned and tin-coated to protect it from rusting in the mould.

In spite of this procedure, the material of the blades does not combine with the cast material, it is not welded to it, even when connected to cast steel. The anchoring of the blades in the disc and rim of the runner is brought about only by clamping the blade ends in the cast material when the latter has cooled down. For this reason, the blades must penetrate rather deeply into the cast material, and disc and rim must be of sufficient thickness. In order to achieve more perfect connection, the cast-in ends of the blades are fitted with dovetail notches and bores, as indicated in

Figs. 133 and 134. For the dimensions of the cast-in parts, the following values may be taken as an approximate guide¹⁾

$$\delta_0 = 1.5 s_2, \delta'_0 = 3.5 s_2, \delta''_0 = 2.5 s_2.$$

The thickness (mm) of the disc and rim (Fig. 134) is selected according to the following formulas:

$$\begin{aligned} \delta &= (20 \text{ to } 25) + 0.01 D_1 \text{ at the circumference} \\ \delta_1 &= (25 \text{ to } 35) + 0.01 D_1 \text{ at the hub} \end{aligned} \quad (154)$$

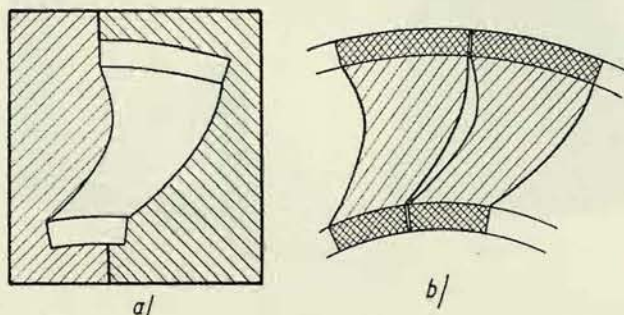


Fig. 136

The thickness of the hub itself is made in dependence of the bore:

$$\delta_n = (10 \text{ to } 20) + \frac{d}{4} \text{ mm.}$$

The pressing dies for the blades are cast according to a wooden pattern, which is made by means of a contour-line plan of the blade. When establishing the dimensions of this plan, the shrinking of the cast dies must be taken into account. The wooden pattern is made according to the pressure side of the blade in such a way that the contour lines are transferred (by piercing pins through the original drawing) to small wooden boards the thickness of which equals the spacing of the contour line planes. According to these contour lines the wooden boards are trimmed and glued on one another (see Fig. 135). The edges of the boards are then removed by means of a rasp and thus a smooth patterns of the die is obtained (see Fig. 135b). According to this pattern the dies are cast from cast iron, one directly according to the pattern, while the other is moulded after fastening to the pattern a lead plate of the same thickness as that of the steel plate from which the blades are to be pressed; the lead plate is adjusted to the shape of the pattern by hammering. Prior to moulding, the pattern is, of course, supplemented by a base plate with risers for bolts and guide pins (Fig. 132) or for fastening it in the press.

¹⁾ From the lectures of Prof. Kieswetter: Vodní stroje lopatkové (Hydraulic Turbomachinery), Donátův fond, Brno, 1939.

The pressed blades need no further machining for hydraulic reasons; they are only cleaned from scale and sharpened at the inlet and outlet edges according to the directions given in the part dealing with hydraulic design.

As already pointed out, this manufacturing process is falling into disuse and only used for turbines of small outputs and dimensions. The reason for this is firstly the imperfect fixing of the blades into the cast material, and secondly the considerable cost of manufacture and storage of the dies. Another shortcoming is presented by the safety factor in using plates of stainless steel (for cavitation reasons – see further), because this material is subjected to heating when being cast-in, and the blades – near the rim and disc – lose their cavitation resistance and may even crack in operation.

Runners are already manufactured with blades fastened to rim and disc by electric welding (Fig. 209.).¹⁾

b) Runners with blades cast as one unit with the wheel are exclusively used for higher heads, large machines and large outputs.

In this case, the runner is cast from cast steel into a mould manufactured by means of a pattern which is made according to the outer contours of the runner and in which the necessary spaces of revolution for placing the core marks are provided. Then the cores are inserted into the mould to fill the spaces of the ducts.

These cores are made in a wooden core box in which the blade surfaces are again composed by means of wooden boards glued together and trimmed according to the contour lines, as described in the manufacture of the dies for pressed blades. Fig. 136a shows such a core box, and Fig. 136b the cores made in it; for better



Fig. 137a

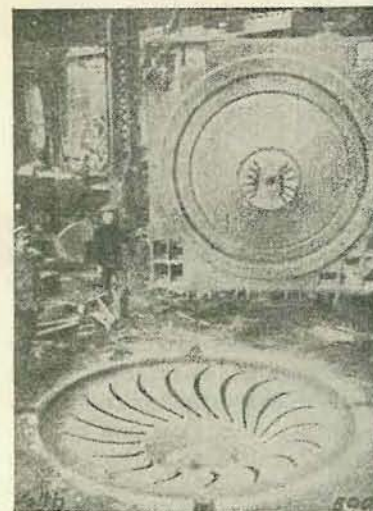


Fig. 137b

¹⁾ Salto de Castro, Water Power (1953), p. 84.

clarity, the core marks are indicated by cross-hatched areas. Fig. 137a shows the insertion of the cores in the mould, and Fig. 137b the mould before closing. After moulding and annealing the castings, the blades and the wetted surfaces

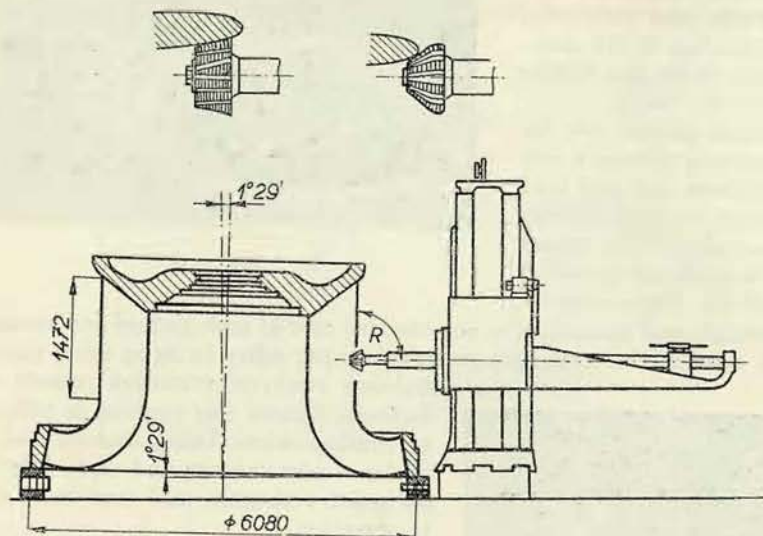


Fig. 138

of the disc and rim must be manually ground in order to obtain the necessary smoothness to secure the smallest possible losses due to the friction of the water along the blade. The inlet edge may be milled¹⁾ (Fig. 138).

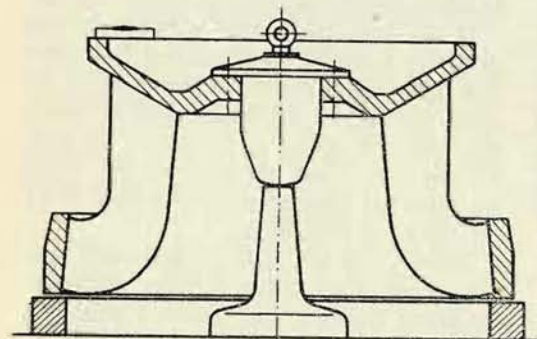


Fig. 139

The other part of the runner is machined to a smooth surface in order to reduce friction losses in the water flow and to facilitate balancing, which (after complete machining) is advantageously carried out, as indicated in Fig. 139.

The walls of the rim and disc are made somewhat thicker than the maximum thickness of the blades; the thickness of

¹⁾ Gamze i Goldsher: *Technologiya proizvodstva krupnykh gidroturbin*, Moskva, Leningrad, Gosudarstvennoye nauchnotekhnicheskoye izdatelstvo, 1950, p. 159.

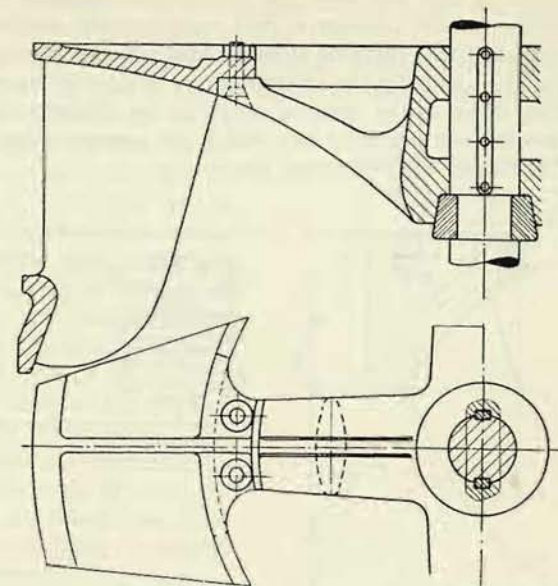


Fig. 140

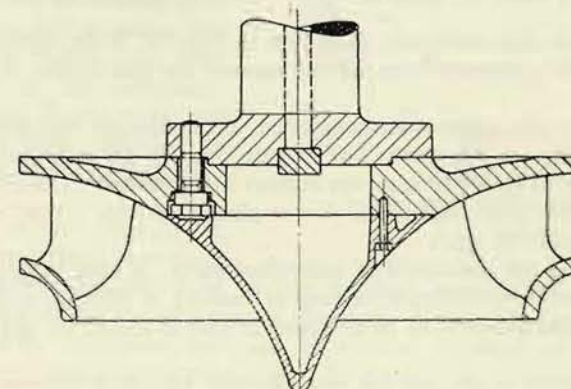


Fig. 141

the disc being greater than that of the rim. Since rim and disc are spatially curved, their strength is high and need not be specially checked.

c) *Further construction rules common to both manufacturing methods.* The outer edge of the disc for low-speed turbines as well as the rim are reinforced (Fig. 36), which, on the one hand, reduces the internal stress in the casting process due to the retarded cooling down of the material, and, on the other hand, provides the possibility of hollowing out a groove into which the counter-weights are placed when balancing the runner after complete machining.

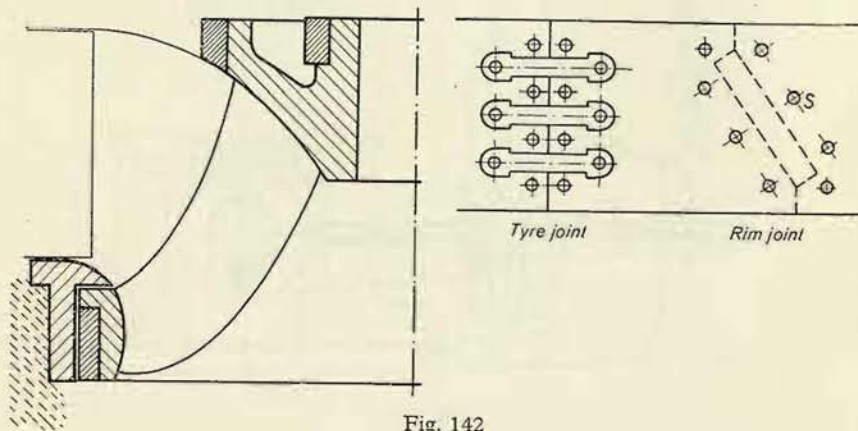


Fig. 142

The hub itself has a thickness of $\frac{d}{4} + (10 \text{ to } 20) \text{ mm}$ and if necessary, is fitted with a reinforced circumference, as shown in Fig. 36. With regard to foundry requirements, the transition from the thickness of the disc to that of the hub must be gradual.

As far as large-size runners are concerned, difficulties are encountered not only in casting but also in transport. The largest runners manufactured as one unit are those of the hydro-electric power station Dnieprostroy (USSR), which have a diameter of 5450 mm¹⁾ and of the power plant Garrison (USA) with diameter 6 m and weight 85 000 kg.²⁾

Larger runners are composed of individual parts. If only weight reduction is concerned in order to facilitate casting or making it altogether feasible, or of savings of stainless steel are to be achieved in case it should be indispensable for

¹⁾ For a description of the machine see: „Turbina LMZ tipa Frensisia moshchnosti 102,000 Ks“. *Viestnik mechinostroeniya* 1947, pp. 25—26. Foundry technology, description of the mould and casting procedure for this runner see in „Osobennosti technologii otlivki rabochego kolesa i statora gidroturbiny Frensisia dlya Dnieprovskoy Ges“, in the same issue on pp. 59—63.

²⁾ Engineering News Record (1955).

the wheel itself, the hub is made separately and the wheel is bolted to it (the bolts must be well secured, most advantageously by point welding). An example of such a construction is presented on Fig. 140.

Subdividing the entire wheel is difficult. Splits are made between the blades, and both halves are joined e. g. by means of hoops. An example of this method is illustrated in Fig. 142 which shows the runner at the power station Conowingo (USA); it has a diameter of 4870 mm and is fitted with 15 blades. The runner consists of three parts connected by steel tyres, two of which, on the hub, are in one-part, whilst the tyre on the rim is split and joined by hoops. The joints of the rim alternate with those of the tyre and are filled with white metal. The joints of the rim are reinforced by screws “S”, the heads of which are countersunk and welded-in. The output of the machine is 54,000 metric horsepower.

A very ingenious method of joining¹⁾ is presented in Fig. 143, where the dividing splits in the disc and hub proceed between the blades along several times rectangularly broken lines, so that the taper pins placed in these splits join both halves firmly in all directions. Since the forces in the joints are transmitted by pins subjected to shearing stress, the connection is very efficient.

Connection of the runner to the shaft may be performed in various ways. The simplest, but also least perfect method, consists in sliding the runner over the cylindrical stepped part of the shaft. Against the axial force, which is composed of the hydraulic pull and in vertical turbines of the weight of the runner, the runner is secured either by a nut (Fig. 144), which in turn must be held in position by means of a setscrew, or by a split ring secured against falling off by a single retaining ring (Fig. 145), which at the same time

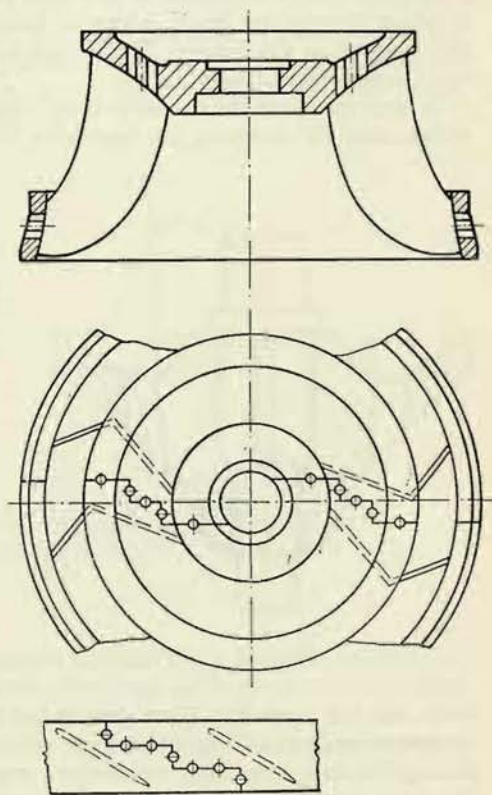


Fig. 143

¹⁾ Swiss Patent No. 239271 (Escher-Wyss A. G., Zurich).

forms the cap of the runner. The torque is taken up by one or two fitted-in feather keys.

Very firm but also rather expensive is the seating on a cone, which ensures a good centering of the runner and is therefore employed for high operating speeds. The cone is made in the ratio 1 : 5 and the runner is secured on it by a nut (Fig. 36). With regard to the large size of the bolt there are no difficulties in taking up the axial forces. A conical extension is slid over the nut as a hydraulic prolongation of the runner. The torque is again taken up by one or still better, two fitted-in feather keys.

In large machines the runner is always fastened to the shaft by means of a flange with a collar for centering (see Appendix VI). The axial forces are transmitted by

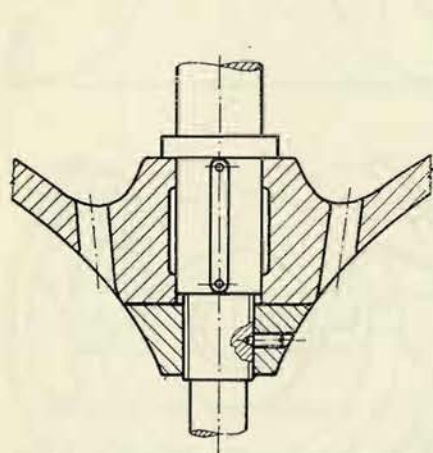


Fig. 144

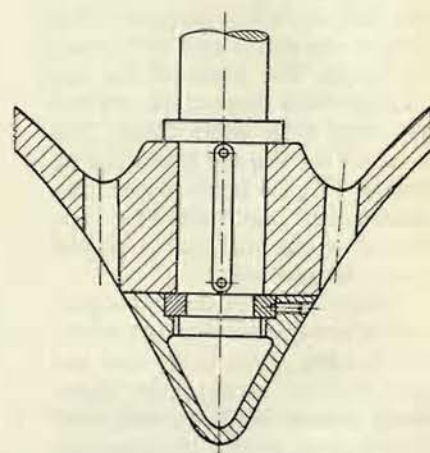


Fig. 145

bolts and the torque by taper pins radial keys formerly used are expensive and no longer employed – Fig. 141). If we have no possibility to manufacture the flange in a sufficiently large size, we can use fitted-in bolts which then transmit both the axial force (tensile stress) and the torque (shearing stress). This type of fastening is less advantageous from the manufacturing point of view.

Dimensioning of the connecting parts. For dimensioning the connecting parts of the shaft and runner we always calculate with double the normal torque (for details see Part I, Chapter X/2). $M_{n, \text{kgm}} = 716 \cdot 20 \frac{N \cdot k}{n}$; the torque can attain

approximately this value when the fully opened turbine would stop by braking, or when with the turbine at rest the guide wheel would suddenly open. With regard to the rarity of such cases we allow here a shearing stress in the keys or conical pins of 1400 to 1600 to (1800) kg/cm², and a wearing pressure stress of 1600 to 1800 kg/cm², for steel of a strength of 60 kg/mm². For bolts carrying only

an axial load we calculate as in other cases with a permissible tensile stress of about 800 kg/cm². For fitted-in bolts we must calculate with the reduced stress¹⁾, $\sigma_r = \sqrt{\sigma^2 + 3\tau^2}$ which must not exceed the permissible value of about 1500 kg/cm².

2. Cavitation and Material of the Runner

In Part I, Chapter V/2, we explained how, on the suction side of the blade, evaporation takes place in the form of bubbles, when the pressure has dropped to the value of the tension of the water vapour. These bubbles burst in places where the pressure is again higher and cause there a considerable deterioration of the blade.

Whether this phenomenon of cavitation will occur or not, depends on the value of the Thoma cavitation coefficient $\sigma =$

$$= \frac{H_b - H_s}{H}. \text{ Its value}$$

varies e. g. with the suction head, so that by a gradual increase of the latter cavitation can be evoked. The transition, from a cavitation-free operation to one with cavitation, is gradual, because as soon as the formation of vapour bubbles starts, heat of vaporization is extracted from the water, the water cools down and so the process of cavitation is stabilized.²⁾

In this way we may follow the transition to cavitation in the cavitation testing room which is equipped so as to permit a gradual increase in the suction head of the model turbine in question. In this test we determine the efficiency, sometimes the flow-rate, too, and at the same time we may observe through a glass extension of the draft tube what happens on the runner blade which we bring to a fictitious standstill by means of stroboscopic illumination.

If we mark off the efficiencies and flow-rates (best in unit values) as function of the cavitation coefficient, we obtain approximately the picture shown in Fig. 146. At a sufficiently high value of σ (low suction head) we do not observe anything

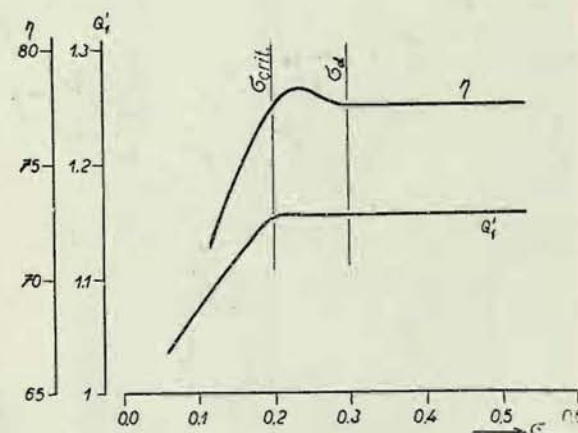


Fig. 146

¹⁾ Technický průvodce – nauka o pružnosti a pevnosti (Technical Guide – Strength of Materials), Prague, SNTL, 1955, p. 12.

²⁾ Kieswetter: Kavitační zjevy na lopatkách vodních turbin (Cavitation Phenomena on the Blades of Hydraulic Turbines), Strojnický obzor (Mechanical Engineering Review), 1937.



Fig. 147. From the cavitation testing room in the Research Institute of Hydraulic Machines at the Engineering Works ČKD, Blansko, Czechoslovakia

particular on the blades, and the efficiency as well as the flow-rate are in relation to σ constant and remain so with a decreasing value of σ (increasing suction head) down to a certain limit. When this limit is passed, as a rule the efficiency and sometimes the flow-rate, too, begin to increase slightly; at the same time, within a certain area on the suction side of the blade vapour bubbles begin to form and

disappear again. Fig. 147 (see plate) presents a picture of the cavitation process on the runner of a propeller turbine, where this phenomenon is better suited for photographing.

With a further decrease of σ the region of the blade surface affected by cavitation increases and later on the bubbles proceed even into the draft tube. After having attained the maximum (about 1 to 2 % above the initial value), efficiency and flow-rate diminish again, and after passing a certain limit value of σ , a rapid fall sets in. This progress may be explained by the circumstance that at the beginning of the cavitation process, a thin vapour layer separates the water from the blade, whereby the friction of the water on the blade is reduced, resulting in a decrease of the losses and an increase of the efficiency and in some cases of the flow-rate, too. But later, as soon as the vapour formation becomes intense enough to disturb the flow through the blade ducts, and the vapour entrained in the draft tube affects the action of the latter, efficiency and flow-rate begin to decrease. This state is termed the critical cavitation limit, and the pertinent cavitation coefficient we denote by σ_{crit} . The beginning of cavitation (beginning of bubble formation) we term lower cavitation limit, giving the corresponding coefficient the symbol σ_d .

These limits need not always be distinctly marked on the efficiency curve. In some cases, no increase of efficiency and flow-rate is observed, but efficiency diminishes immediately from the lower limit, gradually at the beginning and more rapidly later. This is usually a sign of an unsuitable, too intensely diverging draft tube. Then the function of the draft tube begins to be impaired by the influence of the vapour entrained from the blades in the initial phase of cavitation, as well as by the influence of the liberation of air and vapour in the draft tube before the full development of the cavitation on the blades.

It is clear that when designing and installing the turbine, we must never overstep the critical value, because then the turbine would not deliver the required output, apart from the vibration accompanying a strongly developed cavitation. It is advantageous, to select conditions in which the turbine works below the critical limit but still within the range of cavitation as in this way we utilize the increase in efficiency and at the same reduce the excavation work for the draft tube. Such an operation is only feasible if we select for the runner, which is subjected to strong attacks by cavitation, a suitable, cavitation-resistant material.

In order to explain the resistance of material against cavitation, we must, at least briefly, deal with the physical processes encountered in cavitation.

In experiments carried out in a diverging diffuser, shaped so that during the through-flow the pressure dropped and cavitation set in, it was found on specimens of materials inserted that deterioration arose in places where the vapour bubbles were collapsing. These results shook the hypothesis of the chemical action of oxygen absorbed in water and liberated under reduced pressure. This possibility was entirely eliminated in experiments with water freed from absorbed gases and with cavitation attacks upon glass.¹⁾ On the contrary, it could be observed that

¹⁾ Föttinger: Untersuchungen über Kavitation und Korrosion bei Turbinen, Turbopumpen und Propellern. Hydraulische Probleme, VDI, 1925.

deterioration was mainly brought about by mechanical stress due to impacts of the water upon the blade when the vapour was condensing. Theoretical¹⁾ and experimental²⁾ investigations, based upon piezo-electric pressure measurements, confirmed the possibility of creating such high pressures at the disappearance of the cavitation bubbles.³⁾ It is possible to accept this explanation, particularly as here fatigue stress is concerned, the limit of which for most materials is lower in the presence of water (for iron half the normal value, – see later). This theory is further confirmed by microscopically discernible deformations of the crystals in the places affected, as well as by the experiments of Pozdunin⁴⁾, according to which the material is not damaged in so far as no condensation of the vapour bubbles takes place on it but only further on (behind the blade). Experiments with a magnetostriction instrument, in which the specimen is submerged into a liquid and oscillated by the magnetostrictive effect of a nickel rod so as to evoke cavitation on it, have shown that in all probability, considerable local heating takes place in the affected areas (as a result of the impacts), restricted to a thin surface layer only but attaining a temperature of about 300° C.⁵⁾ Experiments with the magnetostriction instrument have further shown that through the action of temperature differences electric currents are generated which electrochemically very intensely attack the cavitated material.⁶⁾

Finally, we must still mention experiments⁷⁾ in which specimens of glass and fusible quartz were enclosed in a rubber cylinder filled with a liquid. When the pressure of the liquid was increased up to 15,000 atm. and immediately reduced, the specimens remained intact. When, however, the specimens were left under pressure for a longer time (about 30 minutes) and then the pressure suddenly reduced, the specimens cracked; when the specimens were submerged into liquids of higher viscosity, they had to remain a longer time under pressure to achieve the same effect. From these experiments it is obvious that the liquid under pressure penetrated into the material and cracked it from inside when the pressure was suddenly reduced. In this way we may also explain the reduction of the fatigue limit of the material in the presence of water; at alternating stress of the materials the water is „sucked“ between the crystals and driven out again, whereby the crystals of the material are gradually loosened.

Considering all the facts mentioned and their interconnection, we arrive at the

¹⁾ Ackeret: Experimentale und theoretische Untersuchungen über Hohlraumbildung im Wasser. Technische Mechanik und Thermodynamik, 1930.

²⁾ De Haller: Untersuchungen über die durch Kavitation hervorgerufenen Korrosionen, Schweizerische Bauzeitung, 1933, p. 243.

³⁾ The bubble is not destroyed at once, but appears again several times, obviously when the water is thrown back by the material; see Knapp & Hollander: Laboratory Investigations of the Mechanism of Cavitation, Transactions ASME, 1948.

⁴⁾ Pozdunin: Fundamentals of the Theory, Construction and Operation of Supercavitating Ship Propellers. Izvestiya Akademiy Nauk SSSR, 1945, No. 10–11.

⁵⁾ Nowotny: Werkstoffzerstörung durch Kavitation, VDI-Verlag, 1942.

⁶⁾ Foltýn: Příspěvek ke katodické ochraně vodních strojů. Disertace na bývalé Vysoké škole technické v Brně, 1951. (Contribution to the Cathodic Protection of Cavitating Parts).

⁷⁾ Poulter: The Mechanism of Cavitation Erosion. Journal of Applied Mechanics, 1942.

following conception of the process of cavitation corrosion of material. For purely hydraulic reasons local pressure reduction down to the tension of water vapour takes place at a given temperature. In consequence of this vapour bubbles are formed, which again condense in places of higher pressure. The collapsing bubbles cause considerable impacts of the water upon the material. When the material is not sufficiently compact and has not a smooth surface, the liquid penetrates at least into the surface layer of the material and at alternation of the pressure loosens the individual crystals. When the material is compact and its surface sufficiently smooth this effect cannot set in immediately. But owing to local temperature rises, caused by the impact of the water, sets in electrochemical corrosion; this corrosion evidently first attacks the less resistant intercrystalline phases and so prepares the way for the action of the liquid as just described. As soon as, by the loosening of the surface crystals, deeper and larger cavities are formed, the effect of the impact of the water on the penetration of the latter into these cavities intensifies (see Part III) and in this way accelerates still more the deterioration of the material.

From these considerations we can establish rules for the selection of the material and its adjustment with regard to resistance against cavitation. An indispensable condition is that the material exhibits, at least on its surface subjected to the effects of cavitation, a fine homogeneous and sufficiently hard and strong structure. A further condition is the smoothest possible surface. Among the presently known types of steel the best cavitation resistance is offered by an alloy steel containing 18 % chromium and 8 % nickel. But in order to save nickel, a chrome-nickel cast steel is currently employed with only slightly less resistance, containing 15 % chromium and 0.5 to 0.8 % nickel. With regard to satisfactory machinability, the carbon content of this steel must be kept below 0.2 %. The properties of this material are approximately as follows: strength at the yield point about 50 to 60 kg/mm², tensile strength 70 to 80 kg/mm², and elongation ($l = 10 d$) about 10 %. After casting, the runner must be subjected to the correct heat treatment and after machining, the blades must be manually ground and polished.

Sometimes, if we know where the blades are attacked by cavitation, the runner is made of normal cast steel, the endangered places are ground to a greater depth (about 2 mm) and covered with a layer of stainless steel by electric welding. The welded-on surface must again be ground to a smooth surface.

3. Recalculation of the Cavitation Coefficient

In the foregoing part we have seen that the magnitude of the coefficient σ characterizes the intensity of cavitation. If we e. g. in the model cavitation test room alter the suction head and thus the magnitude of the cavitation coefficient, the intensity of cavitation varies from the lower cavitation limit up to the critical limit.

As a rule, the head H_m at which we perform the measurements in the cavitation test room will not be the same as the head H_{inst} under which the turbine is to be installed in the power station. Therefore, we must make sure whether the same intensity of cavitation will be characterized by the same value of the cavitation

coefficient also under various heads, and if this should not be the case, we must establish a suitable conversion formula.

The Thoma cavitation coefficient was derived on the assumption that the pressure on the suction side of the blade equals the tension of the vapour (see Part I, Chapter V/2). Therefore, this coefficient holds good for the value σ_{crit} , which consequently will be independent of the head. When the value of the installed runner, σ_{inst} , equals the critical value of the model, i. e. $\sigma_{inst} = \sigma_{crit, mod}$, and when both runners are geometrically similar – in particular with regard to the draft tube – the pressure on the suction side of the blades will in both cases equal the tension of the water vapour, and also the runner installed in the actual turbine will operate at the critical limit.

It is always necessary, however, that the runner of the turbine ordered operates at a certain distance from the critical limit. For a runner of stainless steel it will be sufficient if the pressure on the suction side of the blades equals about two metres of water column; thus we ensure the machine against the consequence of inaccuracies in manufacture. But for a runner of ordinary cast steel it is necessary that the conditions in the actual turbine correspond to those in the model at the lower cavitation limit.

If in the cavitation test room we have adjusted the conditions so as to achieve for a certain value σ the relation $\sigma > \sigma_{crit}$, it means that we have reduced the critical suction head for the model, $H_{s, crit}$ by a certain value ΔH_s , so that we can write with the subscripts *m* for the model and *inst* for the actual machine:

$$\sigma_m = \frac{H_b - H_{s, crit, m} + \Delta H_s}{H_m} = \sigma_{m, crit} + \frac{\Delta H_s}{H_m}. \quad (155)$$

It is evident, that when the runner of the full-size turbine is installed so as to exhibit the same value σ , i. e. $\sigma_{inst} = \sigma_m$, the pressure on the suction side of the blades, ΔH_s will be different when $H_{inst} \neq H_m$, and consequently the cavitation effects will not be the same.

For the same cavitation effects there must hold good $\Delta H_{s, inst} = \Delta H_{s, m}$, so that we can put according to Equation (155):

$$\Delta H_{sm} = H_m (\sigma_m - \sigma_{m, crit}) = \Delta H_{s, inst} = H_{inst} (\sigma_{inst} - \sigma_{inst, crit}),$$

and since

$$\sigma_{m, crit} = \sigma_{inst, crit} = \sigma_{crit},$$

applies

$$\frac{\sigma_{inst} - \sigma_{crit}}{\sigma_m - \sigma_{crit}} = \frac{H_m}{H_{inst}}. \quad (156)$$

From this relation it follows how we have to establish the cavitation coefficient of a full-size machine to achieve the same cavitation effects (intensity) as on the model runner at the value of the cavitation coefficient σ_m .¹⁾

¹⁾ Ténor A.: Turbines hydrauliques et régulateurs automatiques de vitesse, Part III, Paris, Eyrolles, 1935, p. 381.

If we also want to take into account the variation in efficiency caused by the different sizes of the machines (Part I, Chapter XI/2), we must further recalculate the value of the cavitation coefficient σ_{inst} thus obtained according to the efficiency ratio, as has been explained.

4. Sealing of the Runner Gaps

The gaps between the runner and the lids of the turbine must be as small as possible as they exert an influence upon the volumetric efficiency. For low heads and machines of smaller sizes the gap is directly between the machined surfaces of the runner and the lids (see Fig. 34). In this case the clearance must be larger,

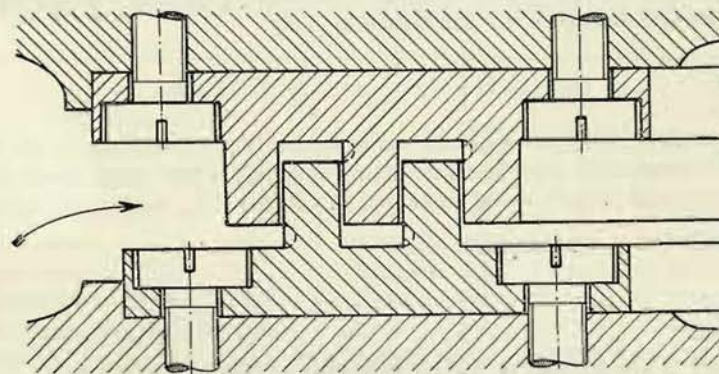


Fig. 148

1 to 2 mm measured at the radius, with regard to the risk of jamming due to rust formation. For higher heads and in larger machines rings of bronze or stainless steel (which better resists erosion by sand) are inserted into the lids and shrunk on the runner; in this case the clearance may be smaller, 0.5 to 1 mm at the radius, according to the size of the runner.

For large heads – exceeding about 100 m – we employ rings which engage comb-like into each other, as shown in Fig. 148 and Appendix VI, and reduce the head corresponding to one gap. Sealing rings of this type, in which wider gaps alternate with narrower ones, so that the through-flow velocity developed in the narrow gap is destroyed in the following wide gap, are termed labyrinths. These rings, which are interchangeable, are made of bronze or stainless steel and fastened to the runner and lids by screws with countersunk cylindrical heads (screws with conical heads can be loosened only with great difficulty after a certain time), which must be secured against loosening. It is best to do this by point welds. The labyrinth rings are centered on the runner and lids by means of centering rings. Rings of large diameters consist of several parts; the centering ring of the runner must be here outside

the labyrinth to take up the centrifugal forces of the individual parts of the labyrinth ring. When the labyrinth is machined, as indicated in Fig. 148 in full lines, the contraction at the entrance into the narrow gap is only one-sided. Therefore, recesses, indicated by dash lines, are made, which bring about two-sided contraction, thus reducing the flow through the labyrinth.

The narrow gaps of large diameter are as a rule arranged so as to permit shifting of the runner in the axial direction, these shifts are caused by thermal deformations of the shaft and a deflection of the supporting structure of the axial bearing at variations of the axial pull.

As already pointed out, that by the action of the labyrinth the through-flow velocity developed in a narrow gap is destroyed in the wider part and so must be created anew in the following narrow gap. The total head of the labyrinth is therefore divided into n stages when the number of sealing gaps is n . The through-flow through the labyrinth then is – see Equation (124):

$$Q_s = \mu_s f_s \sqrt{2g \frac{h_s}{n}} = \frac{\mu_s}{\sqrt{n}} f_s \sqrt{2g h_s}. \quad (157)$$

We see that the discharge coefficient varies inversely proportionally to the square root of the number of gaps. For calculating axial pull when using labyrinths, we therefore proceed entirely in the same way in Chapter I/12, Section *a*, but instead of the coefficient μ_s we substitute $\frac{\mu_s}{\sqrt{n}}$.

5. Shaft

The shaft of the turbine is mainly subjected to torsional stress by the driving torque M . The maximum value of this torque with a fully opened guide apparatus and blocked runner can attain approximately double the magnitude of the torque at normal speed (for details see Part I, Chapter X/2), this must be borne in mind. Tensile stress by axial forces is insignificant and need not be taken into account. On the other hand, the shaft may be subjected to bending stress resulting from: 1. centrifugal forces of the imperfectly balanced runner; 2. forces from the spur or bevel gearing; 3. in horizontal turbines, the weight of the shaft and the weight of the parts seated on it, and maybe also the pull of the belt, should the output be transmitted by a belt drive.

Bending stress is usually small, and, therefore, we only calculate the shaft for torsional stress according to the expressions:¹⁾

$$\text{for a solid shaft } \tau_{\max} = \frac{16 M}{\pi D^3}, \quad (158)$$

$$\text{for a hollow shaft } \tau_{\max} = \frac{16 M D}{\pi (D^4 - d^4)},$$

¹⁾ Technický průvodce, díl 3, Pružnost a pevnost (Technical Guide, Part 3, Strength of Materials), Prague, SNTL, 1955, p. 175.

where M is the maximum torque at the operating speed

$$\left(M = 71,620 \frac{N_{\max, \text{ metr. horsepower}}}{n} \right),$$

D the outer and d the inner diameter (the shafts of Francis turbines are bored firstly for reason of material control, and secondly, in vertical machines to pass a rope through the bore for assembly work in the space of the turbine).

We select a low permissible stress, within the range of 150 to 400 kg/cm², with regard to the circumstance that the starting torque is approximately double the normal torque, and because of the additional bending stress. We calculate with lower values at higher operating speeds with regard to the critical speed.

The following table, containing data from pertinent literature, presents the conditions of some machines actually manufactured (including Kaplan turbines):

Power station	N_{\max} k	n 1/min	$M_{\max} \cdot 10^6$ kgcm	Shaft D/d mm	τ_{\max} atm
Ryburg-Schwörstadt	38000	75	36	800/360	375
Dnyeprostroj	102000	83,3	88	1120/300	320
Hamersforsen	15450	93,8	11,8	500/—	475
Power station in Czechoslovakia	1500	107	1	340/125	146
Power station in Czechoslovakia	10700	150	5,1	480/260	257
Shannon	32500	150	15,5	625/—	323
Power station in Czechoslovakia	7840	300	1,88	320/50	297
Portenstein	12700	600	1,5	375/—	154
Yokawa	2400	900	0,19	200/—	122

The main demand is that the shafts of hydraulic turbines always rotate at lower speeds than the critical one, and this rule applies even to the highest speed which may be encountered in a case of failure of the controller. In turbines with a higher operating speed we, therefore, control the critical speed, and it should be at least 20 % higher than the runaway speed.

Since the turbine shaft is always seated in more than one bearing and carries more than one disc – the turbine shaft is as a rule connected by a coupling with the shaft of the alternator or the shaft of the gear mechanism – by a semi-graphical method we investigate the deflection of the shaft caused by forces equalling the weights of the discs¹⁾; the sense of the forces must be selected so that each of them augments the deflection (they replace the centrifugal forces).

¹⁾ See e. g. Dobrovolný: Pružnost a pevnost (Strength of Materials), Prague, 1944, p. 505 etc.

Having found the deflections y under the individual discs of the weight G , we determine the critical angular velocity of the shaft according to Morley¹⁾

$$\omega_{crit.}^2 = g \frac{\sum G y}{\sum G y^2} \quad (159)$$

and from it the critical speed by means of the relation $n = 9.55 \omega$.

Large shafts are manufactured from basic open-hearth steel with a strength of (50 to 60) to (55 to 65) kg/mm² at an elongation of 18 % and with a yield point of at least 28 kg/mm². Large shafts are always directly connected with the alternator, which is principally performed by means of flanges forged on the shaft. The flange for the runner is likewise forged from the shaft (see Enclosure VI and Fig. 36). The connecting parts of the coupling are made and dimensioned in the same way as those of the flange of the runner.

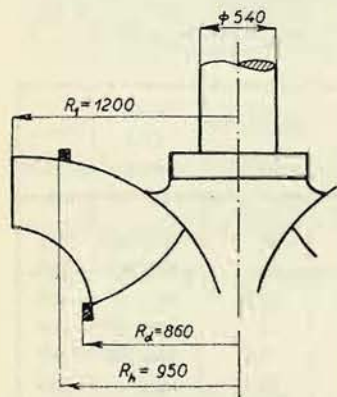


Fig. 149

Small shafts are made from round stock and a coupling of cast iron or cast steel is then pressed on the stepped end of shaft and secured by one or two feather keys for the transmission of the torque. Small shafts are usually fitted with electrically welded-on coupling flanges.

The transitions of the diameters are made as far as possible conical and the stepping with the largest possible radius in order to reduce the scoring effect upon the strength of the shaft.

Example: As an example let us calculate the parts of the turbine illustrated in Appendix VI.

It is a specific low-speed Francis turbine in vertical arrangement. The turbine, which forms part of a pumping station, is by means of a coupling connected on top with an alternator, whilst the bottom end of the shaft, passing through the draft tube is connected to a pump.²⁾

The turbine operates under a maximum head (net) $H = 208$ m, at a flow-rate of 12.5 m³/sec. and a speed of 375 r. p. m.; the diameter of the runner is 2400 mm. The maximum output of the turbine at $\eta = 87$ % is:

$$N = \frac{\gamma Q H \eta}{75} = \frac{1000 \cdot 12.5 \cdot 208 \cdot 0.87}{75} = 30\,200 \approx 30\,000 \text{ h. p.}$$

(h. p. = metric horsepower).

¹⁾ Technický průvodce, 3. díl, Pružnost a pevnost (Technical Guide, Part 3, Strength of Materials), Prague, SNTL, 1955, p. 268.

²⁾ A description of the entire plant is to be found in the paper of Nechleba: Vodní elektrárna ve Štěchovicích (The Hydraulic Power Station at Štěchovice, Strojnický obzor (Mechanical Engineering Review), 1948, No. 9.

a) *Labyrinths.* With regard to the considerable head, the labyrinths are made as shown in Fig. 148. The labyrinth on the rim of the runner has a smaller mean diameter than the labyrinth on the disc (Fig. 149), so that the runner is under the influence of a lifting force. To determine this, it is necessary to know the pressure in the places of the labyrinths.

In the spaces in front of the labyrinths between the runner and the lids the water rotates at half the velocity of the wheel, and for the difference between pressure h_1 at the inlet radius R_l and pressure h_l in the places of the labyrinths there will apply (Chapter I/12):

$$h_1 - h_l = \frac{\omega^2}{8g} (R_l^2 - R_l'^2).$$

In our case $\omega = \frac{n}{9.55} = \frac{375}{9.55} = 39.3$ 1/s; for R_l we substitute the mean value of the diameters of both labyrinths $R_l = \frac{R_d + R_h}{2} = 905 \text{ mm} = 0.905 \text{ m}$. Further we have

$$h_1 - h_l = \frac{39.3^2}{8 \cdot 9.81} (1.2^2 - 0.91^2) = 12 \text{ m.}$$

Overpressure of the runner is obtained with sufficient accuracy from the expression

$$h_p = H - \frac{C_0^2}{2g} = H (1 - c_0^2),$$

where we take c_0 from the velocity triangle in Appendix II (this is containing the hydraulic design of the turbine in question), or determine C_0 according to the discharge from the guide apparatus, $C_0 = \frac{Q}{z_1 B a'}$, where z_1 is the number of guide blades, B the height of the guide wheel, and a' the width of the outlet ducts of the guide apparatus. According to Appendix II, $c_0 = 0.61$ and hence

$$h_p = 208 \cdot (1 - 0.373) = 208 \cdot 0.627 = 131 \text{ m.}$$

Overpressure in places in front of the labyrinths in relation to pressure at the back of the runner hence is

$$h_l = h_p - (h_1 - h_l) = 131 - 12 = 119 \text{ m.}$$

Further we must determine the overpressure behind the upper labyrinth. From Appendix II we can see that immediately behind the upper labyrinth the pipe is connected for the discharge of the water into the draft tube. This pipe opens rather near behind the runner. Therefore, we can write, the resistance of the labyrinth (as in Chapter I/12) by the symbol h_s and by h_0 the resistance of the by-pass pipe (in the cited chapter the resistance of the relief openings): $h_s + h_0 = h_l$. Furthermore continuity equation must hold good.

$$Q_s = \mu_s f_s \sqrt{2g h_s} = \mu_0 f_0 \sqrt{2g h_0}.$$

The through-flow area of the labyrinth gap with a clearance of 1 mm equals

$$f_s = 2\pi R_h \cdot s = 2\pi \cdot 95 \cdot 0.1 = 59.6 \text{ cm}^2 \doteq 60 \text{ cm}^2.$$

As the number of labyrinth gaps is $n = 6$, we take

$$\mu_s = \frac{0.6}{6} = 0.245 \doteq 0.25.$$

The least through-flow area of the by-pass pipe is $f_0 = 375 \text{ cm}^2$; μ_0 we substitute, with regard to the resistances within the pipe itself which we shall later not calculate – with the value 0.6. thus we obtain

$$0.25 \cdot 60 \cdot \sqrt{2g h_s} = 0.6 \cdot 375 \cdot \sqrt{2g h_0},$$

whence

$$h_s = h_0 \left(\frac{0.6 \cdot 375}{0.25 \cdot 60} \right)^2 = h_0 \cdot 225,$$

which, substituted into the equation gives:

$$h_s + h_0 = h_l, \text{ gives } h_0 \cdot 226 = 119,$$

or

$$h_0 = \frac{119}{226} = 0.526 \doteq 0.53 \text{ m}$$

and

$$h_s = 119 - 0.53 = 118.47 \text{ m} \doteq 118.5 \text{ m}.$$

The difference of the areas of the mean diameters of the upper and lower labyrinths amounts to $\Delta F = 5119 \text{ cm}^2$. This annulus is acted upon from below by a pressure 119 m higher than the pressure in the back of the runner, and from above by a pressure 0.53 m higher than the pressure in the back of the runner. The lifting force acting upon the runner is therefore

$$S_s = 5119 \cdot 11.85 = 60,600 \text{ kg}.$$

In addition to this, the runner is raised by the force resulting from the meridional deflection of the water flow according to Equation (128):

$$S_m = - \frac{Q\gamma}{g} \cdot C_s.$$

C_s is the inlet velocity into the draft tube, $C_s = \frac{Q}{F_s} = \frac{12.5}{1.96} = 6.4 \text{ m/sec.}$, so that

$$S_m = - \frac{12.5 \cdot 1000}{9.81} \cdot 6.4 = 8130 \text{ kg}.$$

On the other hand, the runner is pressed downward by the water behind the upper labyrinth with force S_t , which we determine from the relation (126), considering that now $R_0 = R_{s,t}$ (see Fig. 103):

$$S_t = \pi \cdot 1000 (0.95^2 - 0.54^2) \cdot \left[0.53 - \frac{39.3^2 \cdot 0.95^2}{8 \cdot 9.81} + \frac{39.3^2}{16 \cdot 9.81} (0.95^2 + 0.54^2) \right] = -1100 \text{ kg}.$$

From this sign it follows that this force acts in an upward direction, which is clear when we consider that the by-pass pipe is connected immediately behind the labyrinth, i. e. at the edge of the pressure paraboloid, so that here the pressure equals approximately the pressure under the runner; since under the influence of rotation the pressure diminishes towards the shaft, the average pressure above the runner is lower than below it.

The total of all these forces amounts to $69,830 \text{ kg} \doteq 70,000 \text{ kg}$ and must be indispensably less than the total of the weights of the rotating parts, i. e.: rotor of the generator $125,000 \text{ kg}$ + runner of the turbine $10,000 \text{ kg}$ + weight of the shaft $16,000 \text{ kg}$, giving a total of $151,000 \text{ kg}$. Consequently the remaining load upon the axial bearing the full flow-rate through the turbine is $151 - 70 = 81$ metric tons; at no-load run the rotor of the turbine will not be acted upon by lifting forces, and the load upon the bearing will amount to 151 metric tons.

We can also determine the quantity of water leaking through the labyrinth

$$Q_s = \mu_s f_s \sqrt{2g h_s} = 0.25 \cdot 0.006 \cdot 4.43 \cdot \sqrt{118.5} = 0.25 \cdot 0.006 \cdot 4.43 \cdot 10.9 = 0.0725 \text{ m}^3/\text{s} \doteq 75 \text{ litres/sec.}$$

Since there are two labyrinths, the leakage losses amount to $2 Q_s = 150 \text{ litres/sec.}$, and hence the volumetric efficiency of the turbine is

$$\eta_v = \frac{12,500 - 150}{12,500} = 0.988 \doteq 99 \%$$

b) *Connection of the runner.* When the machine is under load, the runner is pressed upon the flange of the shaft; consequently it would be sufficient to calculate the connecting bolts only on the basis of the weight of the runner and the rotating parts under it (only the shaft to the pump when the pump is connected by an axially shiftable clutch). The bolts, however, would be disproportionate. With regard to the dimensions of the flange and the circumstance that wear of the upper labyrinth results in a rise of the water pressure behind it, 10 bolts type M99 have been selected. But these bolts alone would not be sufficient to press the runner so intensely against the flange as to guarantee transmission of the torque merely by friction. For the maximum torque at normal speed is

$$M_k = 71,620 \frac{30,000}{375} = 3,740,000 \text{ kgcm}.$$

Therefore, the peripheral force at the radius $R = 420$ mm of the pitch circle of the bolts should have $T = \frac{5,740,000}{42} = 136,500$ kg, so that with a friction coefficient of 0.2 the flange would have to be drawn to the clutch with the force $S = \frac{136,500}{2} = 684,000$ kg. Consequently we should have to calculate with

a stress of the bolts of $\sigma_t = \frac{S}{zf} = \frac{684,000}{10 \cdot 68} = 1010$ kg/cm², $f = 68$ cm² being the area of the core of the bolt. But this connection would not in any way transmit the twofold moment of the blocked turbine.

For this reason, five taper pins of 65 mm diameter were used for transmitting the torque; each of them had a shearing area $f = 33.1$ cm²; the pins were placed between the bolts on the same pitch circle. Their shearing stress by the torque at normal speed amounts to

$$\tau = \frac{T}{5f} = \frac{136,500}{5 \cdot 33.1} = 825 \text{ kg/cm}^2,$$

and consequently with the runner at rest and the guide apparatus fully opened $\tau_{\max} = 1650$ kg/cm².

Similarly, the flange towards the pump is dimensioned, of course, for the torque taken up by the pump.

c) *Shaft*. Since the shaft is fitted with a bore of only 60 mm diameter for control of material and for pulling a rope from the hook of the crane through it to facilitate assembly of the lower parts, we calculate with the formula for a solid shaft

$$D^3 = \frac{16 \cdot M}{\pi \tau}, \text{ selecting } \tau \doteq 300 \text{ kg/cm}^2, \text{ so that}$$

$$D^3 = \frac{16 \cdot 5,740,000}{\pi \cdot 300} = 97,500 \text{ cm}^3, \text{ and hence } D = 45.8 \text{ cm} \doteq 450 \text{ mm}.$$

Control of critical speed: The shaft is supported by four bearings A, B, C, D , as indicated by the diagram in Fig. 150. The bearing A is the bearing in the elbow of the draft tube (Appendix VI), B is the bearing on the top lid of the turbine, C and D are the bearings of the generator under the rotor and above it. The individual forces in the diagram (Fig. 150) are: $P_1 = 2000$ kg – the weight of the clutch towards the pump; $P_2 = 15,650$ kg – the weight of the turbine runner together with the weight of the shaft towards the pump and one third of the weight of the main turbine shaft; $P_3 = 8000$ kg is the weight of two thirds of the turbine shaft and of part of the alternator shaft; $P_4 = 110,000$ kg – the weight of the rotor of the alternator and the pertinent part of the shaft; $P_5 = 2600$ kg – the weight of the rotor of the main and auxiliary exciters together with the weight of the overhanging end of the shaft.

The statically indeterminate reactions are found e. g. from the condition that

the deflection in the place of such a reaction equals zero. As statically indeterminate we select the reactions B and C . We imagine the supports in the places B and C to be removed and investigate the deflection curves for unit loads of 1000 kg, first in place B and then in place C . We plot the deflection curves by the well-known semi-graphical method as moment curves from the load by the area of the ordinates $M_0 \frac{J_0}{J}$, where the moment of inertia J_0 may be selected e. g. for

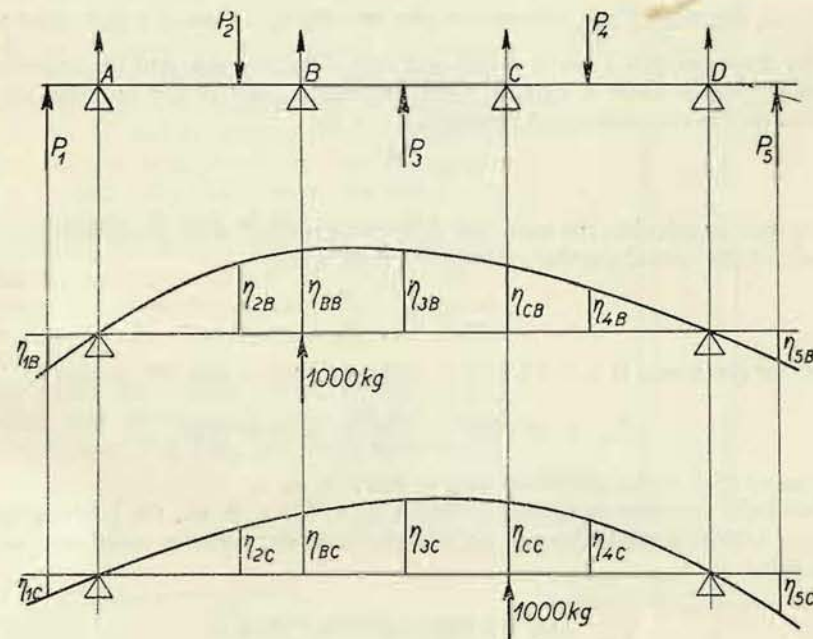


Fig. 150

a shaft diameter of 500 mm. J is the actual moment of inertia of the shaft in the appropriate place and M_0 the bending moment resulting from the selected load.

According to the law of the superposition of displacements, deflections y in places B and C will be given by the relations:

$$y_B = 0 = -P_1\eta_{B1} - P_2\eta_{B2} + P_3\eta_{B3} - P_4\eta_{B4} - P_5\eta_{B5} + B\eta_{BB} + C\eta_{BC};$$

$$y_C = 0 = -P_1\eta_{C1} - P_2\eta_{C2} + P_3\eta_{C3} - P_4\eta_{C4} - P_5\eta_{C5} + B\eta_{CB} + C\eta_{CC}.$$

From these two equations the unknown reactions B and C were calculated, because, according to Maxwell's reciprocal theorem,¹⁾ applies $\eta_{m,n} = \eta_{n,m}$, and the magnitude of the influence coefficients $\eta_{m,n}$ can be measured from the plotted deflection

¹⁾ Timoshenko: *Pružnost a pevnost* (Strength of Materials), Prague, 1952.

lines (e. g. $\eta_{B3} = \eta_{3B}$, see Fig. 150b, c). Both deflection lines must, of course, be represented in the same scale. Then we can easily determine reactions A and D as in the case of a beam on two supports, reactions B and C being counted among the loads.

Furthermore, we draw the progress of the moments $M_0 \frac{f_0}{f}$ for the actual load and plot the appropriate deflection line. When the scale of reduction of the shaft is $1 : m$, the scale of the ordinates of the line $M_0 \frac{f_0}{f} : 1 \text{ cm} = n \text{ kgcm}$, the scale of the force polygon $1 \text{ cm} = p \text{ cm}^2$, the pole distance $e \text{ cm}$, and the modulus of elasticity of the shaft $E \text{ kg/cm}^2$, the enlargement scale of the ordinates of the deflection line over the actual dimensions will be

$$\mu = \frac{E f_0}{e m^2 n p}.$$

If we want to calculate the measured deflections instead of the actual ones, for the square of the critical angular velocity, we must write:

$$\omega_{\text{crit}}^2 = \mu g \frac{\sum P y}{\sum P y^2}.$$

In the given case is $\mu = 25$, $\sum P y = 350,250$, $\sum P y^2 = 935,725$, so that

$$\omega_{\text{crit}}^2 = 25 \cdot 981 \cdot \frac{350,250}{935,725} = 9180 \text{ 1/sec.},$$

$\omega_{\text{crit}} = 95.7 \text{ 1/sec.}$, and hence $n_{\text{crit}} = 915 \text{ r. p. m.}$

Since the runaway speed has the value $n_p = 675 \text{ r. p. m.}$, the critical speed $n_{\text{crit}} = 1.36 n_p$ is approximately 36 % higher than the runaway speed well on the safe side.

III. GUIDE APPARATUS

1. Guide Blades and Their Seating

Internal regulation (Fig. 34) is selected only for low heads and for turbines of smaller size. Therefore, the pressures upon the blades are not high, and the blades for this type of guide mechanism are nearly always cast from gray cast iron. Since the water velocities are likewise not high, the blades, as a rule, are not machined. Only to attain the requisite sealing action of the guide apparatus in its closed position, are the blade ends planed (B in Fig. 151), and in place where the blade contacts the end of the preceding one (A Fig. 151) a bar is cast on; this bar is then planed to provide a clean bearing surface. With regard to tightness it is important that the machined sealing surfaces are parallel with the bore for the pivot of the blade. Larger blades are cast with a cavity in the thicker rear end (see Figs. 151 and 34).

The blades are pivoted on bolts which at the same time hold both turbine lids together. For rotating on the bolts, the blades are provided with pressed-in bronze bushings, which reach from either side into a quarter to a third of the length of the bore. The bolt on which the blade rotates between these bushings is often stepped to a smaller diameter (Fig. 152) to permit easy removal even if the surface has become rusty. In vertical shaft turbines in particular the pivot is fitted with a ring on the bottom end (Fig. 152) which projects about 0.5 mm beyond the turbine lid and supports the blade in the axial direction, eliminating friction of the blade with its full length against the lid and facilitating rotation. A shortcoming of this arrangement is that to replace only one blade, the bolt cannot be pulled out; for this reason, instead of this supporting ring, a special ring slid over the bolt is often employed, so that the bolt can be pulled out in the upward direction. To facilitate rotation, the blades are made about 1 mm shorter than the distance of the lids.

The blades are rotated by the regulating ring to which they are connected by means of steel links and pins. The links are fitted with bronze

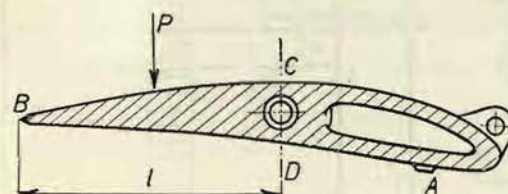


Fig. 151

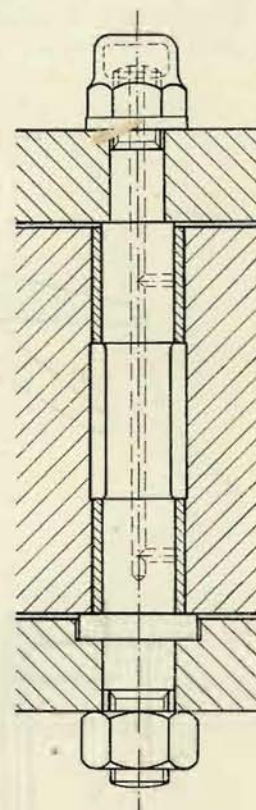


Fig. 152

sleeves for the pins, of which some are pressed into the blades, the others into the shifting ring. It is advantageous to arrange the links in such a way so that in a shut-off position they enclose an angle of 15° to 20° in the radial direction (Fig. 153). Thus it is made possible that by a comparatively small force in the regulating ring large forces in the links are created, providing a good sealing effect of the blades in the closed position. A further advantage of this arrangement is a partial equalization of the progress of the moments from the water pressure upon the blade, which as a rule cannot be fully equalized only hydraulically (by the position of the pivot).

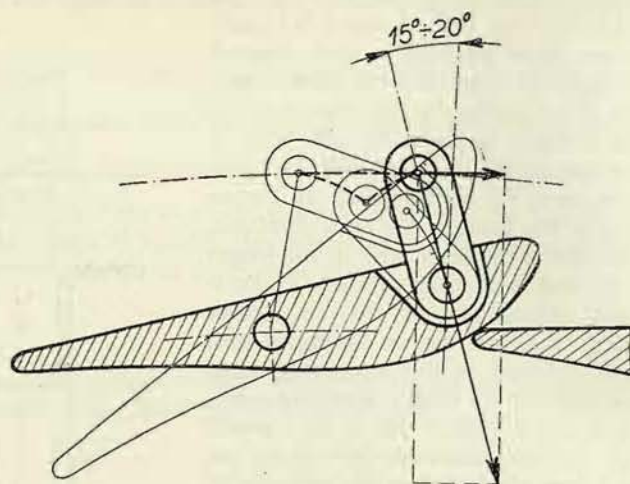


Fig. 153

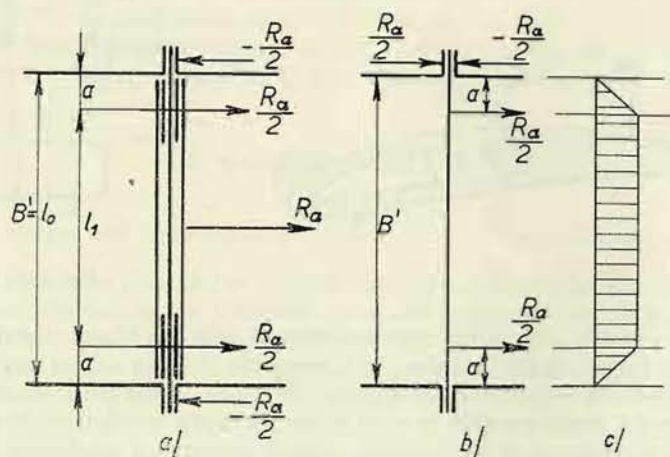


Fig. 154

Since all pivots are in water and cannot be regularly lubricated, only moderate specific pressures in these pivots are selected, the maximum value being 40 to 50 kg/cm².

The strength of the blade must be controlled in the place weakened by the bore for the bolt. We control this cross section as to bending by the moment from the water pressures upon the part of the blade from the point B (Fig. 151) for the cross section C-D in the closed position. The bending moment is (B being the

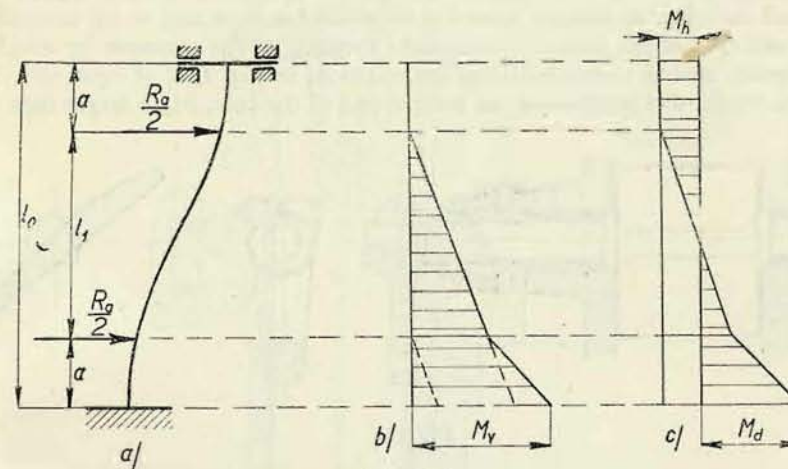


Fig. 155

face of the guide wheel, p the pressure in atm., and l the distance indicated in Fig. 151): $M_0 = \frac{l^2 B}{2} \cdot p$; the modulus of the cross section is (t being the thickness of the blade in the cross section C-D and d the diameter of the bore):

$$W = \frac{B}{6} \frac{t^3 - d^3}{t}.$$

Further we must control the strength of the pivots of the blades. When the lids of the turbine are held together in another way (e. g. by special connecting bolts as shown in Fig. 35), they will be subjected to stress according to the diagram in Figs. 154a, b, and the progress of the bending moment will be as indicated in Fig. 154c. The maximum moment is $M_{\max} = \frac{R_a}{2} \cdot a$, where R_a is the maximum load of the blade. The requisite diameter of the bolt hence is

$$d^3 \doteq 10 \frac{R_a}{2} \frac{a}{\sigma_d}. \quad (160)$$

When the connection of both lids is brought about by the blade bolts alone, then they will be loaded according to the diagram in Fig. 155a. If the bolts were fixed only at the bottom and not at the top, the progress of the bending moments would correspond to Fig. 155b, and the fix-end moment M_v would have the value

$$M_v = \frac{R_a}{2} a + \frac{R_a}{2} (l_1 + a) = \frac{R_a}{2} l_o.$$

But the upper end of the deflection line of the bolt must be parallel to the lower end, and therefore we obtain (according to which has been said in the calculation of the strength of the runners) the correct progress of the moments by dividing the moment area so as to obtain the hatched areas in Fig. 155c of equal size. We see that the fix-end moment of the bottom end of the bolt, M_d is larger than the

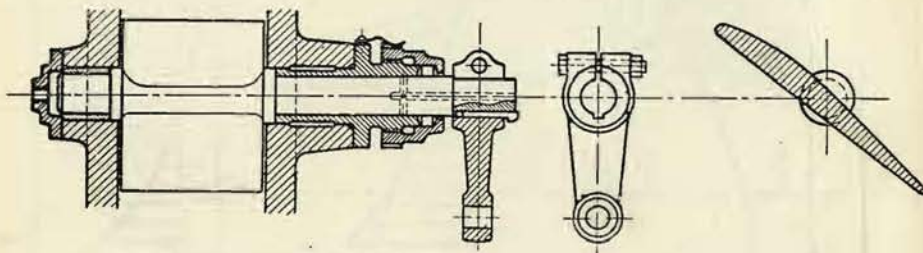


Fig. 156

fix-end moment of the top end, M_h . But with regard to the fact that a is small in comparison with l_o , no great error is made by putting

$$M_d \doteq M_h \doteq \frac{M_v}{2} = \frac{R_a \cdot l_o}{4}, \quad (161)$$

so that the requisite diameter of the bolt is given by the formula

$$d^3 \doteq 10 \frac{R_a \cdot l_o}{4 \sigma_d}. \quad (162)$$

To keep the thickness of the blade within appropriate measures, we select the permissible stress σ_d in the formulas (160) and (162) at a rather high value

$$\sigma_d = 360 \text{ to } 1000 \text{ kg/cm}^2.$$

The diameter of the bolt may also be calculated according to an empirical formula based upon the inlet diameter D_1 of the runner (d and D_1 in mm): $d = \sqrt[3]{10 \cdot D_1}$, giving the round numbers

for $D_1 =$	400	600	800	1000	1500	2000	mm,
$d =$	16	18	20	22	24	26	mm.

But when using these data we must check the strength, and should the stress be inadmissibly high, we must add special bolts connecting both lids (e. g. as shown in Fig. 35), or connect the lids by stay blades.

Should the lids be held firm at the correct distance from each other by another means, even blades with cast-on pivots may be used, as shown in Fig. 166, where

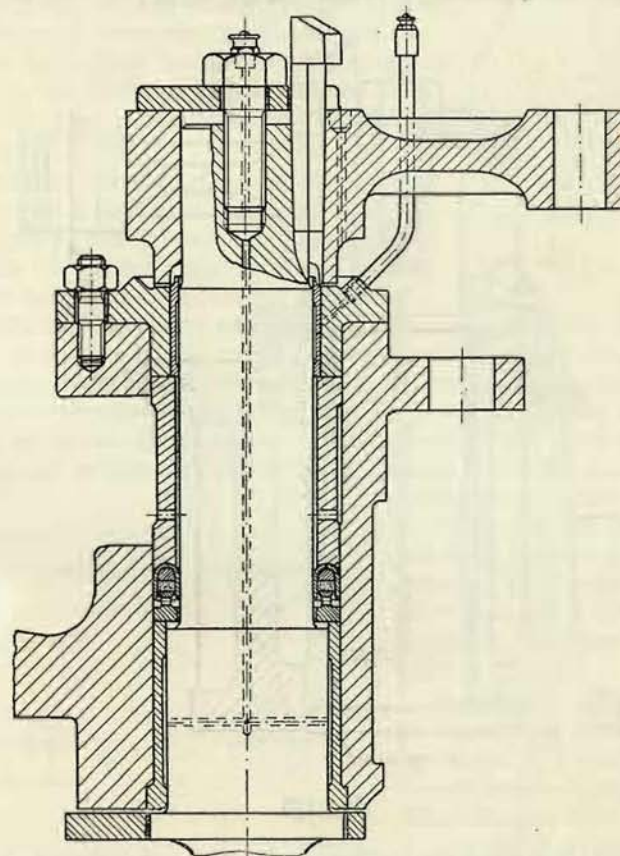


Fig. 157

the spacing of the lids is determined by the concrete spiral. This has the advantage that the pivots of the blades can be lubricated during operation, for which purpose tubes are cast into the lids.

The blades may then have a more slender cross section.

External regulation (Fig. 35, 36, Appendix VI) is employed for turbines of larger size and for higher heads. The blades are cast from steel in one piece with

the pivots. With regard to the higher through-flow velocities, the blades for large heads (low-speed turbines) are usually manually reground; for the highest heads and in particular for installations where the water carries fine sand, the blades are made from stainless steel which resists to erosion. The composition of this steel is the same as that for runners. In (specifically) low-speed turbines, the pin to which the regulating crank is fastened, is the part of the blade subjected to most stress,

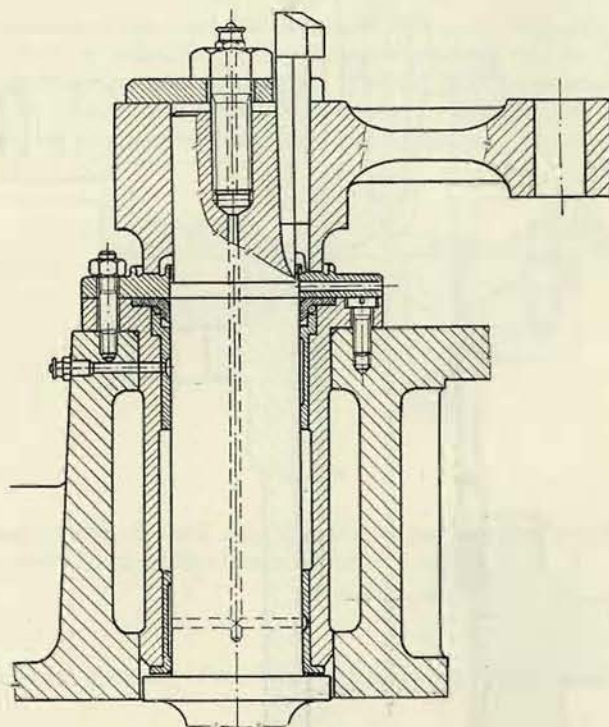


Fig. 158

the most critical place being the bearing nearest the crank, where the pin is acted upon by the torque and at the same time by the bending stress resulting from the force of the ling acting upon the crank. Therefore, this pin is, if necessary, reformed in order to compact the material and render it more resistant to greater stress.

In this case the blade may have a very slender cross section if we provide for a suitable, gradual transition (see Fig. 156) into the rings to restrict the axial shifts of the blade and from which the pins protrude with a greater thickness than that of the blade itself. Clearance is again provided for on either side of the blade, which is again axially held towards the bronze bushings of the bearings by rings to prevent

friction on the lids across the length. In the case of lower heads, only the crank pin is led through the stuffing box into the dry space (Fig. 156), while the other pin remains in water. The blade in this case is axially pressed to the bearing of the crank by a force equalling the product of the water pressure and the area of the pin in the stuffing box. In the case of large heads, this force would be excessive, and, therefore, both pins are led through the stuffing box into the dry space; when these pins in the stuffing boxes are of the same diameters, the blade is axially entirely discharged (Fig. 36, Appendix VI).

The constructional disposition of the stuffing boxes of the pins is illustrated in Figs. 157 and 158. Fig. 157 shows a stuffing box for high heads (detail to Appendix VI), where a leather sleeve packing is used. To provide for good seating of this sleeve and a certain axial flexibility necessary for tightening the body of the bearing under the crank to the lid, the ring of the sleeve packing is split and, between both parts, a rubber ring is inserted. The collar which presses the sleeve into position is provided with openings for the discharge of the leaking water and is in turn held in position by the bearing under the crank. In vertical shaft turbines, the bearing also takes up the weight of the blade by a ring on the hub of the crank; the friction

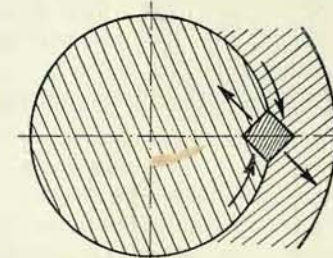


Fig. 159

surface of this ring is moving under oil which fills the pan formed by the body and the bushing of the bearing. The radial bearings are lubricated by a grease pressure lubricator, as shown in the diagram.

The crank is placed on the end of the pin, and the blade is hinged by means of a bolt permitting a correct axial seating of the blade when the machine is assembled. The torque is transmitted by keys or taper pins, which are driven home after the axial positioning of the blade. Here square keys are employed, driven home diagonally (Fig. 159); the bevel is only on one side, but by driving the key home diagonally it is gripped on all four sides and held firmly. Taper pins have the disadvantage that after

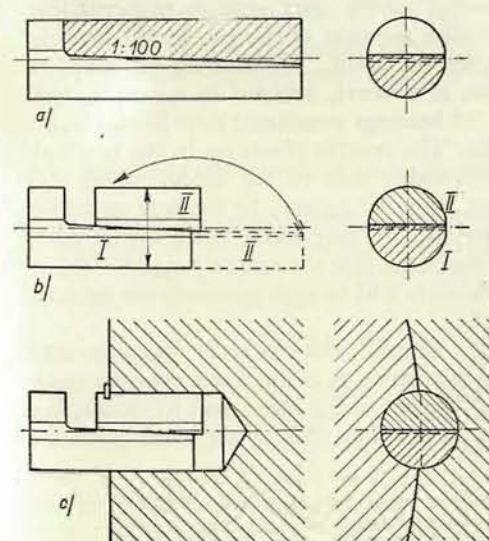


Fig. 160

an axial shift of the blade (when checked after a long operating) the pin is no longer firmly seated and the bore must be adjusted by re-machining. This shortcoming is obviated by employing cylindrical pins which are likewise not expensive. Fig. 160 a-c shows the manufacture and application of such a key.¹⁾ The hatched area in Fig. 160a shows the part which is obtained from round stock by planing; Fig. 160b indicates how two parts I and II of the key are obtained by cutting; Fig. 160c, shows how the keys are applied. When finally fitting and driving home the keys, or when turning the bore and driving home the cylindrical or taper

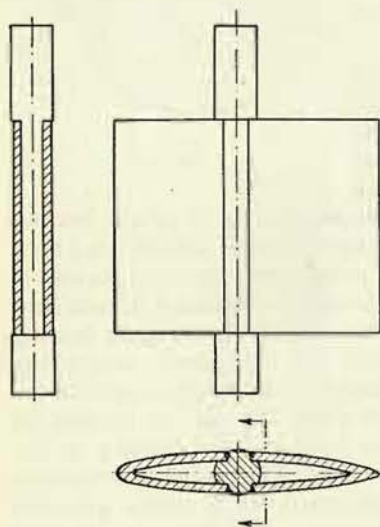


Fig. 161

pins (this is only done after assembling the complete regulating mechanism including the shifting ring), the guide blades are pulled together by means of rope which is put round the guide apparatus and tightened by a pulley block in order to ensure a correct seating of all blades in the shut-off position.

Fig. 158 shows a similar arrangement but for lower heads (up to about 60 m). The difference lies in the location of the stuffing box, which at lower heads may be placed directly under the crank where it is more accessible. At higher heads, and consequently also at higher forces upon the crank, the increased projection of the latter from the bearing would unfavourably augment the bending moment of the pin in the bearing under the crank. The stuffing box consists here of a sleeve, retained by a rubber ring.

All bearings mentioned have bronze bushings. The specific pressures in the bearings from either side of the blade, where the

water has free access, are selected lower, 40 to 50 kg/cm². In the bearing under the lever, where proper lubrication is ensured, we may admit much higher pressures (up to 150 kg/cm²), but as a rule, (regarding that the size of the pin is given by its stress) the value of the specific pressure will be approximately the same as in the afore-mentioned bearings.

When checking the strength, we may simplify the statically indeterminate seating of the blade in three bearings by calculating as if the water pressure upon the blade were taken up by two bearings adjacent to the blade, and by calculating the pull of the link on the blade as if it were taken up only by the bearing nearest the crank.²⁾

¹⁾ Gamze i Golsher: *Technologiya proizvodstva krupnykh gidroturbin*, Moskva, Leningrad, Gosudarstvennoye nauchnotekhnicheskoye izdatelstvo, 1950, p. 258.

²⁾ For an exact calculation and equalization of the stress by means of the clearance in the bearing under the crank see: Granovskiy, Orgo, Smolyarov: *Konstrukcii gidroturbin*, Mashgiz, Moskva, Leningrad, 1953, p. 160.

The bending stress of the blade end by the water pressure must be checked in the shut-off position, similarly as the blade for inside regulation, and further we must control the bending stress of the blade by the reactions of the bearings determined by the method already mentioned (i. e. as in the case of a uniformly loaded beam on two supports), and finally the stress of the pins in the places where fastened to the blade. Here we assume that the reaction in the bearings acts in the centre of the length of the bushings; for the upper pin (towards the crank) we compose this stress with the stress by the torque of the blade. We calculate the pin under the crank for bending by the pull of the link and compose the bending stress again with the stress resulting from the torque.

If we calculate with the forces created by the moment with which the water acts upon the blade, we select as permissible stress about 800 kg/cm² (cast steel). For safety reasons, however, we select the regulator for regulating forces higher than the forces resulting from the hydraulic determination of the pressures upon the blades (see further in this chapter); the regulating mechanism and the blades are not as a rule subjected to stress by these greater forces, because the rectifying screws in the pull rods of the regulating ring are set to ensure that the piston of the servomotor bears against its stop when the blades have returned to a firmly closed position. Despite this arrangement, we must demand, that, even if the lengths of the pull rods of the regulating ring were incorrectly adjusted, the blades and the other parts of the regulating mechanism would still stand these maximum forces, also when we neglect the friction in the mechanism (which is the more unfavourable case). But for such an exceptional case we calculate with a high stress, i. e. for cast steel up to 1500 kg/cm², and for the reformed pins and other forged parts of the mechanism 2000 kg/cm².

It must also be mentioned that it is possible to manufacture welded blades.¹⁾ (See Fig. 161).

2. Regulating Mechanism, Links, Regulating Ring

The composition of the regulating mechanism for inside as well as for outside regulation has been described earlier (Part I, Chapter VI). But we must still emphasize the advantage of utilizing the principle of the bent lever in the shut-off position in the arrangement of the links for both mentioned types of regulation.

In the shut-off position of the blades, the axis of the link is usually selected so as to enclose an angle of 15° to 20° with the radius led from the centre of the runner. This principle, which has already been mentioned in connection with inside regulation, holds good also for outside regulation; for inside regulation see Fig. 153. We must bear in mind that the variation of the through-flow when turning the guide blades by a certain small angle is comparatively smaller if the blades are in a position near full opening than when they are near the shut-off position. By employing the bent-lever principle we can compensate this influence, because to the same rotation of the regulating ring corresponds a smaller rotation

¹⁾ Swiss Patent No. 162526 (Escher-Wyss A. G., Zurich).

of the blades when they are near the shut-off position. In addition, there is a greater force transmission in the closed position of the blades, and this is more advantageous for a tight closing of the blades, as a rule it is less possible when selecting the position of the pivot of the blade to equalize entirely the moments of the water pressures in the open and closed positions; in the closed position the moment is as a rule greater.

Fig. 162 indicates the graphical determination of the forces in the regulating mechanism. The force P_T in the link we determine from the moment acting upon the blade by dividing its magnitude by the perpendicular distance (perpendicular to the axis of the link) of the pivot of the blade. Then we resolve the force in the link into the radial force (which is not indicated in the figure

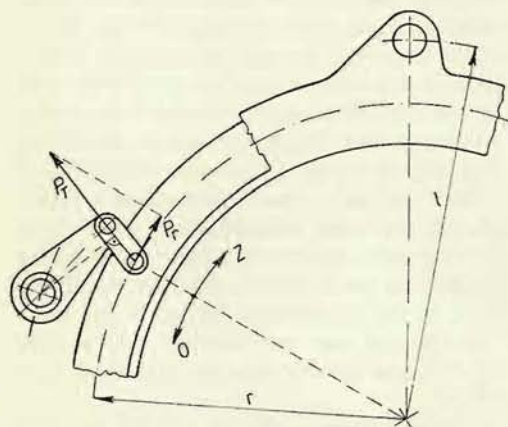


Fig. 162

and is counter-balanced by the equal component on the opposite side of the ring) and the peripheral force P_r on the pitch circle of the pins of the regulating ring. By multiplying the force P_r by the number of blades and the radius r of the pitch circle we obtain the total moment which the regulating ring must develop. If we divide this moment by radius l where the centre of the eye of the regulating ring is located, we obtain the force in the pull rod of the regulating ring; when

this ring is fitted with two pull rods – as it is in the majority of cases – we must, of course, still divide this force by two to obtain the force in one pull rod.

In this way we usually determine graphically the conditions for both extreme positions of the regulating mechanism, whereby at the same time we ascertain the necessary lift of the shifting ring and the extreme positions of the links and cranks, which, of course, must not interfere with each other.

The regulating links are as a rule made from forged material and fitted with bronze bushings for the pins. The pins are of steel, their length equals approximately their diameter. Through a bore in the pin grease is pressed upon the friction surfaces by a pressure lubricator. The pins are pressed into the regulating ring and the cranks of the blades; the diameter of the pressed-in part is somewhat smaller, the stepping determining the depth of pressing-in. The cranks depend on the stress and are made either of cast iron or cast steel.

For outside regulation and when calculations are based on the forces with which the water acts upon the blade, we may admit a specific pressure upon the pins up to about 150 kg/cm².

As already pointed out, the regulator is constructed for greater regulating work – by this we mean the product of the maximum force and lift in any point of the regulating mechanism – other than results from water pressures upon the blade. The reason for this is that we have neither taken into account the friction of the pivots of the blades and other parts of the mechanism, nor that in the course of time the forces required for actuating the blades are increased due to dirt settling on the faces of the blades or clogging by floating ice. Therefore, we must calculate with a certain efficiency of the regulating mechanism, taking for the magnitude of the regulating work 1.5 to 3 times the theoretical value. According to the author's experience, reliably safe values are offered by the expression

$$A_{kgm} = 30 Q_m^{3/5} \sqrt{H_m D_{1,m}}, \quad (163)$$

where D_1 is the largest inlet diameter of the runner in meters, provided that the regulating mechanism is correctly designed.

When checking the specific pressures from the forces in the regulating mechanism selected in this way, we admit values up to 400 kg/cm².

The calculation of the strength of the links, pins and cranks is carried out in the usual way and will be shown, at least partially, by an example.

The regulating links are also used as safety elements against damage of the guide blades or other difficultly replaceable parts by foreign bodies. Such a case can only occur when the installation is equipped with a wide-spaced grid, and, therefore, this safety measure is only for low-pressure machines with wide runner ducts.

Fig. 163 shows a regulating link which is made so as to have the least strength in all parts of the regulating mechanism.

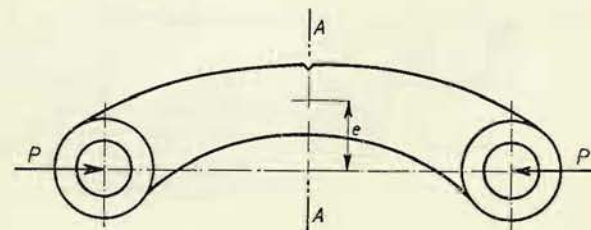


Fig. 163

For this reason it is made of cast iron and is curved, so that in the cross section. $A-A$ it is subjected to bending stress by the moment P . e . The resisting moment here is further adjusted by a notch to cause the link to crack at about double that force which can occur in it when the maximum force of the regulator is distributed to all links; the other parts (pins, cranks) must still stand the corresponding forces. Should a foreign body penetrate between two blades, the excess of the force of the regulator will concentrate upon the two links in question, which will crack and be easily replaced after the removal of the cause of the defect.

A similar principle¹⁾ underlies the design of the links illustrated in Fig. 165, where the safety device consists of a bolt with a recess subjected to tensile stress

¹⁾ Mashinostroyeniye, Part 12, Moskva, Gosudarstvennoye nauchno-technicheskoye izdatelstvo, 1948, p. 294.

when the blades are being closed. In addition, this bolt offers the possibility of adjusting the shut-off positions of the individual blades.

Fig. 164 shows the safety device as a bolt (likewise subjected to stress when the blades are being closed) which transmits the moment from the crank pivoted on its own hub, which in turn is keyed on the pin of the blade. Instead of the bolt subjected to tensile stress a pin subjected to shear stress may be employed.

The function of the regulating ring has already been described. Its shape depends to a certain degree on the general disposition, but mainly on the resisting moment which is required for strength reasons. Various shapes of regulating ring

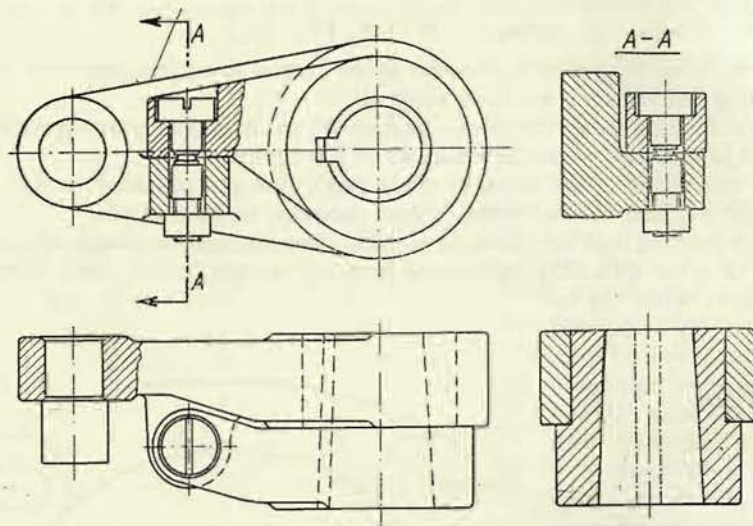


Fig. 164

are presented in Figs. 34, 35 and 36 and in Appendix I, VI and X. In general it is more advantageous to employ two pull rods for turning the ring, because then it is subjected to less strain and the ring can be made of gray cast iron up to considerable size. The use of one pull rod is less advantageous owing to the greater stress on the ring; rings of larger size must be made of cast steel; this construction is only used for smaller machines.

When servomotors, built directly into the turbine pit (Appendix I), are used, where the manual mechanical regulation is eliminated, a latch-bolt must be provided for, by which the shifting ring is secured (blocked) in the closed position before (in case of a longer down-time) the pressure oil supply is cut off; otherwise the water pressure upon the guide blades would open the turbine.

The strength of the latch-bolt must be calculated for the sum of the maximum forces of the regulator and the water pressure when the blades are in the shut-off

position. Such a latch-bolt shaped like a large taper pin, controlled by a handwheel and a spindle, is shown on the left half of Appendix I.

When the latch-bolt is to be hydraulically remote-controlled, it must be equipped with an oil-operated servomotor which, if of the one-sided type, can

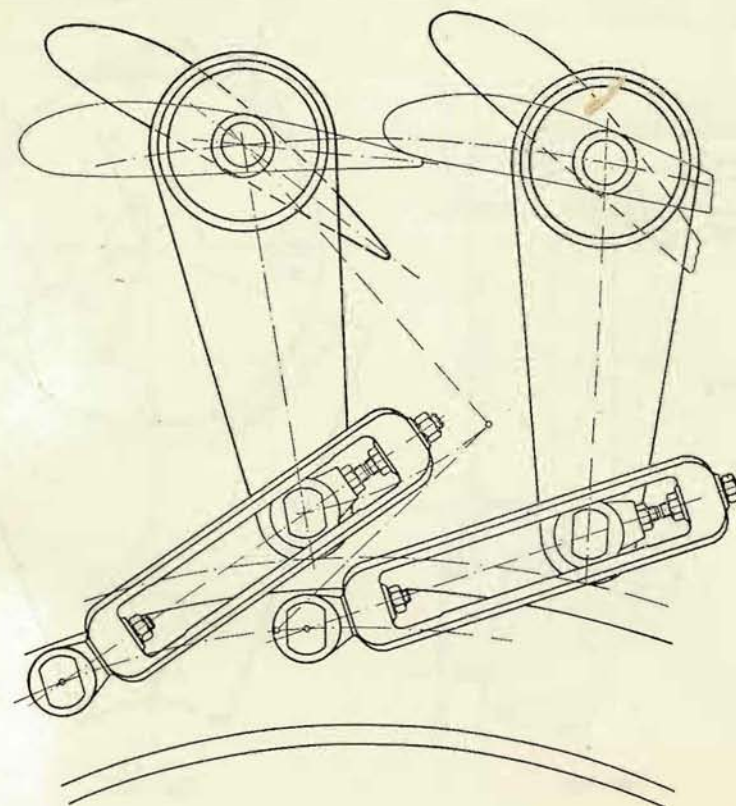


Fig. 165

only act against the force of a helical spring. But whether we employ a single-acting motor with a spring or a double-acting motor, we must always bear in mind that the force required for pulling out the latch-bolt must be decisively greater than that for inserting it. Therefore, when a single-acting servomotor is employed, the latch-bolt is inserted by the spring and pulled out by the oil pressure; in double-acting servomotors, the active area of the piston subjected to the oil pressure in pulling out the latch-bolt must be larger than the active area of the piston which inserts it.

The locking of the shut-off position of the regulating ring may also be arranged on the servomotors.

When a split regulating ring is used, it is with regard to symmetry, divided in the sections lying on the ray which bisects the angles between the eyes of the pull rods. The ring is split either with regard to its large size or with regard to assembly

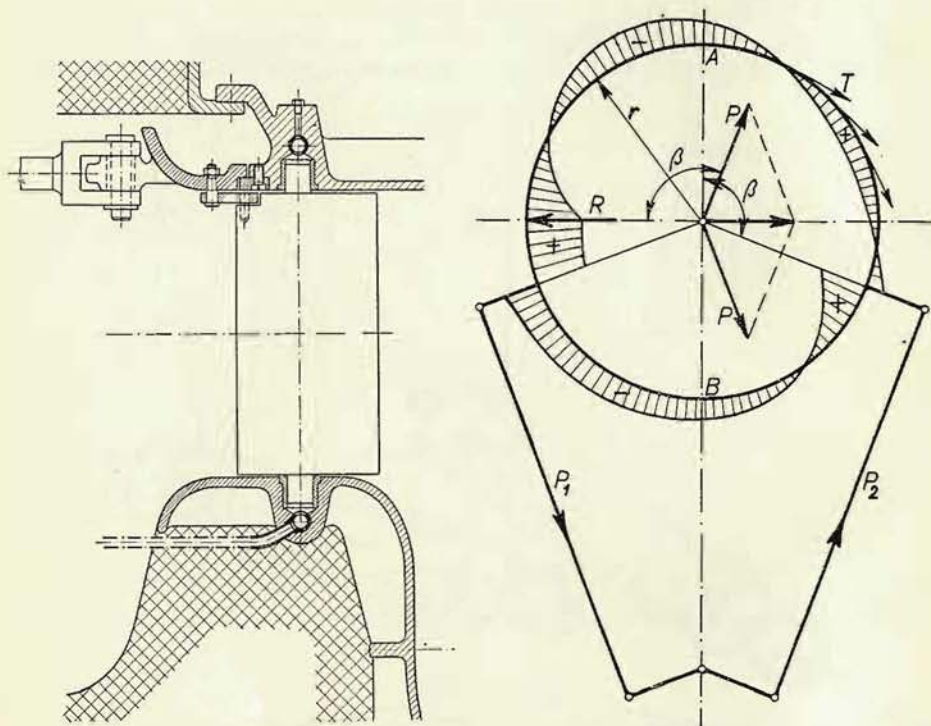


Fig. 166

Fig. 167

considerations. A split ring is inevitable e. g. for the disposition illustrated in Fig. 166 (inside regulation), which otherwise is very advantageous, because by locating the ring on the top lid we obtain a shorter regulating shaft, which does not pass through the concrete spiral and does not disturb the water supply to the turbine.

When the ring is revolved by two pull rods which are not parallel (Fig. 34, on the right side), in turning, it shifts slightly in the direction of the connecting line of the axes of the regulating heart and the turbine, as evident by a kinematic investigation of the mechanism. The seating of the ring must permit this shift and is therefore made with a clearance of 1 to 2 mm, or the ring is guided by two bronze

adaptors placed on the line perpendicular to the mentioned connecting line (or it is guided by more adaptors placed near and symmetrically to this line).

In the strength calculation for the shifting ring¹⁾ we shall consider the general case of a ring with two pull rods, as diagrammatically indicated in Fig. 167. The ring is acted upon by the following external forces:

1. The forces in the pull rods P_1 and P_2 , if we neglect variations caused by inaccuracies in assembly work, friction, etc., will be $P_1 = P_2 = P$.

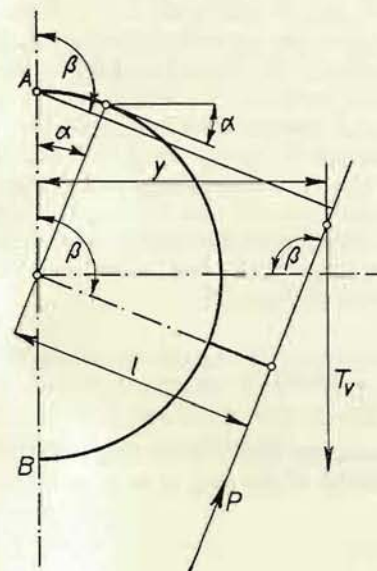


Fig. 168

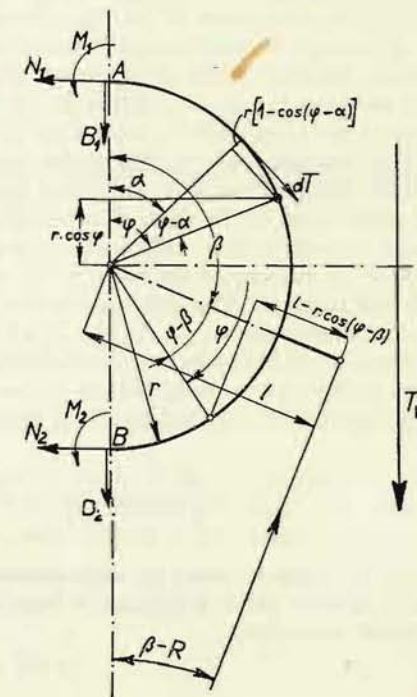


Fig. 169

2. The forces from the regulating links T . Neglecting variations caused by fluctuations of the water pressures upon the blades, fluctuations of the magnitude of the friction, etc., we may consider these forces to be equal. With regard to the large number of links we assume that their total force ΣT is uniformly distributed

¹⁾ Nechleba: Pevnostní výpočet regulačního kruhu s dvěma táhly (Strength Calculation of a Regulating Ring with Two Pull Rods), Strojnický obzor (Mechanical Engineering Review), 1941, p. 317. Also Meyer H.: Calcul des cercles de vannage des turbines hydrauliques, Bulletin technique de la Suisse romande, 1932. Further, Schnyder: Die Festigkeitsberechnung für Wasserturbinen und Pumpen, Dissertation at the Technical University (ETH) of Zurich, 1930.

along the circumference of the ring. To the part of the circumference $r \cdot d\alpha$ therefore falls

$$dT = \frac{z_0 T}{2\pi r} \cdot r d\alpha = \frac{z_0 T}{2\pi} d\alpha,$$

where z_0 is the number of links, r the radius of the shifting ring, and T the force with which each link acts upon the ring.

3. The reaction R of the guide of the regulating ring. If we transfer the forces P_1 and P_2 into the centre of the ring, there arise, on the one hand, the moments of these forces, which are in equilibrium with the moment of the forces of the links T , and, on the other hand, the resultant, which must be taken up by the guide of the ring and creates in it the reaction R . The magnitude of this reaction is known as it is given by the geometrical sum of the forces P_1 and P_2 and equals $R = 2P \cos \beta$.

This reaction acts according to the diagram upon the left half of the ring; in this half we subtract from it the horizontal components of the forces T and the horizontal component of the force P , whereupon the remainder is carried over as the forces N_1 and N_2 (Fig. 169) to the section $A - B$ into the right half of the ring.

Now let us imagine the circle to be cut through along section $A - B$ and the left half removed. The influence of this half upon the remaining part is replaced by the external forces N_1, N_2, B_1, B_2 and the moments M_1 and M_2 (see Fig. 169).

Now let us determine the resultant of the elementary forces dT ; its direction must be vertical as the horizontal components in the upper and in the lower part cancel each other; the magnitude of the resultant is (Fig. 168):

$$T_v = \int_0^\pi (\sin \alpha) \cdot dT = \frac{z_0 T}{2\pi} \int_0^\pi \sin \alpha d\alpha = \frac{z_0 T}{\pi}.$$

If this force has to create the same moment about the centre of the ring as the forces T , it must act at a distance y from the centre of the ring so as to satisfy the moment condition:

$$\int_0^\pi r dT = T_v y,$$

whence follows after substitution

$$r \frac{z_0 T}{2\pi} \int_0^\pi d\alpha = \frac{z_0 T}{\pi} y,$$

hence

$$y = \frac{\pi r}{2}.$$

We express now the bending moment in an arbitrary cross section of the regulating ring, deflected from the section A by the angle φ (Fig. 169). The moment of the force B_1 in the mentioned cross section is

$$\overleftarrow{M}_{B1} = B_1 r \sin \varphi.$$

From the force N_1 results:

$$\overleftarrow{M}_{N1} = N_1 \cdot r (1 - \cos \varphi);$$

from the forces dT :

$$\Sigma \overrightarrow{M}_T = \int_0^\varphi r [1 - \cos (\varphi - \alpha)] dT = \frac{z_0 T r}{2\pi} (\varphi - \sin \varphi);$$

the general moment hence is

$$\overleftarrow{M}_\varphi = B_1 r \sin \varphi + N_1 r (1 - \cos \varphi) - \frac{z_0 T r}{2\pi} (\varphi - \sin \varphi) + M_1$$

and applies from the point A and further on across the angle β . In the proceeding part the moment of the force P must be added:

$$\overleftarrow{M}_P = P [l - r \cos (\varphi - \beta)],$$

and the total moment will be

$$\begin{aligned} \overleftarrow{M}_\varphi = & B_1 r \sin \varphi + N_1 r (1 - \cos \varphi) - \frac{z_0 T r}{2\pi} (\varphi - \sin \varphi) + \\ & + \{P [l - r \cos (\varphi - \beta)]\} + M_1. \end{aligned}$$

From the equation of the moments about the centre of the ring we can ascertain the value P (neglecting the friction). Since the moment of the force P has already been introduced with the appropriate sign, we shall now pay no regard to it. From the equation of the moments

$$2 \cdot l P = z_0 T r$$

follows

$$P = \frac{z_0 T r}{2l}.$$

Thus the expression for the general moment is adjusted to

$$\overleftarrow{M}_\varphi = B_1 r \sin \varphi + N_1 r (1 - \cos \varphi) - \frac{z_0 T r}{2}.$$

$$\left[\frac{\varphi - \sin \varphi}{\pi} - \left\{ 1 - \frac{r}{l} \cos (\varphi - \beta) \right\} \right] + M_1,$$

which holds also in the left half of the ring up to the angle $(2\pi - \beta)$, from where again the moment of the force P must be added:

$$\overleftarrow{M}_P = P [l - r \cos (\beta - 2\pi + \varphi)] = P \cdot [l - r \cos (\varphi + \beta)]$$

and finally, in the place of the reaction R we must further add the moment of this reaction, which equals

$$\vec{M}_R = R r \sin\left(\varphi - \frac{3}{2}\pi\right) = R r \cos \varphi,$$

so that the general expression for the moment in the place rotated from the point A about the angle φ (in a clockwise direction – see Fig. 169) is, the positive moment being counted in the anti-clockwise direction,

$$M_\varphi = B_1 r \sin \varphi + N_1 r (1 - \cos \varphi) - \frac{z_0 T r}{2} \left[\frac{\varphi - \sin \varphi}{\pi} - \int_{\beta}^{2\pi} \left\{ 1 - \frac{r}{l} \cos(\varphi - \beta) \right\} - \int_{2\pi - \beta}^{2\pi} \left\{ 1 - \frac{r}{l} \cos(\varphi + \beta) \right\} \right] - \left[R r \cos \varphi \right] + M_1 \quad (164)$$

or

$$M_\varphi = B_1 r \sin \varphi + N_1 r (1 - \cos \varphi) - P l \left[\frac{\varphi - \sin \varphi}{\pi} - \int_{\beta}^{2\pi} \left\{ 1 - \frac{r}{l} \cos(\varphi - \beta) \right\} - \int_{2\pi - \beta}^{2\pi} \left\{ 1 - \frac{r}{l} \cos(\varphi + \beta) \right\} \right] - \left[R r \cos \varphi \right] + M_1. \quad (165)$$

Now we apply to the mentioned half of the ring the condition that the sums of the forces in the horizontal and vertical directions must equal zero. In the horizontal direction only the forces N_1, N_2 act and the component $P \cos(\pi - \beta)$. Hence it holds good:

$$N_1 + N_2 + P \cos(\pi - \beta) = 0$$

or

$$N_1 + N_2 = P \cos \beta. \quad (166)$$

Similarly applies for the vertical direction

$$B_1 + B_2 + P \sin(\pi - \beta) + T_v = 0$$

or

$$B_1 + B_2 = -P \sin \beta - T_v = P \left(\frac{2l}{\pi r} - \sin \beta \right). \quad (167)$$

We can further determine some other relations. If in Fig. 169 we change the sense of the force T_v , the sense of the force P also changes, as well as that of

moments M in the points A and B , as is the case in the right half of Fig. 170. If we look at this picture on the reverse side of the paper, we see it as it has been drawn in the left part of Fig. 170. If we further let act upon the ring reaction $R = 2P \cos \beta$, counterbalancing this action by introducing the forces $P \cos \beta$ of the opposite sense on both ends of the semi-circle, we obtain the picture of the forces acting upon the left half of the ring. If we compare this picture with the original picture

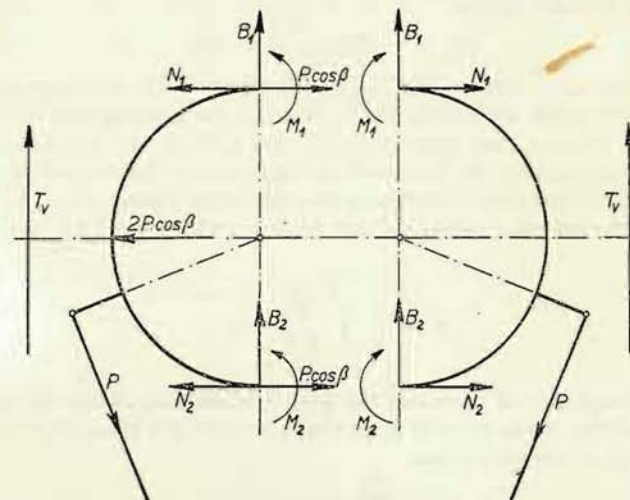


Fig. 170

in Fig. 169, we see that the forces at the ends of the semi-circle constitute the reaction to the forces at the ends of the right half, and at the same time follows from this consideration that $N_1 = N_2 = -\frac{P}{2} \cos \beta$. The minus sign indicates that the sense of the forces N_1 and N_2 must be opposite to that of the component $P \cos \beta$. But if we pay regard to the sign of the function $\cos \beta$, we may write

$$N_1 = N_2 = \frac{P}{2} \cos \beta. \quad (168)$$

We can further ascertain the relation between the moments M_1 and M_2 . We determine the moment in the point B from Equation (164) by substituting $\varphi = \pi$

$$M_{\varphi=\pi} = 2 N_1 r - \frac{z_0 T r}{2} \left[1 - 1 + \frac{r}{l} \cos(\pi - \beta) \right] + M_1,$$

$$M_{\varphi=\pi} = r [(P \cos \beta)] + P r \cos \beta + M_1.$$

The use of parantheses and brackets in the first term on the right side of the equation denotes that the expression enclosed in them does not change its sign

with the function $\cos \beta$, because it represents the force which we put into the equation for the moment, regardless of the sign, as already in establishing the equation the senses of the moments were taken into consideration; on the other hand, the second term changes its sign ($\beta > 90^\circ$), so that

$$M_{\varphi=\pi} = M_1.$$

Since the moment M_2 is in equilibrium with the moment $M_{\varphi=\pi}$, its sign must be opposite, and hence applies

$$M_2 = -M_{\varphi=\pi} = -M_1. \quad (169)$$

At the original six unknowns N_1, N_2, B_1, B_2, M_1 , and M_2 , we have thus already determined two; these are the forces N_1 and N_2 ; for ascertaining the remaining four unknowns we have only equations (167) and (169) at our disposal. Therefore, we determine the moment M_1 by means of Castigliano's theorem of the minimum of the work of deformation of statically indeterminate forces.

Neglecting the influence of the shifting forces upon the work of deformation A , we may write

$$A = \frac{1}{2} \int_0^{2\pi} \frac{M^2}{E \mathcal{J}} r d\varphi,$$

where \mathcal{J} is the moment of inertia of the profile of the ring about the neutral axis and E the modulus of elasticity of the material, whilst the value M_1 can be determined by means of the expression

$$\frac{\partial A}{\partial M_1} = \int_0^{2\pi} M \frac{\partial M}{\partial M_1} d\varphi = 0;$$

since $\frac{\partial M}{\partial M_1} = 1$, we obtain by using Equation (164)

$$\begin{aligned} & \int_0^{2\pi} B_1 r \sin \varphi d\varphi + \int_0^{2\pi} N_1 r (1 - \cos \varphi) d\varphi - \frac{z_0 T r}{2} \int_0^{2\pi} \frac{\varphi - \sin \varphi}{\pi} d\varphi + \\ & + \frac{z_0 T r}{2} \int_{\beta}^{2\pi} \left[1 - \frac{r}{l} \cos (\varphi - \beta) \right] d\varphi + \frac{z_0 T r}{2} \int_{2\pi - \beta}^{2\pi} \left[1 - \frac{r}{l} \cos (\varphi + \beta) \right] d\varphi - \\ & - R r \int_{\frac{3}{2}\pi}^{2\pi} \cos \varphi d\varphi + \int_0^{2\pi} M_1 d\varphi = 0, \end{aligned}$$

and from this relation we obtain after integration and adjustment the simple equation

$$N_1 r + M_1 - \frac{R r}{2\pi} = 0, \quad (170)$$

and by substituting for N_1 and R the corresponding expressions, we arrive at

$$M_1 = \frac{[(Pr \cos \beta)]}{\pi} - \left[\left(\frac{1}{2} Pr \cos \beta \right) \right] = [(Pr \cos \beta)] \left(\frac{1}{\pi} - \frac{1}{2} \right) = -M_2. \quad (171)$$

If we choose the same way for ascertaining the value B_1 , we set out from the expression

$$\frac{\partial A}{\partial B_1} = \int_0^{2\pi} M \frac{\partial M}{\partial B_1} d\varphi = 0.$$

Since applies $\frac{\partial M}{\partial B_1} = r \sin \varphi$, we obtain, immediately cancelling r , the equation

$$\begin{aligned} & \int_0^{2\pi} B_1 r \sin^2 \varphi d\varphi + \int_0^{2\pi} N_1 r \sin \varphi d\varphi - \int_0^{2\pi} N_1 r \cos \varphi \sin \varphi d\varphi - \\ & - \int_0^{2\pi} \frac{z_0 T r}{2} \frac{\varphi - \sin \varphi}{\pi} \sin \varphi d\varphi + \int_{\beta}^{2\pi} \frac{z_0 T r}{2} \left[1 - \frac{r}{l} \cos (\varphi - \beta) \right] \sin \varphi d\varphi + \\ & + \int_{2\pi - \beta}^{2\pi} \frac{z_0 T r}{2} \left[1 - \frac{r}{l} \cos (\varphi + \beta) \right] \sin \varphi d\varphi - \int_{\frac{3}{2}\pi}^{2\pi} R r \cos \varphi \sin \varphi d\varphi + \\ & + \int_0^{2\pi} M_1 \sin \varphi d\varphi = 0, \end{aligned}$$

whence by integration and adjustment it results

$$\begin{aligned} B_1 + \frac{3}{2} \frac{z_0 T}{\pi} + \frac{z_0 T r}{2 \cdot l} \left(\frac{\beta}{\pi} - 1 \right) \sin \beta - \frac{z_0 T}{\pi} (1 - \cos \beta) + \frac{R}{2\pi} &= 0 \\ B_1 = P \left(1 - \frac{\beta}{\pi} \right) \sin \beta - P \frac{l}{r \pi} - P \frac{2l}{\pi r} \cos \beta - [(P \cos \beta)] \frac{1}{\pi}, \end{aligned}$$

where the use of parantheses and brackets for the last term again denotes that a change of the function $\cos \beta$ exerts no influence upon the sign of the complete term as here the insertion of the expression of a force into the equation of the moment is concerned, so that it holds good:

$$B_1 = P \left[\left(1 - \frac{\beta}{\pi} \right) \sin \beta - \frac{l}{r \pi} - \left(\frac{2 \cdot l}{\pi r} - \frac{1}{\pi} \right) \cos \beta \right]. \quad (172)$$

The expression for B_1 has the positive sign, from which it is evident that the moment of the force B_1 has been inserted with the correct sense into the equation of the moment, or in other words that the sense of the force B_1 is the same as indicated in Fig. 169. If we, however, consider the component $P \sin \beta$ as positive, the

minus sign must be taken; this is necessary for further use in Equation (167). Thus we obtain

$$B_2 = P \left[-\frac{\beta}{\pi} \sin \beta + \frac{l}{r\pi} - \left(\frac{2 \cdot l}{\pi r} - \frac{1}{\pi} \right) \cos \beta \right]. \quad (173)$$

In this way we have ascertained all the values necessary for the determination of the general moment according to Equation (164), and thus also the general moment M_φ is determined. Its progress in an actual case is shown in Fig. 167.

By means of relations (171), (172), (173) and (168) the forces and moments in sections A and B are also determined. When in sections A and B the bolt connections are located, as usually is the case in split rings, we must dimension these connections with regard to the forces ascertained in this way.

When $\beta = 90^\circ$, i. e. when the pull rods are parallel, $N_1 = N_2 = 0$ and $M_1 = -M_2 = 0$, and the joint of the split ring, arranged between the eyes lying diametrically opposite each other, will be subjected only to shearing stress by the forces according to Equation (172) for $\beta = \frac{\pi}{2}$:

$$B_1 = B_2 = -P \left[\frac{1}{2} - \frac{l}{r\pi} \right]. \quad (174)$$

The general moment for both halves of the ring will be the same:

$$M = B_1 r \cdot \sin \varphi - \frac{z_0 Tr}{2 \cdot l} \left[\frac{\varphi - \sin \varphi}{\pi} l - l \left\{ 1 - \frac{r}{l} \sin \varphi \right\} \right],$$

or

$$M_\varphi = P \left[\frac{1}{2} r \cdot \sin \varphi - \frac{\varphi}{\pi} l + l \left\{ 1 - \frac{r}{l} \sin \varphi \right\} \right] \quad (175)$$

(here we have introduced the forces regardless of the sign, because the sense of the moments, we have already taken into account in the expression for the moment).

It is evident that a ring with diametrically arranged eyes, with regard to the connection of both halves, is more suitable than a ring with eyes located under an angle $\beta > \frac{\pi}{2}$. When further, in a ring for which applies $\beta > \frac{\pi}{2}$ make (if it is possible

with regard to other reasons) $l = y = \frac{\pi r}{2}$, there will hold good

$$B_1 = B_2 = P \left[\frac{1}{2} - \frac{l}{r\pi} \right] = P \left[\frac{1}{2} - \frac{\pi r}{2\pi r} \right] = 0,$$

and theoretically the connection of such a ring will not be subjected to any stress

These formulas are applicable also to a ring with one eye if we substitute $\beta = \pi$ and thus concentrate both forces (i. e. of the value $2P$) on one arm.

Example. As an example, let us now carry out mathematical control of the parts of the turboset as shown in Appendix VI, above all of the guide blade, the dimensions and seating conditions of which are indicated in Fig. 171. By graphical investigation of the pressures upon the blade according to Part II, Section a, Chapter II, we have found that the maximum force and the maximum moment of the water pressure upon the blade are encountered in the completely closed position.

When the machine operates under a small load, the losses in the supply pipe fall off; therefore, we shall calculate with a head not reduced by these losses, i. e. $H = 220$ m.

Further we must consider the conditions at a sudden discharge of the set and closing of the guide apparatus by the automatic regulator. Since the turbine is equipped with a relief valve (see Part III), the pressure rise does not normally exceed 20 % and the same applies for the increase of the stress of all parts; this circumstance we take into consideration when judging the resultant stresses. On an accidental failure of the relief valve the pressure would rise by 100 %. In such a case the stresses would be doubled. As this would be very exceptional (the relief valve is fitted with a device which in the case of a valve failure extends the closing time of the regulator and which therefore would have to fail at the same time), we may in this case admit a very high stress, nearly up to the yield stress.

The force P with which the water acts upon the closed blade under the head $H = 220$ m is indicated with values in Fig. (171):

$$P = 18 \cdot 54.2 \cdot 22 = 21,500 \text{ kg.}$$

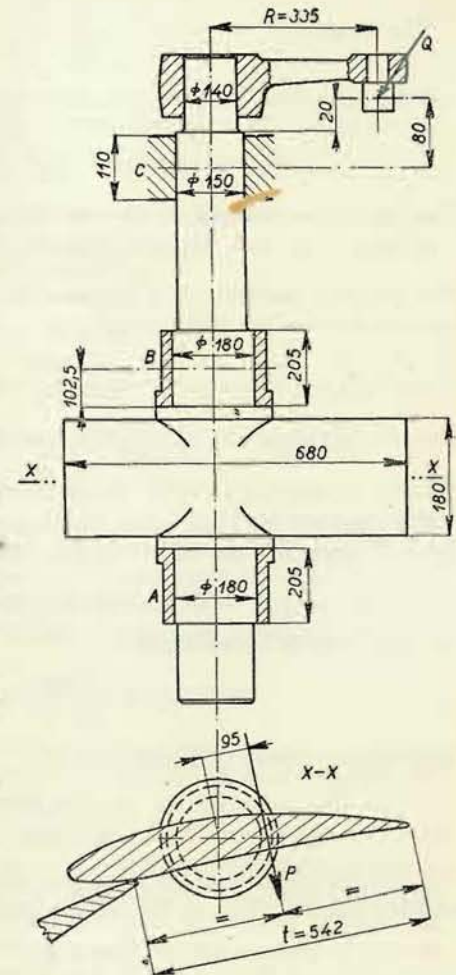


Fig. 171

The reactions in the bearings A and B will consequently be $P_1 = P_2 = 10,750$ kg and the specific pressure in them

$$p_{A,B} = \frac{10,750}{18 \cdot 20.5} = 29.1 \text{ kg/cm}^2.$$

The torque is

$$M_k = 21,500 \cdot 9.5 = 204,000 \text{ kgcm},$$

and the stress from the torque in the pivot B

$$\tau_k = \frac{10 \cdot M_k}{\pi d^3} = \frac{16 \cdot 204,000}{\pi \cdot 5832} = 178.5 \text{ kg/cm}^2.$$

The bending moment of the pivot in the place of the transition into the retainer is

$$M_0 = 10,750 \cdot 10.25 = 110,000 \text{ kgcm}.$$

The resisting moment for a diameter of 180 mm is $W_{180} = 572.6 \text{ cm}^3$ and the bending stress of the pivot equals

$$\sigma_0 = \frac{110,000}{572.6} = 192 \text{ kg/cm}^2.$$

The ideal stress in this section consequently is

$$\sigma_r = \sqrt{\sigma_0^2 + 3\tau_k^2} = \sqrt{37,000 + 3 \cdot 32,000} = 364 \text{ kg/cm}^2.$$

For checking the pivot under the regulating crank we must first determine the force Q upon the pin of the crank; this force will have the magnitude $Q = 21,500 \cdot \frac{9.5}{33.5} = 6100$ kg, and the specific pressure in the bearing C under the crank will be approximately

$$p_C = \frac{6100}{15 \cdot 11} = 37 \text{ kg/cm}^2.$$

The bending stress in this pivot will be

$$\tau_k = \frac{16 \cdot 204,000}{\pi \cdot 3375} = 308 \text{ kg/cm}^2.$$

The bending moment of the force Q is $M_0 = 6100 \cdot 8 = 49,000$ kgcm, and at the resisting moment $W_{150} = 331 \text{ cm}^3$ the bending stress will be

$$\sigma_0 = \frac{49,000}{331} = 148 \text{ kg/cm}^2,$$

so that the ideal stress will be $\sigma_r = 548 \text{ kg/cm}^2$.

A pivot of a diameter of 140 mm will be subjected to torsional stress

$$\tau_k = \frac{16 \cdot 204,000}{\pi \cdot 2744} = 378 \text{ kg/cm}^2,$$

and to bending stress in the weakened place by the moment $M_0 = 6100 \cdot 2 = 12,200$ kgcm; here applies

$$W_{140} = 269 \text{ cm}^3,$$

so that

$$\sigma_0 = \frac{12,200}{269} = 45.4 \text{ kg/cm}^2,$$

which may be neglected.

On a regulating pin with a diameter of 70 mm and a length of 70 mm the specific pressure will be $p = \frac{6100}{7 \cdot 7} = 125 \text{ kg/cm}^2$, and the pin will be stressed by the bending moment $M_0 = 6100 \cdot 3.5 = 21,300$ kgcm. As the cast-in part is stepped down to the diameter of 65 mm, the resisting moment has the magnitude $W_{65} = 27 \text{ cm}^3$, and hence the bending stress of the pin is

$$\sigma_0 = \frac{21,300}{27} = 790 \text{ kg/cm}^2.$$

For reasons already mentioned we shall dimension the regulator for regulating work

$$A = 30 Q \sqrt{H D} = 30 \cdot 12.5 \cdot \sqrt{220 \cdot 2.4} = 8600 \text{ kgm} \doteq 9000 \text{ kgm}.$$

With regard to standardization of regulators the servomotors are selected for the nearest higher stage of regulating work, i. e. $A = 10,000$ kg. The diameter of the pistons of these servomotors is 420 mm and consequently the surface is 1385 cm^2 . Since the turbine is fitted with two servomotors, the total surface is $F = 2770 \text{ cm}^2$, and the regulating work for a stroke of the servomotors of $z = 230$ mm has to be $A = F p z = 2770 \cdot 0.23 \cdot p = 9000$ kg, the required minimum pressure of the oil is

$$p_{\min} = \frac{9000}{2770 \cdot 0.23} \doteq 14 \text{ atm. gauge pressure}.$$

As here a fully automatic turboset is concerned, an automatic cut-off is necessary in case of failure in the supply of the regulator oil; this cut-off must be performed slightly before the oil pressure drops to value p_{\min} , so that there will still be sufficient pressure to shut the turbine, i. e. approximately 16 atm. gauge pressure.

Note: The determination of this pressure is derived from the capacity of an air-vessel which holds 1500 litres (see Part III). When the pressure drops to 16 atm. gauge pressure initiates (by means of a pressure switch) the closing process, the quantity of oil discharging from the air-vessel equals the stroke volume of both servomotors, i. e. the quantity $o = 2570 \cdot 23 \doteq 65,000 \text{ cm}^3 = 65$ litres. That is to say, the pressure in the air-vessel, which is no longer refilled, drops according to the relation (for simplicity reasons we consider here an isothermic process)

$1500 \cdot 17 = 1565 p'$, from which results $p' = \frac{1500 \cdot 17}{1565} = 16.2 \doteq 16 \text{ atm.}$, or 15 atm. gauge pressure, which is with a certain safety factor the required minimum pressure.

With regard to the lag in the repumping action (see Part III), which for safety reasons we consider as equalling three atm. gauge pressure, the upper pressure limit will be 19 atm. gauge pressure. The installation is also equipped with an auxiliary pump which (with regard to automatic action) is designed to work at higher pumping pressures within the range of the repumping lag from 19 to 22 atm. gauge pressure. In the case of failure in the repumping cycle the turboset is cut off when the maximum upper pressure limit of 24 atm. gauge pressure is attained. With this last value we shall further calculate as with safely established upper pressure limit.

Thus we obtain the force of one servomotor as $P_{\max} = 1385 \cdot 24 = 33,200$ kg and the force of both servomotors as $2 P_{\max} = 66,400$ kg. The servomotors act upon the eyes of the shifting ring at the radius $l = 1730$ mm. Since the pitch circle of the regulating pins has the radius $r = 1100$ mm, the total force at this radius equals $P_r = 2 P_{\max} \frac{l}{r} = 66,400 \cdot \frac{1700}{1100} \doteq 10,200$ kg, and as there are 16 guide blades, the force acting upon one pin in the peripheral direction (P_r in Fig. 162) will be

$$P_r = \frac{10,200}{16} = 6400 \text{ kg}.$$

We have determined graphically (see Fig. 162) that this peripheral force corresponds to the force in the link $Q = 21,000$ kg and the torque on the crank, since in the shut-off position the perpendicular distance of the link is 330 mm, $M_k = 21,000 \cdot 33 = 693,000$ kg cm.

When we count with these values, the specific pressure in the bearing under the crank equals

$$p_{C,\max} = \frac{21,000}{15 \cdot 11} = 128 \text{ kg/cm}^2,$$

and the stress in the pin with a diameter of 140 mm by the torque will be

$$\tau_k = \frac{16 \cdot 693,000}{\pi \cdot 2744} = 1300 \text{ kg/cm}^2.$$

The stress in the pin in the bearing C under the crank will be: torsional stress

$$\tau_k = \frac{16 \cdot 693,000}{\pi \cdot 3373} = 1050 \text{ kg/cm}^2,$$

and bending stress

$$\sigma_0 = \frac{21,000 \cdot 8}{331} = 510 \text{ kg/cm}^2,$$

whence $\sigma_r = 1900 \text{ kg/cm}^2$.

With regard to this stress the pin of the blade (blade of cast steel) was reforged.

The specific pressure on the regulating pin is under these conditions $p = \frac{21,000}{7 \cdot 7} = 428 \text{ kg/cm}^2$, and the bending stress of this pin, which is made of steel Type C60 will be

$$\sigma_0 = \frac{21,000 \cdot 3.5}{27} = 2700 \text{ kg/cm}^2.$$

The regulating ring is designed in such a way that theoretically there are no forces in the bolt connection located between the eyes; for this reason we have selected the radius passing through the centres of the eyes of the pull rod with a length $l = 1730$ mm for the radius $r = 1100$ mm of the pitch circle of the pins, so that the shearing force according to Equation (174) equals

$$B_1 = B_2 = -P \left(\frac{1}{2} - \frac{l}{r\pi} \right) = -P \left(\frac{1}{2} - \frac{1730}{1100 \cdot \pi} \right) \doteq 0.$$

The normal forces and bending moments in these connections will likewise equal zero, which follows from the fact that the radii of the eyes of the ring enclose an angle of 90° with the dividing plane. Theoretically, the connection transmits no forces whatsoever, and therefore we select the connecting parts – bolts and fitting taper pins – in accordance with the size of the ring without special calculation.

Further, we ascertain the bending moments in various sections of the ring according to the expression (175)

$$M_\varphi = Pl \left(\frac{1}{2} \frac{r}{l} \sin \varphi - \frac{\varphi}{\pi} + \left[1 - \frac{r}{l} \sin \varphi \right] \right),$$

where for the first quarter of the ring the term in the brackets falls off and we obtain¹⁾

$$M_\varphi = Pl \left(\frac{r}{2l} \sin \varphi - \frac{\varphi}{\pi} \right).$$

If we substitute $\pi/2$ for φ and for P the force of the servomotor the round value $P = 35,000$ kg, we obtain

$$M_{90^\circ} = 35,000 \cdot 173 \cdot (0.318 - 0.5) = -35,000 \cdot 173 \cdot 0.182 = -1,100,000 \text{ kgcm}.$$

We determine further the moments for other angles φ and thus we ensure that the moment in the section $\varphi = \pi/2$ as given above is the maximum value, and calculate with this value. We ascertain graphically the moment of inertia and from

¹⁾ It can be proved that in rings with parallel pull rods the bending moments in the second quarter are equal and symmetrically distributed to those in the first quarter. It will therefore suffice to check only a quarter of the ring. See Pfarr: Die Turbinen für Wasserkraftbetrieb, Berlin, 1912, p. 401.

it the resisting moment of the cross section of the regulating ring. The value of the latter is $W = 4950 \text{ cm}^3$. Hence the maximum bending stress of the regulating ring is

$$\sigma_0 = \frac{1,100,000}{4950} = 220 \text{ kg/cm}^2.$$

Therefore the ring was made of gray cast iron.

Now there only remains to check the eyes of the regulating ring for bending stress and the pins of the main pull rods for bending stress and specific pressure; the pins were selected so as to exhibit a specific pressure of approximately 120 kg/cm^2 and a bending stress of 870 kg/cm^2 under the influence of the maximum force of the servomotor.

IV. EXTENSION OF THE REGULATION

Under the term „extension of the regulation“ we understand the force-transmitting mechanism between the servomotor of the turbine regulator and the shifting ring. This mechanism consists of the following parts: regulating pull

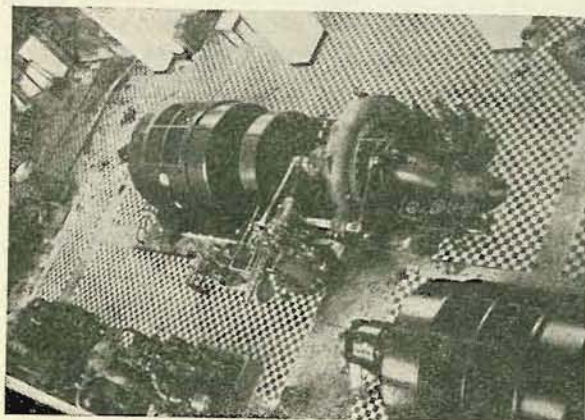


Fig. 172

rods, regulating heart, regulating shaft and seating, or, in large turbines, the servomotors which are built into the turbine pit and equipped with pull rods.

The pull rods are made as a rule of tubes and their length should be adjustable to permit a correct setting of the shut-off position of the guide apparatus; for this reason, the eyes of the pull rods are connected (at least at one end) by means of a thread with

a lock nut (see Figs. 34, 35 and Appendix I). Into the eyes of the pull rods bronze bushings are inserted in which rotate the pins, connecting the pull rods to the regulating ring and heart; the specific pressures in the bushings are the same as the mentioned permissible pressures on the pins of the links. In parts which contain fixed pins and where much higher specific pressure is encountered, the pins must be secured against rotation to prevent abrasion in the pin holes and the development of a clearance which would impair the precision of the regulating action.

The seating of the regulating shaft on a horizontal turbine is seen in Fig. 172,

and presents a view of the turboset a section of which is shown in Fig. 36. The regulating shaft is seated in the bearing on the spiral and in the bearing of the regulator, where it is also secured against axial shift by the keyed-on crank of the regulator. The regulating heart is overhung and also keyed on the shaft.

The regulating shaft must be checked for bending and torsional strength with regard to the place of the seating. We select a low permissible (reduced) stress – about 200 to 400 kg/cm^2 – for the torsion of the shaft, which must not exceed a certain limit, otherwise the accuracy of the regulation would be impaired.

When the regulator begins to move, the regulating lever and the regulating mechanism offers resistance to this action, the part of the shaft between the lever of the regulator and the regulating heart must undergo elastic deformation, so that the lever of the regulator performs part of the lift „unloaded“, with the regulating heart at rest. This „no-load“ lift of the regulating lever in a manual regulation should not exceed 2% of the total lift of the lever (from the open into the closed position) and in an automatic regulation it must not exceed 0.5% of the total path.

If we denote by M_k the maximum torque on the regulating shaft of diameter d , the twisting of two sections spaced 1 cm , measured at a radius of 1 cm , is given by the expression

$$\delta = \frac{32 M_k}{\pi d^4 G}, \quad (176)$$

where G is the modulus of shearing elasticity in kg/cm^2 .

Further, when L is the length in cm of the shaft between the regulating lever and the regulating heart, z the total lift of the regulating lever with the radius r , and x is that permissible part of the total lift so that xz is the „no-load“ lift of the regulating lever in cm , then it holds good that:

$$L \cdot \delta = \frac{xz}{r}.$$

If we introduce the value δ determined from this relation into Equation (176) and ascertain d^4 , substituting for $\frac{32}{\pi}$ the approximate value 10 , we obtain

$$d^4 = \frac{10 \cdot M_k}{G} \cdot \frac{Lr}{xz}.$$

The moment M_k can be expressed by the regulating work A (in kgm), for the regulating work is the product of the force and the lift and consequently also the product of the moment and the angle in circular measure corresponding to this lift. Since z is the lift of the lever measured in cm along the arc of the radius r of the lever, this angle is $\frac{z}{r}$, and consequently applies

$$100 A_{(\text{kgm})} = M_{k(\text{kgcm})} \frac{z}{r},$$

and hence

$$d^4 = \frac{1000 A}{G} \frac{r^2 L}{z^2 x}, \quad (177)$$

where A is expressed in kgm and the other values in the kg-cm system.

Regulating shafts for great regulating work would have considerable diameters which would render practical application impossible. In this case pairs of servo-

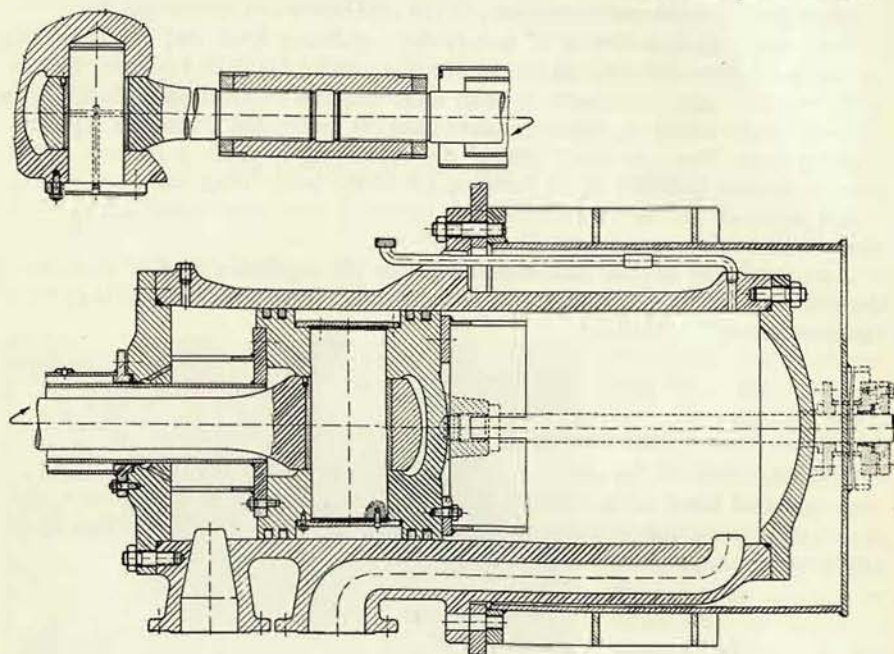


Fig. 173

motors built into the turbine pit are used; these motors are directly connected to the regulating ring by their pull rods (see Appendix I.) Since they are always mounted with their pull rods parallel, the regulating ring also is subjected to less stress. Fig. 173 presents a cross section of such a servomotor. The cylinder of the servomotor is bolted by means of a flange to the welded foundation case, which is held by anchor bolts and concreted into the turbine pit. The pin of the swinging seat of the pull rod is directly inserted into the piston to which is bolted a packing tube, covering the pull rod and passing through the stuffing box. The piston has either no special sealed parts or is fitted with piston rings. The covering tube has a leather sleeve packing. The cylinder as well as the piston are made of grey cast iron (in so far this is compatible with stress by oil pressure); while for high pressures and large sizes, both the cylinder and the piston must be made of cast steel,

supporting rings of grey cast iron (Fig. 174) are fastened to the cylinder to ensure good sliding properties. In order to prevent oil leakage from the pressure spaces of

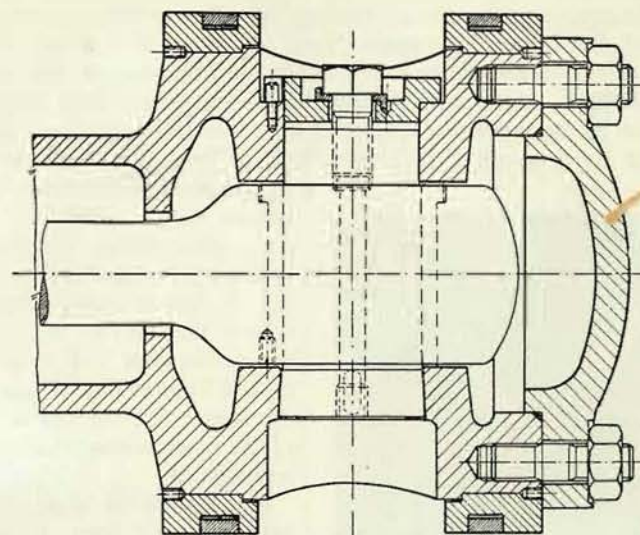


Fig. 174

the cylinder around the pin into the covering tube and through it into the outer space, special sealing of the pin must be provided for (see the flanges in Figs. 173 and 174).

These servomotors, even when their pull rods are parallel, do not act upon the

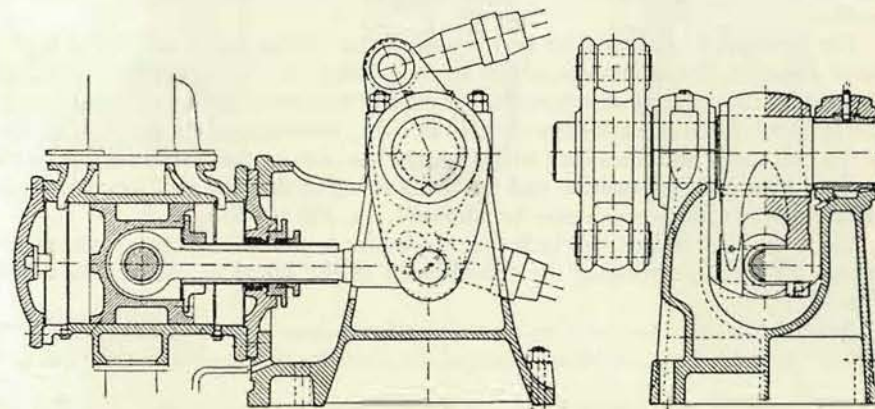


Fig. 175

regulating ring with the net moment. The oil pressure always acts in one servomotor upon the rear side of the piston, while in the other servomotor the pressure is exerted upon the front surface of the piston, which is smaller by the cross section of the covering tube passing through the stuffing box; for this reason, the ring is always acted upon by a certain force (equalling the product of the cross section area of the covering tube in the stuffing box and the oil pressure) directed off the servomotors, which must be taken up by the guide of the regulating ring.

The motion of the regulating ring or of the servomotor must be transmitted to the regulator by a so-called feed back linkage (see Part III). As shown in

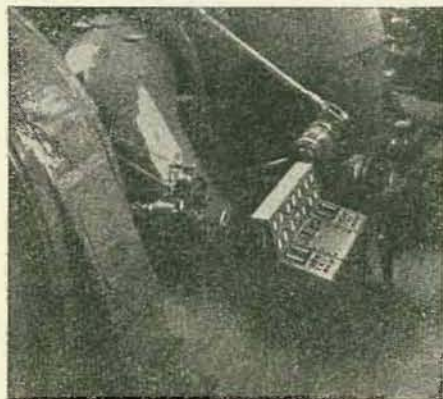


Fig. 176

Appendix I, the motion of the regulating ring is transmitted by means of a sliding block, two-armed lever (indicated by dashed lines in Appendix I) and a rod mechanism. The motion may also be transmitted from the servomotor (as shown by the dashed lines in Fig. 173) or by means of a sleeve slid over the covering tube of the servomotor, which also moves rectilinearly.

For horizontal shaft turbines the installation of two servomotors is unsuitable. Here an arrangement having a regulating heart is employed, but with only a very short regulating shaft, as shown in Fig. 175 (it must be only pointed out that – as can be

seen in the figure – the oil-distributing slide valve of the regulator is placed directly on the servomotor). Fig. 176 illustrates this servomotor in connection with the turbine.

The strength of the cylinder and piston of the servomotor is calculated in the usual manner. The anchorage of the servo-cylinder into the foundation case and the case on the concrete structure must, of course be dimensioned for the maximum forces which the servomotor can develop in either direction of its action. The eye of the pull rod is also lined here with a bronze bushing for the piston pin, and with regard to the good lubrication and the small swing of the pull rod, comparatively rather high specific pressure may be admitted, i. e. 250 to 350 kg/cm².

There are also designs in which the servomotor is placed directly into the regulating ring, thus eliminating the transmission of the forces to the structure (see Fig. 177).¹⁾

Example: In order to obtain an idea of the dimensions of the regulating shaft, we are now going to calculate as an example the diameter of this shaft for the turbine

¹⁾ L. Meissner: Die Kaplanturbinen des Wasserkraftwerkes Neu-Oetting, VDI, Vol. 93 (1951), p. 868.

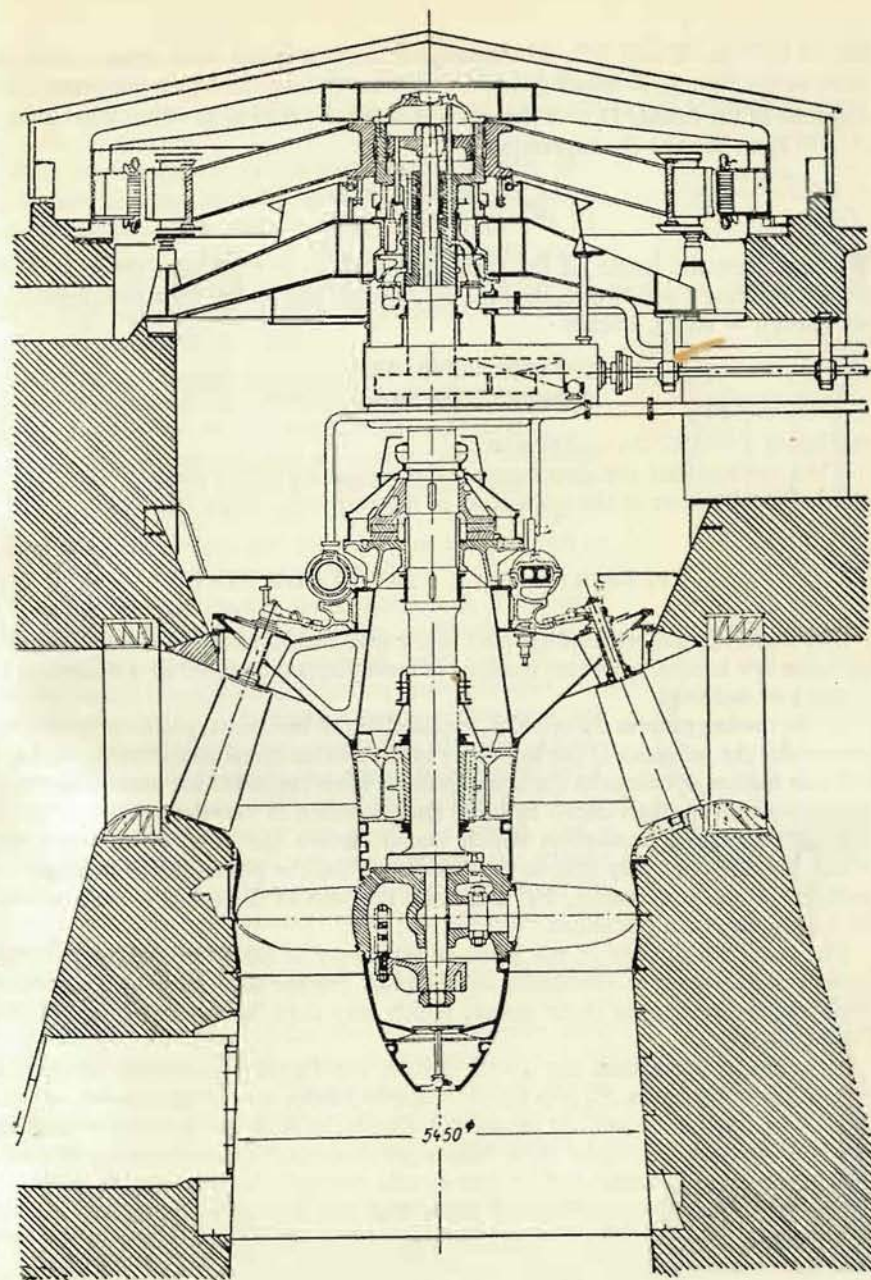


Fig. 177

shown in Figs. 36 and 172, considering for the regulation work again a loss-free head in the piping, amounting to $H = 230$ m, so that the regulation work (inlet diameter of the runner $D_1 = 930$ mm) is $A = 30 Q \sqrt{HD} = 30 \cdot 1.9 \sqrt{230 \cdot 0.93} \approx 850$ kgm. We use the expression (177):

$$d^4 = \frac{1000 A}{G} \frac{r^2 L}{z^2 x}.$$

We have here the length of the regulating shaft $L = 1500$ mm, the arm of the regulating lever $r = 275$ mm, the lift $z = 200$ mm, and for the automatic regulation we select $x = 0.005$, whence

$$d^4 = \frac{1000 \cdot 850}{800\,000} \cdot \frac{760 \cdot 150}{400 \cdot 0.005} = 61000 \text{ cm}^4,$$

and hence $d = 15.7 \text{ cm} \approx 160 \text{ mm}$.

Thus we see that the diameters of the regulating shafts assume considerable values (the diameter of the main shaft of the turbine is about 240 mm).

V. SPIRAL WITH STAY BLADE RING

The metal spirals, which form part of the machine, are either made of grey cast iron (for low heads), or of cast steel, or of steel plates connected to one another by riveting or welding.

In the casting process the spiral is moulded in the horizontal position, so that the core under the influence of the buoyancy in the molten metal tends to shift upward. For this reason, openings in the spiral wall are often made for the anchoring cores; these openings are then closed by blind flanges which fit into the openings so as to eliminate surface irregularities which would disturb the flow within the spiral. When the cores are only held in position by struts, the possibility of deformation must be taken into account, and therefore, the wall of the spiral is made thicker by 5 to 10 mm than calculated.

The mould is divided in the plane of symmetry of the spiral, and the casting then exhibits a seam or a moderate overlapping. For the sake of better appearance, a low rib is fastened in these places, which may then be manually ground (see Figs. 120a, b).

In order to strengthen the spiral against the forces which tend to open it (Fig. 120b – the forces S), it is fitted with stay blades already mentioned or with bolts. The stay blades are cast in one piece with the spiral if cast steel is used for construction material. Since these blades are subjected to tensile stress, grey cast iron is not suitable because of its low tensile strength. In this case, the spiral is reinforced by means of cast-in steel bolts. The cast-in ends of the bolts are fitted with rings, as shown in Fig. 178, to ensure good transmission of the forces between the cast iron and the bolt. In order to reduce hydraulic resistances, sometimes even spirals of cast iron are moulded as one unit with stay blades, but then they are

bored, and steel bolts are inserted, as illustrated in Fig. 179. The cast blades constitute here not only a hydraulic cover for the bolts but at the same time prevent dangerous pre-stress of the spiral which could occur when tightening the nuts of the bolts.

With high-pressure turbines in particular the stay blades are inserted into the spiral in the shape of arcinforced ring which is cast separately (see Appendix VI and Fig. 36). The blades in this case are easily accessible for manual grinding which is advantageous because of the high velocity of the flow; in addition, this design facilitates the casting process.

Large spirals are split into halves in the plane passing through the turbine axis; when a split reinforcing ring is used (Appendix VI) is then made of two pieces, too.

Steel plate spirals consist of circular bent segments joined by riveting or welding. The circumference of the spiral is not exactly circular (see Fig. 176). The stay blade ring is steel-cast, and the segments are fastened to it by riveting or welding (Appendix I).

The spiral of horizontal shaft turbines is fitted with lugs for connection to the base plate, whilst the spiral of vertical shaft turbines is equipped with eyes for the anchor bolts; the spirals are further provided with suspension eyes and in the highest place with a de-airing cock, and sometimes in the lowest place also with a drain cock and a threaded opening for connecting a manometer. The drain cock is not really necessary when the drainage is connected to the piping under the spiral, and it is possible to drill a small opening through the splitter (in horizontal shaft turbines), which does not impair the flow, and ensures at the same time the drainage of the space behind the splitter.

Strength control is concerned with the stay blades or bolts and the spiral proper.

As already mentioned, the stay blades or bolts must render the spiral resistant against the forces S (Fig. 120b) which tend to open it.¹⁾ The greatest stress will be encountered in the blade nearest the inlet (see Fig. 180). The stay blades and the spiral proper are checked for

¹⁾ In large low-pressure vertical-shaft turbines, where these forces are comparatively small, they are exceeded by the effect of the alternator weight which the stay blades must transmit to the foundation (eventually even the weight of the ceiling of the pit when the latter is not self-supporting). In this case, the blades may be subjected to buckling stress, which always occurs when the spiral is without water, see Appendix I.

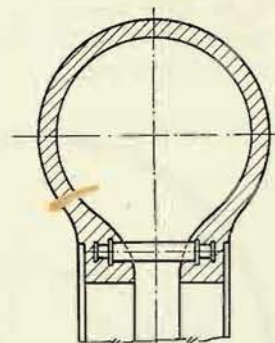


Fig. 178

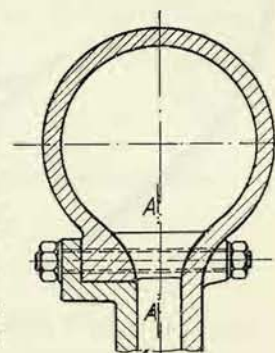


Fig. 179

the same testing pressure as the lower part of the piping. Since when determining testing pressure (see Part III – Pipes) we start from the maximum pressure which can be developed when the guide blades are being closed, we shall consider a uniform distribution of water pressure within the spiral and under the lids up to the pitch diameter of the guide blades. To determine the force acting upon one stay blade, we further delimit this space by the rays bisecting the distance between two adjacent stay blades, thus obtaining the hatched area in Fig. 180.

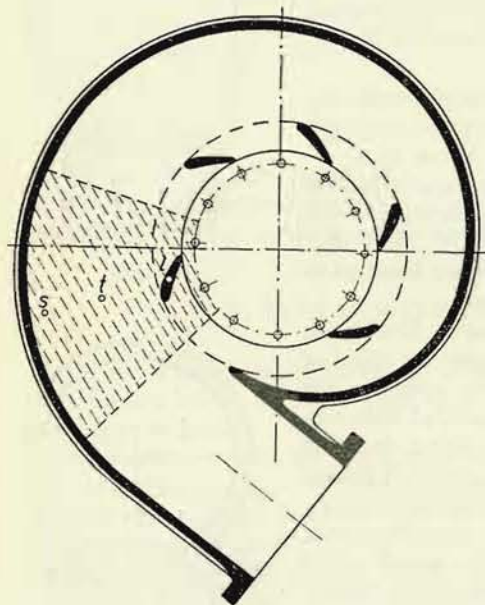


Fig. 180

We measure this area by means of a planimeter, and multiplying it by the water pressure (testing pressure), we obtain the force $T = fp_z$ acting in the centre of gravity t of the hatched area f . This force is taken up on the one hand by the wall of the spiral and on the other hand by the stay blade; we resolve it therefore into the centre of gravity of the wall cross section, s , and into the centre of gravity of the blade, l , and thus we obtain the force acting in the blade (Fig. 180).

$$L = T \frac{ts}{ls}$$

However, not all fibres of the blade are of equal length, because the blade is located in a space which contracts in the radial direction (see Fig. 181). For this reason – we assume here a parallel shift of the limiting surface – the relative

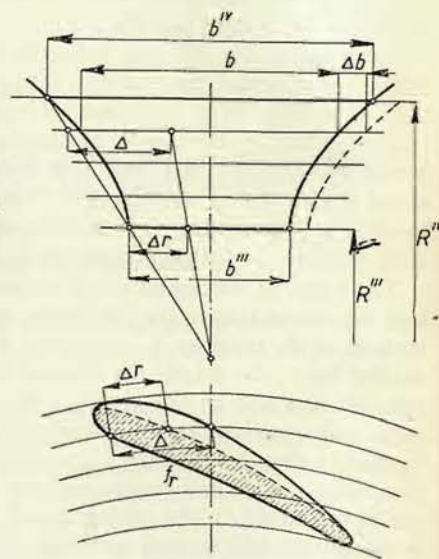


Fig. 181

elongation $\frac{\Delta b}{b}$ will be less in the longer fibre and the same applies to its stress $\sigma_t = \frac{\Delta b}{bE}$. The stresses of two fibres of different length will be in the ratio $\frac{\sigma_1}{\sigma_2} = \frac{b_2}{b_1}$. To determine the maximum stress in the shortest fibre, we calculate with the reduced cross section of the blade which we ascertain by reducing the peripheral dimensions of the blade in the ratio $\frac{b'''}{b}$; we can do this with sufficient accuracy by means of the graphical construction illustrated in Fig. 181, where Δ denotes the actual dimension, and Δr the reduced dimension. Dividing the force L by the area reduced in this way gives the maximum tensile stress in the stay blade:

$$\sigma_{\max} = \frac{L}{f_r}$$

As admissible stress when calculating with the testing pressure we may select 1000 kg/cm² as maximum value for cast steel and for the steel bolts (here, of course, no reduction is made) 1500 kg/cm².

For the selection of the wall thickness of the spiral proper as well as for dimensions of the inlet flange we may use as a guide the Czechoslovak Standard ČSN 1043-1931, Flanges, Part I. According to this standard the wall thickness of a straight pipe is calculated by the formula

$$t = \frac{pd}{200k} + c, \quad (178)$$

where t denotes the wall thickness in mm, p the gauge pressure in atm., d the inner diameter in mm, k the admissible stress in kg/mm², and c an allowance for inaccuracies in the manufacture, eventually for rusting, for which, however, we must take a higher value for the spiral than for the piping, this allowance being – as already mentioned 5 to 10 mm.

The standard mentioned gives for the calculation of the flange (Fig. 182) the following formula

$$a = \sqrt{1.1 \varphi \frac{pdx}{100 k_0}}, \quad (179)$$

$$t_1 = 0.75 a,$$

where a denotes the thickness of the flange in mm, t_1 the thickness of the reducing part in mm, φ a material coefficient which is taken as $\varphi = 1 + \frac{p}{150}$ for cast

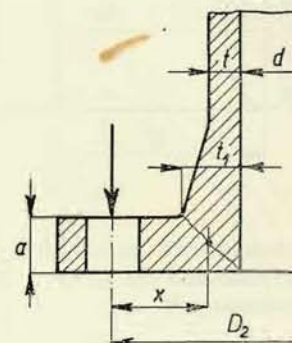


Fig. 182

iron and $\varphi = 1 + \frac{p}{500}$ for cast steel; d is the inner diameter in mm, x the arm of the bending equalling $\frac{D_2}{2} - \frac{d + t_1}{2}$ in mm, k_0 the admissible bending stress in kg/mm², and D_2 the pitch diameter in mm. The standard stipulates here

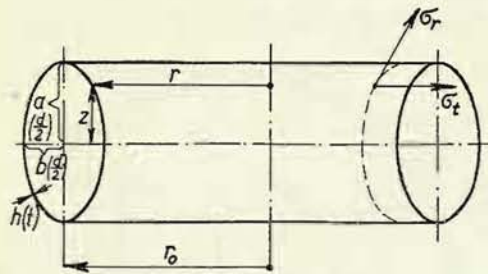


Fig. 183

a permissible stress at the considered rated pressure, $k = 2$ to 2.5 kg/mm² for gray cast iron and 5 to 6 kg/mm² for cast steel, and $k_0 = 1.5 \cdot k$ for gray cast iron and $k_0 = 1.25 \cdot k$ for cast steel.

Formula (178) does not represent the actual conditions as our case is not related to a straight tube. We may rather compare the shell of the spiral with an annuloid of an elliptical, or better still a circular cross section (Fig. 183). For an

$$\sigma_r = \frac{p(r+r_0)}{2ahr} \sqrt{(a^2-b^2)(r-r_0)^2+b^4},$$

$$\sigma_t = \frac{p}{2ah} \frac{2r(a^2-b^2)(r-r_0)+b^4}{\sqrt{(a^2-b^2)(r-r_0)^2+b^4}}.$$

(180)

For a circular cross section we obtain by substituting $b = a$:

$$\sigma_r = \frac{pa}{h} \frac{r+r_0}{2r}$$

$$\sigma_t = \frac{pa}{2h}.$$

(181)

In these expressions the symbols have been left as given in original literature and indicated in Fig. 183; when we take for the circular ring the symbols according to the expression (178) and employ for the diameter the sign d (instead of the radius a) and for the wall thickness the sign t (instead of h , we obtain

$$\sigma_r = \frac{pd}{2t} \frac{r+r_0}{2r}$$

$$\sigma_t = \frac{pd}{4t},$$

(181a)

¹⁾ Föppl: Drang und Zwang, Part 2, Berlin, Oldenbourg, 1928, p. 8.

and putting $\frac{pd}{2t} = \sigma_0$ which is the stress resulting from Equation (178) for a straight pipe, we obtain

$$\sigma_r = \sigma_0 \frac{r+r_0}{2r} = \sigma_0 \frac{1}{2} \left(1 + \frac{r_0}{r}\right),$$

$$\sigma_t = \frac{\sigma_0}{2}.$$

(182)

Thus, we see that the stress in the meridional direction will be the same as the stress σ_0 , resulting from the formula for a straight pipe, only at the radius r_0 . At larger radii the stress will be less, and inversely. The tangential stress will be the same as in straight pipe.

This method of calculation may be advantageously applied to spirals¹⁾ – in this case we divide the spiral into a number of sections with a constant radius of the meridional curve – in so far as the shell of the spiral is directly connected to the stay ring (as indicated in Fig. 184) and no conical part is inserted (as indicated in Fig. 185). Only where the spiral is connected to the stay ring is the stress increased by the action of the bending moments created by the increase in the diameter of the meridional cross section. This stress increase, according to measurements taken by the authors cited below, amounts to about 22 % and rapidly diminishes with the distance from the stay ring, as indicated in Fig. 184.

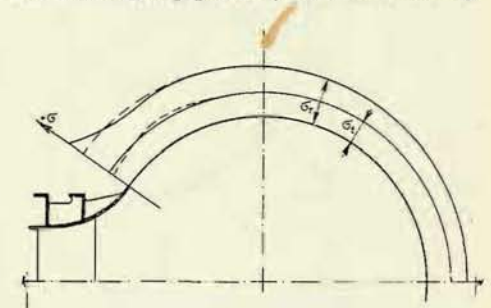


Fig. 184

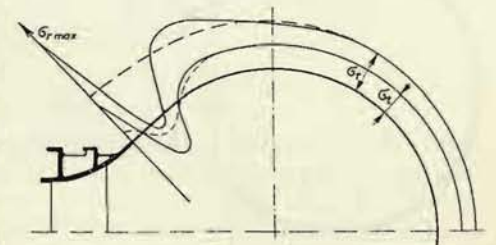


Fig. 185

When, on the other hand, a transitional conical part is inserted (Fig. 185), great bending moments arise and therefore great additional stresses; so it is not advisable to use such shapes of the meridional curve which exhibit a straight transitional part.

In the described way we can determine also the stress σ_r – at the radius R_T – where the spiral is connected to the stay ring (regardless of whether the steel plate wall is connected to the cast steel ring, or whether both parts are cast as in

¹⁾ Salzmann und Süss: Festigkeitsuntersuchungen an Spiralgehäusen, EWAG-Mitteilungen, – 100 Jahre Turbinenbau, 1942/43, p. 164. See also Bovet: Contribution au calcul de résistance mécanique d'une bache spirale, Informations techniques Charmilles, No. 1.

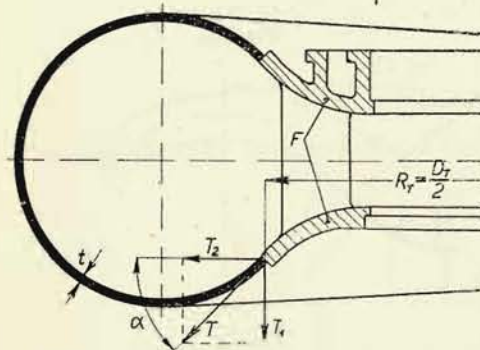
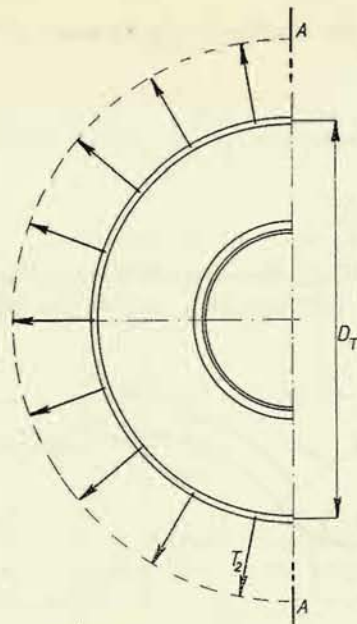


Fig. 186

one piece); see Fig. 186. By multiplying the stress σ_r by the wall thickness t we ascertain the forces T acting upon one linear centimetre of the periphery:

$$T = \sigma_r \cdot t = \sigma_0 \frac{R_T + r_0}{2 R_T} t = \frac{\sigma_0}{2} \left(1 + \frac{r_0}{R_T} \right) t.$$

This force we may resolve, however, according to Fig. 186 into the components T_1 and T_2 , obtaining $T_1 = T \sin \alpha$ and $T_2 = T \cos \alpha$. The forces T_1 subject the stay blades to tensile stress, which has already been taken into account in the previously described method of stay blade control.

By the forces T_2 the stay ring is subjected to stress in the radial direction. We shall assume that the forces T_2 in all radial sections are of the same magnitude corresponding to the largest inner diameter of the spiral. In an arbitrary section A-A (Fig. 186), the rings is then subjected to tearing stress by the force $2 T_2 D_T$ and consequently either of both cross sections are acted upon by the force $T_2 D_T$. The cross section area of the ring, F , – and also the sum of the cross sections of the connecting bolts of the ring – must consequently be of such a magnitude so as to keep the resultant tensile

stress within permissible limits. This stress is hence given by the expression

$$\sigma_t = \frac{T_2 D_T}{F} = \frac{\sigma_0 t \cos \alpha \cdot \left(1 + \frac{2 r_0}{D_T} \right) D_T}{2 F} = \frac{\sigma_0 t (D_T + 2 r_0) \cos \alpha}{2 F} \quad (183)$$

In order to assure ourselves of the satisfactory strength of the spiral (from both strength calculation and quality of material) we always test the spiral of water up to the testing pressure when feasible, under given conditions. As this procedure

is not possible with large spirals, they are tested on a model at a reduced scale. Correct spiral testing requires the use of a special testing implement as shown in Fig. 187.

The testing appliance consists of a cylinder with a flange which is tightly connected by bolts to the flange of the spiral. The outer diameter of this cylinder, D_t , must equal the pitch diameter of the guide blades, so that the load of the

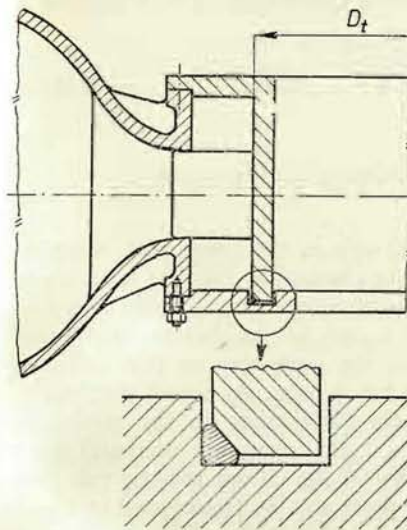


Fig. 187

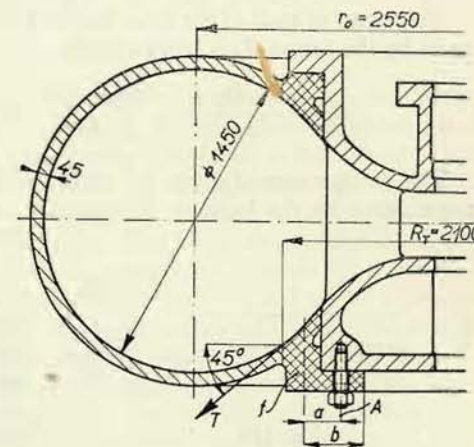


Fig. 188

water pressure during the test corresponds to actual conditions. To the other side of the spiral a counter-flange is bolted, which, however, must not be connected to the cylinder by bolts as this would discharge the stay blades. The sealing between the counter-flange and the flange of the cylinder is done with a rubber string which is inserted into a corner of the recess, as indicated in the detail sketch of Fig. 187.

Example: As an example we now give some control calculations relating to the spiral in Appendix VI.

The main dimensions of the spiral in the cross section of the largest inner diameter are indicated in Fig. 188. At a maximum working gauge pressure of 22 atm., the meridional stress, calculated by means of the formula for a straight pipe when we assume a calculating wall thickness $t = 40$ mm (5 mm, represents the allowance for unsymmetrical casting), as given by

$$\sigma_0 = \frac{pd}{2t} = \frac{22 \cdot 145}{2 \cdot 4} = 400 \text{ kg/cm}^2.$$

At the radius R_T , the maximum meridional stress will be given by formula (182):

$$\sigma_{r, \max} = \frac{\sigma_0}{2} \left(1 + \frac{r_0}{R_T} \right) = 200 \cdot \left(1 + \frac{255}{210} \right) = 443 \div 450 \text{ kg/cm}^2.$$

The force T per 1 cm of the periphery is

$$T = t \sigma_{r, \max} = 4 \cdot 450 = 1800 \text{ kg/cm} \text{ and the component } T_2 = T \cos \alpha = \\ = 1800 \cdot 0.71 = 1280 \text{ kg/cm}.$$

The area f of each of the cross-hatched parts is $f = 350 \text{ cm}^2$. The stress in these parts by the forces T_2 is consequently

$$\sigma_t = \frac{T_2 D_T}{2f} = \frac{1280 \cdot 420}{2 \cdot 350} = 770 \text{ kg/cm}^2 \div 800 \text{ kg/cm}^2.$$

The components T_1 , parallel to the turbine axis in the lower part, must be transmitted by the bolts A . These bolts can be checked as follows: bolts Type M90 with a core cross section area $f = 59.4 \text{ cm}^2$ are uniformly distributed around the periphery so that one stay blade has 6 bolts. As found previously, one stay blade takes up the maximum force (at the operating pressure) $P = 230,000 \text{ kg}$. If we assume that this force must also be transmitted by the 6 bolts, the calculation will be on the safe

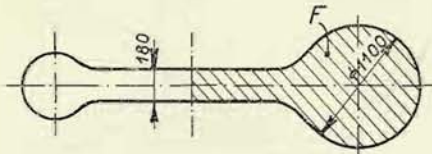


Fig. 189

side (part of the force P results from the pressure upon the stay ring and the lid of the turbine, and this part is not transmitted by the bolts). In this case the stress of the bolts would be $\sigma = \frac{230,000}{6 \cdot 59.4} = 646 \div 650 \text{ kg/cm}^2$. But the bolts

do not take up the force at its point of application but at distance a from it. Since the flange is supported on the inner ring at distance b , it acts as a lever and the stress of the bolts will be increased in the ratio $\frac{b}{b-a} = 2$. The stress thus reduced consequently is $\sigma_{\text{red}} = 1300 \text{ atm}$. With this reduction we count mainly to ensure the least possible stress in the flange by these forces as it is already subjected to the stress resulting from the previously calculated forces T_2 .

As shown in Appendix VI, the spiral consists of two parts. In the place of the cut, the reinforcing flanges, are also split; Fig. 188 shows these flanges as cross-hatched areas. Hence 13 connecting bolts Type M80 with a core cross section area $f = 43 \text{ cm}^2$, distributed around the periphery of the connection, must transmit the total force with which the water acts upon the area $F = 13,300 \text{ cm}^2$ (cross-hatched in Fig. 189). The stress of the bolts therefore is $\sigma = \frac{Fp}{13f} =$

$= \frac{13,300 \cdot 22}{13 \cdot 43} = 525 \text{ atm}$. The bolts in the opposite connection are calculated in a similar way.

The testing gauge pressure was in this case 44 atm. All stresses, which in this case will be doubled, are still below the yield stress, for the spiral is made of cast steel, the bolts of steel with a strength value of 50 kg/mm^2 , the bolts A , however, are made of alloy steel with a strength of 80 kg/mm^2 .

VI. TOP AND BOTTOM LIDS OF THE TURBINE

1. Lids

The lids enclose the space of the runner, and in dependence on the stress, which mainly results from the water pressure on the lids, they are either made of gray cast iron or of cast steel. The guide blades are placed in the lids and their seating and sealing has already been described. It is important that the bores for the blade pins are located exactly opposite to each other to prevent jamming the blades. Therefore, these openings are either bored in both lids simultaneously (with the lids clamped together), or their equal spacing is made by a common pattern. The lids also carry the labyrinth rings, the stuffing box of the shaft, the shifting ring, the bearing, and the extension of the draft tube. All these will be dealt with in the following chapter. The shape of the lids should conform as far as possible to the contour of the runner in order to keep the whirling of the water and the losses resulting from it at a minimum. This has been achieved e. g. with the bottom lid shown in Appendix VI. The shape of the top lid had to be adjusted to other constructional requirements, and for this reason, a cast iron mask has been inserted, adjusted to the shape of the runner.

In a vertical shaft installation, drainage must be provided for the water which leaks not only through the stuffing boxes of the blades but also through the shaft stuffing box to the outer side of the lid; this is achieved by connecting the space above the stuffing box with the outer space of the lid by drainage holes. The water is sucked off by an electric pump controlled by a float or by a small tube connected to the draft tube. If the lid is located below the tail water level (with regard to cavitation), the drain pipe must be fitted with a check valve, and the draining action ceases with a small opening of the machine; i. e. when the lid is below the tail water level, we must always instal a pump to remove the water leaking through the stuffing boxes.

The lids are subjected to stress on the one hand by the pressure of the water up to the labyrinth rings, and on the other hand by the moment resulting from the guide blades which tend to turn the lids, and by the moment from the regulating forces of the shifting ring. These moments, however, are easily counterbalanced by bolting the lids to the spiral and by means of taper pins which are necessary for assembly reasons.

Therefore, mainly control of the stress by the water pressure is to be taken into

consideration. With regard to load conditions, the lids represent plates supported around the periphery and loaded approximately uniformly by the water pressure upon a certain annulus. The calculation will be safer if we assume a support around the periphery instead of clamping.

Best suited for this calculation is the approximate method by Bach,¹⁾ and we use it for the case in question. Fig. 190 shows half of the plate in the plan. The plate is uniformly loaded by pressure p on the annulus (the hatched area in the picture) with radii r_1 and r_2 and supported (held by bolts) on the circle of the radius R (dashed line). The force P is acting upon half of the plate on the annulus of the area F is $P = Fp$ and passes through the centre of gravity T_1 of the half-annulus.

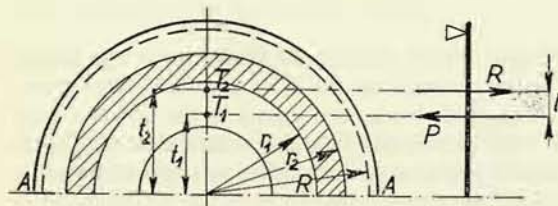


Fig. 190

The total reaction in the support of the plate must be of the same magnitude and will pass through the centre of gravity T_2 of the semi-circle of the radius R .

The external forces (loading and reaction) thus create the moment $M = Pl$, and we must still determine the moment arm l , which equals

the difference of the distances of the centres of gravity from the centre of the plate: $l = t_2 - t_1$. However, the distance of the centre of gravity of the semi-circle is given by the expression $t_2 = 0.637 R$, and the distance of the centre of gravity of the halfannulus from the centre by the expression

$$t_1 = 0.424 \frac{r_2^3 - r_1^3}{r_2^2 - r_1^2},$$

so that for the moment we can write

$$M = P \left(0.637 R - 0.424 \frac{r_2^3 - r_1^3}{r_2^2 - r_1^2} \right). \quad (184)$$

This is the bending moment acting upon the plate in the section $A-A$. When W is the resisting moment of the cross section of the plate in this section, the stress of the material is given by

$$\sigma_0 = \frac{P}{W} \left(0.637 \cdot R - 0.424 \cdot \frac{r_2^3 - r_1^3}{r_2^2 - r_1^2} \right).$$

As a rule, the plate has not the same resisting moment in all sections (see e. g. the bottom lid in Appendix VI, left and right parts); consequently we have to count with the minimum resisting moment. When the lid is made of two parts, we must also check the resisting moment of the bolt connection. For this we

¹⁾ Föpl: Vorlesungen über technische Mechanik, Part III, Berlin, Teubner, 1922, p. 202.

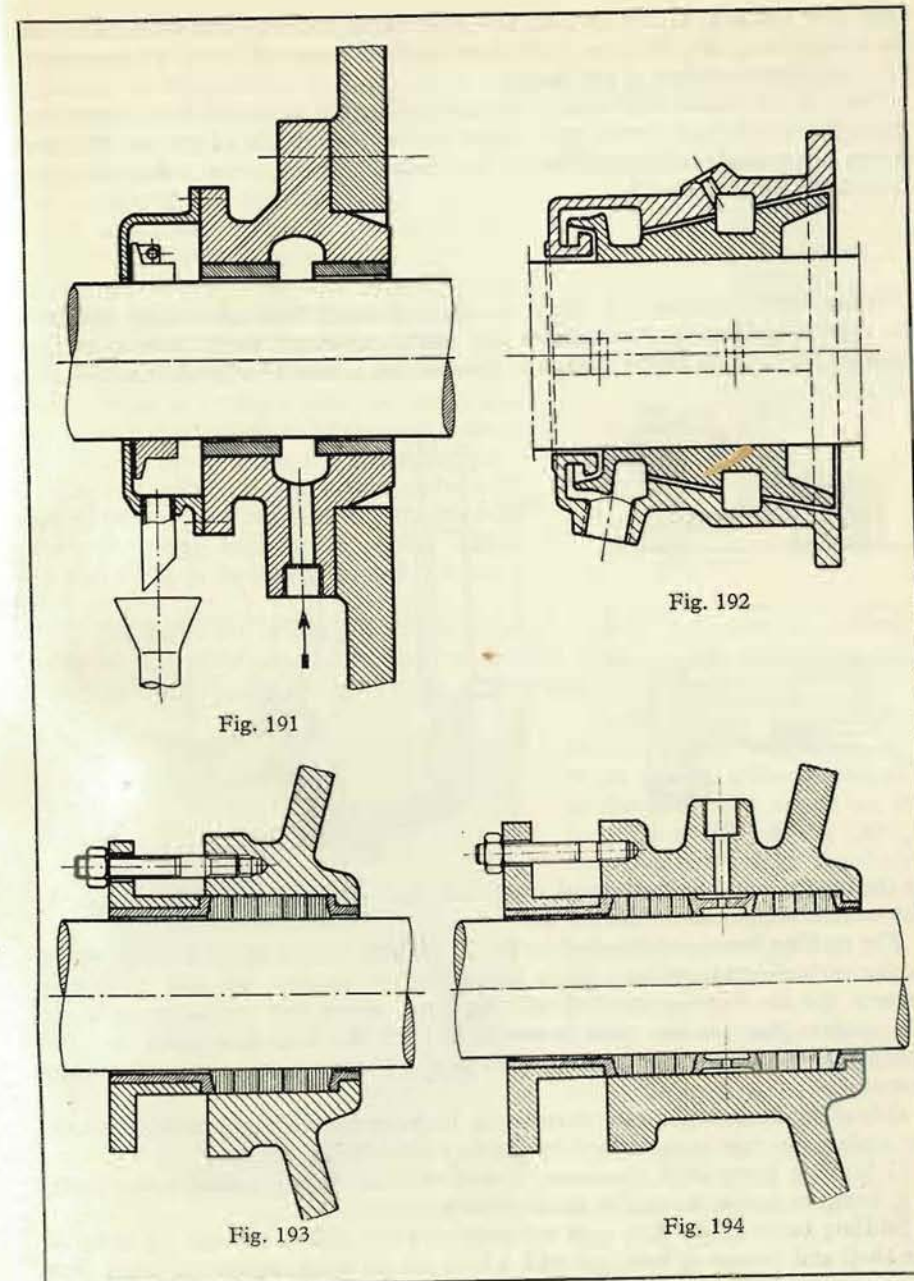


Fig. 191

Fig. 192

Fig. 193

Fig. 194

determine the neutral axis by trial and error in such a way that we consider in the tension part only the cross sections of the bolt cores and in the pressure part the total contact surface of the flange.

Note: In the bottom lid shown in Appendix VI it was not possible to dimension appropriately the bolt connection owing to the small height of the lid. For this reason it was made integral, although dismantling, for inspection would be more convenient with a split lid.

2. Parts of the Lids

In horizontal turbines, the lids as a rule, only carry the shaft stuffing box and the regulating ring, and sometimes the bracket-mounted guide bearing of the turbine (Fig. 34). In larger machines, this bearing is usually separately supported

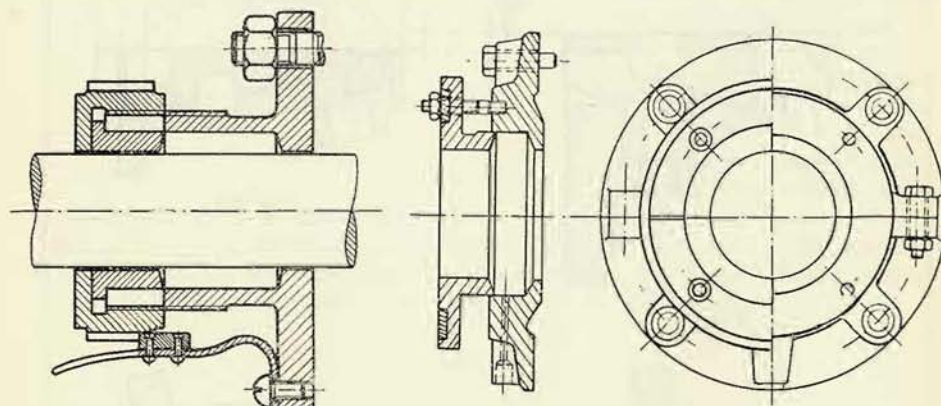


Fig. 195

Fig. 196

on the frame (Fig. 36); in vertical machines, the radial bearing of the turbine is also usually supported on the top lid.

The stuffing boxes seal the shaft in the lid not only against internal overpressure in the turbine, and prevents water leakage to the outside, but they must also prevent the air from penetrating into the space above the runner when there is a vacuum (because this space is connected with the draft tube either by relief openings in the runner or by a by-pass pipe). There are two types of stuffing boxes:

- Stuffing boxes sealing the narrow gap between the shaft and bushing, where the sealing function is performed by the through-flowing water.
- Stuffing boxes with an elastic, flexible packing, fitting tightly to the shaft, e. g. hemp or cotton strings, or metal or carbon rings.

Stuffing boxes of the first type are employed for high peripheral velocities of the shaft and consist of bushings with a bore for the shaft, somewhat larger than

the shaft itself to prevent direct contact between shaft and bushing. Fig. 191 illustrates such a stuffing box. In the middle of the stuffing box is a circular duct; the water discharges from it into stuffing boxes sealed against overpressure, and water is introduced into it in stuffing boxes sealed against underpressure; the water supply is controlled by means of a stop cock. The stuffing box is fitted with a lid on the outside and forms a chamber in which the spray ring is placed; between the ring and lid is a narrow gap to prevent by centrifugal force the sprayed-off water from reaching the opening in the lid. When the stuffing box is sealed against vacuum and for this purpose sealing water is supplied into the chamber, this water is drained off the lid through a small pipe into an open funnel, and the water supply is controlled to maintain continuous drainage; in this way we can ensure that there is always sufficient quantity of sealing water and that no air is aspirated through the stuffing box.

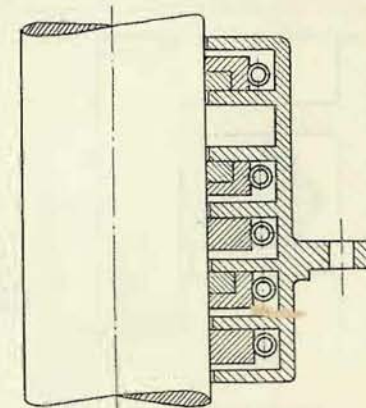


Fig. 197

Fig. 192 shows the design of Voith, in which the sealing clearances are cut into a cone so that their dimensions may be adjusted by axial shift. Sometimes the sealing clearances are made in the form of labvrinths (see Fig. 36).

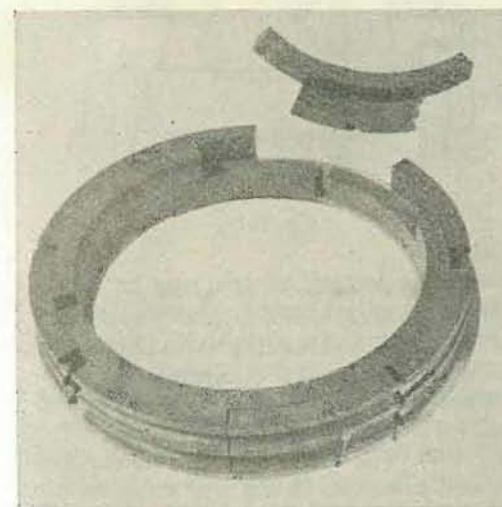


Fig. 198

Stuffing boxes with packing bearing against the shaft, or better against a sleeve shrunk on the shaft and sealed on it (e. g. as shown in Fig. 200), form a cavity around the shaft into which a soft sealing string of hemp or cotton, soaked with tallow is inserted (see Fig. 193). The packing is often divided into two parts by a ring, a so-called lantern ring, through which the packing is supplied with a lubricant (oil or grease) or with sealing water (see Fig. 194).

The cavity for the packing is either in the lid (in smaller machines) or arranged in a special body bolted to the lid, as indicated in Figs. 195 and 196.

The packing is compressed in the cavity by the lid of the stuffing box, which is tightened by bolts or for smaller diameters by the lid which then has the form of threaded nut (Fig. 195). The stuffing boxes are made of cast iron with bronze sleeves, and if necessary for dismantling, they are made of two parts

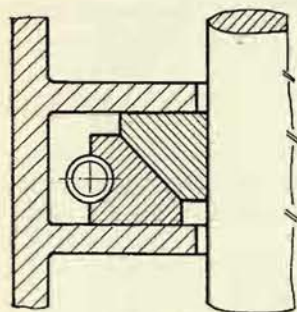


Fig. 199

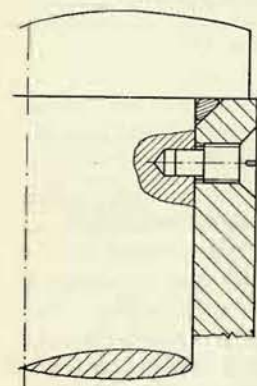


Fig. 200

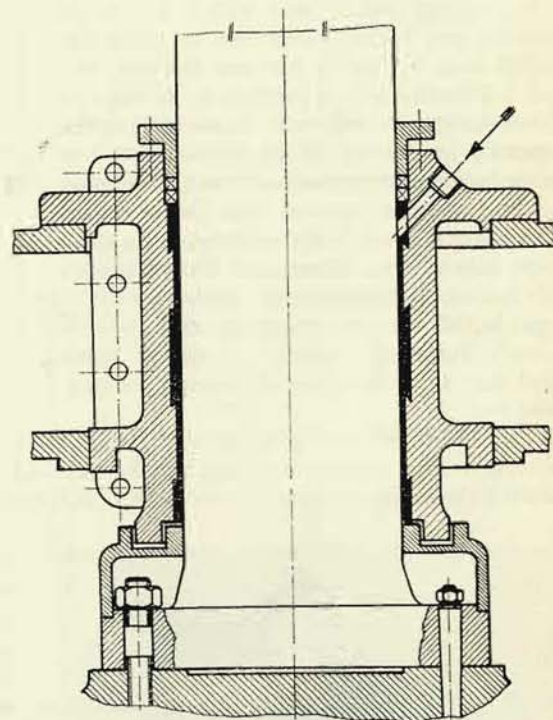


Fig. 201

(Fig. 196). The width of the annulus s for the packing material may be approximately selected according to the relation $(d \text{ in mm}) s = (2 \text{ to } 2.3) \cdot \sqrt{d}$, the maximum value, however, should not exceed 30 mm. Soft stuffing boxes can be used, when the peripheral velocity of the shaft does not exceed 6–8 m/sec.

For large machines carbon packings are used. The seal consists of a stuffing box with chambers for the individual carbon rings which are split and held together by helical brass springs (Fig. 197). The dividing planes of the rings alternate as shown in Fig. 198. In the unit illustrated in Fig. 197 there are four rings as seal against overpressure under the stuffing box, one ring constitutes the seal against vacuum, and the empty chamber serves for the introduction of the

grease which consists mainly of tallow and leaf-like graphite. The number of rings depends on the pressure, one ring per 20 m water column; but at least two or three rings are always employed.

Another arrangement of the rings is shown in Fig. 199, where the dividing surface is conical, so that the pull of the spring does not only presses the rings on the shaft but at the same time expands them against the walls of the chamber.

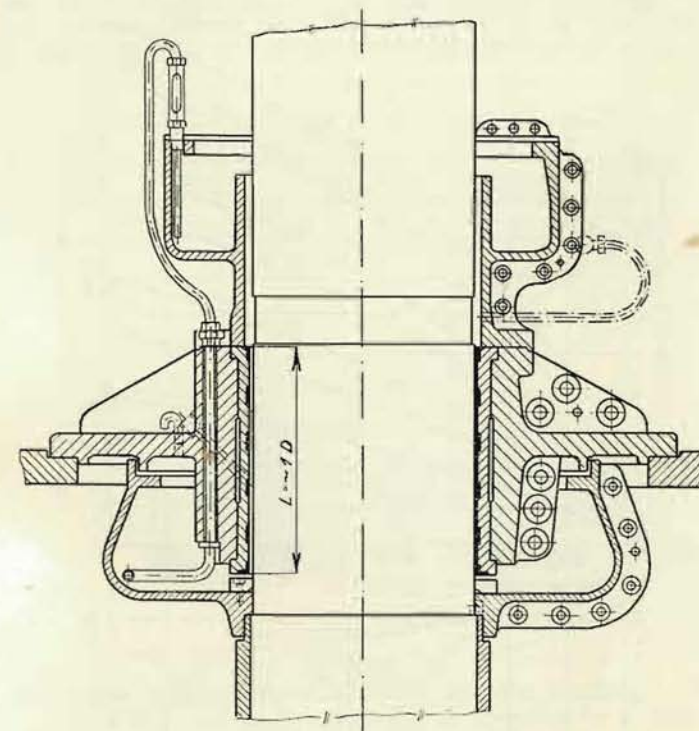


Fig. 202

These stuffing boxes may be employed for peripheral velocities of 20–30 m/sec. (according to instructions given by the manufacturer of the rings).

As a rule, an interchangeable bronze sleeve is slid over the shaft under stuffing box to protect the shaft against erosion from impurities entrained by the water into the stuffing box. Since this sleeve is heated by the friction of the stuffing box, it must only be fastened to the shaft at one end to allow thermal expansion. The sleeve must also be sealed to the shaft. A rubber string pressed against the stepping of the shaft is used for this purpose seen in Fig. 200.

Another arrangement of the sleeve is represented in Appendix VI, where the

sleeve is integral with the labyrinth ring underneath the stuffing box; the clearance of this labyrinth ring can be sealed to the lid by a rubber-lined shift ring when the machine is not in motion, and allows placement of the stuffing box even at a higher tail water level without damming the draft tube.

The bearings of smaller horizontal shaft turbines are usually bracket-mounted (Fig. 34), of standard design and have lubrication; for larger machines they are

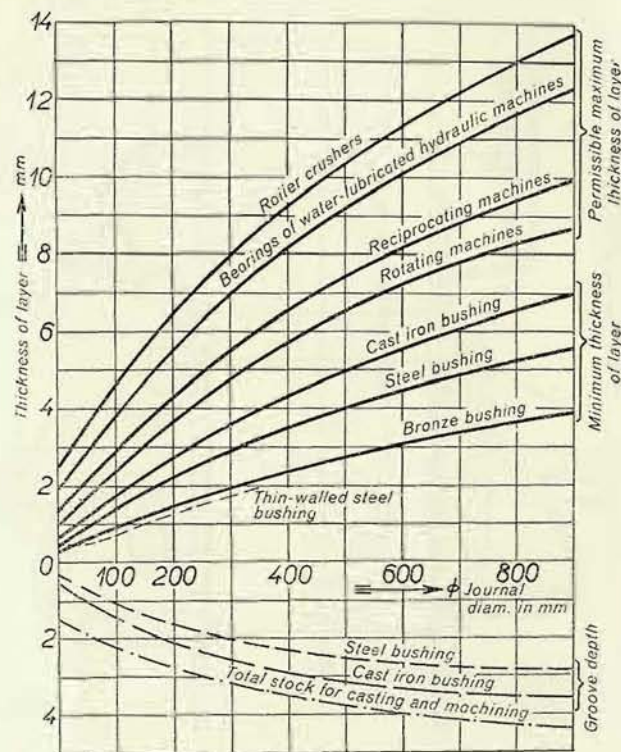


Fig. 203

usually mounted on a separate pedestal (Fig. 36) and combined with the axial thrust bearing.

In vertical shaft turbines a radial bearing is always inserted into the lid and centers the runner. These bearings are loaded only by the reaction resulting from the centrifugal force created by imperfect balancing of the runner. As a rule, we can count on this load maximally 10 % of the runner weight.

When the loading of the bearing is small, so that the product $p \cdot v \leq 10$, where p is the specific load in atm. and v the peripheral velocity in metres per second, grease (vaseline) lubrication by an automatic press may be used. To prevent the

lubricant from being flushed out by the water, the bearing at its upper, accessible end is sealed with a soft packing, and at the bottom end with a plain labyrinth which impedes excessive leakage of the lubricant from the bearing (see Fig. 201).

Large bearings, where lubricant losses would be rather significant, are equipped with circulating oil lubrication, as described in Part I, in the text to Appendix I, and illustrated in Appendix VI.

Another lubricating system is shown in Fig. 202. Here a rotating oil container is arranged under the bearing and a tube introduced into it toward the outer wall in a direction opposite to the rotation which automatically draws the oil into an

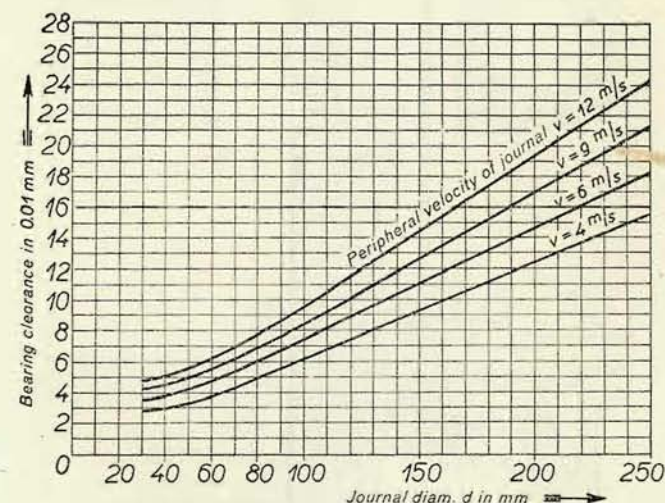


Fig. 204

upper vessel, from where it flows by gravity into the bearing. A by-pass tube (indicated by dot and dash lines), closed during operation by a valve, serves for pre-lubrication from the oil supply in the upper (stationary) vessel prior to starting the machine.

For these oil-lubricated, babbitt-lined bearings should apply $p \cdot v \leq 20$ and $p \leq 18 \text{ kg/cm}^2$.

In both cases bushings of gray cast iron or cast steel with a babbitt lining are employed. The effective length of the bushing may be selected approximately in the range of (0.75 to 1). d , d being the diameter of the bearing. For the selection of the thickness of the babbitt lining and the depth of the grooves, Fig. 203 may serve as a guide, and Fig. 204 for the selection of the bearing clearance.

The split bushing proper with a babbitt lining is always inserted into a housing which is either fastened to the turbine lid by a flange (see Appendix VI) or mounted in the stay ring on a short cylindrical surface which permits small displacements

of the bearing and its adjustment to the position of the shaft (Fig. 205 system ČKD, Blansko).

In installations with a long draft tube and high through-flow velocity, a quick closing of the turbine can result in a rupture of the water flow within the draft tube (see Chapter VII) and a back thrust of the water upon the runner which

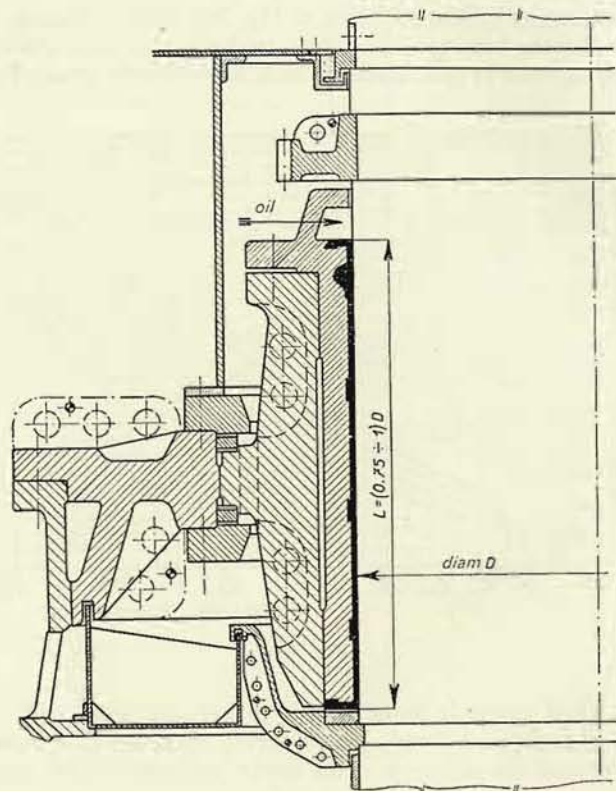


Fig. 205

could even lift the rotor set. In order to eliminate this risk, the ring under the bearing and the bearing itself must be strong enough dimensioned to take up a force in the upward direction of the magnitude of about 10 % of the load on the thrust bearing. Between this ring and the bearing a clearance of about 2 mm must be provided to reduce the impact upon the bearing.

In recent times, increasing use has been made of bearings lined with wood (laminated wood, lignum vitae) or plastic (artificial resins), or rubber. These bearings are lubricated with pure (filtered) water. Their advantages lie in a restricted

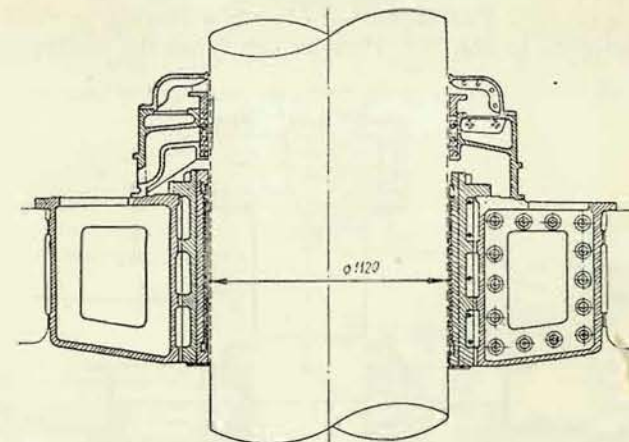


Fig. 206

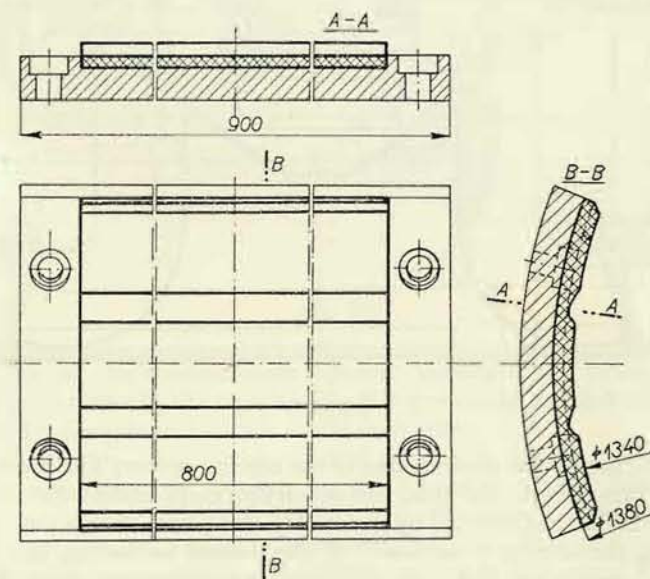


Fig. 207

possibility of defects and simplicity of design which permits a reduction of the overhung of the runner from the bearing; they are used for machines of the largest output (Dnyeprostroy). The disposition of such a bearing, as employed in the USSR, is illustrated in Fig. 206. Here we clearly see the stuffing box with the

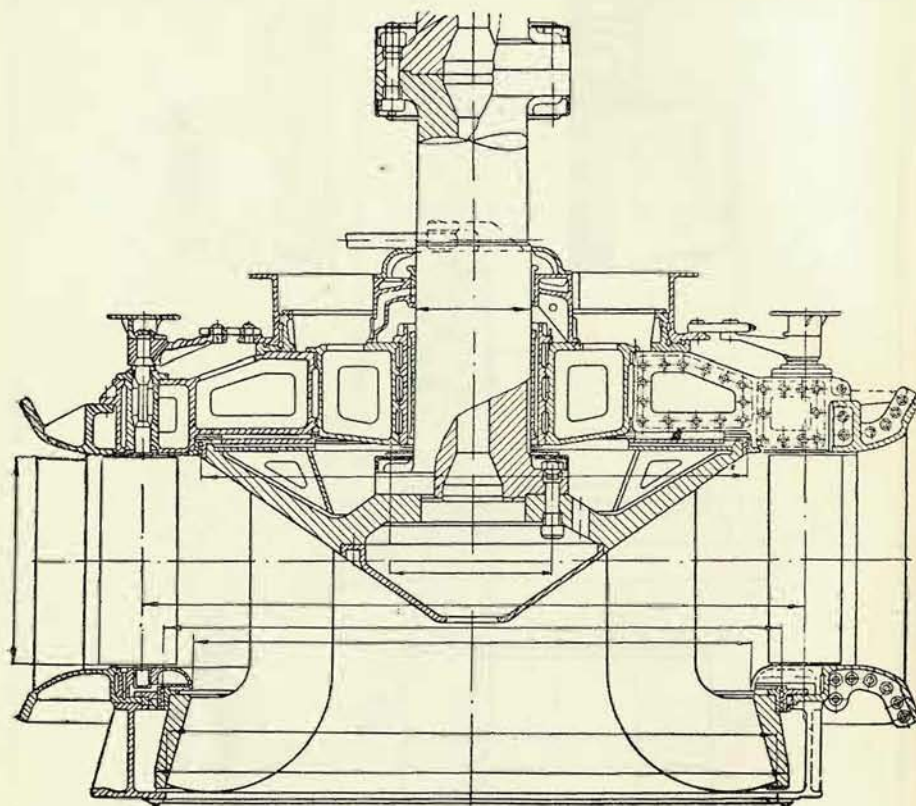


Fig. 208

sealing water supply and the chamber of the bearing proper. The bearing consists of a split bushing of gray cast iron, into which thin metal liners with vulcanized-on rubber are inserted and fastened by screws. Fig. 207 shows such a liner with holes for fastening the screws; in section B-B the grooves for cooling and lubricating water can be seen.¹⁾ Fig. 208 shows this bearing mounted into the turbine.

¹⁾ Gamze i Goldsher: *Technologiya proizvodstva krupnykh gidroturbin*, Moskva, Leningrad, Gosudarstvennoye nauchnotekhnicheskoye izdatelstvo, 1950, p. 203.

VII. DRAFT TUBE AND AIR SUPPLY VALVES

Straight conical draft tubes are made of steel plate. Tubes of other shapes or their parts are cast from gray iron if inspection necessitates dismantling (Appendix VI), otherwise the entire tubes are made of concrete. In the latter case, only the beginning of the tube is armoured with steel plate in places where the flow velocity

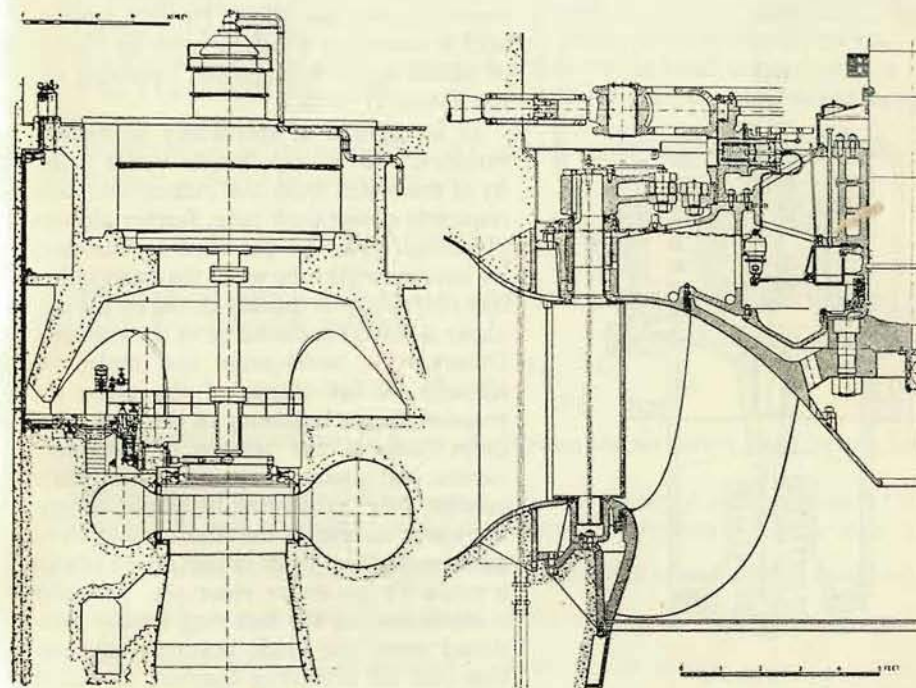


Fig. 209

exceeds 6.5 m/sec. (for extraordinarily resistant concrete up to 9 m/sec.), to prevent erosion of the concrete by the high velocity. Air-proof is an indispensable condition in any case for the proper function of the draft tube.

In Part I, Chapter XII/2, it was pointed out that in Francis turbines unstable air pockets are formed in the back of the runner at smaller flow-rates. This phenomenon, manifesting itself by shocks at partial loads, is eliminated by introducing air into the space behind the runner hub. Aspiration of air is controlled by a valve which is actuated by the regulating ring so as to open at small flow-rates and to close at large flow-rates when the space in back of the runner is completely filled with water.

The air supply for the turboset shown in Appendix VI is similarly designed;

the air is supplied by hollow ribs in the extension of the draft tube into the space around the shaft under the runner.

The air may also be supplied through the top lid of the turbine from where it passes through the relief openings into the space under the runner, or it may be introduced through a bore in the shaft from a chamber in the turbine lid or on

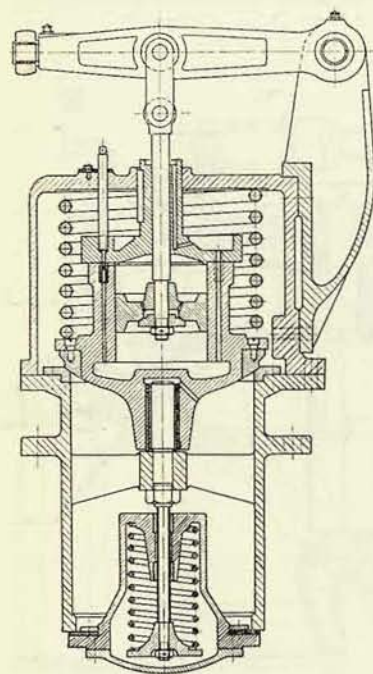


Fig. 210

the top end of the shaft, the air supply into this chamber being in turn regulated by a valve, as described before. Fig. 209 presents such a system on a turbine with an output of 59,000 metric horsepower, operating under a head of 37 m.¹⁾

In installation of specifically high-speed turbines, with a considerable outlet velocity of the water from the runner and consequently a long draft tube, further air supply valves must be provided to introduce air into the draft tube when the water inflow into the turbine is quickly closed by the regulator at a sudden discharge of the machine. Otherwise it could occur that under the influence of the inertia of the water the pressure in the beginning of the draft tube drops down to the tension of the water vapour and causes a rupture of the water column. After exhausting its kinetic energy, the water column in the draft would move backward, where by its impact on the runner it could lift the entire rotor set. This risk is eliminated by the lock ring already mentioned under the guide bearing of the turbine (see the preceding chapter), as well as by introducing air into the draft tube to

form an air cushion and thus to provide for a gradual and elastic stopping of the backward motion of the water.

The air inlet valves are located either directly on the draft tube (see Fig. 36) or on the lid of the turbine; in this case the air is introduced into the space between the guide apparatus and the runner blades (as a rule in Kaplan turbines, see Appendix II).

A cross section through an air valve is presented in Fig. 210. The installation is equipped with two valves. The lower one is a normal check valve with a rubber packing ring, which is pressed to its seat by a spring and automatically opens by the action of the vacuum in the space under the valve when at the same time the upper valve also opens. The upper valve is lifted by an oblique slotted link of the

¹⁾ Salto de Castro, Water Power, 1933, p. 84.

regulating ring, along which travels the roller of a lever which is connected with the piston of the oil cataract of the valve. At a rapid movement of the regulating ring toward the closed position the valve is lifted, whereupon, after a certain time determined by the setting of the by-pass of the cataract, it closes by the movement of the spring. At a downward motion of the lever, the oil flows through the ducts in the piston as the small plate, which has closed the ducts, opens at this downward motion of the lever the passage through the piston. The upper valves function is to permit the aspiration of air only at a rapid closing of the guide apparatus, but to prevent an access of air at normal operation with a small output, when there may be a vacuum in front of the runner and the aspiration of air would impair efficiency.

Underpressure at the beginning of the draft tube during operation has been determined in Part I by expression (26):

$$\frac{p_3}{\gamma} = H_B - H_s - \eta_s \frac{C_2^2 - C_4^2}{2g}.$$

When the guide apparatus is quickly closed, the pressure is further reduced by the value Δh . When this pressure

$$\frac{p_3}{\gamma} = H_B - H_s - \eta_s \frac{C_2^2 - C_4^2}{2g} - \Delta h \quad (185)$$

is approximately the tension of the water vapour, the air valves must be put into action.

The dynamic reduction of the pressure, Δh , may be determined as follows: We assume a draft tube of length L and a mean through-flow area F . In this case, the mass of the water in the draft tube is $\frac{LF\gamma}{g}$. This mass of water flows at velocity C and must be stopped within the time of the closing of the guide apparatus, T_s , and consequently the retardation a of its motion will be $a = \frac{C}{T_s}$. This requires the force

$$P = \frac{LF\gamma}{g} \frac{C}{T_s};$$

and this force is created by the pressure difference $\Delta h\gamma$, acting upon the cross section F of the draft tube, so that the following equation must hold good:

$$F\Delta h\gamma = \frac{LF\gamma}{g} \frac{C}{T_s},$$

whence

$$\Delta h = \frac{LC}{gT_s}. \quad (186)$$

Since the velocity across the length of the draft tube is not uniform, we should have to subdivide the draft tube into individual sections and instead of the product

LC substitute the expression $\Sigma L_n C_n$, in which L_n denotes the lengths of the individual sections and C_n the velocities in them. It will suffice, however, to substitute into Equation (186) for C the arithmetical mean of the initial and the final velocity,¹⁾ so then applies:

$$\Delta h = \frac{L}{gT_s} \frac{C_3 + C_4}{2}. \quad (186a)$$

The through-flow area of all valves should be, as far as possible, so large that the quantity of air admitted through the valves per 1 second equals the through-flow. The through-flow velocity of the air, in this case, must not exceed the critical velocity. If we select the through-flow velocity in the valves as 250 m/sec., this value is approximately the critical velocity, the total through-flow area of all valves should be

$$\Sigma F = \frac{Q}{250}. \quad (187)$$

ΣF is here the total through-flow area of the valves in m^2 and Q the flow-rate of the turbine in m^3/sec . It will not always be possible to attain this value, and in that case we shall employ the largest possible valves so as to ensure the formation of a damping air cushion of sufficient size, however, we must take into account the possibility of a backward, though damped, thrust of the water upon the runner and provide for a retaining ring under the guide bearing of the turbine.²⁾

The draft tubes are as a rule otherwise not subjected to excessive stress, but in some cases the necessity may arise to check their strength. For example, the draft tube of the turboset illustrated in Appendix VI may be subjected to stress at an abnormally high tail water level by the internal overpressure; since the final cross sections are of an oval shape, which is not advantageous in this respect, a partition of sheet metal has been inserted into this part of the draft tube, in the plane dividing both halves, for the purpose of reinforcement (Appendix VI).

The draft tube may be acted upon by forces (Appendix VI) resulting from changes of the momentum of the water and by the weight of the water contained in the draft tube; these forces are readily taken up by the connecting flanges.

Example: As example we are going to determine the hydraulic forces upon the cast iron elbow of the draft tube shown in Appendix VI. The force acting in the vertical direction is according to Equation (11)

$$P_v = \frac{Q\gamma}{g} (C_{3,v} - C_{4,v}) + G,$$

and in the horizontal direction

$$P_h = \frac{Q\gamma}{g} (C_{3,h} - C_{4,h}),$$

¹⁾ L. Grimm: Přednášky o vodních motorech na bývalé české vysoké škole technické v Brně (Lectures on Hydraulic Motors at the Technical University in Brno), p. 57.

²⁾ Fabritz G.: Die Regelung der Kraftmaschinen, Wien, Springer, 1940, p. 120.

where $Q = 12.5 m^3/sec$, $C_{3,v} = C_3 = 6.4 m/sec$ is the vertical component of the velocity at the inlet into the elbow, $C_{4,v} = 0$ is the vertical component of the velocity on the outlet cross section; similarly, $C_{3,h} = 0$ is the horizontal component of the inlet velocity, and $C_{4,h} = C_4 = 4.14 m/sec$ is the horizontal component at the end of the cast iron elbow. $G = 15,000 kg$ is the weight of the water contained in the elbow. Consequently applies

$$P_v = \frac{12.5 \cdot 1000}{9.81} \cdot 6.4 + 15,000 = 8130 + 15,000 = 23,000 kg$$

$$P_h = \frac{12.5 \cdot 1000}{9.81} \cdot 4.14 = 5250 kg.$$

We should further add the forces created by the static overpressures or under pressures acting upon the inlet or the outlet cross section. These forces, however, will act against the afore-mentioned hydraulic forces and may therefore be neglected.

The vertical force is taken up in the flange at the inlet cross section of the elbow by 36 bolts Type M33, each of which has a core area of $f = 7.16 cm^2$. If we now to the vertical force add the own weight of the elbow, i. e. 7000 kg, the stress of the bolts will amount to

$$\sigma_t = \frac{30,000}{36 \cdot 7.16} = 116 kg/cm^2.$$

VIII. GEARCASE WITH AUXILIARY DRIVES

The gearcase, placed on the bearing of the turbine, serves for driving the oil pressure pumps of the regulator and the lubricating pump of the guide bearing of the turbine; on this bearing, as a rule, is also mounted the safety governor (which at regulator failures cuts off the water supply electrically) besides an electric generator for driving the governor of the turboset, or, in some cases, a hydraulic governor (see Appendix VI), and further a lubricating oil pump for the other bearings of the turboset. Thus the function of these auxiliary equipment during operation of the unit is ensured.

In large machines, however, the oil pumps of the regulator and the main lubricating pump are driven electrically; in these cases the gearbox is simpler, because only the generator for the governor is directly driven, eventually the hydraulic governor, the safety governor and the oil pump of the guide bearing of the turbine, if the main lubricating system is not possible (if there is no gradient for the oil discharge; see e. g. Appendix I).

The mentioned parts are driven by toothed gears lubricated from the system of the guide bearing of the turbine. In order to achieve a quiet run, it is advantageous to employ pinions of Textumoid.

When the bearing is water-lubricated and the drive of the generator are designed in another way (separate auxiliary winding on the main generator or drive from the top end of the shaft), the gearcase is eliminated at all, whereby the turbine itself is considerably simplified and easy to inspect (e. g. Fig. 208).

C. GENERAL REMARKS ON ASSEMBLY WORK

The individual parts of the machine (spiral – stay ring – lids – bearing housings) must be connected so that the flanges contact each other “metal on metal”, i. e. without packings which would by its flexibility between the connecting flanges render the alignment of the machine during assembly work unsafe.

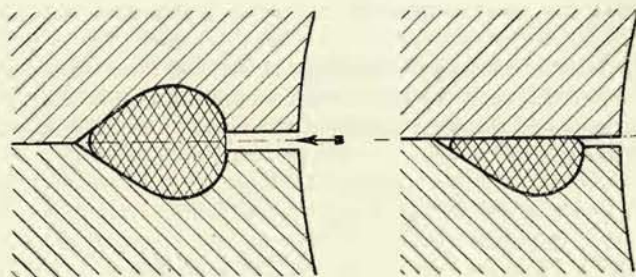


Fig. 211

In case of small heads (up to about 20 m) sealing of the connecting flanges is achieved by coating the contact surfaces prior to tightening with heated tallow which fills up the irregularities of the surfaces.

In installations for large heads and pressures sealing is performed by means of rubber strings which are inserted into grooves machined into the contact surfaces. Appendix VI shows such a groove in the connecting flange of the spiral. The shape

in the cross section is illustrated in Fig. 211.

Either both parts to be connected are fitted with such a groove or only one of them. The groove has the shape of a wedge, so that the rubber is pressed into it by the water pressure, whereby the sealing effect is strengthened. To render this action of the water pressure possible, a gap is left between the surfaces in the part between the sealing groove and the pressure space (see Fig. 211). The diameter of the rubber string, which is round in its original form,

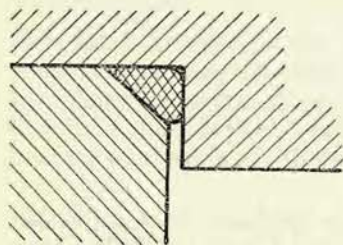


Fig. 212

must be determined so that the groove is properly filled up and the string does not protrude between the bearing surfaces.

When it is feasible to make use of a ring-type connection, a rubber ring consisting of a string cemented together is put over it, and the requested groove is formed by chamfering the edge of the counter-flange, as indicated in Fig. 212; e. g. in this way the sealing between the turbine lids and the spiral may be performed (see also Appendix VI).

These rings, however, serve only for sealing purposes and by no means for mutual centering of the connected parts, because at large diameters there would be excessive clearances. The parts are centered in the course of the assembly and their position is then secured by means of fitting pins, which also transmit the shearing forces in the joint.

The possibility of centering and of measuring during this former operation must already be provided for by the designer. Centering the runner and lid according to the clearances in the labyrinths (Appendix VI) is advantageously made possible by drilling four holes through the lid into one of the channels of the labyrinth, uniformly distributed around the periphery; these holes are subsequently closed with plugs, but during assembly work they permit to measure the clearances in the labyrinths by means of thickness gauges.

For instance, the procedure in assembling the set illustrated in Appendix VI would be approximately as follows: On the runner with the shaft the upper lid is put and by means of the above-mentioned holes in the lid, opening into the channels of the labyrinth, it is centered in relation to the runner so as to obtain a uniform clearance of the labyrinth around the entire periphery. Then the stuffing box and guide bearing are mounted to the shaft; the position of the latter is secured by machined holes through which taper pins are driven home. Above the bearing

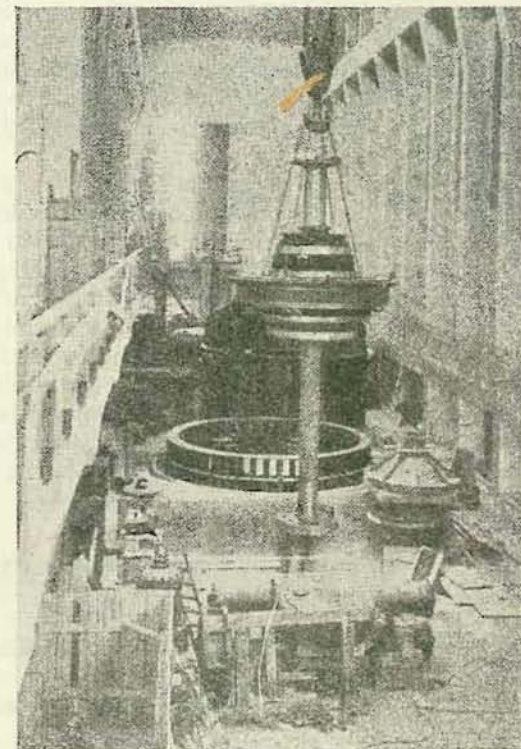


Fig. 213

a gear wheel is mounted, which supports the rotor as long as the coupling in the direction to the rotor of the generator is not connected, and sometimes also the guide blades are placed into the lid and the cranks are mounted. This complete unit is then lowered into the settled spiral (see Fig. 213), centered according to the stay ring and also secured by means of fitting pins.

The bottom lid must be centered according to the pivots of the guide blades to ensure a free motion of the latter. Since the bottom labyrinth must be centered independently of the lid according to the labyrinth of the runner, it is fastened to the extension of the draft tube, permitting this centering, whereupon it is likewise secured by means of fitting pins. Then, after the elbow of the draft tube has been mounted, the bottom bearing with the stuffing box is inserted and centered in conformity with the shaft.

Note: In the set illustrated in Fig. 36 the rear labyrinth ring is placed directly upon the lid. The lid must be centered according to the guide blades, while the labyrinth requires centering in conformity with the runner; for this reason, the labyrinth ring is fastened on the lid so as to permit small radial shifts for centering, and finally it is tightened to the lid by means of bolts which have their threads in the labyrinth ring but their heads outside the lid, to be accessible.

All bolt connections within the turbine must be properly secured. The bolts connecting the runner with the shaft are as a rule secured by metal sheet washers, each for two bolts in common, which after tightening the nuts are bent to the side surfaces of the latter. Smaller bolts (in labyrinths, etc.) are best secured by point welding. Lock nuts provide no reliable fastening as they may become loose.

2. PROPELLER AND KAPLAN TURBINES

A. HYDRAULIC INVESTIGATION

I. RUNNER DESIGN

1. Theoretical Introduction

The hydraulic layout of propeller and Kaplan turbines is in many respects conformable to that of high-speed Francis turbines (establishing of the meridional flow field, design of the guide apparatus, spiral, draft tube), but differs principally in the design of the runner blades themselves.

The runners are here equipped with a small number of blades, from 3 to 4 up to 8 to 10; the spacing of the blades in relation to their length is consequently wide, so that in cases of small numbers of blades the latter do even not overlap one another and form no closed ducts at all – the runner is, as we say, “transparent”. Since the driving force of the water is distributed amongst a small number of blades, there is a great difference between the pressures on the pressure side of the blade and on its suction side. Consequently, according to Bernoulli equation

(for the relative motion – see further), also the velocities on either side of the blade must be different, the higher velocity being encountered on the suction side; these differences will be the greater, the smaller the number of blades is (see Fig. 214). On one and the same cylindrical surface, therefore, neither the relative outlet velocities and consequently nor the absolute outlet velocities will be the same within the range of two successive blades. These differences will be too considerable to be neglected; for this reason, we must resort to a three-dimensional approach to the problem of designing the blade.

One of the possible methods of layout consists in setting out from the velocity triangles; and with regard to the above-mentioned circumstance we ascertain the requisite “exaggeration” of the blade angles at the inlet and the outlet, and in

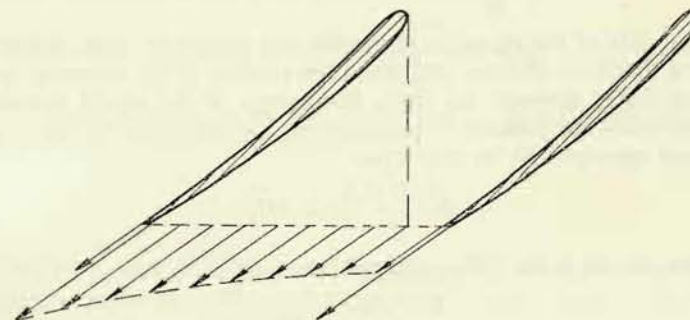


Fig. 214

conformity with the angles thus obtained we design the cross section of the blade. A shortcoming of this procedure¹⁾ is the indeterminateness of the coefficients which must be employed in the calculation.

From this point of view it is more advantageous to select a blade profile conformable to a suitable airfoil of which we exactly know the coefficients of lift and drag (or resistance), enabling us correctly to incorporate it into the blade.

This second method, in which we pay regard also to the distribution of the velocities between two successive blades and which therefore represents a three-dimensional approach, will be explained further. But first let us elucidate some notions of hydromechanics.

α) The Bernoulli Equation in a Relative Motion

We know the Bernoulli equation

$$\frac{C^2}{2g} + \frac{p}{\gamma} + z = \text{const.}, \quad (188)$$

¹⁾ For details see Thomann R.: Die Wasserturbinen und Turbinenpumpen, Part 2, Stuttgart, K. Wittwer, 1931.

which states that the sum of kinetic, pressure and positional energy in a water flow is constant; this equation holds good only when we neglect the losses resulting from friction and whirling, and when the water flows through a stationary duct.

When the duct through which the liquid flows rotates, energy will be either extracted from (turbine) or supplied to (pump) the liquid.

For such a case, we have already in Part I derived the Euler equation (20)

$$\frac{1}{g} (U_1 C_{u1} - U_2 C_{u2}) = H \eta_h.$$

If we neglect the losses – as we do in Equation (188) – then will apply $\eta_h = 1$ and

$$\frac{1}{g} (U_1 C_{u1} - U_2 C_{u2}) = H. \quad (189)$$

The right side of the equation represents the energy of each kilogram of the liquid. It is therefore obvious that when the product $U C_u$ decreases during the flow of the liquid through the duct, the energy of the liquid decreases, too. Conversely, when the product $U C_u$ increases, the energy of the liquid increases likewise, and consequently we may write

$$\frac{\Delta(U C_u)}{g} = \Delta H,$$

which when passing to the differential will be

$$\frac{d(U C_u)}{g} = dH,$$

and by integration we obtain

$$H - \frac{U C_u}{g} = \text{const.}$$

Substituting for the energy H the expression $H = \frac{C^2}{2g} + \frac{p}{\gamma} + z$, we arrive at

$$\frac{p}{\gamma} + z + \frac{C^2 - 2 U C_u}{2g} = \text{const.},$$

and since according to the velocity triangle (fig. 23) holds $W^2 = C^2 + U^2 - 2 U C_u$, we obtain the relation

$$\frac{p}{\gamma} + z + \frac{W^2}{2g} - \frac{U^2}{2g} = \text{const.}, \quad (190)$$

which represents a modification of the Bernoulli Equation for the relative motion of the liquid in a rotating duct.

β) Circulation

Now let us consider a stationary potential flow. As already pointed out earlier, in the case of a potential flow there exists a function, the so-called velocity potential Φ , which, when differentiated with respect to an arbitrary direction, gives with the

opposite sign the velocity in this direction. In the co-ordinate system X, Y, Z , the total differential of the potential is

$$d\Phi = \frac{\partial \Phi}{\partial x} dx + \frac{\partial \Phi}{\partial y} dy + \frac{\partial \Phi}{\partial z} dz,$$

which with regard to the given definition of the potential can be expressed

$$d\Phi = -(C_x \cdot dx + C_y \cdot dy + C_z \cdot dz),$$

where C_x, C_y, C_z are the components of the velocities in the directions of the co-ordinate axes.

The integral along a curve in general from 0 to S , has the form

$$-\int_0^S (C_x dx + C_y dy + C_z dz) = \int_{\Phi_0}^{\Phi_S} d\Phi = \Phi_S - \Phi_0.$$

When the curve along which we integrate is located on a equipotential surface, there is $d\Phi = 0$, $\Phi = \text{const.}$, and hence

$$\int_0^S (C_x dx + C_y dy + C_z dz) = 0.$$

When the curve is closed, so that when integrating we return to the initial point, this integral also equals zero. We mark it as a closed integral with the sign \oint :

$$\oint (C_x dx + C_y dy + C_z dz) = \Phi_0 - \Phi_0 = 0.$$

When the vector of the velocity C encloses with the co-ordinate axes the angles α', β', γ' , and the element of the path along we integrate the angles α, β, γ , there will hold good for the angle δ enclosed by these two vectors

$$\cos \delta = \cos \alpha \cos \alpha' + \cos \beta \cos \beta' + \cos \gamma \cos \gamma',$$

so that applies

$$\int_0^S \vec{C} d\vec{s} = \int_0^S C ds \cos \delta = \int_0^S (C_x dx + C_y dy + C_z dz).$$

This closed integral given above therefore is the integral of the product of the integrating path and the projection of the velocity into the direction of the path, and such a closed integral we term circulation and denote it by the symbol Γ (gamma).

For a potential flow system therefore holds that the circulation equals zero, because we have not made any assumption as to the curve on which we have proved the zero value of this integral, and the result must therefore hold for any curve whatsoever.

There exists only one type of potential flow in which the circulation may differ from zero. This is the so-called potential whirl.

γ) Potential Whirl, Magnus' Effect,
Kutta-Joukowski Theorem.

Let us imagine a circular cylinder of infinite length, rotating in a medium spreading in all directions into the infinite. The cylinder with the radius r_a (Fig. 215) is assumed to rotate with the angular velocity ω . By the action of the viscosity also the surrounding medium is put into a rotary motion. The viscosity of the medium produces on the contact surfaces of the individual layers tangential forces which

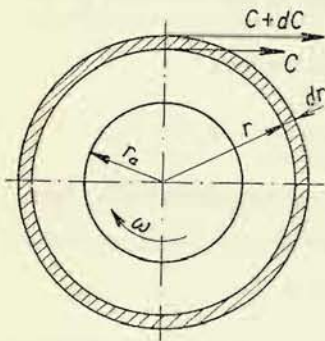


Fig. 215

are proportional to the velocity gradient $\frac{\partial C}{\partial r}$ of the field in the direction normal to the direction of the relative motion of the considered neighbouring layers, C denoting the velocity of the circular layer and r its radius. Terming the tangential force per surface unit τ , we can write

$$\tau = \mu \frac{\partial C}{\partial r}, \quad (191)$$

where μ is the coefficient of the dynamic viscosity or briefly the viscosity of the liquid.

The moments of the tangential forces about the axis of the cylinder, acting after the equilibrium of the motion has been established upon the concentric layer of the radius r and the thickness dr ,

must be in equilibrium, and consequently for the length of the cylinder equalling one must hold good

$$M - M + \frac{\partial M}{\partial r} dr = 0,$$

or

$$M = \text{const.} = 2\pi r \tau r = 2\pi r^2 \tau.$$

If we substitute for τ the corresponding expression from Equation (191), we obtain

$$M = 2\pi r^2 \mu \frac{dC}{dr} = \text{const.},$$

so that

$$dC = \frac{\text{const.}}{r^2} dr,$$

and hence

$$C = -\frac{K_1}{r} + K_2.$$

Since for $r = r_a$ holds $C = C_a$, i. e. the medium adheres to the cylinder, and for $r = \infty$ holds $C = 0$, applies $K_2 = 0$, $K_1 = -r_a C_a$, and hence

$$C = \frac{r_a C_a}{r} = \frac{k}{r},$$

which means that the medium is put into such a motion that the following relation applies:

$$Cr = C_a r_a = k, \quad (192)$$

and this represents the already known circulating flow (Section 1/A, Chapter I/3).

We know from earlier considerations (see the cited chapter) that such a motion can exist even in a non-viscous liquid, and we term it therefore potential whirl,

because the velocity $C = \frac{k}{r}$ has a potential (see also Section 1/A, Chapter I/1, β).

If we know the velocity, we can inversely determine the value of the velocity potential Φ . There will hold good

$$C = \frac{k}{r} = -\frac{d\Phi}{ds},$$

so that

$$d\Phi = -\frac{k}{r} ds = -\frac{k}{r} r d\varphi,$$

because $ds = r d\varphi$ is a circular arc, and, consequently, the potential has the value

$$\Phi = -k\varphi.$$

In a potential motion, the value of the circulation differs from zero only then when the axis of the whirl lies within the curve on which the circulation is determined. In our case, the circulation about the cylinder is

$$\Gamma = \oint C r d\varphi = k \oint d\varphi = 2\pi k = 2\pi r_a C_a = 2\pi r_a^2 \omega. \quad (193)$$

As already said, the whirling motion is brought about by the tangential forces in the liquid. For this reason, it cannot arise in a non-viscous liquid. If it, however, existed in such a liquid, it could not disappear by itself, because its destruction would again require tangential forces (Helmholtz-Thomson theorem). Therefore, if we disregard the viscosity, the whirl in the liquid can arise and cease only on the surface of the liquid or on the wall, or form a closed curve. This whirl then passes from the place of its origin to the place of its disappearance as the so-called whirl fibre formed by rotating particles. The other particles move in circles around the fibre, undergoing deformations but not rotating about their own axes, and for their motion Equation (192) holds good; their circulation around the fibre is therefore constant. If we tried to determine the velocity of the particles at the radius r according to this relation, the value ∞ would result. This is impossible from the viewpoint of physics. We therefore assume that a certain internal part, given by the radius r_0 , the so-called whirl core or whirl fibre, rotates as a solid body with the constant angular velocity ω . The circulation then is according to Equation (193), when f is the area of the core in the plane perpendicular to its axis

$$\Gamma = 2\pi r_0^2 \omega = 2f\omega.$$

The expression $f\omega$ is also termed the whirl moment.

We have so far considered a cylinder rotating in a stationary medium. Apart from the moment opposing the rotation (due to the viscosity), in this case the medium does not bring forth any forces acting upon the cylinder. When, however,

the cylinder rotates in a medium flowing at the velocity V , it will be acted upon, on the one hand, by a force in the direction of the velocity V , given by the resistance of the cylinder, and, on the other, hand by a force normal to the direction of the velocity V .

The creation of this force, normal to the velocity, has been explained¹ qualitatively by Magnus (after whom this phenomenon has been termed) as follows: On

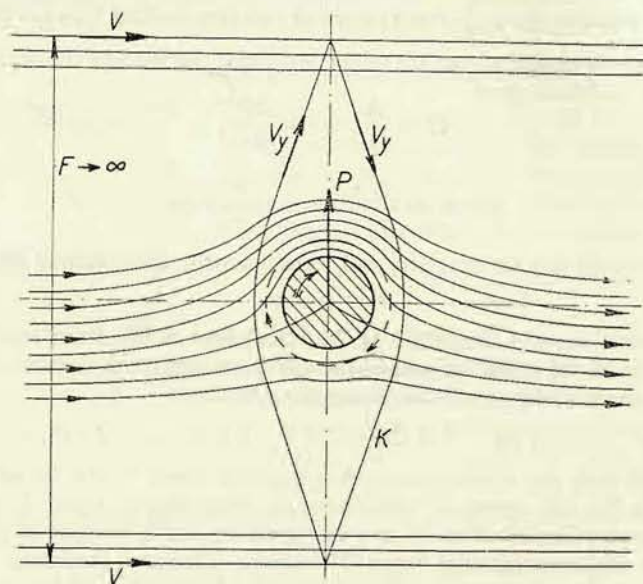


Fig. 216

that side of the cylinder (Fig. 216) where the cylinder creates by its rotation in the medium a velocity of the same sense as that of the velocity V of the flow, both velocities, i. e. the velocity V and the circulation velocity C are added. On the opposite side they are subtracted. For this reason, on one side of the cylinder the velocity of the medium is higher and therefore the pressure lower (according to the Bernoulli equation) than on the other side, and thereby a force is created which acts upon the cylinder perpendicularly to the direction of the velocity V .

The magnitude of this force is given by the expression by Kutta-Joukowski¹), which may be most conveniently derived according to Erhart²) as follows:

¹) Kutta: Auftriebskräfte in strömenden Flüssigkeiten. Illustr. aeron. Mitt., 1902. Über ebene Zirkulationströmungen, Münchener Ber. 1910 and 1911.

Joukowski: Über die Konturen der Tragflächen der Drachenflieger. Zeitschr. für Flugtechnik und Motorluftschiffahrt, 1910; by the same author: Aérodynamique, Paris, 1916.

²) Erhart F.: Kritická a zvuková rychlost media (Critical and sound velocity of the medium), Prague, Tech. knihkupectví, 1937.

We express the value of the circulation on the closed oblong curve K (Fig. 216) occupying the total width F of the flow field. The width of the flow field is assumed to be at least so large that the cylinder encompassed by the flow influences the latter on its boundaries so little that this effect may be neglected. We must therefore imagine the curve K to be much more oblong than it has been possible to indicate in the figure. If we consider the unit depth of a layer of the flow field, the width F assumes also the significance of the cross section. In the vertical direction we select a very oblong shape of the curve K , so that we need not count with the influence of the horizontal components of the velocity upon the circulation. The average value of the velocities on the curve K we then denote by V_y . The circulation on the curve K is the same as the circulation on an arbitrary other curve in which the base of the rotating cylinder is enclosed, because the circulation is given by the circular motion brought about by this cylinder. The circulation determined on the curve K is $\Gamma = 2 F V_y$. The average vertical variation of the velocity imparted to the medium flowing around the rotating cylinder therefore is $2 \cdot V_y = \frac{\Gamma}{F}$. This

velocity is imparted to the complete flow, whose mass through the cross section F per second is given by the expression $\frac{\gamma}{g} F V$. From the momentum theorem (Part I, Chapter III/1) then the magnitude of the force P is derived, necessary for effecting the change of the flow, which as reaction of the flow acts upon the cylinder:

$$P = \frac{\gamma}{g} F V 2 V_y = \frac{\gamma}{g} F V \frac{\Gamma}{F} = \frac{\gamma}{g} \Gamma V;$$

this holds for the considered layer of a thickness equalling one. For a layer of the thickness L consequently holds good

$$P = \frac{\gamma}{g} L V \Gamma, \quad (194)$$

which is the expression given by Kutta and Joukowski.

The force in the direction of the velocity is given by the imperfect flow around the immersed cylinder, resulting in a work-absorbing whirl behind the cylinder. In a non-viscous liquid the cylinder would be flown around without the creation of whirls – potentially – and the force in the direction of the velocity would disappear. But also the force normal to the velocity, the so-called lift, would disappear as in a non-viscous liquid no circulating flow around the cylinder would be created.

The lift acting upon the cylinder will therefore be

$$P = \frac{\gamma}{g} L V \Gamma = \frac{\gamma}{g} L V 2 \pi r_a^2 \omega.$$

On the base of the circulation around the body, we therefore can express the lifting forces upon any body, in so far, of course, it is altogether possible to ascertain the circulation around the profile. This can be done also for the blades

of a hydraulic turbine which are densely spaced and thus form closed ducts.¹⁾ We arrive in this case at results which are also obtained by the one-dimensional theory.

δ) Airfoils and the Creation of the Lift Acting upon the Wing

When designing axial-flow propeller and Kaplan turbines, we may select the profile of the blade in the cylindrical section in conformity to an airfoil. From tests in aerodynamic tunnels we know the coefficients for the resistance P_x (Fig. 217) as well as for the lift P_z for these airfoils.

The resistance of the airfoil is represented by the expression

$$P_x = \frac{k_x}{2} \frac{\gamma}{g} V^2 S, \quad (195)$$

and the lift by

$$P_z = \frac{k_z}{2} \frac{\gamma}{g} V^2 S, \quad (196)$$

where V is the velocity of the medium in relation to the airfoil at a sufficient distance in front of the latter, beyond the range of its influence on the flow. S is the

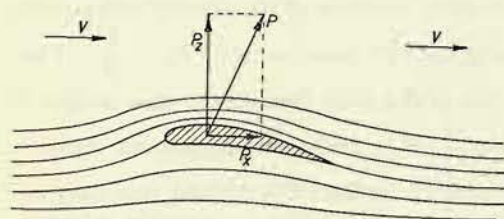


Fig. 217

largest projection of the area of the airfoil, and k_x and k_z are the coefficients of the resistance and the lift respectively. These coefficients are for a certain shape of the airfoil only functions of the Reynolds number Re . The number Re , at which the tests in aerodynamic tunnel are usually carried out, is as a rule of the same order of magnitude as the number Re for the flow around the profile in hydraulic turbines; therefore, we can directly employ these coefficients for designing the turbine blades.

According to Kutta and Joukowski, the lift acting on the airfoil may also be expressed by means of the circulation around it:

$$P_z = \frac{\gamma}{g} L V \Gamma,$$

where L is again the length (span) of the wing.

The circulation Γ , producing the lift, is given by the difference of the relative velocities of the medium below the wing and above it, by the influence of which – similarly as we have seen in the case of the rotating cylinder – a pressure drop above the airfoil arises, and an increase of the pressure below it.

According to Prandtl, this circulation is produced by the action of the boundary

¹⁾ Kaplan-Lechner: Theorie und Bau von Turbinen-Schnellläufern, Berlin, Oldenbourg, 1931, p. 81.

layer.¹⁾ When namely a liquid flows along a wall or body, the particles near the wall adhere to it owing to the influence of the viscosity, so that the velocity of the liquid diminishes in the direction toward the wall down to zero. This velocity drop proceeds within a very thin layer, the so-called boundary layer. Since the velocity of the particles of this layer which are nearest to the wall is zero, while the velocity of the particles at a greater distance from the wall is the same as the velocity of the other part of the medium, the mean velocity of the layer, determining its kinetic energy, equals half the velocity of the medium. From this follows that when the velocity of the liquid decreases at a sudden enlargement of the through-flow cross section, which is connected with an increase of the pressure of the liquid, the pressure in the boundary layer cannot increase to the same extent as in the main flow as its kinetic energy is smaller. Therefore, its particles are by the action of the surrounding liquid of higher pressure put into a reverse motion and thus a whirl arises.

This is the case with an airfoil in a streaming medium. When the motion of the medium relative to the airfoil starts from the stationary state, we have in the initial phase the case of a potential flow (Fig. 218a). Behind the edge A , however, a sudden velocity drop sets in, by the influence of which the boundary layer is stopped, the particles of the medium begin to stream backward from places of higher pressure and thus a so-called starting whirl is produced (Fig. 218b), which rapidly expands, separates from the wing, and is entrained by the stream.

Simultaneously with the generation of the starting whirl, circulation around the airfoil arises as reaction to this whirl, the sense of this circulation being opposed to that of the starting whirl. The circulation gradually shifts the splitting point B to the point A and is of the same magnitude as the starting whirl. The total circulation within the space containing both the airfoil and the starting whirl equals invariably zero. Theoretically, the starting whirl is entrained by the flow into the infinite and permanently in equilibrium with the circulation around the airfoil. Actually, however, in a liquid, the whirl disappears by the action of the internal friction of the medium. On the other hand, when the motion is stopped the circulation concentrates around the airfoil into a so-called stopping whirl which counterbalances

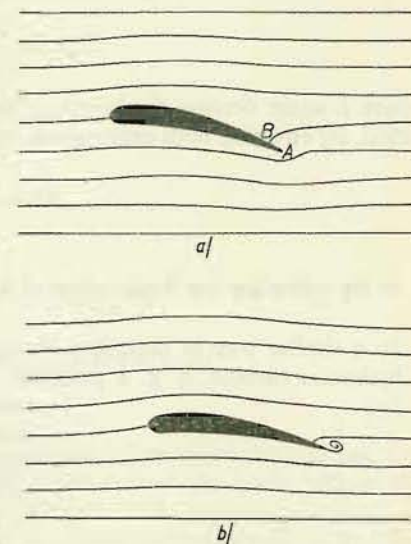


Fig. 218

¹⁾ Tietjens: Hydro- und Aeromechanik nach Vorlesungen von L. Prandtl, Berlin, Springer, 1929–1931.

the starting whirl, so that the total circulation within the considered space again equals zero. The creation of the starting whirl, as well as of the stopping whirl was experimentally ascertained and photographed by Prandtl.¹⁾

Simultaneously with the creation of the circulation, there also arises the lift acting upon the airfoil, which is defined, on the one hand, by Equation (196):

$$P_z = \frac{k_z}{2} \frac{\gamma}{g} V^2 S = \frac{k_z}{2} \frac{\gamma}{g} V^2 L l,$$

and, on the other hand, by the Kutta-Joukowski Equation:

$$P_z = \frac{\gamma}{g} L V \Gamma,$$

where L again denotes the length of the airfoil (the span) and l the depth of the airfoil. By equating both expressions, we obtain the value for the circulation:

$$\Gamma = \frac{k_z l V}{2}.$$

2. Equation for the Application of Airfoils to the Design of Turbine Blades

In a similar way as described above also the circulation around the blade of a hydraulic turbine, e. g. a propeller turbine (Fig. 219), is created. The water approaches the blade at the velocity C_1 which incorporates a certain peripheral component C_{u1} , i. e. in the form of a whirl with its axis in the turbine axis and the circulation $\Gamma_1 = 2\pi r C_{u1}$.

As long as the runner is still at rest, the water impinges upon the blade under an incorrect angle, roughly perpendicularly to the surface of the blade. In back of the leading edge A of the blade and the trailing edge B whirls of opposite senses are created, which are torn off (system of Kármán vortices) and entrained by the flow which leaves in an unchanged direction, i. e. with the original circulation Γ_1 . The water pressure puts the runner into a rotary motion, and the direction of the water relative to the blade shifts with the rising speed continuously into the direction W_1 .

Thereby the whirl at A gradually diminishes; the whirl at B , assuming the character of a starting whirl at an airfoil, creates, on the one hand a circulation

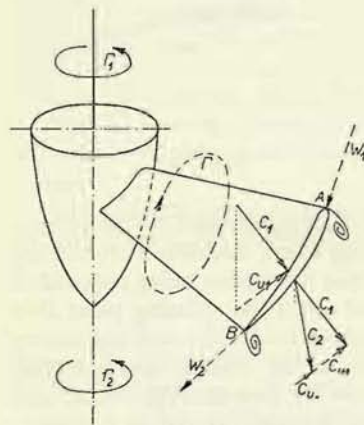


Fig. 219

¹⁾ See the quoted work by Tietjens, Tables 18 to 22.

around the blade, and, on the other hand, the longer the more, reduces the circulation in back of the runner down to the final value Γ_2 which is encountered in this place at normal speed. The total circulation in the entire turbine is always the same, and when full speed is attained, there applies, the number of runner blades being denoted by z_2 :

$$\Gamma_1 = z_2 \Gamma + \Gamma_2,$$

that is to say that the circulation around the blade is

$$\Gamma = \frac{\Gamma_1 - \Gamma_2}{z_2}.$$

Since the circulation in front of the runner is

$$\Gamma_1 = 2\pi r C_{u1},$$

while the circulation in back of the runner is

$$\Gamma_2 = 2\pi r C_{u2},$$

the circulation around the blade is

$$\Gamma_2 = \frac{2\pi r}{z_2} (C_{u1} - C_{u2}),$$

and since $\frac{2\pi r}{z_2} = t$ is the spacing of the blades, it holds good

$$\Gamma = t (C_{u1} - C_{u2}). \quad (197)$$

This value of the circulation can also be ascertained directly by determining the value of the integral $\oint W_s ds$ for the closed curve around the blade, where W_s denotes the projection of the velocity W into the path of the integration s .¹⁾ Let us select a curve along which we carry out the integration as indicated in Fig. 220: $a-b-c-d-a$, which is formed by the stream lines $b-c$ and $a-d$ whose distance from each other is just the spacing of the blades and which therefore exhibit in correspondingly located points the same velocity, and further by the lines $a-b$ and $c-d$, parallel to the plane of the runner, at so great a distance from the runner that the velocities on them are constant. Then will apply

$$\Gamma = \oint W_s ds = \int_a^b W_s ds + \int_b^c W_s ds + \int_c^d W_s ds + \int_d^a W_s ds.$$

Since on the lines $b-c$ and $a-d$, in correspondingly located points, there are the same velocities, but in forming the closed integral, we travel along the lines $b-c$ and $a-d$ in opposite directions, we can write

$$\int_b^c W_s ds = - \int_d^a W_s ds$$

¹⁾ Spannake. Kreisräder als Pumpen und Turbinen. Berlin, Springer, 1931, p. 81.

and hence

$$\Gamma = \int_a^b W_s ds + \int_c^d W_s ds,$$

or

$$\Gamma = t(W_{u2} - W_{u1}).$$

In an axial-flow turbine, there is according to Fig. 221, as we, by the way, already know,

$$W_{u2} - W_{u1} = C_{u1} - C_{u2},$$

and consequently

$$\Gamma = t(C_{u1} - C_{u2}).$$

The value $(C_{u1} - C_{u2})$ occurs in the design of the runner. We know it from the diagram of the turbine, or we determine it by means of Euler's energy equation, which for an axial-flow turbine has the form

$$U(C_{u1} - C_{u2}) = \eta h g H.$$

By the circulation Γ around the blade a lifting force acting on the blade is produced. In order to ascertain the velocity W which in the Kutta-Joukowski equation is decisive for the lift, we determine the force on the blade from the momentum equation, selecting the delimited area as indicated in Fig. 220. In the horizontal direction, the pressures p of the medium and forces resulting from the internal friction counterbalance each other. The relative velocity

of the water changes in the horizontal direction from the value W_{u1} in front of the runner to the value W_{u2} in back of the runner. The mass per second to which this flow variation is imparted (we consider here only the part of one blade of the radial length equalling one), is in this case given by $t \frac{\gamma}{g} W_m$, where the subscript m again indicates the meridional component. Consequently, the horizontal component of the force acting upon the part of the blade of the radial length equalling one, is

$$P_h^1 = W_m t \frac{\gamma}{g} (W_{u1} - W_{u2}).$$

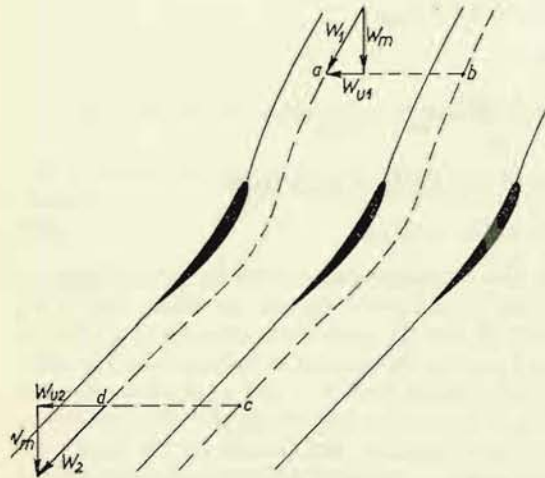


Fig. 220

In the vertical direction, the same part of the blade is acted upon, with regard to the circumstance that the vertical component of the velocity, W_m , does not change its magnitude, by the force

$$P_v^1 = t(p_1 - p_2),$$

where $(p_1 - p_2)$ is the overpressure of the runner. If we denote by h_z the loss of head within the space of the runner, we may write according to the Bernoulli equation (190) for the relative motion, since $U_1 = U_2$ and $W_{m1} = W_{m2}$,

$$\begin{aligned} \frac{p_1 - p_2}{\gamma} &= \frac{W_{u2}^2 - W_{u1}^2}{2g} + h_z = \frac{W_{u2}^2 - W_{u1}^2}{2g} + h_z = \\ &= \frac{W_{u2}^2 - W_{u1}^2}{2g} \left(1 + \frac{2g h_z}{W_{u2}^2 - W_{u1}^2} \right). \end{aligned}$$

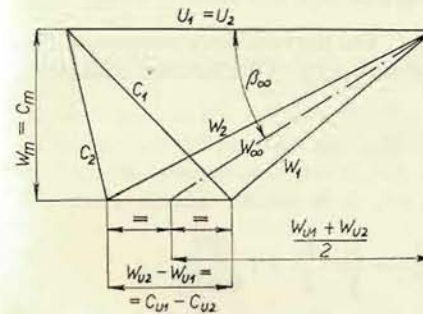


Fig. 221

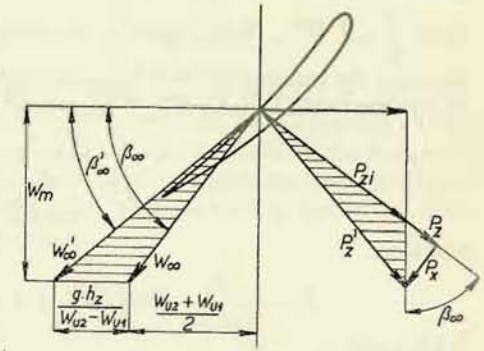


Fig. 222

The resultant force on the blade is then determined as the geometric mean:

$$\begin{aligned} P_z^1 &= \\ &= \sqrt{t^2 \left(\frac{\gamma}{g} \right)^2 \left\{ W_m^2 (W_{u1} - W_{u2})^2 + (W_{u2} - W_{u1})^2 \left(\frac{W_{u2} + W_{u1}}{2} \right)^2 \left(1 + \frac{2g h_z}{W_{u2}^2 - W_{u1}^2} \right)^2 \right\}} \\ P_z^1 &= \frac{\gamma}{g} t (W_{u2} - W_{u1}) \sqrt{W_m^2 + \left\{ \frac{W_{u2} + W_{u1}}{2} \left(1 + \frac{2g h_z}{W_{u2}^2 - W_{u1}^2} \right) \right\}^2}, \quad (198) \end{aligned}$$

Since $t(W_{u2} - W_{u1}) = \Gamma$ and the expression under the radical sign have the dimension of a velocity, we may write

$$P_z^1 = \frac{\gamma}{g} \Gamma W_\infty,$$

and for the full width of the blade

$$P_z = \frac{\gamma}{g} \Gamma W_\infty L.$$

As is obvious from Equation (198), for the ideal case of a loss-free through-flow of the water through the runner, i. e. for $h_z = 0$, we obtain the velocity W_∞ , decisive for the determination of the lift, and the inclination β_∞ of this velocity, as indicated by the construction in Fig. 221. The force $P_{z,i}$ resulting from this velocity is normal to it. Actually, however, the through-flow is connected with a certain loss h_z , and in this case, as follows from Equation (198), the horizontal component of the velocity W_∞ is increased by the value $\frac{g h_z}{W_{u2} - W_{u1}}$, whereby the velocity W_∞ increases to the value W'_∞ , and its inclination changes from β_∞ to β'_∞ , because the vertical component does not change if we assume that the through-flow is constant. Also the resultant force acting upon the blade is more inclined (Fig. 222) and increases its value so that the peripheral component is again the same. The resultant force P'_z is again perpendicular to the velocity W'_∞ , and here applies.

$P'_z = \frac{\gamma}{g} L \Gamma W'_\infty$. With regard to the circumstance that this force is at the same time also the resultant of the lifting component P_z and the resistance component P_x , in relation to the velocity W_∞ , follows from the similarity of the hatched triangles¹⁾

$$\frac{P'_z}{P_z - \frac{P_x}{\tan \beta_\infty}} = \frac{W'_\infty}{W_\infty},$$

and since

$$P_z - \frac{P_x}{\tan \beta_\infty} = \frac{\gamma}{g} \frac{k_z}{2} L l W_\infty^2 - \frac{\gamma}{g} \frac{k_x}{2} L l \frac{W_\infty^2}{\tan \beta_\infty},$$

holds good

$$\frac{\gamma}{g} L \Gamma W'_\infty W_\infty = \frac{\gamma}{g} \frac{k_z}{2} L l W_\infty^2 W'_\infty - \frac{\gamma}{g} \frac{k_x}{2} L l \frac{W_\infty^2}{\tan \beta_\infty} W'_\infty,$$

or

$$\Gamma = \frac{1}{2} \left(k_z - \frac{k_x}{\tan \beta_\infty} \right) l W_\infty.$$

Therefore, we need not know the velocity W'_∞ and the angle β'_∞ , but we can calculate with the values W_∞ and β_∞ , which we readily determine according to the construction in Fig. 221. Since we know that the circulation around the blade has according to Equation (197) the value $\Gamma = t (C_{u1} - C_{u2})$, we may write

$$t (C_{u1} - C_{u2}) = \frac{1}{2} \left(k_z - \frac{k_x}{\tan \beta_\infty} \right) l W_\infty,$$

whence

$$k_z - \frac{k_x}{\tan \beta_\infty} = 2 \frac{C_{u1} - C_{u2}}{W_\infty} \frac{t}{l} = \frac{2 \Gamma}{l W_\infty}.$$

¹⁾ Nechleba: Cirkulace kolem lopatky turbíny (Circulation around the Turbine Blade), Strojnický obzor (Mechanical Engineering Review), 1943, No. 15—16, p. 284.

By introducing the specific velocities, we transform the expression to

$$k_z - \frac{k_x}{\tan \beta_\infty} = 2 \frac{C_{u1} - C_{u2}}{w_\infty} \frac{t}{l}.$$

Substituting for $(C_{u1} - C_{u2})$ the values from the Euler equation

$$u (C_{u1} - C_{u2}) = \frac{\eta_h}{2},$$

we obtain

$$k_z - \frac{k_x}{\tan \beta_\infty} = \frac{\eta_h}{u w_\infty} \frac{t}{l},$$

and from this results the expression for the hydraulic efficiency of the turbine

$$\eta_h = u w_\infty \frac{l}{t} \left(k_z - \frac{k_x}{\tan \beta_\infty} \right). \quad (199)$$

From this expression it is evident that at higher specific speed, i. e. at higher values u and w_∞ , the length l of the blade must be reduced, or the spacing t must be increased or the number of blades reduced, in order to maintain the hydraulic efficiency according to Equation (199) at the value with which has been calculated and which, as experience has shown, is attainable. Thus the specific load of the blade increases, as also follows from the expression

$$\Delta p = \frac{P_z}{S} = \frac{\gamma}{g} \frac{k_z}{2} W_\infty^2$$

because with rising speed also W_∞ increases. This pressure difference, however, is determined by the difference of the squares of the velocities on the pressure and suction sides of the blade. With rising speed, the velocity distribution within the spacing becomes steadily less uniform. This circumstance impairs the efficiency of the draft tube, because equalizing the differing velocities to a common value causes whirls in the draft tube. This is one of the factors which restrict the reduction of the ratios $\frac{l}{t}$ and the possibility of increasing the specific speed.

The derived expression (199) may be used for determining suitable airfoils from which the turbine blade can be formed, and for their setting with regard to the velocity W_∞ . When the lift and resistance coefficients of the airfoils, k_z and k_x respectively, satisfy Equation (199), then the selected airfoils exhibit such properties that the created circulation around the blades meets the requirement of a correct utilization of the energy of the water.

The coefficients k_z and k_x express the properties of the airfoils in their sequence in the blade field of the turbine, i. e. the properties of airfoils of infinite span, acting upon one another. When values ascertained in aerodynamic tunnels for individual airfoils (each separately) are employed, certain corrections will be required. The coefficient of resistance will have to be reduced by the induced resistance due to

the finiteness of the tested airfoil, and the coefficient of lift must then be altered with regard to the mutual interaction of the airfoils arranged in a line. These relations will be explained in the following chapter.

Note: From the expression (199) also the fact follows that when varying the number of blades in a propeller turbine, but leaving their shape unaltered, we must vary the product $uv\omega$ to maintain a good efficiency. In principle, we therefore can with only one blade form build a number of runners with different specific speeds by changing the number of blades.¹⁾

3. Aerodynamic Properties of Airfoils

For a more detailed study of the properties of airfoils we refer to the work Letecký průvodce, díl 2 (Aeronautical Guide, Part 2), Prague, ČMT, 1939. For completeness of the present book, some chapters of this work which are of special interest to the turbine designer are to be reproduced here.

α) On the Aerodynamic Properties of Airfoils in General

The fundamental aerodynamic properties of airfoils are characterized by the coefficients of resistance c_x , of lift c_z and moment c_m ²⁾ which are defined by the equations

$$P_z = \frac{c_z}{2} \frac{\gamma}{g} V^2 S, \quad P_x = \frac{c_x}{2} \frac{\gamma}{g} V^2 S, \quad M = \frac{c_m}{2} \frac{\gamma}{g} V^2 S l, \quad (200)$$

where S is the supporting surface, i. e. the area of the plan of the airfoil, given by its largest projection in the plan. P_z is the lift, i. e. the component of the resultant aerodynamic force in the axis of lift, always normal to the direction of the relative velocity of the flow; P_x is the resistance, i. e. the component of the resultant aerodynamic force in the direction of the velocity V of the flow relative to the airfoil. M is the moment of the aerodynamic forces about a certain axis normal to the plane of symmetry (the position of this axis in relation to the airfoil must be exactly defined); when there is no further information at disposal, the moment M , or its coefficient c_m , relates to the leading edge. When the coefficient of the moment is related to the point located on the chord at a quarter of the depth of the airfoil, it is denoted by $c_{m, 0.25 l}$; when it is related to the aerodynamic centre, it is marked c_{mac} ; the moment, and consequently also the coefficient, is positive when it acts as tilting moment, i. e. against the positive sense of the angle of attack α (see also Fig. 223).

The dependences of the coefficients c_z , c_x , c_m on the angle α are in the majority

¹⁾ For details see Nechleba: Kaplan Turbine Blading, Report to the 4th World Power Congress in London, 1950. Further, Druckmüller: Důsledky změny počtu lopatek Kaplanových turbin (Consequences Resulting from Changes of the Number of Blades in Kaplan Turbines), Strojírenství (Mechanical Engineering Review) 2, 1952, No. 7, p. 295.

²⁾ For single airfoils of finite length we employ the symbols c as in the Aeronautical Guide; for values already recalculated for the conditions in the turbine we use the symbols k . Similarly, the velocity of approach to the airfoil we shall denote by V , but the relative velocities in the turbine by W .

of cases experimentally determined for certain airfoils and given in the literature numerically and graphically.¹⁾

Apart from graphical and tabular representations of the aerodynamic coefficients of airfoils, we may also advantageously employ equations expressing the relations between the individual coefficients and the angle of attack. Most important are the following equations which hold good in the range of the usual angles of attack, when the flow around the wing is continuous, without rupture:

$$\begin{aligned} c_z &= \frac{\partial c_z}{\partial \alpha} (\alpha - \alpha_0) \\ c_x &= c_{x0} + \frac{\partial c_x}{\partial c_z^2} c_z^2 \\ c_m &= c_{m0} + \frac{\partial c_m}{\partial c_z} c_z. \end{aligned} \quad (201)$$

In these equations $\frac{\partial c_z}{\partial \alpha}$ denotes the gradient of the straight line which characterizes the dependence of the coefficient c_z on the angle α ; α_0 is the angle of attack at which $c_z = 0$; c_{x0} is the length on the c_x axis cut off by the straight line characterizing the progress of the coefficient of resistance of the airfoil in dependence on c_z^2 , and

$\frac{\partial c_x}{\partial c_z^2}$ is the gradient of this straight line; c_{m0} is the coefficient of the moment at the zero lift coefficient; the expression $\frac{\partial c_m}{\partial c_z}$ denotes the gradient of the straight line characterizing the dependence of the moment coefficient on the lift coefficient.

β. Geometric Characteristics of Airfoils

The most important geometric characteristics of the airfoil are indicated in Fig. 224. These are:

- m – maximum deflection of the central curve of the airfoil,
- L – distance of the maximum deflection of the central curve from the leading edge,
- t – maximum thickness of the airfoil.

The geometric characteristics m , L and t are usually given as fractions of the length l of the chord of the airfoil.

¹⁾ Letecký průvodce, 2. díl (Aeronautical Guide Part 2), Prague, ČMT, 1939, or Ergebnisse der Aerodynamischen Versuchsanstalt zu Göttingen, Serial Parts 1–4, Berlin, Oldenbourg, 1925–1932.

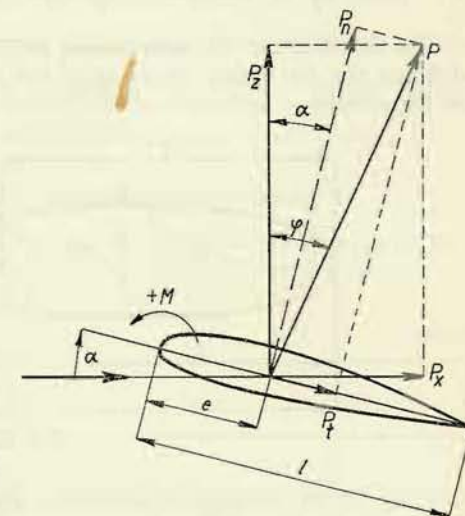


Fig. 223

For determining the influence of the enumerated characteristics of the airfoil on its aerodynamic properties, systematic experiments were carried out in various aerodynamic laboratories. The most complete picture of these influences is presented by test results obtained with a series of American airfoils.¹⁾ In this series, the geometric characteristics were systematically varied in the following ranges:

$$\frac{m}{l} = 0 \text{ to } 0.06; \quad \frac{L}{l} = 0.2 \text{ to } 0.6; \quad \frac{t}{l} = 0.06 \text{ to } 0.21.$$

The airfoils are in this case marked with numbers of four places, the first figure defining the maximum deflection of the central curve, the second the distance of the maximum deflection of the central curve from the leading edge, and the

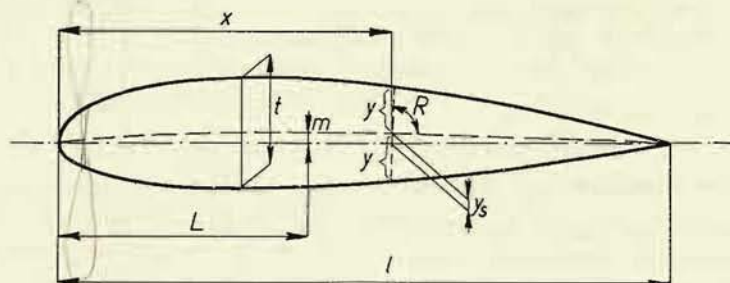


Fig. 224

last two figures indicate the thickness. Thus e. g. the number 2412 denotes an airfoil exhibiting the following ratios:

$$\frac{m}{l} = 0.02; \quad \frac{L}{l} = 0.40; \quad \frac{t}{l} = 0.12.$$

The co-ordinates y and y_s (Fig. 224) are defined by equations, but as the

Table 1

$x \%$	$y \%$	$x \%$	$y \%$	$x \%$	$y \%$
0	0	15	8.909	60	7.606
1.25	3.157	20	9.563	70	6.107
2.5	4.358	25	9.902	80	4.372
5.0	5.925	30	10.000	90	2.413
7.5	7.000	40	9.672	100	0.210
10.0	7.805	50	8.823		

¹⁾ NACA Rep. 460.

calculations based upon them are rather time-consuming, we give here tables replacing these equations.

The first table presents half the thickness of the airfoil, y , in dependence on the distance from the leading edge, x , expressed in percents of the length of the chord.

The table holds good for airfoils of the relative thickness $\frac{t}{l} = 0.2$, but may be used for any ratio $\frac{t}{l}$ when we multiply the number in the column y by the factor $5 \frac{t}{l}$.

The second table defines the co-ordinates of the central curve of the airfoil with the relative deflection $\frac{m}{l} = 0.1$. Here y_{s2} denotes the ordinates of the central curve whose maximum deflection is at one fifth of the length of the chord ($\frac{L}{l} = 0.2$), y_{s3} denotes the ordinates of the central curve whose ratio is $\frac{L}{l} = 0.3$, etc.; for other maximum deflections $\frac{m}{l}$ we use the values of the table multiplied by $10 \frac{m}{l}$.

Table 2

$x \%$	$y_{s2} \%$	$y_{s3} \%$	$y_{s4} \%$	$y_{s5} \%$
0	0	0	0	0
5	4.38	3.06	2.34	1.90
10	7.50	5.56	4.38	3.60
15	9.38	7.50	6.09	5.00
20	10.00	8.89	7.50	6.40
25	9.95	9.72	8.60	7.50
30	9.84	10.00	9.38	8.40
40	9.38	9.80	10.00	9.60
50	8.59	9.18	9.73	10.00
60	7.50	8.16	8.89	9.60
70	6.09	6.74	7.50	8.40
80	4.38	4.90	5.56	6.40
90	2.34	2.65	3.06	3.60
100	0	0	0	0

When drawing the airfoil, we proceed as follows: First we draw the central curve in conformity with the co-ordinates by the method described above. Through the individual points of the central curve we then lay verticals on which we plot on

both sides the corresponding halves of the thickness y . By connecting the points ascertained in this way we obtain the required airfoil of the series NACA.

Correct drawing of the airfoil is aided by the knowledge of the curvature r of the airfoil at the leading edge, which is given by the relation $\frac{r}{l} = 1.10 \left(\frac{t}{l}\right)^2$.

γ. Interdependence of the Geometric and Aerodynamic Characteristics of the Airfoil

The tests results given in NACA Rep. 460 may be summarized in the diagrams shown in Figs. 225 to 230, which define the dependence of the most important aerodynamic characteristics on the geometric characteristics of the airfoil.

These diagrams have been plotted on the base of tests on rectangular wings exhibiting a slenderness (i. e. the ratio of the span to the mean length of the chord, or the ratio of the square of the span to the area of the wing) of $\Lambda = 6$, at a Reynolds number of $3.5 \cdot 10^6$.

Fig. 225 illustrates the dependence of the angle of attack α_0 at zero lift upon the maximum relative deflection $\frac{m}{l}$ of the central curve and upon the relative distance $\frac{L}{l}$ of this deflection

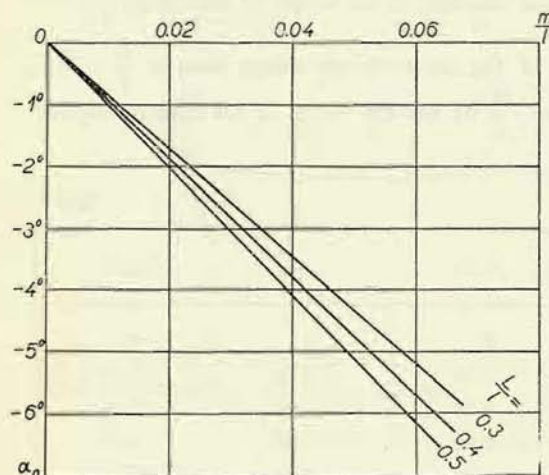


Fig. 225

from the leading edge. The absolute value of the angle α_0 increases with the deflection m and the distance L . When employing these diagrams, we must bear in mind that the angle of attack α_0 is here measured from the connecting line between the initial and end points of the central curve and that this connecting line is in general not identical with the chord of the airfoil.

Fig. 226 presents graphically the dependence of the value $\frac{\partial c_z}{\partial \alpha}$ on the relative length $\frac{t}{l}$. The ratio $\frac{\partial c_z}{\partial \alpha}$ diminishes with rising thickness almost linearly.

Fig. 227 shows the increase of the coefficient of viscous resistance, c_{xv} , with the thickness and deflection of the airfoil.

Fig. 228 presents the dependence of $\frac{\partial c_x}{\partial c_z^2}$ on the relative thickness of the

profile. The value of the ratio $\frac{\partial c_x}{\partial c_z^2}$ increases almost linearly with increasing thickness.

The dependence of the moment coefficient at zero lift, c_{m0} , upon the ratios $\frac{m}{l}$, $\frac{L}{l}$, $\frac{t}{l}$ is illustrated in Fig. 229. The coefficient rises with increasing deflection

of the central curve, $\frac{m}{l}$, and

with an increasing ratio $\frac{L}{l}$;

on the other hand, this coefficient diminishes with rising relative thickness for the same central curve.

The dependence of the ratio $\frac{\partial c_m}{\partial c_z}$ is represented in Fig. 230 which shows a moderate decrease of this ratio with an increasing relative thickness $\frac{t}{l}$ of the airfoil.

δ. Influence of the Finite Length of the Supporting Whirl and Wing

In a two-dimensional stream line flow, the whirl core or the wing replacing this core is infinitely long, thus satisfying the Helmholtz law, which states that in a non-viscous fluid a whirl can neither arise nor cease, but must either end on restricting walls or be closed.

If we cut of a cylindrical whirl only a part of finite length, it would be necessary to restrict the core by walls perpendicular to the axis of the whirl, so that

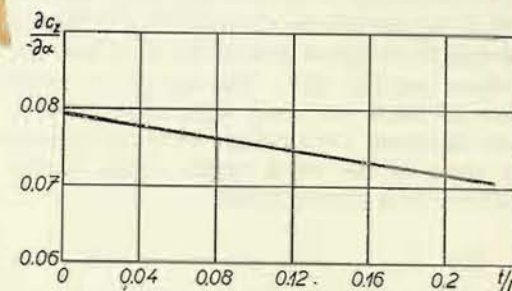


Fig. 226

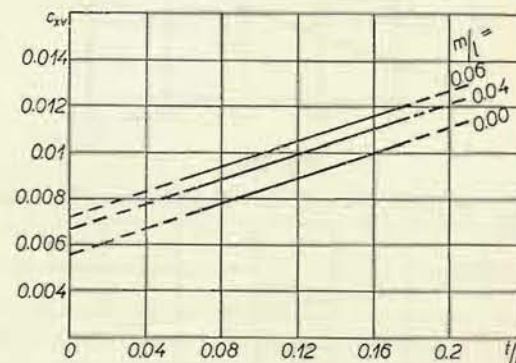


Fig. 227

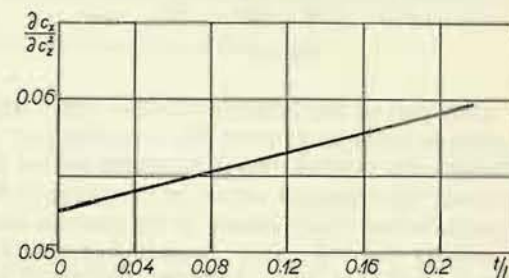


Fig. 228

only the part of the medium between these walls would be put in motion. The influence of the walls would manifest itself only by friction on the boundary layer and would be insignificant to the stream line motion between the walls. When the core or the wing ends freely, pressure is different on both sides and a flow arises in the direction of the axis of the whirl, connected with the whirl. There arise whirls normal to the direction of the flow which approximately coincides with the whirl axis (the axis of the supporting whirl – the wing), i. e. whirls normal to this axis, which in principle are a continuation of the supporting whirl and would in a non-viscous fluid extend behind the wing into the infinite (see Fig. 231). The axis of the whirl does not break but passes along an arc into the new direction. Thus a single whirl, in the proper sense of the word, arises, closed in the infinite (by a starting whirl).

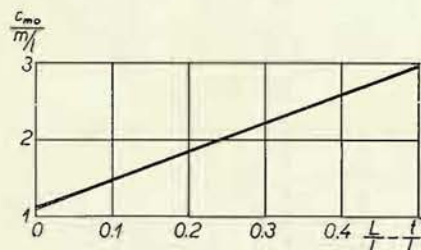


Fig. 229

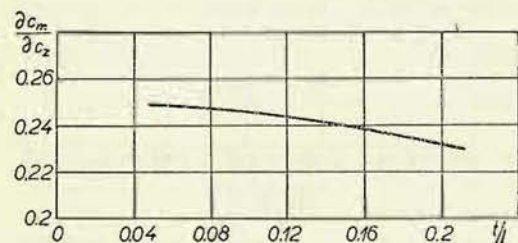


Fig. 230

Only part of this horseshoe-shaped whirl, appertaining to the actual whirl core (wing) is supporting, while the remaining part increases the resistance. This part changes the original two-dimensional stream line field and renders the motion spatial. The resistance caused by the change is termed induced resistance, because the ineffective whirls induce in the space in back, as well as in front of the wing, a velocity directed against the action of the lift, thus creating a deflection of the flow; the stream line is deflected downward by the so-called downflow angle ε (see Fig. 232).

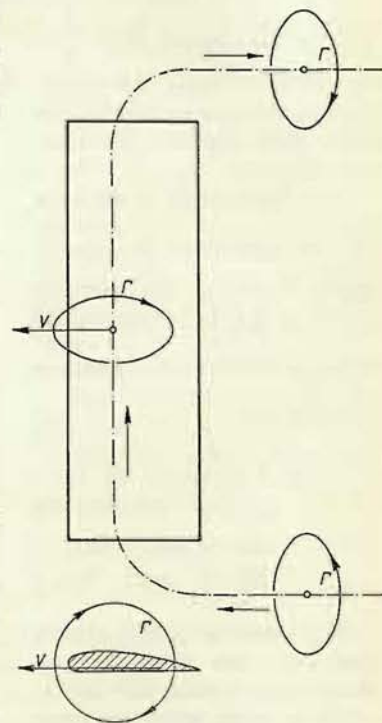


Fig. 231

Far in front of the wing the deflection is zero, so that at the wing itself we can approximately count with a deflection equalling the arithmetical mean, i. e. with the angle $\frac{\varepsilon}{2}$. This angle of the deflection of the airflow is termed induced angle of attack α_i .

Owing to the inclination of the airflow by the angle α_i , also the direction of the lift, or of the lift axis which is always normal to the relative velocity of the approaching flow, is tilted by the same angle, so that the lift further contains a component in the initial direction of the velocity of the airflow, which is termed induced

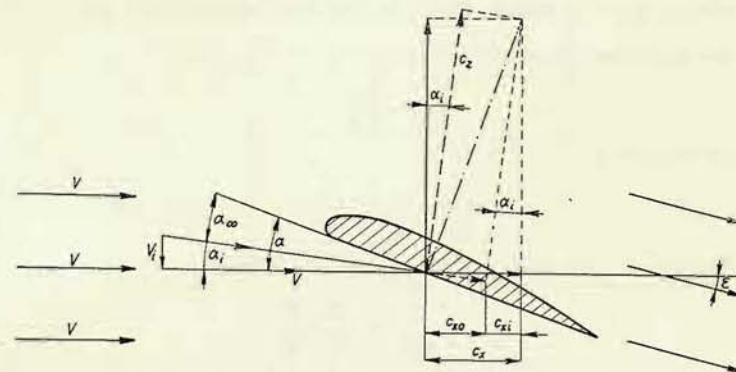


Fig. 232

resistance or induced drag. Denoting the coefficient of the induced drag by c_{xi} there applies according to Fig. 232:

$$c_{xi} = c_z \sin \alpha_i \doteq c_z \alpha_i, \quad (202)$$

where α_i is the induced angle of attack in circular measure.

The total drag coefficient of wing of finite span is then given by the sum of the following components:

a) Drag coefficient of the wing of infinite span, termed profile drag coefficient c_{x0} for the angle of attack $\alpha_\infty = \alpha - \alpha_i$, where α is the angle of the chord with the direction of the relative velocity of the undeflected flow.

b) The induced drag coefficient c_{xi} .

Therefore we can write for the total drag

$$c_x = c_{x0} + c_{xi} \quad (203)$$

and for the pertinent angle of attack

$$\alpha = \alpha_\infty + \alpha_i. \quad (204)$$

For an elliptical distribution of the lift across the span of the wing, as e. g. encountered on a wing of an elliptical plan, with the same profile in all sections

parallel to the plane of symmetry and with a constant angle of attack across the span, the induced velocity across the span is constant and defined by the expression

$$V_i = V \frac{c_z}{\pi A}, \quad (205)$$

where A is the slenderness or aspect ratio of the wing, i. e. the ratio of the span to the mean length of the chord, $\frac{b}{l_{mean}}$, which may also be defined by the expression $A = \frac{b^2}{S}$.

The induced angle of attack, too, is in this case constant and given in circular measure by the ratio $\frac{V_i}{V}$, i. e.

$$\alpha_i = \frac{c_z}{\pi A};$$

its value in degrees is

$$\alpha_i^0 = 57.3 \cdot \frac{c_z}{\pi A}. \quad (206)$$

From Equations (202) and (206) we obtain the relation

$$c_{xi} = \frac{c_z^2}{\pi A} = \frac{S}{\pi} \frac{c_z^2}{b^2}. \quad (207)$$

The induced drag coefficient is directly proportional to the square of the lift coefficient and inversely proportional to the aspect ratio of the wing.

Equations (203) and (207) enable us to determine the drag coefficient of a wing of an arbitrary aspect ratio A_2 from the known coefficient of a wing of the aspect ratio A_1 , provided that both wings exhibit the same profile and the same elliptical distribution of the lift across the span. We denote the drag coefficients of the wings by c_{x1} and c_{x2} respectively and express the equality of the profile drag in both cases, the coefficient c_z being the same:

$$c_{x1} - \frac{c_z^2}{\pi A_1} = c_{x2} - \frac{c_z^2}{\pi A_2}.$$

From this equation we obtain after adjustment

$$c_{x2} = c_{x1} + \frac{c_z^2}{\pi} \left(\frac{1}{A_2} - \frac{1}{A_1} \right),$$

and by recalculation for an infinite span, we obtain the drag coefficient of a wing of infinite span – the profile drag c_{x0} – which will be introduced into the expression (199) and therefore identically denoted by k_x :

$$k_x \equiv c_{x0} = c_x - \frac{c_z^2}{\pi A}. \quad (208)$$

The angle of attack α_2 , the aspect ratio being A_2 , we determine from the angle of attack α_1 of a wing of the aspect ratio A_1 (the lift coefficient being again c_z), by expressing the equality of the angle α_∞ in both cases by means of Equations (206) and (204): to represent the angles in degrees, we put

$$\alpha_1^0 - 57.3 \cdot \frac{c_z}{\pi A_1} = \alpha_2^0 - 57.3 \cdot \frac{c_z}{\pi A_2},$$

from which we obtain the sought angle of attack

$$\alpha_2^0 = \alpha_1^0 + 57.3 \cdot \frac{c_z}{\pi} \left(\frac{1}{A_2} - \frac{1}{A_1} \right),$$

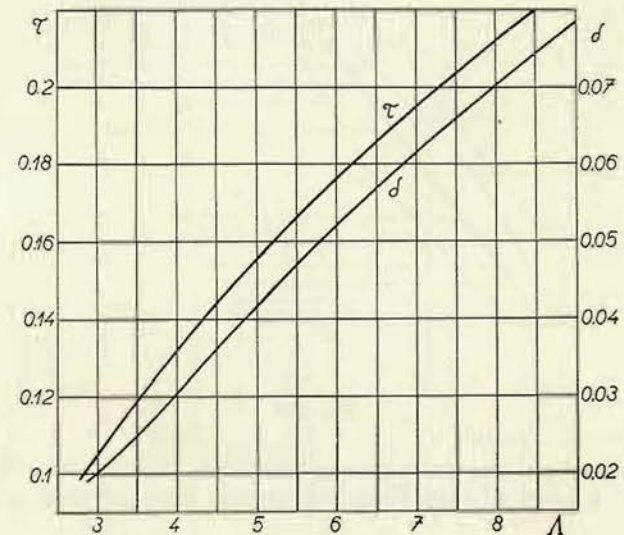


Fig. 233

and when we recalculate it for an infinite span, we obtain the angle of attack for infinite span

$$\alpha_\infty^0 = \alpha^0 - 57.3 \cdot \frac{c_z}{\pi A}. \quad (209)$$

In general, the distribution of the lift across the span of the wing is not elliptical, and the conversion formulas will be somewhat different. E. g. for a rectangular wing we must introduce the correction coefficients τ and δ , whose progress is shown in Fig. 233, and when recalculating the drag coefficient for an infinite span, we must according to Equation (203) deduct the induced drag coefficient given by the expression

$$c_{xi} = \frac{c_z^2}{\pi A} (1 + \delta), \quad (210)$$

or when determining the angle of attack for an infinite span, deduct according the Equation (204) the induced angle of attack defined by the expression

$$\alpha_i = \frac{c_z}{\pi A} (1 + \tau). \quad (211)$$

For a wing of another plan shape, exhibiting a geometrically similar profile and the same angle of attack across the entire span, the circulation around the wing (see the expression for the circulation as previously derived, $\Gamma = \frac{k_z l v}{2}$) will

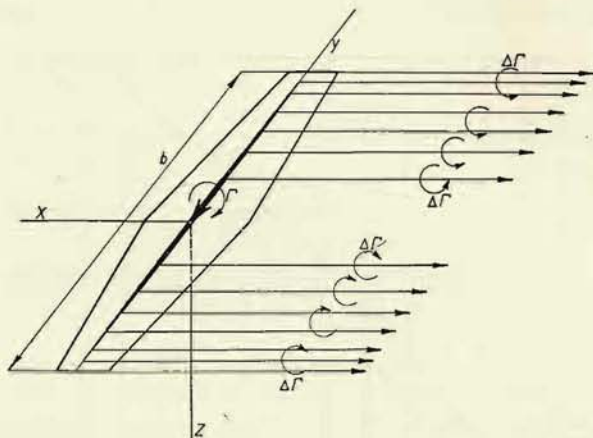


Fig. 234

not be the same across the entire span and therefore, in addition to the horseshoe-shaped whirl, a series of whirl fibres will separate from the wing, as indicated in Fig. 234.

When utilizing these results for the application of airfoils to the blades of propeller turbines, we must bear in mind:

1. That the blade is at both ends of its span enclosed by flow surfaces; at one end by the hub, and at the other end by the runner casing. The formation of a horseshoe-shaped whirl, characteristic for wing of finite span, is therefore not possible.

2. That the circulation along the span of the blade (i. e. the wing) is constant, because it is given by the expression $\Gamma = t C_{u1} - C_{u2}$, and the expression $U (C_{u1} - C_{u2})$, in which U is proportional to the spacing t , has an approximately constant value equalling $\eta_h gH$; the circulation along the span of the blade is therefore constant. Consequently, no separation of whirl fibres, not even along the blade, will take place.

That means that we have here the case of an analogue to a wing of rectangular shape and infinite span. Since the properties of airfoils are currently given for

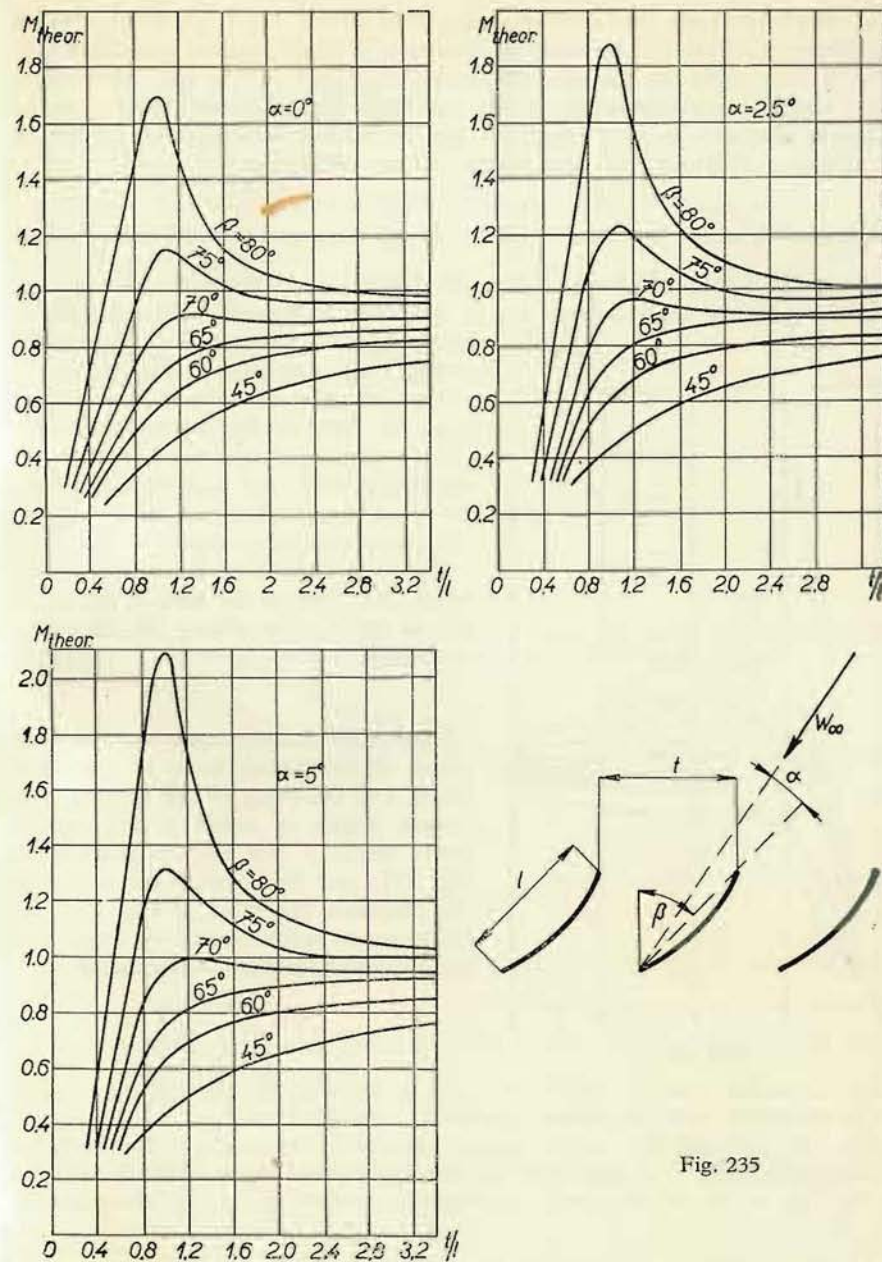


Fig. 235

wings of a rectangular plan and the usual aspect ratio of 5 or 6, we should employ the relations (210) and (211) for our recalculation. We make no great error, however, if we directly apply the relations (208) and (209); this is all the more permissible as not even the recalculation of the lift coefficient – which is to be explained in the following chapter – is quite exact; but also the more exact procedure employing the relations (210) and (211) does not present any difficulties.

4. Variation of the Lift Coefficient for Wings Arranged into a Lattice System

If we pass a cylindrical section through the blades and develop it into a plane (Fig. 220), we see that we have not to deal with an isolated wing but with an infinite series of wing profiles, successively arranged into a so-called profile lattice.

The influences of the individual profiles upon the flow interfere with one another, and the lift coefficient k_z of one wing in the lattice will have another value than the respective coefficient c_z of an isolated wing, and may be greater or smaller.

Denoting the lift on the isolated wing by P_1 and that on the wing in the lattice system by P_r , we obtain for the same conditions

$$\frac{P_r}{P_1} = \frac{k_z}{c_z} = M.$$

Proskura¹⁾ has theoretically derived these values M for various ratios of the chord length l of the wing to the spacing t , at various angles of attack α and various lattice angles β (see the designations in Fig. 235), and has plotted the results in the diagrams presented in Fig. 235. By experimental verification he has found that these values multiplied by the factor

$$\left[1 + \frac{0.75}{\left(\frac{t}{l} \right)^2} \right]$$

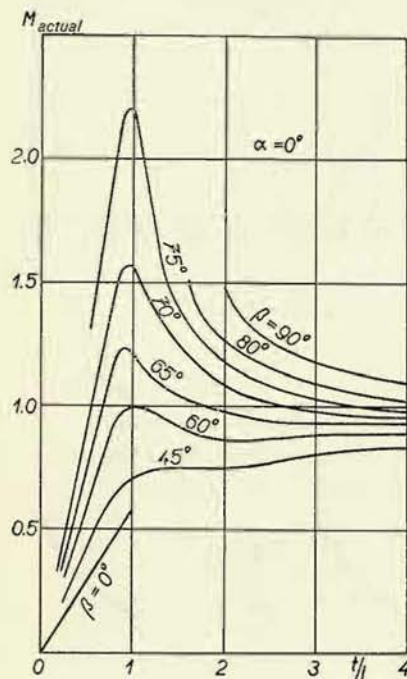


Fig. 236

are in agreement with the values obtained by measurements.

Fig. 236 shows likewise such a diagram recalculated according to Proskura, for an angle of attack $\alpha = 0$. Since the diagrams for different angles of attack, as given in Fig. 235, do not exhibit significant differences within the range of the generally

¹⁾ Proskura: Gidrodinamika turbomachin, Moskva, ONTI, Energoizdat, 1934.

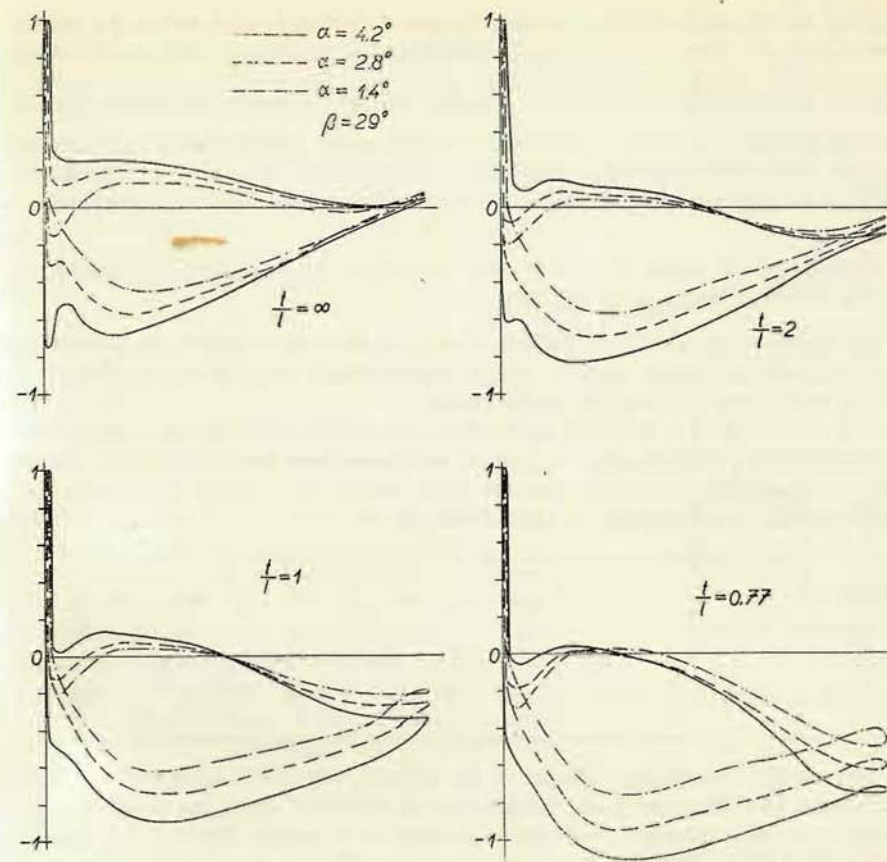


Fig. 237

used lattice angles, the diagram in Fig. 236 may be used also for other angles of attack.¹⁾

The value $M = \frac{k_z}{c_z}$ will evidently also depend on the shape of the profile and somewhat vary for different profiles, but no considerable differences are to be expected.

For the reason of completeness it should be noted that with the ratio $\frac{t}{l}$, repre-

¹⁾ A theoretical derivation of such a diagram has also been presented by Weinig in his book Strömung um die Schaufeln von Turbomaschinen, Leipzig, Barth, 1935; however, without experimental verification and necessary corrections.

senting the density of the lattice also the pressure distribution across the profile varies. Fig. 237 represents the pressure distribution according to Thomann¹⁾ along profiles of four different ratios $\frac{t}{l}$. We see that in the case of an isolated wing at greater angles of attack a considerable underpressure peak appears immediately behind the beginning of the profile, diminishing with an increasing density of the lattice, so that the progress of the underpressure assumes a parabolic shape.

5. Shape of the Space of the Turbine, Meridional Flow Field and Interrelation of the Velocity Diagrams on the Flow Surfaces

The space of the turbine is delimited by the hub of the runner and the shell of the casing of the runner, both of which pass gradually into the planes of the lids which enclose the space of the guide blades.

The ratio of the hub diameter to the diameter of the runner casing is determined by the number of blades so as to provide sufficient space for anchoring the blades and accommodating the mechanism for their setting (in Kaplan Turbines); this ratio is given approximately by the following table:

Head H_m	5	20	40	50	60	70
Number of blades	3	4	5	6	8	10
d/D	0.3	0.4	0.5	0.55	0.60	0.70
Specific speed about	1000	800	600	400	350	300

The transition from the cylinder of the hub, or that of the runner casing, into the planes enclosing the guide blades has the shape of an ellipse quadrant, the distance of the runner axis from the inner edges of the guide blades being usually $\lambda = 0.25 D$ (Fig. 238). The height of the runner blades is as a rule approximately $B = 0.4 D$ and depends on the specific speed (see Fig. 54a).

The hub and the shell of the runner casing are only for low heads of cylindrical shape. In this design there is a large gap between the hub and the blade in the closed position, and between the blade and the casing in the open position, and this circumstance exerts an unfavourable influence upon the volumetric efficiency and gap cavitation (see later). For higher heads (and frequently even for low heads) the hub is therefore fitted with a spherical surface and the same is done with the lower part of the runner casing (see Appendix I). In the design represented in Fig. 177, the shell of the casing is spherical throughout; for disassembling the runner blades must be turned entirely into the axial direction, and from the upper half of the casing special insertions must be removed, which fill recesses through which the blades may be passed in lifting the runner.

¹⁾ Thomann R.: Wasserturbinen und Turbinenpumpen, Part 2, Stuttgart, K. Wittwer, 1931, p. 99.

With regard to its considerable curvature, the meridional flow field must be established by the two-dimensional method. As a rule, however, no complete layout is required, because when the runner axis is located at a sufficient distance from the guide wheel, according to the rule $\lambda = 0.25 D$, the flow surfaces in the space of the runner exhibit with sufficient accuracy a cylindrical shape and the same meridional velocity. The flow field must therefore be established only to ascertain the conditions at the discharge from the guide apparatus if we want to lay out the linkage between the velocity triangles on the various flow surfaces so as to prevent inlet shock (see Section 1, A, Chapter I/7).

As far as high-speed Francis turbines are concerned, we have seen, however, that in such a case there are considerable differences in the directions and magnitudes of the velocities at which the water on the various flow surfaces enters the draft tube. The equalization of these velocities to a common value is necessarily connected with losses (whirls) reducing the efficiency of the draft tube. In propeller turbines (and in express Francis turbines, too), the outlet velocities from the runner, and consequently also the inlet velocities into the draft tube, are extraordinarily high; and the circumstance that a great part of the energy must be regained in the draft tube justifies the selection of such a mutual linkage of the velocity triangles which ensures the conditions for a satisfactory function of the draft tube.

For propeller turbines, as well as for express Francis turbines, it will therefore be more advantageous to select the velocity triangles on the various flow surfaces so as to have on them the same value of $C_{u2} R_2$, i. e. the same circulation, with which the water enters the draft tube. This will all the more advantageous as the shock on the inlet edges of the blades will be moderated in these turbines by the large blade-less space in front of the runner, because, similarly as in the flow through an elbow the action of the bend manifests itself already far in front of it, influencing the arrangement of the stream lines, we may expect also here that the runner will exert an influence upon the conditions in the space in front of it.¹⁾

¹⁾ During his activities in the Engineering Works ČKD-Blansko, the author had the opportunity to design two propeller wheels, determined for the same conditions, and to test them on models. One wheel was designed for constant circulation in back of the runner, $C_{u2} R_2 = \text{const.}$, while the other wheel was designed so as to eliminate the inlet shock on all flow surfaces simultaneously, i. e. by the method as described for high-speed Francis turbines. The first runner exhibited a better efficiency.

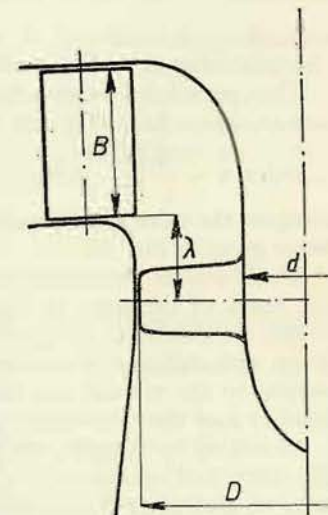


Fig. 238

In order to reduce the losses due to the friction of the water across the blades, we shall endeavour to decrease the relative velocities (Section 1, A, Chapter I/7) and therefore principally select isocles outlet triangles.

6. General Procedure in Designing the Runner of a Propeller (Kaplan) Turbine

According to the specific speed we select the number of runner blades and the ratio $\frac{d}{D}$ between the diameter of the hub and that of the runner.

Similarly as in the case of Francis turbines, we determine by means of Fig. 54b the unit values n_1' and Q_1' which correspond to the given specific speed.

Then we select a runner diameter D , suitable from the point of view of design and a suitable head H . From the value n_1' we ascertain the speed and the angular velocity, $n = \frac{n_1' \sqrt{H}}{D}$ and $\omega = \frac{n}{9.55}$ respectively. For control purposes we may compare the value of the specific peripheral velocity at the largest diameter with the value given in Fig. 75b.

We determine the face of the guide wheel, the diameter of the hub, and lay out the shape of the space of the turbine in conformity with the given directions.

Into the picture of the space of the runner we draw the flow field which will be given with sufficient approximation by the cylindrical surfaces that on the plane normal to the turbine axis define annuli of equal areas, because the meridional velocity may with satisfactory accuracy be considered constant.

According to Fig. 54b, we select the unit flow-rate Q_1', η for the optimum efficiency, and by dividing it by the through-flow area between the casing and the hub, we ascertain the meridional velocity $C_{m,\eta}$ which will be the same for all flow surfaces and which we recalculate to the specific value.

On each flow surface we know now the specific peripheral velocity $u_1 = u_2$ and the specific meridional velocity. Then we draw the isocles outlet velocity triangle corresponding to these values, and by means of the Braun construction we determine the inlet velocity triangle.

By means of the construction illustrated in Fig. 221 we determine w_∞ , whereupon we select a suitable profile—always with regard to a gradual transition to the adjacent profiles—and according to Equation (199) we determine to it such an angle of attack in relation to the direction of the velocity w_∞ as to satisfy Equation (199).

As an approximate guide in the selection of the profiles, the following directions may be employed:

The deflection of the central line of the profile should be selected so as to achieve an approximate agreement between the deviation angle of the central line and the deviation angle resulting from the velocity diagram. This will be easily feasible for the outer profiles, but it will not always be possible to fulfil this condition for the profiles near the hub, which sometimes must have a straighter shape. The thickness of the profile should be the least possible, just sufficient to meet the strength requirements. The reason is that thick profiles cause a considerable

velocity increase of the passing flow and consequently a material pressure reduction which is unfavourable with regard to cavitation.

We shall prefer profiles with the place of greatest thickness shifted as far as possible toward the trailing edge. On such profiles there is a shorter path on which a retardation of the boundary layer takes place, and therefore they contribute less to a rupture of the flow.¹⁾

When ascertaining the velocity of the flow, we principally do not count with the restriction of the through-flow profile due to the blades as in our further design we calculate with the velocity w_∞ in front of them.

Then we arrange the profiles into the continuous blade surface, adjusting the strengthened transition into the ring of the pivot. We select a spherical hub and adjust the adjacent part for the blade without otherwise altering its shape.

For checking the continuity, we draw the contour line plan, which may also be used for the manufacture of the blade, although cylindrical sections are better suited.

The procedure will be shown later on an example.

7. Control of the Cavitation Coefficient

The ratio of the drag coefficient to the lift coefficient in values already recalculated for the turbine, i. e. the ratio $\frac{k_x}{k_z}$, should be the least possible in order to achieve the highest possible efficiency. The value of the coefficient k_z , however, is here confined to a certain range with regard to cavitation, as will be explained now.

The force acting upon the profile results from the difference of the velocity on the pressure and suction sides of the blade. The specific overpressure on the profile can be expressed by the difference of the velocity heads,²⁾ the velocity on the pressure side being assumed equal to W_∞ (Fig. 221). Thus the specific overpressure Δh in metres of water column will be

$$\Delta h = \frac{W^2 - W_\infty^2}{2g},$$

and the force acting upon the profile of the area S

$$P_z = S \Delta h \gamma = S \gamma \frac{W^2 - W_\infty^2}{2g}.$$

But according to Equation (196) also applies

$$P_z = \frac{k_z}{2} \frac{\gamma}{g} W_\infty^2 S,$$

and hence

$$W^2 = W_\infty^2 (1 + k_z). \quad (212)$$

¹⁾ Prandtl: Führer durch die Strömungslehre, Braunschweig, Vieweg, 1944, p. 176
Analogous Trends in the Design of Rapid Aircraft.

²⁾ Hýbl J.: Vodní motory, 3. díl (Hydraulic Motors, Part 3), Prague, ČMT, 1928, p. 336.

Actually the underpressure across the entire length of the suction side of the profile will not be the same, and consequently also the velocity W on the suction side will not be uniform across the entire length. In the place of the lowest pressure h_{\min} the velocity of the passing flow will be maximum, and we denote it by W_{\max} . The greatest underpressure will therefore be

$$\Delta h' = \frac{W_{\max}^2 - W_{\infty}^2}{2g}.$$

The maximum velocity of the passing flow may be expressed by the relation

$$W_{\max}^2 = W_{\infty}^2 (1 + Kk_z). \quad (213)$$

A certain profile tested by Betz exhibited the following values

$c_z = 0.71$	1	1.26	1.46
$K = 1.33$	1.37	1.75	2.12

The magnitude of K depends on the shape of the profile and will be the less the more slender the profile is, but it will always be greater than unity.

According to Equation (26), the pressure at the beginning of the draft tube, and hence at the discharge from the runner, is

$$\frac{p_3}{\gamma} = \frac{p_2}{\gamma} = h_2 = H_B - H_s - \eta_s \frac{C_2^2 - C_4^2}{2g},$$

where H_B is the barometric pressure in terms of water column and H_s denotes the suction head up to the outlet profile of the runner, i. e. up to the outlet edges of the runner blades.

Substituting into the Bernoulli equation for the relative motion ($U = \text{const.}$)

$$h_{\min} + \frac{W_{\max}^2}{2g} = h_2 + \frac{W_2^2}{2g}$$

leads to

$$\frac{p_{\min}}{\gamma} = h_{\min} = H_B - H_s - \eta_s \frac{C_2^2 - C_4^2}{2g} - \frac{W_{\max}^2 - W_2^2}{2g}.$$

Thus we have arrived at the expression (27), but with the value

$$\Delta h' = \frac{W_{\max}^2 - W_2^2}{2g}.$$

From Fig. 221, however, follows

$$C_2^2 = C_m^2 + C_{u2}^2,$$

$$W_2^2 = C_m^2 + (U - C_{u2})^2 = C_m^2 + U^2 - 2UC_{u2} + C_{u2}^2,$$

so that

$$h_{\min} = H_B - H_s - \frac{W_{\max}^2 - \eta_s C_4^2 - U^2 + 2UC_{u2} - (1 - \eta_s)(C_m^2 + C_{u2}^2)}{2g},$$

and by substituting for W_{\max}^2 the value according to Equation (213), we obtain

$$h_{\min} = H_B - H_s - \frac{W_{\infty}^2 (1 + Kk_z) - \eta_s C_4^2 - U^2 + 2UC_{u2} - (1 - \eta_s)(C_m^2 + C_{u2}^2)}{2g}.$$

Putting now $h_{\min} = H_t$, where H_t as previously denotes the tension of the water vapour, and forming the expression $\frac{H_B - H_t - H_s}{H}$, we obtain the critical value of the Thoma cavitation coefficient

$$\sigma_{\text{crit}} = w_{\infty}^2 \cdot (1 + Kk_z) - \eta_s c_4^2 - u^2 + 2uc_{u2} - (1 - \eta_s)(c_m^2 + c_{u2}^2). \quad (214)$$

From this expression it is evident that large values of the lift coefficient k_z increase the value of the cavitation coefficient and consequently reduce the permissible suction head.

The value k_z in Equation (214) is the lift coefficient, already recalculated with regard to the arrangement into a lattice system.

Note: For vertical turbines of large diameter, operating under a low head, σ_{crit} is no constant. This will be easily understood when we imagine two vertical propeller turbines of the same type but different diameters, both with the same suction head H_s (up to the outlet edges of the blades). It is obvious from Fig. 239 that the similarly located points M and M' have different static suction heads owing to the influence of the different distances h and h' of these points from the outlet edge. The underpressure at the point M of the large turbine is therefore greater than at the point M' of the small turbine. The maximum underpressures in both turbines will not be at corresponding points of the blades and also their values will be different. Under the assumption of a parabolical distribution of the underpressures between the inlet and outlet edges, we may conclude¹⁾ that σ is a function of the ratio $\frac{D}{H}$;

$$\sigma = A + B \left(\frac{D}{H} \right) + C \left(\frac{D}{H} \right)^2.$$

¹⁾ Nechleba: Sur la fonction de cavitation, La Houille Blanche 1947, p. 117 where also a method for ascertaining the individual coefficients A , B and C of the function is described.

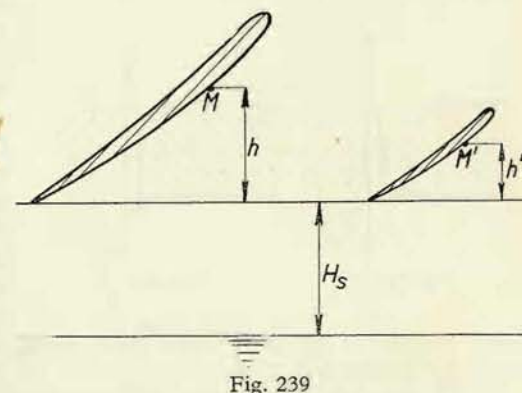


Fig. 239

For large ratios of the head to the runner diameter, the last two coefficients lose their significance, and σ may be considered a constant.

In propeller turbines we encounter, apart from cavitation on the suction side of the blade, also the so-called gap cavitation. This phenomenon is connected with the circumstance that propeller turbines have no rim. This is advantageous for the efficiency, because along the stationary wall of the runner casing the water streams at the absolute velocity which is in turbine of such a high speed always considerably lower than the relative velocity; the losses due to friction of the water on the wall of the runner casing are therefore smaller than the losses due to friction of the water on the rotating rim of the runner would be.

Objectionable effects, however, are encountered with regard to cavitation. The pressure and suction sides of the blade are separated only by the gap between

the casing and the end of the blade which is very short. For this reason, a high through-flow velocity is created in the gap, and this is connected with a reduction of the pressure which sometimes attains even the tension of the water vapour. This results in cavitation corrosion, unless at least the edge of the blade is made of a cavitation-resistant material; the cavitation manifests itself on the one

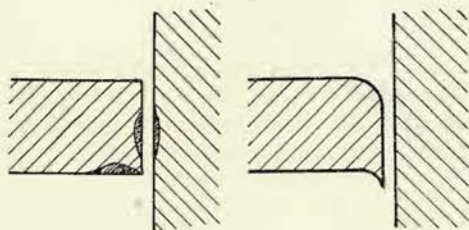


Fig. 240

Fig. 241

hand, within the gap and, on the other hand, on the bottom side of the blade, as indicated in Fig. 240.

The problem of gap cavitation has been treated theoretically and experimentally by Shalnev,¹⁾ according to whose investigations cavitation within the gap may be prevented by rounding off the inlet edge, and the cavitation in back of the gap by extending the edge. Consequently, it would be advantageous to give the blade edge the shape as indicated in Fig. 241.

Example: As example of designing a propeller runner we mention here the somewhat extraordinary case of a runner of very low specific speed. Our task is to construct a Kaplan runner for a head of 50 to 60 m.

We select eight runner blades and a specific speed of $n_s = 300$ r. p. m. at the full flow-rate. For a Francis turbine the unit flow-rate would be, according to Fig. 54, $Q_1' = 1.1$ m³/sec. We have no experience with this design and assume for the time being an optimum efficiency at about $0.55 Q_1'$, and therefore we select $Q_1'_{\eta} = 0.6$.

For drawing the runner we select the outer diameter $D_1 = 0.5$ m and the head $H = 10$ m, and thus a theoretical outlet velocity $\sqrt{2gH} = 14$ m/sec. Then, employing Figs. 75a and 75b, we select for Q_{η} the specific inlet velocity into the draft

¹⁾ Shalnev: Shchelevaya kavitatsiya. Inzhenernyi sbornik. Akademiya nauk SSSR, tom VIII, 1950.

tube equal to the meridional velocity in the runner $c_s = 0.3$ and the specific peripheral velocity at the largest diameter $u_e = 0.92$. The actual values of these velocities will therefore be $C_m = C_s = 14 \cdot 0.3 = 4.2$ m/sec. and $U_e = 14 \cdot 0.92 = 12.9$ m/sec.

From the peripheral velocity we determine the speed

$$U_e = R_e \omega; \omega = \frac{12.9}{0.25} = 52 \text{ 1/sec}; n = 495 \text{ r. p. m.}$$

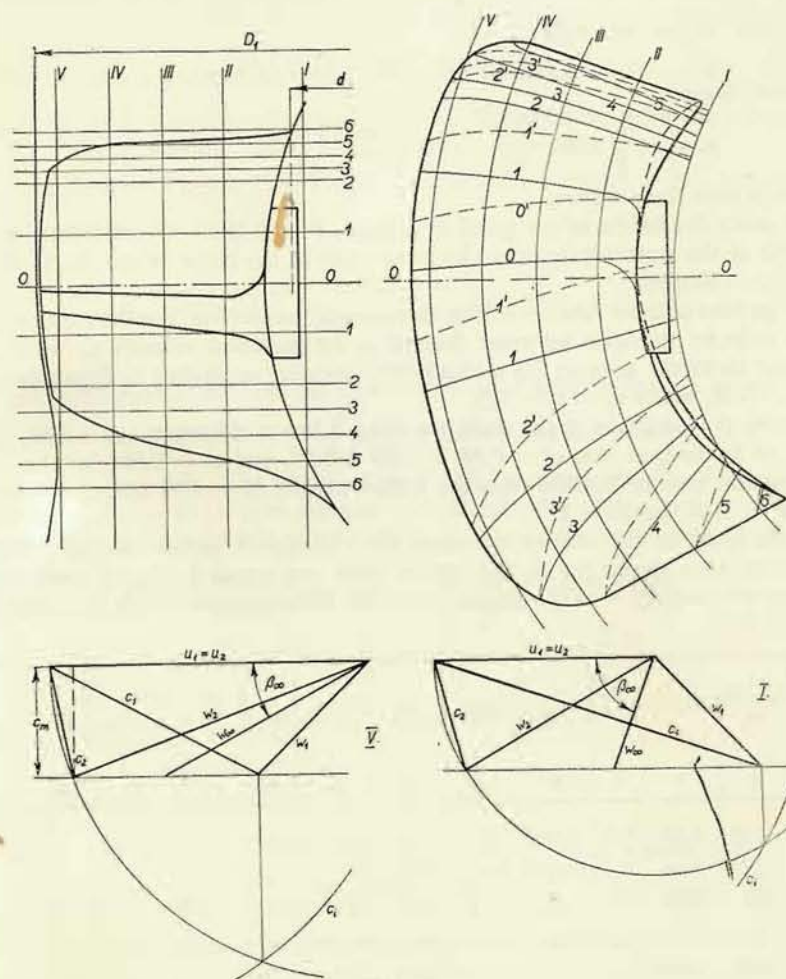


Fig. 242

From the meridional velocity we ascertain the flow-rate; we select first the diameter of the hub as equalling 60 % of the outer diameter, so that the through-flow area is

$$F = \frac{\pi}{4} D^2 (1 - 0.6^2) = 1963 \cdot 0.64 = 1230 \text{ cm}^2,$$

and hence

$$n'_1 = \frac{495 \cdot 0.5}{3.17} = 79 \text{ r. p. m.},$$

$$Q_\eta = 0.123 \cdot 4.2 = 0.518 \text{ m}^3/\text{sec.}, \quad Q'_{1,\eta} = \frac{0.518}{0.25 \cdot 3.17} = 0.65 \text{ m}^3/\text{sec.}$$

With these values we obtain

$$Q'_{1,\max} = 1.82 \cdot 0.65 = 1.18 \text{ m}^3/\text{sec.},$$

and consequently

$$n_s = n'_1 \sqrt[3]{1000 \frac{Q'_{1,\eta}}{75}} = 79 \sqrt[3]{\frac{1180 \cdot 0.87}{75}} = 293 \text{ r. p. m.}$$

and we accept these values.

We select the height of the guide apparatus, $B = 0.35 D_1 = 175 \text{ mm}$, and the distance of the runner axis from the inner edge of the guide wheel, $0.25 \cdot D_1 = 125 \pm 130 \text{ mm}$.

On the base of these values we draw the space of the turbine. For the construction of the velocity triangles we must determine the indicated velocity c_i , which we ascertain from the relation for a shock-free entrance according to Equation (58) $c_i^2 = \eta_h + c_s^2$, where $c_s = c_2 = 0.3$.

For the flow surfaces at the walls we select a lower efficiency, $\eta_h = 0.88$, with regard to friction, so that $c_i^2 = 0.88 + 0.09 = 0.97$, and $c_i = 0.98$; for the flow surfaces at a greater distance from the walls we select $\eta_h = 0.91$ and $c_i^2 = 0.91 + 0.09 = 1$, so that $c_i = 1$.

In the space of the runner we select five cylindrical sections as indicated in Fig. 242 so as to obtain the anulli between them with equal areas, and their values we enter successively – in the sequence of their determination – into the following table:

Cylindr. section	$R_1=R_2$ m	$u_1=u_2$	c_m	c_{u2}	w_∞	β_∞	t	l	$\frac{l}{t}$	$k_z - \frac{k_x}{\tan \beta_\infty}$	β	Profile No.
1	2	3	4	5	6	7	8	9	10	11	12	13
I	0.146	0.54	0.3	0.099	0.31	75°	113.9	215				
II	0.177	0.66	0.3	0.082	0.41	50.5°	139.8	235				
III	0.201	0.75	0.3	0.072	0.51	38°	158.0	250				
IV	0.223	0.83	0.3	0.065	0.60	31°	174.5	260	1.5	1.2		
V	0.243	0.90	0.3	0.06	0.69	27.5°	190.0	230	1.2	1.17	66°	6404

In the first column, the number of the section is recorded in conformity with Fig. 242. The second column contains the radii of the individual sections, and the third the corresponding specific peripheral velocity. The fourth column presents the specific meridional velocity (by laying out the meridional flow field we can check whether some correction is required; at the selected distance of the runner from the guide apparatus, the corrections will be insignificant). The fifth column gives the specific value c_{u2} , selected so as to have in all sections $R_2 c_{u2} = \text{const.}$ Columns No. six and seven contain the values w_∞ and β_∞ respectively, as resulting from the velocity triangles. In Fig. 242 their construction is reproduced for the sections I and V. Column eight shows the spacing as resulting for the selected number of eight blades.

Now we begin with the determination of the individual cross sections. We apply Equation (199) $\eta_h = w w_\infty \frac{l}{t} \left(k_z - \frac{k_x}{\tan \beta_\infty} \right)$. We select e. g. for the cross section on the cylindrical section V the length $l = 230 \text{ mm}$, so that $\frac{l}{t} = 1.2$, and ascertain the value in the brackets

$$\left(k_z - \frac{k_x}{\tan \beta_\infty} \right) = \frac{\eta_h}{w w_\infty \frac{l}{t}} = \frac{0.88}{0.9 \cdot 0.69 \cdot 1.2} = 1.17.$$

The coefficients in the brackets apply to a wing of infinite span in a lattice system; hence $k_z = M c_z$ and $k_x = c_x - \frac{c_z^2}{6\pi}$. The value M we ascertain from the Proskura diagram in Fig. 236. The lattice angle β will be greater by the angle of attack than $90^\circ - \beta_\infty = 62.5^\circ$; we estimate provisionally the angle of attack as equalling 4° and thus we obtain $\beta = 62.5 + 4 = 66^\circ$. For this value and for the ratio $\frac{t}{l} = \frac{1}{1.2} = 0.84$ we read $M = 1.3$. Therefore, we may write

$$c_z M \tan \beta_\infty - c_x + \frac{c_z^2}{6\pi} = 1.17 \cdot \tan \beta_\infty,$$

and since $\tan \beta_\infty = 0.521$, we obtain after substitution of M

$$0.676 \cdot c_z - c_x + \frac{c_z^2}{6\pi} = 0.612.$$

We select the profile NACA Rep. 460, No. 6404, which means that the profile will exhibit the values $\frac{m}{l} = 6\%$; $\frac{L}{l} = 40\%$; $\frac{t}{l} = 4\%$ (t here denotes the thickness of the profile; since no confusion with the spacing of the blades is possible, we have left the same designation as employed in the Aeronautical Guide), which satisfy the given directions for the selection of the cross section, which is defined

by the following relations (201):

$$c_x = \frac{\partial c_z}{\partial \alpha} (\alpha - \alpha_0), \quad c_x = c_{xv} + \frac{\partial c_x}{\partial c_z^2} c_z^2.$$

From the diagrams in the Figs. 225 to 228 we read

$$\alpha_0 = -5.8^\circ; \quad \frac{\partial c_z}{\partial \alpha} = 0.078; \quad c_{xv} = 0.0081; \quad \frac{\partial c_x}{\partial c_z^2} = 0.054.$$

Now we try to select the angle of attack $\alpha = 6^\circ$. Thus we obtain

$$c_z = 0.078 \cdot 11.8 = 0.92, \\ c_x = 0.0081 + 0.54 \cdot 0.85 = 0.054,$$

and by substituting into the relation

$$0.676 c_z - c_x + \frac{c_z^2}{6\pi} = 0.612$$

we arrive at

$$0.676 \cdot 0.92 - 0.054 + \frac{0.85}{6\pi} = 0.611,$$

which satisfactorily approximates the original value 0.612, i. e. the angle of attack was selected correctly. Now we recalculate it for an infinite span

$$\alpha_\infty^0 = \alpha^0 - 57.3 \cdot \frac{c_z}{6\pi} = 6^\circ - 57.3 \cdot \frac{0.92}{6\pi} = 6^\circ - 2.8^\circ = 3.2^\circ.$$

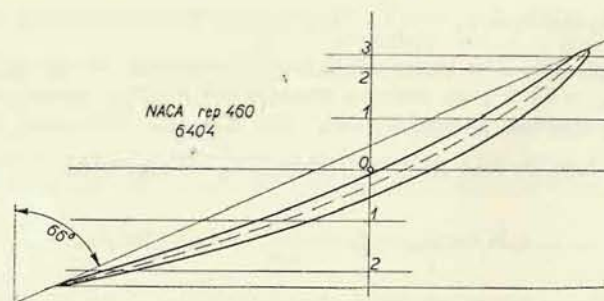


Fig. 243

The chord of the cross section must be inclined to the velocity w_∞ under this angle (see the sketch in Fig. 235), and the lattice angle will therefore be

$$\beta = 90^\circ - \beta_\infty + \alpha_\infty = 62.5 + 3.2 = 65.7^\circ \approx 66^\circ.$$

We enter the obtained values into the corresponding columns of the table and draw the profile under this angle β (see Fig. 243). We select the point O which will lie on the blade axis $O-O$ in Fig. 242, and mark in this diagram both the extreme points of the profile (height of the blade) and the points of intersection with the

meridional plane. We mark the extreme points also in the plan of the blade and this enables us to select the length of the profiles in the further section IV.

In this way we determine stepwise all profiles on all cylindrical sections. In direction towards the hub we select successively thicker cross section with regard to the strength of the blade.

In the circular projection we then select the parallel planes 1 to 6, normal to the axis of rotation, above and below the blade axis, and transfer them into the pictures of the profiles (see Fig. 243) and construct the contour lines to them in the plan of the blade. The shape of the contour lines provides a control whether the surface of the blade exhibits sufficient continuity. Finally, we adjust the blades at the outer diameter, as well as at the hub.

For the manufacture of the pattern of the blade we can then use this contour line plan or, still better, directly the cylindrical sections (see later).

We shall check the cross sections for cavitation on two or three outer cylindrical sections where the highest velocities are encountered.

E. g. for the investigated cross section on the cylindrical section V, we obtain from the expression (214), where we put $\eta_s = 0.9$ and $c_4 = 0.06$, for the flow-rate at optimum efficiency

$$\sigma_{crit} = w_\infty^2 (1 + Kk_z) - \eta_s c_4^2 - u^2 + 2uc_{u2} - (1 - \eta_s) (c_m^2 + c_{u2}^2).$$

With the value $K = 1.1$ (dense lattice) and $k_z = Mc_z$ holds good

$$\sigma_{crit} = 0.69^2 (1 + 1.1 \cdot 1.3 \cdot 0.92) - 0.9 \cdot 0.06^2 - 0.9^2 + \\ + 2 \cdot 0.9 \cdot 0.06 - 0.1 \cdot (0.3^2 + 0.06^2) = 0.39.$$

For the full flow-rate we should substitute the values from the velocity diagram established for the maximum through-flow (see Part I, Chapter XII/3). But already for the optimum through-flow we obtain with the value of the cavitation coefficient determined above for $H = 50$ m a permissible suction head of

$$H_s = H_b - \sigma H = 9.5 - 0.39 \cdot 50 = -10 \text{ m},$$

i. e. an unacceptable value.

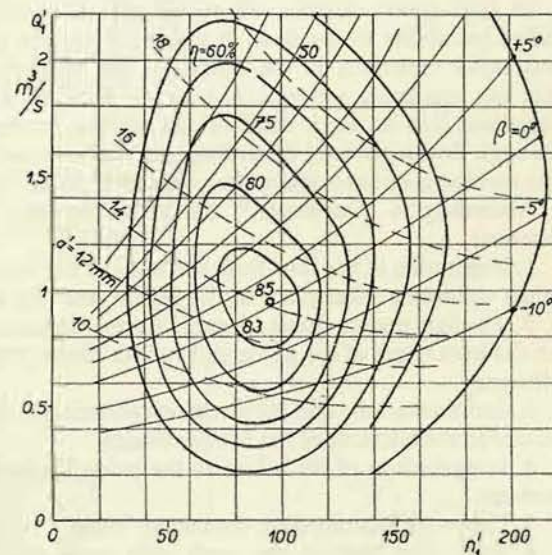


Fig. 244

For this reason, we had to select longer runner blades (peripherally) in order to reduce their specific load. Nevertheless, this runner in its original design was examined for efficiency in the test station and the result is presented in Fig. 244. The efficiencies are given as measured on a model with a runner diameter of 200 mm.

8. Stability of the Flow along the Blade

In high-speed turbines we sometimes encounter the phenomenon of the so-called instability of the flow. It manifests itself in practical operation by more or less rapid variations in the output of the turbine without any external change and any regulating action, i. e. with the position of the blades unchanged. These variations can attain a third of the normal output and even more. When the through-flow is reduced by shifting the blades toward the closed position, and then the turbine is opened again, the output will attain its original value.¹⁾

According to Kieswetter,²⁾ the instability may be caused by the following reasons:

1. Separation of the flow from the walls of the ducts of the machine, in particular when streaming takes place in the region near the cavitation (critical) limit.
2. Foreign matter (grass, leaves, fibres) entrained by the water and retained on the inlet edges of the guide and runner blades, causing changes of the hydraulic efficiency.
3. Sedimentations and incrustations adhering to the walls of the ducts, in particular to the surfaces of the runner blades.
4. Irregularities of the inflow to the guide blades in the chamber in front of the turbine.
5. Excessive local load on the runner blade.
6. Turbulent flow in the draft tube itself and in the tail race immediately behind it.
7. Unsuitable shape of the runner blades (or even of the guide blades) or temporary objectionable deformation of their shape owing to the reasons given in points 2 and 3.

From the investigations of the cited author follows that the main reason of an instable flow in the turbine is presented by the circumstance that in some designs the path of the flow is not secured so as to guarantee its stabilized progress in the laid-out flow surface. This happens when the shape of the duct walls do not prevent flowing over the runner blades on various ways (see Fig. 245), or when the instability of the flow is caused by circumstances outside the runner, i. e. instable flow within the guide blades and in the bladeless space, or when accidental or

¹⁾ See also Thomann R.: Wasserturbinen und Turbinenpumpen, Part 2, Stuttgart, K. Wittwer, 1931, p. 114.

²⁾ Kieswetter: Ustálení vodního proudu v kanálech lopatkových strojů (Stabilization of the Water Flow in the Ducts of Turbomachines), Strojnický obzor (Mechanical Engineering Review), 1941, pp. 105—113.

temporary deformation of the blade surface is brought about by adhering solid or gelatinous deposits.

More susceptible in this respect are turbines with a higher specific speed, having only moderately curved blades.

The flow proceeds along the blade on the path of least resistance, that means it takes the way of the least possible deflection from the direction of the incoming flow approaching the inlet edge at shockless entrance.

Therefore, when on the path 1—2' (Fig. 245) the deviation angle is of a smaller value than that corresponding to the angle as defined by the energy equation $u_1 c_{u1} - u_2 c_{u2} = \frac{\eta_h}{2}$, the

flow will tend to assume this way on which less energy is extracted from it, i. e. the way of less resistance, but on which also the output of the turbine will be smaller.

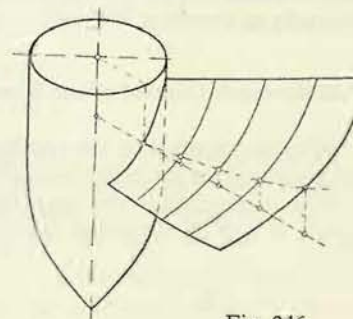


Fig. 246

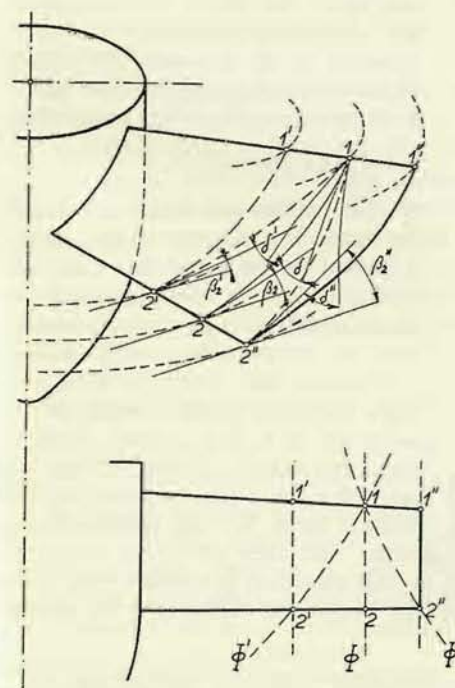


Fig. 245

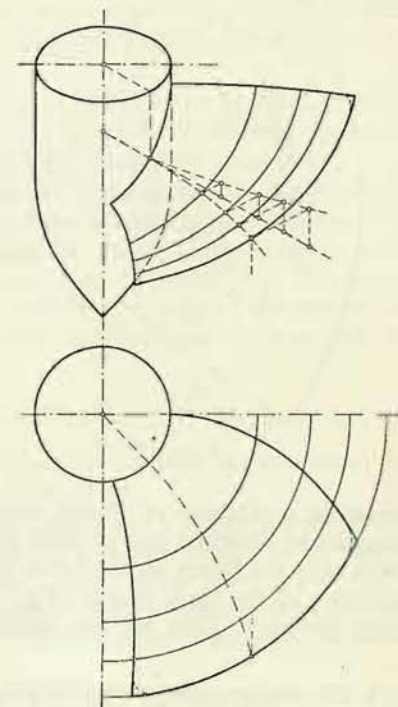


Fig. 247

In order to avoid this situation, we must try to achieve greater deviation angles of the blade in other sections than with the considered flow surface. This can be realized by a suitable selection of the directrix on which the individual profiles are located with their significant points determined by the same principle on all profiles.

For this purpose, the directrix is either deflected so that its outer end is elevated as indicated in Fig. 246 (see also Fig. 242) or even simultaneously shifted peripherally as shown in Fig. 247.

9. Strength Control of the Runner Blade

We must control on the one hand the strength of the connection of the blade to its pivot and on the other hand the strength of the blade proper.

The connection to the pivot will be subjected to various stress: At the runaway speed it will be subjected mainly to tensile stress by the centrifugal force.¹⁾ At

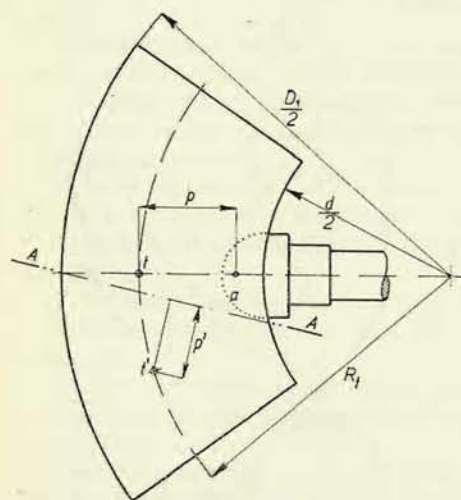


Fig. 248

normal speed it will be subjected to tensile stress by the centrifugal force and to bending and shearing stresses by the force with which the water acts upon the blade. We determine the centrifugal force with the same accuracy as we ascertain the weight G_L of the blade proper and the radius R_t of its centre of gravity. By dividing the centrifugal force $O_L = \frac{G_L}{g} R_t \cdot \omega^2$ by the smallest area F through which the blade is connected to the pivot, indicated by the dotted line a in Fig. 248, at which the enlargement of the transition into the pivot ends, we obtain the corresponding tensile stress.

The force with which the water acts upon the blade we can exactly determine on each flow surface, because from the design of the profiles we

¹⁾ The pressure of the water on the blades at the runaway speed amounts to only about 30 % of the pressure at normal speed, while the centrifugal forces rise to more than four times the normal value.

force P from the output (in metric horsepowers) and the speed of the machine by means of the relation

$$P_u = \frac{M}{R_t z_2} = \frac{1}{z_2 R_t} 716.2 \frac{N}{n},$$

where R_t is given in metres and z_2 denotes the number of runner blades. The force P acts almost perpendicularly (see Fig. 222) upon the blade inclined to the meridional plane under the angle β . The value of the force P will therefore be

$$P = \frac{P_u}{\cos \beta} = \frac{716.2 N}{z_2 R_t n \cos \beta}. \quad (215)$$

If we divide this force by the previously defined area F , we obtain the shearing stress. If we multiply the force P by the arm p which extends from the centre of gravity of the line a , we obtain the bending moment, and dividing this by the resisting moment, we calculate the bending stress.

Apart from these forces, the water brings about the rotation of the blade. The moment with which the water acts on the blade, we determine either by testing the model or by means of the later given relation (218). With this moment we shall calculate when checking the stress in the pivot, which, apart from this, is simultaneously subjected to tensile stress by the centrifugal force and to bending stress by the force P .

By composing these three stresses, namely the tensile stress by the centrifugal force, and the bending and shearing stresses by the force P , we obtain a correct survey of the stresses of the blade in the place of its connection to the pivot.

The stresses of the blade proper must be checked in the section $A - A$ (Fig. 248). We shall assume that either half of the blade proper (when we divide it by the blade axis) is in its centre of gravity t' loaded by half the force P . This, however, is not quite correct, because the pressure distribution along the profile (Fig. 237) is such that the pressures diminish in the direction towards the ends of the profile; our calculation therefore will assume less favourable conditions than there actually are and thus be all the safer.

By multiplying the force $\frac{P}{2}$ by the arm p' (Fig. 248), we obtain the bending moment in the section $A - A$, and by dividing it by the resisting moment of this section, we determine the corresponding bending stress.

In Kaplan turbines with adjustable runner blades and a longer supply line we must further take into account the possibility of a sudden closing of the runner while the guide apparatus is open. This may happen either when the turbine is equipped with a safety device which on an objectionable increase of the speed due to a failure of the guide wheel regulation closes the runner by means of the safety governor, or even by accident.

In such a case, the runner blades close almost entirely the through-flow, and due

to the rapid stoppage of the latter, the head rises to the value H' (see Part III, "Water Shock"). Each runner will therefore be acted upon by the force

$$P' = \frac{\pi}{4} (D_1^2 - d^2) H' \gamma \left(\frac{1}{z_2} \right),$$

where D_1 is the outer diameter of the runner and d the diameter of the hub (Fig. 238); or, when we introduce all values in metres,

$$P' = 785 \cdot (D_1^2 - d^2) \frac{H'}{z_2}. \quad (216)$$

When we assume the same points of application of the forces on the blade, we can perform the control in the same way as before, but with the value of the acting force P' instead of the former value P .

In blades of cast steel we admit a stress of up to 1600 kg/cm² in the blade proper, and up to 2500 kg/cm² when stainless steel is employed.

10. Hydraulic Load of the Runner

The hydraulic load of a propeller runner is given by the sum of the vertical components of the forces on the blades, increased by the overpressure on the runner hub up to the shaft stuffing box, and by the overpressure of the atmosphere over the pressure in the draft tube on the cross section area of the shaft in the stuffing box. This last component is comparatively small and may therefore be neglected.

When we, in conformity with the preceding chapter, determine the resultant P of the action of the water upon the blade in the centre of gravity of its surface, the vertical component of this resultant defines rather exactly the hydraulic axial load of the blade, so that by multiplying its magnitude by the number of blades, we calculate that part of the hydraulic load which results from the runner blades. Since we know the overpressure of the runner, we can ascertain the remaining part of the hydraulic load by multiplying the magnitude of the overpressure by the area of the annulus up to the shaft stuffing box.

In the case of Kaplan turbines with adjustable runner blades the hydraulic load determined in this way cannot be considered the maximum value. Again, as in the preceding chapter, we must take into account a closing of the runner blades with the guide apparatus open, may it be intended or accidental.

In this case, the through-flow is almost completely cut-off by the runner blades, and the full head H , temporarily increased to the head H' , will act upon the blade on the annulus defined by the outer diameter D_1 of the runner blades and by the inner diameter d of the shaft in the stuffing box. When we introduce all values in metres, the maximum hydraulic load will be expressed by the relation

$$S = 785 (D^2 - d^2) H'. \quad (217)$$

II. DESIGN OF THE RUNNER, SPIRAL AND DRAFT TUBE

This procedure is the same as described for Francis turbines in Chapters II to IV, Section 1. A.

B. ACTUAL DESIGN

I. LAYOUT OF THE MACHINE AND CONSTRUCTIONAL UNITS

The procedure in laying out the machine is the same as for Francis turbines. The subdivision into constructional units is likewise the same (see Section 1, B, Chapter I).

For this reason we pass immediately to the first constructional unit, i. e. runner and shaft.

II. RUNNER AND SHAFT

1. Runner

The blades of the runner are usually cast from plain or stainless steel, according cavitation conditions. The pattern is made either on the base of the contour line plan or in conformity to the cylindrical sections.

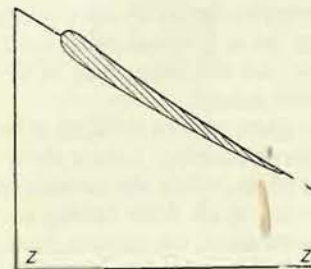


Fig. 249

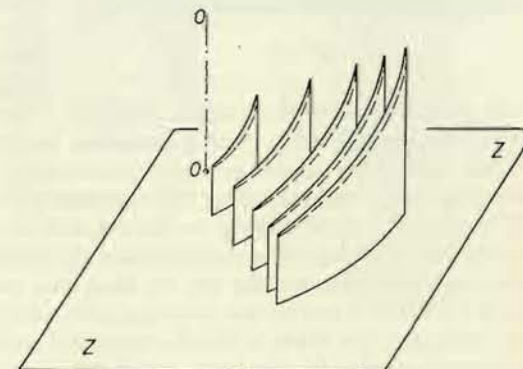


Fig. 250

With a drawing of the contour lines at disposal, the procedure in manufacturing the pattern is the same as in making the core box for the blades of Francis turbines. Small wooden boards exhibiting a thickness equalling the spacing of the contour line planes are trimmed according to the contour lines, glued together in the correct mutual positions, and the edges are removed. Thus we obtain the pattern of the

blade, which is supplemented by the pattern of the pivot. In the axis of the pivot, but on the opposite side of the blade, the pattern of a riser is attached for the centre of the lathe.

In making the model according to the cylindrical sections, all these sections in the drawing must be dimensioned from their common base $Z - Z$ (Fig. 249), and the radii of the cylindrical surfaces in which the sections lie must be given.

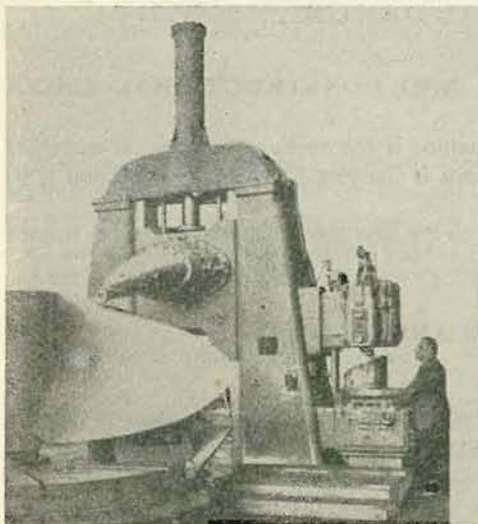


Fig. 251

of the pressure side of the blade is obtained. This is supplemented by the pattern of the pivot and the riser, then a moulding box is put on it, rammed with sand, and one half of the mould is ready. In a similar way also the other half of the pattern is made, and according to it the other half of the mould.

The sheet metal for making the pattern and the complete pattern itself must be dimensioned with regard to the necessary allowances for machining. Larger allowances are only provided for on the inlet and outlet edges, while the remaining part of the blade is cast with a very small allowance or none at all. After casting and heat treatment, the blade is cleanly machined and smoothed, on the one hand, to prevent excessive friction losses which otherwise would be caused by the comparatively high velocity of the water along the blade, and on the other hand, to attain a higher cavitation resistance (see Section 1, A, Chapter II/2).

The blade is manually smoothed by means of a grinding machine; rough machining is conveniently carried out on special copying lathes (see e. g. Fig. 251).

The pivots of the blades of propeller turbines with fixed blades differ from those of Kaplan turbines. Also the blades of propeller turbines (which are fitted with fixed runner blades), although sometimes cast integral with the hub, are mostly

cast separately and then bolted to the hub. In this case, the pivot is very short, as e. g. to be seen in Fig. 252. The blade is centered by the pivot and tightened by one central bolt and several bolts with countersunk heads along the periphery of the pivot. In a Kaplan turbine the pivot is much longer as it is usually seated in two bearings (see Appendix I), between which the crank for rotating the blades is

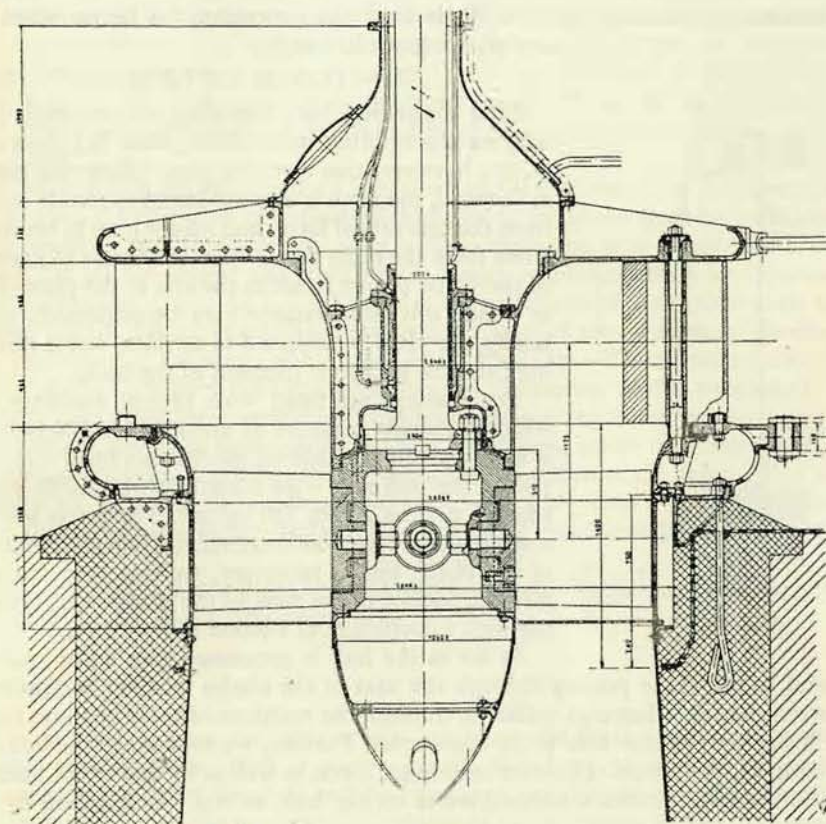


Fig. 252

located; this crank is with its hub supported on the bushing of the outer bearing and thus takes up the centrifugal force. The crank is either mounted on the cylindrical surface and secured by a taper pin (which thus transmits both the centrifugal force and the torque of the blade) or by a feather-key and a split ring, whose both halves, after having been turned by 90° , are held together by the collar of the hub of the crank (Fig. 256), or the crank is mounted on the conical part of the pivot on a feather and axially secured by a nut (Appendix I).

If we know the magnitude and direction of the water pressure on the blade (Section 2, A, Chapter I/9), we can easily determine the reactions in the bearings. To these reactions are added the reactions resulting from the force on the crank, which are likewise readily ascertained when this force is known. We determine it by dividing the maximum moment of the blade by the radius of the crank. The maximum moment is ascertained either by direct measurement on the model, or approximately calculated for one blade from the expression (in kgcm, when H and D_1 are given in metres)

$$M = (1200 \text{ to } 1500) H D_1^3. \quad (218)$$

After composing both reactions, we can easily determine the bending stress in the pivot. We must not forget, however, that up to the place where the crank is fastened, the pivot is also subjected to tensile stress from the centrifugal force, and maybe even to bending stress from the same force, when the centre of gravity of the blade proper is not in the axis of the pivot (but as a rule, this circumstance may be neglected), and, finally, the pivot is subjected to torsional stress resulting from the hydraulic moment of the blade.

The bearings are fitted with bronze bushings, in which a specific pressure of about 150 to 200 kg/cm² is admitted. In the shifting mechanism itself – in the pins of the pull rods – we admit higher specific pressures, i. e. from 250 to 330 kg/cm². The forces in this mechanism are likewise determined from the moment of the blade, but, if necessary, we take into account also the friction in the pins of the mechanism, counting with a coefficient of friction of $\mu = 0.16$.

As far as the hub is concerned, we must mainly control in the plane passing through the axes of the blades whether the profiles between the outer bearings suffice to transmit the reactions of these bearings from the lower part of the hub to its upper part. Further, we must check the hub for bursting by the action of its own centrifugal force, as well as by that of the blades, which, moreover, exerts a bending stress on the hub, as will be explained by an example.

The hub is usually made of cast steel, and only for smaller machines and low heads of gray cast iron.

The connection of the hub with the flange of the shaft is calculated in the same way as for Francis turbines, but the force resulting from the shifting rod must be taken into account; when acting downward, this force is added to the weight of the runner and to the hydraulic pull which subject the connecting bolts to tensile stress.

Lubrication of the shifting mechanism is provided for by filling the runner hub with oil. In turbines for low heads – up to about 6 m – where the specific pressures in the pins of the mechanism are small, the runner hub is filled with regulator oil

having a viscosity of about 3 to 4°E/50°C. For high specific pressures, we select a lubricating oil of high viscosity (45 to 50°E/50°C), to which fatty components may be added; these form an emulsion with small quantities of water leaking into the hub and thus secure lubricating effect and sealing.

Otherwise, we prevent penetration of water into the hub and, inversely, escaping of oil from the hub by fitting the pivots of the blades with packings. Fig 253 illustrates a proved packing consisting of conical leather cups pressed-on by means of a bronze ring and springs located in the hub. From outside they are held in position by a segmental ring whose parts are inserted into a bayonet-catch in the wall of the hub; the last part is fastened by countersunk screws. When the leather cups are split, they can be replaced without dismounting the blade; the cuts in the cups are staggered.

When the shifting rod is moved into the hub, part of the oil is displaced. For this reason, the hub must be connected with the cavity in the shaft by sufficiently large openings, and through this cavity with an expansion tank (Appendix I) into which the oil can escape and from which it may be refilled. Such an expansion tank is shown in Appendix I; it is located at the upper end of the turbine shaft and rotates with it. Since, owing to the rotation, the level of the oil assumes the shape of a paraboloid of rotation – as indicated by a dotted line – it is connected with the cavity of the shaft by a tube extending beyond the surface of this paraboloid. In order to prevent the servomotor oil from penetrating along the piston rod into the cavity of the shaft and mixing with the hub oil, there is under the piston rings, at the end of the liner, a sealing sleeve from which the oil from the space above it is sprayed off, or, when the machine is at rest, flows freely into a special collecting tank, from which it is either discharged or repumped into the tank for the regulator oil.

Refilling of the oil into the runners of turbines in which regulator oil is employed will be described in the next chapter.

2. Shaft

To the shaft applies the same which has been said in the part dealing with Francis turbines. The shaft is always bored. When the servomotor is located between the flanges of the shaft and the alternator, the shifting rod passes through the shaft; but when the servomotor is placed in the extension of the runner hub (Fig. 254),¹ the hollow shaft houses the oil supply tubes. Arranging the servomotor in the runner affords the advantage of a very short shifting rod, not subjected to buckling stress; such a disposition, however, is not suited for high heads as here the diameter of the servomotor exceeds that of the hub.

The oil supply tubes pass also through the bore of the alternator shaft. The supply line consists of two concentric tubes. The inner tube – screwed into the end

¹ Gamze i Goldsher: *Technologiya proizvodstva krupnykh gidroturbin*, Moskva, Leningrad, Gosudarstvennoye nauchnotechnicheskoye izdatelstvo, 1950, Fig. 3.

of the shifting rod (see Appendix I) – leads the oil under the piston, while the oil supply to the upper side of the piston passes through the space between both tubes. To ensure centering of the tubes over their full length, they are fitted with uniformly distributed welded-on spacers by which also centering in relation to the

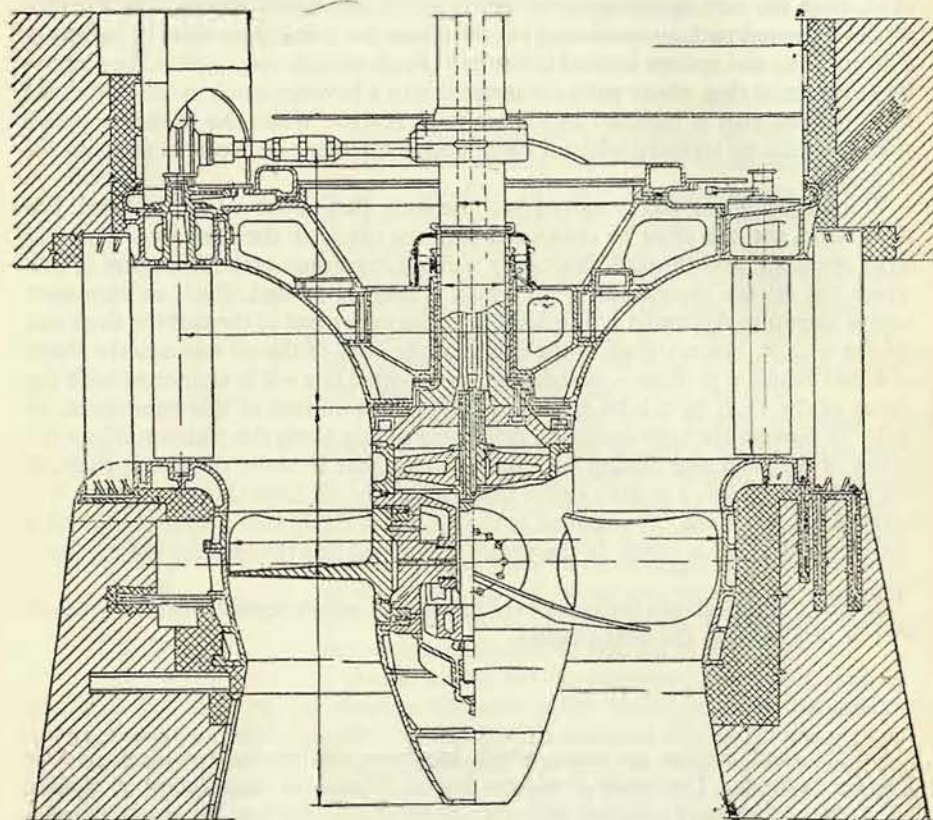


Fig. 254

shaft is realized. In the distributing head, the tubes pass through a stuffing box, and, therefore, threads at the ends of both tubes are arranged so as to effect tightening of the tubes by the friction in the stuffing box. Since the tubes should have the least possible diameter, we must reckon with a rather high velocity of the oil when the servomotor is in operation; this velocity amounts to 6, 10 and even 14 m/sec.

In smaller turbines, where the runner is filled with regulator oil, the space between the outer tube and the alternator shaft on the one hand and the space of

the shifting rod on the other hand are connected by a tube passing outside the servomotor. In this way, the oil in the hub is refilled by the oil leaking through the stuffing box of the distributing head (see Fig. 255).

Example: We have to calculate a runner with five blades. Its diameter is $D_1 = 4800$ mm, the diameter of the hub $d = 2400$ mm, the maximum head under which the runner should still operate $H = 25$ m; the normal speed is $n_n = 135$ r. p. m., the run-away speed $n_p = 302$ r. p. m.; the inclination of the blade to the peripheral circle at the full output $N = 31,000$ metric horsepower is 29° .

The force acting upon the runner blades – the hydraulic pull – is

$$S = \frac{\pi}{4} (D_1^2 - d^2) \gamma H = \\ = 785 (4.8^2 - 2.4^2) 25 = \\ = 340,000 \text{ kg.}$$

1. One blade is acted upon by the force resulting from the water pressure

$$P_v = \frac{S}{5} = 70,000 \text{ kg.}$$

We assume that this force acts in the centre of gravity of the blade proper, which lies at the radius (measured from the runner axis) $R_l = 1740$ mm.

2. When the centre of gravity of the complete blade lies at the radius $R_T = 1600$ mm and when the weight of the blade has been estimated (by comparing with already manufactured blades) to be $G = 3000$ kg, the centrifugal force at normal speed equals

$$O_n = \frac{G}{g} R_T \left(\frac{n_n}{9.55} \right)^2 = \frac{3000}{9.81} \cdot 1.6 \cdot \left(\frac{135}{9.55} \right)^2 = 98,000 \text{ kg,}$$

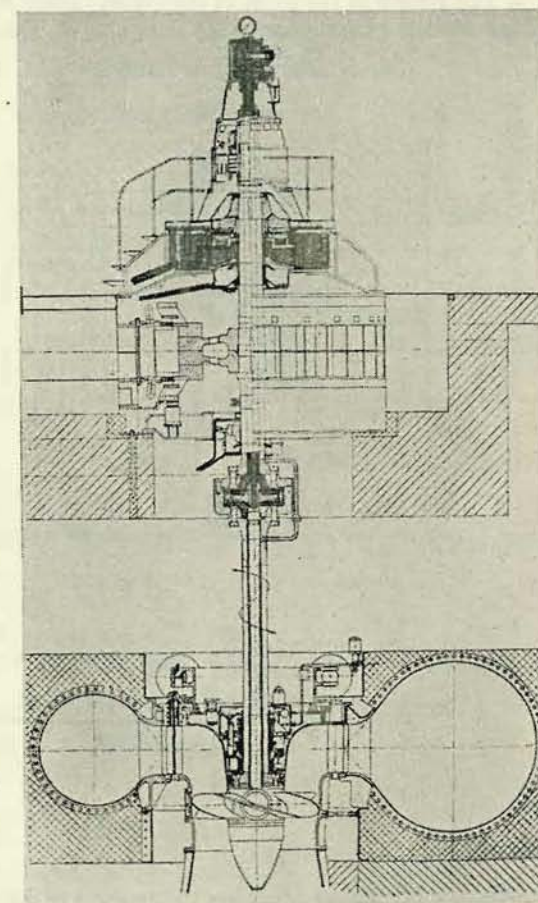


Fig. 255

Section II

$$O_n = 98,000 \text{ kg}; \quad F = 1017 \text{ cm}^2; \quad \sigma_{t,n} = 97 \text{ kg/cm}^2; \\ O_p = 490,000 \text{ kg}; \quad \sigma_{t,p} = 480 \text{ kg/cm}^2.$$

Section III

$$O_n = 98,000 \text{ kg}; \quad F = 1452 \text{ cm}^2; \quad \sigma_{t,n} = 68 \text{ kg/cm}^2; \\ O_p = 490,000 \text{ kg}; \quad \sigma_{t,p} = 337 \text{ kg/cm}^2.$$

Section IV

$$O_n = 98,000 \text{ kg}; \quad F = 1662 \text{ cm}^2; \quad \sigma_{t,n} = 59 \text{ kg/cm}^2; \\ O_p = 490,000 \text{ kg}; \quad \sigma_{t,p} = 265 \text{ kg/cm}^2.$$

Section A

$$O_n = 98,000 \text{ kg}; \quad F = 1964 \text{ cm}^2; \quad \sigma_{t,n} = 50 \text{ kg/cm}^2; \\ O_p = 490,000 \text{ kg}; \quad \sigma_{t,p} = 250 \text{ kg/cm}^2.$$

At normal speed, the reduced stresses in the individual cross sections consequently are:

Section I

$$\Sigma\sigma = 520 \text{ kg/cm}^2; \quad \tau = 0 \text{ kg/cm}^2; \quad \sigma_{\text{red}} = \sqrt{\sigma^2 + 3\tau^2} = 520 \text{ kg/cm}^2.$$

Section II

$$\Sigma\sigma = 747 \text{ kg/cm}^2; \quad \tau = 0 \text{ kg/cm}^2; \quad \sigma_{\text{red}} = 747 \text{ kg/cm}^2.$$

Section III

$$\Sigma\sigma = 668 \text{ kg/cm}^2; \quad \tau = 213 \text{ kg/cm}^2; \quad \sigma_{\text{red}} = 763 \text{ kg/cm}^2.$$

Section IV

$$\Sigma\sigma = 609 \text{ kg/cm}^2; \quad \tau = 174 \text{ kg/cm}^2; \quad \sigma_{\text{red}} = 687 \text{ kg/cm}^2.$$

Section A

$$\Sigma\sigma = 510 \text{ kg/cm}^2; \quad \tau = 136 \text{ kg/cm}^2; \quad \sigma_{\text{red}} = 562 \text{ kg/cm}^2,$$

and at the runaway speed, the reduction of the water pressure upon the blade not being taken into account:

Section I

$$\Sigma\sigma = 520 \text{ kg/cm}^2; \quad \tau = 0 \text{ kg/cm}^2; \quad \sigma_{\text{red}} = 520 \text{ kg/cm}^2.$$

Section II

$$\Sigma\sigma = 1130 \text{ kg/cm}^2; \quad \tau = 0 \text{ kg/cm}^2; \quad \sigma_{\text{red}} = 1130 \text{ kg/cm}^2.$$

Section III

$$\Sigma\sigma = 937 \text{ kg/cm}^2; \quad \tau = 213 \text{ kg/cm}^2; \quad \sigma_{\text{red}} = 1010 \text{ kg/cm}^2.$$

Section IV

$$\Sigma\sigma = 815 \text{ kg/cm}^2; \quad \tau = 174 \text{ kg/cm}^2; \quad \sigma_{\text{red}} = 869 \text{ kg/cm}^2.$$

Section A

$$\Sigma\sigma = 710 \text{ kg/cm}^2; \quad \tau = 136 \text{ kg/cm}^2; \quad \sigma_{\text{red}} = 748 \text{ kg/cm}^2.$$

The split ring *a* (Fig. 256), taking up the centrifugal force of the blade, is by this force subjected to shearing stress, and we shall control it for the case of runaway speed when the centrifugal force attains the value $O_p = 490,000 \text{ kg}$. The ring would be sheared off at the radius 420 mm, so that the shearing area $f = \pi \cdot 42 \cdot 6 = 790 \text{ cm}^2$; and the shearing stress amounts to

$$\tau = \frac{490,000}{790} = 620 \text{ kg/cm}^2.$$

On the other hand, the ring pivot with the outer diameter of 420 mm would be sheared off at the diameter of 360 mm, so that the shearing area is

$$f = \pi \cdot 36 \cdot 7 = 790 \text{ cm}^2,$$

and the shearing stress equals

$$\tau = \frac{490,000}{790} = 620 \text{ kg/cm}^2.$$

The specific pressure between the pivot and the ring is

$$p = \frac{490,000}{\frac{\pi}{4}(42^2 - 36^2)} = \frac{490,000}{367} = 1330 \text{ kg/cm}^2.$$

The specific pressure between the ring of the outer bronze bushing and the hub of the crank is at runaway speed

$$p = \frac{490,000}{\frac{\pi}{4}(62^2 - 50^2)} = 465 \text{ kg/cm}^2,$$

this is admissible as at normal speed it will equal one fifth of this value.

The specific pressures in the bearings *A* and *B* are

$$p_A = \frac{200,000}{50 \cdot 19} = 210 \text{ kg/cm}^2, \quad p_B = \frac{120,000}{30 \cdot 21} = 190 \text{ kg/cm}^2,$$

and thus likewise within admissible limits.

All stresses in the blade are of such values that we may employ plain carbon steel, provided that this is feasible with regard to cavitation.

As far as the hub is concerned, we must check the tensile stress in the cross section f_1 (Fig. 258). This cross section with the area $f_1 = 1450 \text{ cm}^2$ is subjected to tensile stress by the reaction of the bearing *A*, amounting to 200,000 kg, and hence the tensile stress will be

$$\sigma = \frac{200,000}{1450} = 138 \text{ kg/cm}^2.$$

Similarly, we determine the stress for the cross section f_2 when the force R acts downward:

$$\sigma = \frac{62,000}{258} = 240 \text{ kg/cm}^2.$$

The hub is further stressed by its own centrifugal force, as well as by that of the blades. We ascertain the corresponding stress for the runaway speed.

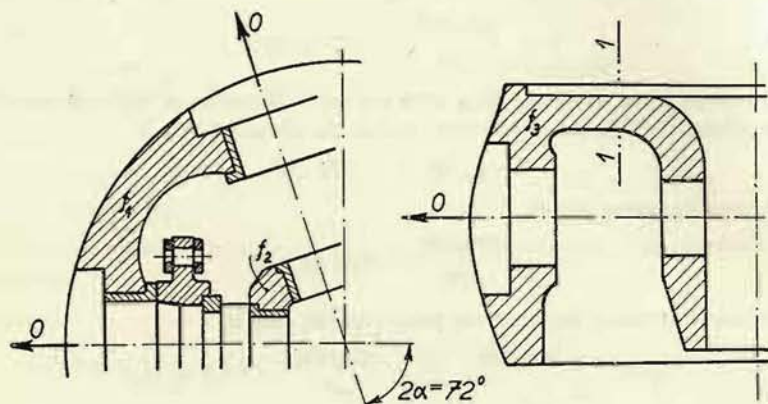


Fig. 258

The stress resulting from the centrifugal force of the hub itself can be calculated by means of the expression¹⁾

$$\sigma_1 = \frac{\gamma}{g} U^2,$$

where U is the peripheral velocity of the hub and has the value

$$U = r \omega_p = 1.2 \cdot \frac{302}{9.55} = 38 \text{ m/sec.} = 3800 \text{ cm/sec.}$$

Hence there will apply

$$\sigma_1 = \frac{7800}{9.81} \cdot 1444 = 1,150,000 \text{ kg/m}^2 = 115 \text{ kg/cm}^2.$$

The hub is also subjected to tensile stress resulting from the centrifugal forces of the blades and amounting to $O_p = 490,000 \text{ kg}$. If we assume these forces to be uniformly distributed along the periphery, the proportion corresponding to 1 cm is

$$O_0 = \frac{5 \cdot 490,000}{\pi \cdot 240} = 3250 \text{ kg/cm,}$$

¹⁾ Dobrovolný: Pružnost a pevnost (Strength of Materials), Prague, 1944, p. 796.

and the stress in the cross section $f_3 = 3380 \text{ cm}^2$ consequently amounts to

$$\sigma_2 = \frac{o \cdot d}{2 \cdot f_3} = \frac{3250 \cdot 240}{2 \cdot 3380} = 115 \text{ kg/cm}^2.$$

By the centrifugal forces, however, the hub will be subjected also to bending stress, like a ring for which the greatest bending moment is given by the expression²⁾

$$M_0 = \frac{P \cdot R}{2} \left(\cot \alpha - \frac{1}{\alpha} \right),$$

where α is half the angle enclosed by the forces P .

In our case therefore will be (Fig. 258) $\alpha = 36^\circ$ and

$$M_0 = \frac{490,000 \cdot 120}{2} 0.214 = 6,300,000 \text{ kg/cm.}$$

The resisting moment of the hub up to the section 1—1, i. e. without its internal part which is not connected by ribs and therefore ineffective, has been determined graphically as equalling $W = 15,000 \text{ cm}^3$; and hence the bending stress in the hub is

$$\sigma_0 = \frac{6,300,000}{15,000} = 420 \text{ kg/cm}^2.$$

The total tensile stress in the hub therefore equals

$$\Sigma \sigma = \sigma_1 + \sigma_2 + \sigma_0 = 115 + 115 + 420 = 650 \text{ kg/cm}^2.$$

Consequently, the hub will be made of cast steel.

The thickness of the outer wall must be determined so as to resist safely the centrifugal force resulting from the outer bearing.

To the other parts of propeller and Kaplan turbines applies the same as has been said concerning Francis turbines. Only from the viewpoint of strength control, we must pay special regard to the inner lid.

III. INNER LID

The inner lid of the propeller or Kaplan turbine differs in its shape considerably from a plate; apart from this, it is usually reinforced according to requirements by a greater or smaller number of ribs which are located in the planes passing through the axis of rotation.

For this reason, we do not calculate the strength of these lids as that of plates, but we divide the lid into segments by planes passing through the axis of rotation (taking as many segments as there are ribs and placing each rib into centre line of the appropriate segment). We then may consider each of these segments an inde-

²⁾ Loc. cit., p. 568.

pendent beam, not connected with the adjacent segments and uniformly loaded by the pressure of the water (or by the overpressure of the atmosphere at a sudden closing of the guide blades). This procedure is indicated diagrammatically in

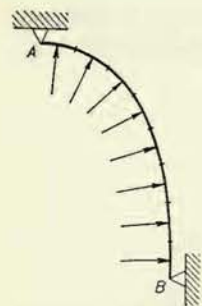


Fig. 259

Fig. 259. If we divide the length of such a beam into a number (preferably equal) sections, we can easily determine the magnitude and direction of the resultant of the pressures acting upon these sections. Without difficulty we ascertain their moments about the supports and thus we find the reactions in the supports *A* and *B*, represented by the flanges of the lid. Then we can determine the bending moment and bending stress in any arbitrarily selected place of the beam.

This method is only approximate, and the calculated stresses will be greater than the actual ones, because we have not taken into account the circular stresses in the lid.

The inner lid is also in this case fitted with a stuffing box, a bearing and other accessories. Fig. 254 shows the disposition of a large Kaplan turbine in the USSR with a rubber bearing, the use of which permits a material simplification of the turboset.

C. GENERAL ASSEMBLY PROCEDURE

As in the case of Francis turbines, also here a separate assembly unit is presented by the runner with the shaft, inner lid, stuffing box, and guide bearing, the latter and the stuffing box being mounted according to the requirements of centering the inner lid with the runner (labyrinths in front of the stuffing box).

This unit (see Fig. 260) is then lowered into the assembled „bottom part“ of the turbine, formed by the extension of the draft tube, the casing of the runner, the bottom lid (the lower blade ring), the stay blade ring, and sometimes the spiral, the guide blades, and maybe even the outer part of the top lid (Fig. 261).

The runner with the inner lid is then centered in relation to the runner casing, and the inner lid is secured by fitting pins in its correct position. If the casing of the runner is not entirely cast-in, it is fitted with staybolts with left-hand and right-hand threads, enabling the casing to be given a circular shape by supporting it against the concrete foundations and appropriately adjusting the staybolts (see Appendix I).

Since these turbines are designed for lower heads, sealing can be realized by coating the flanges with molten tallow which fills up surface irregularities and thus seals the flanges.

Fig. 260

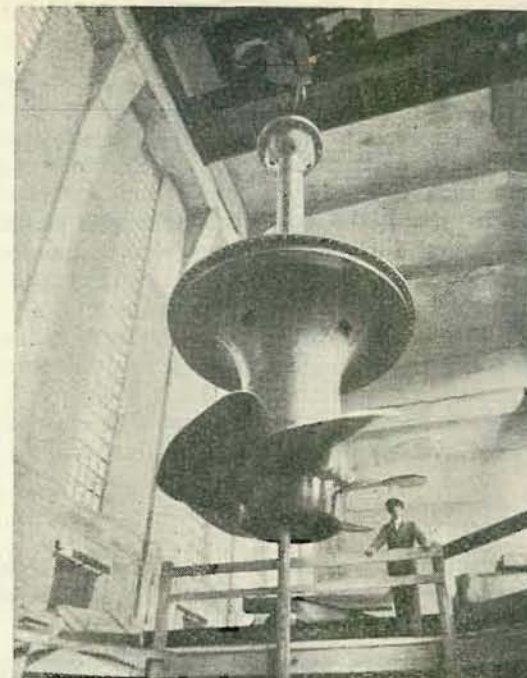
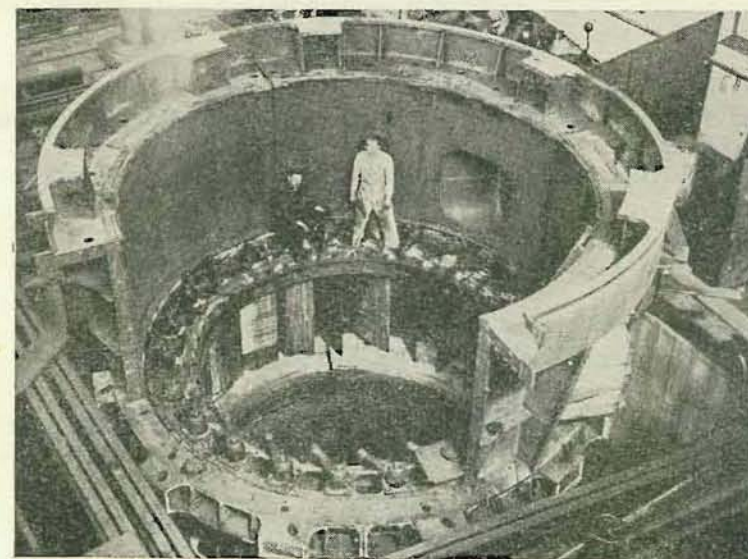


Fig. 261



3. PELTON TURBINES¹⁾

Pelton wheels are impulse turbines. The guide apparatus consists of a nozzle, from which the water emerges as a compact jet and enters the runner. To the rim of the runner disc are fastened bucket-shaped blades which are for a better discharge of the water divided by a ridge or splitter into two symmetrical parts. The water jet is deflected by the bucket and thus transfers its energy to the wheel. In order to achieve the most efficient position of the bucket for the impinging water, i. e. normal to the jet, a notch is made into the edge of the bucket at the largest radius. This notch is carefully sharpened to ensure, as far as possible, a loss-free entrance of the bucket into the jet.

Pelton turbines are regulated by decreasing or increasing the diameter of the jet, and this is effected by means of a needle or spear which closes or opens the throat of the nozzle.

The specific speed of Pelton turbines with one nozzle is $n_s = 4$ to 35 r. p. m. and defined by Equation (44), derived in Part I:

$$n_s = 576 u_1 \frac{d_0}{D} \sqrt{c_0 \eta}.$$

If we substitute $u_1 = 0.45$ and $c_0 = 0.97$, as usually selected (see later), and for η the value 0.85, the expression (44) can for the purpose of rough calculation be simplified to the form

$$n_s = 576 \cdot 0.45 \frac{d_0}{D} \sqrt{0.97 \cdot 0.85} = 235 \frac{d_0}{D}$$

$$n_s \doteq 235 \frac{d_0}{D}.$$

From this follows that high specific speeds are achieved by means of a small diameter D at large jet diameter d_0 , and vice versa. But increasing the specific speed is limited by the circumstance that the runner, or the blade connections, cannot be dimensioned so as to meet the strength requirements at high specific speeds.

A. HYDRAULIC INVESTIGATION

I. WATER JET

1. Free Jet

When a particle of a free jet moves in absolute vacuum (this is only a theoretical assumption as actually a cavitation would occur), its motion equals that of a mass point.²⁾

¹⁾ The section on Pelton turbines has been prepared by Ing. M. Druckmüller.

²⁾ Dubs R.: Angewandte Hydraulik, Zürich, Rascher Verlag, 1947, p. 218.

For an oblique projection under the angle of elevation α and with the initial velocity C_0 , the co-ordinates of the mass point can be calculated from the following equations (see Fig. 262):

$$x = C_0 t \cos \alpha,$$

$$z = C_0 t \sin \alpha - \frac{1}{2} g t^2,$$

where t is the time.

Eliminating the time t from both equation, we obtain:

$$z = C_0 \frac{x}{\cos \alpha}$$

and thus

$$z = x \tan \alpha - \frac{g}{2 C_0^2 \cos^2 \alpha} x^2, \quad (219)$$

or expressed generally

$$z = ax - bx^2, \quad (219a)$$

because α , g and C_0 may be considered constant for a given case.

The maximum height z_{\max} is obtained by differentiation:

$$\frac{dz}{dx} = a - 2bx_m = 0.$$

Hence the abscissa of the highest point is given by

$$x_m = \frac{a}{2b} = \frac{\tan \alpha C_0^2 \cos^2 \alpha}{g}.$$

By substituting into Equation (219a), we obtain

$$z_{\max} = \frac{(C_0 \sin \alpha)^2}{2g}. \quad (220)$$

From this relation follows that the maximum height for $\alpha = \frac{\pi}{2}$ equals

$$z_{\max} = \frac{C_0^2}{2g}.$$

To calculate the length of the projection, x_{\max} , we substitute $z = 0$, and from Equation (219) we obtain

$$x_{\max} = 4 \frac{C_0^2}{2g} \sin \alpha \cos \alpha, \quad (221)$$

or

$$x_{\max} = 2 \frac{C_0^2}{2g} \sin (2\alpha). \quad (221a)$$

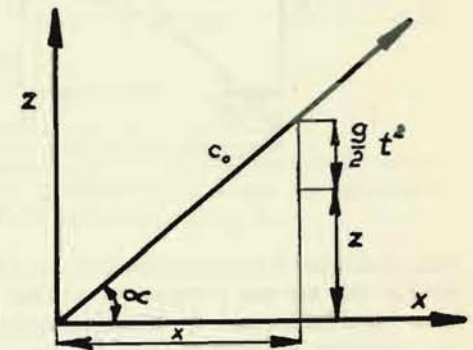


Fig. 262

According to this equation the length of the projection is greatest when $\alpha = 45^\circ$, and then holds good

$$x_{\max} = 2 \frac{C_0^2}{2g},$$

which is double the maximum height. Equation (219) represents a series of parabolas with the angle α and the velocity C_0 as parameters. Fig. 263 shows one of

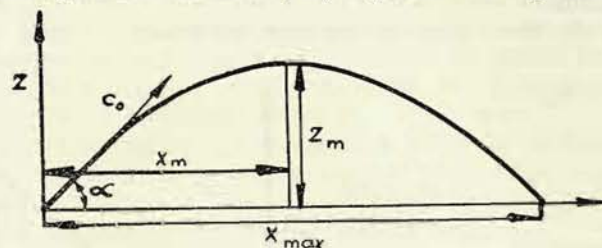


Fig. 263

these parabolas. Quite other relations, however, hold good for the oblique projection when it does not take place in vacuum but in a medium as e. g. in air. The flying mass particles entrain air particles, resulting in interchange of momentum, i. e. the resistance to the motion of the mass particle, and this resistance becomes a function of the velocity and depends also on the shape and size of the particle.

By the action of the resistance of air the maximum height of the path is considerably reduced in comparison with Equation (220), as well as the maximum length of the projection in comparison with Equation (221). The same is the case with the particles of the liquid jet, which, as experience has shown, after a longer flight is scattered into individual droplets in consequence of the exchange of impulses (Fig. 264). From the theoretical point of view it is difficult to determine the path of the individual particles as their motion cannot be exactly expressed in a mathematical form.

For this reason, purely experimental investigations were undertaken already long ago, and Freeman was the first who occupied himself with a systematic study of this phenomenon. In a series of experiments with varying pressures and jet diameters the height and length of the projection were measured



Fig. 264

It was found that at higher velocities scattering of the water jet sets in earlier. The influence of the jet diameter upon the length of the projection is materially greater than the influence of the velocity, or of the pressure. In order to attain greater lengths of the projection, the water must emerge from the nozzle without a circular motion. For realizing this condition, it is recommended to mount a rectifier into the nozzle; this, however, results in a pressure loss and thus in a reduction of the velocity head $h = \frac{C_0^2}{2g}$.

When the jet impinges perpendicularly upon a straight plate of sufficient area the plate will be acted upon by a force in the direction of the jet, defined according to Equation (11) by the expression

$$P_x = \frac{\gamma Q}{g} C_0;$$

here, however, we must place the control surface, serving as a base for the calculation of the impulse, in such a position that the transversing jet is not yet influenced by the wall and all its particles move in the same direction (Fig. 265).

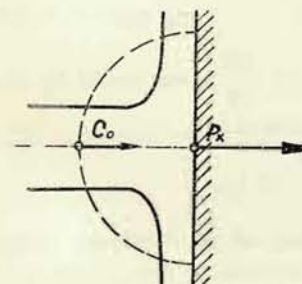


Fig. 265

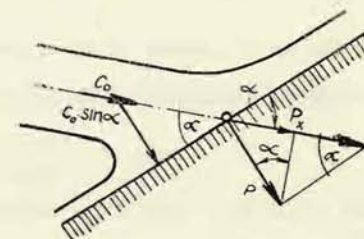


Fig. 266

When the plate moves in the direction of the jet at the velocity U , the jet will impinge upon it at the relative velocity $W = C_0 - U$, and the force will then be

$$P_{x1} = \frac{\gamma Q}{g} W = \frac{\gamma Q}{g} (C_0 - U). \quad (222)$$

And since the plate moves, the jet does work every second, and hence its power equals

$$N = P_{x1} U = \frac{\gamma Q}{g} (C_0 U - U^2). \quad (223)$$

By differentiation we find:

$$\frac{dN}{dU} = \frac{\gamma Q}{g} (C_0 - 2U),$$

and for $U = \frac{C_0}{2}$ the differential coefficient is zero and consequently the power attains the maximum value.

In conformity with Equation (223) the maximum power then equals

$$N_{\max, ef} = \frac{1}{2} \gamma Q \frac{C_0^2}{2g}.$$

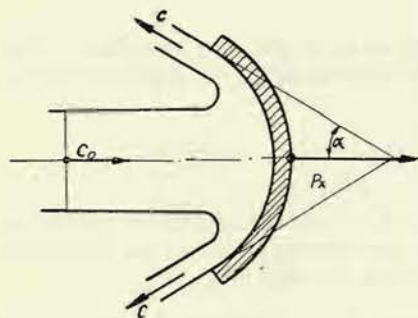


Fig. 267

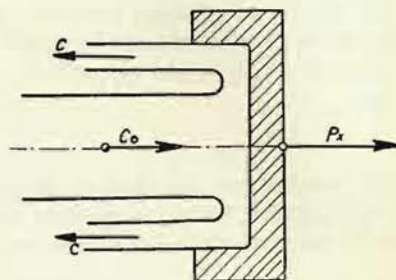


Fig. 268

Since the jet is capable of the power $N_{th} = \gamma Q \frac{C_0^2}{2g}$, we would by means of the described equipment attain a maximum efficiency of

$$\eta_{\max} = \frac{N_{\max, ef}}{N_{th}} = 0.5 = 50 \%,$$

and this would be a very unsatisfactory utilization of the hydraulic power at disposal.

When the jet impinges upon the plate at an oblique angle (Fig. 266), the force P acting perpendicularly to the plate is expressed by the value

$$P = \frac{\gamma Q}{g} C_0 \sin \alpha, \quad (224)$$

where $C_0 \sin \alpha$ represents the velocity component perpendicular to the plane of the plate. In the direction of the plane of the plate we have the velocity component $C_0 \cos \alpha$ and the corresponding discharge of the water with a deflection exceeding 90° and depending on the angle α . In order that the jet might act with the force defined by Equation (224), the plate must have a sufficiently large diameter ($D > 6d$). The force P_x in the direction of the jet then will be given by:

$$P_x = P \sin \alpha = \frac{\gamma Q}{g} C_0 \sin^2 \alpha. \quad (225)$$

We see from this equation that with a diminishing value of α the force P_x diminishes, too. For $\alpha = 0$, P and P_x equal zero.

When the water jet impinges upon a surface of rotation (Fig. 267), the force created in the direction of the jet is

$$P_x = \frac{\gamma Q}{g} C_0 (1 + \cos \alpha). \quad (226)$$

When the jet is deflected by 180° (Fig. 268), P_x assumes the maximum value

$$P_x = 2 \frac{\gamma Q}{g} C_0, \quad (227)$$

as can be calculated from Equation (226) for $\alpha = 0^\circ$.

When α is less than 90° , the actual force is reduced by the influence of friction. This influence of friction must be estimated. When a body moves in the direction of the jet at the constant velocity U , the relative velocity W of the particles with regard to the body will be $W = C_0 - U$, and for the deflection of the flow by 180° we obtain the force

$$P_x = 2 \gamma \frac{Q}{g} (C_0 - U) \quad (228)$$

and the power

$$N = 2 \gamma \frac{Q}{g} (C_0 U - U^2).$$

The maximum power will be attained when $U = \frac{C_0}{2}$ and amount to

$$N_{\max, ef} = \gamma Q \frac{C_0^2}{2g}.$$

Since the power at disposal is

$$N_{th} = \gamma Q \frac{C_0^2}{2g},$$

the maximum efficiency, under the assumption of a loss-free flow along the wall, will be

$$\eta_{\max} = \frac{\gamma Q \frac{C_0^2}{2g}}{\gamma Q \frac{C_0^2}{2g}} = 1 = 100 \%.$$

Owing to friction this value cannot be attained, and, apart from this, it is not possible in practical operation to realize a deflection of the flow by 180° (i. e. $\alpha = 0$). For instance, in Pelton wheel, the discharging water would impinge on the following blade. The actually achievable efficiency is

$$\eta_{\max} = 92 - 93 \%.$$

2. Diameter of the Jet

When the water jet emerges from the nozzle of a Pelton turbine, its diameter somewhat decreases due to contraction, and its velocity increases up to its least cross section (Fig. 269).¹⁾

From this place, the diameter of the jet begins to increase again gradually, because under the influence of the exchange of impulses between the jet and the ambient air, the velocity of the outer particles of the jet is gradually reduced. Since the velocity, in particular of the outer particles, diminishes, the diameter

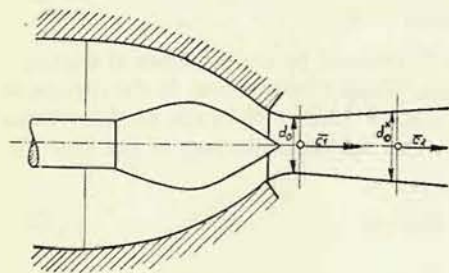


Fig. 269

of the jet must increase to preserve the continuity. The jet widens the farther the more until it is entirely dispersed. Denoting the least diameter of the jet by d_0 , we obtain from the continuity equation

$$Q = \frac{\pi}{4} d_0^2 C_0. \quad (229)$$

For evaluating this expression, we must, of course, know the mean velocity C_0 of the jet. Since we have here to deal with an impulse turbine,

the entire head H is converted into velocity, so that the velocity of the free outflow is given by the equation

$$C_0 = \varphi \sqrt{2gH}, \quad (230)$$

where φ represents the efficiency of the nozzle and amounts to 0.95 to 0.98.

By substitution into Equation (229) we obtain

$$\frac{d_0^2 \pi}{4} = \frac{Q}{C_0} = \frac{Q}{\varphi \sqrt{2gH}},$$

whence follows

$$d_0 = \sqrt{\frac{4}{\pi} \frac{Q}{\varphi \sqrt{2gH}}},$$

and by substituting $\varphi = 0.97$ as mean value we arrive at

$$d_0 = 0.55 \sqrt{\frac{Q}{\sqrt{H}}} = 0.55 \sqrt{Q_1},$$

$$d_0 = 550 \sqrt{Q_1}, \quad (231)$$

where d_0 appears in millimetres when we express the flow-rate for the head of 1 m in m³/sec.

¹⁾ Dubs R.: *Angewandte Hydraulik*, Zürich, Rascher Verlag, 1947, p. 229.

Example:

$$H = 520 \text{ m}$$

$$Q = 349 \text{ litres/sec.}$$

$$C_0 = 0.97 \sqrt{2gH} = 0.97 \sqrt{2 \cdot 520g} = 98 \text{ m/sec.}$$

$$\text{The cross section of the jet is } F = \frac{Q}{C_0} = \frac{349}{980} = 0.356 \text{ dm}^2.$$

The diameter of the jet is $d_0 = 67.3 \text{ mm}$.

Or, from Equation (231) we obtain

$$d_0 = 550 \sqrt{Q_1} = 550 \sqrt{\frac{Q}{\sqrt{H}}} = 550 \sqrt{\frac{0.349}{\sqrt{520}}},$$

$$d_0 = 67.8 \text{ mm.}$$

II. RUNNER

1. Diameter of the Runner

From Equation (20)

$$\eta_h H = \frac{1}{g} (U_1 C_{u1} - U_2 C_{u2})$$

we can under the assumption of a perpendicular discharge, i. e. $C_{u2} = 0$, calculate the permissible velocity

$$U_1 = \frac{\eta_h g H}{C_{u1}}.$$

In the case of Pelton turbines, this relation passes for the values $C_{u1} \doteq C_0$ and $H = \frac{C_0^2}{2g\varphi^2}$ into

$$U_1 = \frac{\eta_h g \frac{C_0^2}{2g\varphi^2}}{C_0},$$

whence follows after cancelling

$$U_1 = \frac{\eta_h C_0}{2\varphi^2} \doteq \frac{C_0}{2}.$$

From the inlet velocity triangle (Fig. 270) follows:

$$W_1 \doteq C_0 - U_1 = C_0 - \eta_h \frac{C_0}{2\varphi^2}$$

and then

$$W_1 = \left(1 - \frac{\eta_h}{2\varphi^2}\right) C_0 \doteq \frac{C_0}{2},$$

and hence

$$W_1 \doteq U_1;$$

according to Equation (230) here applies $C_0 = \varphi \sqrt{2gH}$.

At the discharge of the water from the blade, there is $W_2 \doteq W_1$ and further $U_2 = U_1$. By composing the velocity W_2 directed by the blade angle β_2 and the velocity U_2 we obtain the absolute outlet velocity C_2 at which the water leaves the blade.

The value of the angle β_2 is usually selected between 4 and 10°, because, as already pointed out, it is not possible to deflect the water flow by 180° as in this case the water would impinge upon the following blades.

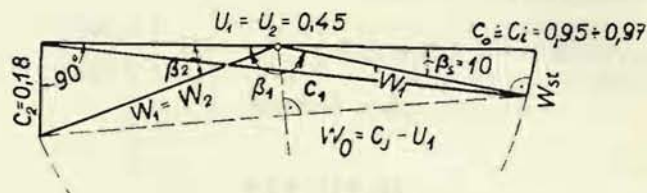


Fig. 270

Since the height of the runner above the tail water level represents a loss, the wheel is arranged above this level at the least possible height, i. e. about from 0.5 to 3 m, according to the possibilities given by construction and design, and in dependence on the fluctuations of the tail water level.

From the expression

$$U_1 = \frac{\eta_h C_0}{2 \varphi^2} = \frac{\eta_h \varphi \sqrt{2gH}}{2 \varphi^2}$$

and by introducing the mean value $\varphi = 0.97$, we obtain the peripheral velocity

$$U_1 = 2.28 \eta_h \sqrt{H}. \quad (232)$$

or also $U_1 = \frac{\eta_h}{1.94} \sqrt{2gH}$, and when taking the safely attainable value $\eta_h = 0.88$,

$$U_1 = 0.45 \sqrt{2gH}.$$

The speed n of the turbine having been selected, the diameter D of the runner is determined from the relation

$$U_1 = \frac{\pi n D}{60}, \text{ where } U_1 = 2.28 \eta_h \sqrt{H},$$

whence

$$D = \frac{U_1 60}{\pi n} \text{ or } = \frac{2.28 \cdot 60 \cdot \eta_h \sqrt{H}}{\pi n} = 43.5 \frac{\eta_h}{n_1},$$

and for the diameter expressed in mm holds good

$$D = \frac{43,500 \eta_h}{n_1}. \quad (233)$$

Example:

$$H = 520 \text{ m}$$

$$Q = 349 \text{ litres/sec.}$$

$$n = 1000 \text{ r. p. m.}$$

$$U_1 = 0.45 \sqrt{2gH} = 0.45 \sqrt{2g \cdot 520} = 45.5 \text{ m/sec.}$$

$$\text{The diameter of the runner then is } D = \frac{60 U_1}{\pi n} = \frac{60 \cdot 45.5}{1000 \pi} = 870 \text{ mm.}$$

Or from Equation (233)

$$D = \frac{43,500 \eta_h}{n_1} = \frac{43,500 \cdot 0.89}{\frac{1000}{\sqrt{520}}} = 870 \text{ mm.}$$

When a turbine has been ordered, the diameter of the runner is determined from the characteristic obtained by a braking test of the model of the turbine in the testing station. For instance, on the horizontal

axis we mark off $n'_1 = \frac{nD}{\sqrt{H}}$,

and on the vertical axis $Q'_1 = \frac{Q}{D^2 \sqrt{H}}$ (see Fig. 271).

The values of n'_1 and Q'_1 are then selected from the characteristic so that at the given head the turbine operates in the range of optimum efficiency, i. e. that the selected value of n'_1 passes through the region of the optimum efficiencies. In our case we select

$$n'_1 = 38 \text{ r. p. m.,}$$

$$Q'_1 = 20.5 \text{ litres/sec.;}$$

the diameter is then defined by:

$$D = \sqrt{\frac{Q}{Q'_1 \sqrt{H}}} =$$

$$\sqrt{\frac{349}{20.5 \sqrt{520}}} = 870 \text{ mm;}$$

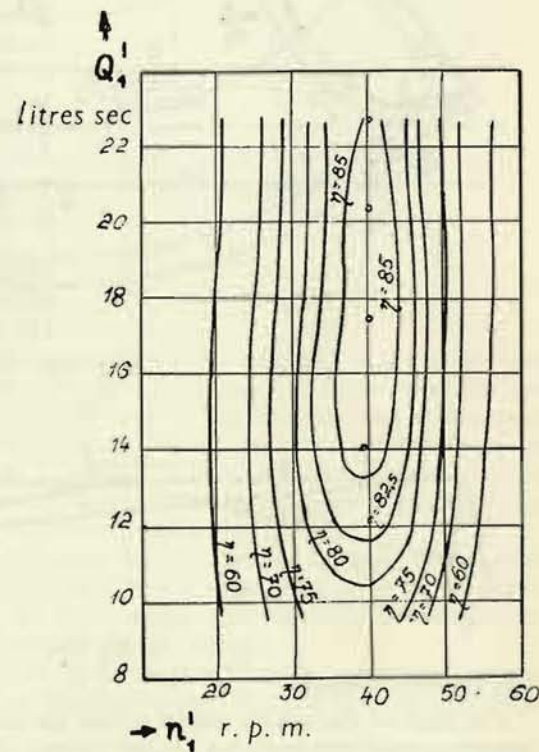


Fig. 271

and the speed by:

$$n = \frac{n'_1 \sqrt{H}}{D} = 980 \sim 1000 \text{ r. p. m.}$$

From the characteristic we then determine the guaranteed values of the turbine for $\frac{3}{4}Q$, $\frac{1}{2}Q$ and $\frac{1}{4}Q$.

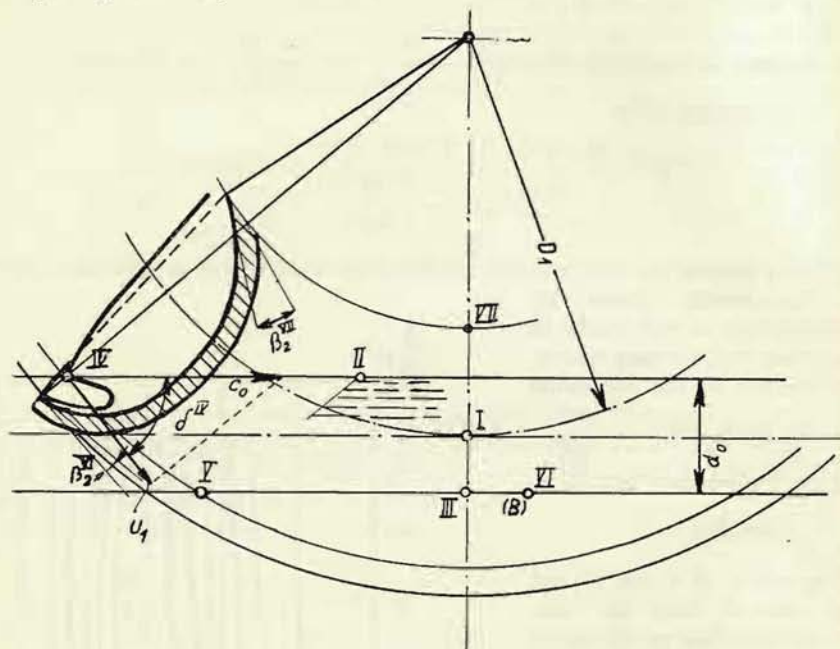


Fig. 272

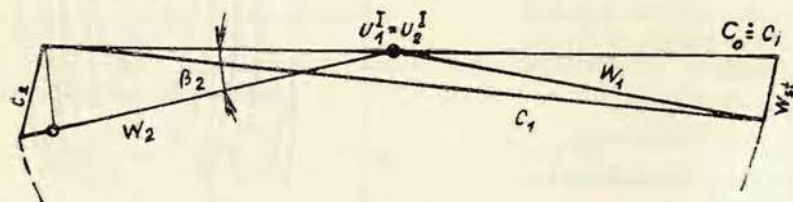


Fig. 273

2. Velocity Diagrams

The work of the water particles within the wheel is not uniform and depends upon the conditions and place of their contact with the blade. It is advantageous to draw the diagrams for the extreme points, as e. g. the points *I* to *IV* in Fig. 272.

The losses ϱ in the entire turbine, caused by friction and vorticity,¹⁾ vary in dependence on the shape and material of the blade, the conditions of the approach of the water, etc. Without making a significant error, we may, independently of all variables, select for the indicated velocity c_i a value in the region from (0.9) to 0.93 to 0.95.

The angle δ , enclosed by the specific velocity c_0 and the peripheral velocity, equals zero for the point *I* and also for the points *III* and *VII* which lie on the radius passing through point *I* (Fig. 272). For all other points this angle must be derived from the figure. The relative velocity w_0 is ascertained from the triangle defined by u_1 , c_0 and δ . The direction of w_1 departs from the vector w_0 by half the angle of the ridge, β_s , when w_0 is directed perpendicularly to the ridge. When w_0 is directed obliquely to the ridge, the angle β_s will be replaced by the angle β'_s , which is somewhat smaller and can be easily determined according to Figs. 274 and 275; here we take the inlet velocity c_0 as equalling the indicated velocity (i. e. we count with a lower value), thus taking into account that the velocity of the water decreases along the blade owing to friction.

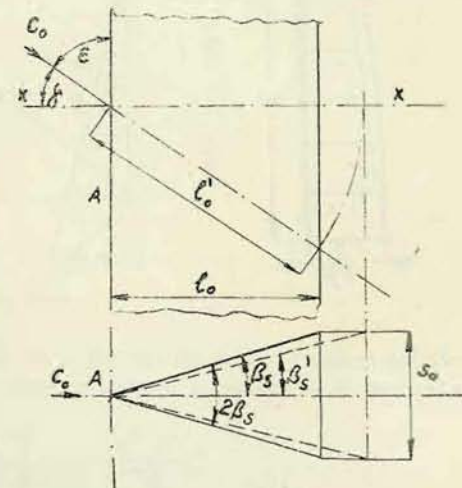


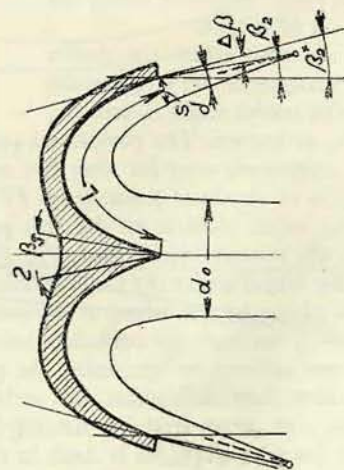
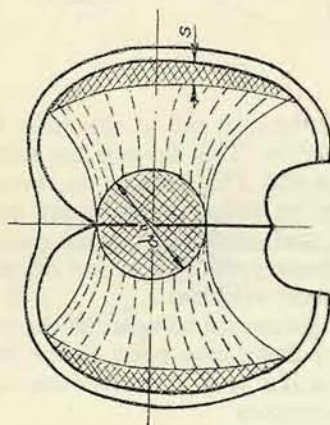
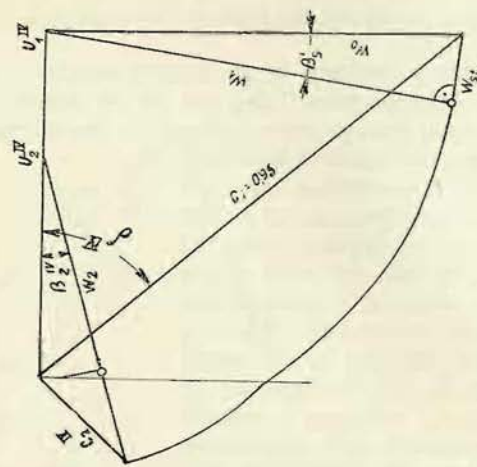
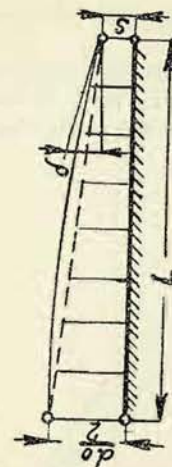
Fig. 274 275

We could also draw the outlet velocity triangles if we e. g. would consider the outlet angle α_2 and the value of u_2 as known. The peripheral velocity at the inlet and at the outlet is of the same magnitude only for very few water particles. This depends not only on the position of the inlet point (e. g. IV or V in Fig. 272) but also on the position of the water particle in the free jet. This jet widens considerably on its way over the runner blade (Figs. 276 and 277), and consequently water particles entering the wheel under the same conditions assume various paths and discharge in various places of the wheel at various peripheral velocities.

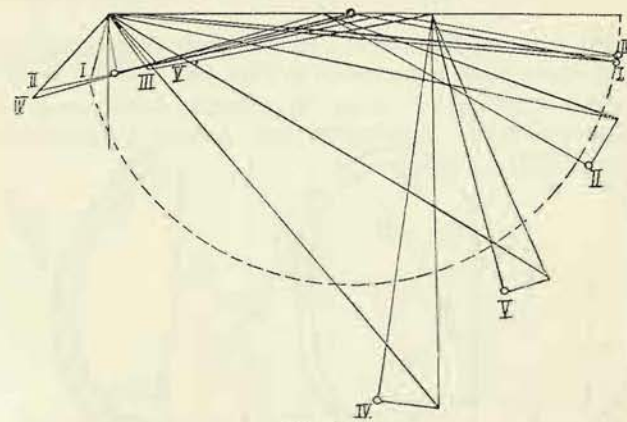
But even if we base our considerations upon the mutual influence of the water particles and attempt to determine the path of a single mass point on the blade, we encounter great difficulties. We arrive at our goal only after laborious calculations and only when applying simplifying assumptions.

One of these assumptions is dealt in the chapter "Free Jet (pressure on various plates)". But we can estimate the deflection created by an oblique position of the

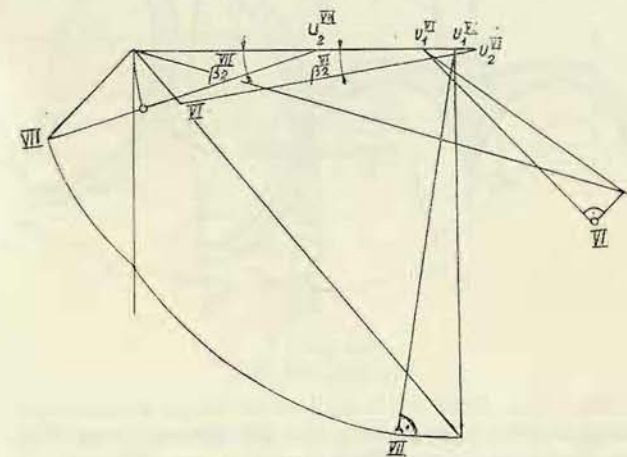
¹⁾ Thomann R.: Die Wasserturbinen und Turbinenpumpen, Part 2, Stuttgart, K. Wittwer, 1931, p. 274.



blade and even draw the path of the particle on the blade. The direction β_2 for the outlet point I we then consider first so that the outlet velocity c_2 or its meridional component equal a value in the range from 0.12 to 0.2. The discharge loss amounts



in this case to 1.5 to 4 %. The direction of w_2 for the other outlet points are then ascertained most advantageously so that all vectors w_2 intersect in one point



which lies either on the vertical passing through the origin of the diagram or at the distance $w_{2I} = u_{2I}$ from the origin of w_2 (Fig. 280). Since there would be different diagrams for each particle, also the discharge losses for each particle

are different. Their mean value for all particles would have to be calculated, as for pressure turbines, from the equation

$$c_{2st}^2 = \frac{\int c_2^2 dQ}{Q}. \quad (234)$$

Figs. 279 to 281 show the diagrams of a runner whose characteristic is illustrated in Fig. 271, and whose blade is presented in Figs. 282 to 284.¹⁾ In the diagrams,

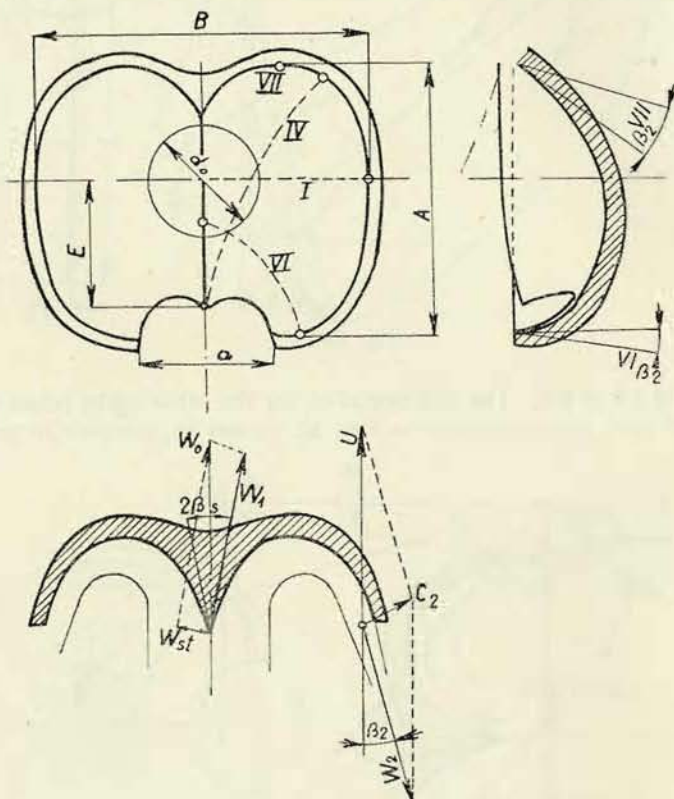


Fig. 282, 283, 284

w_1 has been rotated about w_0 as the axis into the plane of the picture. The Pelton turbine exhibits no overpressure. When u_1 and u_2 are different, the value of w_2 is therefore determined from Equation (25)

$$w_2^2 = w_1^2 - u_1^2 + u_2^2.$$

¹⁾ Thomann R.: Die Wasserturbinen und Turbinenpumpen, Part 2, Stuttgart, K. Wittwer, 1931.

Frequently, however, we draw only the velocity diagram for the particle I , disregarding the friction of the water along the blade, thus putting $w_2 = w_1$ and leaving along the entire periphery of the blade the outlet angle β_2 , which we ascertain from the diagram (Fig. 273).

3. Number of Blades

The most advantageous number of blades is ascertained from quite another point of view than it is done for Francis turbines. As far as Francis turbines are

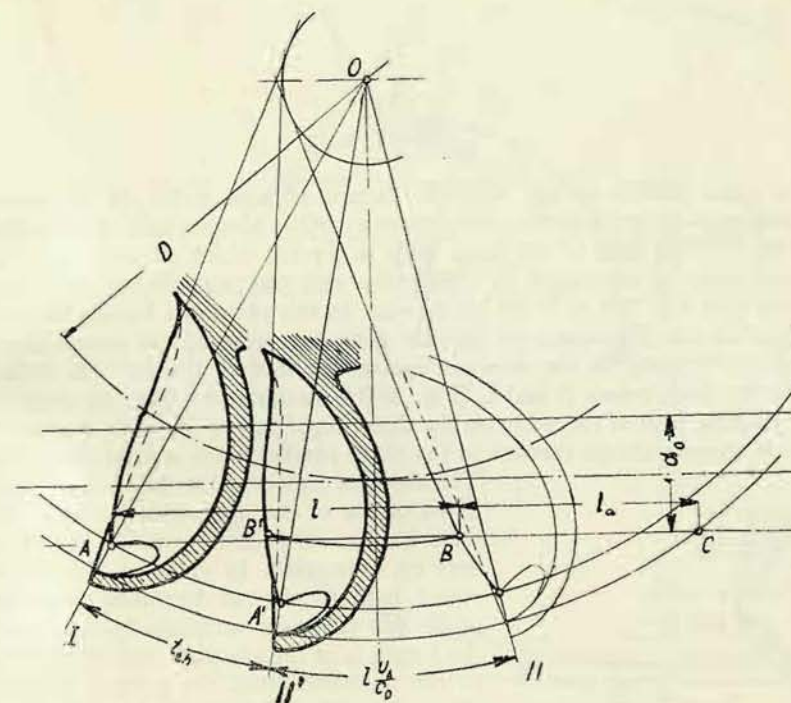


Fig. 285

concerned, we must pay regard to the load of the blades and a satisfactory guiding of the water. These considerations are insignificant for Pelton turbines.¹⁾

On the other hand, however, our greatest care must be directed to establishing such conditions that the blade does not frequently interfere with the water jet and that all water particles are forced to give off all their kinetic energy to the wheel.

¹⁾ Thomann R.: Die Wasserturbinen und Turbinenpumpen, Part 2, Stuttgart, K. Wittwer, 1931, p. 283.

As will be described in more detail in the chapter on the notch in the blade, the entering of the blade into the jet causes considerable disturbance owing to the unfavourable outward deflection of part of the water. For this reason, we never take a greater number of blades than indispensably necessary. This least, still permissible number is determined on the base of the second requirement, i. e.

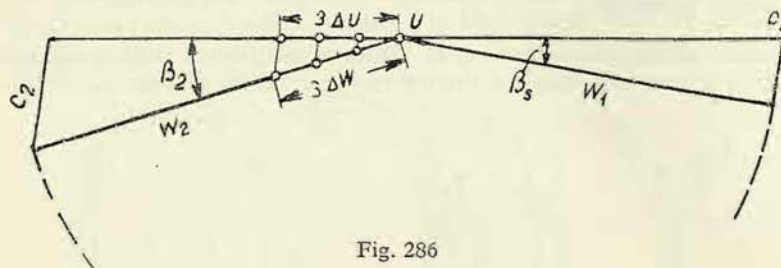


Fig. 286

that no water particle should leave the turbine without giving off the greatest possible part of its energy to the runner. Such a particle does not fulfil this condition, when the absolute path of the water ends in a point which already lies beyond the outer circle of the wheel. In conformity with this requirement we consider the point *C* in Fig. 285 to be the limit point. In this point, the last particle must leave the runner. Therefore, the particle must have entered the runner already at the point *B* lying in the direction against the flow of the jet. The distance between the both points *B* and *C* (Fig. 285) is nothing else than the projection of the absolute path of the water on the direction of the jet. Here we assume that the water particle always remains in the plane parallel to the axis of the turbine.

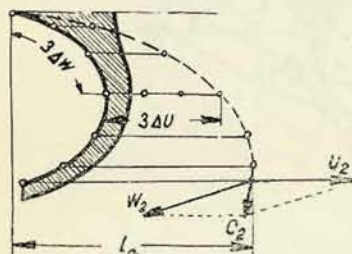


Fig. 287

point *A* (Fig. 285). Before it impinges on the following blade in the point *B*, it still must travel along the path \overline{AB} at the velocity C_0 , for which it takes the time $\Delta t = \frac{\overline{AB}}{C_0}$. During this time, the extreme point *A* of the blade edge travels along a certain path at the velocity U_A (corresponding to the radius r_a). Both

these velocities are constant, consequently the lengths of the paths are proportional to the velocities, and, therefore, the point *A* of the blade covers in the observed time the path

$$\overline{AB} \frac{U_A}{C_0} = l \frac{u_A}{c_0}.$$

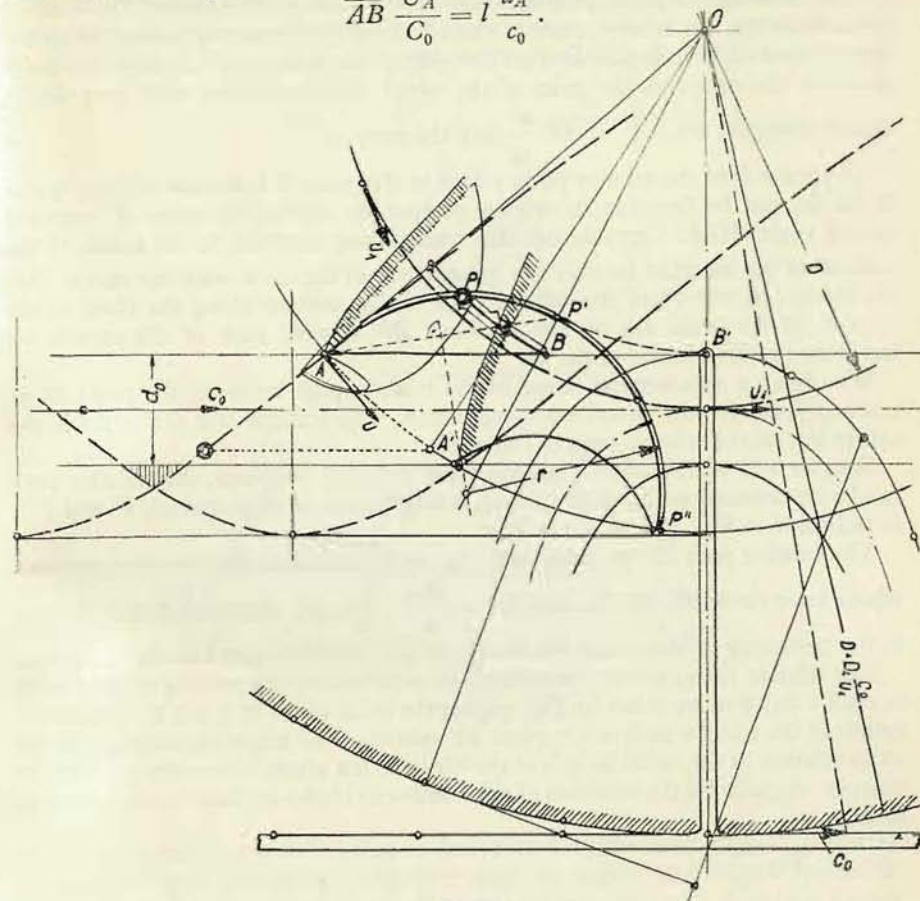


Fig. 288

At the moment when the water particle passes the point *A* of the blade *I*, the blade *II* must therefore be in the position *II'*, which lags behind the position of *II* by the distance $l \frac{u_A}{c_0}$, which defines the theoretical spacing of the blades, t_{th} .

In a wheel with a wider spacing of the blades, the energy of some water particles will not be utilized, and, on the other hand, when the spacing is too narrow, the jet will be superfluously disturbed by the interfering blades.

It is self-understood that the number of blades determined by the spacing must be rounded off to an integer, and, if necessary, the calculated spacing must be reduced. The spacing of the blades may also be established from the relative path of the jet along the plane perpendicular to the axis of the runner. The method of ascertaining the relative path of the jet along the plane perpendicular to the axis of rotation is indicated in Fig. 288. While the water particle from the point A covers the path AB , the point of the wheel which coincides with the point A rotates along the arc $\widehat{AA'} = \overline{AB} \frac{u}{c_0}$ into the point A' .

The point P of the relative path, which in the point B coincides with the point of the jet, can be found in its original position by rotating the point B backward by the angle AOA' . Carrying out this construction stepwise for all points of the contour of the jet, in so far they are located within the circle with the radius \overline{OA} , we obtain the picture of the relative path of this contour along the plane of the runner. In the same way we also establish the relative path of the particle on the other (outer) contour of the jet.

We obtain a symmetrical shape of the relative path by using the point B' as starting point for the described construction. The straight line OP' then is the centre line of the relative path of the water.

Simpler and with sufficient accuracy for practical purposes, this relative path can be represented as the circle passing through three of its points (A , P' and P''), as indicated in Fig. 288 by a thin line.

The relative path of the water may also be expressed as the extended involute whose basic circle has the diameter $D^x = \frac{Dc_0}{u_1}$, i. e. the diameter which belongs to the periphery of that circle which revolves at the same speed as the jet moves.

The relative path can now be utilized for establishing the spacing of the blades in such a way that we select for the spacing the value of 0.7 to 0.8 of the peripheral length of the relative path of the outer jet contour. The larger the diameter of the jet in relation to the radial length of the blade is, the greater the number of blades must be. A guide for the selection of the number of blades is given by the following table:

For $\frac{d_0}{D} =$	$\frac{1}{6}$	$\frac{1}{8}$	$\frac{1}{10}$	$\frac{1}{15}$	$\frac{1}{20}$	$\frac{1}{25}$
-----------------------	---------------	---------------	----------------	----------------	----------------	----------------

Number of blades $z = 17$ to 21, 18 to 22, 19 to 24, 22 to 27, 24 to 30, 26 to 33.

4. Inclination of the Blade to the Radius

The jet is not deflected from the direction of the generatrices of the blade only then when the flow impinges perpendicularly on the leading edge of the blade, i. e. when this edge is normal to the axis of the jet. This condition cannot be fully satisfied, because the direction of the leading edge in relation to the axis of the jet varies with the rotation of the blade. For this reason, we attempt to achieve

a perpendicular incidence of the stream at least in the time of its full action upon the blade by selecting the position of the leading edge perpendicular to the jet at the moment which halves the duration of the full approach of the flow.

The same condition may also be applied to the outlet edge which comes into action later, according to the length of the absolute path of the water, l_a (see Fig. 287). The inlet and the outlet edge are then mutually distorted. As we want

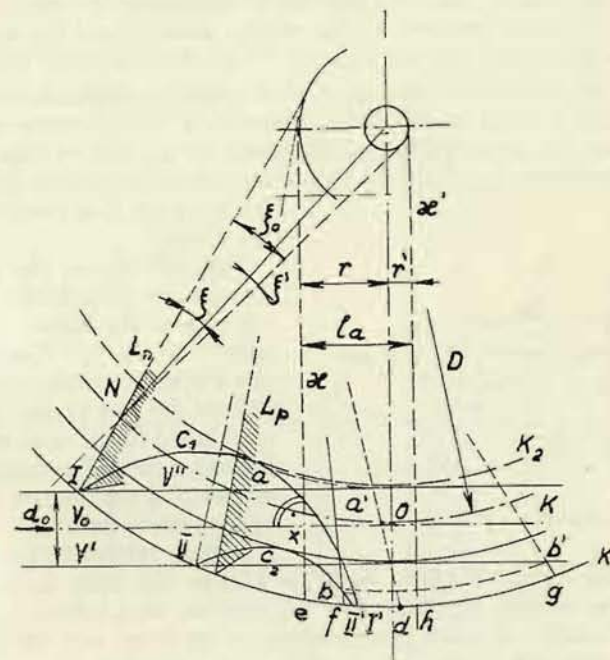


Fig. 289

them to be parallel, the inclination is determined by the inlet edge, and in this case we select it perpendicular to the jet just in the middle between the beginning of the entrance and the end of the discharge of the full jet, i. e. in the centre between the beginning and the end of the relative path of the outer jet contour. Always, however, there is only one position of the bucket which causes no deflection of the jet radially inward or outward.

Consequently, we set out from the fundamental condition that the direction of the leading edge in the region of its interference with the full jet should exhibit in its central position the least possible deflection from the perpendicular to the jet.

This will be achieved when the point x , in which the leading edge N is normal to the axis of the jet, lies in the centre of the path of the approaching full flow onto the bucket, given by the position of the path II and d . For this solution of the

problem, requiring to have the spacing of the blades established beforehand, the position of the blade is first selected empirically and subsequently adjusted in dependence on the results.¹⁾ (See Fig. 289.)

The beginning of the onflow path of the water particle in the filament V'' of the jet nearest the centre of the wheel is in the point I , and its end is in the point a' , at which the last water particle reaches the edge of the preceding bucket Lp (Fig. 289). The point a' (absolute position) is determined in such a way that the intersection a (relative position) of the relative path C_1 and the edge N of the bucket Lp is transferred into the filament V'' by rotation about the runner axis along the arc aa' . By drawing the edge N in the point a' , we obtain the intersection d with the circle K_1 . The arc IId defines the range of the full stream of the corresponding bucket Lp ; in the point e , which bisects the arc IId , we raise the perpendicular z to the centre line V_0 of the jet and thus obtain the sought direction of the

leading edge N at the distance r from the Y -axis.

Fig. 289 shows for the sake of interest also the position of the leading edge of the bucket when the last particle of the flow corresponding to one bucket impinges; this position is defined by the point g , which is established in the same way from the starting point II as beginning of the approach of the filament V' by means of the relative path C_2 .

It must further be noted that at the approach of the central filament V_0 to the edge in the point x , the peripheral velocity u_1 has another direction than the absolute inlet velocity c_0 , so that the relative inlet velocity w_1 is not perpendicular to the edge, and that therefore the bucket shifts normally to the jet at the velocity c_h (Fig. 290). Since it is assumed that the splitter of the bucket is in the region of the approach of the flow formed by cylindrical surfaces, this circumstance has no influence upon the deflection of the path of the relative flow from the plane perpendicular to the central plane of the runner and passing through the filament of the stream. Therefore, this shift may be disregarded.

The projection of the trailing edge into the central plane of the wheel is as a rule made as a straight line. For small ratios $\frac{d_0}{D}$, the trailing edge is as a rule made parallel with the leading edge. In other cases its position is established in the same way as that of the leading edge, but we must bear in mind, of course, that the trailing edge comes into action later than the leading edge and therefore it is

¹⁾ Kieswetter: Vodní stroje lopátkové (Hydraulic Turbomachinery), Part I, Brno, 1939, p. 28.

in the projection shifted in the direction of the rotation of the absolute path l_a of the water flow on the surface of the blade (Fig. 289). The projection of the trailing edge, z' , into central plane of the wheel, normal to the axis of the jet,

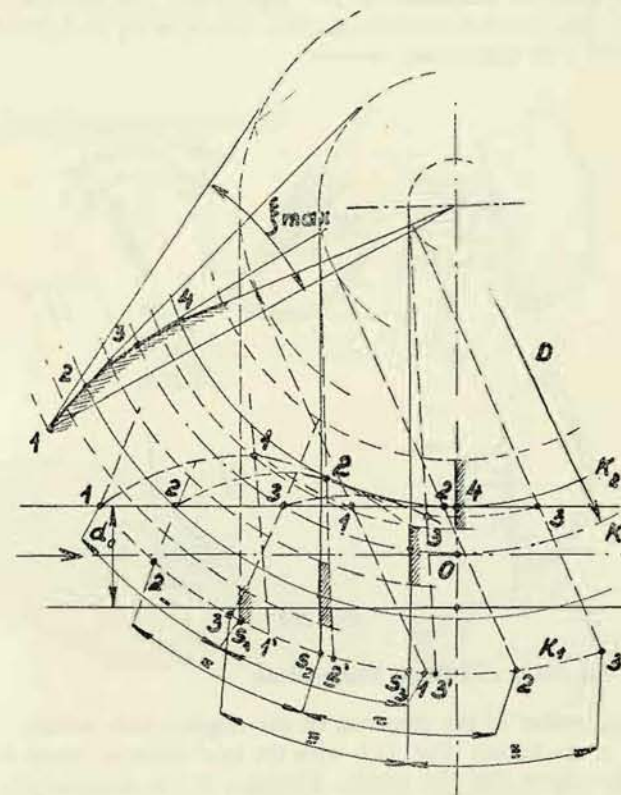


Fig. 291

V_0 is at the distance l_a from z and parallel to the Y -axis; its distance from this axis is r' .

The inclination of the projections of both edges, the trailing edge as well as the leading edge, is given by the angle (Fig. 289)

$$\xi_0 = \xi \pm \xi'.$$

For larger values of the ratio $\frac{d_0}{D}$, the leading edge is made with a curvature.

Its shape is ascertained in the same way as the position of a straight edge, but the described method is applied only for parts of the full length of the blade, and these

individual parts are connected by a broken line whose curve of contact defines the leading edge 1 2 3 4 (Fig. 291).

At present, the angle of the ridge is in the majority of cases 18° (Fig. 292a), instead of the formerly used angle of 10° (Fig. 292b). The strongly curved ridge shown in Fig. 292d exhibits a certain increase of the spacing (Δp), which, however, must be applied with appropriate reserve.

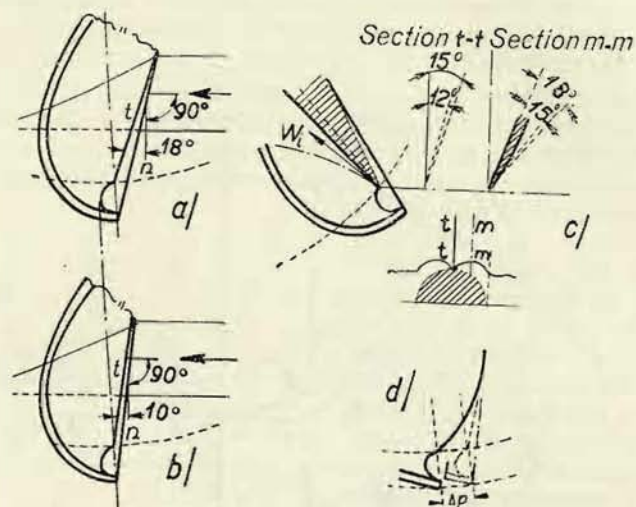


Fig. 292

5. Notch of the Blade and Blade Dimensions

From a comparison of the direction of the relative inlet velocity at the most distant point of the bucket (Fig. 272) with the inlet angle β_2 (given by the shape of the bucket) follows that the relative direction of the entrance of the jet is in the outer part of the bucket much more inclined than the surface element of the bucket at its contour. If we left the elliptic shape of the bucket unchanged even in this place, the jet would here enter with a stronger impact and the efficiency would notably decrease. Therefore, the outer part of the bucket must be cut according to the width of the jet.

Formerly, the shape of the notch was simply established in such a way that in the point A, where the jet first contacted the ridge was plotted the curve of the penetration of the cylinder of the jet with the surface of the bucket. This was done by passing the individual plane sections normal to the turbine axis through the jet and the bucket surface. Such a notch exhibits the property that all its points enter the jet simultaneously. First, partial layers of the jet are cut off and directed onto the surface of the bucket, while the remaining part of the jet strikes the preceding bucket. Then the ridge penetrates faster forward than the outer

points, whereby the cross sections of the jet which impinges on the preceding bucket assume, the longer the more, an unfavourable shape. Notches less deep farther from the leading part of the ridge are better suited, because they disperse the jet less in its splitting by the ridge of the bucket. The bucket first catches

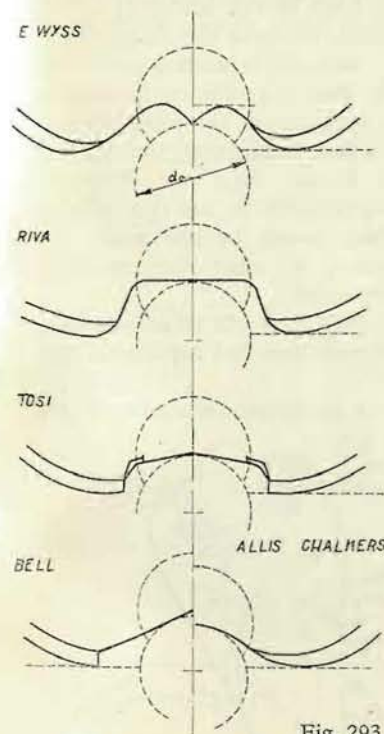


Fig. 293

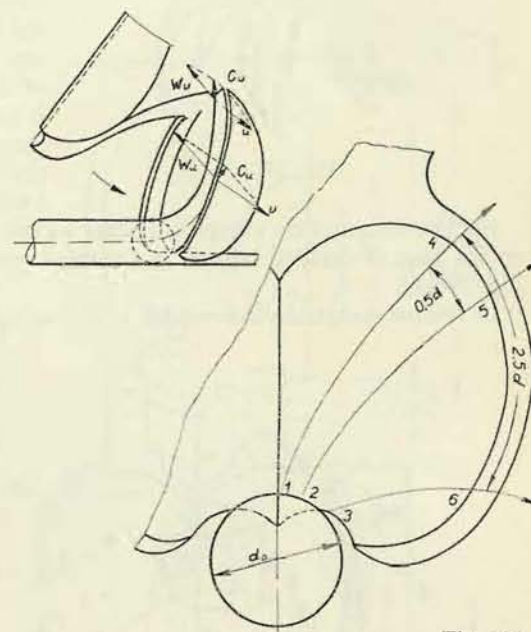


Fig. 294

the water particles which are further from the splitter and the latter enters the jet only later (Figs. 293 and 294).

The width of the notch must be larger than the diameter d_0 of the jet as we must take into account inaccuracies in the manufacture of the blades and in their mounting in relation to the centre line of the jet. It is recommended to make the width of the notch according to the formula

$$a = 1.2 d_0 + 5 \text{ mm.} \quad (235)$$

A principal rule for the design of the notches is that the water particles which are not retained by the edge of the notch should stream without obstructions and without any deflection onto the preceding bucket.¹⁾ This case is illustrated in

¹⁾ Thomann R.: Die Wasserturbinen und Turbinenpumpen, Part II, Stuttgart, K. Wittwer, 1931, p. 289.

Fig. 295, where e. g. in the position *I* the generatrix is created in conformity with the relative path pertaining to this position. When the notch is cut out according to this path, the water particle slides along the surface created in this way without pressure, and the jet is not deflected by the back of the blade. It is advantageous to have the shape of the notch designed in such a way that, in so far there is a sufficient air supply, the jet separates at the edge without any further contacting the surface of the bucket. As a rule, however, it is not possible to use this way as the blade would be too weak. For this reason, we must often resort to a compromise.

For the design of the complete bucket we can employ reference values obtained on the base of detailed layouts and verified by experiments and experience (see Fig. 296).¹⁾

In routine design the dimensions of the bucket are determined according to the

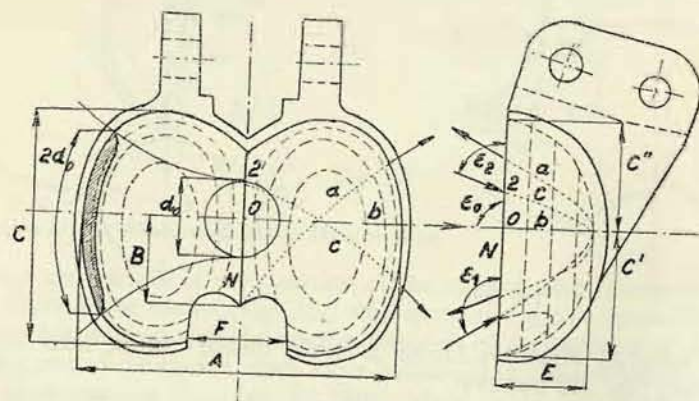


Fig. 296

diameter of the cross section of the jet, d_0 . The shape of the bucket is approximately defined by the following dimensions:

Length of the bucket $C \doteq 2.5 - 2.8$ times jet diameter

Width of the bucket $A \doteq 2.8 - 4.0$ times jet diameter

Depth of the bucket $E \doteq 0.95$ of the jet diameter.

¹⁾ Kieswetter: Vodní stroje lopatkové (Hydraulic Turbomachinery), Part I, Brno, 1939, p. 19.

Fig. 297 illustrates four examples of bucket shapes which are at present mostly used. The size of the buckets has no influence upon the magnitude of the maximum efficiency but only on the progress of the efficiency. Small buckets give the maximum efficiency at lower flow-rates, larger buckets at higher flow-rates (Fig. 298).

The stream on the bucket surface flattens and toward the discharge widens to such an extent that its width on the outlet edge amounts to about double the jet

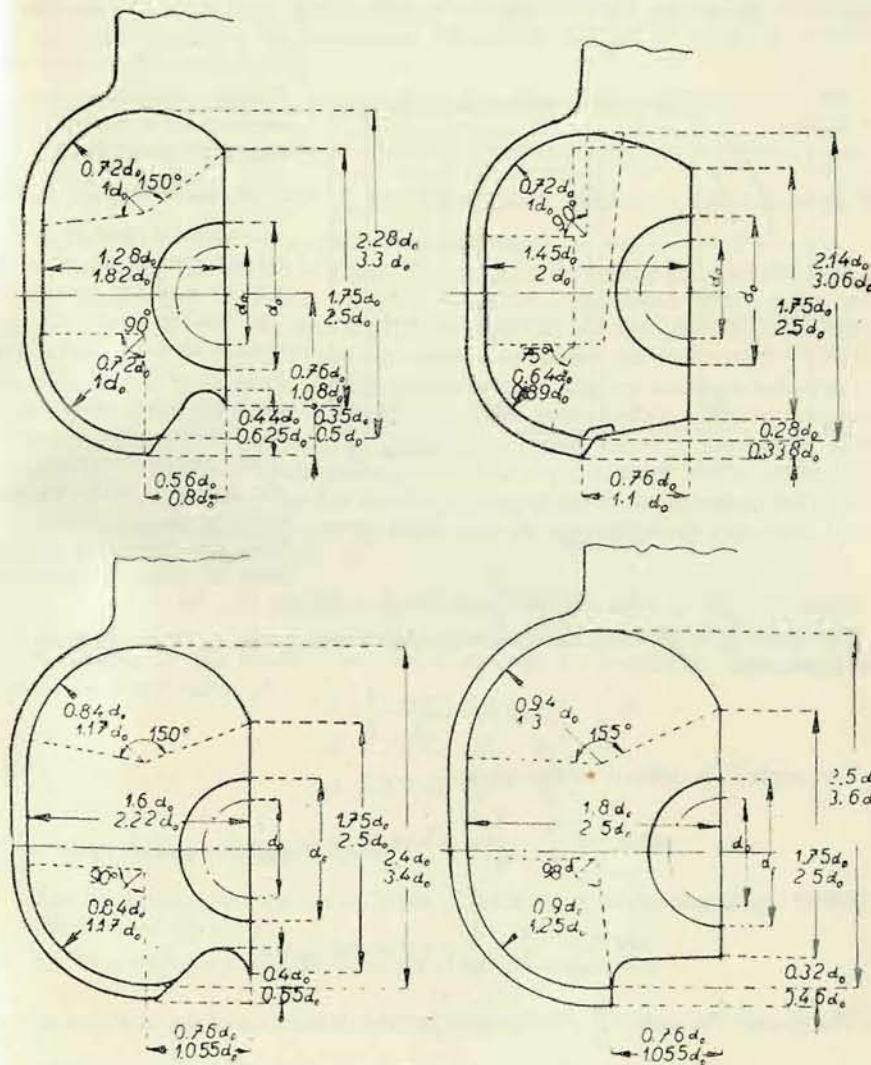


Fig. 297

diameter ($S = 2d_0$) and even more. Looked at in the peripheral direction, the path of the flow appears at the beginning of the entrance of the blade into the jet, when the angle ε is greater than 90° , approximately in conformity with the line a , in its further progress, when ε equals 90° , as indicated by the line b , and at the end of the entrance of the bucket into the jet, when ε is less than 90° , in conformity with the line c (Fig. 296). The paths of the flow along the bucket are the more scattered, the greater the distance of the end of the ridge from the innermost filament of the jet is; for this reason, the distance of the point O (where the jet

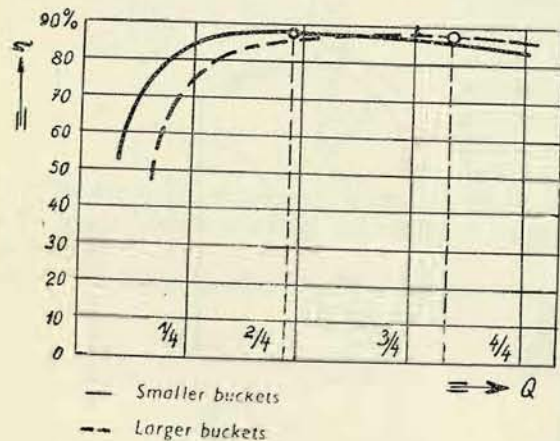


Fig. 298

Angle $\gamma = 90^\circ - \varepsilon$ for $\varepsilon < 90^\circ$, and $\gamma = \varepsilon - 90^\circ$ for $\varepsilon > 90^\circ$.

The angle β_s is given by the constructional values l_0 and s_0 , interconnected by the expression

$$\tan \beta_s = \frac{s_0}{2} \cdot \frac{1}{l_0}.$$

The angle β'_s is defined by the relation

$$\tan \beta'_s = \frac{s_0}{2} \cdot \frac{1}{l'_0}, \text{ where } \beta'_0 = l_0 \frac{1}{\cos \gamma},$$

whence

$$\tan \beta'_s = \frac{s_0}{2} \cdot \frac{1}{l_0} \cos \gamma = \tan \beta_s \cos \gamma.$$

The greater the ratio $\frac{d_0}{D}$, the greater are the deflections of the direction of the onflowing stream (given by the angle γ) from a perpendicular approach. Therefore,

strikes the ridge perpendicularly) from the beginning of the ridge is made according to the formula

$$B = (0.9 \text{ to } 1.2) \cdot d_0.$$

Further it must be pointed out that at an oblique approach of the stream to the leading edge of the bucket also the inlet angle β_s (Figs. 274 and 275) in the plane x perpendicular to the leading edge changes. This angle decreases to the angle β'_s with an increasing angle γ which defines the deflection of the inlet jet into the plane x .

we pay attention to the magnitude of $\frac{d_0}{D}$ and select

$$\frac{d_0}{D} = \frac{1}{16} \text{ to } \frac{1}{14} \text{ for current cases of normal design,}$$

$$\frac{d_0}{D} = \frac{1}{10} \text{ to } \frac{1}{6} \text{ for extreme cases of very carefully and specially designed buckets.}$$

Sometimes, the ratio $\frac{d_0}{D}$ is also taken according to the relation $d_0 = \frac{75 D}{1000} + 5 \text{ mm}$, where D is given by the selected speed and the given peripheral velocity.

If for the given case the ratio $\frac{d_0}{D}$ assumes a higher magnitude than indicated, two or more inlet nozzles are employed for one wheel.

In designing the bucket it is also important to determine the magnitude of the outlet blade angle β_2 , which is smaller than the actual mean value of the outlet angle β_2^+ , because the flattened stream converges at the discharge from the bucket under the angle δ (Fig. 277) and its central jet proceeds under the angle β_2^+ , which is greater than the angle of its outermost filament with the inclination β_2 . For this reason, we must design the discharge end of the guide surface of the bucket under a smaller angle β_2 - corrected or exaggerated - than the calculated angle of the stream β_2^+ . This leads to the consequence that the discharge loss at lower loads, when the angle of flattening δ is smaller, is comparatively smaller than at full load.

The correction of the discharge angle may be approximately expressed by the relation

$$\beta_2^+ - \beta_2 = 15^\circ \frac{d_0}{A} = \Delta\beta.$$

According to this formula we can determine the correction of the angle for various bucket widths A :

$$A = 2.8 d_0, \Delta\beta = 5\frac{1}{2}^\circ,$$

$$A = 3.5 d_0, \Delta\beta = 4\frac{1}{3}^\circ,$$

$$A = 4.0 d_0, \Delta\beta = 3\frac{3}{4}^\circ.$$

6. Force Acting upon the Bucket

The bucket is subjected to two kinds of forces, i. e. to the centrifugal force and to the force of the jet.¹⁾

1. The centrifugal force acts radially and has the magnitude

$$O = \frac{G}{g} \frac{U^2}{R}, \quad (236)$$

¹⁾ Thomann R.: Die Wasserturbinen und Turbinenpumpen, Part II, Stuttgart, K. Wittwer, 1931, p. 290

where G is the weight of the bucket, U the peripheral velocity, R the radius of the centre of gravity of the bucket, including the ribs and the fastening lugs.

As a rule, the centre of gravity is located approximately on the pitch circle D , and we can determine the centrifugal force O with sufficient accuracy from the equation

$$O = \frac{2 G u_1^2}{g D} 2 g H = \frac{4 G H u_1^2}{D} \quad (237)$$

When at normal speed the specific velocity is $u_1 = 0.45$, the centrifugal force amounts to

$$O = 0.8 \frac{G H}{D},$$

and for an arbitrary speed

$$O = 0.8 \frac{G H}{D} \left(\frac{n}{n_n} \right)^2 \quad (238)$$

At the runaway speed, which is about double the normal speed, the centrifugal force assumes the highest value:

$$O_{\max} = (3 \text{ to } 3.2) \frac{G H}{D} \quad (239)$$

It is clear that for the blocked wheel the centrifugal force equals zero. Since the speed does not vary considerably during operation, we may assume the load of the blade by the centrifugal force to be static.

2. *The force of the jet.* The force of the jet acts in the tangential direction and its magnitude is given by the impulse equation

$$P_0 = \frac{\gamma Q}{g} (C_{u0} - C_{u2}) \quad (240)$$

P_0 acts at the radius $\frac{D}{2}$, and here we assume that the water particles are not led away in the plane normal to the turbine axis. If we want to determine the force acting upon one bucket, we cannot take Q as the flow-rate of the turbine but must introduce the quantity corresponding to one blade. We may write

$$Q_{bl} = Q \frac{W_0}{C_0} = Q \frac{C_0 - U_1}{C_0} = \frac{\pi}{4} d_0^2 c_0 \frac{c_0 - u_1}{c_0} \sqrt{2 g H},$$

and into Equation (240) we substitute: $C_{u0} = c_0 \sqrt{2 g H}$;

$$C_{u2} = [u_1 - (c_0 - u_1) \cos \beta_2] \sqrt{2 g H}.$$

The discharge angle β_2 is so small that we may put $\cos \beta_2 = 1$. We obtain

$$P_0 = \frac{\gamma}{g} \frac{\pi}{4} d_0^2 (c_0 - u_1) [c_0 - (u_1 - c_0 + u_1)] \sqrt{2 g H} = \gamma H \pi d_0^2 (c_0 - u_1)^2 \quad (241)$$

in the specific values, or expressed in the actual values

$$P_0 = \frac{\gamma}{g} \frac{\pi d_0^2}{4} 2 (C_0 - U_1)^2 \quad (242)$$

The maximum value is attained at $U_1 = 0$, i. e. with the wheel blocked, and amounts to

$$P_{0 \max} = \gamma H \pi d_0^2 c_0^2 = 4 P_0.$$

At the runaway speed, the force of the jet equals zero.

The total stress of the buckets is composed of the stresses resulting from the action of both forces. The maximum stress is encountered either with the wheel blocked or at the runaway speed. Therefore, we must calculate the stress for both these cases, as well as for the case of normal speed. When ascertaining the influence of both forces, we must bear in mind the difference in their character. Whilst the stress resulting from the centrifugal force may be considered static, the stress exerted by the force of the jet changes very rapidly with time. For instance, the progress of the forces acting upon the blades of a turbine with two nozzles operating under a head of 360 m is illustrated by the diagram in Fig. 299. We have here a pulsating stress, not proceeding from the maximum value to zero and back again; it is an alternating stress. That is to say that the bucket after leaving the jet – under the influence of its own inertia – is deflected to the side opposite to that deflected by the load from the jet, so that in it a stress of the same magnitude but opposite sign arises.

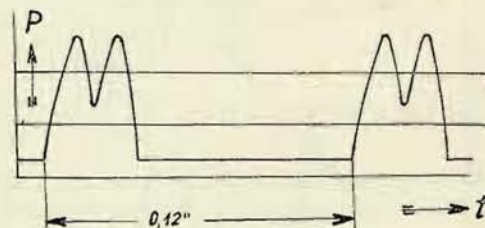


Fig. 299

We must also be aware of the fact that the fatigue strength of steel is in the presence of water reduced to about half the normal value; therefore, even for cast steel buckets we shall not admit a stress exceeding about 200 to 300 kg/cm².

The resistance of the blade against fatigue is materially impaired by small cracks caused by machining. For this reason, we must very thoroughly control the blade prior to machining, as well as after this operation. The control must be mainly directed to arising cracks on the edge and notch of the bucket. Detected cracks must be fully bored out and the attacked places restored by welding.

Example (see Fig. 300):

The calculation is carried out for two positions of the bucket.

a) Position K, when the bucket is for the first time subjected to the full action of the jet.

b) Position N, in which the bucket is for the last time subjected to the full action of the jet, and further for three speeds under the highest head:

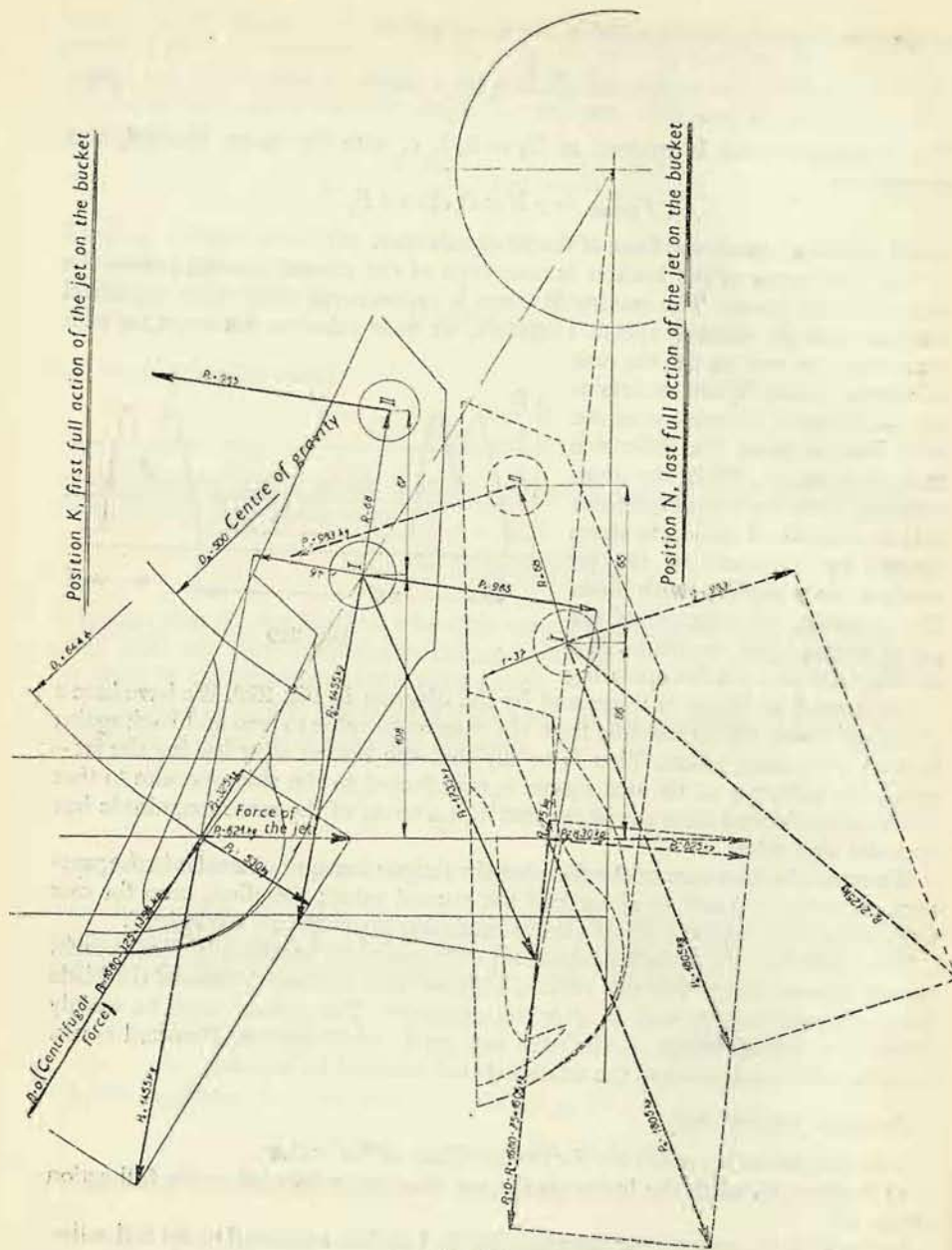


Fig. 300

1. Normal speed ($n = 1000$ r. p. m.);
2. Runaway speed ($n_p = 1800$ r. p. m.);
3. With the wheel fully blocked ($n = 0$ r. p. m.).

The stress is caused by the centrifugal force and the force of the jet.

The centrifugal force is taken up by the outer bolt as through it passes the connecting line between the centre of gravity and the centre of the wheel.

a) Calculation of the forces in position K.

1. At normal speed, $n = 1000$ r. p. m.

We assume that the force of the jet acts in the intersection with the centrifugal force, i. e. at the diameter $D = 0.644$ m; then holds good:

$$U_1 = \frac{0.644 \cdot \pi \cdot 1000}{60} = 33.7 \text{ m/sec.},$$

$$C_0 = 64.6 \text{ m/sec.},$$

$$P_0 = \frac{\gamma}{g} \frac{d_0^2 \pi}{4} 2 (C_0 - U_1)^2 = \frac{1000}{9.81} \cdot \frac{0.0637^2 \pi}{4} 2 (64.6 - 33.7)^2 = 612 \text{ kg.}$$

The force of the jet is resolved into the direction of U_1 and into the direction of the connecting line with the centre, i. e. into the forces $P_1 = 530$ kg and $P_2 = 325$ kg respectively.

Against the force P_2 acts the centrifugal force created by the weight of the bucket, $G = 6$ kg, at the centre of gravity lying at the diameter $D_t = 500$ mm ($R = 0.25$ m), whose peripheral velocity is

$$U_t = \frac{\pi D_t n}{60} = \frac{0.5 \pi \cdot 1000}{60} = 26.2 \text{ m/sec.}$$

The centrifugal force amounts to

$$O = \frac{GU_t^2}{gR} = \frac{6 \cdot 26.2^2}{9.81 \cdot 0.25} = 1680 \text{ kg,}$$

whence we obtain $P_3 = O - P_2 = 1355$ kg.

The resultant force P_4 then is $P_4 = \sqrt{P_3^2 + P_1^2} = \sqrt{1355^2 + 530^2} = 1455$ kg. P_4 acts in the centre of the bolt I at the radius $r = 46$ mm. If we select the centre of I as the moment centre, the moment of the force P_4 exerts in the centre of the bolt II, at the radius $R = 68$ mm, the force

$$P_5 = \frac{P_4 r}{R} = \frac{1455 \cdot 46}{68} = 985 \text{ kg.}$$

The forces P_4 and P_5 give in the centre of I the resultant force $P_6 = 1735$ kg.

At normal speed, the pin I is subjected to stress by the force $P_6 = 1735$ kg, and the pin II by the force $P_5 = 985$ kg.

2. At the runaway speed $n_p = 1800$ r. p. m.
The data are the same as in the preceding calculation.

$$U_p = \frac{0.644 \cdot \pi \cdot 1800}{60} = 60.7 \text{ m/sec.},$$

$$C_0 = 64.6 \text{ m/sec.}$$

The force of the jet equals

$$P_{0p} = \frac{\gamma}{g} d_0^2 \frac{\pi}{4} 2 (C_0 - U_p)^2 = \frac{1000}{9.81} \cdot \frac{0.0637^2 \cdot \pi}{4} \cdot 2 (64.6 - 60.7)^2 = 99 \text{ kg.}$$

The force of the jet is insignificant and may therefore be disregarded. Theoretically, it equals zero, the jet flies freely through the runner. The force is just great enough to overcome the friction losses in the bearings and the losses resulting from the ventilation of the runner and the rotor of the generator. The bucket then is acted upon only by the centrifugal force at the peripheral velocity of the centre of gravity:

$$U_{pt} = \frac{D_t n_p \pi}{60} = \frac{0.5 \cdot \pi \cdot 1800}{60} = 47.1 \text{ m/sec.}$$

The centrifugal force equals

$$O_p = \frac{G U_{pt}^2}{gr} = \frac{6 \cdot 47.1^2}{9.81 \cdot 0.25} = 5430 \text{ kg}$$

and is taken up by the pin *I*, in the pin *II* it is zero.

3. With the wheel fully blocked, $n = 0$ r. p. m.

$$U_1 = 0; C_0 = 64.6 \text{ m/sec.}$$

The force of the jet is

$$P_7 = \frac{\gamma}{g} \frac{d_0^2 \pi}{4} 2 (C_0 - U_1)^2 = \frac{1000}{9.81} \frac{0.0637^2 \pi}{4} 2 (64.6 - 0)^2 = 2720 \text{ kg.}$$

The pin *I* is acted upon by the force $P_8 = \frac{2720 \cdot 175}{67} = 7100 \text{ kg.}$

The pin *II* is acted upon by the force $P_9 = \frac{2720 \cdot 108}{67} = 4380 \text{ kg.}$

- b) Calculation of the forces in the position *N* (last full action of the jet on the blade):

1. At normal speed, $n = 1000$ r. p. m.

We assume again that the force of the jet acts in the intersection with the centrifugal force, i. e. at the diameter $D_3 = 0.552$ m; then holds good

$$U = \frac{0.552 \cdot \pi \cdot 1000}{60} = 28.9 \text{ m/sec.},$$

$$C_0 = 64.6 \text{ m/sec.}$$

The force of the jet equals

$$P_0 = \frac{1000}{9.81} \cdot \frac{0.0637^2 \pi}{4} \cdot 2 (64.6 - 28.9)^2 = 830 \text{ kg}$$

and is resolved into the components $P_1 = 825$ kg and $P_2 = 75$ kg.

The force P_2 is counteracted by the centrifugal force $O = 1680$ kg, and we obtain $P_3 = O - P_2 = 1680 \text{ kg} - 75 \text{ kg} = 1605 \text{ kg.}$

The resultant force then is

$$P_4 = \sqrt{P_1^2 + P_3^2} = \sqrt{825^2 + 1605^2} = 1805 \text{ kg.}$$

The force P_4 acts to the centre of the pin *I* at the radius $r = 37$ mm; the centre of *I*, selected as moment centre, gives in the centre of the pin *II* at the radius $R = 68$ mm the force

$$P_5 = \frac{P_4 r}{R} = \frac{1805 \cdot 37}{68} = 983 \text{ kg.}$$

The forces P_4 and P_5 give in the centre of *I* the resultant $P_6 = 2125$ kg.

The pin *I* is subjected to stress by $P_6 = 2125$ kg.

The pin *II* is subjected to stress by $P_5 = 983$ kg.

2. At the runaway speed $n_p = 1800$ r. p. m. The condition are the same as given in paragraph a/2.

3. With the wheel fully blocked, $n = 0$ r. p. m.

According to a/3 the force of the jet is $P_7 = 2720$ kg. The pin *I* is acted upon by the force $P_8 = \frac{2720 \cdot 145}{65} = 6070$ kg. The pin *II* is acted upon by the force

$$P_9 = \frac{2720 \cdot 80}{65} = 3350 \text{ kg.}$$

- c) Determination of the dimensions of the outer pin *I* (selected diameter 28 mm):

The pin is subjected to shearing stress, the load acts upon two cross sections.

1. Stress at normal speed:

Load in position *K*, $P_6 = 1735$ kg.

Load in position *N*, $P_6 = 2125$ kg.

The greatest force acting upon one cross section is $P = \frac{2125}{2} = 1063$ kg.

$$F = \frac{\pi \cdot 2.8^2}{4} = 6.16 \text{ cm}^2,$$

$$\tau = \frac{1063}{6.16} = 173 \text{ kg/cm}^2,$$

and with regard to the circumstance that the pin is at the same time subjected to bending stress,

$$\sigma = \frac{173}{0.8} = 216 \text{ kg/cm}^2,$$

the stress is within the permissible limits.

2. Stress at runaway speed:

Load in position K , $O_p = 5430 \text{ kg}$.

Load in position N , $O_p = 5430 \text{ kg}$.

The greatest force acting upon one cross section is $P = \frac{5430}{2} = 2715 \text{ kg}$.

$$F = 6.16 \text{ cm}^2,$$

$$\tau = \frac{2715}{616} = 442 \text{ kg/cm}^2,$$

$$\sigma = \frac{442}{0.8} = 525 \text{ kg/cm}^2.$$

The force is static and therefore these stresses are permissible.

3. Stress with the wheel fully blocked:

Load in position K , $P_8 = 7100 \text{ kg}$.

Load in position N , $P_8 = 6070 \text{ kg}$.

The greatest force acting upon the cross section equals $P = \frac{7100}{2} = 3550 \text{ kg}$.

$$F = 6.16 \text{ cm}^2,$$

$$\tau = \frac{3550}{6.16} = 576 \text{ kg/cm}^2,$$

$$\sigma = \frac{576}{0.8} = 720 \text{ kg/cm}^2.$$

The force is static and consequently these stresses, too, are permissible.

The material selected is steel exhibiting a strength of 60–70 kg/mm², or better with regard to fatigue and the importance of a reliable connection, steel Type Poldi having a strength of 80 kg/mm².

d) *Determination of the inner pin II (selected diameter 24 mm):*

The shearing stress acts again upon two cross sections.

1. Stress at normal speed:

Load in position K , $P_5 = 985 \text{ kg}$.

Load in position N , $P_5 = 983 \text{ kg}$.

The greatest force on one cross section

$$P = \frac{985}{2} = 492.5 \text{ kg acts upon the area}$$

$$F = \frac{\pi \cdot 2.4^2}{4} = 4.52 \text{ cm}^2, \text{ so that}$$

$$\tau = \frac{492.5}{4.52} = 190 \text{ kg/cm}^2,$$

$$\sigma = \frac{109}{0.8} = 136 \text{ kg/cm}^2.$$

2. Stress at runaway speed:

Load in position K , $P = 0$.

Load in position N , $P = 0$.

3. Stress with the wheel fully blocked:

Load in position K , $P_9 = 4380 \text{ kg}$.

Load in position N , $P_9 = 3350 \text{ kg}$.

The greatest force acting upon one cross section equals $P = \frac{4380}{2} = 2190 \text{ kg}$.

$$F = 4.52 \text{ cm}^2,$$

$$\tau = \frac{2190}{4.52} = 485 \text{ kg/cm}^2,$$

$$\sigma = \frac{485}{0.8} = 606 \text{ kg/cm}^2.$$

The material selected is steel of a strength of 60–70 kg/mm².

e) *Control of the pins for wear pressure:*

1. Wear pressure of the outer pin at normal speed:

Area of the pin in the blade, $F_{BI} = 2 \cdot 2.8 \cdot 2.6 = 14.5 \text{ cm}^2$,

$$d = 28 \text{ mm}, l = 26 \text{ mm}.$$

Greatest stress in position N : $P_6 = 2125 \text{ kg}$.

$p = \frac{2125}{14.5} = 147 \text{ kg/cm}^2$. The blade is made of cast steel having a strength of 52 kg/mm².

Plan area in the ring, $F_{RI} = 2.8 \cdot 4 = 11.2 \text{ cm}^2$, $p = \frac{2125}{11.2} = 192 \text{ kg/cm}^2$.
The ring is made of steel having a strength of 60–70 kg/mm².

2. Wear pressure of the outer pin at runaway speed:

Greatest stress in position $N = K$, $O_p = 5430 \text{ kg}$.

Wear pressure in the blade, $p = \frac{5430}{14.5} = 375 \text{ kg/cm}^2$.

Wear pressure in the ring, $p = \frac{5430}{11.2} = 485 \text{ kg/cm}^2$.

3. Wear pressure of the outer pin with wheel fully blocked:

Greatest load in position K , $P_s = 7100 \text{ kg}$.

Wear pressure in the blade, $p = \frac{7100}{14.5} = 490 \text{ kg/cm}^2$.

Wear pressure in the ring, $p = \frac{7100}{11.2} = 634 \text{ kg/cm}^2$.

4. Wear pressure of the inner pin at normal speed:

Plan area in the blade, $F_{BII} = 2 \cdot 2.4 \cdot 2.2 = 10.5 \text{ cm}^2$,

$$d = 24 \text{ mm},$$

$$l = 22 \text{ mm}.$$

Plan area in the hub, $F_{RII} = 2.4 \cdot 4 = 9.6 \text{ cm}^2$,

$$d = 24 \text{ mm}, l = 40 \text{ mm}.$$

Greatest load in position K , $P_s = 985 \text{ kg}$.

Wear pressure in the blade, $p = \frac{985}{10.5} = 94 \text{ kg/cm}^2$.

Wear pressure in the ring, $p = \frac{985}{9.6} = 103 \text{ kg/cm}^2$.

5. Wear pressure of the inner pin at runaway speed:

The load is taken up by the pin I .

6. Wear pressure of the inner pin II with the wheel fully blocked:

Greatest load in position K , $P_s = 4380 \text{ kg}$.

Wear pressure in the blade, $p = \frac{4380}{10.5} = 417 \text{ kg/cm}^2$.

Wear pressure in the ring, $p = \frac{4380}{9.6} = 655 \text{ kg/cm}^2$.

7. Control of the stem of the blade:

The greatest stress is encountered in sections I .

$H = 7.1 \text{ cm}$, $h = d = 2.8 \text{ cm}$, $B = 3 \text{ cm}$, 2 links,

$$W = 2 \cdot \frac{B \cdot (H^3 - h^3)}{6H} = 2 \cdot \frac{3 \cdot (7.1^3 - 2.8^3)}{6 \cdot 7.1} = 47.2 \text{ cm}^3,$$

$$M_0 = P_r l = 2720 \cdot 10.8 = 29,400 \text{ kgcm}.$$

$$\sigma_0 = \frac{29,400}{47.3} = 620 \text{ kg/cm}^2.$$

Since the load on the blocked turbine is static, these stresses are permissible. (The stems of the blade are made of cast steel having a strength of 52 kg/mm².)

III. OUTPUT REGULATION

1. Deflector and Deviator

The output of Pelton turbines is regulated as that of other turbine types by varying the flow-rate, and this is effected by closing or opening the mouth of the nozzle by means of a needle or spear. The prevention of an excessive increase of the speed, e. g. when the full through-flow is cut off, would require rather a rapid movement of the needle, that means that the needle would have to close the through-flow within a few seconds. Since, however, excessive pressure rises in the supply line must be avoided, the turbine would have to be equipped with a pressure regulator to discharge into the free space the same flow which has streamed through the turbine. This type of regulation was formerly employed and is still in use in America. In Europe, Pelton turbines are now generally constructed with double regulation. Single regulation is no longer employed as double regulation is simpler in construction and besides that, more reliable. The principle of the latter consists in a deflector or deviator, which is installed behind the mouth of the nozzle and rapidly enters the jet, deflects it from its path and directs it into the tail race. In this case, the closing action of the needle is gradual, so that no water hammer arises in the supply line. When the needle has closed the nozzle, the deflector moves out of contact with the jet. The deflector acts in such a way that it begins to cut off the jet from outside and therefore must cover a stroke equalling the diameter of the full jet in order to achieve complete deflection. The deviator, on the other hand, enters the jet from inside and requires only half the stroke for destroying the output as by dissipating the upper half of the jet also its lower half is scattered. At present, the deflector is mostly used as the regulation is more exact.

The problem of double regulation has also been solved in another way. For instance, Seewer installed movable ribs in the nozzle, and by their appropriate setting the jet was put into fast rotation, dispersing conically immediately behind the nozzle. A very small shift of the ribs was sufficient to scatter the jet and to reduce the output to nearly zero.

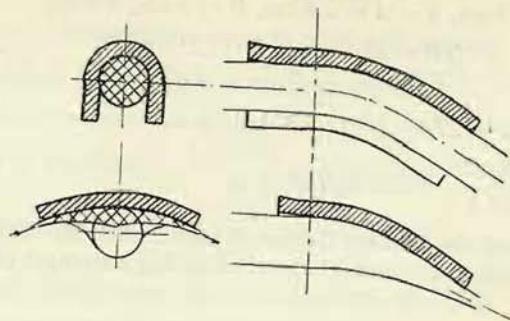


Fig. 301

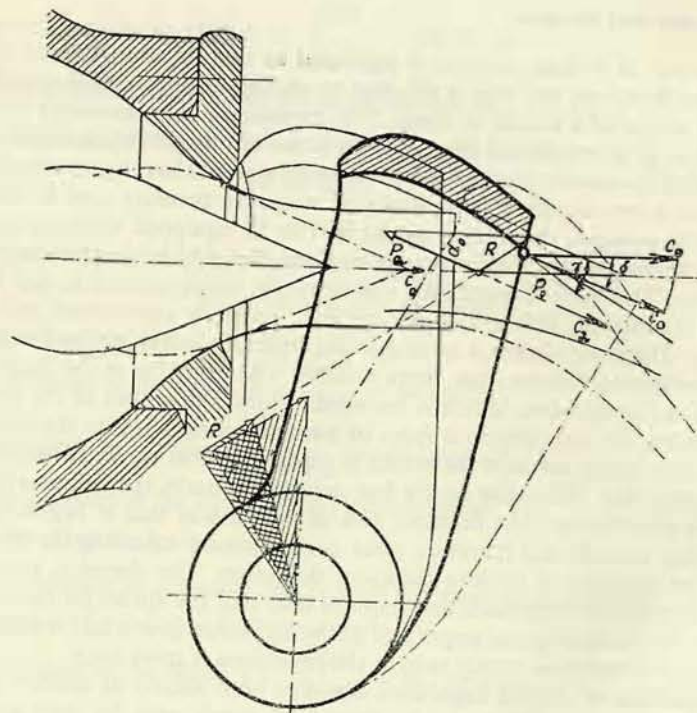


Fig. 302

A shortcoming of this arrangement was that the sealing of the pins in the space of the high pressure water was connected with difficulties, and further, that after a certain wear of the pins and increase of the lost motions in the regulating leverage, setting of the ribs into the axial plane of the jet was no longer ensured, so that the jet was not entirely compact and consequently its efficiency was impaired. Another design of this system was based upon oblique ribs mounted in the head of the needle. These ribs were shifted out and pulled in again. Of all these mentioned designs, double regulation by means of a deflector is at present mostly employed.

The force with which the retained jet acts upon the deflector depends to a considerable degree on its shape. Let us as-

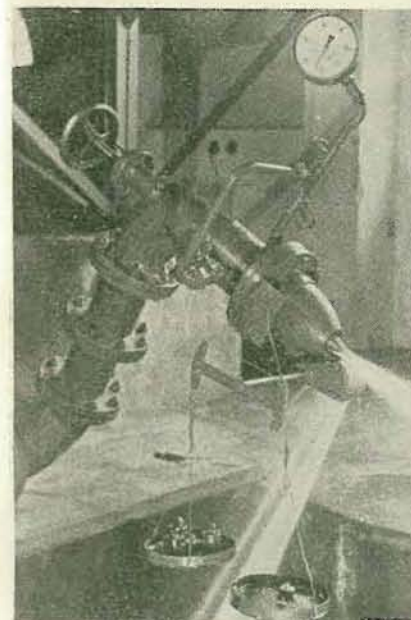


Fig. 303

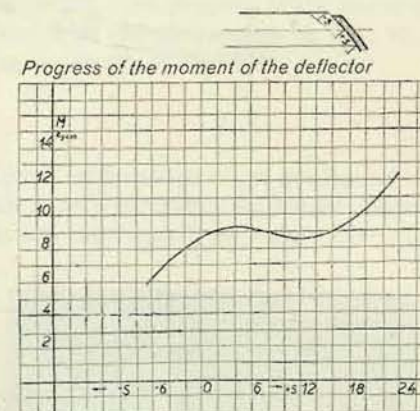


Fig. 304

sume that the deflector encompasses the jet so closely that the latter cannot spread toward the sides (Fig. 301). We may then assume that all water particles will be deflected to the same degree, retained in the direction of the jet axis at the velocity c_0 and deflected into the direction of the outlet tangent of the deflector. The force acting upon the deflector is then determined according to the momentum theorem (12).

The resultant R is then established graphically (Fig. 302). The moment is given by the resultant R and its perpendicular distance from the axis of rotation of the deflector. With a certain shape of the deflector and a certain position of its axis of rotation, the progress of the moment can pass through zero; that means that after covering a certain stroke, the deflector can be pulled into the jet. Such a progress is undesirable, because the lost motion in the leverage and in the deflector might

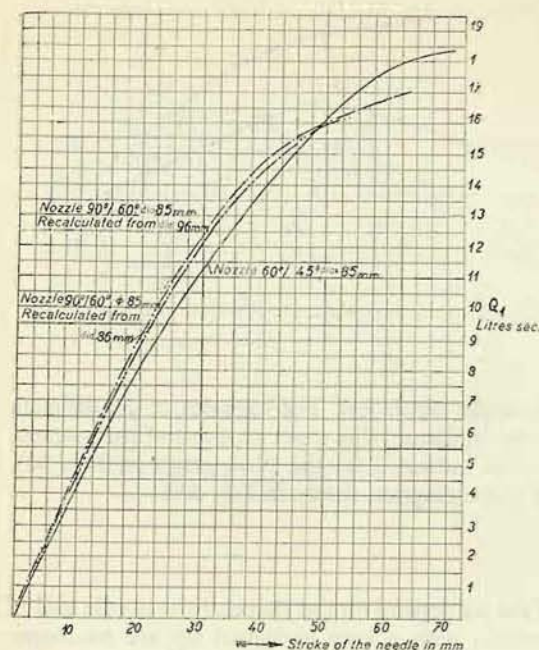


Fig. 310

are plotted in the diagram (Fig. 310). The deflector must always be close to the jet. When, for instance, it is required to reduce the output instantaneously from 100 % to 90 %, the regulator tilts the deflector, which cuts off the necessary portion of the jet and directs it into the discharge (Fig. 311). For the previously mentioned reasons, the needle closes the nozzle gradually, and the jet contracts until finally the deflector separates from it. The stroke of the deflector is derived from a slotted link, whose curvature is determined just by the dependence of the jet diameter on the stroke of the needle.

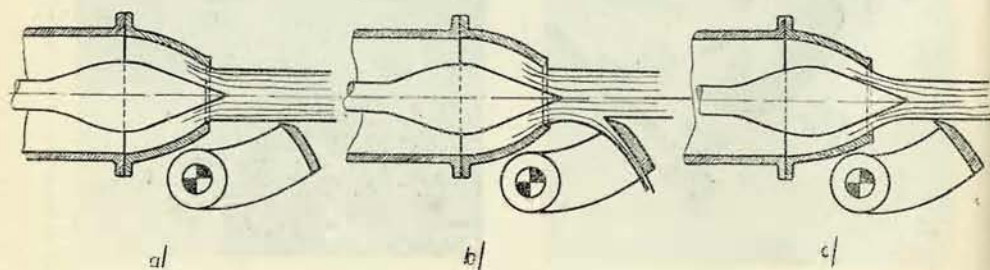


Fig. 311

needles of this type the jet is strongly contracted and the tip of the needle is subjected to considerable erosion. At present are generally used needles and nozzles with the angles $45^\circ/60^\circ$ (Fig. 306), or $60^\circ/90^\circ$ and $55^\circ/80^\circ$, the latter being in the literature considered best suited (Fig. 307). This shape of the conical needles and nozzles is more advantageous as the jet rapidly converges without being disturbed by the tip and the needle is less subjected to erosion.

The design of the regulating leverage (drive) of the deflector requires to know the diameter of the jet at various strokes of the needle. The measuring method is illustrated on the photographs (Figs. 308 and 309); the through-flows of the nozzles $45^\circ/60^\circ$ and $60^\circ/90^\circ$, ascertained at the same time,

The magnitude of the outlet cross section of the nozzle must be established in such a way¹⁾ that at the given head H it allows the given flow-rate Q to pass. The outlet cross section of the nozzle at the position of the needle according to Fig. 312 is given by the relation

$$F = \pi \frac{d_1 + d_2}{2} a,$$

where

$$a = \frac{d_1 - d_2}{2} \cdot \frac{1}{\sin \alpha}$$

and the flow-rate through the nozzle equals

$$Q = \mu \frac{\pi}{4} \frac{d_1^2 - d_2^2}{\sin \alpha} c_0 \sqrt{2gH}, \quad (243)$$

where μ is the efflux coefficient, depending on the design of the nozzle and usually being $\mu = 0.8$ to 0.88 ; this coefficient depends on the angles φ and ψ and on the magnitude of the nozzle opening, as it is evident from the diagram in Fig. 314. As a rule, the needle opens the nozzle to such an extent that at the maximum opening z_{\max} applies $d_2 = \frac{d_1}{2}$ (or somewhat more), whence follows the maximum through-flow for F

$$F = \frac{\pi}{4} \left[d_1^2 - \left(\frac{1}{2} d_1 \right)^2 \right] = 0.75 \frac{\pi}{4} d_1^2,$$

$$Q = \mu \frac{\pi}{4} d_1^2 \cdot 0.75 c_0 \sqrt{2gH} \cdot \frac{1}{\sin \alpha} = \mu 2.66 \cdot d_1^2 c_0 \sqrt{H} \cdot \frac{1}{\sin \alpha} \quad (244)$$

$$d_1 = \sqrt{\frac{Q \cdot \sin \alpha}{2.66 \mu \cdot c_0 \sqrt{H}}}. \quad (245)$$

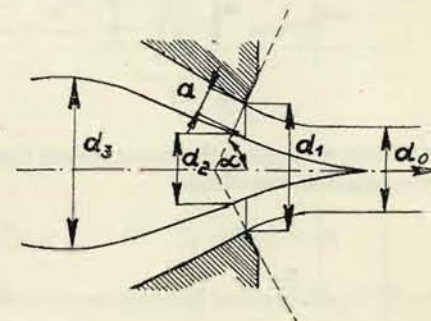


Fig. 312

3. Forces Acting upon the Needle

For designing the drive of the needle, we must know the forces with which the water flow acts upon the needle. First we must know the forces resulting from the pressure of the water, and then we determine the external forces so as to achieve mutual counterbalancing of the forces of the water pressure to greatest possible extent, i. e. the least possible magnitudes of the regulating work and of the regulator size. In the open position of the needle the resultant force of the water pressure consists of two parts, which we can assume to be distributed approximately within

¹⁾ Kieswetter: Vodní stroje lopatkové (Hydraulic Turbomachinery), Part I, Brno, 1939, p. 36.

the largest diameter of the needle, d_{\max} .¹⁾ In the region between this diameter and the passage of the rod of the needle through the stuffing box, the water has an almost uniform and comparatively low velocity. We may consider the pressure in this section as being approximately constant and proportional to the head. On the front part of the needle, the pressure varies continuously from the diameter d_{\max} to the tip. The pressure p_x at an arbitrary radius r_x from the axis is easily ascertained as follows: We draw the perpendicular to the stream lines from the latter to the nozzle (Fig. 313), measure the length of this perpendicular (a) and the diameter d_x on which its centre of gravity lies, and then we find the through-flow area $f = \pi d_x a_x$ and calculate the mean velocity:

$$C_x = \frac{Q}{\pi d_x a_x} = \frac{\frac{\pi}{4} d_0^2 C_0}{\pi d_x a_x} = \frac{d_0^2}{4 d_x a_x} C_0.$$

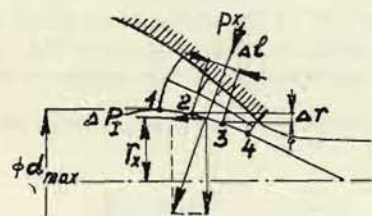


Fig. 313

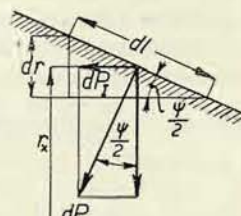


Fig. 314

When we neglect the losses arising from the inlet cross section to the point under examination, we obtain:

$$p_x = \gamma H - c_x^2 \gamma H = (1 - c_x^2) \gamma H = \left[1 - \left(\frac{d_0^2}{4 d_x a_x} \right)^2 c_0^2 \right] \gamma H,$$

or, if we assume that approximately applies $c_0 = 1$,

$$p_x = \left[1 - \left(\frac{d_0^2}{4 d_x a_x} \right)^2 \right] \gamma H.$$

The component of the axial force (Fig. 314) created by this pressure and acting upon the surface differential of the length dl equals

$$dP_I = 2 \pi r_x dl p_x \sin \frac{\psi}{2},$$

or, since $dl \sin \frac{\psi}{2}$ equals dr ,

$$dP_I = 2 \pi (r_x p_x) dr.$$

¹⁾ Thomann R.: Die Wasserturbinen und Turbinenpumpen, Stuttgart, K. Wittwer, 1931, p. 314.

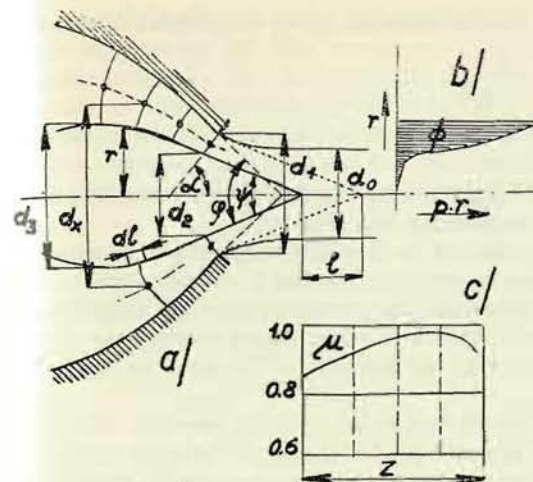


Fig. 315

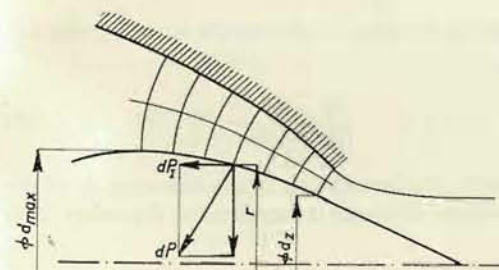


Fig. 316

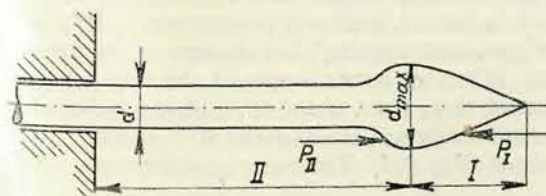


Fig. 320

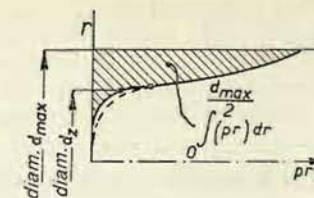


Fig. 317

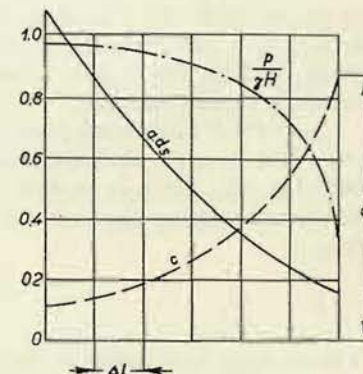


Fig. 318

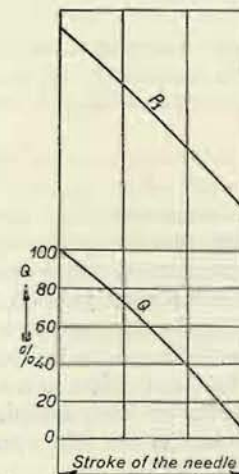


Fig. 319

The total force acting upon the needle from the tip to the largest diameter equals

$$P_I = 2\pi \int_0^{\frac{d_{\max}}{2}} (p_x r_x) dr. \quad (246)$$

The integral is easily determined graphically by plotting the product $p_x r_x$ as function of r_x and measuring the corresponding area (Fig. 315).

In general, the progress of the pressure can be calculated according to Equation (246) only for the outlet area itself. But we further know that $p_x r_x$ must equal zero in the axis of the jet. Therefore, we can delimit the corresponding small part of the area of $p_x r_x$ rather exactly by the transition curve which passes through the zero point. In Figs. 316 to 319, these forces are ascertained for the same needle and nozzle at various openings.

To the just established force P_I , which acts in the opening direction, further comes the force P_{II} along the section from the head of the needle up to the stuffing box (Fig. 320). Since we may here assume the pressure being constant, the force P_{II} acting in the closing direction, equals, d being the diameter of the rod in the stuffing box,

$$P_{II} = \frac{\pi}{4} (d_{\max}^2 - d^2) \gamma H. \quad (247)$$

The resultant force acting in the opening direction of the needle is then given by:

$$P = P_I - P_{II} = 2\pi \int_0^{\frac{d_{\max}}{2}} (p_x r_x) dr - \frac{\pi}{4} (d_{\max}^2 - d^2) \gamma H. \quad (248)$$

When the nozzle is completely closed, the pressure up to the diameter d_1 of the throat is constantly γH , and in back of this diameter it equals zero; Equation (248) thus assumes the simpler form:

$$P = -\frac{\pi}{4} (d_1^2 - d^2) \gamma H.$$

The magnitude of the force depends exclusively upon the position of the needle, i. e. only upon the progress of the force P_I on the head of the needle. By calculation or measurements we can establish the following progress of the forces: When the nozzle is completely closed, the needle is pressed, as already pointed out, by a force equalling the pressure on the area of the nozzle opening¹⁾ less the area of the cross section of the rod in the stuffing box. When the nozzle is opened, the force acting upon the needle rises to a small extent, then, from about 10 % of the stroke of the needle, the force diminishes almost linearly and attains about 40 % of its initial magnitude for the fully opened position (Fig. 321). The water pressure acts upon

¹⁾ Meissner L. & Rudert M.: Einige Konstruktionsmerkmale neuzeitlicher Grossfreistrahlturbinen, Wasserkraft und Wasserwirtschaft, 38, 1943, p. 153.

the needle during the entire stroke with a force which only tends to close the nozzle, and overcoming this force would require great regulating forces. Practically, the linear progress of the forces permits to reduce the shifting forces considerably by means of a counterbalancing device and to lessen the regulating work to a fraction of its initial value, or to a fraction of the work required for a Francis turbine of the same output. Fig. 321 shows the progress of the forces in an arrangement with a relief piston which is acted upon by a force equalling about half the maximum

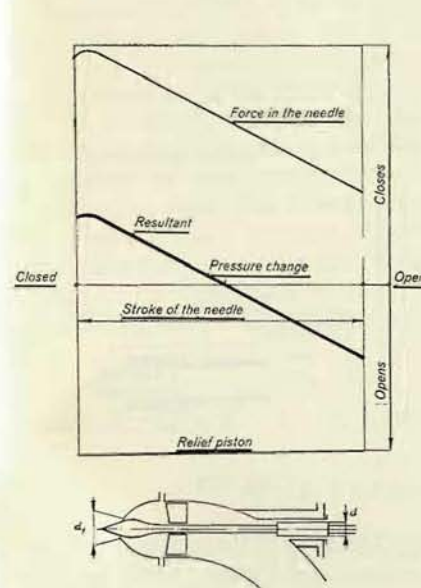


Fig. 321

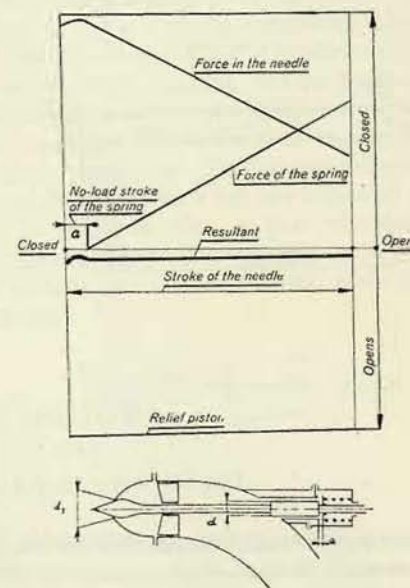


Fig. 322

force acting upon the needle. Both forces give a resultant which equals about 30 % of the greatest force and tends to close when the nozzle is closed; on the other hand, when the nozzle is fully opened, the force tends to open with about the same intensity. The force which we demand from the regulator is considerably smaller, and approximately in the middle of the stroke the needle is balanced. This device is entirely sufficient for smaller turbines. We can achieve a considerably more efficient counterbalancing of the forces if we load the relief piston with a helical spring in such a way that this spring is most compressed when the nozzle is open, and relieved shortly before the closure of the nozzle (see Fig. 322).

Now let us consider this arrangement in which the relief piston, in contradistinction to the preceding case, is so large that its force on the shank of the needle for opening somewhat exceeds the force of the needle tip in the closing cycle. For this purpose, the force of the helical spring is selected so that in the fully opened position it

equals approximately the difference between the opening force of the relief piston and the closing force of the needle in this position. The resultant will then exhibit

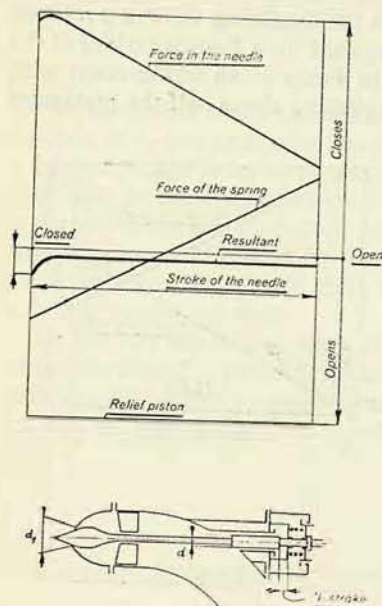


Fig. 323

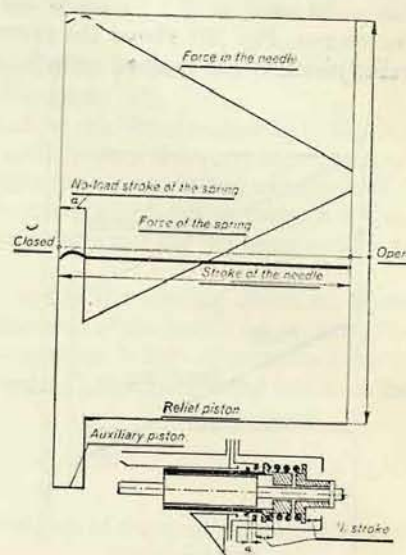


Fig. 325

only a very small force, as indicated in Fig. 322. The work of the regulator will consequently be very small, even if we take into account the friction, which has been neglected in all the respective figures. The possibility of utilizing this relief system is unfortunately very much restricted by manufacturing considerations as the springs must be extraordinarily strong; a balancing system of this type is therefore feasible only for turbines of medium size. The great forces of the springs are here indispensable owing to the size of the relief piston.

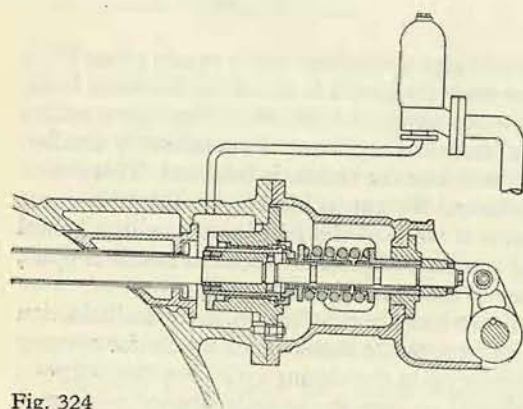


Fig. 324

More convenient dimensions of the springs are possible when the latter are arranged in such

a way that in the closed position they develop an opening force, that they are relieved in the middle of the stroke of the needle, and finally, that in the fully opened position they develop a closing force (Fig. 323).

Here, a considerably smaller piston will suffice in comparison with the disposition shown in Fig. 321, as follows from the resultant created by the force in the needle and the force of the spring. Only within the first 10 % of the stroke, the resultant exhibits a very objectionable peak, which did not appear in the preceding design. This undesirable force at the beginning of the stroke can be eliminated by an arrangement in which, in addition to the relief piston, during the initial part of the stroke there is a ring piston effective; this latter piston is with the proceeding stroke of the needle retained by a stop and thus put out of action, while the smaller (relief) piston continues in his travel. Fig. 324 shows the design, and Fig. 325 the progress of the forces and the resultant. This double-piston system has given very good results in large machines. The described balancing device permits to employ a regulator of normal size even in the largest installations. In dimensioning the regulator, however, the forces resulting from friction, which are not indicated in the diagrams, must be taken into account. In large machines, in particular those with more than one nozzle, the regulation is arranged in such a way that the servomotor for the drive of the needle is placed directly on the needle shank, while the distributing slide valve is located in the regulator.

B. ACTUAL DESIGN

I. FRANCIS OR PELTON?

Advancing research has resulted in a steadily extending application of the individual types of hydraulic turbines. A Kaplan turbine works now under a head of about 60 m, and a Francis turbine has already been constructed for a head of about

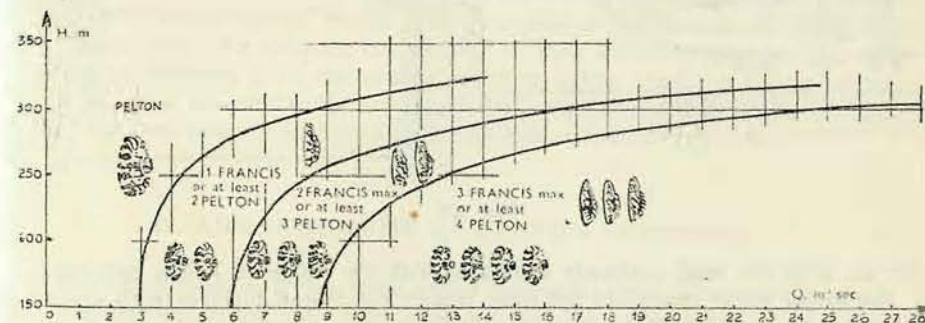


Fig. 326

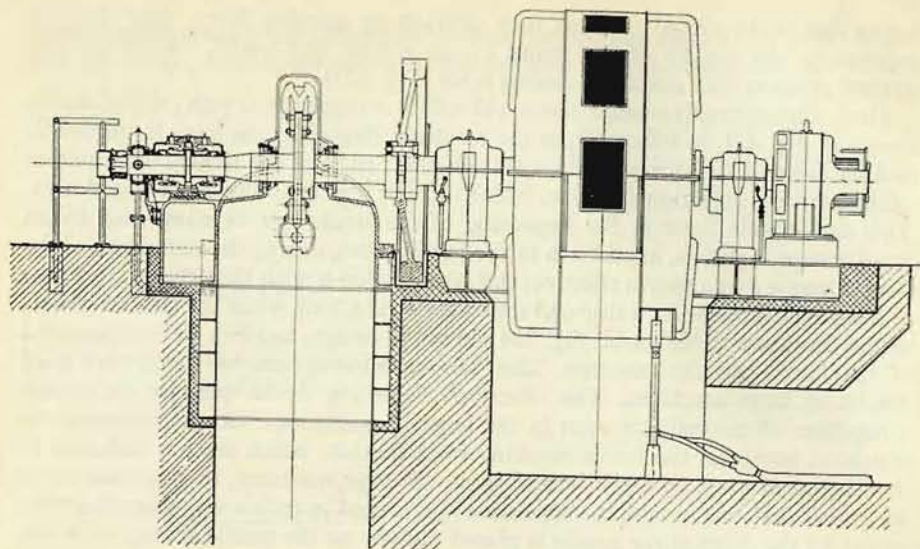


Fig. 327

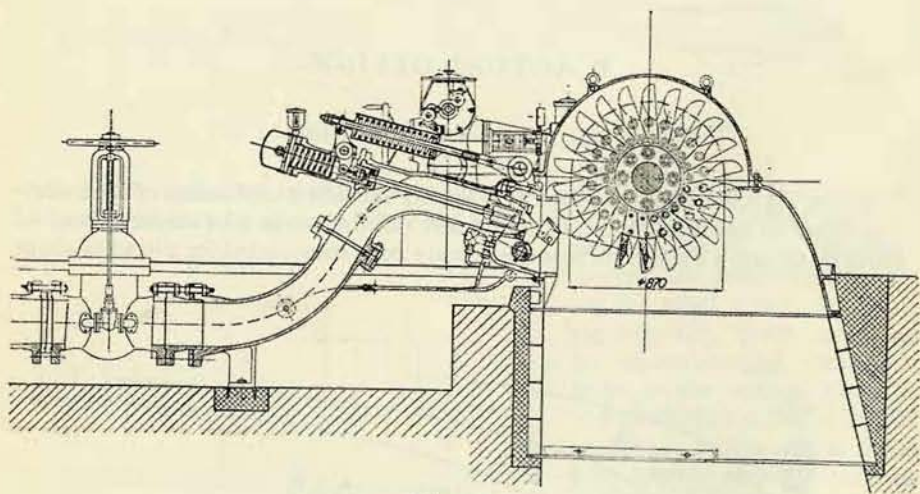


Fig. 328

400 m. With this head it already interferes with the range of Pelton turbines.¹⁾

For larger water quantities we must design the Pelton turbines with several wheels and a greater number of nozzles. In laying out power stations we must pay

¹⁾ Puyo M. A.: Francis ou Pelton, La Houille Blanche, 1949, No. 4.

attention to installation possibilities, i. e. we must take into account the erection of the plant, the operating conditions and the first costs. Concerning installation possibilities we must be aware of the fact that a Francis turbine for such a high head requires with regard to cavitation a negative suction head, which means higher building costs. The operating conditions must be judged with regard to water supply and stability of the water level. Pelton turbines have in the

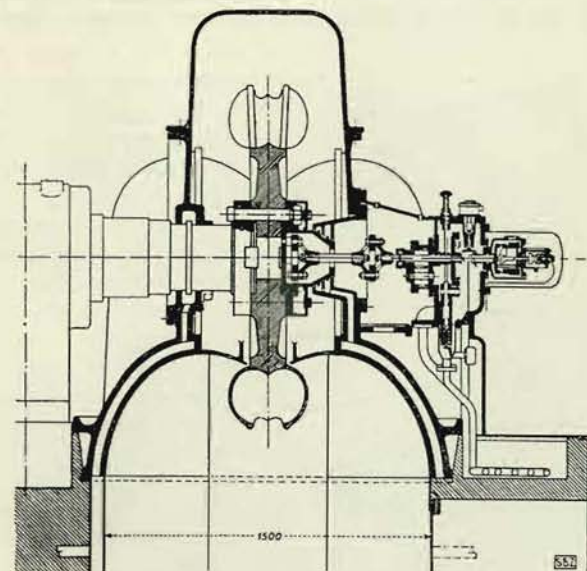


Fig. 329

case of variable flow-rate a flatter progress of the efficiency curve and are consequently advantageous where level fluctuations are encountered. On the other hand, when we compare the weights of both turbine types, we see that the Francis turbine, in the same conditions lighter than the Pelton wheel. When all these circumstances are considered, the application of both types within the same range is indicated in the diagram shown in Fig. 326.

II. ARRANGEMENT OF PELTON TURBINES

Pelton turbines are as a rule made with a horizontal shaft. The simplest case is that with one nozzle and one wheel (Figs. 327 and 328). The turbine shaft is here seated in one bearing and the other bearing is for the generator, or the runner may be fastened in an overhung position on the generator shaft (Fig. 329).

The disposition with one wheel and two nozzles (Fig. 330) is used for greater outputs and for increasing the specific speed of the turbine. A vertical arrangement (Fig. 331) is advantageous from the viewpoint of construction and permits a simple design with more than one nozzle. With this disposition it is possible to attain a specific speed n_s of 60 r. p. m. and even more. The maximum number of nozzles is selected as follows: Two for horizontal turbines, and four to six for vertical turbines.¹⁾ In this case, attention must be paid to the requirement that the bucket should enter the next jet only after the water from the preceding has run out.

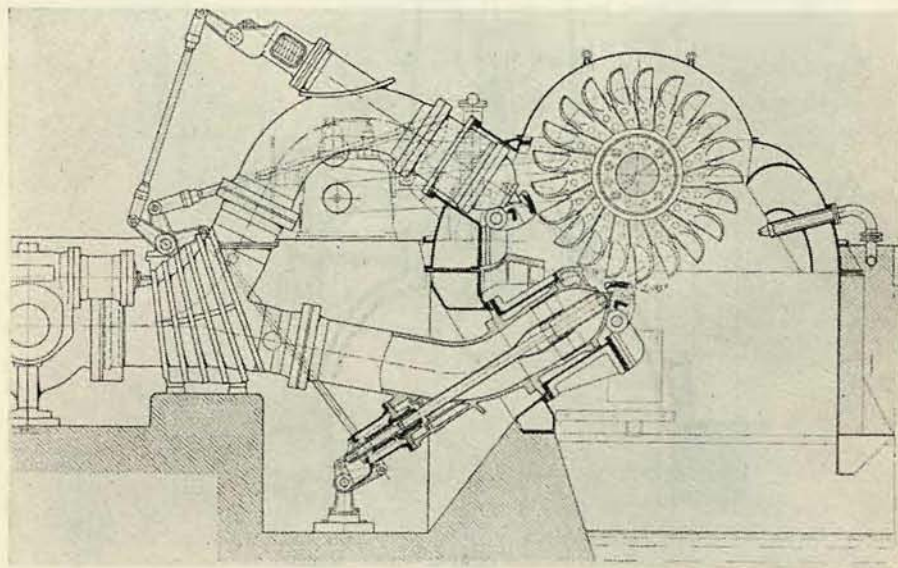


Fig. 330

III. PARTS

1. Casing

The casing of the Pelton turbine has not only the function of collecting and leading away the water which discharges from the wheel, but in some cases it also must take up the reaction of the nozzles. In the places projecting above the ground, the casing is as a rule made with such a wall thickness as is required by casting technique. In the axis of the wheel, the case is split so that after removal of the top cover the runner is accessible. In the place of contact between the jet and the wheel, the width of the casing should equal 12 to 18 jet diameters and that of the upper

¹⁾ Boyle, White: 62,000 HP Vertical Six Nozzle Impulse Turbines for the Bridge River Hydrodevelopment, ASME, 1952, p. 289.

cover 3 to 5 jet diameters. In order to reduce the ventilation losses in the casing owing to rotation of the air and dispersed water particles, a wiper must be arranged behind the discharge of the water from the wheel. This wiper is made very exactly in conformity with the contour of the bucket as the clearance between the wheel and the wiper must be of the least possible width, i. e. about 0.5 to 1 mm. The bottom part of the casing, as a rule bedded into concrete, is usually welded. The place on which the jet might impinge at the runaway speed of turbine must be well armoured. At the passages of the shaft through the casing, there are mounted spray rings which prevent spraying of the water and its escaping along the shaft. As a rule, bearing pedestals are cast to the casing; they are not necessary when the runner is fastened in an overhung arrangement on the generator shaft. Braking of the turbine for stopping the turboset is usually realized by arranging a braking jet which acts against the sense of rotation. It is frequently put into action automatically when the regulator fails and consequently the turbine exceeds the permissible speed. The runaway speed can also be reduced so that in the casing, in the places on which the jet impinges at the runaway speed, a device is mounted which turns the jet against the sense of the rotation of the turbine. In vertical turbines, which are mostly fitted with several nozzles, the casing is welded and forms the supporting structure of the generator (Fig. 332).

Below the runner, an easily removable grate is located, providing access to the wheel and nozzle without any dismantling. A manhole must be provided for in the casing or in the discharge duct.

2. Runner

The runners may be manufactured integrant with the buckets, the material of construction being either cast iron for a peripheral velocity $U = 30$ m/sec., or cast steel for $U = 70$ m/sec. (Fig. 333). Most frequently, however, the buckets are cast

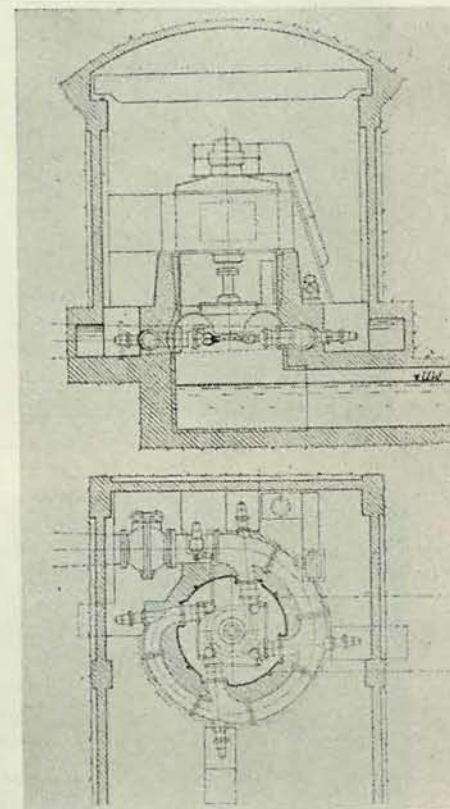


Fig. 331

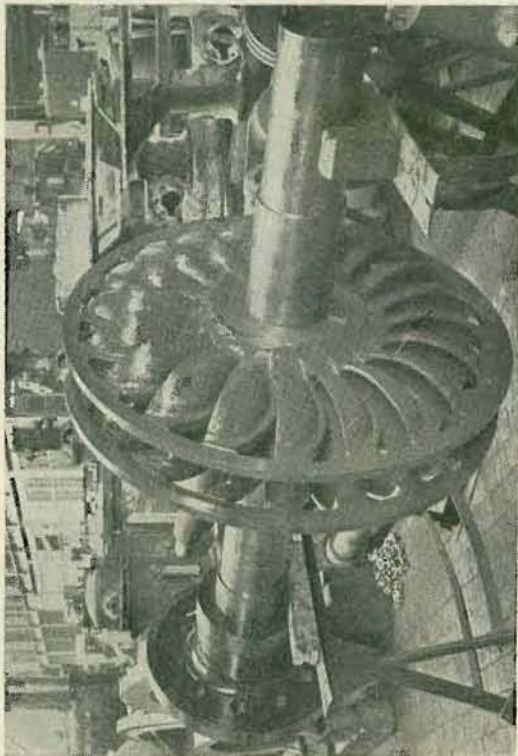


Fig. 334.

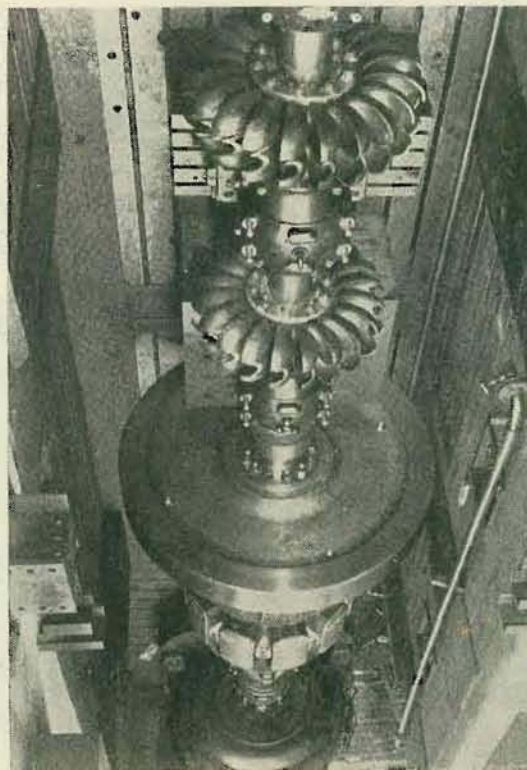


Fig. 335

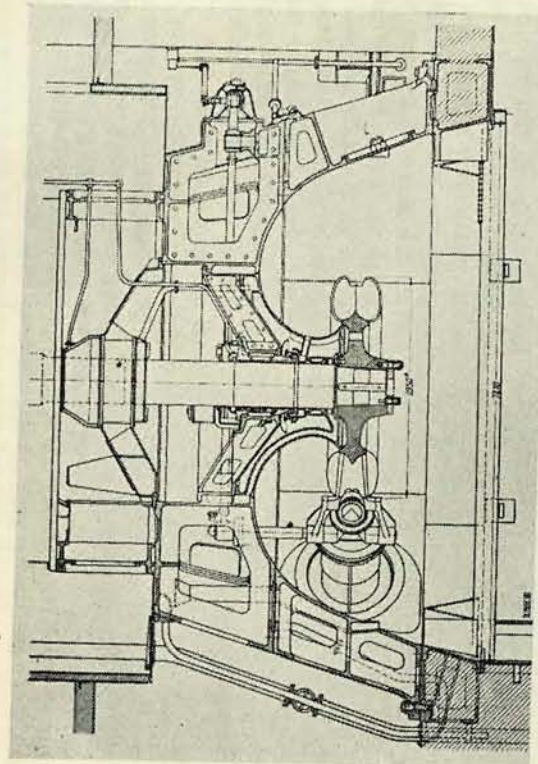


Fig. 332

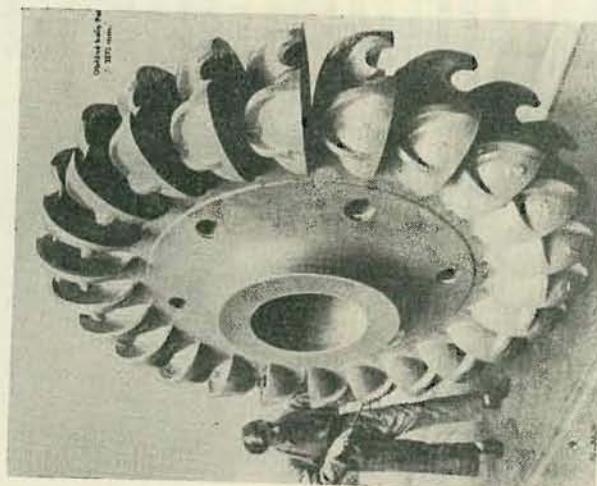


Fig. 333

integrant with the stems, and these are bolted to the disc of the wheel. This manufacturing method is more expensive but facilitates exact grinding and polishing of the buckets, their replacement in case of defect and the casting process itself. The buckets are in this case easier machinable than on a runner cast integral with them. With regard to the alternating stress, the buckets are fastened to the wheel by

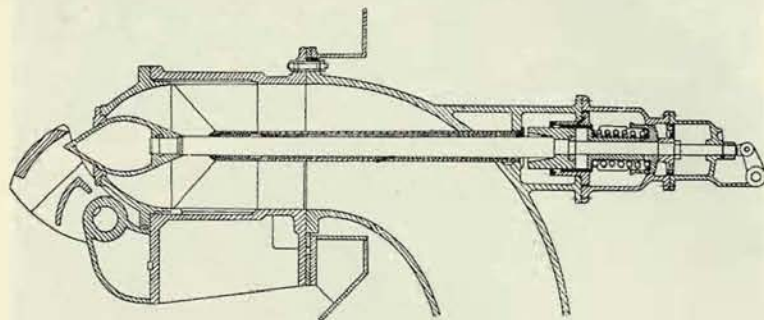


Fig. 336

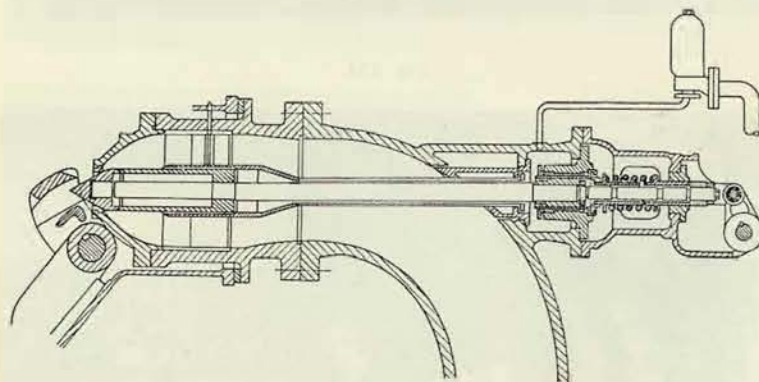


Fig. 337

means of fitted bolts, preferable with conical shanks. Difficulties are encountered in dimensioning the connections of the buckets to high-speed runners (n_s exceeding 30 r. p. m.). In these cases it is recommended to shrink two heated steel hoops on the buckets as indicated in Fig. 334.

The runner is fastened on the shaft by means of a key or feather, and in an overhung arrangement by a flange.

As already mentioned the blades are made of cast iron or of cast steel. For high heads alloyed cast steels are employed. Special operating conditions are encountered when the water contains acids or fine sand. In such a case the runner must be made of alloyed cast steel withstanding corrosion and erosion. The lips of the buckets

are most subjected to wear, and when the sand content of the water is not too high, the buckets are made of standard material and for economy's sake only lips of alloyed cast steel are inserted.

Great care must be devoted to the manufacture of the buckets. Their inner surface must exactly ground to shape and finally polished. The buckets must be free of cracks. The assembled runner must be carefully balanced statically and for higher speeds also dynamically (see Fig. 335).

3. Nozzles - Needles

The nozzle with the needle is usually mounted in an elbow of the supply pipe, whose diameter equals three to four times the jet diameter, while its radius of curvature is two to three times the pipe diameter. The throat of the nozzle and the

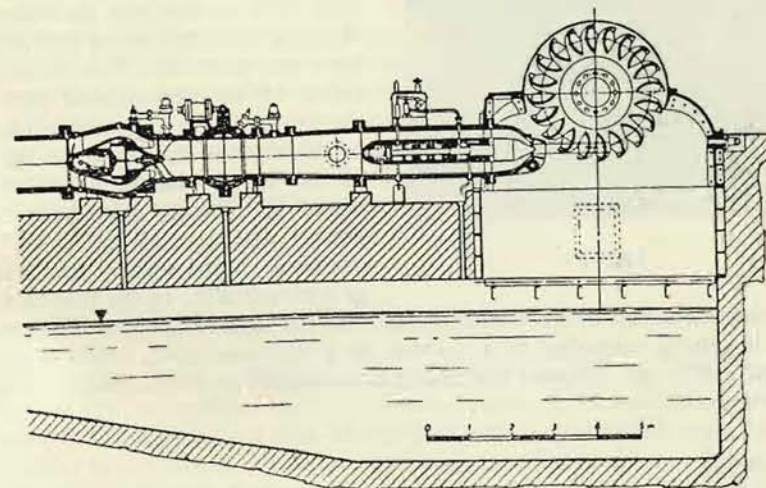


Fig. 338

tip of the needle are replaceable. The tip of the needle is replaced either from inside the case, or the tip with the shank is pulled through the elbow and re-inserted after replacement. In the first case, the needle has a bulbiform shape and a slender shank which moves in a guide tube (Fig. 336). In the second case, the cylindrical part of the needle is guided, passing into the slender shank outside the guide. The elbow is fitted with an opening of sufficient width for pulling out the needle (Fig. 337). In some designs the needles are protected from sand by an outer tube filled with pressure water. Since the elbow in front of the turbine causes losses even when its radius of curvature is large, a straight supply pipe is adopted in modern designs for high heads and outputs (Fig. 338).

The supply pipe in larger turbine installations is located in a duct under the

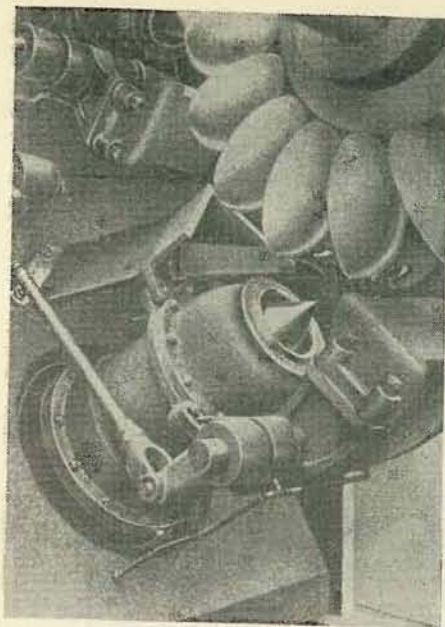


Fig. 339

motion is transmitted by a rod mechanism from the regulating shaft. The time of closure is usually controlled by a dashpot. In a hydraulic drive, which is usually employed for larger outputs, the needle is controlled by a servomotor operating with pressure oil.

4. Deflector

The deflector is of rugged design as it is subjected to great forces and reliable operation must be ensured. The part coming into contact with the jet is usually made replaceable as it is exposed to erosion (Fig. 339).

floor. Vertical arrangements of the turboset are mostly fitted with more than one nozzle. The supply pipe is circular and stepped according to the number of nozzles. When two nozzles are employed, they are located at an angle of 180° to eliminate any resultant force of the jets acting on the shaft. In turbines with more than one nozzle, the second and further jets must be protected by cover plates against the water spraying the wheel.

Vertical turbines must be equipped with such buckets that the water discharging from the upper does not fall back into the wheel. This is achieved either by an asymmetrical shape of the bucket or by a greater inclination of the plane of the bucket to the axis of the jet. A suitable shape of the upper lid likewise contributes to a correct discharge of the water. The needle is shifted either mechanically or hydraulically. In the first case, the

PART III

EQUIPMENT OF HYDRAULIC TURBINES

A. CONTROLLERS

The speed of hydraulic turbines is regulated exclusively by indirect controllers. Self-actuated controllers are not suitable for this purpose, because of the great forces required to operate the control gear. Unsufficient sensitivity is another reason why self-operated controllers are not used for the regulation of turbines.

The control gear is operated by a servomotor which is controlled by the centrifugal governor. The servomotor is normally driven by pressure oil supplied from the control valve operated by the governor. The pressure oil acts upon the piston of the servomotor.

I. BASIC PRINCIPLES OF CONTROLLERS

The simplest operation of a servomotor is shown in Fig. 340. The servomotor consists of a power cylinder with a differential piston P , i. e. each side of the piston has a different acting surface area. The surface area in contact with space a is half of that acting upon space b . Oil under pressure is supplied to space a , from which it flows to space b through the bore v . From here the oil can escape through the gate o (if open) into the central bore of the piston to be discarded therefrom. The gate valve S placed in the bore of the piston is connected to the sleeve of the governor. When the gate valve reaches the position shown in Fig. 340 a pressure drop will occur in the chamber b , because the discharge hole o is larger than the supply bore v . Pressure in chamber a will remain almost constant and therefore the piston will move to the left, i. e. it will follow the valve. By this movement of the piston the gate o will gradually be closed and subsequently the oil pressure in chamber b will rise until a pressure equilibrium on both sides of the piston is reached. If the gate valve should be driven by the gov-

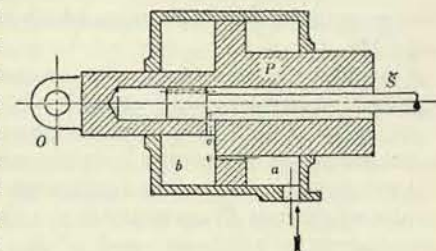


Fig. 340

error in the opposite direction, the discharge hole o will be closed and the specific pressure in both chambers will be equalized. However, the acting surface area of the piston in chamber b is twice as large as in chamber a , and therefore the piston will start to move to the right, i. e. it will again follow the movement of the valve. By this movement of the piston the gate o will be gradually opened and pressure in chamber b will decrease until an equilibrium is reached again.

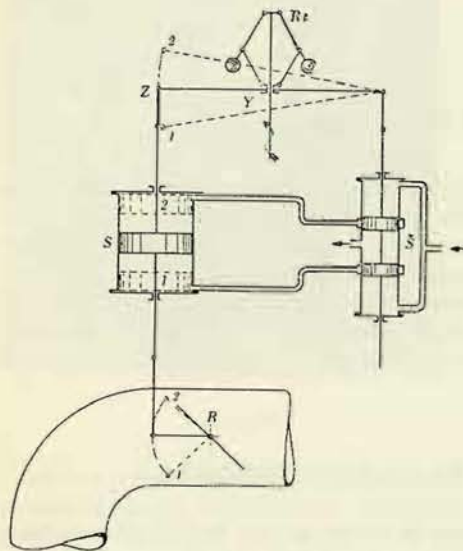


Fig. 341

Piston P copies the movement of the gate valve and consequently also the movement of the governor sleeve. The eye O , which is part of the piston, is then used for driving the regulating mechanism of the turbine.

This simple method is seldom used for servomotors regulating hydraulic turbines. It may be used only in very small controlling units. The method is frequently used as an intermediary element, which actuates the control valves of large controlling units.

A standard arrangement of a control unit is illustrated in Fig. 341, where governor, servomotor and control valve are separated. The diagram illustrates a proportional feed-back arrangement (called also primary compensation); the piston rod of the servomotor is rigidly connected with the lever of the governor so, that any given position of the servomotor piston (and thus any given position of the regulating element R) corresponds to a definite position of the governor sleeve and consequently to a definite speed of the regulated machine. A completely relieved machine will run at maximum speed, a machine running under full load will have

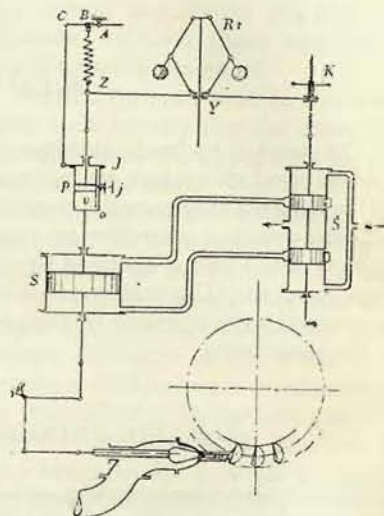


Fig. 342

a minimum speed. If we denote n_2 the speed of the relieved machine, n_1 the speed of the fully loaded machine and $n_s = \frac{n_1 + n_2}{2}$ the medium speed, then the value $\frac{n_2 - n_1}{n_s}$ is called the permanent droop denoted as δ_i and usually expressed in $\%$. If we denote n_{II} the speed corresponding to the highest position of the governor sleeve (which may be considered for the purpose of control in accordance with the lift y_{\max} in Fig. 344) and n_I the speed corresponding to the lowest position of the governor sleeve, the value $\frac{n_{II} - n_I}{n_s}$ is called the useful droop of the governor; it is denoted δ and expressed in $\%$. It is obvious, that in the case of an indirect controller with rigid feed-back $\delta_i = \delta$.

Hydraulic turbines require a stable control and, therefore, the value δ must be greater than the value δ_i . (A control is called stable, when the controller after deviation is automatically restored to the correct equilibrium position; on the contrary, in the case of a labile control deviation from the equilibrium, position steadily increases and the control is unstable). The condition $\delta_i < \delta$ cannot be fulfilled with a proportional feed-back arrangement (stabiliser with droop) and therefore the elastic arrangement of a stabiliser (called also secondary compensation) is applied in the control of hydraulic turbines (See Fig. 342.).

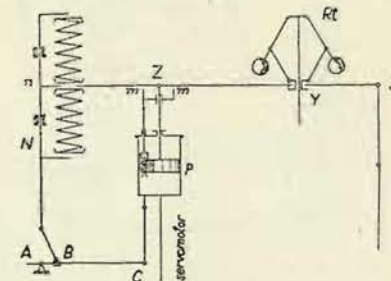


Fig. 343

The restoring mechanism contains the oil dashpot \mathcal{F} with a by-pass controlled by the throttle valve j . The left end Z of the lever is held in position by the spring BZ . When the control valve S is moved from its neutral position, the piston of the servomotor is also moved by the pressure oil, the piston of the dashpot is carried by the dashpot cylinder, the spring BZ is compressed or stretched (according to the direction of the movement of the dashpot piston), the left end of the lever is lowered or lifted and the control valve is restored to the neutral (dead-beat) position bringing to a standstill the servomotor and the whole mechanism. The force of the compensating spring causes an additional movement of the dashpot piston, the control valve is moved again and the whole regulating process is repeated until the dashpot piston is in a position in which the spring BZ is neither compressed nor stretched. After the regulating process has been completed, the permanent speed droop δ_i is in accordance with the displacement of the point B caused by the servomotor. By shifting the hinge B along the lever BCA the displacement can be changed from positive (shown in Fig. 342) to negative values (hinge B is to the right hand of the fulcrum A). In the latter case point Z and governor sleeve Y are lowered under no-load conditions and the turbine under full load has a greater speed than a re-

lieved machine. When the hinge B is placed into the fulcrum A (i. e. no displacement takes place during regulation), the speed is constant at any position of the servomotor and, thus, the revolutions of the turbine do not change with a changing load. This special arrangement is called an isodromous control.

The small handwheel K shown in Fig. 342 is not illustrated in the remaining diagrams. By this handwheel revolutions can be changed or the turbine stopped. The hub of the wheel forms the nut of the control valve spindle so that by turning

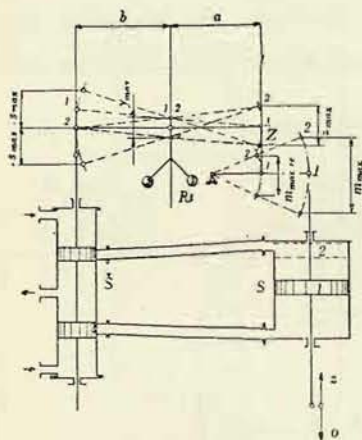


Fig. 344

the handwheel the control valve is moved from the normal position. The pressed oil flows into the cylinder of the servomotor and the whole mechanism is brought into action; it is brought again to a standstill after the restoring mechanism and the new position of the governor sleeve (resulting from the changed speed) has moved the control valve into neutral position. This handwheel can be connected also with other elements of the mechanism, e. g. with the rod connecting point C with the dashpot cylinder, J , or with the governor sleeve, etc.

The arrangement described has two disadvantages: the reverse point Z is not suitably fixed and the permanently open valve j of the dashpot J together with the slow movement of the servomotor prevents an intensive action of the restoring mechanism. Fig. 343. shows an improved design of the arrangement (the diagram illustrates only the governor and the return-motion gear – also called the isodrome). The compensating springs are prestressed and placed in carrier N . The reverse end of the lever (point Z) is suitably fixed by the plates of the springs. When one spring is compressed, the other is retained by the nose n so that the first one acts immediately with sufficient force. The by-pass of the dashpot is mounted in piston p and is normally closed by a spring valve (the spring acts and closes the valve in an upward direction). The valve opens only after point Z has been moved from the

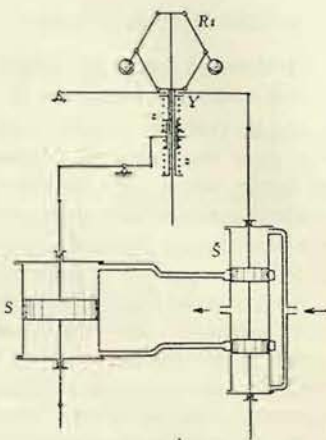


Fig. 345

neutral position, the inclining lever presses down one of the stops m and so opens the valve.

Fig. 344 presents the relations between the individual lifts of the control valve, governor, reverse point Z and the servomotor. In an elastic compensating device piston p of the oil dashpot (called also isodrome) slides in the cylinder of the dashpot during the movement of the servomotor. Point Z will therefore travel a smaller lift as the isodrome cylinder or the piston of the servomotor. If $m_{\max, re}$ is the lift of the servomotor reduced to the reverse point, i. e. the real lift increased by the preceding travel of the dashpot piston, and z_{\max} is the lift of the reverse point derived from the full value of the governor lift, we can write the relation $m_{\max, re} > z_{\max}$. An elastic compensating device in which

the relation $\beta = \frac{m_{\max, re}}{z_{\max}} > 1$ holds good,

is called an accelerated stabilisator. Here the restoring mechanism acts more intensively and the stability of the regulation is increased.

Fig. 345 is a diagram of Fröll's indirect controller. The load of the governor sleeve is changed by the restoring mechanism in accordance with the position of the servomotor. The position of the sleeve remains constant at all positions of the servomotor (i. e. at any load of the turbine); with a larger load of the turbine, however, the force acting upon the sleeve is smaller and the controller reduces the speed of the machine.

Fig. 346 shows Gagg's improvement of the controller in Fig. 345. This arrangement permits the setting of a permanent speed. The governor sleeve is subjected to the action of pressure springs placed in the piston t ; the stabilisator actuates the springs of the sleeve by means of a hydraulic transmission gear consisting of pump p and piston t . Any change of the position of the servomotor is transmitted via pump p to the piston t and so the governor sleeve is subjected to an additional pressure exerted by the springs. The adjustable gate v connects the space under the piston with the oil container N . At the moment when oil pressure in both spaces is equalized, the pressure exerted upon the governor sleeve ceases. The permanent droop is positive when the coupling V is on the left side of the fulcrum, equals zero when the coupling is in the fulcrum (isodromous regulation) and is negative when the coupling is on the right side of the fulcrum.

Stability of the regulation can also be achieved by forces of inertia. Fig. 347 is a diagram of an indirect revolving mass controller. Apart from the centrifugal weight (flyball) G the governor is equipped also with revolving mass M_n . The

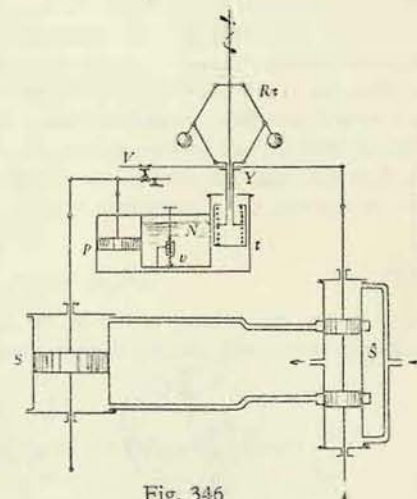


Fig. 346

controller must rotate in such direction that during speed rising (i. e. with a relieved machine), the force of inertia P_n exerted by the mass M_n acts in the same direction as the centrifugal force of the fly-ball G . In this phase of increasing speed the revolving mass shows a tendency to retain the original low speed and the force of inertia acts in the same direction as the centrifugal force. After the speed of the governor has reached its maximum, the revolutions start to decrease. In this phase of

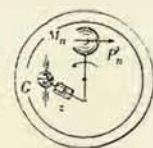
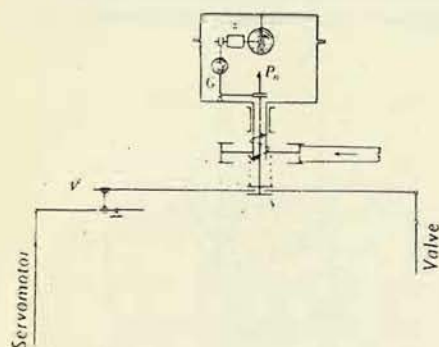


Fig. 347

decreasing speed the revolving mass (which in the meantime has also attained the maximum speed) shows a tendency to retain the high number of revolution and acts in the opposite sense: it tends to rotate at a higher speed, than the governor. The force of inertia acts against the centrifugal force and causes a sooner return of the sleeve to the neutral position. The described behavior of the force of inertia increases the stability of the regulation. The restoring mechanism V permits the setting of the permanent droop δ_i .

In all diagrams hitherto described the floating lever which actuates the control valve was shown as directly connected with the governor sleeve. In standard arrangements a multiplying intermediary element (see Fig. 340) is mounted between the governor and the floating lever. The lever is then connected to the eye O and the governor only actuates the light and balanced gate valve S . This arrange-

ment excludes the adverse effect of the forces of inertia of the lever (and all parts connected with it) upon the movement of the governor sleeve. Similar multiplying relays are used for actuating (pilot) valves of large dimensions, which cannot be directly connected with the lever.

Indirect controllers are divided into two main groups:

1. Straight flow controllers without air vessels; a safety valve maintains the prescribed oil pressure and the oil pump works constantly at full pressure. The oil pump must be able to supply pressure oil in a quantity corresponding to the volume of the maximum stroke of the servomotor piston and within the time prescribed for the closing of the gates. This type is used for smaller hydraulic turbine units up to a controller performance of 200 kgm. If controllers equipped with pumps without air vessel were used for greater performances, their design would be too complicated.

2. Controllers with air vessels, where the oil is accumulated under pressure in the air vessel. The oil pump supplies oil into the air vessel only during a pressure

drop (otherwise it pumps without pressure into the oil sump), a smaller rate of flow is required than in the previous case and consequently there is a smaller increase of the oil temperature.

II. PARTICULARS OF DESIGN

1. Oil Pumps

Oil pumps are almost exclusively of the gear or screw type; they usually work against a pressure head of 2—10 atm. g. with straight controllers and 20, 25 (up to 30) atm. g. with controllers with air pressure vessels. The gear usually consists of two identical spur pinions with more than 14 teeth (to avoid the necessity of correction). The gear is carefully machined, inter-meshing is without clearance so that the pulsation of the pump is reduced to a minimum and the highest possible volumetric efficiency is attained.¹⁾ When these conditions are fulfilled and the pressure angle is 20° (the pressure angle has little influence), the theoretical discharge Q in cm^3/sec is given by the equation²⁾

$$Q = 0.104 n b m^2 (z + 0.28), \quad (249)$$

n is the rotational speed r. p. m., b = the width of the pinions in cm, m = the module of gearing in cm, z = number of teeth in each pinion. The actual discharge is then

$$Q_{ef} = \eta_v \cdot Q,$$

where η_v is the volumetric efficiency according to the following table³⁾

pressure in atm. g.	5	10	15	20	25	30
η_v	0.95	0.93	0.91	0.89	0.87	0.83

The table contains average values which depend upon the quality of machining (clearance). The values apply to suitable circumferential velocities; volumetric efficiency increases with rising velocity.

The mechanical energy input of the pump is given by the equation

$$N = \frac{Q p}{7500 \eta}, \quad (250)$$

In this equation N is the input in metric h. p., p is the delivery head in atm. g. and η is the total efficiency given in the following table⁴⁾.

¹⁾ Kieswetter: Výpočet a konstrukce zubových pump. (Calculation and design of gear-wheel pumps) Technical Reports of the Škoda Works No. 3 (1939), No. 1. (1940) and No. 1. (1942).

²⁾ Nekolný: Výpočet a návrh zubové pumpy. (Calculation and draft of a gear-wheel pump.) Strojnický Obzor (1941), p. 260.

³⁾ Fabritz G.: Die Regelung der Kraftmaschinen, Wien, Springer, 1940, p. 25.

⁴⁾ Loc. cit. p. 25.

Circumferential velocity at pitch diameter in m/sec		1	2	3	4
Delivery head atm. g.	5	0.81	0.76	0.68	0.62
	10	0.63	0.77	0.76	0.71
	15	0.47	0.71	0.72	0.73
	20	0.30	0.55	0.58	0.72

Fig. 348 shows the design of the pump. In order to ensure a noiseless work, the circumferential velocity of the gear-wheels must not exceed 4.5–5.6 m/sec (the

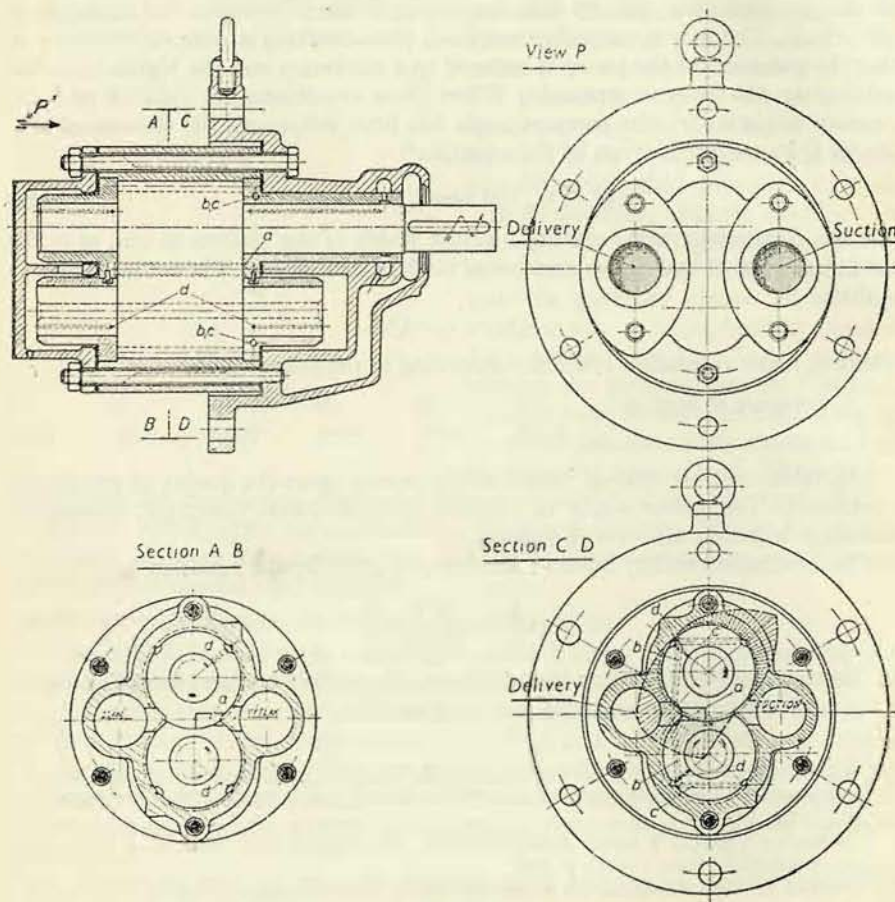


Fig. 348

smaller figure applies to the higher pressure). Oil discharged by churning between the gear teeth is collected in slots on the faces of the bearing bushings, see Fig. 348, channel *a*. The oil pressure acts upon each wheel with the force $P = 0.75 p \cdot D \cdot b$. (D is the outer diameter of the wheel). This force represents the load which must be carried by the bearings. The bearings are made of bronze or gray cast iron with babbitt lining. The latter ones are better, because their thermal expansion is the same as that of the pump casing. Specific load of the bearings should not exceed the value $p = 20$ to 24 kg/cm^2 . Ball and roller bearings are also used, especially at higher rotation speeds. The force acting upon the wheel has a bending effect upon the journals, the contact and fit in the bearings becomes worse. Therefore the width of the wheels should never exceed the dimensions of the diameter (especially at higher pressures). The same ratio applies to the dimensions of the bearing journals. At higher pressures relief ducts are applied (*b-c-d* in Fig. 348) by which pressure - oil is lead to the wheels opposite to the delivery zone and regions opposite to the suction zone are opened toward the sump (simultaneous lubrication of the journals). The load upon the wheels is partially balanced by this arrangement of the ducts. The volumetric efficiency is somewhat lower, than given in the table, but the bearings are relieved and we may use wider wheels. Where large quantities of oil must be supplied (and the gear-wheel would be too wide), the oil pumps are arranged in a duplex system. Two pairs of pinions are used with a third bearing between them, or a third wheel is added; in extreme cases a combination of both these arrangements can be used.

Screw pumps, known as "IMO" pumps, are used for high rotational speeds and large deliveries. The pump consists of two or three inter-meshing screws according to Fig. 349.¹⁾ The parallel run of the screws is sometimes ensured by spur pinions running in oil on the suction or delivery side. Axial forces acting upon the screws are balanced hydraulically. Screw pumps are designed for rotational speeds 1000–3000 r. p. m. The quantity of fluid delivered by one screw in one revolution is²⁾

$$V = \frac{\pi}{4} (d^2 - d_1^2) \frac{t}{2} - \left[\frac{\pi}{4} d^2 \frac{4\alpha}{360} - \left(\frac{d + d_1}{4} \right)^2 \cdot 2 \tan \alpha \right] \frac{t}{2}, \quad (251)$$

where $\cos \alpha = \frac{1}{2} + \frac{d_1}{2d}$; all other dimensions can be seen in Fig. 349. Volumetric efficiency increases with an increased length of the screws, it amounts to about 95 %. Total efficiency is about 90 %.

¹⁾ A. Ribaux: Pompes à vis, Bulletin technique de la Suisse romande (1943), p. 256.

²⁾ For inter-meshing, the profile of the thread must be backed off at the base.

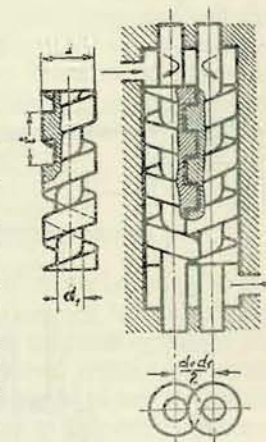


Fig. 349

Fig. 350 shows a section of an actual vertical screw pump. The delivery branch of the pump is placed on the drive side so that the other end of the driving or driven shaft is available for the mounting of pistons used to balance the axial loads. In order to secure the position of the screws, the axial load is not fully balanced; the

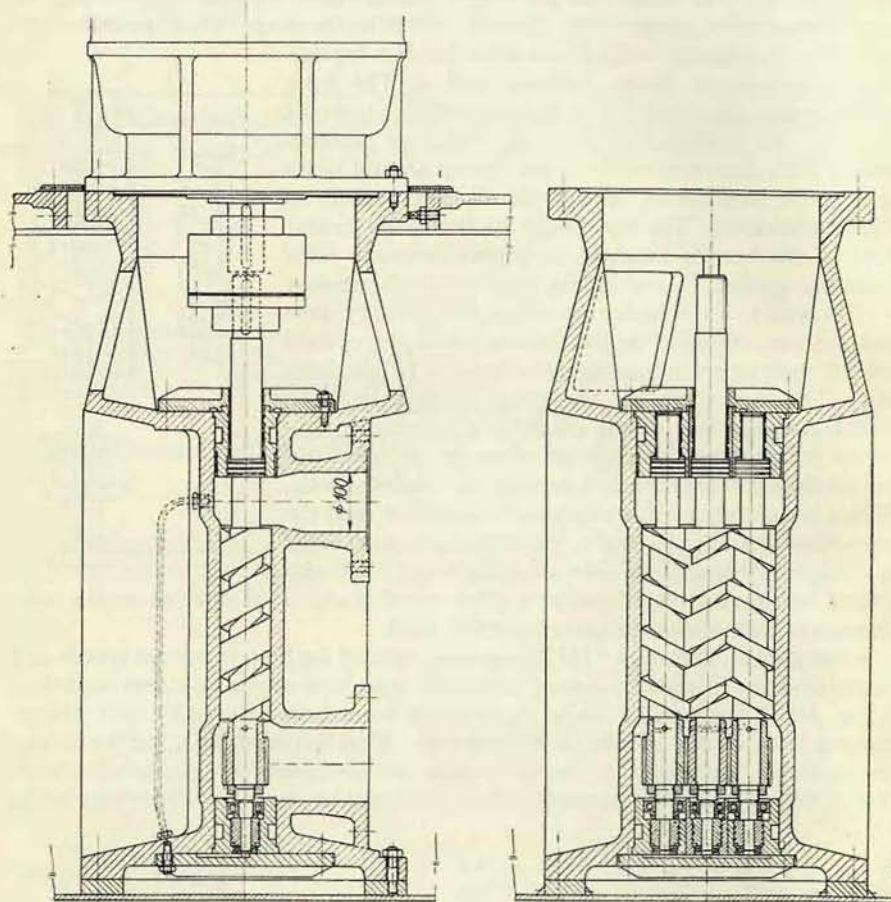


Fig. 350

unbalanced part of the axial forces is utilized for pressing the screws against the axial ball bearings.

The quantity of oil delivered (liters/sec) in straight flow controllers equals the stroke volume of the servomotor (in liters) divided by the time required for the

closure of the controller (in seconds). Controllers with air pressure vessels are equipped with oil pumps dimensioned for a delivery per minute equalling 3.5 to 10 times the volume of the servomotor (lower figures for larger controllers and vice versa).

The oil pump can be either belt-driven from the shaft of the turbine (smaller units) or motordriven. If the controller oil pump is put out of operation, the guide apparatus of the turbine must be closed and secured in the closed position. This precaution is necessary, because with the oil pump at standstill complete absence of oil pressure occurs, the water opens automatically the guide apparatus and the turbine may run away. In the case of an electrically driven oil pump, current supply must be secured from several independent sources. The drive of oil pumps and other auxiliary plant in large power stations is provided by an independent motorgenerator. The generator is driven by its own impulse wheel or by another motor or it is mounted directly on the shaft of the turbine.

2. Unloading valve (Controller of the oil pressure in the air vessel)

In straight flow controllers the oil is supplied directly from the oil pump to the control valve. The required pressure is adjusted and maintained by a regulating valve through which the superfluous oil is readmitted from the pressure pipe to the oil receiver tank. These valves are designed as spring valves similarly to safety valves. Noiseless operation of the regulating valve is secured either by special damping pistons or by countersinking the cylindrical part of the valve cone into the valve seat. (Fig. 351).

By this arrangement the conical sealing surface is sufficiently lifted during the working stroke above the valve seat, so that no contact is possible between them during vibration. Equally good results are obtained by an alternative design of Pop's safety valve with an increased lift.

In controller systems with air pressure vessels the pumps are provided with unloading valves which at a certain pressure open the discharge to the oil tank, close it again when the pressure in the air vessel drops below a desirable minimum so that the pump delivers through the check valve again to the air vessel. The function of the unloading valve is frequently combined with the replacement of air in the pressure tank. Air in the pressure tank is under pressure absorbed by oil and escapes from it under atmospheric pressure in the receiver tank. There is a constant reduction of air content in the pressure vessel and this loss must be replaced.

According to previous methods, air was sucked into the suction pipe of the pump and air bub-

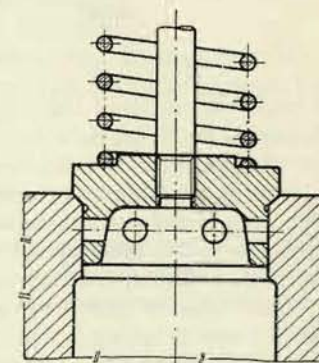


Fig. 351

bles had been in close contact with oil producing the undesirable result of intensive oil oxidation and premature ageing. New methods admit, therefore, the air into the delivery branch of the pump. A design of this type is shown in Fig. 352 (ČKD Works - Blansko). Oil from the pressure tank flows below the pilot valve *a* which is loaded by the spring *b*. When oil is pumped into the pressure tank, the pressure rises until the pilot valve *a* is moved in an upward direction. Now the oil is admit-

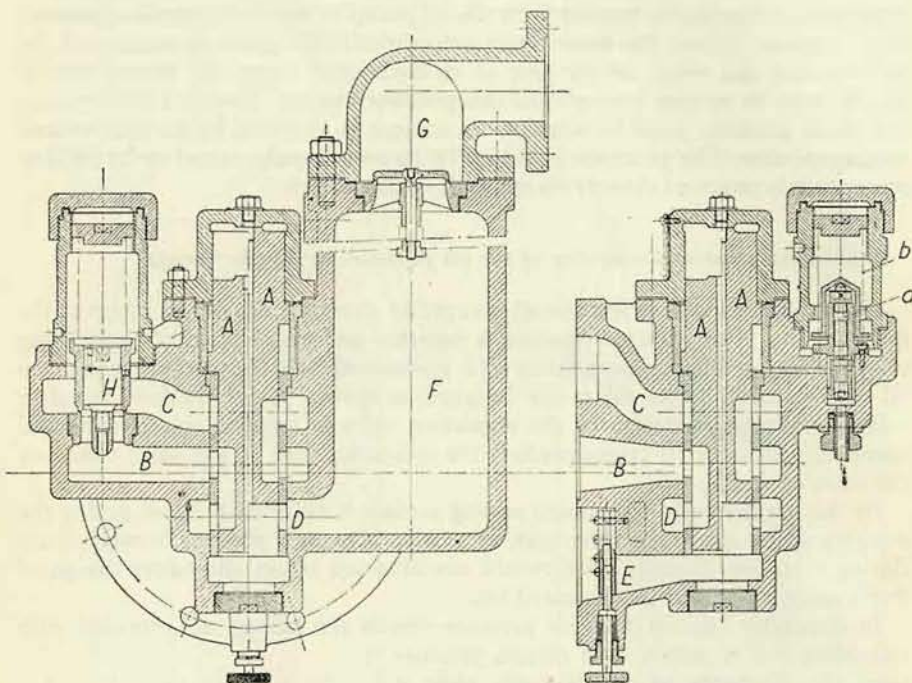


Fig. 352

ted below the piston of the control valve *A*, and the piston moves upward into a position shown on the right side of Fig. 352. The pump delivers oil into the duct *B* from which it enters the discharge channel *C*—the oil pump floats idly, i. e. it works under no appreciable oil pressure. In this position of the control valve the gate *D* is also opened and permits the discharge of oil from air chamber *F* according to the adjustment of the hand operated valve *E*. Through the oil stream escaping from this valve bubbles up a certain quantity of air into the air chamber. When pressure in the air pressure tank drops below the required minimum, the pilot valve *a* is pushed down by spring *b*, the oil below piston *A* escapes and the control valve *A* is pushed down by the oil from the pressure tank acting upon the upper annular face of the piston *A* (see position drawn on the left side of Fig. 352). The delivery

side of the oil pump is now connected with air chamber *F*. Oil is delivered from the pump to this chamber and supplied through the check valve *G* into the air pressure vessel. Obviously the air accumulated in the air chamber enters the pressure tank first. The safety valve *H*, mounted in the branch connecting the unloading valve with the pump, relieves the air pressure tank in the event of a break-down of the unloading valve; no second safety valve is then required for the air pressure vessel.

The pilot valve *a* is set off at its lower end in order to permit a rapid adjustment (See Fig. 353, diameter 1 is larger than diameter 2). After an initial lift of the valve the oil acts upon a larger surface area and simultaneously the discharge from this space is closed by a ring mounted on the upper end of valve. By this arrangement a rapid displacement of the valve is attained and the same applies to the downward move of the valve; the pressure range is sharply limited and this prevents a possible stoppage of the control valve *A* in an intermediate (medium) position.

The unloading valve operates within a pressure range of 1 to 2.5 atm. g. The volume of the air chamber should amount to about 1—2 % of the total volume of the air pressure tank. Velocity of oil in the delivery branch of the pump is about 2 m/sec.

3. Pressure Tank

The total volume of the air pressure vessel should be determined as follows. Oil content: equals five times the stroke volume of the servomotor. Air content equals: twice the oil content. Pressure tanks for small controlling units are made of cast iron; larger tanks are riveted or welded. Stresses are calculated as in normal pressure vessels. Smaller pressure tanks are mounted on a common base with the controller, only their pressure gauge is mounted separately. In large units the air vessel is separated from the controller and equipped with liquid level gauge, pressure gauge, mud valve and manhole.

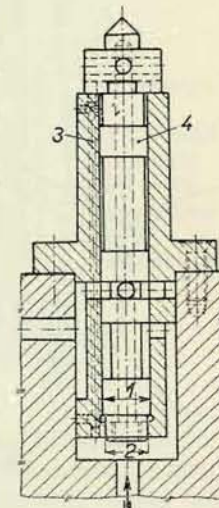


Fig. 353

4. Controller of Air Content in the Pressure Tank

A certain quantity of air is steadily supplied to the pressure tank. Superfluous air is automatically discharged into the receiver tank by the controller of air content. The air must not be discharged into the machine room atmosphere, because fog forming oil vapours escape simultaneously.

Fig. 354 illustrates a controller which acts as a float. At a certain minimum oil level the float opens an air discharge valve and the volume of the discharged air is replaced by an equal volume of oil supplied from the oil pump.

Fig. 355 shows another controller of air content of a simple design. It is based upon the principle that oil and air show different resistances against flow through a labyrinth, because at a given pressure in the air vessel their respective velocities are different due to the different specific weights. The controller is so adjusted,

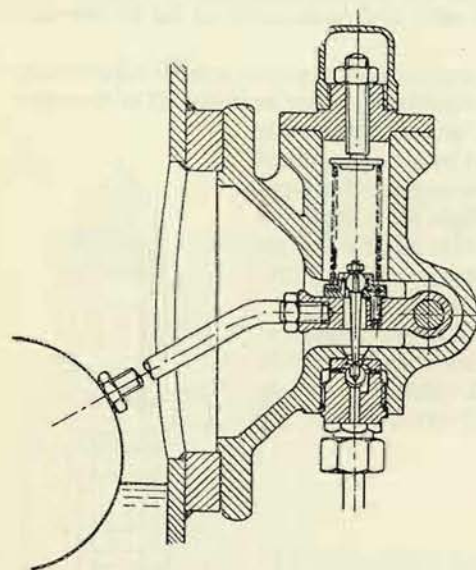


Fig. 354

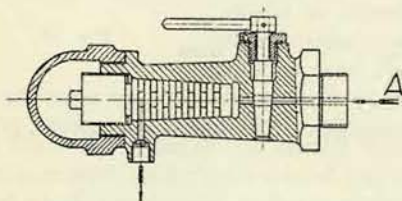


Fig. 355

tank and servomotor, should not exceed 20 to 60 % of the inlet oil pressure (smaller values apply to higher operating pressure of the control system). The gate valve and the bushing must be precisely machined, the bore of the bushing and the outer surface of the gate valve ground and covering edges worked to tolerances admitting a maximum overlapping of 0.2 mm. Large gate valves operating under high pressures would not seal properly with this small overlapping and this is, therefore, increased up to 2 mm. Two or four slots oppositely placed and serving

that at normal pressure a certain small quantity of oil flows from the pressure tank (direction *A*) into the controller and is discharged therefrom. If the oil level in the pressure tank drops, air instead of oil flows into the controller. The air passes the labyrinth with a greater velocity and so the superfluous air is discharged.

In both systems described a suitable closing of the air content controller must be provided for, because in the event of the speed controller out of operation (e. g. stoppage of the turbine) the total air content of the pressure vessel could escape during the shut-down.

5. Control Valve

The function of the control valve is to distribute oil under pressure to one side or the other of the servomotor piston according to the impulses of the governor. The control valve consists essentially of the gate valve, its bushing and the ducts or gates. It must have such dimensions that the total loss in oil pressure, occurring during the passage through the control valve and the piping between pressure

the purpose of a hydraulic radial balancing are machined, however, to the minimum overlapping of 0.2 mm.

Small control valves have gate valves made of steel and bushings of bronze or grey cast iron. In large control valves both parts are made either of bronze or of grey cast iron. Small control valves are connected directly to the driving mechanism (lever), larger ones through the intermediary of pilot valves. Fig. 356 shows a smaller control valve in combination with the pilot valve. The driving mechanism is connected with rod *A* (the internal slide of the pilot valve). By adjusting rod *A* against the main gate *B*, oil is admitted from the inlet channel through the ducts *a*, *b* above or below the gate valve. In both cases the opposite end of the valve is connected with the discharge. Therefore the main gate valve will exactly follow the movements of the rod (this is clearly illustrated in the picture).

In the illustrated design the regulating rings are extended by a collar on the discharge end so that the edge is not entirely exposed even at a maximum stroke. The time T_s required for closing the valve and the time T_o required for opening can be adjusted by the width of slots *x*, *y* which have an overlapping of 0.2 mm. An exact and safe adjustment of these times is absolutely necessary for protecting the turbine against hydraulic shocks. In this design the velocity of the piston is directly related to the stroke of the gate valve. This is a disadvantage. The above times can be adjusted better by orifice plates placed in the piping leading to the servomotor (as will be described in a later paragraph). The gate valves can be then designed without collars, so that the total edge of the regulating rings is exposed even at small strokes. The velocity of the servomotor piston is then of constant value. Here the gate valve is made of steel, the bushing of grey cast iron and the rod is hardened.

Fig. 357 shows a large control valve for a 100 liter stroke volume of the servomotor. The gate valve and the bushing are made of grey cast iron. The gates are opened simultaneously by two edges, which, for the sake of better sealing, have an overlapping of 1.5 mm. This overlapping is reduced in the slots to 0.2—0.5 mm. The upper part of the gate valve is designed again as a pilot valve. Pressure oil is admitted through a filter and it enters the pilot valve axially. The pilot valve is based upon the principle explained in Fig. 340 with the difference, that the function of the gate valve *S* is performed here by a plate mounted on the dog *a*. The gate covers a larger or a smaller part of the bore in the uppermost part of the gate valve. The dog *a* is actuated by the governor (direction *A*) with a compensating device. Hand wheel *B* is used for the adjustment of speed changes.

It has been stated in the previous paragraph that the time intervals required for the closure and opening the controller must be always safely adjusted. It is un-

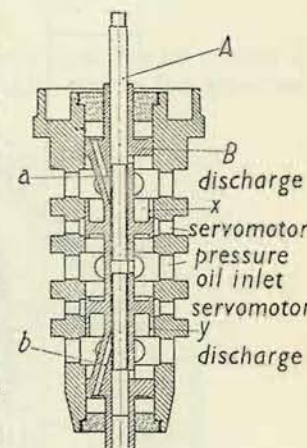


Fig. 356

suitable to limit these time intervals by the application of the gate valve slots. This holds good particularly in the case of large controllers. It is more suitable to adjust the time intervals by applying a simple orifice plate in the pipe connecting the control valve with the servomotor. The time of closure is limited by means of a simple orifice plate placed in the pipe, through which (during closure) the oil flows

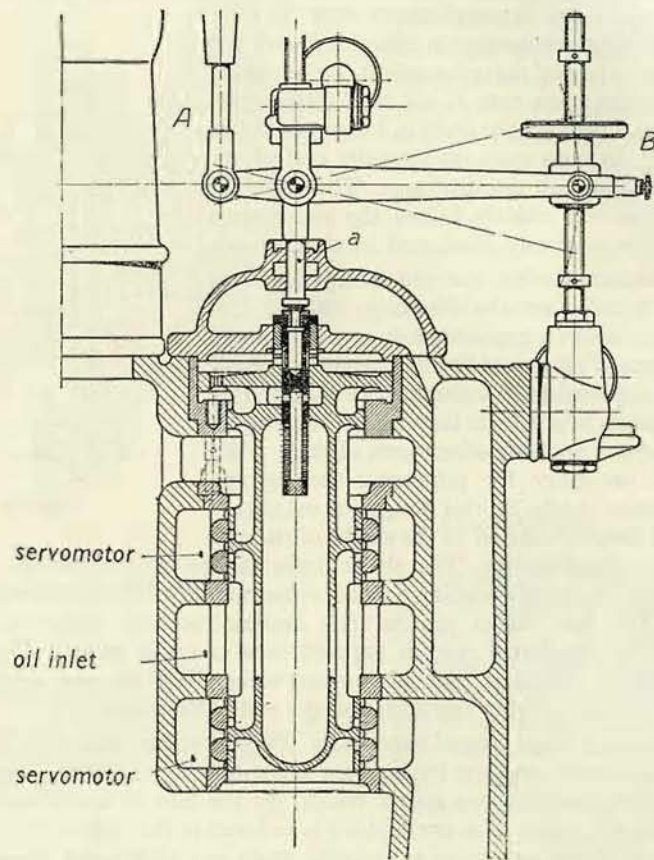


Fig. 357

from the servomotor. This arrangement is more suitable, as it has a throttling effect acting by overpressure against the tendency of the water to close the turbine. (The value of underpressure is limited to 1 kg/cm²). We then limit the time interval required for opening by a smaller orifice plate (T_0 is always greater as T_s) mounted in the second branch of the piping. This orifice plate acts as a check valve; it is pressed by a spring to the seat from which it is lifted by the oil stream occurring

during the closure of the water inlet to the runner of the turbine. By lifting the orifice plate from the seat the required increased flow is obtained. Another device for lengthening the opening interval is built into the servomotor, as shown in Fig. 358. During the opening stroke of the servomotor piston of the ball valve reduces the flow area so that the oil can pass only through the opening of the adjustable valve.¹⁾

6. Servomotor

The control valve is connected to the servomotor by a pipe. The oil velocity in the connecting pipe may be selected between 2.5—6 (to 10) cm/sec. It is important

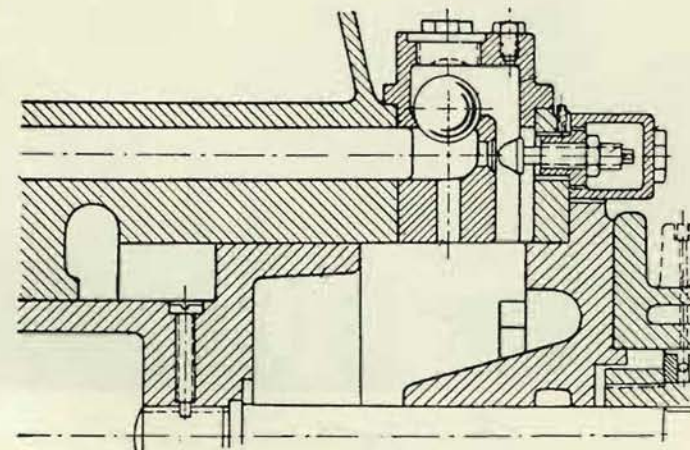


Fig. 358

to prevent an accumulation of air in the servomotor, as this would slow down its action. The gate valve is, therefore, always placed above the servomotor and the connecting pipe enters the servomotor at its highest point. The air then escapes automatically through the unsealed gaps of the gate valve.

The pistons of small servomotors are mounted in the cylinders without special packing, the piston rod is sealed by a soft packing. In large servomotors the pistons are also mounted without special packing, or they have piston rings, the piston rods are packed by one or two leather cups — see Fig. 361. The suitable ratio between bore and stroke is $D/z = 1 - 0.65$ (the smaller value applies to smaller servomotors).

In small controllers the servomotor is mounted on a common base with the controller and the movement of the piston rod is transmitted to the control shaft

¹⁾ Fabritz G.: Regelung der Kraftmaschinen, Wien, Springer, 1940, p. 50.

by a crosshead and a crank (Fig. 361). Large controllers have two servomotors placed normally near the turbine in the turbine pit. (Fig. 369). Details of this arrangement have been described in Part II. Chapter IV. (Extension of the regulation).



Fig. 359

7. Receiver Tank

This oil tank is mounted on a common base with other parts of the controller (Fig. 361). For large capacity units it is separated from the controller, but it is used as a mounting base for the air pressure tank and the motor-driven oil pump (Fig. 359). The tank contains about eight times the oil quantity delivered by the pump per minute so that an ageing of the oil is prevented. The oil temperature in large units is kept at 60° C by means of a cooling coil.

8. Governor

Governors (speed responsive devices) for control units of hydraulic turbines are made with a minimum reduced lift,¹⁾ which amounts to about 1/30 to 1/50 of the actual lift and does not exceed 1 mm. For this purpose we choose high

¹⁾ Nechleba: *Theorie indirektní regulace rychlosti*. (The theory of indirect speed control) Prague, Technicko-vědecké vydavatelství, 1952.

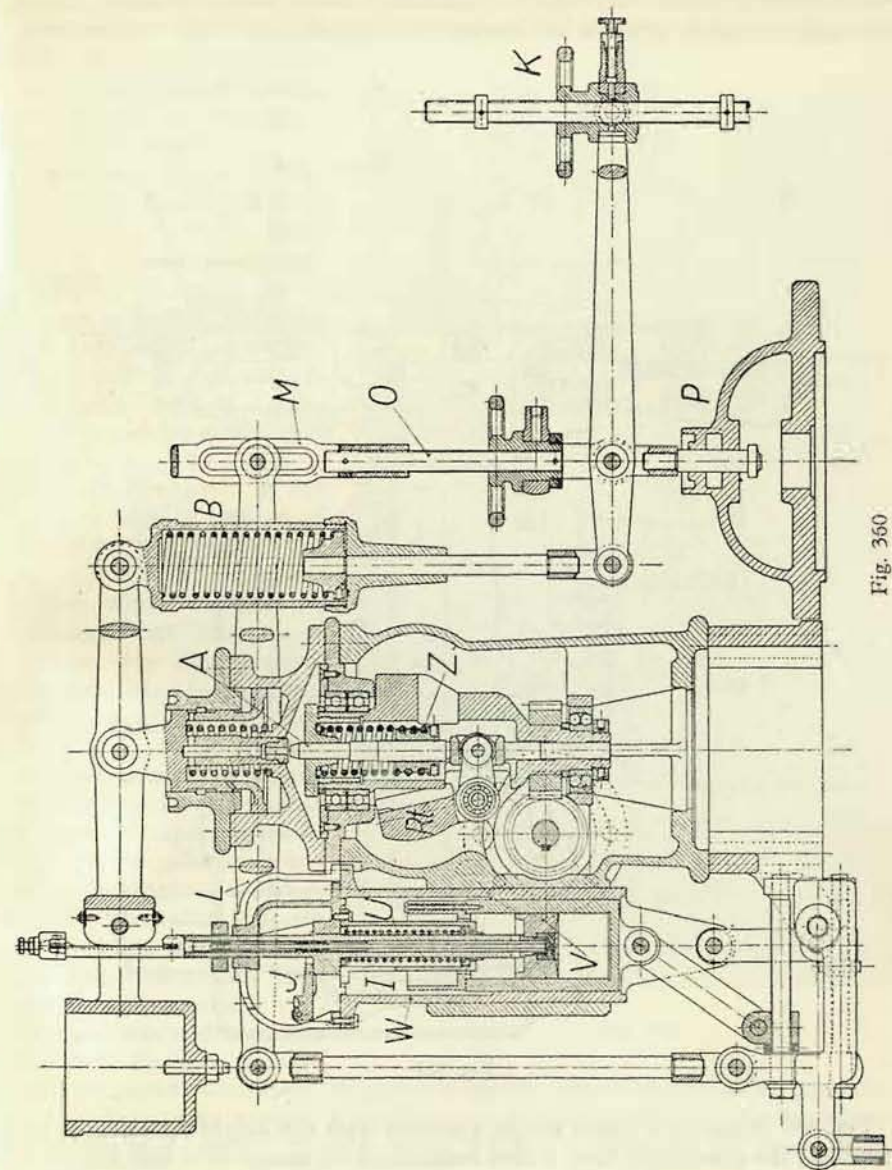


Fig. 360

Fig. 360 illustrates a single weight governor with the weight R_1 seated in ball bearings; the centrifugal force is also transmitted by means of a ball bearing to the light rod A which is loaded by the compensating spring Z . The governor is the original design of the Escher-Wyss Works in Zürich.

Governors can be driven by various means: belt drive (e. g. in Fig. 172), gear-wheels with auxiliary shaft (Fig. 363) or electric drive.

¹⁾ Maschinostroyeniye, tom 12, Gosudarstvennoye nauchnotekhnicheskoye izdatelstvo. Moscow 1948, p. 299.

the turbine. All auxiliary electric machines must be overdimensioned so that they remain in phase in spite of the large accelerating moments occurring during sudden changes of speed. Permanent magnets become demagnetized after a certain time and they must be remagnetized.



Fig. 363

a voltage drop to 25 % of the rated voltage. The loss of voltage caused by the action of a field-discharge switch cannot be prevented even by overdimensioning. The controller must, therefore, be equipped with a device which will automatically close the guide apparatus of the turbine when a voltage loss occurs in the driving electric motor.

Governors are sometimes driven by standard asynchronous electric motors connected to the main shaft generator. Such induction motors must be liberally rated, so that their slip is negligible. A break down of the drive occurs again at a voltage

The arrangement described can be simplified by connecting the electric motor with permanent magnets to the terminals of the main generator; the connection can be either direct or through potential transformers. The auxiliary alternating current generator and its drive are not necessary any more. However, a new serious disadvantage appears: a voltage drop in the main shaft generator puts the governor drive out of action. This may be caused either by the action of the protecting devices (field-discharge switch) or by a short circuit in the vicinity of the power station. This means that the controller often breaks down at the moment, when it is most needed. This disadvantage can be partly eliminated by overdimensioning of the electric motor. According to Fabritz a ten times overdimensioned electric motor does not fall out of step at

drop, but an inserted matching transformer keeps the drive in operation even if the generator voltage drops to 20 %. As in the former case, the electric motor starts only after the generator has been excited. The drive depends again upon the voltage of the main shaft generator.

The ČKD-Blansko Works use hydraulic transmission¹⁾. Speed of the controlled machine can be transformed into pressure changes in a suitable fluid, usually oil. We speak of oil under control pressure. The oil is supplied to a measuring installation which consists of, e. g. a piston loaded by strings and suitably placed at a distance from the controlled machine. The system is diagrammatically illustrated in Fig. 364, which also shows the simplest method of transforming speed into pressure by means of a gear-wheel pump. The fluid is pumped into a pipe branch with a constant discharge orifice.

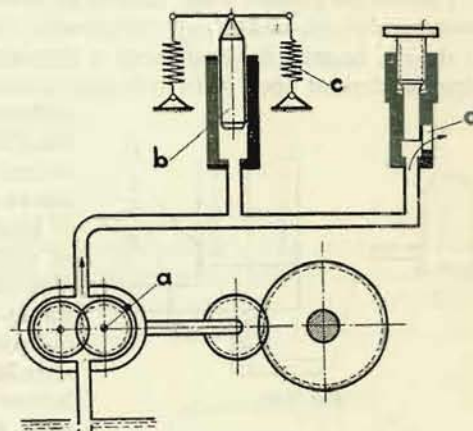


Fig. 364

Gear wheel pump *a* delivers the oil into the piping connected with piston *b* and with discharge (orifice) *d*. The piston carries the load of spring *c* and measures the oil pressure. The pump is driven by the shaft of the controlled machine and therefore the quantity *Q* of oil delivered by the pump is in direct relation to the rotational speed *n* and to the angular velocity ω of the controlled machine.

$$Q = kn = K\omega.$$

This quantity will be discharged through orifice *d* of the area *f*. If φ is the coefficient of discharge, then

$$\frac{Q}{f} = \frac{kn}{f} = v = \varphi \sqrt{2g \frac{p}{\gamma}}.$$

The oil pressure is proportional to the square of the rotational speed or to the

¹⁾ Nechleba: Nový hydraulický regulátor vodních turbin ČKD. (New hydraulic controller of the ČKD hydraulic turbines). Strojírnoství 1 (1951), No. 7—8, p. 264.

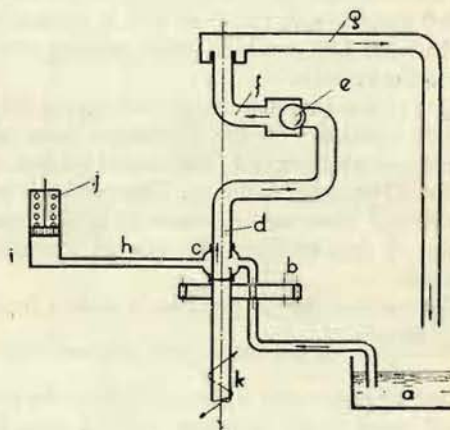


Fig. 365

square of the angular velocity and so is the centrifugal force. The position of the piston is thus determined by the same law, as the position of the governor sleeve. Changes in the position of the piston can be used for controlling purposes.

This simple method is not suitable for controller unit of hydraulic turbines. The position of the piston also depends upon the viscosity and thus upon the temperature of the oil, because the coefficient of discharge and the head loss occurring in the pipe also depend upon it. In hydraulic turbines we must take into account the great

difference between the oil temperature at the start and after a long run. The effect of viscosity has been eliminated by the design shown in Fig. 365.

Gear-wheel pump *b* mounted on shaft *k* of the hydraulic governor is driven by the controlled machine either directly or by means of a reduction gear. The pump draws oil from auxiliary vessel *a* and delivers it into chamber *c*. The oil enters the U shaped, hollow part *d* of the governor shaft. Both parts, *k* and *d*, of the governor shaft are made

of one piece and part *d* rotates at the same speed as part *k*. The oil flowing through the cranked part of the shaft must overcome the resistance offered by the ball *e* which rotates with the shaft and is pushed by centrifugal force against the inner wall of the hollow shaft. After passing this obstacle the oil returns via pipes *f*, *g* into the vessel *a*.

Due to the fact, that the oil had to pass the above described obstacle, its pressure is only controlled by the centrifugal force without regard to viscosity. If *p* is the specific oil pressure and *f* the area of the seat of the ball *e*, the total pressure exerted by the oil upon the ball is *fp*. This pressure must under all circumstances equal the centrifugal force $mr\omega^2$, where *m* is the mass of the ball, *r* the distance of its center of gravity from the axis of rotation and ω the angular velocity of the rotation.

We see that the oil pressure is only a function of the angular velocity, because $p = \frac{mr\omega^2}{f}$. If oil under this control pressure is led below a measuring piston loaded by the spring *j*, the position of the piston will depend only upon the rotational speed of the governor without regard to the viscosity of the oil. Viscosity will only influence the flow area, i. e. the distance of the centrifugal ball from its seat.

It is of great importance that the oil pump forms one unit with the hydraulic governor and rotates at the same speed. Due to this fact the position of the centrifugal ball does not change with a change of speed; it changes only with a change of the viscosity of the oil. The quantity *Q* delivered by the pump may be expressed as $Q = kn = K\omega$, where *k* and *K* are constants determined by the design of the gear-wheel pump. An equal quantity of oil must pass through the flow area of the

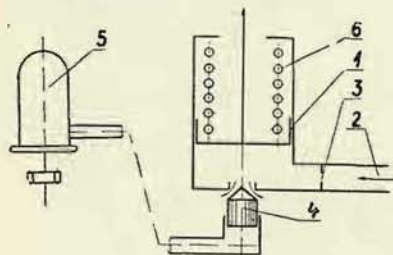


Fig. 366

centrifugal ball $f' = oz$, where *o* is the circumference of the seat and *z* the lift of the ball. If φ is the coefficient of discharge, then

$$Q = f' \varphi \sqrt{2g \frac{p}{\gamma}} = f' \varphi \sqrt{2g \frac{mr\omega^2}{f\gamma}} = f' \varphi \omega \sqrt{2g \frac{mr}{f\gamma}}$$

and because this quantity equals that delivered by the pump, it follows that:

$$f' \varphi \omega \sqrt{2g \frac{mr}{f\gamma}} = K\omega, \text{ or } f' = oz = \frac{K}{\varphi \sqrt{2g \frac{mr}{f\gamma}}}$$

The equations above show that the term expressing the value of the flow area *f'* (and that of the lift *z*) does not contain the angular velocity. The lift does not depend upon the angular velocity and does not change with a change of speed. The flow area *f'* depends, however, upon the coefficient of discharge and the lift of the centrifugal ball changes with a change of viscosity. This means that the lift eliminates the influence of viscosity.

The conclusion that the centrifugal ball does not change its position during the controlling process is of great importance. It means that the governor has no parts which are brought into motion by a change of speed and which, due to their mass, cause a retardation of its function. The hydraulic governor operates as an ideal governor without mass.

Different conditions apply to the piston and to the oil in the connecting pipe *h*. In order to change the position of the piston, the piston and the oil must be accelerated. The mass of the oil in connecting pipe *h* has a harmful effect and its influence has been, therefore, eliminated by the arrangement shown in Fig. 366. Piston *I* is actuated by oil flowing either from the air pressure tank of the controller or from an auxiliary pump. The oil flows through pipe *2* and orifice plate *3*. It leaves the installation through the valve *4* which is pressed to the seat by the oil under

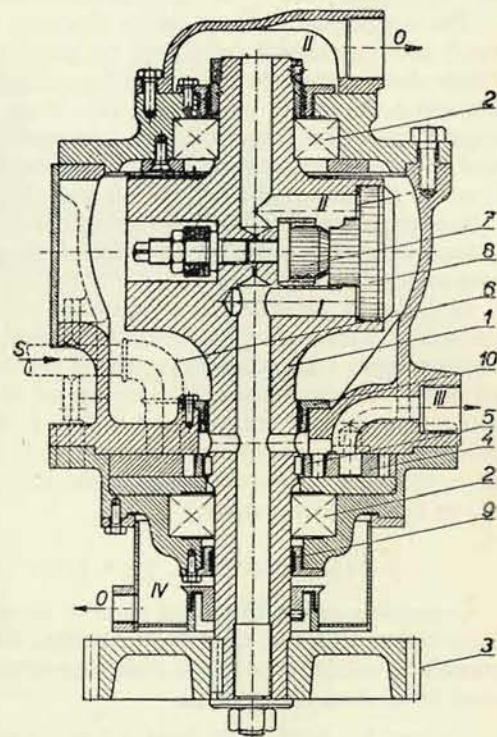


Fig. 367

control pressure from the hydraulic governor 5. The oil pressure in the regulating cylinder below the piston 1 is adjusted automatically so that the downward thrust upon the valve equals the force exerted in the opposite direction by the oil under control pressure. If the contact surface of the valve is equal to the area exposed to the oil under control pressure, the pressure below the piston will be the same as the control pressure of the oil. During control valve 4 has only very small lifts, so that the oil in the connecting pipe moves only very slightly and the inertia of the oil mass becomes negligible. At a diameter of the measuring piston = 5 cm, stroke = 2 cm and the diameter of valve 4 = 15 mm, the average lift of the valve is 0.3 mm. The reduced lift for a 10 m long connecting pipe is then 0.05 mm, i. e. a negligible value. The whole installation operates as an ideal governor without mass.

Hydraulic governors are mounted on the lids of turbines and driven by a reduction gear from the main shaft; the gear drives simultaneously the lubricating pump for the lower guide bearing of the turbine. The hydraulic governor shown in Fig. 367 is mounted in a vertical position; the vessel containing the control pressure oil is placed below. In smaller turbines the governor is mounted horizontally in the casing and driven by a gear from the jack shaft.

The central part of the governor illustrated in Fig. 367 is the casing 1 seated in two¹⁾ ball bearings 2 and driven by gear 3 from the main shaft of the turbine. Gear-wheel pump 4, 5 draws oil by the suction pipe 6 from the oil tank and delivers it through the duct 7 towards the centrifugal piece 7 which is pressed by centrifugal force against the seat 8. This arrangement causes a throttling of the oil flow and an increase of pressure in space I. The oil pressed around the piece 7 enters space II and flows back into the oil tank from which it was drawn by the pump. The space containing the oil under control pressure is connected by duct III and a connecting pipe with the pilot valve of the controller. The oil pump is sealed by two sealing bearings 9 and 10.

In order to increase the sensitiveness of the control, the governor space is excited by pressure impulses created by a periodical regular connection established between space I and discharge space IV by means of the smaller gear-wheel of the oil pump. Discharge space IV is connected by a pipe with the oil tank of the governor. The size of the pressure impulses and also the vibration of the control valve can be adjusted by a needle valve. This adjustment is of great importance for an exact setting of the overlapping in the main gate valve. The oil flows from space III to the controller proper.

III. GENERAL LAY-OUT OF CONTROLLERS

Controllers represent special parts of turbines and several types are produced according to different controller capacities. In present day practice the intention prevails to use one type of the main controlling elements (governors and stabilisers) for all sizes of controllers.

¹⁾ Němec K.: Konstrukční provedení hydraulického regulátoru vodních turbin ČKD. (Construction of hydraulic controllers of the ČKD water turbines), Strojirenství 1 (1951), No 7—8, p. 268.

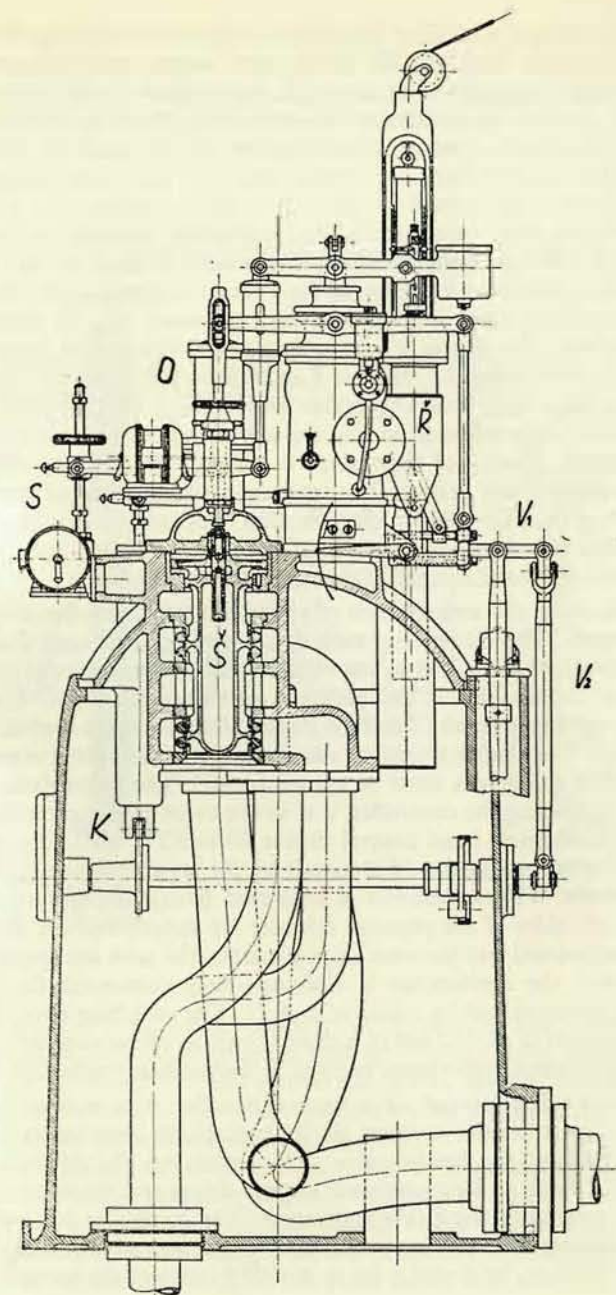


Fig. 368

Fig. 360 illustrates a controller installation with a compensating device according to the diagram in Fig. 343. We can see the single weight governor R_t with a vertical stem and compensating spring Z . The dog A of the governor actuates the amplifier designed according to the principle explained in Fig. 340. The amplifier has a separate oil pump which is driven by the governor. If the drive of the governor breaks down (belt or electric drive), the pilot valve ceases to supply oil, its piston is pressed upward by the spring and thus the turbine is closed. One end of the floating lever connected with the amplifier actuates the suspension of the pilot valve P which is connected also with the hand wheel K for setting the speed change (the hand wheel can be arranged for a remote control by an electric motor). The other end of the lever is connected with the isodrome (oil dashpot) I . The inner cylinder with the piston V and spring U constitutes the isodrome proper with the needle valve lifted by the arm J and the outer cylinder W represents the carrier N (See Fig. 344). Rod O together with lever L limit the opening of the turbine. If stirrup M is adjusted so that the upper end of its slot is in contact with the bolt of lever L , opening of the turbine is limited. Even if rotational speed decreases, the controller cannot open the turbine any further, because lever L prevents the movement of the pilot valve in the direction of opening the turbine (the spring in bushing B is compressed). In the event of increasing rotational speed, lever L does not prevent the closure of the guide apparatus of the turbine.

Fig. 361 illustrates the arrangement of a medium size controller with a capacity of about 500 kgm. The oil receiver tank 3, and the pressure tank 2 are mounted inside the controller base 1. Unloading valve 63 and the controller of air content 62 are also visible. Servomotor 13 and piston 14 are shown in section. Piston rod 15, crosshead 16, regulating crank 17 and the guides 18 transmit the control work to the regulating shaft. The shaft is shown in a horizontal position; for a vertical arrangement of the shaft the guides must be turned by 90° . The belt-driven oil pump is not visible. For starting the controller, i. e. in the event of complete absence of oil pressure, the mechanical hand control device 20 to 22 is used. Worm gear 20 is driven by a hand wheel. Piston 14 is moved by the jaws 22 which form the nut of the worm spindle. The servomotor is separated from the pressure tank by the cock 11 and both sides of the pressure cylinder are interconnected. After the turboset has been started and pressure oil is available, the jaws are opened by a lever (not visible) and the servomotor is simultaneously connected through control valve 12 to the pressure tank by means of cock 11. The switching over from hand to automatic operation is carried out in a closed position of the controller. The main gate valve of the control valve must be fixed in the position marked: "closed".

Fig. 368 shows the lay-out of a large controller with a capacity of about 20 000 kgm. The controller consists of the controlling installation \bar{R} (shown in detail in Fig. 360) and the control valve \bar{S} (for details see Fig. 357) with the speed setting device S (with an electromotoric remote drive) and the stroke regulator O (limiting the opening of the guide apparatus). The controller has no mechanical hand control device. The pressure oil supply from the pressure tank to the controller must, therefore, be closed prior to any shut down of the turbine. Due to the

absence of oil pressure in the servomotor the water pressure can automatically open the turbine; this is prevented by locking the guide apparatus during stoppage by a safety bolt. The oil pump is mounted directly on the turbine and for starting the turbine a special starting pump, driven by an electric motor or by a small impulse wheel, is installed. The pressure and receiver tanks equipped with the

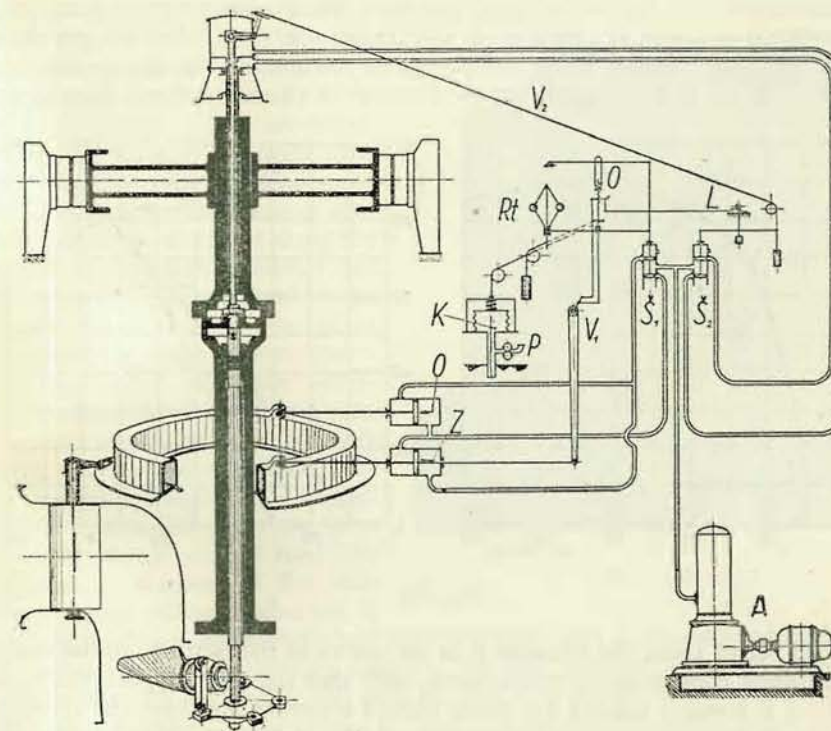


Fig. 369

necessary armature are mounted separately on a common base. The servomotors are mounted on the turbine. Regulating rods serving as a restoring mechanism are connected with the servomotor and actuate the bolt V_1 . Rod V_2 actuates the slotted piece K connected with the control valve regulating the setting of the runner blades of a Kaplan turbine (for more details see Fig. 369).

The complete lay-out of the controller unit is diagrammatically illustrated in Fig. 369. The complete pumping station A consists of an electrically driven oil pump (sometimes a second pump, driven directly by the turbine shaft, is connected in parallel), receiver tank unloading valve and pressure tank. Oil from the pressure tank flows to the control valve S_1 of the guide wheel and control valve S_2 of the

runner. In order not to complicate the diagram, pilot valves are not shown in the picture. Control valve \mathcal{S}_1 is actuated by the governor Rt and the stabiliser with the stroke regulator O . For a simplification of the diagram a rigid feed-back is shown in the picture.

The picture also shows an example of secondary control derived from the head race level. The auxiliary air pump p delivers air into the elastic chamber K and simultaneously to a float on the head race level. With a change of the head race level, the air pressure in chamber K will change too. The lid of the chamber loaded by a compensating spring will change its position and this change is transmitted by means of a rope to the stroke regulator O . (To simplify the diagram an

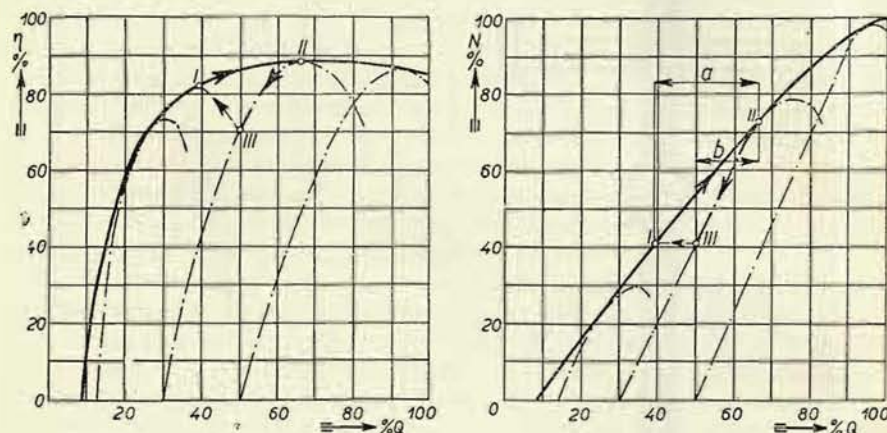


Fig. 370

amplifier placed above the chamber K is not shown in the picture). In the event of the turbine consuming too much water, more than the river supplies, the head race level is lowered and the secondary control automatically closes the turbine. The loss in output must then be compensated by another machine working in parallel.

The runner controller with control valve \mathcal{S}_2 is driven by the mechanism of the guide wheel controller via slotted piece L and rope V_2 . The servomotor of the runner controller is built in the main shaft of the turbine.

The normal equipment of a turbine contains also a safety governor driven directly by the main shaft of the turbine. This governor comes into action in the event of a random overstepping of the permissible rotational speed, it closes the turbine gates or it closes the runner by means of an auxiliary gate valve (which simultaneously puts out of operation control valve \mathcal{S}_2), or it inclines the deflector of a Pelton turbine.

Runner wheels are normally slowly closed by the controllers (with the exception of the safety governor which closes the runner rapidly). This is attained by a one

sided limitation of the stroke of the gate valve. The advantages of the system are illustrated in Fig. 370. The left side diagram shows the efficiency curve of the Kaplan turbine, constructed as an envelope of the efficiency curves for various settings of the runner blades (see Part I., Chapter X/1.), in relation to the flow rate Q . The right side diagram shows the output curve.

Let us assume that the turbine operating under conditions represented by the point I is suddenly loaded corresponding to point II . The guide and runner blades will be simultaneously opened and the stroke of the servomotor will be increased, according to the increased flow rate, by the value a . The point representing instantaneous operating conditions will move along the envelope curve from position I into position II . If the load drops again to the value I the point representing instantaneous operating conditions will move downward along the dot and dash line, because the runner is closed only very slowly. The servomotor will restore an equilibrium by a smaller stroke in accordance with the value b of the change of flow rate. The temporary increase of the rotational speed will be smaller too. If

output fluctuates permanently between the values I and II , the servomotor swings in accordance with the smaller value b of the change of the flow rate; changes of rotational speed are smaller and so is the oil consumption. In the event of a load stabilized at value III , the runner is steadily closed to the required extent and the point representing instantaneous operating conditions is moved to position I of higher efficiency.

Fig. 371 shows the section of a modern „duplex“ controller for Kaplan turbines (ČKD). The controller is located in a cabinet shown in Fig 372, together with the hydraulic controller (ČKD system). Oil pressure is controlled according to the rotational speed of the turbine by the method described in a preceding paragraph. Oil is delivered to valve 1 located in the cabinet. (Fig. 371.) The cabinet can be most suitably placed in the machine hall without regard to the auxiliary equipment and independently from the turbine, so that the requirements of an easy and efficient manipulation can be fully respected. Pressure changes are transmitted by the valve 1 which is placed in the cast iron casing 2 . Both parts can be easily dismantled by loosening the screw 3 . The valve closes the exactly calibrated opening of the nozzle 4 .

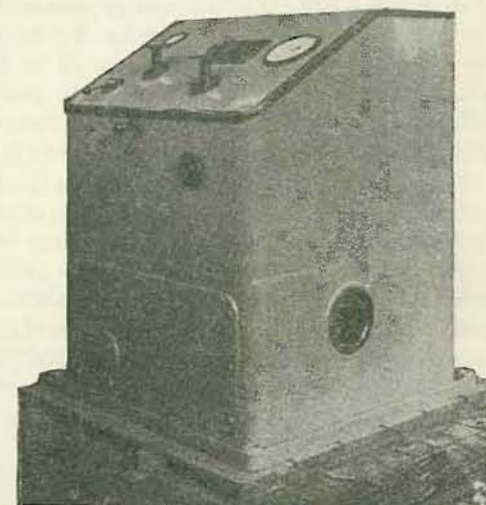


Fig. 372

Pressure head differences between the governor and cabinet can be compensated by the flow area of the nozzle. At the rated rotational speed 3 atm. g. oil pressure is normally maintained under the piston 5. The movement of piston 5 is transmitted to the control mechanism by means of the stem 6 which actuates the differential piston of the amplifier. The formation of air bubbles under the valve 1 is prevented by the needle valve 7 which is suitably mounted into the oil inlet pipe. The needle valve is permanently open (the opening is very small), so that it permits the escape of air which is present in the control pressure oil circuit during the starting period. Oil under control pressure is supplied by the pipe 9 and that part of it which passes the needle valve is returned by pipe 10 to the oil tank. Pressure oil is delivered below the measuring piston 5 from the pumping unit through a suitably sized orifice plate. Differential piston 11 is connected with the upper floating lever; the remaining parts are arranged according to Fig. 360.

The controller of the guide wheel is directly connected with the emergency installation. In the event of a break down of the hydraulic governor, pressure drop in the pressure tank or piping, defects or any other faults, the emergency installation closes the gates and brings the turbine to a standstill. Pressure oil is supplied to the differential pilot valve through this installation. When the turbine is at a standstill, gate valve 23 and slide sleeve 24 are pressed down by springs 25 and 26. The connection between ducts 31 and 32 is interrupted and, therefore, the differential pilot valve is without oil. Spring 12 holds the pilot valve in the position marked „closed“. When starting the machine, first of all the current supply to the D. C. electromagnet 27 must be switched on. The magnet lifts the sleeve 24. However, the connection between the ducts is not yet established, because duct 32 remains closed by the gate valve 23 which is lifted by the control pressure oil only after the rotational speed has reached about 75 % of its rated value. Therefore during the starting period the ducts are connected manually by means of the lever 30 and the cam 29: gate valve 28 is lifted and the ducts are interconnected. After the machine has attained full speed and the gate valve 23 has been lifted by the control pressure oil, gate valve 28 is returned to the lower position, the bypass is interrupted and the protecting installation is brought into action. In the event of a break down of the hydraulic governor when pressure of the control pressure oil drops to a value corresponding to 75 % of the rated rotational speed, gate valve 23 pressed by the spring 25 closes the oil supply to the pilot valve. Spring 12 moves the pilot valve into the „closed“ position. In the event of any other serious defect, the electrical protecting installation (contact pressure gauge, thermometer, oil flow indicator, controller protectings, etc.) transmits the necessary impulse to the relay which actuates the field breaking switch of the main generator, breaks the power circuit and breaks the current supply to the magnet 27. Spring 26 presses down the sleeve 24 which interrupts the oil supply to the pilot valve, and by this the turbine gates are closed.

Runner control is illustrated in Fig. 373. The controller of the runner is actuated by the restoring mechanism of the guide wheel. The movement is transmitted to shaft 42 with the keyed-on cam 43. The gate valve of the runner is actuated by

this cam through the lifter 44 and floating lever 45. The left end of the floating lever is suspended by the rope of the restoring mechanism 46 connected with the lever of the distributing head (See Appendix I). The control valve 22 of the runner operates in the slide sleeve 34. The assembly drawing shows the sleeve in operational

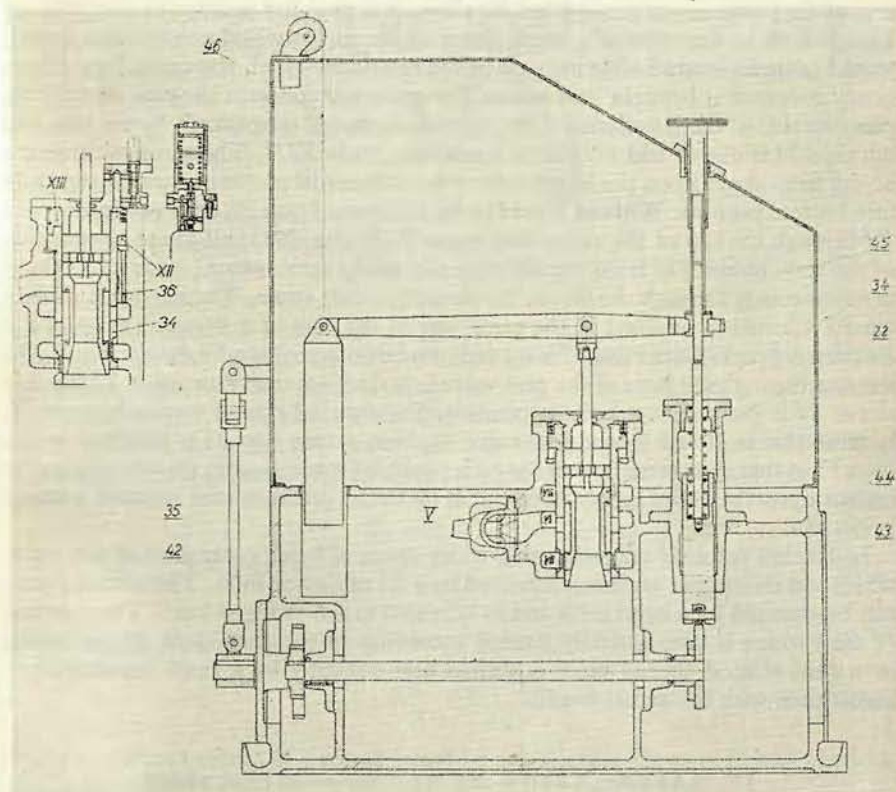


Fig. 373

position, the enlarged detail in a position in which it closes the gates. Pressure oil is delivered through duct V and check valve 35 into space VI from which it flows, at the first moment of pressure admission, through the slot of sleeve 34 to the space VIII and to the closure side of the servomotor. Oil flows simultaneously through the port 36 into space XII (Fig. 371). Here presses the piston and sleeve 34 upward into the working position, so that the oil supply to the closure side of the servomotor is interrupted and the runner blades are opened according to the position of gate valve 22. However, at the first moment oil streamed also through

the bore of the differential gate valve 37 (Fig. 371) and through duct 38 into the space XIII above the piston. This oil stream has been stopped in turn by the rapidly increasing pressure in the inlet pipe by which the differential gate valve 37 has been pushed in an upward direction against the pressure of spring 40. At this moment duct 38 has been connected with the discharge opening, so that the larger area of the piston is not pressed and the sleeve is kept in top position by the pressure from below. In the event of a break down of the guide wheel control unit, which would cause an inadmissible increase of the rotational speed, the centrifugal emergency governor is brought into action. The governor connects the pipe 39 with the pressure side of the installation. Gate valve 41 is moved downwards by the pressure oil, pipe 38 is closed and oil passes freely into space XIII. The same oil pressure acting from above upon the larger area of the differential piston pushes the sleeve 34 into bottom position. Without regard to the position of gate 22, oil flows from space VI through the slot of the sleeve into space VIII (Fig. 371) and to the closure side of the servomotor. Oil from the opening side of the servomotor (space VIII) flows simultaneously through the slot of the sleeve into free space. The runner is rapidly closed. Closure is attained in the same way in the case of a pressure drop in the air pressure tank. Gate valve 37 is moved into bottom position by the spring 40. Oil streams through the bore of the gate valve into duct 38, then into space XIII; slide sleeve 34 is pushed into bottom position. Pressure oil cannot escape by pipe 39, because this is closed by the gate valve 41. Non-return flap 35 is mounted in the duct V, so that no reverse flow of the oil is possible; consequently the water pressure cannot open the runner gates in case that oil in the pressure tank remains without pressure.

In Kaplan turbines operating at a wider range of head, controllers of the guide wheel and the runner are interconnected by a set of slotted links. The slotted pieces can be changed by a hand lever and so adjusted to the changed head. The opening of the turbine is automatically limited according to the conditions of cavitation, or a cone-shaped slotted piece is shifted automatically by a small servomotor in accordance with the actual head¹⁾.

IV. CALCULATION OF SPEED REGULATION

As far as theory is concerned, the reader of this book is advised to peruse the work of the author concerning this subject.²⁾ For completeness's sake this chapter deals with basic conceptions, denotations and directions for the calculation of speed control.

If a turbine, set working at a certain load, is suddenly relieved (to no-load) or

¹⁾ Němec K.: Konstrukční provedení hydraulického regulátoru vodních turbin ČKD. (Construction of hydraulic controllers of the ČKD water turbines.) Strojírnoství 1 (1951), No 7—8, p. 18.

²⁾ Nechleba: Theorie indirektní regulace rychlosti. (Theory of indirect speed control) Prague, Technicko-vědecké nakladatelství, 1952. The book contains derivations of the formulas.

partly relieved (part load), or inversely loaded suddenly from no load to full load, the controller cannot instantaneously adjust the gates to the new position called for by the change of load, because the servomotor piston moves with a definite velocity and it needs a definite time to travel a given stroke. A transitory state occurs, during which the input of the wheel is higher (or lower in the event of a sudden load increase) than the output of the generator. The surplus (deficiency) energy is consumed (supplied) by the revolving masses of the set which are being accelerated (retarded). Temporarily the set acquires higher (lower) speed which is later brought to a final value by the controller. Fig. 374 shows the shape of the speed curve against time in the case of a relieved set.

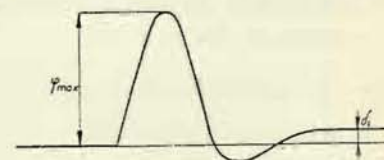


Fig. 374

The maximum deviation from the initial speed is denoted φ_{\max} , called the temporary speed increase and expressed as a percentage of the rated speed. The permanent droop δ_t has been discussed in a previous chapter; it is expressed also in percents of the rated speed and its value can be either positive or negative. The negative droop has had some significance in the drive of D. C. dynamos, to-day it is no longer used.

The value of the temporary speed increase occurring in the course of relieving or loading, is best expressed by Braun's formula

$$\varphi_{\max} = \frac{1}{2} \frac{T_s + 1.5 T_l \left(1 - 0.4 \frac{T_l}{T_s}\right)}{T_a + \frac{1}{4} T_s} \quad (252)$$

or by a simpler formula of the author

$$\varphi_{\max} = \frac{1}{2} \frac{T_s + T_l}{T_a}, \quad (253)$$

The proportional values of the temporary speed increase for partial load changes are the following:

$$\text{for a change } \lambda = 0.5 \quad \varphi = 0.45 \varphi_{\max} \quad (254)$$

$$\text{for a change } \lambda = 0.25 \quad \varphi = 0.20 \varphi_{\max}$$

In the above and following equations the following symbols are used:

$T_a = \frac{GD^2 n^2}{270,000 N_{\max}}$ = the starting time of the machine required to increase the speed from zero to the rated value — in seconds. N is expressed in metric horsepower.

T_s (or T_0) time in seconds desired for the full stroke of the piston of the servomotor. The piston travels the full stroke at the adjusted maximum speed in the direction of closure (or opening).

T_i — falling time of isodrome, during which the piston of the isodrome travels 2/3 of its stroke — in seconds.

T_n — half starting time of the mass of inertia during which the revolving mass of inertia of the governor changes its speed from zero to normal under the influence of the force of the compensating spring — in sec.

$T_l = \frac{\Sigma LC}{gH}$ starting time of the pipe, during which the water flowing through the pipe increases its velocity from zero to the normal value C under the influence of the head H — in seconds.

L — length of pipe in meters.

$C = \frac{Q}{F}$ velocity of water in pipe — in m/sec.

g = gravitation — in m/sec².

H — head in meters.

τ with the respective suffixes — relative time — any of the above times divided by the time of closure T_s — without dimensions.

$\frac{GD^2}{4g}$ — moment of inertia of the revolving mass — in kgm.²

n — speed of the machine — in r. p. m.

δ — droop of the governor without dimension.

δ_i — permanent droop — without dimension.

$\lambda = \frac{N}{N_{\max}}$ relative change of load — without dimension.

$\beta = \frac{m_{\max}}{z_{\max}}$ — acceleration coefficient of the stabilisator (see Fig. 344). — without dimension.

$\varphi = \frac{\Delta n}{n_s}$ — relative change of speed — without dimension.

$\Delta n = n - n_s$ deviation from the medium speed — in r. p. m.

n_s — medium speed — in r. p. m.

Results derived from Braun's formula are clearly visible in the diagram Fig. 375. In order to reduce the number of variables, so that a graphic representation is made possible, relative times τ were introduced.

For the case of a stabilized control, i. e. for the stabilisation of the controlled parameter the following relations must apply:

$$T_i = 2.36 T_l,$$

$$\delta T_a > 3.74 \frac{T_i^2}{\beta T_l}, \quad (255)$$

where $\beta T_i \cong T_s$, i. e. the time of closure adjusted by the orifice plate. If the dashpot has a special by-pass which is opened when the full stroke of the reverse points is reached, the product βT_i may exceed the value of T_{ss} . According to another work of the author¹⁾ it is advantageous to select

$$T_i = 3 T_l,$$

$$\delta T_a = \frac{2 T_l}{\beta}. \quad (255a)$$

Equations (255) and (255a) hold good also for controllers with stabilization by

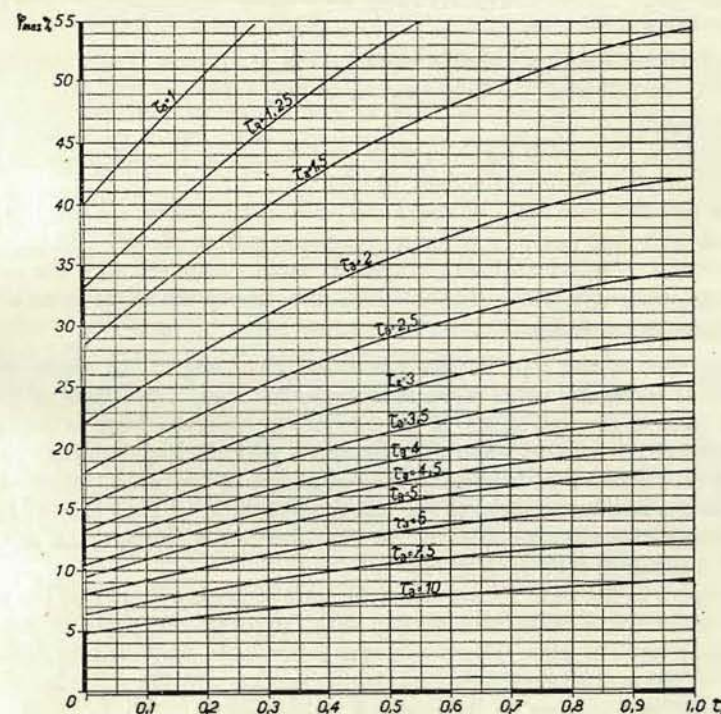


Fig. 375

forces of inertia (e. g. according to Fig. 347), provided that we substitute the half-time T_n for the isodrome time T_i and the time of closure T_s for the product βT_i .

The properties of the network into which the alternator is connected generally

¹⁾ Nechleba: Doplnění diagramu Višněgradského (Supplement to Vishnyegradsky's diagram), Strojřenství 3 (1953), No 11.

improve the stability of the control unit by their selfregulating qualities. Equations in which this effect of the network is respected, are, however, far more complicated.¹⁾

Correct calculation should give a resultant GD^2 of a minimum value, a rotor of smallest weight (an increase of weight above the minimum is justified only by construcional reasons), safe stability of the control and the prescribed values of the temporary speed increase. With regard to the forces of inertia of the control mechanism, the time of closure and the opening time respectively must remain within the admissible limits. This limiting value is $T_s \geq 1.5$ to 2 seconds for turbines with regulating ring and guide blades, a shorter time of closure may be applied for Pelton wheels with deflectors. The time of closure and the opening time respectively must also be within the limits established with regard to the increase or reduction of the head race level.

First of all we select a suitable value of the temporary speed increase for a rejection of the full load; the following values may serve as a guide:

Pelton wheels 12—16 %,

small Francis or Kaplan turbines with short penstock 16—20 %,

large Francis and Kaplan turbines 20—25 %,

Francis turbines with long penstocks and pressure regulators (see later) 20—25 %,

turbines with long penstock without pressure regulator 22—25—30 %,

largest turbines at which load changes are small compared with the output of the turbine (output 60,000—100,000 h. p. and above) the short duration speed increase may be up to 30—50 %.

Starting time of the pipe is then calculated according to the above equation, velocity C is taken at a value corresponding to full load. The length of the spiral casing is taken as the half length of the central stream-line, owing to the fact, that the quantity of the moving water mass decreases with the length of the spiral. The length of the suction pipe is taken as the full length of the central stream-line, the velocity as the arithmetic mean of the velocities of water at both ends of the tube. Starting time is separately calculated for the inlet pipe with the spiral as the time T_{11} and for the draft tube as time T_{12} .

With regard to the time T_{11} we select the time of closure T_s so that the pressure increase in the spiral casing will comply with the prescribed pressure tests of the spiral casing and the pipe. The pressure is determined according to Allievi, Michaud or by the graphical method (see chapter dealing with the water hammer).

The total starting time of the water is calculated as $T_l = T_{11} + T_{12}$ and its relative values as $\tau_l = \frac{T_l}{T_s}$; further the starting time of the machine is determined according to the selected value of the temporary speed increase φ . The moment of inertia GD^2 is calculated from the starting time of the machine, which is determined from the relative time τ_a (the value of the relative time is taken from the

¹⁾ Theorie indirektní regulace rychlosti, 2. vydání (Theory of indirect speed control, 2nd edition), Prague, Technicko-vědecké nakladatelství, 1952. This edition includes the derivations of equations (255).

diagram 375). By multiplying the relative time by the time of closure T_s we receive the time T_a in seconds.

The above calculating method is applicable also to Francis and Kaplan turbines, provided, that the time of closure of their runner equals the time of closure of the guide wheel. If the time of closure of the runner is considerably longer than that of the guide wheel, the open runner blades act as a break and they reduce the short duration speed increase by about 20 % of the value shown in the diagram. This fact is to be born in mind, because it reduces the necessary GD^2 of the turbine set.

For part load runs we can calculate the values according to Equation (254).

Then follows a control calculation of sudden load increase. The opening time T_0 is selected so that the head is reduced by no more than 25 (up to 30) %, because otherwise the output increases slowly and the control hunts. Normally we select $T_0 = 2 T_s$. If the location of the conduit is established so that the first part of the pipe line is laid with a smaller slope than the second, it is necessary to determine separately the starting time of the less inclined part and the opening time of the controller must be longer than this starting time, because otherwise the water column in the first part of the pipe must be accelerated by the underpressure created in the bend and the column disrupted. Abnormal cases must be investigated specially.

From diagram 375 we can read the speed reduction for $\tau_l = \frac{T_l}{T_0}$ and $\tau_a = \frac{T_a}{T_0}$.

These values should correspond to a sudden application of the full load, but this is never the case. For a 50 % load we take half of the diagram value and for 25 % part load 0.2 of the value established from the diagram.

We must not forget to check if there is no danger of disruption of the water column in the draft tube at the established time of closure T_s .

If turbines with a long penstock are equipped with pressure regulators, the pressure regulator is adjusted so that the pressure rise amounts to 20 % of the rated pressure. Pressure drop during load increase is the same as before, because it is not influenced by the pressure regulator. Similarly the pressure regulator does not effect the stability of the control and the criteria (255) must be adhered to as in the case of a turbine without pressure regulator. Therefore stability of control is checked according to the relations (255). The second inequality must be complied with and, with regard to the sufficient sensitiveness of the governor, the value δ must not be higher than 24 % up to 30 % (in exceptional cases). Should the inequality remain unfulfilled even at this high value of δ , it is necessary to select a longer starting time T_a of the machine, i. e. heavier revolving masses.

Finally it is necessary to consider the type of plant with regard to the selection of the correct permanent droop. We select the permanent droop for autonomous plants, or plants operating in parallel. In the latter case we make different selection for base-load hydro plants and for peak-load hydro plants. We select

for autonomous plants $\delta_i = 3$ to 4 %,

for peak-load plants $\delta_i = 1$ to 3 % and

for base-load plants $\delta_i = 5$ to 8 %.

These values influence the distribution of the rise or drop of output upon the individual machines of the system. Generators working in parallel are kept in step by equalizing currents. If the total output of the network is sufficiently high compared with the output of the unit considered, the speed of the machine will not change by an adjustment of its speed controlling device (e. g. by adjusting the controller to the position „more rapid“). The speed remains constant (it changes only very slightly), because it is determined by the electric alternator. However, by the adjustment of the controller the filling of the turbine has been increased and,

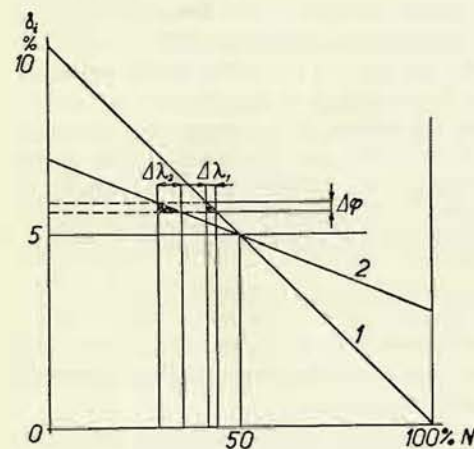


Fig. 376

this change depends upon the permanent droop of the controller as can be seen from Fig. 376.

If speed is reduced by the values $\Delta\varphi$, the load of the machine with the less inclined characteristic curve (2) is increased by the value λ_2 and that of the machine with the more inclined curve (1) is increased by a smaller value λ_1 . The controllers of machines working at permanent loads are set, therefore, to a high value of δ_i and those working at peak are set to small values of δ_i .

A machine with a permanent droop equalling zero (represented by a characteristic curve running parallel to the N axis) or with a negative permanent droop opens its control valve completely even at the slightest drop of the system frequency. Such machines are not suitable for parallel operations. A machine with a permanent droop equalling zero can work in parallel only in case that there is only one such machine in the whole system and provided its output is sufficiently high. All load changes of the system will be taken up by this single machine (the remaining machines will work at constant load) and its output must be, therefore, sufficiently high to comply with this condition.

The slope of the characteristic curve determines thus the stable and definite

therefore, the output of the alternator is increased too. (In order to return the control valve to neutral position, the servomotor and restoring mechanism must change their position, because the sleeve of the governor does not move.) After synchronisation with the network the alternator can be brought to the full rated output by adjusting the controller to the „more rapid“ position. The adjustment represents the value corresponding to the permanent droop δ_i .

If, on the other hand, the frequency of the network changes during operation and so does the speed of the turbine the governor sleeve changes its position and the load of the turbine is increased or reduced. The range of

distribution of load changes occurring in the system to the individual machines. The relative changes of load of the individual machines are indirectly proportional to the permanent droops. Therefore it follows, that

$$\frac{\Delta N_1}{N_1} : \frac{\Delta N_2}{N_2} = \frac{1}{\delta_{i1}} : \frac{1}{\delta_{i2}} \text{ or } \frac{\Delta N_1}{\Delta N_2} = \frac{N_1}{N_2} : \frac{\delta_{i2}}{\delta_{i1}} = \text{const.}$$

The ratio $\frac{N}{\delta_i} = \cot \alpha = L$ determines the slope of the characteristic curve of the controller. The slope of the characteristic curve of the whole system is given by the sum total of all cots. characteristic curves of the individual machine sets $\frac{\Delta N}{\Delta \varphi} = \Sigma L$. The change of frequency of the system at a given change of load is then determined by this characteristic curve.

Example. Spiral Francis turbine, head 42 m, $n = 300$ r. p. m., flow rate $Q_{\max} = 16.2$ m³/sec., output $N_{\max} = 7800$ h. p. The turbine is connected to a pipe line having a diameter 2600 mm and a length 35,000 mm. A conical reduction part 8 600 mm long follows so that the last cylindrical part has a diameter 1800 mm and is 11,000 mm long. This length includes also half the length of the spiral casing in which velocity of the flow is the same as in the pipe line. The upper end of the draft tube has a diameter 1700 mm and the lower end has a cross section 2360 · 5200 mm². Length of the draft tube = 13 000 mm. The turbine is equipped with a controller with elastic compensating device. Pressure rise in the spiral should not exceed 50 % and the temporary speed increase should be maximum 20 %.

Water velocity in cylindrical parts of the pipe is $C_1 = \frac{16.2}{5.3} = 3.05$ m/sec.,

$C_2 = 6.35$ m/sec.; by calculating the velocity in the conical part as the arithmetic mean of these values, the starting time of the total pipe conduit is

$$T_{11} = \frac{3.05 \cdot 35 + 4.7 \cdot 8.6 + 6.35 \cdot 11}{9.81 \cdot 42} = 0.525 \text{ sec.}$$

For the draft tube we established $C_3 = 7 \cdot 15$ m/sec and $C_4 = 1.32$ m/sec and the starting time

$$T_{12} = \frac{4.23 \cdot 13}{9.81 \cdot 42} = 0.134 \text{ sec.}$$

The relative pressure rise can be calculated according to Michaud's formula (353):

$$\alpha = \frac{\Delta H}{H} = 2 \tau_1 = 0.5,$$

from which follows

$$\tau_{11} = 0.25 = \frac{T_{11}}{T_3},$$

so that the time of closure is

$$T_s = \frac{T_{l1}}{0.25} = \frac{0.525}{0.25} = 2.15 \pm 2.5 \text{ s.}$$

The total relative starting time of the pipe line is then

$$\tau_l = \frac{T_{l1} + T_{l2}}{T_s} = \frac{0.525 + 0.134}{2.5} = 0.263.$$

According to (Fig. 375) diagram for this value of the relative time and for $\varphi_{\max} = 20\%$, $\tau_a = 3.2$ and the starting time of the turbine set must be $T_a = 3.2 \cdot 2.5 = 8$ seconds. Therefore the necessary moment of inertia is

$$GD^2 = \frac{270,000 \cdot 7800 \cdot 8}{300 \cdot 300} = 185,000 \text{ kgm}^2.$$

Let us select according to (255a)

$$T_i = 3 T_l = 3 \cdot 0.659 \pm 2 \text{ sec.},$$

$$\text{and } \delta \beta = 2 \frac{T_l}{T_a} = 0.16,$$

and if we select $\delta = 18\%$, it follows

$$\beta = \frac{0.16}{0.18} = 0.9 \pm 1.$$

According to (255) the following relations should apply:

$$T_i = 2.36 \cdot 0.659 = 1.55 \text{ sec.},$$

$$\text{and } \delta T_a > 3.74 \frac{0.44}{1.55} = 1.06$$

and considering the value $T_a = 8$ sec., we arrive at $\delta > \frac{1.06}{8} = 0.13$, so that the values T_a and δ are in conformity with this condition.

By the application of an orifice plate we reduce the time of closure to $T_s = 2.5$ sec.

Let us now assume that the turbine is equipped with a pressure regulator. We may then select $T_s = 2$ seconds. The pressure rise (controlled by the pressure regulator) would be $\kappa = \frac{\Delta H}{H} = 0.2$. From the Michaud's expression written in the form $\kappa = 2 \tau_l$ we find the fictitious starting time of the pipe $\tau_{l1} = \frac{\kappa}{2} = \frac{0.2}{2} = 0.1$. With regard to the draft tube we select the total $\tau_l = 0.15$. We plot this value in the diagram 375 against the value $\varphi_{\max} = 20\%$ and find the value $\tau_a = 2.8$. Consequently

$$T_a = 2.8 \cdot 2 = 5.6 \text{ sec} = 6 \text{ seconds.}$$

The criteria of stability must be calculated, as before, with the actual τ_l :

$$T_i = 2.36 \cdot 0.659 = 1.55 \text{ sec.}$$

and thus at $\beta = 1.2$ it follows:

$$\delta T_a > 3.74 \frac{0.44}{1.6 \cdot 1.2} = 0.85,$$

so that

$$\delta > \frac{0.85}{6} = 0.14,$$

which is satisfactory at the usual setting of $\delta = 18\%$.

In the event of applying the relations (255a) the selection would be

$$T_i = 3 T_l = 3 \cdot 0.659 \pm 2 \text{ sec.}$$

$$\delta \beta = \frac{2 T_l}{T_a} = \frac{2 \cdot 0.659}{6} = 0.22,$$

so that with $\delta = 0.18$ it is necessary to set

$$\beta = \frac{0.22}{0.18} \pm 1.22.$$

In this case the necessary moment of inertia is

$$GD^2 = \frac{270,000 \cdot 7800 \cdot 6}{300 \cdot 300} = 140,000 \text{ kgm}^2.$$

V. CHECKING OF CONTROLLERS

Controller operations are normally checked by a tachograph which automatically records the course of the speed values in relation to time. Fig. 377 shows the reprint made by Horn's tachograph. Three types of recording springs can be used in the apparatus; one dash represents then a change of speed by 2 %, 1 % or 0.5 %. The movement of the strip chart can be adjusted for various speeds. Recordings for acceptance tests are generally made with 2 % springs and a chart movement of 2 mm/sec. With a correctly working controller and an even load the record speed line should be a straight line without undulations, because the insensitivity of good controllers lies below 0.1 % ($\pm 0.05\%$) and this cannot be apparent with a 2 % springs used.

Therefore the servomotor piston should not change its position at an even load. Vibrations of the governor proper, however, are admissible, because the minute forces cannot cause a wear of the pivots and the vibration reduces the insensitivity of the governor.

The record permits the following readings: the temporary speed increase $a\%$ from the initial position, $c\%$ permanent droop and the time of closure T_s required to

bring the servomotor from the initial position to the position of the new equilibrium (but not to the position of complete closure or of the dead point of the piston); further we can read from the chart the time T_x necessary for the control operation

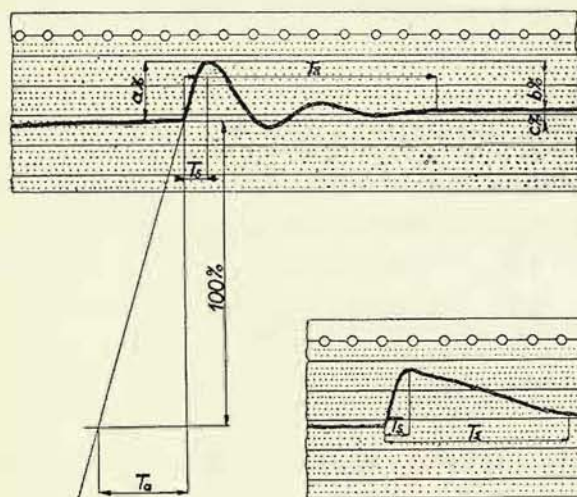


Fig. 377

and the starting time T_a of the machine. The latter time can be established by measuring a straight line at a distance of 100 % from the line of the normal speed (if 1 mm — 1 %, the straight line is at a distance of 100 mm), see Fig. 377.

Pelton turbines have

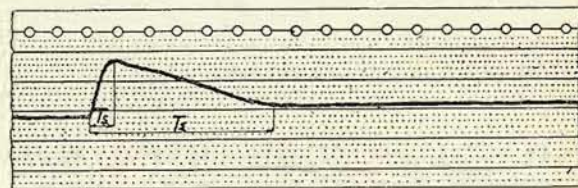


Fig. 378

small passive resistances and their speed line, after complete load rejection and speed increase, runs according to the straight line. (Fig. 378). With a relieved machine (e. g. from full load to 50 % part load) where the remaining load has a braking effect, the speed line runs according to real regulating conditions.

Controllers of hydraulic turbines are supplied and accepted in this country according to the Standard Specification ČSN 08 5010 – 1951: „Water turbines, instructions for tests and guarantees of hydraulic and regulating properties.“

B. THRUST BEARINGS¹⁾

I. PURPOSE AND LOCATION OF THRUST BEARINGS

Axial loads of a vertical turbine set transmitted by the main shaft are carried by the thrust bearing. The axial load consists of (see Appendix I):

1. The weight of the rotating parts, i. e. the weight of the runner, the turbine shaft (in Kaplan turbines the weight of the oil charge must be added), the generator shaft, the rotor and the weight of the revolving parts of the thrust bearing. In turbines with reduction gears the weight of the latter must be added to the axial load.

¹⁾ The Section on Thrust Bearings has been prepared by Ing. J. Urban.

2. The hydraulic thrust of the water on the blades of the runner. The calculation of the hydraulic thrust has been described in Part II., for Francis turbines in Chapter 1, A, I/12, for Kaplan turbines in Chapter 2, A, I/10.

3. In case of a transmission gear being mounted between the turbine and the alternator, the thrust of the bevel gear must be added to or subtracted from the axial load according to the arrangement of the gear.

In a turbine unit with a horizontal shaft the weights enumerated in point 1. will not appear, because they are carried by the radial bearings.

The established axial load is the basis for the dimensioning of the sliding surface of the bearing as described later. The calculation of the axial load is not entirely exact. The calculated axial load is, therefore, checked on an actual machine; this check shows what effect, if any, has the deviation from the calculated value upon the function of the bearing. Such practical checks are also best source of data for future design.¹⁾

The dimensioning of the bearing and its lubricating sets also depends upon the speed of the unit. If the turbine is directly coupled with the driven electric alternator, the synchronous speed of the set is calculated according to the current frequency as follows:

$$n = \frac{60 \cdot f}{p},$$

where n is the speed in r. p. m., p is the number of pole pairs (half the number of the pole pieces) and f is the current frequency (in Europe $f = 50$). If the turbine is used for driving transmission shafts or other plant, its speed may be chosen arbitrarily.

The bearing and the lubrication sets must be dimensioned also with regard to the runaway speed which the turbine can attain at a sudden rejection of load and a breakdown of the controller. The ratios of runaway speeds to operational speeds for different types of turbines have been given in Part I., Chapter X/2.

Further factors necessary for the bearing design are: general lay-out of the turbine set, arrangement of the bearing and hanger structure with regard to the turbine and the alternator respectively. The following arrangements are possible:

1. The thrust bearing with the hanger structure is located above the alternator and the guide bearings of the alternator are above and underneath the rotor. This is the usual classical arrangement, see Fig. 379. The principal justification for this arrangement is the requirement, that the most exposed part of the unit, i. e. the thrust bearing, should be easily accessible for demounting in case of a break down (in the case of the main shaft carrying the whole turbine set, only the exciter of the alternator is dismounted; with Kaplan turbines only the distribution head). Nowadays the bearing is a part of the turbine which is as reliable, as any other part and, therefore, it is not necessary to adhere to the classical arrangement. The arrangement is most frequently used for units with high operational speeds, because the

¹⁾ E. g. Casacci, Peuchmaur: Études expérimentales sur le fonctionnement des pivoteries industrielles, La Houille Blanche, 1951, p. 23.

hanger structure can be easily dimensioned owing to the small diameter of the stator casing to which the hanger structure is attached. The arrangements described further sub 2. and 3. are far more complicated from the designer's point of view. The lower guide bearing of the alternator is carried by a separate cross-beam which supports also the hydraulic brakes. With short shafts the lower guide bearing may

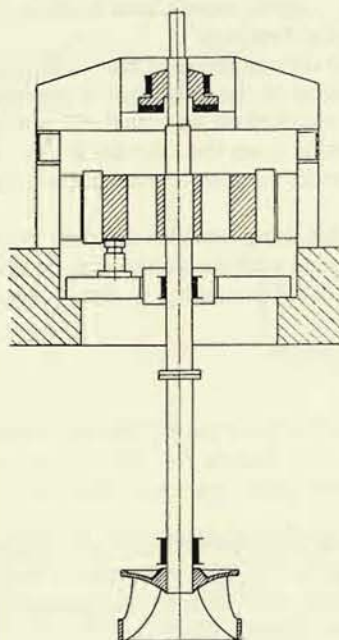


Fig. 379

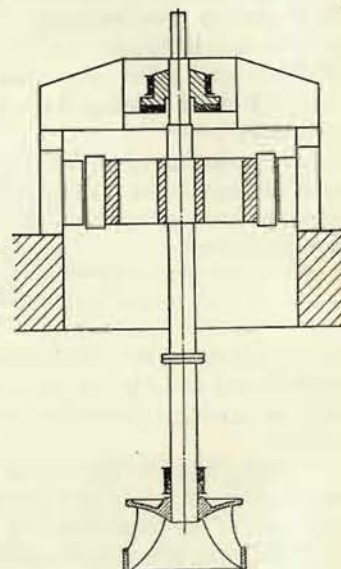


Fig. 380

be left out and the critical speed will be still satisfactory (see Part II, Chapter 1, B, II/5) - (Fig. 380).

2. The thrust bearing with the hanger structure can be located also underneath the rotor of the alternator (Fig. 381). This arrangement is used for units with low operational speeds, i. e. with large machines. The hanger structure of the bearing is lighter and less expensive, because its span is smaller. The design of the bearing is, however, more complicated (the bearing is made of two parts), because dismantling must be carried out in a downward direction (without dismantling the alternator). The rotor must be arranged so that it permits the passing of suspension bars used for dismantling the thrust bearing by means of the main mounting crane. Dismantling can be done also by means of an auxiliary installation located in the pit above the turbine. The upper guide bearing of the alternator is supported by the upper cross-beam which carries the exciter (if this is mounted on the main

shaft) and the distribution head (in the case of Kaplan turbines). Hydraulic brakes are located directly on the hanger structure (Fig. 381).

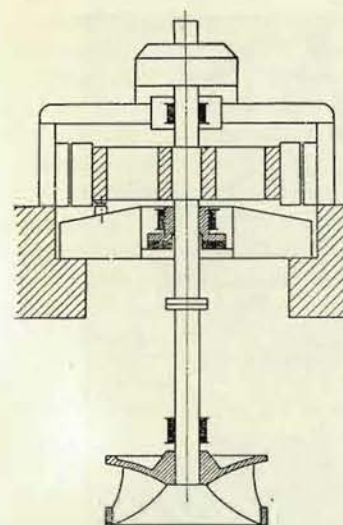


Fig. 381

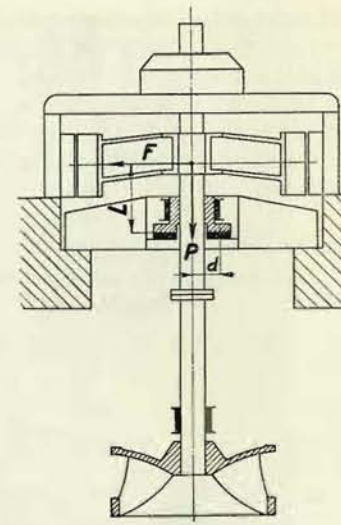


Fig. 382

3. Another possible arrangement is the so called „umbrella“ type. (Fig. 382). The rotor is mounted in an overhung position on the upper end of the shaft. Then there is no need for the upper guide bearing, so that the unit has only two guide bearings.

For ensuring the stability of the rotor the following condition must be complied with:

Bending moment $F \cdot l =$ Stabilizing moment $P \cdot d$, where F is the magnetic pull and the centrifugal force resulting from the unbalanced revolving mass, l is the distance of the plane passing through the centre of gravity of the rotor from the plane of the segments, P is the total axial load and d is the diameter of the circle passing through the centers of gravity of the segments.

This condition shows, that the arrangement is suitable only for units with low operational speed. This arrangement has, however, the same advantage as the previous one, i. e. there is no danger of damaging the coil windings by percolated oil, because the oil tank of the bearing is underneath the rotor. The bearing need not be electrically insulated (for details see Chapter VI) and it has a smaller weight. If the exciter (or the distributing head in Kaplan turbines) must be mounted on the main shaft and supported by the upper cross-beam, the arrangement described sub 2. is more

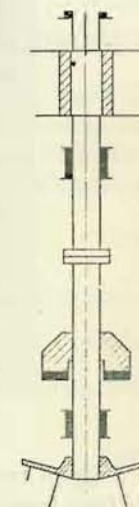


Fig. 383

suitable. The distributing head need not be always above the rotor, see Fig. 177. The hydraulic brakes are mounted on the hanger structure.

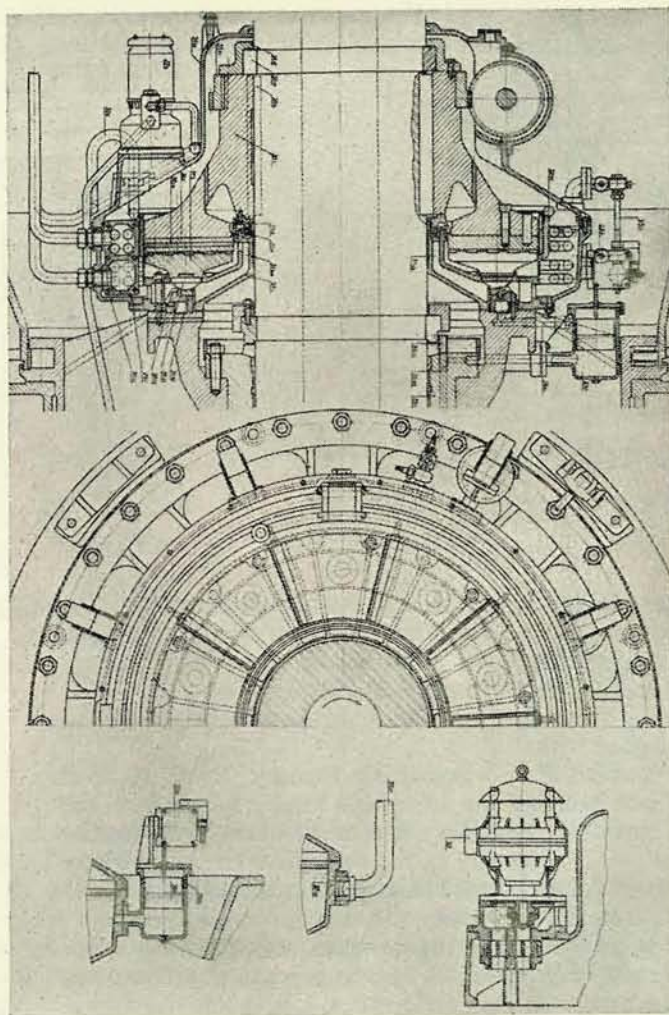


Fig. 383a

4. Up to date designs show frequently an arrangement where the thrust bearing without hanger structure is located directly on the cover plate of the turbine (Figs. 383, 383a and 177). The main advantage of this arrangement is, that no hanger

structure is necessary. The axial load is transmitted by the bearing through the guide vanes directly to the foundations of the turbine; the cover plate must be slightly strengthened, because the hydraulic forces acting upon the runner of the turbine in the axial direction are to a large extent outbalanced by the water pressure upon the cover plate of the turbine. This arrangement also requires a more complicated design of the bearing (made of two parts). Guide bearings are located according to the rotor arrangement. The solution of the lay-out of the cover plate is rather difficult. The cover plate contains packings, labyrinths, the guide bearing, the pumping installation for the discharge of the leakage water. The thrust bearing must be located above these parts, the height of the cover plate is increased and the above enumerated installations are not easily accessible.

Last not least we must remember the important factor of the stability of the shaft. From this point of view arrangement No. 1. seems to be the most suitable.

II. THE HYDRODYNAMIC THEORY

In sliding bearings the following frictions can occur: dry friction, fluid friction and the semifluid or limit friction. The considerations in this chapter will deal with the theory of fluid friction as the basic factor for the design and calculation of bearings. Dry or semifluid friction occurs only during the starting¹⁾ or closing period when there is no bearing oil layer formed yet between the sliding surfaces. This factor will be considered in the paragraph dealing with the selection of materials for the sliding surfaces.

1. Viscosity of oil

Before embarking upon the theory proper, we have to discuss the viscosity of liquids more thoroughly than hitherto.

Viscosity (cohesion or internal friction) is the property of liquids, based on molecular movements, which enables them to resist the final forces of pressure and shear. The relative movement of two parallel adjacent layers is opposed by friction on the contact planes. The value of this friction is expressed by Newton's relation (191).

$$\tau = \pm \mu \frac{dC}{dy}, \quad (256)$$

where τ is the viscous shear stress, μ denotes the coefficient of dynamic cohesion or viscosity and $\frac{dC}{dy}$ is the velocity gradient or the relative velocity of two adjacent layers for an infinitely small perpendicular distance dy . The dynamic viscosity is then expressed by the relation

$$\mu = \tau \frac{dy}{dC}. \quad (257)$$

¹⁾ Performance of Vertical Water Wheel Thrust Bearing during the Starting Period; Transactions ASME, 69 (1947), No 40, p. 543—547.

If the components on the right side of the equation are expressed in technical units, i. e. τ in kg/m², the gradient $\frac{dC}{dy}$ having the dimension of angular velocity in 1/sec., the technical unit of dynamic viscosity is then kg · sec/m².

Kinematic viscosity ν is an established physical conception defined by the ratio of two mutually independent physical values: the dynamic viscosity μ and the density of the liquid $\rho = \frac{\gamma}{g}$ in terms of mass per unit volume.

$$\nu = \frac{\mu}{\rho} = \frac{\mu g}{\gamma}$$

By inserting dimensions in technical units we receive the technical unit of kinematic viscosity (with no special denotation) as m²/sec.

Viscosity of the liquid is rapidly reduced with increasing temperature; the effect of pressure changes need not to be considered in calculations. An apparent rise of viscosity of liquids can be observed at pressures above 150–200 atm. g. Viscosity of air starts to increase at 25 atm. g.

In the C. G. S. system – centimeter as unit of length, gram as unit of mass, second as unit of time and dyne as unit of force – the unit of dynamic viscosity is named the poise. Thus

$$1 \text{ Poise} = 1 \text{ P} = 1 \frac{\text{dyn} \cdot \text{sec.}}{\text{cm}^2} = 1 \frac{g}{\text{cm} \cdot \text{sec.}}$$

Smaller units are 1 centipoise = 1 cP = 0.01 P

1 micropoise = 1 μ P = 1/10⁶ P.

The unit of kinematic viscosity in the C. G. S. system is the stoke:

1 Stoke = 1 St = 1 $\frac{\text{cm}^2}{\text{sec.}}$ = 1 P/ ρ , where ρ is the density in g/cm³.

The smaller unit is the centistoke:

$$1 \text{ cSt} = 0.01 \text{ St.}$$

Relations between various units of viscosity are given in the following table:

Dynamic viscosity	Unit in the C. G. S. system	Technical unit	Relations of units
μ	1 P = 100 cP = = 1 $\frac{\text{dyn} \cdot \text{sec.}}{\text{cm}^2}$	1 $\frac{\text{kg} \cdot \text{sec.}}{\text{m}^2}$	1 $\frac{\text{kg} \cdot \text{sec.}}{\text{m}^2} = 98.067 \text{ P}$ 1 P = 0.010197 $\frac{\text{kg} \cdot \text{sec.}}{\text{m}^2}$
kinematic viscosity	= 1 $\frac{g}{\text{cm} \cdot \text{sec.}}$		
$\nu = \frac{\mu}{\rho}$	1 St = 100 cSt = = 1 $\frac{\text{cm}^2}{\text{sec.}}$	1 $\frac{\text{m}^2}{\text{sec.}}$	1 $\frac{\text{m}^2}{\text{sec.}} = 10^4 \text{ St}$ 1 St = 10 ⁻⁴ $\frac{\text{m}^2}{\text{sec.}}$

Measurement of viscosity by a viscometer is based upon the time taken for a definite volume of the liquid under test to flow at a given temperature through an opening of definite dimensions and shape. Results of measurements by viscometers are expressed in empirical units of viscosity. The relations between the different empirical units of viscosity are given in the following table:

	E	R ₁	R ₂	S	SF	
E	1	30.8	30.8	36.7	3.67	°Engler
R ₁	0.032	1	0.1	1.19	0.119	Redwood 1
R ₂	0.32	10	1	11.9	1.19	Redwood 2
S	0.028	0.84	0.084	1	0.1	Saybolt Universal
SF	0.28	8.4	0.84	10	1	Saybolt Furol all in seconds

The table is arranged so that that the comparative values are in one horizontal line, e. g. 1 °E = 30.8 °R₁ = 3.08 °R₂ = 36.7 °S = 3.67 °SF.

All units of viscosity included in the above table are frequently used in the oil industry and they also have a definite relation to kinematic viscosity. Transfer coefficients can be determined as follows (stokes):

For Engler degrees E:

$$\nu = \frac{E}{100} 7.6^{(1-E^{-3})} \text{ valid up to } 7^\circ \text{E}$$

$$\nu = \frac{E}{100} 7.6 \text{ valid above } 7^\circ \text{E.}$$

For degrees Redwood R₁ sec:

$$\nu = 0.0026 t - \frac{1.9}{t} \text{ valid for } t = 40-85 \text{ seconds}$$

$$\nu = 0.00248 t - \frac{0.65}{t} \text{ valid for } t = 85 \text{ to } 2000 \text{ seconds.}$$

For degrees Redwood R₂ sec:

$$\nu = 0.0248 t \text{ valid for } t \text{ above } 100 \text{ seconds.}$$

For degrees Saybolt Universal S sec:

$$\nu = 0.0023 t - \frac{1.95}{t} \quad \text{valid for } t \text{ up to 100 seconds}$$

$$\nu = 0.0022 t - \frac{1.35}{t} \quad \text{valid for } t \text{ above 100 seconds.}$$

For degrees Saybolt Furol SF sec:

$$\nu = 0.0225 t - \frac{1.9}{t} \quad \text{valid for } t = 25 \text{ to } 40 \text{ seconds}$$

$$\nu = 0.0215 t \quad \text{valid for } t \text{ above 40 seconds.}$$

Units of the Engler degree are most frequently used in present day lubrication practice. The units are related to the viscosity of water established in Engler's viscometer. Units of the C. G. S. system: the St and cSt have been recently used on a wider scale.

2. Hydrodynamic Theory of Bearings¹⁾

Fluid friction must be established in the thrust bearing because otherwise an excessive wear of the sliding surfaces occurs with the formation of large quantities of friction heat which cannot be disposed of simultaneously. Sliding surfaces must be dimensioned and shaped, so that the following three basic conditions are complied with: safe operation, low losses and simple production. Let us discuss now the conditions under which the movement of the sliding surfaces takes place.

Two surfaces divided by a thin layer of the lubricant perform a mutual relative movement with a constant velocity U so that the shape of the cross section of the interstice does not change during the movement. (Fig. 384). The flow in the direction parallel to the Y axis, compared with the far greater flow in the direction parallel to the X axis may be neglected, because the value of the ratio $\frac{h_0}{a}$ may be considered as being very small. Pressure p in the liquid does not depend on the ordinate y . Let us assume further that the surfaces are sufficiently wide and sealed on sides so that oil does not escape in a sideways direction, i. e. no flow exists in the direction perpendicular to the plane XY .

A unit volume of a depth equal unity is exposed to the action of the liquid pressure reduced by the force of internal friction (viscosity) $dp \cdot dy - d\tau \cdot dx$

¹⁾ V. ten Bosch: Vorlesungen über Maschinenelemente, chapter: Reibung und Schmierung, Berlin, Springer 1929.

For the original work of O. Reynolds see Phil. Trans. Roy. Soc. 1886, Part I, Papers II, p. 228.

which accelerates the mass particle $dx \cdot dy \cdot \rho$ by the acceleration $\frac{dC}{dt}$; ρ is the density of the liquid $\frac{\gamma}{g}$. The equation of the movement of the unit volume is:

$$dp \cdot dy - d\tau \cdot dx = \rho \cdot dx \cdot dy \cdot \frac{dC}{dt}. \quad (258)$$

The value of the accelerating force $\rho \cdot dx \cdot dy \cdot \frac{dC}{dt}$ may be neglected, because

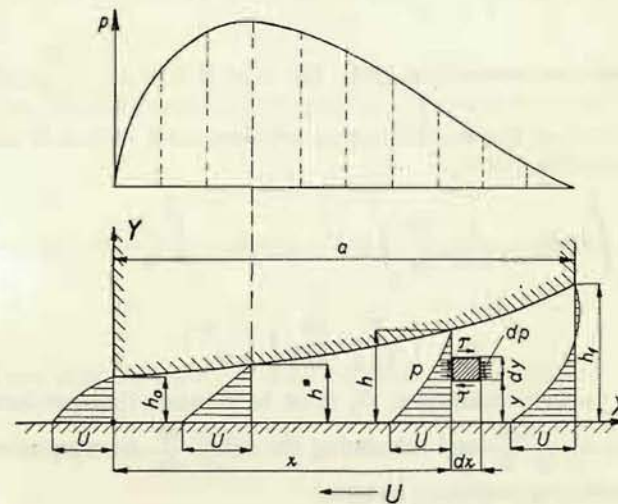


Fig. 384

the influence of viscosity is many times larger. The equation is then simplified into the form:

$$\frac{dp}{dx} = \frac{d\tau}{dy}. \quad (259)$$

By using the expression (256) we can write

$$\frac{dp}{dx} = \mu \frac{d^2C}{dy^2}$$

so that

$$\frac{1}{\mu} \frac{dp}{dx} = \frac{d^2C}{dy^2}. \quad (260)$$

By integration in the plane y , where $\frac{dp}{dx} = \text{const.}$ and assuming a constant viscosity in the direction y , it follows:

$$C = \frac{1}{\mu} \frac{dp}{dx} \frac{y^2}{2} + K_1 y + K_2. \quad (261)$$

The constants of the integral are given by the limiting condition that oil adheres to both sliding surfaces (see later paragraph on oil adsorption).

For $y = 0$, $C = -U = K_2$ and for

$$y = h \text{ is } C = \frac{h^2}{2\mu} \frac{dp}{dx} + K_1 h - U = 0.$$

The velocity

$$C = \frac{1}{2\mu} \frac{dp}{dx} (y^2 - hy) - U \left(1 - \frac{y}{h}\right) \quad (262)$$

has thus a parabolic course (Fig. 384). For $U = 0$ $C = \frac{1}{2\mu} \frac{dp}{dx} (y^2 - hy)$

The quantity of oil flowing through an arbitrary cross section of unit width is denoted by the suffix 1 as G_1 :

$$\begin{aligned} G_1 &= \int_0^h C dy = \frac{1}{2\mu} \frac{dp}{dx} \int_0^h (y^2 - hy) dy - \int_0^h \frac{U}{h} (h - y) dy = \\ &= - \left(\frac{h^3}{12\mu} \frac{dp}{dx} + \frac{U h}{2} \right). \end{aligned} \quad (263)$$

In order to preserve continuity, G_1 must be constant (independent of x). By substituting $G_1 = -\frac{U h^*}{2}$ and calculating the value $\frac{dp}{dx}$ from equation (263) we arrive at the following important relation:

$$\frac{dp}{dx} = -\frac{6\mu U}{h^3} (h - h^*) = 6\mu U \left(\frac{h^*}{h^3} - \frac{1}{h^2} \right), \quad (264)$$

from which it follows, that h^* is the height of the interstice for which $\frac{dp}{dx} = 0$, i. e. the height in the place of maximum pressure. By substituting $\frac{dp}{dx}$ from Equation (264) into Equation (262), we receive

$$-C = \frac{3U}{h^2} \left(1 - \frac{h^*}{h}\right) (y^2 - hy) + U \left(1 - \frac{y}{h}\right) \quad (265)$$

and for $h = h^*$

$$-C = U \left(1 - \frac{y}{h}\right). \quad (266)$$

In the place of maximum pressure the course of velocity in relation to y is thus linear, in all other places parabolical. See Fig. 384.

If the function $h = f(x)$ determining the height of the interstice along the sliding

surface is known, the liquid pressure in place x is determined (after the intergration of Equation (264) by the expression

$$p_x = \int_0^x \frac{6\mu U}{h^3} (h^* - h) dx$$

and after a second integration we receive the total perpendicular force acting upon the sliding surface of unit width, as:

$$P_1 = \int_0^a p_x dx. \quad (267)$$

For the shifting of the sliding plane we require a force which is great enough to overcome the tangential stress on the surface. For a unit width of the sliding surface it follows:

$$R_1 = \int_0^a \tau_0 dx.$$

By using the derivation of the relation (262) we obtain from Equation (256)

$$\tau = \mu \frac{dC}{dy} = \frac{1}{2} \frac{dp}{dx} (2y - h) + \frac{U}{h} \mu.$$

For $y = 0$ and with the value $\frac{dp}{dx}$ from Equation (264) it follows

$$\tau_0 = -\frac{h}{2} \frac{dp}{dx} + \frac{U}{h} \mu = \mu U \left(\frac{4}{h} - 3 \frac{h^*}{h^2} \right). \quad (268)$$

The resistance

$$R_1 = \int_0^a \left[\frac{1}{2} \frac{dp}{dx} (2y - h) + \frac{U}{h} \mu \right] dx$$

apparently depends on y . The difference of its value for $y = h$ is then

$$\tau_h = \frac{h}{2} \frac{dp}{dx} + \frac{U\mu}{h} = \mu U \left(\frac{3h^*}{h^2} - \frac{2}{h} \right)$$

and for $y = 0$

$$\tau_0 = h \frac{dp}{dx}.$$

If oil flows away without overpressure the difference of resistances

$$R_h - R_0 = \int_0^a h \frac{dp}{dx} dx = \left[h p - \int_0^a p dh \right]_0^a = - \int_0^a p dh$$

equals the component of the force P in the direction of the movement. Therefore resistance has the same value for $y = h$, as for $y = 0$.

The coefficient of friction is defined, similarly as for the friction of solid substances, by the ratio

$$\frac{R_1}{P_1} = \mu U \frac{\int_0^a \left(\frac{4}{h} - 3 \frac{h^*}{h^2} \right) dx}{P_1} \quad (269)$$

Assuming a viscosity which does not depend on x (this, however, is never exactly the case, because viscosity changes slightly with the liquid pressure), the following relation for parallel sliding surfaces with constant h can be derived from Equation (267):

$$p_x = \frac{6 \mu U x}{h^3} (h^* - h) + K, \quad (270)$$

which shows a linear course of the pressure line.

If oil flows off at the spot $x = 0$ without overpressure, $K = 0$ and the pressure on the edge of the plane ($x = a$) is given by the equation

$$p_a = \frac{6 \mu U a}{h^2} \left(\frac{h^*}{h} - 1 \right) \quad a \quad p_x = p_a \frac{x}{a}. \quad (271)$$

This equation shows, that the planes can be parallel only in the event, when oil is supplied under overpressure. The pressure p_a for instance can be determined by the oil pump and it may have an arbitrary value; the given value of p_a determines the value of the ratio $\frac{h^*}{h}$.

Pressure decreases along the bearing surface in a linear relation down to zero and, therefore, the carrying capacity of the oil layer of unit width is

$$P_1 = \frac{p_a a}{2} = \frac{3 \mu U a^2}{h^2} \left(\frac{h^*}{h} - 1 \right) = \mu \frac{U a^2}{h^2} \Phi. \quad (272)$$

However, the condition must be fulfilled, that both sliding surfaces remain separated by the oil film. The interstice h must be always higher, than the sum total of all uneven projections of the surfaces caused by roughness of machining. The value of h can be determined from Equation (272):

$$h = a \sqrt{3 \left(\frac{h^*}{h} - 1 \right)} \sqrt{\frac{\mu U}{P_1}} = a \sqrt{\Phi} \sqrt{\frac{\mu U}{P_1}}. \quad (273)$$

This is a simple mathematical expression of the condition, that the oil must not be squeezed out of the interstice between the sliding surfaces.

Generally for calculating purposes we use the "medium" specific pressure p_{mean} - in kg/cm^2 (atm) according to the equation

$$P = a b p_{\text{mean}} \quad (274)$$

where a is the length (in cm) and b the width (also in cm) of the sliding surface.

Pressure in the direction of b is not constant either and therefore the value p_{mean} of the medium specific pressure does not give sufficient information concerning the actual distribution of the specific pressure and its maximum value.

By substituting from Equation (268), we obtain

$$R_1 = \int_0^a \tau_0 dx = \frac{\mu U a}{h} \left(4 - 3 \frac{h^*}{h} \right) = \frac{\mu U a}{h} \vartheta \quad (275)$$

and by comparison with Equation (272) we may calculate the coefficient of friction from the equation:

$$f = \frac{R_1}{P_1} = \frac{4 - 3 \frac{h^*}{h}}{3 \left(\frac{h^*}{h} - 1 \right)} \frac{h}{a} = \frac{\vartheta}{\Phi} \frac{h}{a} = K \frac{h}{a} \quad (276)$$

f equals zero for $h^* = \frac{4}{3} h$.

The value $\frac{h}{a}$ is substituted from Equation (273) and then follows:

$$f = \frac{4 - 3 \frac{h^*}{h}}{\sqrt{3 \left(\frac{h^*}{h} - 1 \right)}} \sqrt{\frac{\mu U}{P_1}} = \frac{\vartheta}{\sqrt{\Phi}} \sqrt{\frac{\mu U}{P_1}} = x \sqrt{\frac{\mu U}{P_1}} = x \sqrt{\frac{\mu U}{a p_{\text{mean}}}}. \quad (277)$$

The values Φ , ϑ , K and x for different values of the ratio $\frac{h^*}{h}$ are given in the following table.

The ratio $\frac{h^*}{h}$ is determined by the pressure of the pump according to Equation (271).

For $\frac{h^*}{h}$	1	1.05	1.1	1.2	1.3	$\frac{4}{3}$
is Φ	0	0.15	0.3	0.6	0.9	1
$\sqrt{\Phi}$	0	0.387	0.548	0.775	0.949	1
ϑ	1	0.85	0.7	0.4	0.1	0
x	∞	2.18	1.28	0.52	0.105	0
K	∞	5.67	2.33	0.667	0.111	0

For $U = 0$ we may calculate from Equation (262) the maximum velocity for $y = \frac{h}{2}$ as

$$C_{\text{max}} = \frac{h^2}{8 \mu} \frac{dp}{dx} \quad (278)$$

and the medium velocity from equation (263) as

$$C = \frac{h^2}{12\mu} \frac{dp}{dx}.$$

From the above consideration we can draw the conclusion, that a bearing oil layer is formed in the interstice of two sliding surfaces whenever the layer is wedge shaped with a tapering in the direction of the movement.

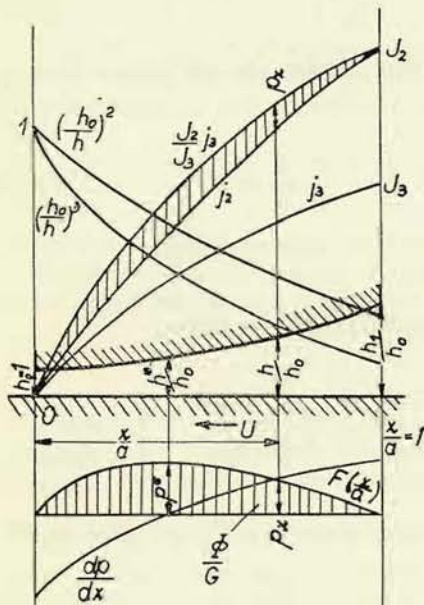


Fig. 385

After integration of the Equation (264) we must obviously know the relation between the size of the interstice h and the distance $x : h = f(x)$. (See Fig. 384). For different interstices and for different sliding surface lengths the integration will give different results for the values of load P , resistance R and thus also a different coefficient of friction f . In order to obtain general relations which are independent on the absolute size of the sliding surface, dimensionless values are introduced in the equations. The equation

$$\frac{h}{h_0} = f\left(\frac{x}{a}\right), \quad (279)$$

where h_0 is the narrowest interstice and a is the dimension of the sliding surface in the direction of the movement, holds good for all "similar" interstices. By substituting into Equation (264), we receive

$$dp = \frac{6\mu U a}{h_0^2} \left[\frac{h^*}{h_0} \frac{1}{f^3\left(\frac{x}{a}\right)} - \frac{1}{f^2\left(\frac{x}{a}\right)} \right] d\left(\frac{x}{a}\right). \quad (280)$$

This expression can be integrated for simpler relations analytically and for complicated ones graphically. (Fig. 385). Zero point lies in the narrowest spot of the interstice and coincides with the edge of the sliding surface.

Different integrations are expressed by the following symbols:

$$j_1\left(\frac{x}{a}\right) = \int_0^{\frac{x}{a}} \frac{d\left(\frac{x}{a}\right)}{f\left(\frac{x}{a}\right)} \quad \mathcal{J}_1 = \int_0^1 \frac{d\left(\frac{x}{a}\right)}{\left(\frac{x}{a}\right)} = j_1(1)$$

$$j_2\left(\frac{x}{a}\right) = \int_0^{\frac{x}{a}} \frac{d\left(\frac{x}{a}\right)}{f^2\left(\frac{x}{a}\right)} \quad \mathcal{J}_2 = \int_0^1 \frac{d\left(\frac{x}{a}\right)}{f^2\left(\frac{x}{a}\right)} = j_2(1)$$

$$j_3\left(\frac{x}{a}\right) = \int_0^{\frac{x}{a}} \frac{d\left(\frac{x}{a}\right)}{f^3\left(\frac{x}{a}\right)} \quad \mathcal{J}_3 = \int_0^1 \frac{d\left(\frac{x}{a}\right)}{f^3\left(\frac{x}{a}\right)} = j_3(1)$$

At a given interstice $\frac{h}{h_0} = f\left(\frac{x}{a}\right)$ the symbols j_1, j_2, j_3 depend only upon the ratio $\frac{x}{a}$ whereas the symbols $\mathcal{J}_1, \mathcal{J}_2, \mathcal{J}_3$ are absolute values which depend on the shape of the interstice. Therefore we can write

$$p_x = \frac{6\mu U a}{h_0^2} \left[\frac{h^*}{h_0} j_3\left(\frac{x}{a}\right) - j_2\left(\frac{x}{a}\right) - K_0 \right]. \quad (281)$$

The constants K_0 and $\frac{h^*}{h_0}$ are unknown until now and they can be determined from the limiting conditions:

a) If for $\frac{x}{a} = 0$ also $p_0 = 0$ and for $\frac{x}{a} = 1$ $p_1 = 0$, which means that oil may freely move into or off the interstice, then it follows

$$K_0 = 0 \text{ and } \frac{h^*}{h_0} = \frac{\mathcal{J}_2}{\mathcal{J}_3}. \quad (282)$$

b) If for $\frac{x}{a} = 0$ also $p_0 = 0$ and for $\frac{x}{a} = 1$ $p_1 \neq 0$, which means, that oil is supplied under overpressure, then $K_0 = 0$ and

$$p_1 = \frac{6\mu U a}{h_0^2} \left(\frac{h^*}{h_0} \mathcal{J}_3 - \mathcal{J}_2 \right) \text{ or } \frac{h^*}{h_0} = \frac{\mathcal{J}_2 + \frac{p_1 h_0^2}{6\mu U a}}{\mathcal{J}_3}. \quad (283)$$

c) If for $\frac{x}{a} = 0$ $p_0 \neq 0$ and for $\frac{x}{a} = 1$ $p_1 = 0$, which means that oil flows off under overpressure, then it follows:

$$K_0 = \frac{h^*}{h_0} \mathcal{J}_3 - \mathcal{J}_2 \text{ and } p_0 = \frac{6\mu U a}{h_0^2} \left(\mathcal{J}_2 - \frac{h^*}{h_0} \mathcal{J}_3 \right)$$

or

$$\frac{h^*}{h_0} = \frac{\tilde{f}_2 - \frac{p_0 h_0^2}{6 \mu U a}}{\tilde{f}_3} \quad (284)$$

The bracketed expression in Equation (281) is now unequivocally determined; at a given interstice it depends only on the ratio $\frac{x}{a}$, for simplicity it will be written as $F\left(\frac{x}{a}\right)$, so that it follows

$$p_x = \frac{6 \mu U a}{h_0^2} F\left(\frac{x}{a}\right) \quad (285)$$

The carrying capacity of the oil film a unit width is then:

$$P_1 = \int_0^a p_x dx = a \int_0^1 p_x d\left(\frac{x}{a}\right) = \frac{6 \mu U a^2}{h_0^2} \int_0^1 F\left(\frac{x}{a}\right) d\left(\frac{x}{a}\right) = \mu \frac{U a^2}{h_0^2} \Phi, \quad (286)$$

where the symbol $\Phi = 6 \int_0^1 F\left(\frac{x}{a}\right) d\left(\frac{x}{a}\right)$ is a value which depends only on the shape of the interstice.

From Equation (286) we calculate then the minimum thickness of the oil layer as

$$h_0 = a \sqrt{\Phi} \sqrt{\frac{\mu U}{P_1}} \quad (287)$$

which must be greater than the sum total of all projections resulting from machining roughness.

The resistance $R_1 = \int_0^1 \tau_0 d\left(\frac{x}{a}\right)$, can be expressed according to equation (268) in the following way:

$$\begin{aligned} R_1 &= a \int_0^1 \tau_0 d\left(\frac{x}{a}\right) = \mu U a \int_0^1 \left(\frac{4}{h} - 3 \frac{h^*}{h^2} \right) d\left(\frac{x}{a}\right) = \\ &= \frac{\mu U a}{h_0} \int_0^1 \left[\frac{4}{\frac{h}{h_0}} - \frac{3 \frac{h^*}{h_0}}{\left(\frac{h}{h_0}\right)^2} \right] d\left(\frac{x}{a}\right) = \\ &= \frac{\mu U a}{h_0} \left(4 \cdot \tilde{f}_1 - 3 \frac{h^*}{h_0} \tilde{f}_2 \right) = \frac{\mu U a}{h_0} \vartheta, \end{aligned} \quad (288)$$

where ϑ is a value which depends only on the shape of the interstice.

The coefficient of friction is then

$$f = \frac{R_1}{P_1} = \frac{h_0}{a} \frac{\vartheta}{\Phi} = K \frac{h_0}{a}, \quad (289)$$

By substituting for $\frac{h_0}{a}$ the value from Equation (287) and for the carrying capacity

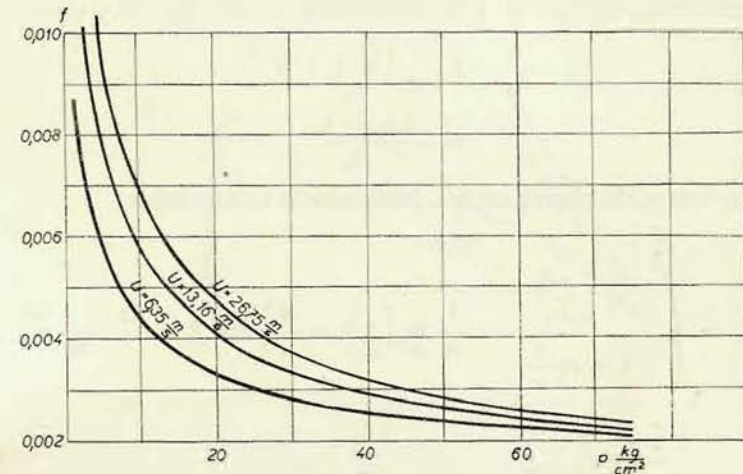


Fig. 386

P_1 the value from Equation (274), the value of the coefficient (for unit width) may be expressed as¹⁾

$$f = \frac{\vartheta}{\Phi} \sqrt{\frac{\mu U}{P_1}} = \kappa \sqrt{\frac{\mu U}{a p_{\text{mean}}}} \quad (290)$$

The equation shows, that the coefficient of friction f depends only on the ratio $\frac{h_0}{h}$ and on the shape of the interstice. Two surfaces which slide one upon the other can have the same coefficient of friction regardless to whether oil or air is used as a lubricant. However, the distance of the surfaces, i. e. ratio $\frac{h_0}{h}$ depends on P_1 , U and μ and therefore, the coefficient of friction is influenced by these values. It is obvious, that the coefficient of friction increases with a rising medium specific pressure p_{mean} . Fig. 386 shows diagrams which

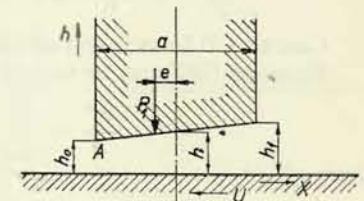


Fig. 387

¹⁾ See also Prandtl: Führer durch die Strömungslehre, Braunschweig, Vieweg, 1944, p. 142.

are the results of tests carried out by the Brown-Boveri Works. They clearly illustrate how the coefficient of friction decreases with a rising medium specific pressure.

When applying these relations we must bear in mind, that the values Φ , ϑ , κ and K depend not only on the shape of the interstice, but also on the limiting conditions.

1. For a general example of an inclined sliding surface (Fig. 387), where

$$\frac{h}{h_0} = f\left(\frac{x}{a}\right) = 1 + m \frac{x}{a}, \quad (291)$$

and

$$m = \frac{h_1 - h_0}{h_0} \quad (292)$$

is the gradient of the sliding surface, integration is rather simple:

$$j_1 = \int_0^{\frac{x}{a}} \frac{d\left(\frac{x}{a}\right)}{1 + m \frac{x}{a}} = \frac{1}{m} \ln \left(1 + m \frac{x}{a}\right) \text{ and } j_1 = \frac{\ln(1+m)}{m}$$

$$j_2 = \int_0^{\frac{x}{a}} \frac{d\left(\frac{x}{a}\right)}{\left(1 + m \frac{x}{a}\right)^2} = \frac{\frac{x}{a}}{1 + m \frac{x}{a}} \quad j_2 = \frac{1}{1+m}$$

$$j_3 = \int_0^{\frac{x}{a}} \frac{d\left(\frac{x}{a}\right)}{\left(1 + m \frac{x}{a}\right)^3} = \frac{\frac{x}{a} \left(2 + m \frac{x}{a}\right)}{2 \left(1 + m \frac{x}{a}\right)^2} \quad j_3 = \frac{m+2}{2(1+m)^2}$$

Case a): Oil flows in and off without overpressure.

Equation (282) can be written as

$$\frac{h^*}{h} = \frac{j_2}{j_3} = \frac{2(m+1)}{m+2}, \quad K_0 = 0$$

$$F_a\left(\frac{x}{a}\right) = \frac{h^*}{h_0} j_3 - j_2 = \frac{m \frac{x}{a} \left(1 - \frac{x}{a}\right)}{(m+2) \left(1 + m \frac{x}{a}\right)^2} \quad (\text{Fig. 388})$$

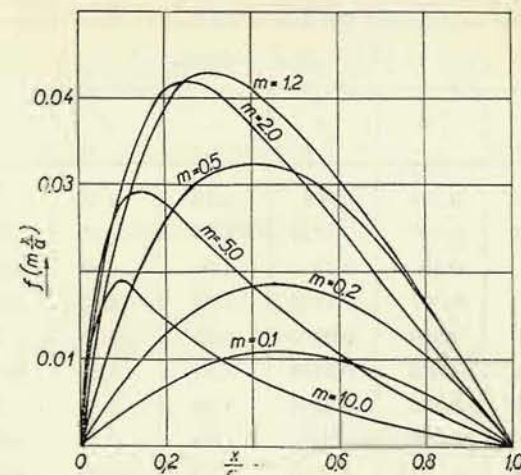


Fig. 388

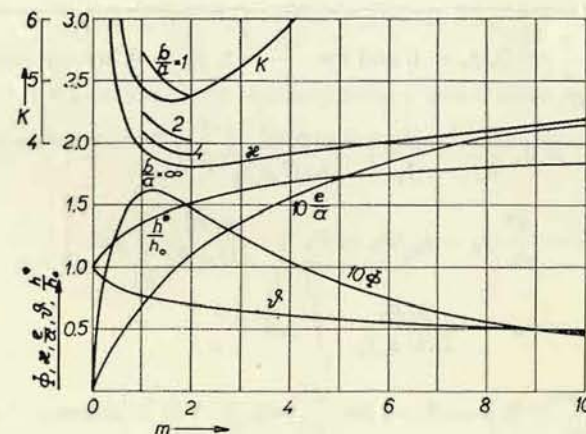


Fig. 389

$$\Phi_a = 6 \int_0^1 F\left(\frac{x}{a}\right) d\left(\frac{x}{a}\right) = \frac{6 \ln(m+1)}{m^2} - \frac{12}{m(m+2)} \quad (\text{Fig. 389}).$$

$$\vartheta_a = 4 j_1 - 3 \frac{j_2^2}{j_3} = \frac{4 \ln(m+1)}{m} - \frac{6}{m+2} \quad (\text{Fig. 389}).$$

Values Φ , ϑ and K are given in the following table:

Values for calculating friction of sliding surfaces in case a)

$b = \infty$; $\mu = \text{const.}$

m	Φ	$\sqrt{\Phi}$	ϑ	α	K	$\frac{e}{a}$	$\frac{h^*}{h_0}$
0.7	0.1476	0.384	0.808	2.10	5.48	0.052	1.259
1	0.15894	0.399	0.7726	1.94	4.86	0.068	1.333
1.2	0.16	0.40	0.76	1.90	4.80	0.078	1.378
1.5	0.15773	0.397	0.7292	1.84	4.62	0.090	1.428
2	0.14790	0.384	0.6970	1.82	4.71	0.108	1.500
3	0.12426	0.352	0.6498	1.84	5.24	0.134	1.600
4	0.10350	0.322	0.6094	1.90	5.89	0.154	1.667
5	0.08718	0.295	0.5803	1.95	6.53	0.169	1.715
10	0.04386	0.2095	0.4592	2.19	10.45	0.214	1.833
100	0.0016	0.04	0.1258	3.14	79	—	1.985

Case b): for $\frac{x}{a} = 0$, $p_0 = 0$ and for $\frac{x}{a} = 1$, $p_1 \neq 0$, we can write according to Equation (281):

$$K_0 = 0, \frac{h^*}{h_0} = \frac{j_2}{j_3} + \frac{p_1 h_0^2}{6\mu U a j_3}$$

$$F_b = \frac{h^*}{h_0} j_3 - j_2, \Phi_b = \Phi_a + \frac{p_1 h_0^2}{\mu U a j_3} \int_0^1 j_3 d\left(\frac{x}{a}\right)$$

$$\vartheta_b = \vartheta_a - \frac{p_1 h_0^2}{2\mu U a j_3} \int_0^1 j_3 d\left(\frac{x}{a}\right).$$

Case c): for $\frac{x}{a} = 0$, $p \neq 0$ and for $\frac{x}{a} = 1$, $p_1 = 0$, it follows:

$$K_c = \frac{h^*}{h_c} j_3 - j_2, \frac{h^*}{h} = \frac{j_2}{j_3} - \frac{p_0 h_0^2}{6\mu U a j_3}$$

$$F_c = \frac{h^*}{h_0} j_3 - j_2 - K_0; \Phi_c = \Phi_a - \frac{p_0 h_0^2}{\mu U a j_3} \int_0^1 j_3 d\left(\frac{x}{a}\right)$$

$$\vartheta_c = \vartheta_a + \frac{p_0 h_0^2}{2\mu U a j_3} \int_0^1 j_3 d\left(\frac{x}{a}\right).$$

2. For parabolically rounded sliding surfaces the following relations apply:

$$h = h_0 + \frac{x}{2\varrho}, \text{ then } f\left(\frac{x}{a}\right) = \frac{h}{h_0} = 1 + \left(\xi \frac{x}{a}\right)^2, \quad (293)$$

where ϱ is the parameter of the parabola and $\xi^2 = \frac{a^2}{2\varrho h_0^2}$, can be written as

$$\xi \frac{x}{a} = \tan \gamma, \text{ then } \xi \cdot d\left(\frac{x}{a}\right) = \frac{d\gamma}{\cos^2 \gamma},$$

so that

$$\frac{h}{h_0} = f\left(\frac{x}{a}\right) = 1 + \tan^2 \gamma = \frac{1}{\cos^2 \gamma}, \quad (294)$$

and

$$\frac{dp}{d\gamma} = \frac{6\mu U a}{\xi h_0^2} \left(\frac{\cos^4 \gamma}{\cos^2 \gamma^*} - \cos^2 \gamma \right). \quad (295)$$

By integration we receive

$$p_\gamma = \frac{6\mu U a}{\xi h_0^2} \left(\frac{j_3(\gamma)}{\cos^2 \gamma^*} - j_2(\gamma) - K_0 \right), \quad (296)$$

the pressure p is a function of the auxiliary value γ and it must be recalculated so that it will be expressed as $F\left(\frac{x}{a}\right)$. Integration gives then the following result:

$$j_1 = \int_0^\gamma \frac{d\left(\frac{x}{a}\right)}{\frac{h}{h_0}} = \frac{1}{\xi} \int_0^\gamma d\gamma = \gamma \cdot \xi, \quad j_1 = \frac{\gamma_1}{\xi},$$

$$j_2 = \int_0^\gamma \cos^2 \gamma d\gamma = \frac{1}{\xi} \left(\frac{\sin 2\gamma}{4} + \frac{\gamma}{2} \right), \quad j_2 = \frac{1}{\xi} \left(\frac{\sin 2\gamma_1}{4} + \frac{\gamma_1}{2} \right),$$

$$j_3 = \frac{1}{\xi} \int_0^\gamma \cos^4 \gamma d\gamma = \frac{1}{\xi} \left(\frac{1}{4} \sin \gamma \cos^3 \gamma + \frac{3}{16} \sin 2\gamma + \frac{3}{8} \gamma \right), \quad j_3 = j_2(\gamma_1).$$

Case a): Oil flows in and off without overpressure.

$$\frac{h^*}{h_0} = \frac{1}{\cos^2 \gamma^*} = \frac{j_2}{j_3}; K_0 = 0; F_a = \frac{h^*}{h_0} (j_3 - j_2) = \frac{j_3}{\cos^2 \gamma^*} - j_2. \quad (\text{Fig. 390}).$$

$$\Phi_a = 6 \int_0^{\gamma_1} F d\gamma = \frac{6}{\xi} \left(\frac{A}{\cos^2 \gamma^*} - B \right), \text{ where}$$

$$A = \frac{1}{16} \sin^2 \gamma_1 (1 + \cos^2 \gamma_1) - \frac{3}{32} \cos 2\gamma_1 + \frac{3}{16} \gamma_1^2 + \frac{3}{32} \text{ and}$$

$$B = \frac{\gamma_1^2}{4} - \frac{\cos 2\gamma_1}{8} + \frac{1}{8},$$

$$\vartheta_a = 4 \cdot \mathcal{J}_1 - \frac{2 \mathcal{J}_2}{\cos^2 \gamma^*}.$$

Case b): for $\frac{x}{a} = 0$, or $\gamma = 0$, $p_0 = 0$ and for $\gamma = \gamma_1$, $p_1 \neq 0$.

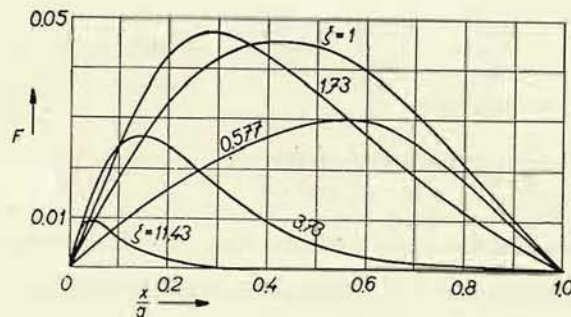


Fig. 39c

$$K_0 = 0, \frac{h^*}{h_0} = \frac{\mathcal{J}_2}{\mathcal{J}_3} + \frac{p_1 h_0^2}{6\mu U a \mathcal{J}_3} = \frac{1}{\cos^2 \gamma^*},$$

$$F_b = \frac{h^*}{h_0} j_3 - j_2 \text{ and } p_1 = \frac{6\mu U a}{h_0^2} \left(\frac{\mathcal{J}_3}{\cos^2 \gamma^*} - \mathcal{J}_2 \right),$$

$$\Phi_b = \frac{6}{\xi} \left[\frac{A}{\cos^2 \gamma^*} - B + \left(\frac{\mathcal{J}_3}{\cos^2 \gamma^*} - \mathcal{J}_2 \right) \gamma_1 \right],$$

$$\vartheta_b = 4 \cdot \mathcal{J}_1 - \frac{3 \cdot \mathcal{J}_2}{\cos^2 \gamma^*}.$$

Case c): for $\gamma = 0$, $p \neq 0$ and for $\gamma = \gamma_1$, $p_1 = 0$

$$K_0 = \frac{\mathcal{J}_3}{\cos^2 \gamma^*} - \mathcal{J}_2 < 0 \text{ and } \frac{h^*}{h_0} = \frac{\mathcal{J}_2}{\mathcal{J}_3} - \frac{p_0 h_0^2}{6\mu U a \mathcal{J}_3} = \frac{1}{\cos^2 \gamma^*},$$

$$F_c = \frac{j_3}{\cos^2 \gamma^*} - j_2 - K_0 \text{ and } p_0 = -\frac{6\mu U a}{h_0^2} \left(\frac{\mathcal{J}_3}{\cos^2 \gamma^*} - \mathcal{J}_2 \right),$$

$$\Phi_c = \frac{6}{\xi} \left[\frac{A}{\cos^2 \gamma^*} - B - \left(\frac{\mathcal{J}_3}{\cos^2 \gamma^*} - \mathcal{J}_2 \right) \gamma_1 \right] \text{ and}$$

$$\vartheta_c = 4 \mathcal{J}_1 - \frac{3 \mathcal{J}_2}{\cos^2 \gamma^*}.$$

Values for calculations are given in tables on pages 503 and 504.

When designing a sliding surface we know the load $P_1 = \frac{P}{b}$ and the sliding velocity U in m/sec. Viscosity of oil may be selected. From equations (287) and (290) and by using the respective tables of numerical values we can calculate

$$f = \sqrt{\frac{\mu U}{P_1}} \text{ and the minimum oil layer is determined from } \frac{h_0}{a} = \sqrt{\Phi} \sqrt{\frac{\mu U}{P_1}}.$$

For designing purposes we endeavour to obtain the lowest possible value of the coefficient of friction and therefore we select a smaller value of K . With regard to production possibilities we must not count with a too small interstice. The value $h_0 = 0.01$ mm is suitable for a very good make and $h_0 = 0.005$ and less for very exact makes. For this reason Φ should be as great as possible. It can be seen from the respective tables, that it is not possible to comply with the condition of a minimum coefficient of friction and a simultaneous maximum thickness of the oil film. At a given or selected h_0 the coefficient of friction is calculated from Equation (289), so that we must select the lowest value of K .

At a given length a of the sliding surface the most favourable coefficient of friction is directly proportional to h_0 and it depends only very little on the shape of the interstice. The coefficient of a parabolic sliding surface is by about 10 % lower, than that of an inclined plane sliding surface.

Owing to the fact, that the viscosity of oil at 20 °C (which is about the temperature at which the turbine unit is being started after a longer shut down) is 6 to 10 times greater than at operational temperature, fluid friction will be attained at a speed which is about 1/6 to 1/10 of the operational speed. On the contrary, during closure of the machine the oil has, at a smaller sliding velocity, the same or lower viscosity as during operation, because the oil in the interstice streams more slowly and has a worse heat conducting capacity. Therefore, during this period a semi-fluid type of friction occurs which is always dangerous. The final run of the machine is shortened by the application of closure brakes.

Sliding surfaces must be calculated generally so that fluid friction is established already at a speed amounting to 10 % of the normal sliding speed or even sooner in cases, where the shaft is running in the bearing frequently for longer periods and at a low speed.

We can see from the equation

$$\frac{h_0}{a} = \sqrt{\Phi} \sqrt{\frac{\mu \frac{U}{10}}{P_1}} \quad (297)$$

that at the same value h_0 the carrying capacity is about 1/10 of the normal. The

thinnest oil layer and thus also the coefficient of friction are higher, i. e. the normal values multiplied by the square root of ten.

The carrying capacity of the bearing is somewhat reduced by a factor hitherto not considered: part of the oil escapes along the side walls of the segment. Pressure diminished then not only towards the front and rear edge of the segment, but also in the direction of the side edges, so that the distribution of pressure corresponds to that illustrated in Fig. 391.

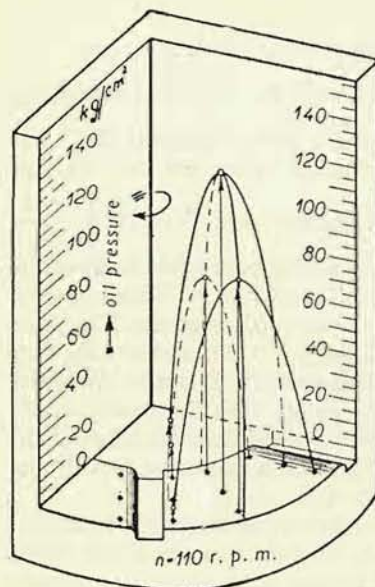


Fig. 391

The practical arrangement of the required interstice between the sliding surfaces is by far more difficult, than its calculation. The machining of the extremely small tapers demanded by the results of calculation is very difficult. If solid segments are produced at all, they have normally a taper of 2 per mille.¹⁾ The wedge shaped interstice which is indispensable for carrying the load is obtained by tiltable supports of the segments according to Michell²⁾. It can be seen from Fig. 384 that owing to the length of the sliding surface, the load is distributed asymmetrically and the resultant force acts excentrically.

We can calculate the excentricity from the condition that the moments acting upon edge A (Fig. 387) must produce a state of equilibrium. It follows then:

$$P_1 \left(\frac{a}{2} - e \right) = \int_0^a p_x x dx. \quad (298)$$

The curve of the calculated relative excentricity $\frac{e}{a}$ is shown in Fig. 389. The value $\frac{e}{a}$ rises with an increasing gradient m - see relation (292). If the sliding surface is supported at a certain point, a definite gradient is established. If, for any reasons, the gradient is increased, the excentricity e of the resultant force increases too and the sliding surface returns automatically into its initial position. Thus the gradient of the sliding surface is stable.

¹⁾ Thomann R.: Die Wasserturbinen und Turbinenpumpen, Stuttgart, K. Wittwer, 1931. Table 32.

²⁾ A. G. H. Michell: Zeitschrift f. Math. und Physik 52 (1905), p. 123, where the effect of the side-escape of oil is also discussed.

Suitably rounded edges are used on all surfaces connected with lubrication. It has been proved, as shown by the above considerations, that the shape of the interstice has only lesser importance. Rounding off the oil inlet edge thus should suffice to make a parallel sliding surface capable of carrying load (Fig. 392).

In interstices combined of differently shaped parts the expression for the load carrying capacity and coefficient of friction can be easily established from the relations derived previously (Fig. 393).

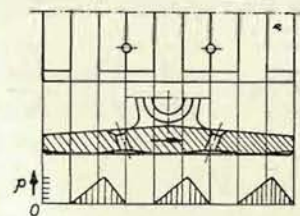


Fig. 392

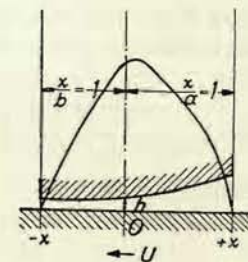


Fig. 393

For the parallel part ranging from $\frac{x}{b} = -1$ to $\frac{x}{b} = 0$ it follows from Equation (271):

$$p_0 = \frac{6\mu U b}{h_0^2} \left(\frac{h^*}{h_0} - 1 \right) \quad \text{a} \quad p_x = p_0 \frac{x}{a}.$$

For the parabolic part ranging from $\frac{x}{a} = 0$ to $\frac{x}{a} = 1$ it follows from Equation (284):

$$p_0 = \frac{6\mu U a}{h_0^2} \left(\mathcal{J}_2 - \frac{h^*}{h_0} \mathcal{J}_3 \right).$$

If the terms on the right sides of the above two equations are equal, then

$$\frac{h^*}{h_0} = \frac{1}{\cos^2 \gamma^*} = \frac{\mathcal{J}_2 + \frac{b}{a}}{\mathcal{J}_3 + \frac{b}{a}} \quad (299)$$

and from this equation it is possible to determine the value $\frac{h^*}{h}$.

The carrying capacity of a combined sliding surface consists of the carrying

capacity of the parabolic and that of the parallel part, i. e.:

$$P_1 = \frac{6\mu U a^2}{h_0^2} \left[\frac{\frac{A}{\xi} + \frac{b}{a} \gamma_1 + \frac{b^2}{2a^2}}{\cos^2 \gamma^*} - \frac{B}{\xi} + \frac{b}{a} \gamma_1 - \frac{b^2}{2a^2} \right] = \frac{\mu U a^2}{h^2} \cdot \Phi, \quad (300)$$

The values A and B in this equation are taken from the table of numerical values. Resistance and the coefficient of friction can be determined from the following equations:

$$\text{Resistance } R_1 = \frac{\mu U a}{h_0} \left[\frac{1}{\xi} \left(4\gamma_1 - \frac{3\gamma_2}{\cos^2 \gamma^*} \right) + \left(4 - \frac{3}{\cos^2 \gamma^*} \right) \right] = \frac{\mu U a}{h_0} \quad (301)$$

and coefficient of friction

$$f = \frac{R_1}{P_1} = \kappa \sqrt{\frac{\mu U}{P_1}} = \kappa \sqrt{\frac{\mu U}{a p_{\text{mean}}}}. \quad (302)$$

Equations valid for an interstice combined of a parabolic and inclined plane sliding surface can be derived in a similar way.

Until now we have not taken into account the oil temperature which changes in the direction of the movement because oil becomes heated by friction work.

Significant temperature differences can occur at high specific pressures. We do not know the relation between the temperature change (and thus also the viscosity) and the distance x from the inlet edge. By assuming a linear course

$$\mu = \mu_0 \left(1 + n \frac{x}{a} \right), \quad (303)$$

the Equations (280) and (286) can easily be integrated. Experiments carried out by E. Barber and C. C. Davenport¹⁾ have shown, that this assumption holds good for sliding velocities up to about 2.6 m/sec, while deviations increase with a rising speed.

The centre in which the resulting force acts upon the sliding surface is shifted by the change of viscosity, i. e. the excentricity $\frac{e}{a}$ is changed. This factor must be considered particularly in the case of bearings at which the inclination of the sliding surface is obtained by an excentric support.

In practical calculations we may use a certain "medium" viscosity which is constant and corresponds with the average temperature in the oil layer. We may also substitute the mean values of the inlet and outlet viscosity.

Until now we have dealt only superficially with the effect of the side-escape of oil. The flow rate for a unit width, i. e. the quantity of fluid which flows in the

¹⁾ V. ten Bosch: Reibung und Schmierung, p. 248.

Numerical values for parabolically rounded surfaces

Degrees	γ circular measure	$\frac{1}{4} \sin 2\gamma$ + $\frac{\gamma}{2}$	$\frac{1}{4} \sin \gamma \cos^3 \gamma$ + $\frac{3}{16} \sin 2\gamma$ + $\frac{3}{8} \gamma$	$\frac{h^*}{h_0}$	B	A	$\tan \gamma_1$ = ξ
5	0.0872566	0.0870453	0.08685	1.0017	0.0038028	0.0037980	0.08749
10	0.1745329	0.1727715	0.17042	1.0138	0.0151538	0.0150777	0.17633
15	0.2617994	0.2558997	0.25043	1.0219	0.0338815	0.0335041	0.26795
20	0.3490658	0.3352298	0.32403	1.0346	0.0597061	0.0585466	0.36379
25	0.4363323	0.4096773	0.38616	1.0619	0.0922480	0.0895180	0.46631
30	0.5235988	0.4783057	0.43992	1.0873	0.1310389	0.1256229	0.57735
35	0.6108652	0.5403558	0.48408	1.1162	0.1755365	0.1660115	0.70021
40	0.6981317	0.5952678	0.51881	1.1473	0.2251409	0.2098330	0.83910
45	0.7853982	0.6426991	0.54452	1.1804	0.2792125	0.2562844	1.0
50	0.8726646	0.6825342	0.56276	1.2129	0.3370918	0.2899977	1.19175
55	0.9599311	0.7148856	0.57504	1.2432	0.3981194	0.3543247	1.42815
60	1.0471976	0.7401051	0.58214	1.2713	0.4616557	0.4048355	1.73205
65	1.1344640	0.7586431	0.58630	1.2940	0.5271006	0.4538316	2.14451
70	1.2217305	0.7715622	0.58807	1.3120	0.6046496	0.5151318	2.74748
75	1.3089969	0.7794985	0.58881	1.3239	0.6616219	0.5584754	3.73205
80	1.3962634	0.7836367	0.58902	1.3305	0.7298491	0.6098301	5.67128
85	1.4835299	0.7853982	0.58905	1.3333	0.7983035	0.6612238	11.43005
90	1.5707963	$\frac{\pi}{4}$	$\frac{3}{16} \pi$	$\frac{4}{3}$	$\frac{\pi^2}{16} + \frac{1}{4}$	$\frac{3\pi^2}{64} + \frac{16}{3}$	∞

direction X of the movement of the sliding surfaces, can be calculated from Equation (263) as follows:

$$G_1 = \frac{h^3}{12 \mu} \frac{dp}{dx} + \frac{U h}{2}. \quad (304)$$

Flow rate for a unit width in the direction Z , i. e. in the direction perpendicular to the sliding movement ($U = 0$ in this direction) is:

$$G_{1z} = \frac{h^3}{12 \cdot \mu} \frac{dp}{dz}. \quad (305)$$

At a state of equilibrium the total quantity of the fluid must be constant, i. e. the sum of the flow rates in directions X and Z must equal zero. Therefore:

$$\frac{\partial}{\partial x} \left(\frac{h^3}{12\mu} \frac{dp}{dx} \right) + \frac{\partial}{\partial z} \left(\frac{h^3}{12\mu} \frac{dp}{dz} \right) + \frac{U}{2} \frac{\partial h}{\partial x} = 0. \quad (306)$$

As has been stated before, the carrying capacity of the sliding surfaces is reduced by the side-escape of oil. This reduction of the carrying capacity can be expressed by a correction coefficient (Fig. 394).

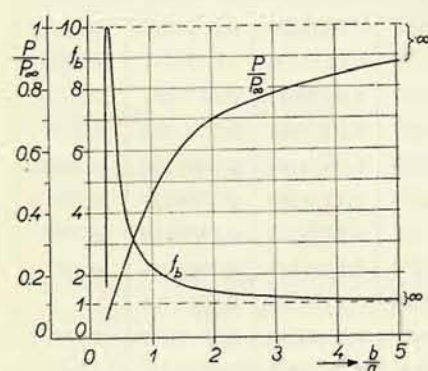


Fig. 394

For a bearing of finite width the following equation holds good:

$$P = \frac{P_{\infty}}{f_b}, \quad (307)$$

The coefficient of friction in this bearing is calculated from the same relation, as applied in the case of a bearing of infinite width, i. e.:

$$f = \kappa' \sqrt{\frac{\mu U}{P_1}}. \quad (308)$$

The values κ' have been calculated by Boswall for $m = 1$ and $m = 2$ (Bosch V.:

Vorlesungen über Maschinenelemente, Berlin, Springer, 1929).

Values for calculating friction of parabolic sliding surfaces

γ	ξ	ϕ	ϑ	$\sqrt{\phi}$	κ'	K
30	0.57735	0.05739	0.92640	0.240	3.87	6.1
45	1	0.13977	0.80575	0.374	2.32	6.25
55	1.428	0.17799	0.8219	0.422	1.96	4.62
60	1.732	0.18360	0.7887	0.4285	1.84	4.3
65	2.145	0.17555	0.7426	0.419	1.77	4.23
70	2.747	0.15549	0.6980	0.3943	1.77	4.49
75	3.732	0.12479	0.5881	0.353	1.67	4.7
80	5.671	0.08625	0.4332	0.294	1.47	5.0
85	11.430	0.04374	0.2440	0.209	1.17	5.5
90	∞	0	0	0	0	6.28

Further mathematical solutions for different values of m and different ratios $\frac{b}{a}$ have been calculated, apart from Michell, by Stodola¹⁾, Kingsbury²⁾ and others. However, the simplified approximative methods and tests with models have produced results which always differ from experience gained in actual operation.

The Swedish firm ASEA carried out tests, the results³⁾ of which suitably complement the previously discussed theoretical considerations. Thus certain rules have been established which must be observed by the designer of bearings.

It is obvious from what has been stated before, that a thick layer of oil is desirable for the interstice between the sliding surfaces; this layer ensures a reliable operation also in the case of sliding surfaces machined less exactly. However, the requirement to reduce friction losses to a minimum is contradictory to the condition of a thick oil layer. Results obtained by the above mentioned tests have shown, that optimum conditions can be achieved by selecting the dimensions of the segment for a given load and a given speed, so that the ratio of the theoretically lowest thickness of the oil layer to the coefficient of friction multiplied by the mean diameter of the bearing has a maximum value. The ASEA Company introduces into the respective formulas the mean sliding velocity U (hitherto we have considered a rectilinear sliding movement), i. e. the velocity of a point moving along the mean diameter of the segment circle, and the mean segment length l , i. e. the mean circumference divided by the number of segments less the width of the gaps between the individual segments. Results of calculations made with these formulas differ only slightly from the results of measurements carried out on actual installations in operation. In any case the differences are by far smaller, than those resulting from the superpositions considered in the previous theoretical section.

Thus the coefficient of friction can be calculated from the formula:

$$f = K_f \sqrt{\frac{\mu U}{l p_{\text{mean}}}} \quad (309)$$

¹⁾ Stodola A.: Die Dampf- und Gasturbinen, Springer, 1932, p. 1111.

²⁾ Kingsbury: On Problems in the Theory of Fluid-Film Lubrication with an Experimental Method of Solution, Transactions ASME 53/1931.

³⁾ S. Gynt: Recent Development of Bearings and Lubrication Systems for Vertical Generators, ASEA-Journal, 1947, pages 72—87.

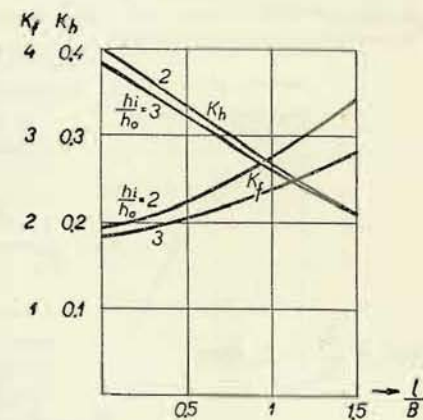


Fig. 395

and the minimum thickness of the oil film from the formula:

$$h_0 = K_h \sqrt{\frac{\mu U l}{p_{\text{mean}}}}, \quad (310)$$

where U is the mean sliding velocity in m/sec, p_{mean} the average value of the specific pressure in kg/m², μ = viscosity of oil in kg sec/m², l = mean length of the segment in m.

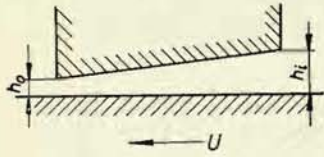


Fig. 396

Symbols K_f and K_h are functions of the ratio $\frac{l}{B}$ and of the ratio of oil film thickness h_0 and h_i . They are illustrated in Figs. 395 and 396, where B is the radial width of the segment.

The relation between K_f and K_h is expressed by the equation

$$K_f = K_h \left[\frac{1}{K_h^2} \frac{\ln \frac{h_i}{h_0}}{\frac{h_i}{h_0}} + \frac{\frac{h_i}{h_0} - 1}{2} \right]. \quad (311)$$

and if $\frac{h_i}{h_0} = 2$, then

$$K_f = K_h \left(\frac{0,69}{K_h^2} + 0,5 \right)$$

for $\frac{h_i}{h_0} = 3$:

$$K_f = K_h \left(\frac{0,55}{K_h^2} + 1 \right). \quad (312)$$

The previously quoted ratio which is characteristic for the establishment of optimum conditions and which should have a maximum value, can be calculated from Equations (309) and (310) as follows:

$$\frac{h_0}{f d} = \frac{K_h}{K_f} \frac{l}{d} = \frac{K_h}{K_f} \frac{l}{B} \frac{B}{d} = \frac{K_h}{K_f} \frac{l}{B} \frac{B}{d_i + B}. \quad (313)$$

In Equations (311) to (313) the following denotations are used: h_i the thickness of the oil film at the front edge of the segment, h_0 the minimum thickness of the oil film, d the mean diameter of the bearing in m and d_i the internal diameter of the bearing in m.

The right side term in Equation (313) consists of two factors. The first $\frac{K_h}{K_f} \frac{l}{B}$ depends only on the ratio $\frac{l}{B}$ and on the wedge-shape coefficient of the oil layer $\frac{h_i}{h_0}$.

In the second factor $\frac{B}{d_i + B}$ we can consider d_i as constant for each individual case. The value of this constant is increased, whenever the value B increases. Therefore in the event of a reduction of the specific load of the bearing, the thickness of the oil layer will increase more rapidly than the friction losses.

Fig. 397. shows the first factor $\frac{K_h}{K_f} \frac{l}{B}$ plotted against $\frac{l}{B}$ within the limits of $\frac{h_i}{h_0} = 2$ to 3. It is clear, that the most favourable value can be obtained for $\frac{l}{B}$ slightly greater than 1. However, a closer investigation has shown, that the majority of producers use segments with dimensions

$\frac{l}{B} = 0.6$ to 1. The reasons justifying this practice are the following: longer segments and thus a smaller number, cause higher temperatures of sliding surfaces; there exists an increased danger of corrosion of the contact surfaces between the bearing sleeves and the shaft.¹⁾ or between the sleeve and the collar.

An alternation of minimum and maximum pressures will cause mat corroded spots appearing on the contact surfaces between sleeve and collar as well, as between sleeve and shaft. This corrosion has been previously thought to be caused by an insufficient electric insulation (see the next pages of this book), but recently the opinion has prevailed that it is caused by the pressure pulsation on these surfaces. By increasing the number of segments, the number of impacts is increased (at the same operational speed, i. e. at the same mean circumferential speed U), but their amplitude is reduced. We can increase the number of segments by reducing their mean length. A further reason for the increase of the number of segments and thus the reduction of their length is given by the consideration of thermal and mechanical deformations which always increase the unevenness of the surface. This question is discussed in the next chapter.

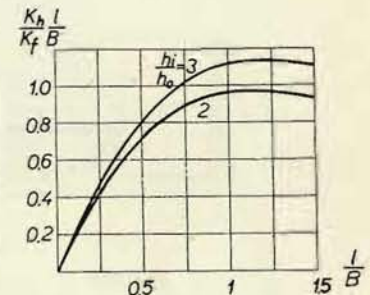


Fig. 397

III. DESIGN OF THRUST BEARINGS

1. Methods of Supporting the Segments, their Shape and Numbers

Fig. 398. shows the most usual arrangement. The segments are stationary and the thrust collar rotates. The reverse arrangement, rotating segments and stationary thrust collar, is used in cases where the centrifugal force of the segments has

¹⁾ O. M. Laffoon: Hydraulic Turbine Generators, Water Power, March-April 1949, p. 64. Here the expression „fretting corrosion“ is introduced.

no adverse effect upon their tilting, i. e. where the mean circumferential velocity does not exceed 10 m/sec. This second arrangement has the advantage, that the gaps between the segments perform a centrifugal pumping action which ensures a reliable internal oil circulation in the base of the bearing. This advantage is not very significant, because a similar circulation can be easily ensured also in the

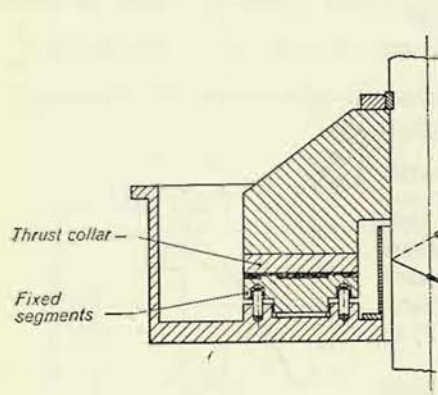


Fig. 398

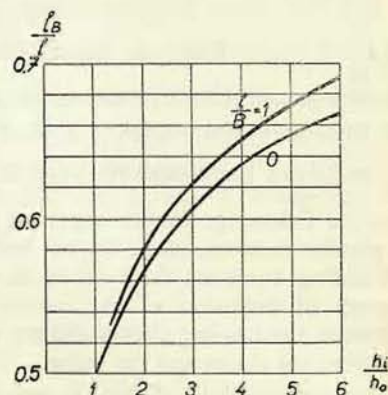


Fig. 399

first arrangement, but the fixing of the rotating segments, on the other hand, is very difficult.

Numbers and shapes of segments have been dealt with in the preceding chapter. Let us discuss the thickness of segments and methods of supporting. Thickness must be dimensioned so that the unevenness of the sliding surface should not be increased by mechanical deformation above an admissible limit. Thickness of segments is discussed in more detail in the next chapter.

As has been explained previously, the main condition of a proper supporting of segments is the possibility of tilting around a suitable edge, so that the formation of a wedge-shaped interstice is ensured. The tilting edge is determined according to Equation (298). An empirically established relation determining the distance of the tilting edge from the inlet edge is shown in Fig. 399 (ASEA diagram). ČKD Blansko locate the tilting edge according to Fig. 400.

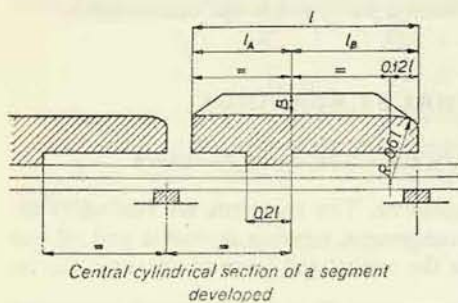


Fig. 400

The inlet edge of the segments is slightly beveled. The parabolic surface is substituted by a cylindrical one (Fig. 400), in former constructions it has been substituted by a plane chamfer.

Segment supports can vary considerably. A survey of the most important methods used by leading manufacturers is shown in the following figures.

Fig. 401 shows the so called „System Kieswetter“ support used by the SKODA Works in Pilsen. The segments are undercut and tilted according to the flexibility of the material. This arrangement is suitable from the point of view of assembling, but production is not simple. The system is more suitable for horizontal shafts.

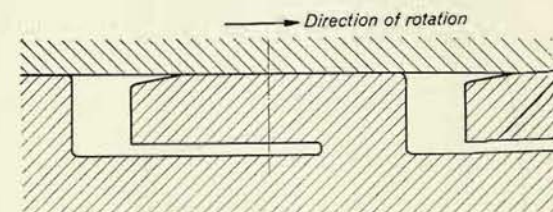


Fig. 402 illustrates an arrangement used by the Ateliers de Charmilles. Tilting is also made possible by the flexibility of the material in the lug. (This method of supporting has been used for turbine bearings in the Ryburg-Schwörstadt power station for an axial load of 900 metric tons).

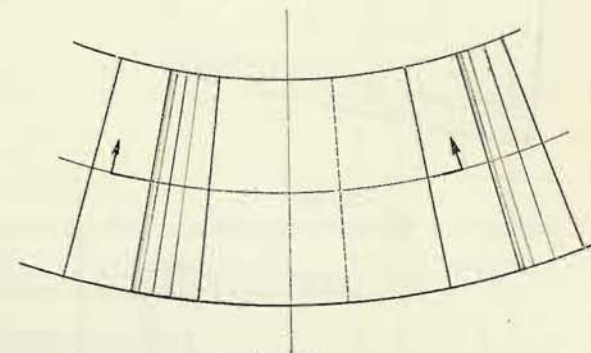


Fig. 401

Figs. 403 and 404 show the methods used by the firm of Voith and recently also by the Brown-Boveri Works. Segments are supported by flexible plates made of an oil-resisting material. The maximum admissible pressure on the flexible plate must not be exceeded. One or two pins secure the segments against a circumferential shifting. Fixing by

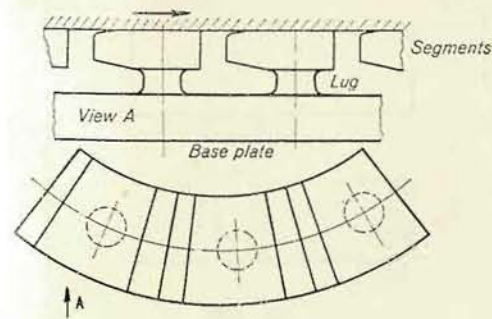


Fig. 402

a radially located pin is possible also. Simple production is a great advantage of this arrangement. Flexible metal plates have been used by the Siemens Works.

A former design of the Siemens Works consisting of a spherical pivot and a hardened plate, shown in Fig. 405, is no longer used.

Fig. 406 shows a ball-support design of the Brown-Boveri Works. This arrangement has been abandoned too.

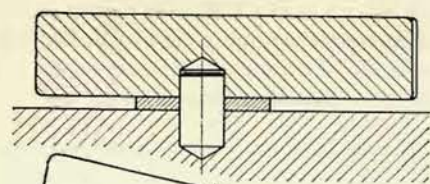


Fig. 403

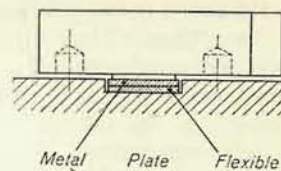


Fig. 404

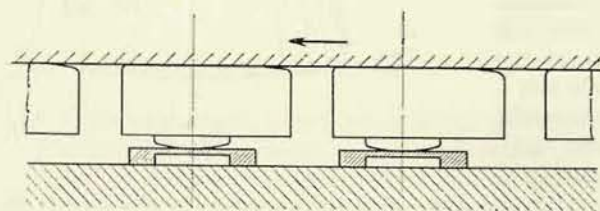
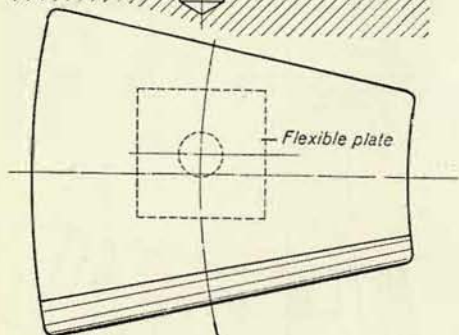


Fig. 405

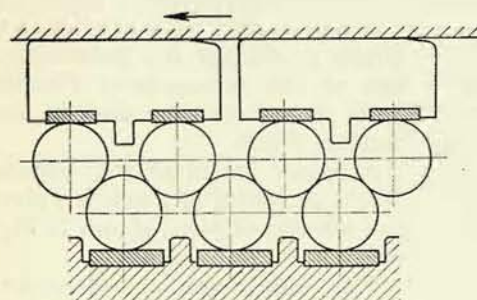


Fig. 406

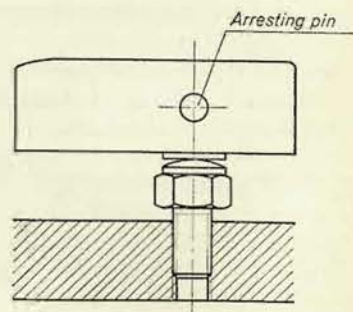


Fig. 407

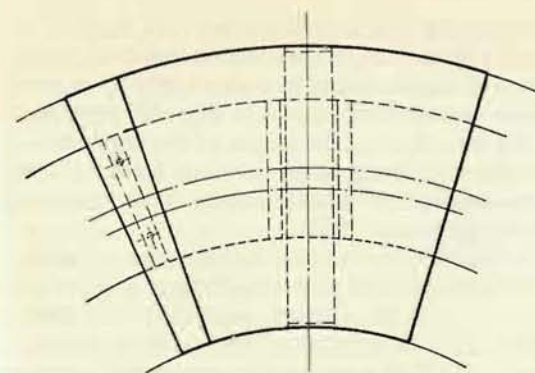


Fig. 408

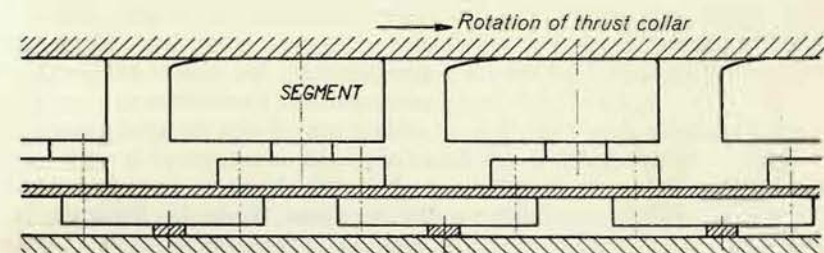
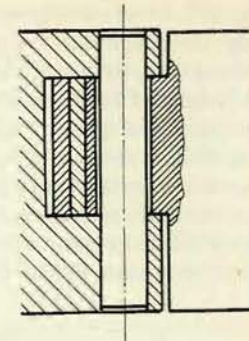
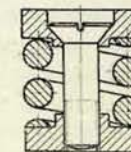
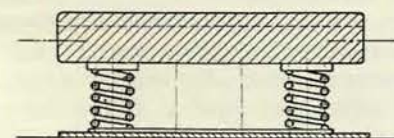
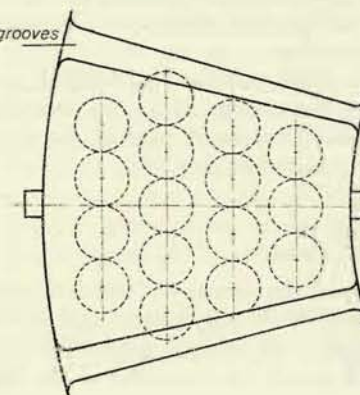


Fig. 409



Radial grooves



Arresting pins

Fig. 410

Fig. 407. shows a support arrangement with a setting screw. All supports previously described have required a rather exact production method, because a uniform distribution of load upon all segments can be assured only by an exactly equal height of the segments. The arrangement shown in Fig. 407 permits the compensation of production faults by adjusting the height of the segments. The setting of the screw is checked by a pressure gauge or the necessary force for turning the screw is measured and compared with that of other segments. This arrangement is used in newly manufactured bearings in the USSR.

The Hoffman system shown in Fig. 408 is used by ČKD Blansko and recently also by the Brown-Boveri Works. The segments rest upon flexible annular plates

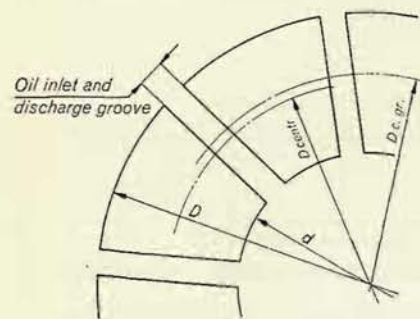


Fig. 411

made of sheet metal supported between the seating of two adjacent segments. This arrangement guarantees a uniform load distribution over all segments, because differences in heights caused by imperfect production are automatically compensated; the elastic annular plates must maintain a contact upon their whole surface area. From the production point of view this arrangement is very simple.

Fig. 409 shows an arrangement used by the Ganz Works in Budapest. It is based upon the same principles as shown in Fig. 408.

Fig. 410 illustrates a new arrangement not yet used in Czechoslovakia. The comparatively thin segment is supported by springs and, therefore, this arrangement is called „the mattress support“. It is widely used in the USA, USSR, Switzerland and Sweden. The mechanical deformation of the segment is of the opposite sense, than the thermal, so that under certain conditions both deformations can be compensated. This is an advantage of the arrangement which also is less sensitive in respect of the angle enclosed by the planes of the sliding surfaces and the axis of rotation. The production of the ground springs, however, is very expensive.

Segments are shaped according to the division of the load carrying annular ring by radial grooves through which the oil flows. (Fig. 411). The inner diameter is determined by the diameter of the shaft. Centers of supports lie on the circle passing through the center of gravity of the annular ring.

2. Material of Segments and Adhesion

Thrust bearings must be lubricated by oil the viscosity of which does not change very much with temperature, i. e. the curve of viscosity plotted against temperature has a flat course. Further the viscosity should not cause an increase of the coefficient of friction f , on the other hand it should permit the formation of the thickest pos-

sible oil layer. It is rather difficult to find a type of oil which could fulfil these contradictory conditions even partially. Highest possible lubricating capacity is required also. This can be obtained by various chemical additives. Oil must not foam, i. e. it must not absorb air; it must be chemically and physically stable, etc. Mineral oils are used exclusively and never oil of animal or vegetable origin.¹⁾

Due attention must be paid, however, to other oil circuits also. In the case of a common oil circuit installed for lubrication and regulation (control), a suitable compromise must be found. Turbines equipped with a reduction gear have a common oil circuit for both lubrications. Reduction gears require oil of a higher viscosity. Oils used in Czechoslovakia for the lubrication of thrust bearings have a viscosity 6 to 6.5 °E/50 °C or 45 to 50 cSt/50 °C.

Apart from the oil, also the material of the sliding surfaces has a great influence upon the coefficient of friction and friction losses in general. Oil adhesion to different materials varies considerably and so does the thickness of the oil film which remains on the sliding surfaces. Exact relations between these factors have not been established mathematically, but they can be practically observed on actual tests carried out with models.²⁾ A bearing made of graphitic grey cast iron has a much smaller coefficient of friction than a babbitted bearing.

This is one point of view which must be respected when selecting the material. Apart from this, we also must bear in mind the so called emergency properties of the sliding materials. As stated before, the oil film ceases to be formed at a certain moment of the starting or closing period when conditions of a semi-fluid friction are created. Therefore we must consider the properties of materials at such conditions. Impurities can also find their way into the interstice between the sliding surfaces, and we must consider the resistance of materials against the effect of impurities. Finally, heat conducting properties of materials must be also considered.

Excellent emergency properties were observed in segments babbitted with white metals having a tin or lead base. The thrust collar proper is made of steel or cast steel. Some manufacturers, e. g. Ganz, Ateliers de Chammilles, Brown-Boveri, ČKD Blansko, etc., use sliding surfaces made of grey cast iron.

White metal has good emergency properties; small impurities between the sliding surfaces are easily pressed into the white metal. At identical conditions seizure occurs later than with grey cast iron. On the other hand, as stated before, it has a higher coefficient of friction and thus also higher friction losses.

Though grey cast iron has worse emergency properties – impurities cut grooves in the sliding surface and this may cause a seizure of the bearing – it stands higher temperatures than babbitt and has a smaller coefficient of friction. It requires better maintenance, greater purity of oil and oil ducts; the necessity of increased care, however, is compensated for by smaller friction losses. Surface hardnesses of the sliding surfaces of the segments and collar must be different; this can be

¹⁾ For details see: Havlíček: Mazání strojů a hospodaření oleji v průmyslových podnicích (Lubrication of machines and oil economy in industrial undertakings). Práce, 1947.

²⁾ Šmerák: Prüfung und Bewertung von Lagerwerkstoffen, Škoda-Mitteilungen (1943), Heft No 1, 2.

achieved by casting a thinner, thus harder, collar. Homogeneous, faultless surface of a fine pearlitic structure is rather difficult to obtain particularly with large castings. Waste in production is increased by this requirement.

White metal shows a special resistance against seizure during small sliding velocities when no oil film is yet formed. Apparently this can be explained by adhesion. Šmerák's experiments have shown¹⁾, that seizure with white metal occurs at specific pressures of 80—240 kg/cm² (according to composition), while seizure of grey cast iron occurs already at a mean specific pressure of 40 kg/cm². This, however, is not so important, because no hydraulic pull exists during starting and closure of the turbine. In Francis turbines the blades are designed for full opening and there is no overpressure at a small opening of the guide wheel. In Kaplan turbines the runner is opened to 30 % or more before we start to open the guide apparatus for starting or before we start reducing the speed during closure. This is done in order to eliminate the hydraulic thrust during the starting or closing period. As the hydraulic thrust represents about 50 % of the load carried by the bearing and the highest operational pressure is about 40 kg/cm², the specific pressure during starting and closure amounts to about 20 kg/cm² which is well below the value at which cast iron is seized.

Selection of materials depends to a certain extent, on the requirements of the customer and the manufacturing possibilities and practice of the manufacturer.

Another combination of sliding surface materials could be the bronze-steel couple. This has been used hitherto only sporadically. Sliding surfaces made of basalt, textgumoid, etc. need not to be considered because of their bad heat conducting capacity.

Specific pressure influences, as the thickness of the oil film, as well the coefficient of friction. The selection of the specific pressure determines thus the losses of the bearing. Small specific pressure means large diameters of the segments, great mean circumferential velocity and consequently large friction losses. With regard to the material and due to the fact, that maximum specific pressure is about 2.5 times the mean value, we select the mean specific pressure within the range of 40—50 (up to 60) kg/cm²; sometimes it is not more than 30 kg/cm².

In bearings with exceptional high loads (above 1200 tons axial thrust) the dimensions of the sliding surfaces would be very large. For reason of easier production we divide the sliding surfaces into two concentric sets and increase simultaneously the specific pressure.²⁾ In order to prevent a seizure of the bearing during starting or closure, the rotor can be relieved electromagnetically during these periods. At normal operation — when the oil film is already formed — this relief is not necessary and it could not be maintained, because it cannot be secured (would cause an inadmissible loss of voltage).

¹⁾ Šmerák: Prüfung und Bewertung von Lagerwerkstoffen, Škoda Mitteilungen (1943), Heft No 1, 2.

²⁾ Alexeyev A. E.: Konstrukciya elektricheskikh mashin, Moskva-Leningrad, Gos-energoizdat, 1949, p. 234.

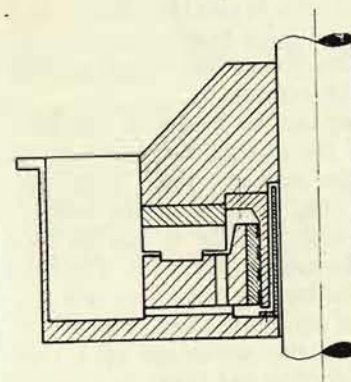


Fig. 412

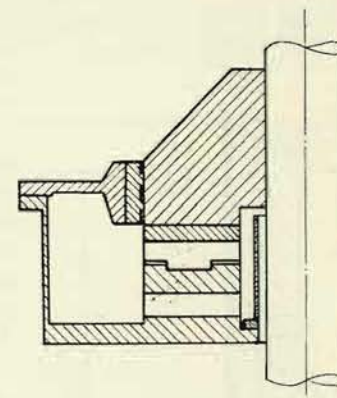


Fig. 413

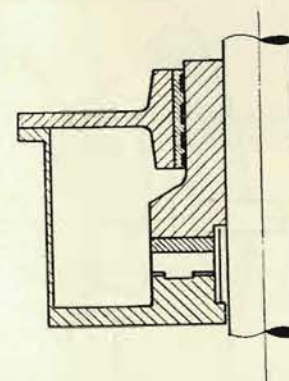


Fig. 414

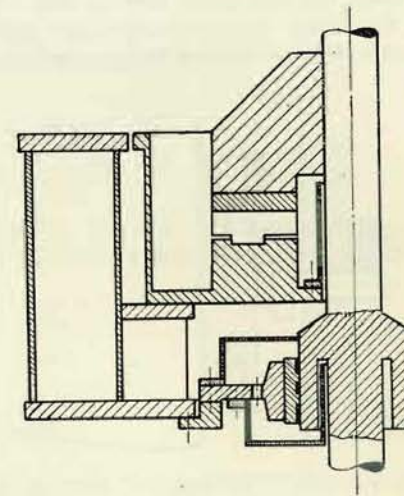


Fig. 415

IV. GUIDE BEARINGS AND THEIR LOCATION

The upper guide bearing (above the rotor of the generator) is usually combined with the thrust bearing. It carries the respective part of the magnetic pull and centrifugal forces of the unbalanced masses of the rotor in case that there is another guide bearing below the rotor. If there is no second guide bearing underneath the rotor, the above forces are carried entirely by the upper guide bearing.

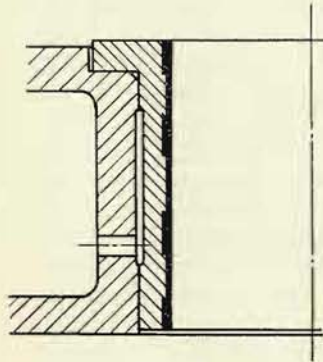


Fig. 416

Finally the type of the bearing used is determined also by the operational speed and the general lay-out of the thrust bearing. In units running at low speeds easy access is decisive and the designer will put the guide bearing on the collar. On the

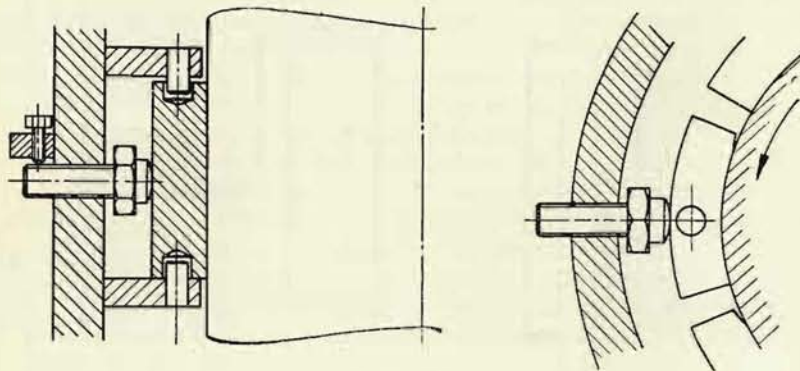


Fig. 417

contrary, in the case of high operational speed, friction losses are the decisive factor and the guide bearing must be designed with a smallest possible diameter regardless to difficulties of assembling and mounting.

Calculation and design of the normal split bearing is not discussed here, because ample literature is available on this subject. The calculating method of a guide bearing containing shoes is given in some detail. (Fig. 418).¹⁾

Let us denote the thickness of the oil film at the inlet edge as h and on the other end of the shoe as h_0 . The resultant of forces acts at the point of support and is denoted by F ; the shoe turns about this point and the thickness of oil film in this point is h^* .

If the supporting point is located so, that $\frac{h}{h_0} = K$,

we can calculate the minimum thickness of the oil layer for the shoe marked 1.

$$h_0 = \frac{2}{1+K} h^*. \quad (314)$$

For calculating purposes it is advantageous to insert the apparently thinnest layer h_0 and the respective excentricity of the shaft $\delta - h_0$.

The minimum thickness for the shoe with the thinnest layer is then:

$$h_{0,\min} = \frac{2}{1+k} h_0. \quad (315)$$

In the case of a bearing with six or more shoes, we may, with admissible exactness, use for the minimum thickness of the oil film the same formula, as used for plane shoes:

$$h_0 = K_h \sqrt{\frac{\mu U l}{p_{\text{mean}}}}, \quad (316)$$

from which we derive

$$p = \frac{K_h^2}{h_0^2} \mu U l. \quad (316a)$$

Taking the value K_h from Fig. 395 we can calculate the total load of the shoe, as:

$$F = p B l = \frac{K_h^2}{h_0^2} \mu U l^2 B = \frac{(1+K)^2}{4 h^{*2}} K_h^2 \mu U l^2 B. \quad (318)$$

¹⁾ Gynt S.: Recent Development of Bearings and Lubrication Systems for Vertical Generators, ASEA Journal (1947), p. 72—87.

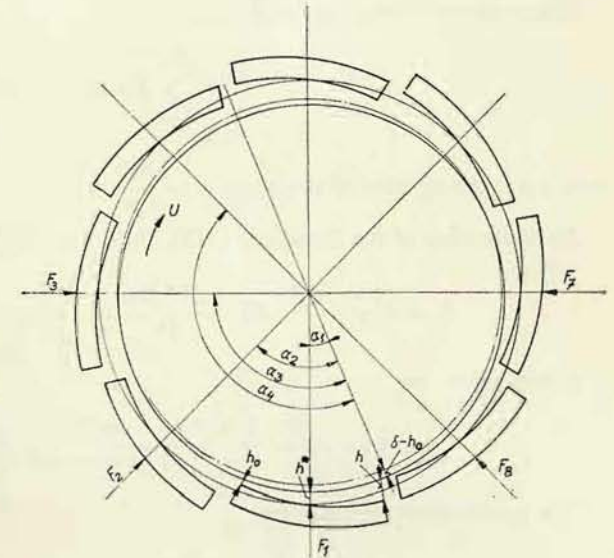


Fig. 418

With sufficient exactness we can write also:

$$h^* = \delta - (\delta - h_0) \cos \alpha = \delta (1 - m \cos \alpha), \quad (319)$$

where

$$m = \frac{\delta - h_0}{\delta} \quad (320)$$

is the relative excentricity of the shaft.

The total load of the bearing is then:

$$F = \sum_{i=1}^n F \cos \alpha, \quad (321)$$

where n is the number of shoes and $\alpha = \frac{360^\circ}{n}$.

By application of the Equations (318), (319) and (321), we receive:

$$F = \frac{(1 + K)^2}{4} \cdot K_h^2 \cdot \frac{\mu B l^2 B n}{\delta^2} \cdot \frac{1}{n} \sum_{i=1}^n \frac{\cos \alpha}{(1 - m \cos \alpha)^2}. \quad (322)$$

Let us substitute

$$\psi = \frac{1}{n} \sum_{i=1}^n \frac{\cos \alpha}{(1 - m \cos \alpha)^2}. \quad (323)$$

If n is sufficiently great, then

$$\psi_{1..n} = \frac{1}{\pi} \int_0^\pi \frac{\cos \alpha}{(1 - m \cos \alpha)^2} d\alpha = \frac{m}{(1 - m^2)^{\frac{3}{2}}}. \quad (324)$$

Fig. 419. shows, that the value resulting from the integration is practically exact even in the case of 8 shoes only.

By using Equation (322), Fig. 419 and the expressions (320) and (315) we can determine the respective values of the bearing load and the minimum thickness of oil layer for a particular bearing.

The coefficient of friction of the n -th shoe can be calculated from the equation:

$$f_n = K_f \cdot \sqrt{\frac{\mu U}{p_n l}}, \quad (325)$$

The value K_f in the above equation is calculated according to Fig. 395.

The value of the friction force for a given shoe is calculated from Equations (325) and (317) as:

$$F_{f,n} = f_n p_n l B = K_f K_h \mu U l B \frac{1}{h_0}. \quad (326)$$

The values K_f and K_h are the same for all shoes. The total friction is:

$$F_f = K_f K_h \mu U l B n \frac{1}{n} \sum_{i=1}^n \frac{1}{h_0} \quad (327)$$

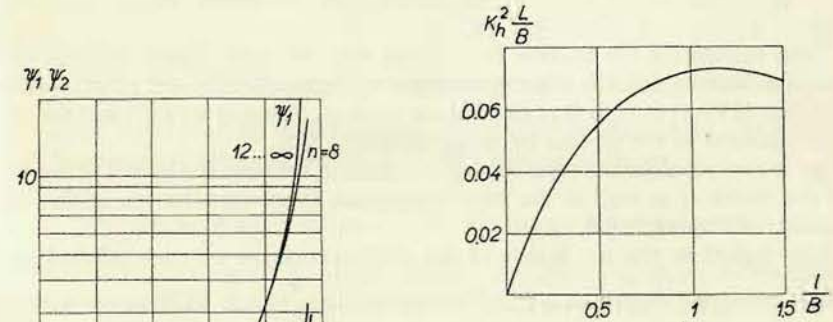


Fig. 420

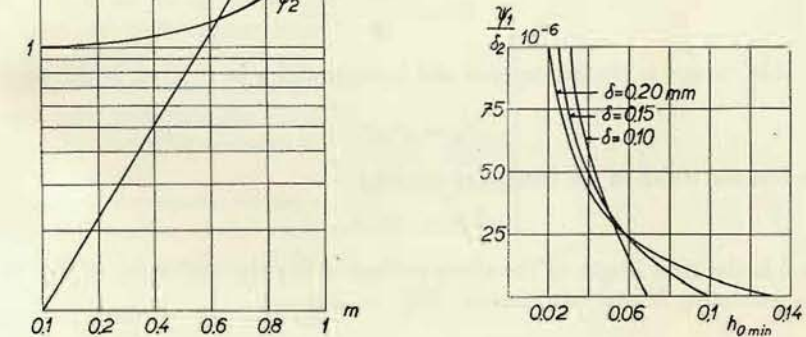


Fig. 421

By using Equations (319) and (314) we can write:

$$F_f = \frac{1 + K}{2} K_f K_h \frac{\mu U l B n}{\delta} \cdot \frac{1}{n} \sum_{i=1}^n \frac{1}{1 - m \cos \alpha}. \quad (328)$$

Let us substitute

$$\psi_2 = \frac{1}{n} \sum_{i=1}^n \frac{1}{1 - m \cos \alpha}. \quad (329)$$

If n is great enough, it follows:

$$\psi_{2,\infty} = \frac{1}{\pi} \int_0^\pi \frac{1}{1 - m \cdot \cos \alpha} d\alpha = \frac{1}{(1 - m^2)^{\frac{1}{2}}} \quad (330)$$

In Fig. 419 the values ψ_1 and ψ_2 are illustrated as functions of m for the following numbers of shoes: $n = 8.12$ and ∞ .

When calculating the friction for a given load we shall follow this procedure. First of all we establish the value ψ_1 by applying Equation (322), the value m is taken from Fig. 419 and from it we calculate the value ψ_2 . From m we calculate the minimum thickness of the oil film by using Equation (316).

Let us now consider the most favourable relation between the length of the shoe l and the width B as well as the basic conditions from the selection of the radial clearance of the bearing δ .

With regard to the machining of the sliding surfaces we may select $h_{0,\dots} = 0.04$ mm and the value of the friction $K = \frac{h}{h_0} = 2$. Further we make the following substitutions:

$$U = \frac{\pi d n}{60}$$

where d in metres is the diameter of the bearing and n in r. p. m. is the normal speed,

$$A_p = d \cdot B,$$

where B is the width of the bearing in metres;

$$n l B = \pi \lambda A_p,$$

where λ is the total length of the shoes related to the circumference of the shaft.

By substituting $K = 2$ into relation (322), we receive:

$$F = \frac{9 \pi^2}{4} \frac{\mu n}{60} \lambda A_p^2 K_h^2 \frac{l}{B} \frac{\psi_1}{\delta^2} \quad (331)$$

The expression $K_h^2 \frac{l}{B}$ is illustrated in Fig. 420. Its maximum value, which is also the most favourable as far as the carrying capacity of the bearing is concerned, lies within the range $\frac{l}{B} = 0.8$ to 1.5 . The curves in Fig. 421 have been constructed by using Fig. 419 and equations (315) and (320) and they represent changes of the factor $\frac{\psi_1}{\delta^2}$ in dependence on $h_{0,\min}$ and δ . For a selected $h_{0,\min} = 0.04$ mm, the carrying capacity of the bearing is practically the same within the range $\delta = 0.1$ to 0.15 mm. For the selected values $\mu = 0.002$, $\lambda = 0.85$, the minimum thickness

of the oil layer = 0.04 mm, the carrying capacity in kg of this type of bearing is expressed by the following formula, according to Equation (331):

$$F = 220\,000 \frac{n}{100} A_p^2 \quad (332)$$

Friction losses will be as follows:

$$F_f = \frac{K' \mu U A_c}{\delta} \quad (333)$$

where $K' = \frac{1 + K}{2} K_f K_h \lambda$ and $A_c = \pi d B$ is the contact surface of the shaft in m^2 .

The guide shoes are lined with white metal, because the shaft of the collar (which forms the journal of the guide bearing) is made of steel or cast steel.

V. GENERAL LAY-OUT OF THRUST BEARINGS

Axial load is transmitted from the shaft to the sliding surfaces by the thrust runner or collar. The design of the thrust collar must comply with the following requirements:

- it must be sufficiently rigid, i. e. it must not be deflected by the load to such extent; that would cause an additional unevenness of the sliding surfaces;
- it must withstand the stress caused by centrifugal forces at runaway speed;
- it must be capable to carry the double torque of the shaft in the event of a seizure of the bearing
- the plane of the sliding surfaces must be perpendicular to the axis of rotation
- it must be well designed from the point of view of foundry practice.

Thrust runner 1 (see Appendix VII) is generally cast of grey cast iron or steel. Its shape may vary (see Fig. 422 and 423) according to the above enumerated requirements. On the periphery it has oil grooves. It is connected with the shaft by one

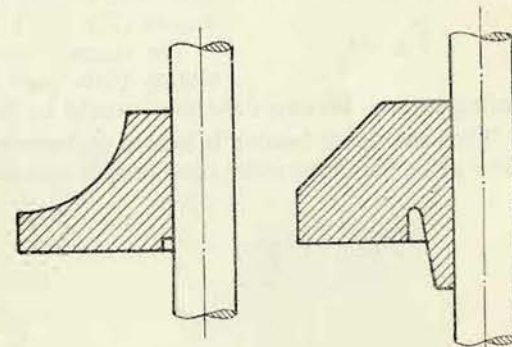


Fig. 422

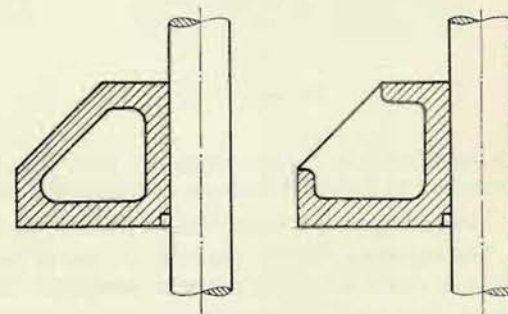


Fig. 423

or two fitted keys. Mounting is either with a sliding fit or interference fit. In the latter case the runner is put on the shaft in a slightly heated state. At large dimensions the bore is relieved and the lower part has a recess of a larger diameter to permit a better mounting on the shaft.

Some runners have been forged and produced in one piece with the shaft. In this case the lower part of the bearing is split.

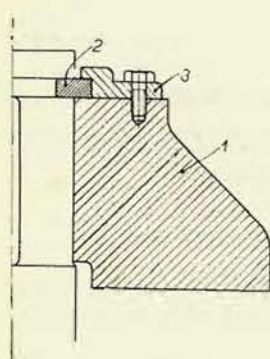


Fig. 424

Split ring 2 mounted in the cylindrical slot of the shaft secures the runner in axial direction. Cap ring 3 secures the split ring against opening. (Fig. 424). If a bevel reduction gear (Fig. 35) is used, the runner is axially secured by a nut (Fig. 425) which permits the proper setting of the engagement of the larger wheel.

The sliding surface could be formed directly on the runner, but this is never done, because the sliding surface should be exchangeable when it is damaged. An annular plate fixed to the runner by cylindrical bolts and screws (Fig. 426) or by radial keys and screws (Fig. 427), forms the sliding surface (collar).

The contact surface of the thrust collar and its sliding plate must be machined as exactly as the sliding surface, because deflections would be transmitted to the sliding surface.

When the thrust bearing is located underneath the generator or on the turbine cover plate, the thrust collar must be split into two parts. The halves are connected

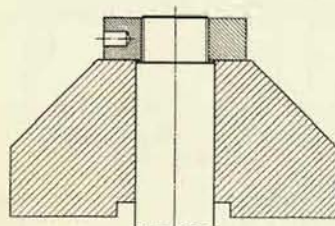


Fig. 425

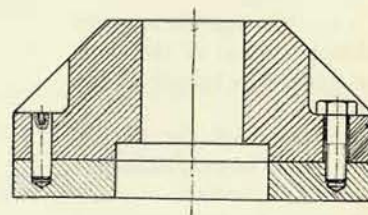


Fig. 426

by bolts, bands or simultaneously by both. The split sliding plate must be bevelled according to Fig. 428, because otherwise the oil film could be disrupted.

The sliding plate has radial openings serving the inner circulation of oil.

The segments fixed in position by pins or radial bolts are supported on a base plate (as described in the previous paragraph) which permits the tilting of the segments. Base plate 5 (Appendix VII) can be variously shaped. It must be sufficiently rigid, so that its deformation cannot affect the position of the segments. Flowing

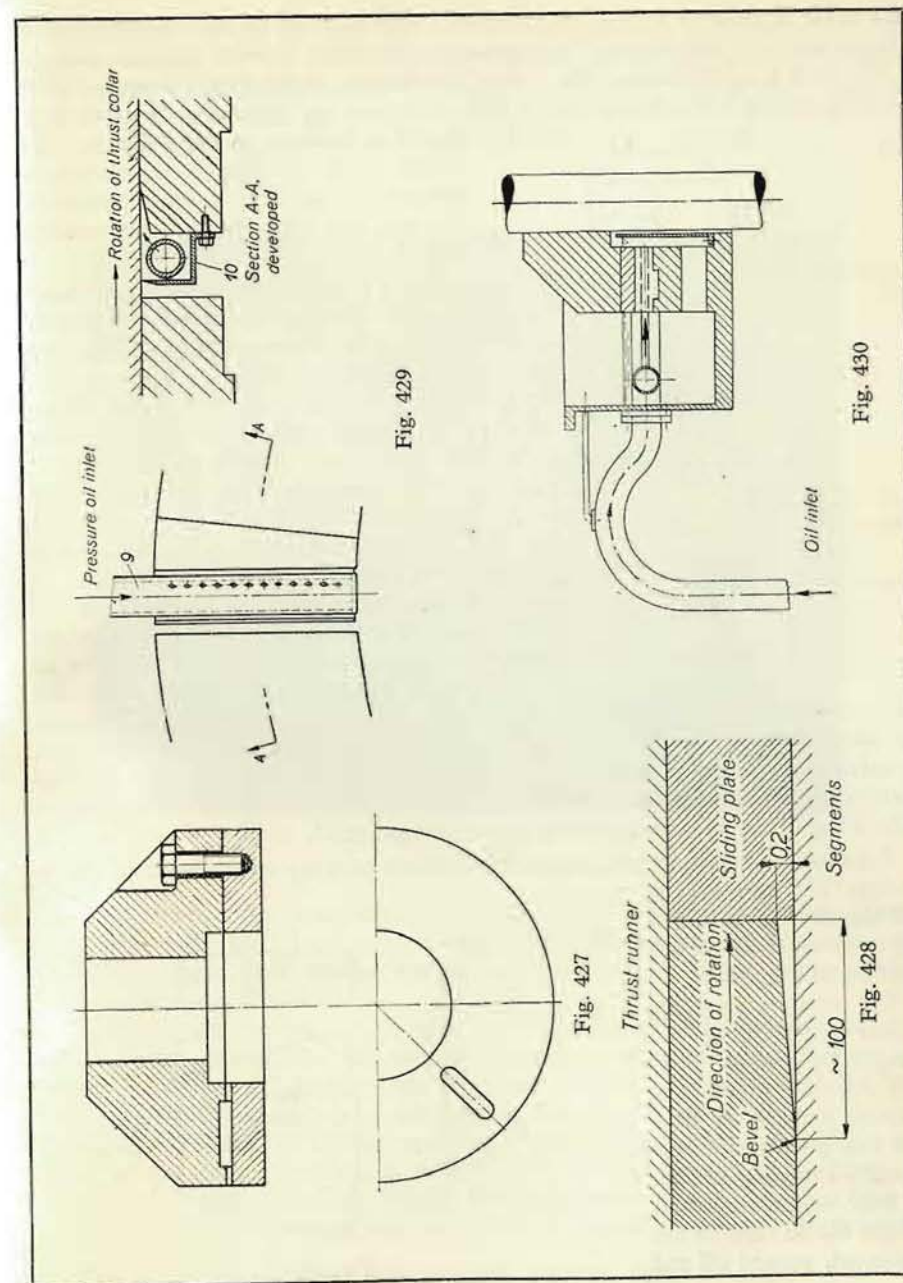


Fig. 429

Fig. 430

Fig. 427

Fig. 428

of cold oil to the lower parts of the segments is prevented by the base plate; different temperatures on both sides of the segments could cause harmful deformations.

Oil level is maintained in the tank of the bearing by the pipe 6 at such a level that the sliding surfaces are always kept under oil. In the event of an overflow, the oil is retained in the oil tank 7 by means of the oil ring 8. Oil discharge piping is richly dimensioned, because of the low viscosity during the starting period.

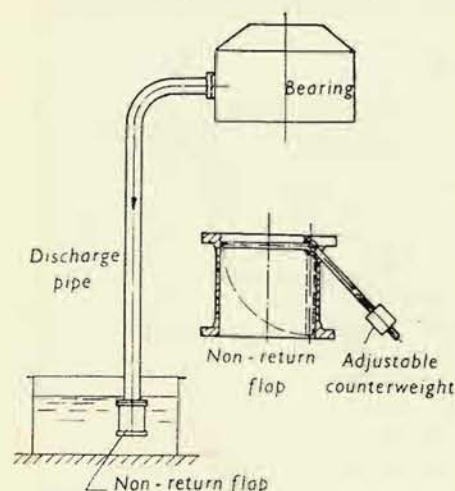


Fig. 431

shows an arrangement where the flap mounted in the discharge pipe is balanced, so that the pipe is filled up to the bearing. The oil does not fall from a great height, it does not disperse and is not aerated. The discharge pipe must be suitably overdimensioned with regard to the cold oil which enters during the starting period. The filling of the oil tank is checked by oil level gauge 11.

Segment temperatures are measured by remote mercury and resistance thermometers 12. Pressure of the oil film can be measured by a pressure gauge according to Fig. 432.

Oil vapours escaping from the bearing are caught by metallic packing 13, sometimes also carbon packing is used for this purpose. Exceptionally a special chamber is built around the shaft where the oil vapours are collected, sucked off and

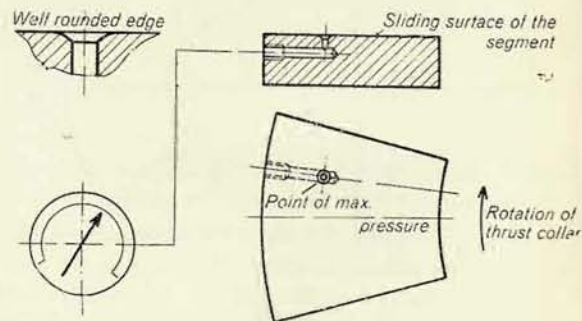


Fig. 432

condensed outside the bearing. The oil level in the bearing tank should be maintained so that the wetted surface area of the rotating parts is the smallest possible with regard to the losses caused by vortices; however, the oil level must be sufficiently high to keep the sliding surfaces under oil during rotation. Radially placed calming sheets in the oil tank prevent the spreading of oil and the formation of a rotational paraboloid.

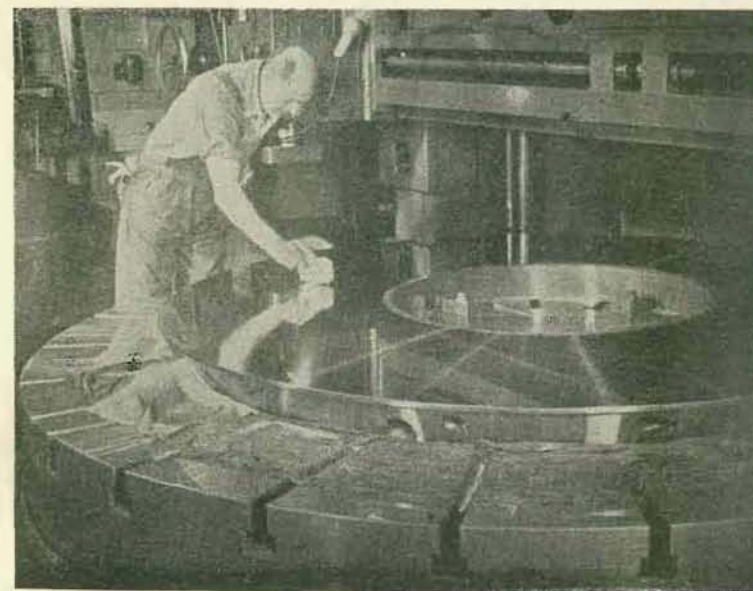


Fig. 433

Lid 14 prevents the penetration of impurities into the bearing. A cast oil tank must be properly cleaned and coated with an oil resistant lacquer before assembling. The design shown in Appendix VII has an oil tank which is part of the welded hanger structure.

The whole unit consisting of the split base plate, thrust collar, sliding plate, and segments must be produced with utmost precision in order to attain perfectly exact perpendicularity, parallelism, concentricity and levelness. Therefore the individual parts should be mounted for machining on the shaft or an auxiliary mandrel. Sliding surfaces must be finished to a mirror-like high polish. (See Fig. 433.) Levelness of the sliding surfaces is determined for various types of machining.¹⁾ Owing to the small thickness of the oil film unevenness must be less than 0.01 to 0.02 mm. The machined parts must be free of all internal stresses and the finishing

¹⁾ Falz: Grundzüge der Schmiertechnik, Berlin, Springer, 1926.

of the sliding surfaces must be carried out in a special room with constant temperature. Absolute care and cleanliness must be maintained throughout production and assembling.

VI. HANGER STRUCTURE

The hanger structure must transmit the axial load from the bearing to other parts, i. e. either to the skeleton of the stator or to the concrete foundations.

For smaller loads bridge-structures according to Fig. 434 are suitable; for higher loads star-shaped constructions are recommended. Attention must be paid

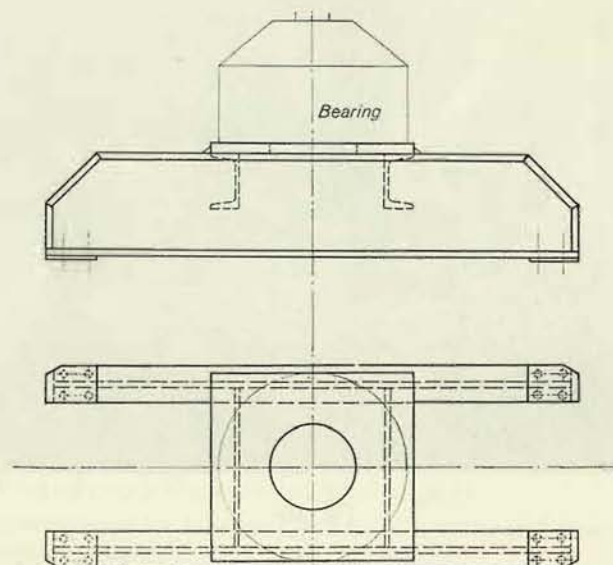


Fig. 434

to the admissible deflection which amounts to 1 mm for large turbines. Structures formerly cast have been recently replaced by welded constructions. The casing of the hanger structure can be advantageously used as the bearing oil tank. The design shown in Fig. 435 is less advantageous because the oil tank is separated by two shells and two air gaps from the surrounding space with very bad conditions for heat radiation.

The number of the brackets of the star structure is determined by the axial load. If the structure is located above the rotor, the lugs must be insulated from the stator. Specific load on insulating plates must not exceed 150 kg/cm². An increased number of brackets ensures evenly distributed stresses in the rings of the casing.

The rings may be smaller but the total weight is increased by the additional brackets. Brackets are fixed to the casing by means of keys and screws (Fig. 436). With smaller dimensions and suitable conditions of transport the brackets may be welded to the casing (Fig. 437). In other cases they may be only fixed by screws (Fig. 438). Lugs of the brackets are machined only after mounting and are fixed to the structure by pins and screws.

If the thrust bearing is placed above the rotor of the alternator, it forms together

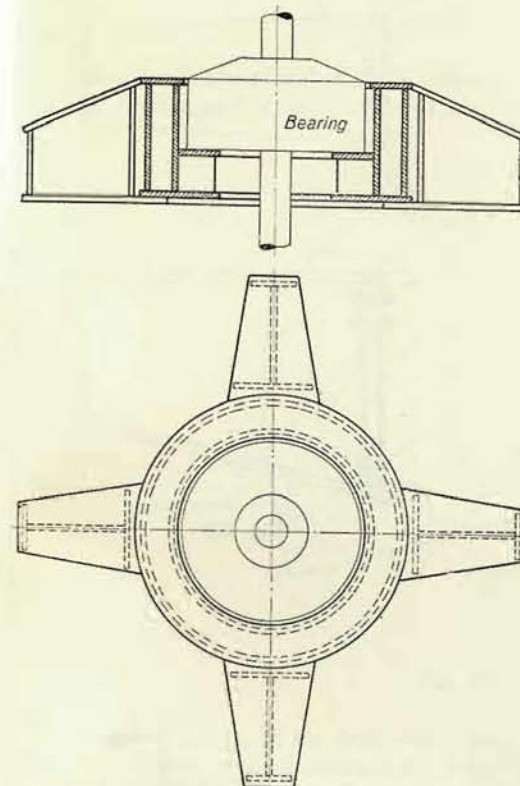


Fig. 435

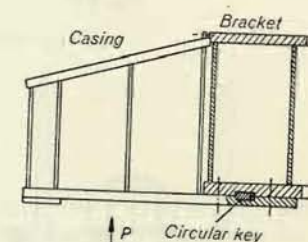
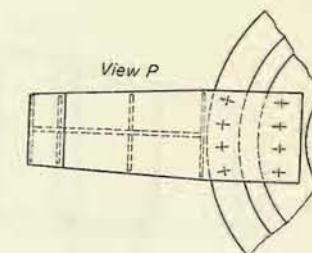
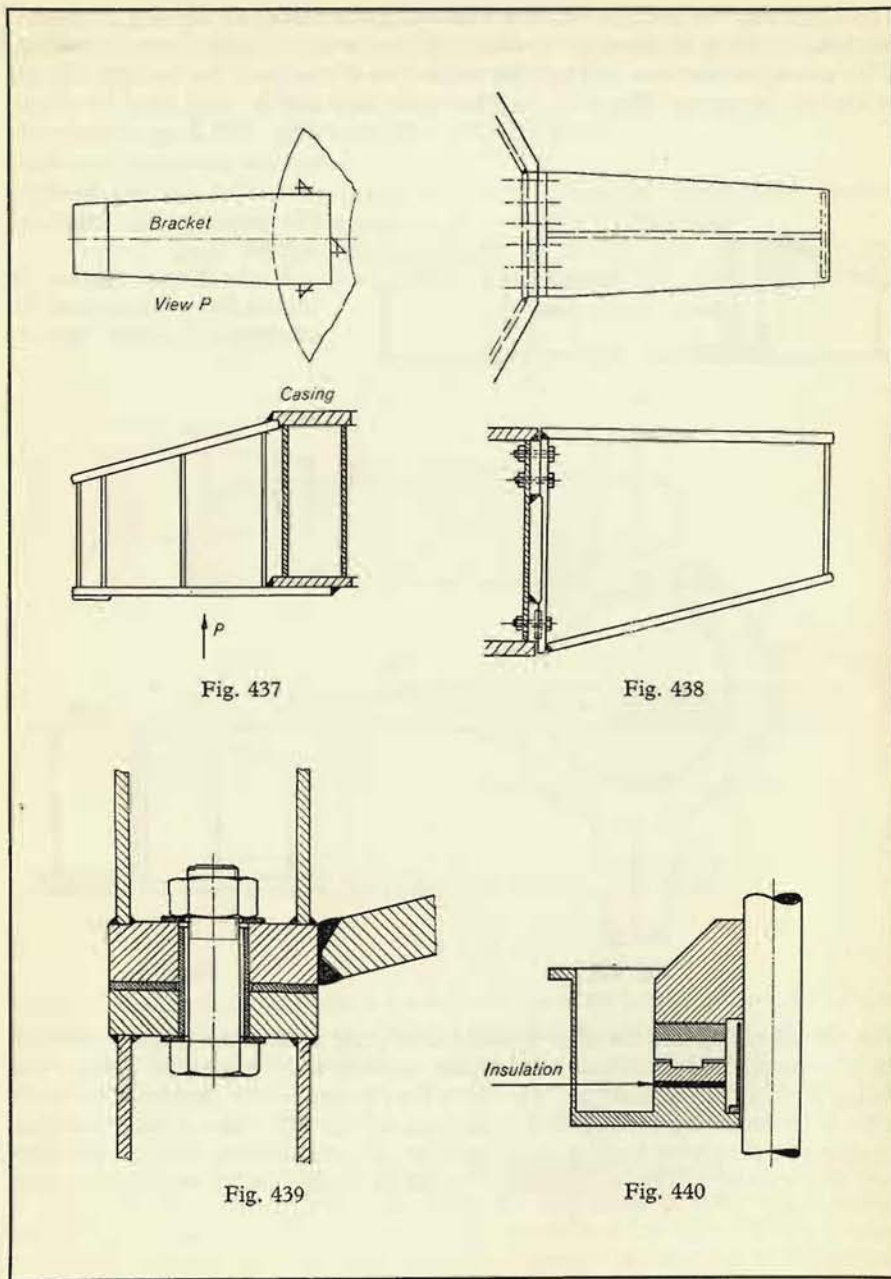


Fig. 436

with the oil piping and the shaft a closed conductor around the magnetic field of the alternator. Eddy currents would pass through this circuit and destroy the sliding surfaces of the bearings. Therefore the circuit must be broken. The break is made by insulating the lugs e. g. according to Fig. 439. Then it is necessary to insulate also the piping leading to the structure and the capillary tubes of the mercury thermometers. The insulation can be placed directly in the bearing according to Fig. 440.



VII. LUBRICATING AND COOLING INSTALLATIONS

Friction in the bearing produces heat. Temperatures are distributed over the segment approximately according to Fig. 441. The heat evolved can be expressed by the equation:

$$Q_s = \frac{PUf}{427} \text{ kcal/s} = \frac{102N}{427}, \quad (334)$$

where P is the axial load in kg, U the mean peripheral velocity in m/sec. f the coefficient of friction and N the friction work in kw.

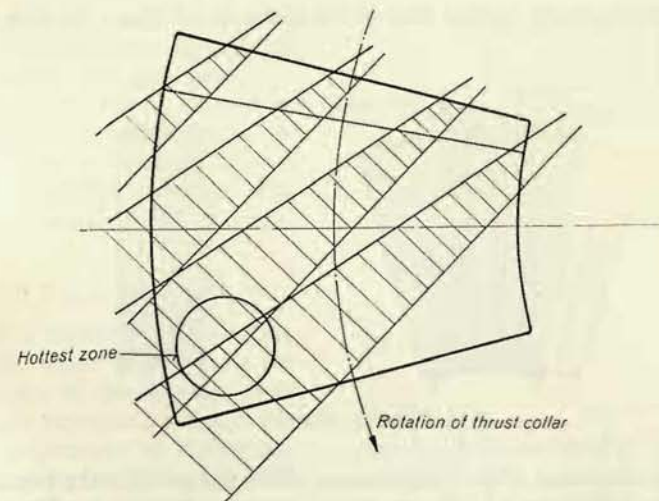


Fig. 441

If $p_{\text{mean}} \cdot U_{\text{mean}} \leq 90$ the heat evolved is so small, that under normal conditions and with a secured internal oil circulation in the bearing tank, it can be disposed of by radiation from the bearing into the surrounding space. If the above product is greater than 90, the heat evolved must be carried off by oil and the oil must be cooled. In this case we do not take into account radiation and calculation is based upon the assumption that the total heat is taken off by the oil. The flow rate of oil per second which is necessary to take off the heat evolved during this time, is given by the equation:

$$O_0 = \frac{Q_s}{\gamma c \Delta t}, \quad (335)$$

where $\gamma = 0.8 \text{ kg/dm}^3$ is the specific weight of oil, $c = 0.4 \text{ kcal/kg } ^\circ\text{C}$ is the specific heat of the oil and Δt is the number of $^\circ\text{C}$ by which the temperature of oil has been increased by the accepted heat. The same relation holds good for the flow rate of

water necessary for cooling the oil in the cooler. Specific heat and specific weight of water equal one and therefore the equation for water is simplified in the following way:

$$O_v = \frac{Q_s}{\Delta t} \quad (336)$$

The necessary surface area of the cooler is calculated from the equation:

$$F = \frac{Q_{\text{hour}}}{k \Delta_m}, \quad (337)$$

where F is the necessary surface area of the cooler in m^2 , Q_{hour} the heat in kcal/h

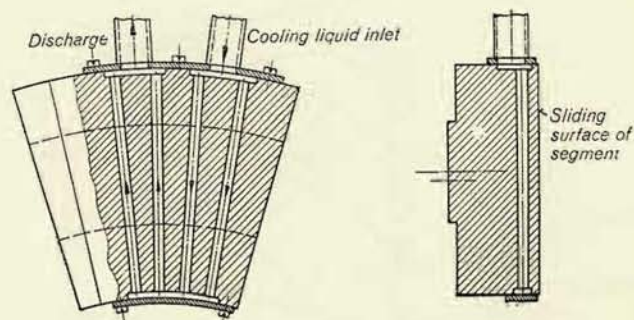


Fig. 442

Δ_m the mean difference of the temperatures of water and oil at the beginning and end of the heat transfer and k is the thermal coefficient of the cooler. The value of k for coolers of a simple design is about 180; for coolers with higher flow velocities (1 — 1.5 m/sec), with well placed cooling tubes without dead corners, the value of k amounts to 420 to 500.

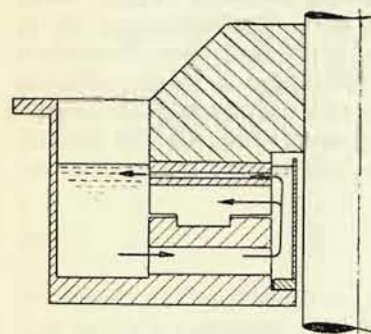


Fig. 443

The quantity of oil determined by equation (335) which is necessary for the conducting of the heat evolved, must actually pass the heated surfaces of the segments and thrust collar. If the thickness of the oil film is so small, that (considering an average velocity equal half of the mean peripheral velocity) this quantity cannot pass through the interstice between the sliding surfaces, the oil must be brought into contact with the segments also by other means. E. g. the oil can be pressed through ducts bored in the seg-

ments underneath the sliding surfaces and located preferably in places of the highest heat evolution.

Artificial cooling can be arranged, in principle, by three methods: 1. to conduct the heat directly off the sliding surfaces, 2. to conduct the heat off the bearing oil tank and 3. to conduct the heat off the oil in the circulating system outside the oil tank.

1. Direct heat conduction off the sliding surfaces is illustrated in Fig. 442.¹⁾ The segments have radial borings placed near to the sliding surface, water is pressed through the borings and circulates through inlet and discharge collecting chambers located on the inner and outer diameter of the segments. The quantity of the carried off heat may be apparently calculated by the same equation as used for the calculation of heat conducted by tubes cast-in into the bearing brass of journal bearings, i. e.:

$$Q = 1070 F (t_1 - t_2) \text{ kcal/h}, \quad (338)$$

where F is the surface area in contact with water in m^2 , t_1 is the temperature of the bearing (here that of the segments) and t_2 is the mean temperature of the water.

This cooling method is very efficient, but there exists the danger that water can penetrate into the bearing if the material of the segments is porous or the inlet and discharge chambers of water are insufficiently packed. The fact, that heat is conducted off the place of its evolution, is a great advantage. There is almost no thermal deformation of the segments. However, this advantage can be obtained also in the previously described system of pressing cold oil through the segments.

2. In the course of the inner circulation of oil in the oil tank (Fig. 443) the oil heated on the sliding surfaces enters the oil tank. Here the heat can be conducted off by a cooling coil with a suitable cooling liquid (usually water). The cooling water circulates either in a closed circuit (Fig. 444) or it is discharged (Fig. 445).

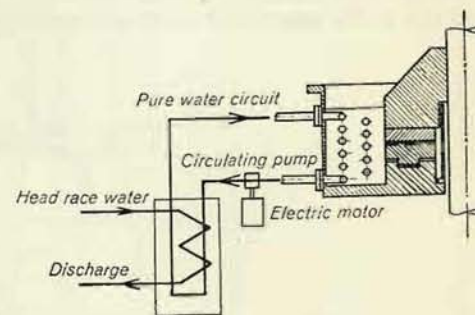


Fig. 444

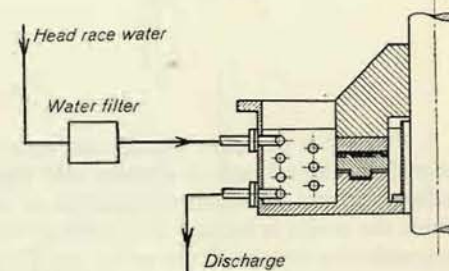


Fig. 445

¹⁾ Swiss patent.

An advantage is, that oil does not flow through pipes, so that there is no danger of loose packing or contamination of oil in an unclean piping. A disadvantage is the small value of the specific thermal conductivity which, according to Hoffman, is 0.008 kcal/sec dm² for low velocities of water and 0.01 for higher velocities. Therefore larger cooling surfaces are required. Another disadvantage is the possibility of an incrustation of the pipes. This is avoided by the arrangement shown in Fig. 444 (Ganz, Budapest) where the closed circuit of the cooling water is filled by distilled water. In both cases an absolute tightness of the piping in the oil tank is required and this is the reason why some manufacturers have no confidence in this system.

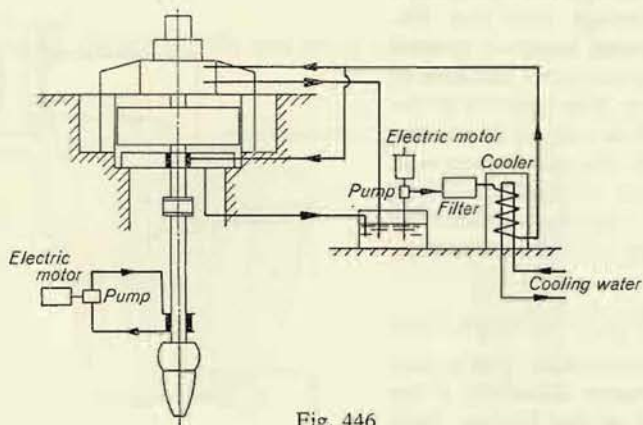


Fig. 446

3. Fig. 446 is the most widely used heat conducting arrangement. The heated oil flows from the oil tank to a cooler and therefrom it returns through a filter to the sliding surfaces. A simple alternative of this arrangement is shown in Fig. 447, where the cooler is located in streaming water. In a tubular cooler the water passes by gravitation (taken off the spiral) or it is pumped to a duplex filter which can be cleaned during operation. Pumps must be used if the head is not sufficient to overcome the resistance of the cooler. In the opposite case of very high head the use of head race water may not be economical.

Oil circulation is secured by circulating pumps or by a pump, formed in the thrust collar of the bearing. The latter arrangement (see Fig. 448) is practicable in the case of high operational speeds, so that the pressure created in the radial borings of the thrust collar is sufficiently high to overcome the resistance of the oil circuit. For a normally composed oil circuit (cooler, filter, piping, armatures) a pressure of 3 atm. g. should suffice to deliver the oil to the sliding surfaces. The pressure created in the borings of the thrust collar can be calculated from the following equation:

$$p = \frac{\gamma}{2g} (U_2^2 - U_1^2) 10^{-4}, \quad (339)$$

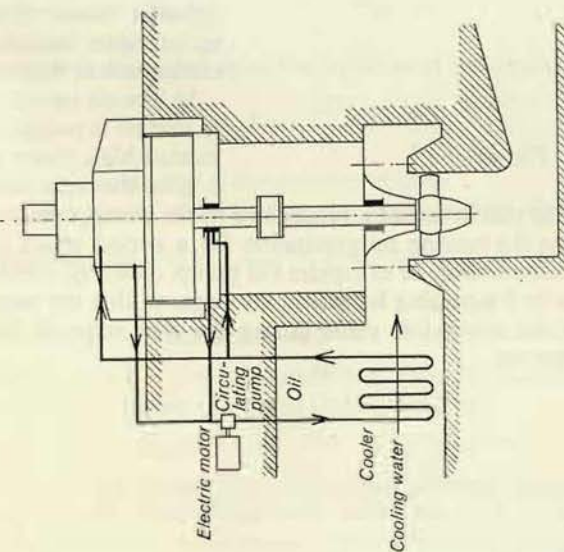


Fig. 447

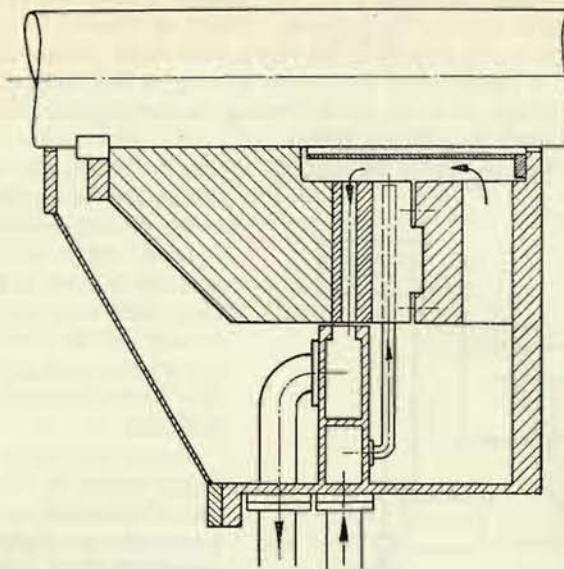


Fig. 448

where p is the pressure in atm. g., γ the specific weight of the oil in kg/m^3 and g acceleration due to gravity in m/sec^2 ; U_2 the peripheral velocity at the outlet of the pumping borings in m/sec , U_1 the same velocity at the inlet in m/sec . Volumetric efficiency of the pump formed in this way is very small (about 0.2), however, the great advantage is a guaranteed circulation as long, as the turbine remains in operation. Lubrication cannot break down. During the starting and closing periods the circulation is assisted by a starting pump.

With circulation pumps driven by electric motors we must bear in mind to

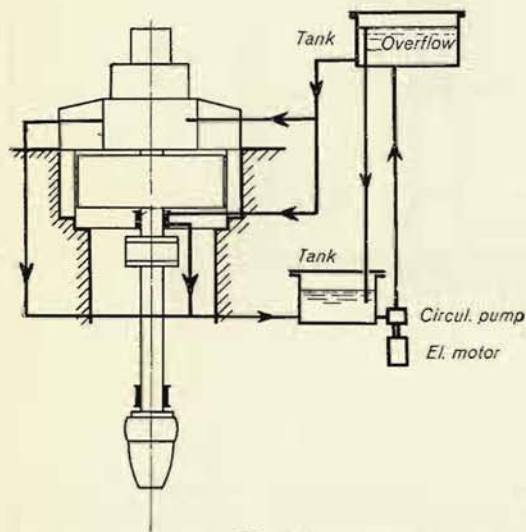


Fig. 449

tank is dimensioned so that in case of a breakdown of the pump, there is a sufficient supply of oil entering the bearing by gravitation for a period which is sufficient either to shut down the turbine or to repair the pump. (See Fig. 449.)

c) The oil charge in the bearing is sufficiently large, so that the temperature of oil will not exceed the admissible value during the time required for a normal closure of the turbine set.

ensure the oil circulation in the event of a breakdown of the current supply. The circulation must be ensured at least for the time necessary for a normal closure of the turbine. There are several methods by which the above condition can be fulfilled:

a) arrangement of a stand-by pump which is connected, in case of a shut down of the main pump, automatically by a flow controller. The driving motor of the stand-by pump has a different source of current: an accumulator battery, local generating unit or the exciter circuit.

b) The oil circuit is arranged so that oil is pumped into a tank located high above the bearing e. g. on the crane runway). This

C. CONDUITS

I. PIPES

1. Generally

Piping is used to carry the water to the turbines in cases of higher heads (above 10 m) or great distances of the reservoir from the power house.

For the approximately horizontal part of the conduit (Fig. 450) open canals (B) or flumes are used, for the strongly inclined part piping E must be used. Water from the open conduit passes into the pressure conduit through the surge tank G. The entire section of a pipe is filled with water. Pipes are made of wood, concrete, cast iron steel according to the pressure to which it is exposed.

The size of a pipe is determined by its cross section area F or diameter D (inner diameter), the wall thickness s and the length L .

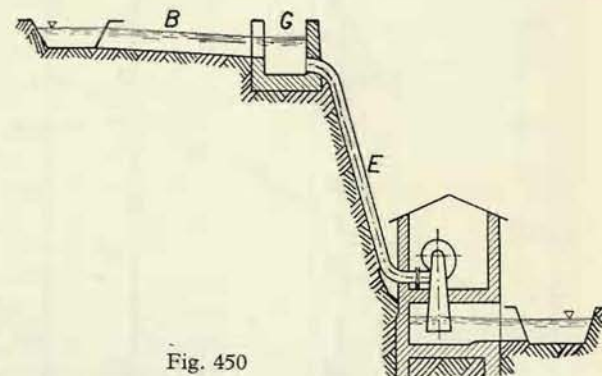


Fig. 450

The diameter is calculated from the equation of continuous flow:

$$F = \frac{\pi D^2}{4} = \frac{Q}{C},$$

where Q is the flow rate and C the velocity of flow.

Velocity C is selected according to the length of the pipe L and the head H .

For $\frac{L}{H}$ smaller than 1 to 2, $C_{\max} = 4$ to 3 m/sec.

$$= 2 \text{ to } 4 \quad = 3 \text{ to } 2.5 \text{ m/sec.}$$

$$= 5 \text{ and more} = 2 \text{ to } 1 \text{ m/sec.}$$

For diameters $D = 0.6 - 4$ m, heads less than 90 m and pipes shorter than 300 m, the velocity may be calculated from the relation

$$C_{\max} = 4.3 - 0.5 \cdot D. \quad (D \text{ in metres}).$$

With an increasing diameter the price of the pipe increases also. The cost of pipe forms a considerable part of the total investment cost of the system and it can influence the rentability of the whole project. Therefore with longer pipe conduits the pipe diameter must be established with regard to cost and the most economical pipe diameter must be selected. Higher velocity means smaller pipe diameter,

smaller first cost and smaller cost of depreciation. On the other hand smaller diameter entails higher losses and reduced output of the turbine. It is obvious that there exists a certain economical diameter (optimum) of the pipe. This economical diameter is influenced by the cost of material, cost of the current produced, cost of installation. These costs are not always the same, but, in spite of this, we can make the first estimate of an economical diameter on the basis of the chart in Fig. 451.¹⁾

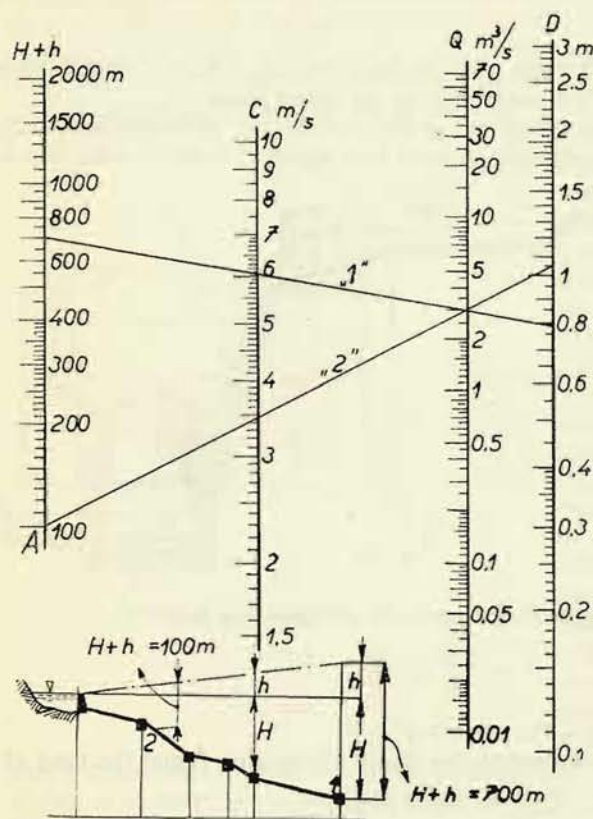


Fig. 451

eters with smaller diameters of pipes nearer to the turbine, so that no excessive wall thickness is obtained in the lower part of the pipe line. First we establish from the chart the diameter in the lower part, then in the upper part up to a head of 100 m, further gradation is made for sections according to economic considerations.

Loss of head by friction in the pipe must be established for calculating the econo-

mic diameter is influenced by the cost of material, cost of the current produced, cost of installation. These costs are not always the same, but, in spite of this, we can make the first estimate of an economical diameter on the basis of the chart in Fig. 451.¹⁾

The chart is used in the following way. First of all we draw the longitudinal section of the pipe into which we plot the line of the highest operational heads (the static head increased by the pressure rise caused by changes of flow conditions in the pipe – see Chapter II). If the maximum operational head is throughout less than 100 m, the pipe is made of a uniform diameter as we can see from the chart. The connecting line starts always from the point A. If the total head exceeds 100 m the pipe line is made of different diam-

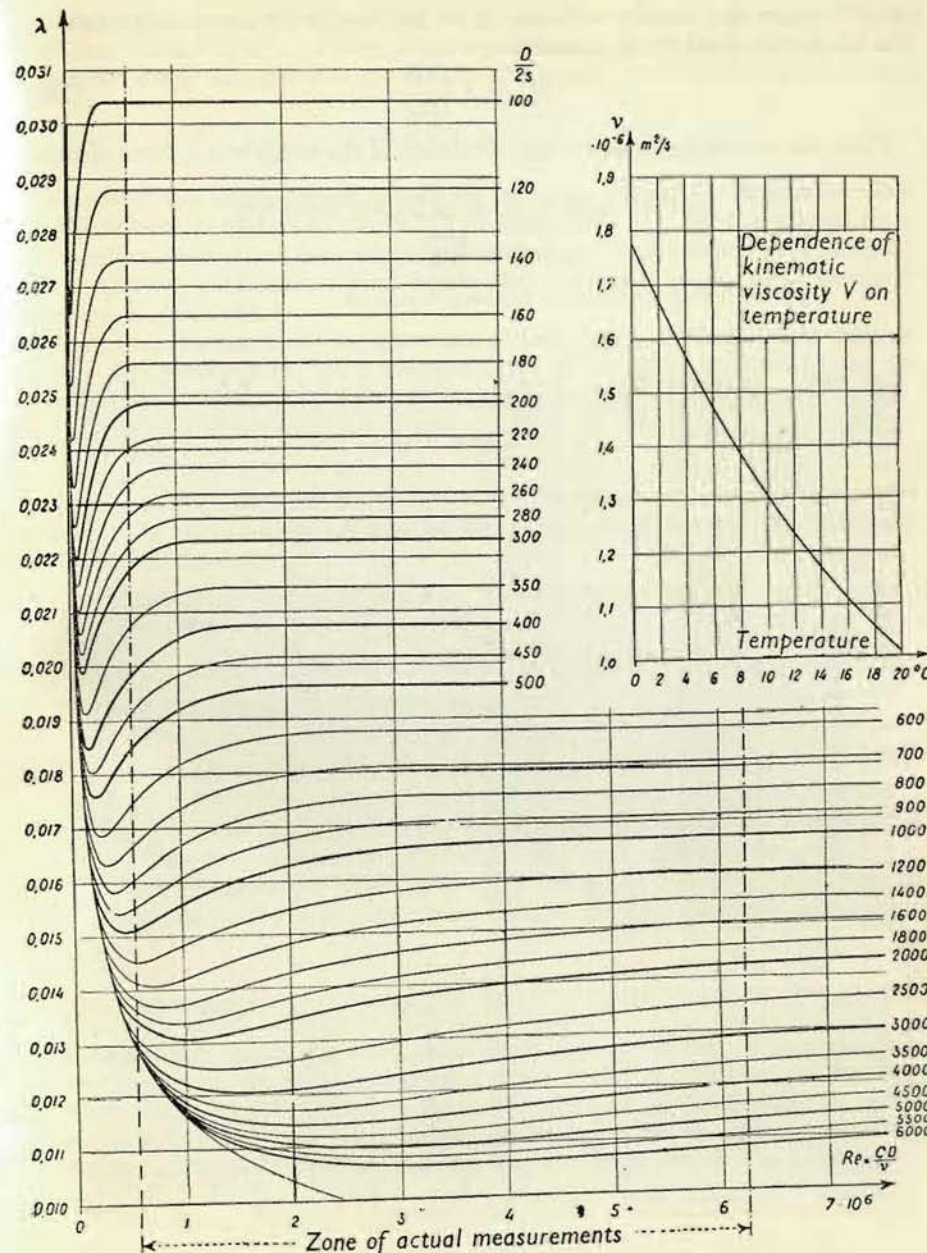


Fig. 452

¹⁾ See Bundschu: Wirtschaftlicher Entwurf von Turbinenrohrleitungen, Wasserkraft und Wasserwirtschaft (1931), p. 56.

mical diameter and also for establishing the net head for purposes of projection. The loss is calculated by the formula:

$$H_{z1} = \lambda \frac{LC^2}{D2g}. \quad (340)$$

There are several formulas for the calculation of the coefficient λ , some of them

SPECIFIC HEAD LOSS IN OLD CAST IRON PIPE

$$h_1 = 1.776 \frac{q^{1.965}}{d^{5.285}}$$

WATER TEMPERATURE 15°; h_1 in m/km, q in m³/s, d in m, u in m/s

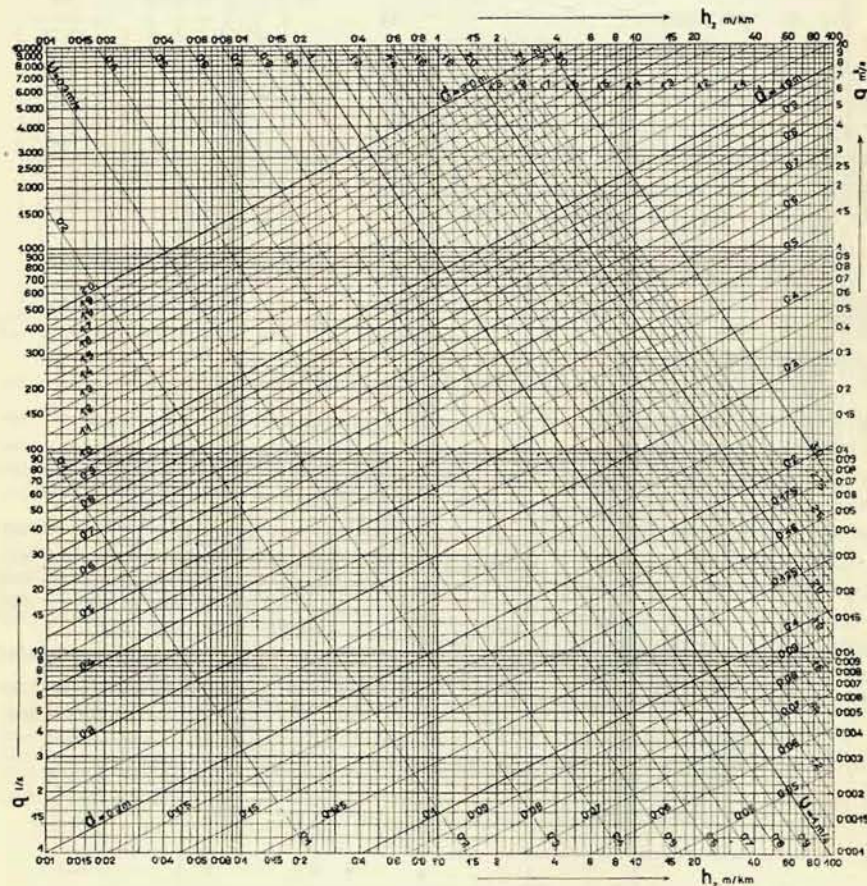


Fig. 453

are not used any more (Blasius, Mises, Biel, etc.). The following formula of Weisbach has been derived from numerous measurements carried out on pipes of a diameter range 27—490 mm and at velocities ranging from 0.0436 to 4.6 m/sec.

$$\lambda = 0.01439 + \frac{0.00947}{\sqrt{C}}. \quad (341)$$

Results of new measurements carried out on power-station pipe lines in Switzerland have been published by Hoeck.¹⁾ The Diagram in Fig. 452 is reprinted from this publication. It shows the values of the coefficient λ related to Reynolds numbers and roughness coefficients s . First information on friction losses can be obtained from the diagram 453.

Apart from friction losses we encounter in pipe lines also losses due to changes of flow direction (elbows, bends, tee-pieces, etc) which can be calculated from the equation:

$$H_{z2} = \xi \frac{C^2}{2g}. \quad (342)$$

The values ξ for standard connecting pieces are given in all text books on Hydraulics. The values ξ for bends (elbows) are given in the following table²⁾ (ϱ is the radius of curvature):

$\frac{D}{\varrho}$	0.2	0.5	0.8	1	1.2	1.5
ξ	0.132	0.145	0.205	0.294	0.436	0.805

The total loss of head in the pipe is then:

$$H_z = H_{z1} + H_{z2} = \sum \left(\lambda \frac{L}{D} \frac{C^2}{2g} \right) + \sum \left(\xi \frac{C^2}{2g} \right). \quad (343)$$

Losses of head in the pipe line are established according to the values given above. Now we can calculate the net head for which the turbine is designed.

For stress calculation we must know the location and method of anchorage of the pipe, because these factors determine some of the external forces acting upon the pipe.

2. Seating of Pipes

Pipes are laid upon the ground either freely (not buried), upon concrete piers above the ground or in open trenches and finally buried in trenches. The pipe line is firmly anchored at both ends — one end is anchored in the foundations of the intake and the other in the foundations of the power house. Apart from these, anchorages are installed at bends and also near the expansion joints of long straight

¹⁾ Hoeck: Druckverluste in Druckleitungen großer Kraftwerke, Leeman and Co. Zürich.

²⁾ According to Escher (Die Theorie der Wasserturbinen, Berlin, Springer, 1924).

sections. Pipes in these places are equipped with ring girders made of rolled sections, see Fig. 454. Axial forces acting upon pipes are taken up by the anchors. The pipe is axially fixed to the anchor blocks and, therefore, an expansion joint is mounted between two blocks. The expansion joint permits a dilatation of the pipe due to changes of temperature. These changes are rather great particularly in the case of unburied pipes. Between the anchor blocks the pipe is supported by concrete piers which take up reactions acting perpendicularly to the axis of the pipe and they

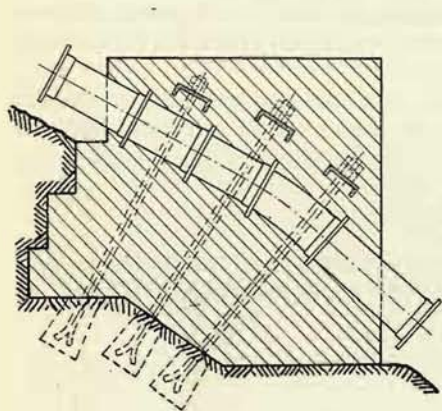


Fig. 454

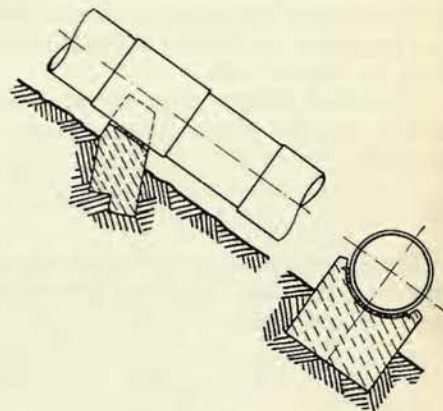


Fig. 455

permit shifting in axial direction. For a better shifting the surface of the pier is covered by sheet metal (Fig. 455). Pipes of large diameters are frequently seated on supports placed on rollers (Fig. 456).

Special attention must be paid to the upper end of the pipe line. As far as the head is concerned the thickness of the pipe wall can be very small. There exists the danger that due to the weight of water and own weight of the pipe the cross section could be deformed from a circular shape to an elliptical one. Such deformed pipes are very sensitive to pressure changes and they easily start to vibrate.¹⁾ The pipe is, therefore, reinforced by ring girders made of rolled sections which are used for fixing the pipes to the supports by frames placed on rollers and fixed against lifting by pendulum screws (Fig. 457).

Buried pipes have no expansion joints, because temperature changes are not great. Pipes are generally buried in soft ground. Danger of freezing is avoided even during shut downs (no flowing water) by burying the pipe to a depth of 1 to 1.5 m

¹⁾ For Calculations of stresses and deformations see Hruschka A: Druckrohrleitungen der Wasserkraftwerke, Wien-Berlin, Springer, 1929, p. 121—124.

See also Federhofer: Zur strengen Berechnung liegender weiter Rohre, Wasserkraft und Wasserwirtschaft, 1943, Heft 10, p. 237.

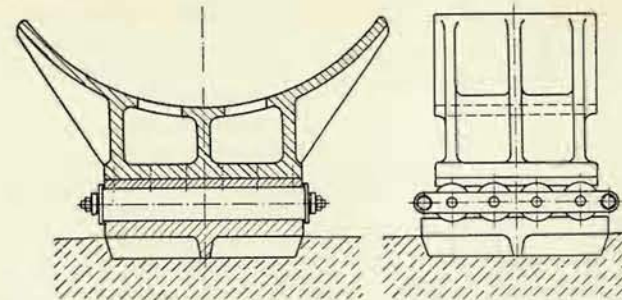


Fig. 456

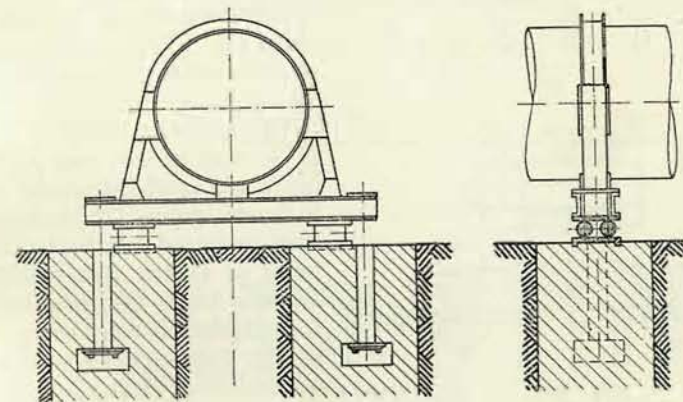


Fig. 457

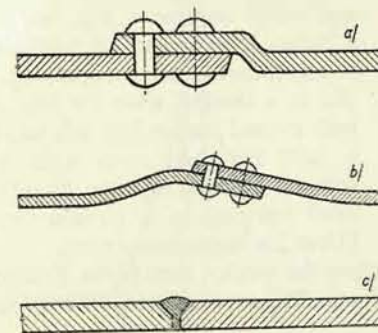


Fig. 458

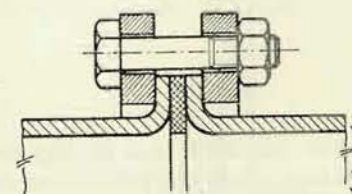


Fig. 459

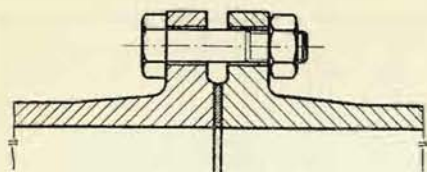


Fig. 460

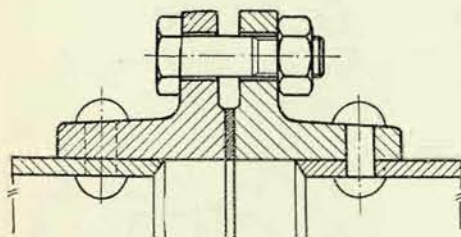


Fig. 461

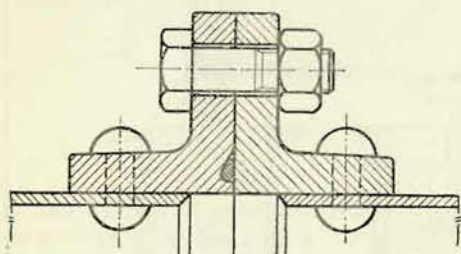


Fig. 462

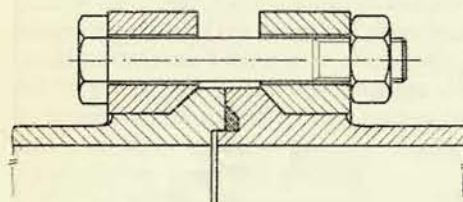


Fig. 463

Figs. 463—465 show joints for high pressures for welded steel pipes. Flanges are welded to one section and seated loose on the mating section, (465) or both flanges are loose (Fig. 463).

¹⁾ For the necessary calculations see Hruschka: Druckrohrleitungen der Wasserkraftwerke, Wien-Berlin, 1929, p. 125—128.

(position of the highest point of the pipe). The disadvantage of the buried pipe is, that no inspection and maintenance of coating is possible. The pipe is laid in its whole length upon a concrete base which is designed according to the nature of the soil. At both ends and in sharp bends the pipe is anchored in the same way as an over-ground pipe. At the upper end of the pipe line the buried pipe must be carefully checked against external pressure of the soil (large diameter, thin walls¹⁾).

Protection against corrosion is provided by a bituminous coat. Pipe sections laid in concrete are protected by a lime coating.

Pipes are manufactured in lengths of 3—4 m of cast iron pipes (small heads and small diameters) and of 10 m for steel pipes. The sections of pipes steel are joined together by riveted lap joints or electric butt-welded joints. Sections inside the power house have flanged joints. Riveted joints are shown in Fig. 458a and b, a welded joint is shown in Fig. 458c.

Fig. 459 illustrates a flanged joint with loose flanges for smaller heads and small diameters. Fig. 460 shows a flanged joint of cast iron sections with plain surfaces and flat packing. Fig. 461 is a flanged joint for steel pipes with riveted flanges. Fig. 462 illustrates a joint for steel pipes with riveted flanges. Packing is done by a rubber cord inserted in a circular groove. (Used for larger diameters).

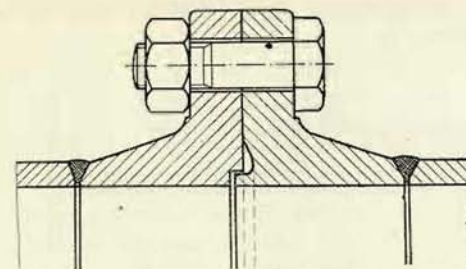


Fig. 464

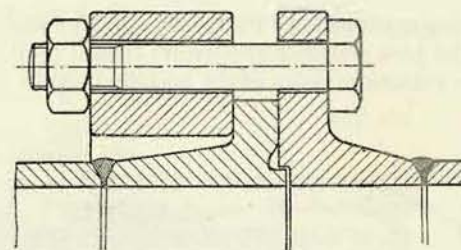


Fig. 465

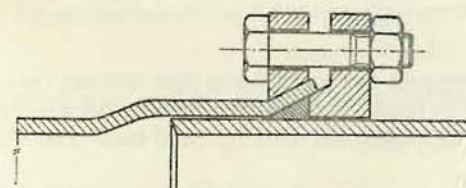


Fig. 466

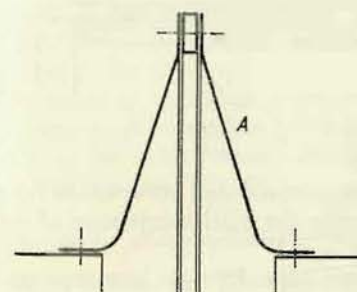


Fig. 467

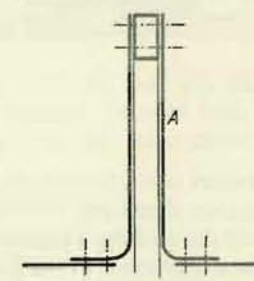


Fig. 468

Fig. 466 illustrates a spigot and cosket joint with loose flanges tightening the jointing ring. This joint is used for pressures up to 10 atm. g. provided, that no axial load is transmitted by the joint.

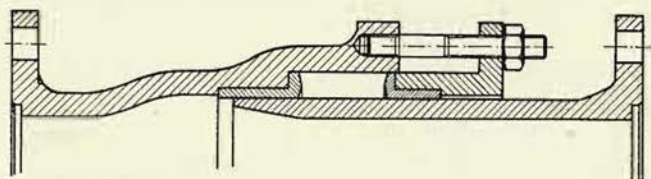


Fig. 469

Flange bolts are calculated for tensile stress by axial reactions (by the axial component of the pipe weight respectively) caused by the hydraulic pressure. Forces required for the compression of the packing must be added to these reactions. The

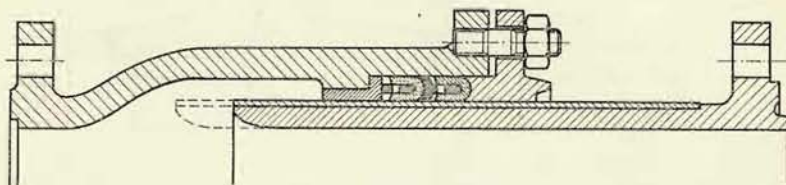


Fig. 470

maximum possible hydraulic pressure has to be taken into account (increase by water hammer see II). Admissible tensile stress of the bolts is 700 kg/cm². If the pipe section is equipped with an expansion joint no axial loads resulting from

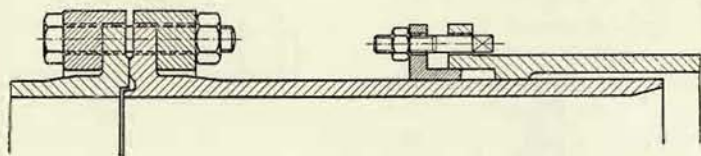


Fig. 471

water pressure occur (unless the diameter has been reduced between the flange and the expansion joint) and the joint carries only the axial component of the pipe weight and the packing compression forces.

All joints hitherto described are of the rigid type. Pipe sections exposed to the influence of temperature changes (freely laid pipe) must be connected between two supports by a flexible joint which permits an alteration of the pipe length, but simultaneously keeps the connection tight. This so called expansion joint is known

to be arranged in two basic types: the flexible joint and the slip joint. The relative shifting of two pipe sections connected by a flexible joint is made possible by inserting an elastic coupling *A* into the joint (Figs. 467 and 468). The coupling seals completely the gap between the pipe ends and permits the mutual movement of the pipe ends by its own elastic deformation.

In the case of a slip joint the gap between the pipe ends is sealed by hemp or leather mounted in a stuffing box. Corrosion of the sliding surface is prevented by bronze bushings.

Fig. 469 illustrates the design of a cast expansion joint with hemp packing. Fig. 470 shows a similar joint for higher pressures packed by leather cups. Fig. 471 is a welded expansion joint with leather cups.

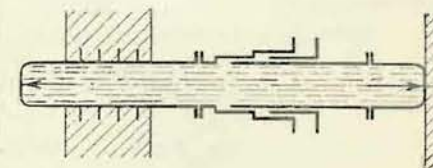


Fig. 472

Expansion joints are not used for buried pipes, as such pipe is not exposed to great extremes of temperature. Neither are expansion joints used in pipes located in the power house building, nor for short pipe sections. Let us calculate the stresses created in the wall of a pipe without expansion joint.

Temperature of the pipe is t °C; if we denote the coefficient of the thermal expansion as α , the pipe length at a temperature difference of Δt °C will increase by the value $\lambda = \pm \alpha \cdot \Delta t$. If the pipe cannot increase its length, a stress is created in the walls of the pipe which is determined by the above calculated elongation: $\sigma = E \cdot \lambda$ and after substituting for λ we may express the stress as:

$$\sigma = \pm E \alpha \Delta t.$$

By substituting for steel $E = 2,120,000$ kg/cm² and $\alpha = \frac{1}{85,000}$, we can write:

$$\sigma = \pm 25 \Delta t. \quad (344)$$

If the temperature of the pipe deviates by ± 20 °C from a temperature at which no stress is present in the pipe wall, the stress created by the temperature change amounts to ± 500 kg/cm² which is not very high. The foundations of the anchor block must carry, however, the significant reaction $R = f \cdot \sigma$, where f is the cross section area of the pipe wall.

When using an expansion joint we must bear in mind, that the axial forces acting upon the pipe must be taken up by the foundation, because both pipes are subjected to the water pressure which tries to tear open the joint (water pressure acts as upon a piston (Fig. 472)).

3. Calculation of the stability of anchor blocks

As stated before, the pipe line is anchored in blocks which take up mainly the axial forces, because the supporting piers between the blocks permit a longitudinal movement of the pipe and take up only forces perpendicular to the pipe axis.

An anchor block must take up the following forces (Fig. 473):

1. The component of the weight of pipe G acting in the center line of the pipe, i. e. its branch G_1 on the upstream side and G_2 on the downstream side of the anchor. If q_t is the weight of the pipe per linear metre and $L = L_1 + L_2$ the length of the pipe section supported by the anchor block, then

$$G = G_1 + G_2 = L_1 q_t + L_2 \cdot q_t = L \cdot q_t.$$

The components of these weights act in the center line of the pipe, if the re-

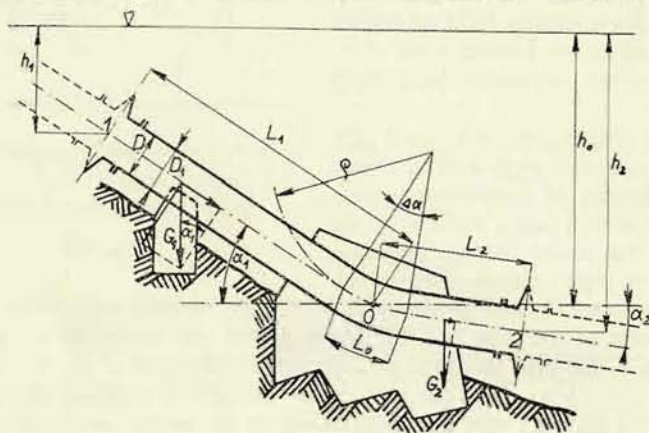


Fig. 473

spective slopes if the pipe are expressed by the angles α_1 and α_2 respectively, then the above components have the following values:

$$\text{acting in center line } \overline{0-1} \quad G'_1 = G_1 \cdot \sin \alpha_1$$

$$\text{acting in center line } \overline{0-2} \quad G'_2 = G_2 \cdot \sin \alpha_2$$

2. Weight of water V is composed of

$$\text{the weight } V_1 \text{ in the branch } L_1 \quad V_1 = 1000 \pi D^2 / 4 L_1$$

$$\text{the weight } V_2 \text{ in the branch } L_2 \quad V_2 = 1000 \pi D^2 / 4 L_2.$$

The components acting in the center line of the pipe are calculated similarly as the components of the pipe weight. We can write

$$V'_1 = V_1 \cdot \sin \alpha_1 \text{ and } V'_2 = V_2 \cdot \sin \alpha_2.$$

3. The hydrostatic water pressure acting in the end cross sections of the pipe in the expansion joints of an inner diameter D . In the upstream joint this force is $P'_1 = 1000 \frac{\pi D^2}{4} h_1$ and in the downstream cross section — $P'_2 = 1000 \frac{\pi D^2}{4} h_2$.

The latter force has a minus value because it acts against the direction of the flow.

Further axial forces act in the case of slip joints, i. e. the water pressure upon the annular parts of the joint of an outer diameter D_1 and the inner diameter D (equal the inner diameter of the pipe). In the upstream branch $\overline{1-0}$ this force amounts to

$$U'_1 = \frac{\pi}{4} (D_1^2 - D^2) h_1 \gamma \text{ acting in the direction of the flow, in the branch } \overline{0-2}:$$

$$- U'_2 = \frac{\pi}{4} (D_1^2 - D^2) h_2 \gamma \text{ acting in the opposite sense.}$$

4. The centrifugal force acting in the bend with a curvature radius and with angles of the end cross sections $\Delta\alpha = \alpha_1 - \alpha_2$. This force acts only during the flow of the water. At a velocity C the force can be calculated from the equation:

$$O = \frac{m \cdot C^2}{\rho}, \text{ where } m \text{ is the mass of water in the bend}$$

$$m = L_0 \frac{\pi D^2}{4} \frac{\gamma}{g} \text{ and for a length of the bend } L_0 = \pi \rho \frac{\Delta\alpha^\circ}{180^\circ}$$

$$O = \pi \rho \frac{\Delta\alpha^\circ}{180^\circ} \frac{\pi D^2}{4} \frac{\gamma}{g} \frac{C^2}{\rho}, \text{ and because } \frac{\pi D^2}{4} C = Q$$

and $\gamma = 1000 \text{ kg/m}^3$, we can write the final value of the force as:

$$O = \frac{\gamma}{g} Q C \pi \frac{\Delta\alpha^\circ}{180^\circ} \doteq 1.78 Q C \Delta\alpha^\circ.$$

5. Friction between water and pipe walls. In the branch $\overline{1-0}$ at a loss of head h_z per linear metre the total loss of head is $H_{z1} = L_1 \cdot h_z$ and the friction force is $T_1 = H_{z1} \gamma \frac{\pi D^2}{4}$ acting in the direction of the flow. Similarly for the branch $\overline{0-2}$, $H_{z2} = L_2 \cdot h_z$ and $T_2 = H_{z2} \gamma \frac{\pi D^2}{4}$, the direction of the flow.

6. Friction of the pipe upon the supporting piers is caused by the component perpendicular to the pipe axis. It is composed of the weight of pipe and that of the water and it is denoted as R_k . Coefficient of friction for pipe sliding upon concrete can be taken as 0.45 and for pipe upon sheet metal or cast supports as 0.2. The force in the direction of the pipe axis is then $T_r = f \cdot R_k$. This force calculated for the branch $\overline{1-0}$, where $R_{k1} = (G_1 + V_1) \cdot \cos \alpha_1$, is $\pm T_{r1} = f(G_1 + V_1) \cos \alpha_1 = -fL_1 \cdot \left(q_t + 1000 \frac{\pi D^2}{4} \right) \cos \alpha_1$. The sign $+$ applies to the expansion of the pipe and $-$ to its contraction.

For the downstream branch $\overline{0-2}$ $R_{k2} = (G_2 + V_2) \cdot \cos \alpha_2$ and the friction force $\mp T_{r2} = f(G_2 + V_2) \cdot \cos \alpha_2 = fL_2 \left(q_t + 1000 \frac{\pi D^2}{4} \right) \cos \alpha_2$. Here the sign $-$ applies to the expansion of the pipe and $+$ to its contraction.

These forces can be complemented by the effects of the pipe movements in the expansion joints (in both types). These forces are denoted as U_1 and U_2 . Their

sense of action is for U_1 : — for expansion and — for contraction and for U_2 — for expansion and + for contraction.

7. In pipes with a reduced inner diameter a further force appears which can be calculated from the following equation

$$P'' = 1000 \frac{\pi}{4} (D^2 - D_0^2) h,$$

where D_0 is the reduced diameter and h is the pressure head acting in the place of reduction. (Fig. 474).

All formulas have been derived after substituting the values in the technical units kg, m, sec.

The forces described act upon the anchor block by which they are taken up. Their magnitude and effect depends upon the type of pipe and upon its seating.

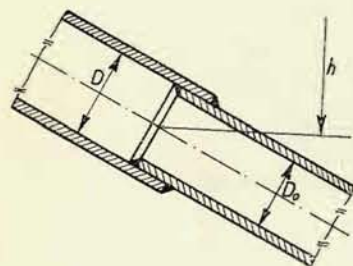


Fig. 474

The weight of the block foundation is denoted as Z . It takes up the resultant of all forces acting upon the block so, that the condition of stability is complied with, i. e. the resultant R_0 of all forces (including the weight Z) acting upon the block must act in a point inside the core of the loading surface of the foundation, so that this surface is exposed to compressive forces only.¹⁾

Stability is better with a steep resultant R_0 , i. e. the angle enclosed between this force and the vertical is as small, as possible. This position of the resultant R_0 can be obtained by arranging the branches L_2 so, that they are short compared with the branches L_1 .

When investigating the stability of the foundations we must consider normal conditions as well as extreme cases, i. e. no flowing water and increased pressure. Pipe expansion is calculated for the most unfavourable case.

Example. We consider forces acting upon the pipe according to Fig. 475. The resultant of forces acting upon the first (upstream branch) is expressed by the equation:

$$S_1 = G'_1 + V'_1 + P'_1 + T_1 \pm T_{r1} \pm U_1 + U'_1$$

and those acting in the center line of the downstream branch:

$$S_2 = G'_2 + V'_2 - P'_2 + T_2 \pm T_{r2} \pm U_2 + U'_2.$$

The resultant R of these forces (Fig. 475a) acts in point m . Let us first consider the case of water at rest. The forces S_1 and S_2 are somewhat reduced by the value of the components T_1 and T_2 . Apart from the resultant R also the weight Z acts

¹⁾ Timoshenko: Pružnost a pevnost, díl I. (Elasticity and Strength Part I.), Vědecko-technické vydavatelství, Prague 1952.

upon the foundation. Z acts in the centre of gravity t . The forces R and Z produce the resultant R_0 which acts upon the load carrying surface of the foundation ab . For a correct stability the resultant must act within the inner third of this surface, i. e. within the section $a'b'$.

This example shows, how the component S_2 became negative due to small values of G'_2 and V'_2 compared with the force $-P'_2$.

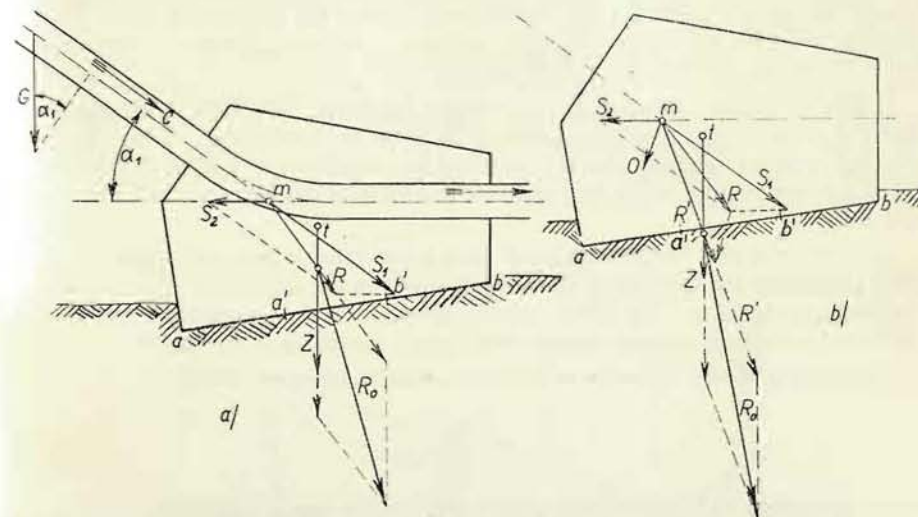


Fig. 475

By adding to R the centrifugal force O we receive the resultant R' (Fig. 475b). Forces R' and Z give the resultant R_0 which in this case is less inclined, than in the previous one. We can see, that the centrifugal force has a stabilizing effect. This influence can be felt, however, only in cases of higher velocities.

4. Calculation of wall thickness

The thickness s of the wall is determined by the stress conditions and is calculated from the admissible stress in the meridional cross section:

$$\frac{Dp_z}{2} = s \frac{K}{\mu}, \quad (345)$$

where $\frac{K}{\mu} = k_1$ is the safe stress in the unweakened cross section, μ is the safety factor and P_z is the pressure at which the pipe is tested.

When selecting the test pressure we must consider the pressure rise caused by the sudden closure of the gates by an automatic controller (See Water hammer in

Chapter II), whether the turbine has an installation to prevent such a pressure rise (see chapter on pressure regulators) and finally the reliability of this installation.

a) The turbine is not equipped with a pressure regulator. The pressure rise can occur rather frequently and we must take it into account as a maximum operational pressure. If we denote this pressure as p_{\max} , then the test pressure of the pipe is $p_z = 1.5 p_{\max} + 1 \text{ atm. g.}$ The stress caused by this pressure must be below the yield point, because no permanent deformation must remain after the test. The admissible stress is generally fixed at 0.6 to 0.8 times the yield point stress. (According to the Société Hydrotechnique de France the working pressure multiplied by 2.5 should be still below the yield point).¹⁾

b) The turbine is equipped with a pressure regulator. The latter is adjusted so that the pressure rise should not exceed 20 % of the static head. With a safely working pressure regulator this increase may be considered as the maximum operational pressure from which test pressure and stresses can be calculated as in the first case.

c) In the case of a turbine equipped with a non-reliable pressure regulator, we must determine the increase of pressure occurring in the event of a breakdown of the pressure regulator. This pressure is considered to be the test pressure provided, that it is higher than the test pressure established according to the case b).

The calculated wall thickness is then (according to equation (345)):

$$s = \frac{D p_z}{2 k_1},$$

where k_1 is 60 to 80 % of the yield point stress. In the case of a pipe line supplying several turbines, we may assume that a breakdown of all pressure regulators is not probable. Higher value is then taken as the admissible stress.

With regard to corrosion and the possibility of damage caused by external effects the actual wall thickness is somewhat greater, than the calculated one: $s_k = s + 1 \text{ to } 2 \text{ (or up to 2.5) mm}$ (the higher figures apply for larger diameters).

Wall thickness determined in this way is calculated with regard to stresses in the peripheral direction σ_θ ; the stress in axial direction is one half of this value:

$$\sigma_x = \frac{D p_z}{4 s}, \quad (346)$$

This holds good only in the event of the pipe being supported upon the whole length. In pipes seated on individual supports at a distance l (Fig. 476) this stress is increased by the influence of the bending moment caused by the load of the pipe weight and the weight of water in the respective section of the pipe.

Let us denote this load as q per linear centimeter. The maximum bending moment for a horizontally laid pipe (for an inclined pipe the same considera-

tions and formulas hold good, we calculate, however, the moment caused by the component perpendicular to the pipe axis $q' = q \cdot \cos \alpha$) is then calculated from:¹⁾

$$M_{\max} = \frac{q l^2}{12}. \quad (347)$$

This moment causes an additional stress in the cross section perpendicular to the pipe axis σ'_x . The maximum value $\sigma'_{x,\max}$ appears in the lowest (tension) and highest (compression) place of the mean cross section. It is distributed similarly (but with opposite signs) in the cross section above the support.

We can determine the value of this stress by assuming a linear course of the stresses throughout the cross

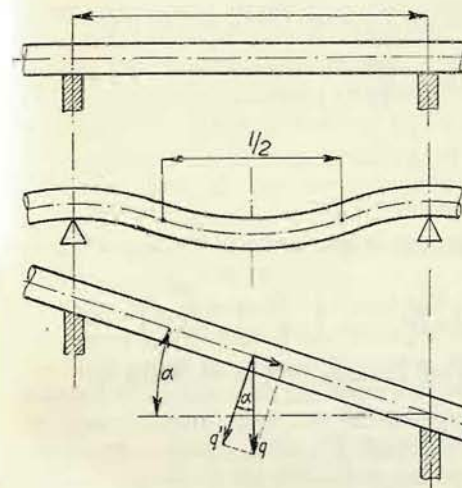


Fig. 476

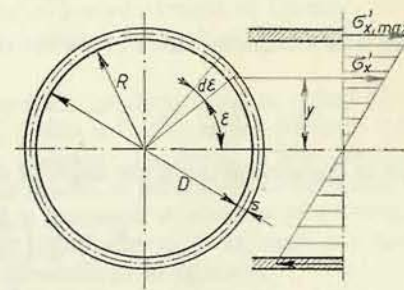


Fig. 477

section. By applying the annotations from Fig. 477, we can write:

$$\sigma'_x = \sigma'_{x,\max} \frac{y}{R} = \sigma'_{x,\max} \sin \varepsilon. \quad (348)$$

Further the following holds good:

$$dM = dF y \sigma'_x = R d\varepsilon s R \sin \varepsilon \cdot \sigma'_x$$

and after substituting from Equation (348):

$$dM = R^2 s \sin^2 \varepsilon d\varepsilon \sigma'_{x,\max},$$

so that:

$$M = R^2 s \sigma'_{x,\max} \int_0^{2\pi} \sin^2 \varepsilon d\varepsilon = R^2 s \pi \sigma'_{x,\max}, \quad (349)$$

¹⁾ See e. g. Černoch: Strojné technická příručka, díl I. (Engineering Manual, Part I.), 1947, p. 744.

for by using the relation

$$\cos \alpha = 1 - 2 \sin^2 \frac{\alpha}{2},$$

we can write:

$$\int_0^{2\pi} \sin^2 \varepsilon d\varepsilon = \frac{1}{2} \int_0^{2\pi} (1 - \cos 2\varepsilon) d\varepsilon = \frac{1}{2} \left[\varepsilon - \frac{\sin 2\varepsilon}{2} \right]_0^{2\pi} = \pi.$$

By substituting the value M from (347) into the Equation (349), we receive:

$$R^2 s \sigma'_{x, \max} \cdot \pi = \frac{ql^2}{12},$$

and from this the value of stress:

$$\sigma'_{x, \max} = \frac{ql^2}{3\pi s D^2}. \quad (350)$$

The total maximum stress above the support or in the center of the span is then:

$$\sigma_{\Sigma x} = \sigma_x + \sigma'_{x, \max} = \frac{Dp_z}{4s} + \frac{ql^2}{3\pi s D^2} = \frac{1}{s} \left(\frac{Dp_z}{4} + \frac{ql^2}{3\pi D^2} \right).$$

For an economical use of the material we shall put this stress as equalling k_1 :

$$\begin{aligned} k_1 &= \frac{1}{s} \left(\frac{Dp_z}{4} + \frac{ql^2}{3\pi D^2} \right), \\ sk_1 - \frac{Dp_z}{4} &= \frac{ql^2}{3\pi D^2}, \\ l &= D \sqrt{\left(sk_1 - \frac{Dp_z}{4} \right) \frac{3\pi}{q}}. \end{aligned} \quad (351)$$

We have thus determined the suitable distance between the supporting piers. At this distance the material of the pipe is subjected to equal stresses in both directions.

In the case of a riveted pipe we must calculate the joint according to the rules valid for riveting and with regard to the weakening of the cross section by the rivet holes. In welded pipes we take into consideration the weakening by welds.

5. Pipes for Extremely High Heads and Large Diameters

As stated before, the wall thickness is determined by the expression

$$s = \frac{Dp_z}{2k_1}.$$

where k_1 is a certain part of the strength of the material K which must remain

below the yield point also during the application of the test pressure, so that we can express it as a proportion of the yield point stress, i. e. $k_1 = \frac{P}{\mu_1}$.

The wall thickness can then be written as:

$$s = \frac{Dp_z \mu_1}{2P}.$$

It can be seen that for large diameters and high pressures the wall thickness is very great and the cost of the pipe very high. The calculated thickness can attain values so high, that it is impossible to produce the required pipe at all. The wall thickness can be reduced by selecting a material with higher yield point or by increasing the yield point of a given material by a suitable treatment.

The production of large pressure pipes has been greatly advanced in France where the material used for pipe production has been improved from steel of a strength 35 kg/mm², yield point 20 kg/mm² to a steel strength 48 kg/mm², yield point 28 kg/mm² and finally to a steel type having a strength of 54 kg/mm² and a yield point of 34 kg/mm².

Pipes have been produced by a special process producing the so called pipes "surpressé". The pipe is placed into a mould with a slightly larger diameter than the diameter of the pipe. The pipe is then "inflated" by water, so that the shell makes full contact with the inner wall of the mould. A permanent deformation of the material takes place and the yield point is increased. A material of a strength 54 kg/mm², deformed by 2 % increases the yield point to 40 kg/mm², and after a 5 % deformation the yield point has been increased to 50 kg/mm².

Bandaged pipes present a further progress in pipe production. Thin walled steel pipes are wound over by bandages made of steel strips having a yield point 60—105 kg/mm². The inner diameter of the bandages is slightly larger than the outer diameter of the pipe. The pipe is again "inflated" by water pressure, so that it firmly adheres to the bandage (these pipes are called autofretté).

Instead of steel bandages steel ropes have been used recently (pipes are called cablé). Yield point of the steel rope is 150 kg/mm². The process is the same as with the autofretté pipes. The ropes are made of tinned wires in order to prevent corrosion. Localized loads in supports reduce the strength of the ropes by 10 % as a maximum.

According to Ferrand¹⁾ the piping produced for the Vénéon power station has an inner diameter of 2 meters, wall thickness 7 mm, operational pressure 23 atm. g. It is bandaged by a 7 strand rope made of 3 mm wires with a bandage pitch 120 mm. During a pressure test only one rope burst at a pressure of 76.5 atm. g.

¹⁾ Ferrand: La conduite forcée unique pour hautes chutes à grand puissance, La Houille Blanche (1946), p. 245.

II. WATER HAMMER

1. Basic Relations and Calculation

Water hammer is a pressure rise occurring in a pipe, filled with a liquid flowing at the velocity C , during the closure of the pipe. Velocity of the liquid particles before the closing gate is reduced and their kinetic energy changes into pressure energy. Particles are compressed by the pressure, so that velocity reduction and pressure rise does not occur in the whole length of the pipe simultaneously, but proceeds as a pressure wave gradually from the closing gate towards the inlet.

No pressure rise occurs at the inlet, because here pressure is determined by the level head of the reservoir and particles which did not enter yet the pipe, have no kinetic energy. On the contrary, as the pressure rise decreases towards the reservoir, particles at the inlet soon begin to move backwards and this reverse movement spreads inside the pipe. Particles at the closing gate continue to move in the original direction until they are caught by the underpressure wave proceeding from the inlet. A reverse flow has been started and when the underpressure wave has reached the closing gate, all particles in the pipe acquired velocity again (directed oppositely) and

also kinetic energy. By changing pressure into kinetic energy a pressure drop occurs at the closing gate which proceeds gradually towards the inlet in the same way as the pressure rise proceeded before. This process is repeated. After completed closure the water in the pipe acquires an oscillating movement which is gradually damped down by the effect of friction.

During the compression of the liquid a simultaneous expansion of the pipe takes place: the liquid, therefore, appears to be more compressible, than it is actually. At this stage of our investigation we do not take into account the apparently increased compressibility and calculate with a liquid having a modulus of elasticity ε .

Under the influence of a pressure rise $\gamma \cdot h$ the liquid column x is shortened by Δx . The value of this compression is given by the equation:

$$\Delta x = h\gamma \frac{x}{\varepsilon}.$$

Let us consider an infinitely long horizontal pipe, where no return wave exists and where the total kinetic energy had been transformed into pressure. Under these circumstances the whole length of the column x is subjected to the same pressure h . (Fig. 478.) Pressure increase during compression is linear and, therefore,

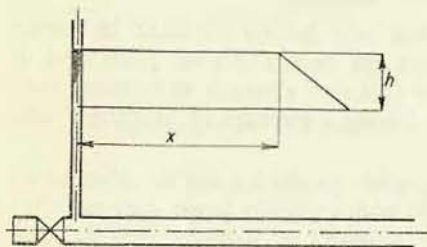


Fig. 478

compression work equals half the product of the pressure rise and final compression. Compression work is then given by the following equation:

$$A = \frac{1}{2} Fh\gamma\Delta x = \frac{1}{2} Fh^2\gamma^2 \frac{x}{\varepsilon},$$

where we considered that the work A is the product of the force $F \cdot h$ multiplied by the compression distance Δx .

This work has been produced by the kinetic energy of the column x . The energy E can be expressed as:

$$E = m \frac{C^2}{2} = Fx \frac{\gamma}{g} \frac{C^2}{2},$$

where C is the initial velocity of flow. By assuming that work A equals the energy E , we may write:

$$\frac{1}{2} Fh^2\gamma^2 \frac{x}{\varepsilon} = \frac{1}{2} Fx \frac{\gamma}{g} C^2.$$

From this equation we arrive at the value h , as:

$$h = C \sqrt{\frac{\varepsilon}{g\gamma}}.$$

According to Newton the velocity of sound in elastic bodies is given by the formula

$$a = \sqrt{\frac{g\varepsilon}{\gamma}}.$$

By dividing the last two expressions, we receive:

$$h = C \frac{a}{g}.$$

It can be seen, that in this case of the so called total impact, the pressure rise is determined by the product of sound velocity divided by gravity acceleration and of the original velocity of the water. For a partial velocity change ΔC , we may obviously write:

$$h = \frac{a}{g} \Delta C. \quad (352)$$

Sound velocity in pipes amounts to about 1000 m/sec, so that each unit (1 m/sec) of velocity destroyed produces a pressure rise of 100 metres, i. e. 10 atm. g. These are values which cannot be overlooked.

Relation (352) has been first derived by Zhukovski (also written as Joukovski) and is called, therefore, Zhukovski's (Joukovski) expression.¹⁾

¹⁾ Zhukovski N. E.: O gidravlicheskom udare v vodoprovodnikh trubakh, Trudy IV, russkovo vodoprovodnovo syezda, Odessa 1901.

The above considerations show, that this expression holds good for pipes, where closure is terminated before the return underpressure wave reaches the closing gate. The underpressure wave may be considered as being the original pressure wave reflected from the inlet cross section (see further). Pressure waves move with a velocity a and the time in which the wave returns to the closing gate (the so called time of one interval or critical time of the pipe) is given by the following formula:

$$T_{2L} = \frac{2L}{a}.$$

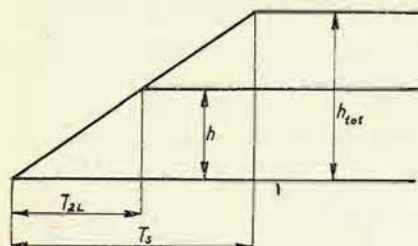


Fig. 479

Formula (352) holds good as long as the time of closure T_s is smaller than the time of one interval: $T_s < T_{2L}$.

Pressure increase is linear, if velocity decrease during closure is linear also. If $T_s > T_{2L}$ and the return wave reaches the closing gate before closure is terminated, i. e. before the total kinetic energy has been changed into pressure, the

increase of pressure is interrupted by the return wave. In case that $T_s \geq T_{2L}$ the maximum increase is $h_{tot} = \frac{a}{g} \cdot C$. It can be seen from Fig. 479, that this value will be now reduced to

$$h = h_{tot} \frac{T_{2L}}{T_s}$$

or we may write also:

$$h = \frac{a}{g} C \frac{2L}{aT_s} = 2 \frac{CL}{gT_s}.$$

This expression can be written in the form:

$$\frac{h}{H} = 2 \frac{T_l}{T_s}. \quad (353)$$

The left hand side of this equation represents the ratio of the pressure rise to the original head, i. e. "the relative increase of the pressure head" on the right hand side we have used the time constant

$$T_l = \frac{LC}{gH},$$

which is the starting time of the pipe, i. e. the time in which the pressure head H increases the velocity of the water from zero to the value C .

The mass of water contained in the pipe is $m = \frac{L \cdot F \cdot \gamma}{g}$, the force which accelerates this mass is $P = F \cdot H \cdot \gamma$, where F is the cross section area of the pipe

and H the normal head. The acceleration of water caused by the head H is then:

$$a = \frac{P}{m} = \frac{gH}{L}.$$

The time required to bring the water by this acceleration from a resting state to the velocity C is

$$T_l = \frac{C}{a} = \frac{LC}{gH}.$$

In pipes with different cross sections the velocity C is different also. We can write analogically:

$$T_l = \frac{\sum_1^m L_n C_n}{gH}, \quad (354)$$

where L_n are the lengths of pipe sections with a constant cross sections and C_n is the respective velocity in these sections.

Expression (353) is the Michaud formula which is in accordance with practical experience and with the more exact relations of Allievi (see further) as long as $2 \cdot \frac{L \cdot C_0}{g \cdot T_s \cdot H_0} < 2.2$, where the suffix o denotes operational values – before closure.

The expression holds good for closure and opening, in the latter case h denotes the pressure drop. The constant 2.2 is applied instead of the constant 2 in expression (353), because the velocity change is not linear.

Hitherto we have considered a horizontal pipe; if the pipe is not horizontal superposition of pressures applies.

Allievi¹⁾ has described the phenomenon of water hammer more exactly and proved that the velocity a at which the pressure wave moves, is given by the formula:

$$a = \sqrt{\frac{\frac{g}{\gamma}}{\frac{1}{\varepsilon} + \frac{1}{E} \frac{D}{s}}} = \sqrt{\frac{9900}{48.3 + k \frac{D}{s}}}, \quad (355)$$

where $\varepsilon = 2.07 \cdot 10^8$ is the modulus of elasticity of water in kg/m².

$E = 2 \cdot 10^{10}$ is the modulus of elasticity of steel

$1 \cdot 10^{10}$ the modulus of elasticity of cast iron,

$\gamma = 1000$ is the specific weight of water in kg/m³,

D, s = pipe diameter and wall thickness in m,

$k = \frac{10^{10}}{E} = 0.5$ for steel, and 1 for cast iron.

¹⁾ Allievi, Dubs, Battaillard: Allgemeine Theorie über die veränderliche Bewegung des Wassers in Rohrleitungen, Springer.

a = is the velocity in m/sec. The average value is $a = 1000$ m/sec. If axial deformations are prevented, we may write according to Thoma:

$$\frac{1}{a^2} = \frac{\gamma}{g} \left(\frac{1}{\varepsilon} + \frac{2R}{s} \frac{m^2 - 1}{Em} \right),$$

where m is Poisson's constant of the material of the pipe.¹⁾

Allievi investigates further the constant flow suddenly stopped by closure. By applying to an elementary particle of the flow the rule that mass multiplied by acceleration equals force, we may write:

$$\underbrace{\frac{R^2 \pi dx \gamma}{g}}_{\text{mass of the particle}} \underbrace{\frac{\partial}{\partial t} \left(C - \frac{\partial C}{\partial x} dx \right)}_{\text{acceleration of the moving particle}} = R^2 \pi \underbrace{\left(p + \frac{\partial p}{\partial x} dx \right)}_{\text{pressure upon farther cross section}} - R^2 \pi \underbrace{p}_{\text{pressure upon nearer cross section (to closing gate)}}$$

It is assumed that velocity C decreases and pressure p rises with an increasing x . It follows:

$$\frac{R^2 \pi dx \gamma}{g} \left(\frac{\partial C}{\partial t} - \frac{\partial C}{\partial x} \frac{\partial x}{\partial t} - \frac{\partial^2 C}{\partial x^2} \frac{\partial x}{\partial t} dx \right) = R^2 \pi \left(p + \frac{\partial p}{\partial x} dx \right) - R^2 \pi p.$$

If we neglect $\frac{\partial^2 C}{\partial x^2} \frac{\partial x}{\partial t} dx$, and because $\frac{\partial x}{\partial t} = C$,

it follows:

$$\frac{R^2 \pi dx \gamma}{g} \left(\frac{\partial C}{\partial t} - C \frac{\partial C}{\partial x} \right) = R^2 \pi \left(p + \frac{\partial p}{\partial x} dx \right) - R^2 \pi p$$

$$\frac{\gamma}{g} \left(\frac{\partial C}{\partial t} - C \frac{\partial C}{\partial x} \right) = \frac{\partial p}{\partial x}. \quad (356)$$

The second equation can be derived by assuming that the shortening of the elementary column dx is caused by the compression of the liquid and by the expansion of the pipe due to the pressure rise and adding both values together.

The shortening of the elementary column dx caused by the compression of the liquid, is:

$$\delta_1 = \frac{dx}{\varepsilon} \frac{\partial p}{\partial t} dt, \quad (357)$$

where ε is the modulus of elasticity of the liquid.

The expansion of the pipe diameter is expressed as

$$\varrho = \frac{R^2}{E} \frac{p}{s},$$

¹⁾ Thoma: Zur Theorie des Wasserstosses in Rohrleitungen, Zeitschrift für das gesamte Turbinenwesen (1918), p. 293.

because

$$\varrho = \frac{R}{E} \sigma \quad \text{and} \quad \sigma = \frac{pD}{2s} = \frac{pR}{s},$$

where σ is the peripheral stress in the pipe wall of a thickness s .

At a change of pressure ∂p in time dt the radius is changed by:

$$\partial \varrho = \frac{R^2}{Es} \frac{\partial p}{\partial t} dt. \quad (358)$$

If at this change of diameter the volume of the liquid particle remains constant, it follows:

$$\pi D \partial \varrho dx = R^2 \pi \delta_2,$$

where δ_2 is the shortening of the column dx caused by the expansion of the pipe.

$$\delta_2 = \frac{D \partial \varrho dx}{R^2}$$

and substituting for $\partial \varrho$ we arrive at:

$$\delta_2 = \frac{dx}{E} \frac{D}{s} \frac{\partial p}{\partial t} dt.$$

Velocity at both faces of the elements must differ by the sum of both changes $\delta_1 + \delta_2$ (because we have calculated the changes of length occurring in time dt). This can be expressed by the following equation:

$$-\left(C - \frac{\partial C}{\partial x} dx \right) dt + C dt = \delta_1 + \delta_2.$$

and it follows:

$$dx \frac{\partial C}{\partial x} dt = \delta_1 + \delta_2.$$

By substituting for the values δ_1 and δ_2 (contraction of the water column) we receive:

$$dx \frac{\partial C}{\partial x} dt = \frac{dx}{\varepsilon} \frac{\partial p}{\partial t} dt + \frac{dx}{E} \frac{D}{s} \frac{\partial p}{\partial t} dt$$

and subsequently

$$\frac{\partial C}{\partial x} = \left(\frac{1}{\varepsilon} + \frac{1}{E} \frac{D}{s} \right) \frac{\partial p}{\partial t}. \quad (359)$$

Let us substitute $\frac{\gamma}{g} \left(\frac{1}{\varepsilon} + \frac{1}{E} \frac{D}{s} \right) = \frac{1}{a^2}$, where a , as we shall see further on, is the velocity of the pressure wave.

Let us further denote as y the pressure in metres of the liquid column which equals the original head H increased by the pressure rise h (Fig. 480). We may write

$$\frac{p}{\gamma} = H + h = y,$$

and also

$$\frac{\partial p}{\partial x} = \gamma \frac{\partial y}{\partial x} \quad \frac{\partial p}{\partial t} = \gamma \frac{\partial y}{\partial t},$$

The Equation (356) may be written in the following form:

$$\frac{\partial C}{\partial t} - C \frac{\partial C}{\partial x} = g \frac{\partial y}{\partial x}. \quad (360)$$

With the same substitution from Equation (359) we arrive at:

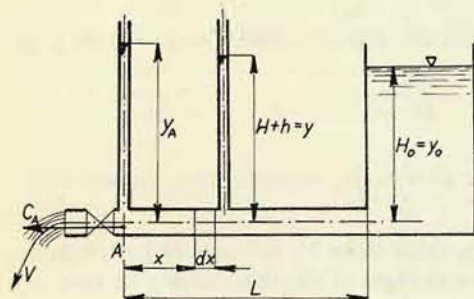


Fig. 480

$$\frac{\partial C}{\partial x} = \left(\frac{1}{\varepsilon} + \frac{1}{E} \frac{D}{s} \right) \gamma \frac{\partial y}{\partial t},$$

$$\frac{\partial C}{\partial x} = \frac{\gamma}{g} \left(\frac{1}{\varepsilon} + \frac{1}{E} \frac{D}{s} \right) \frac{g}{\gamma} \frac{\partial y}{\partial t},$$

and by using the relation for the velocity a we can write:

$$\frac{\partial C}{\partial x} = \frac{g}{a^2} \frac{\partial y}{\partial t}.$$

Now we have received two basic equations:

$$\begin{aligned}\frac{\partial C}{\partial t} - C \frac{\partial C}{\partial x} &= g \frac{\partial y}{\partial x} \\ \frac{\partial C}{\partial x} &= \frac{g}{a^2} \frac{\partial y}{\partial t}.\end{aligned}\quad (361)$$

By deriving these equations we have neglected the pressure loss caused by the friction of water in the pipe. However, this loss need not to be taken into account particularly in the case of rapid changes. Equations (361) cannot be integrated, on the other hand the flow velocity C is small, compared with the velocity of pressure distribution a , so that we may neglect the term $C \frac{\partial C}{\partial x}$, because

$$\frac{\partial C}{\partial t} - C \frac{\partial C}{\partial x} = \frac{\partial C}{\partial t} - C \frac{\partial C}{a \partial t} = \frac{\partial C}{\partial t} \left(1 - \frac{C}{a}\right) = \frac{\partial C}{\partial t}.$$

Thus we arrive at the equations

$$\frac{\partial C}{\partial t} = g \frac{\partial y}{\partial x} \quad (362)$$

Now let us imagine that an observer moves in the direction $+x$ along the pipe

at a velocity a . Then we may write $x = a \cdot t + \text{const.}$ and also $\partial x = a \cdot \partial t$. By putting these expressions into the second Equation (362), we receive:

$$\frac{\partial C}{\partial t} = \frac{g \partial y}{a \partial x},$$

which means that the second equation has been transformed into the first one. We can further re-write it into the form:

$$\frac{\partial C}{\partial t} = \frac{g}{a^2} \frac{\partial y}{\partial t},$$

and we see, that by the above substitution the equation has been transformed into a relation which is independent upon time. It describes a stationary flow and the above mentioned observer conceives a constant pressure rise. The velocity a , at which he travelled along the pipe, is equal to the velocity at which the pressure wave moves in the pipe. This velocity is expressed by the relations (355).

It can be seen, that the relation $x = a \cdot t + \text{const.}$ lends a constant value to the function $y = f(x, t)$. Therefore y must be a function of the expression $a \cdot t - x$ or of the expression $t - \frac{x}{a}$. Equations (362) are, therefore, complied with by the relations

$$y = y_0 + F\left(t - \frac{x}{a}\right),$$

$$C = C_0 - \frac{g}{a} F\left(t - \frac{x}{a}\right),$$

where the suffix o is attached to values before the pressure rise, i. e. to those valid before the process of closure had started. As we did not attach any condition concerning the sense of the velocity a , the relations will be complied with, as far as the reflected wave is concerned, also for a wave motion in the direction $-x$.

In the case of the reflected wave a pressure drop occurs and therefore the sign - appears in the first equation

$$y = y_0 - f\left(t + \frac{x}{a}\right),$$

$$C = C_0 - \frac{g}{a} f\left(t + \frac{x}{a}\right),$$

The common integral of the Equations (362) is the sum of partial integrals. It reads:

$$\begin{aligned} y &= y_0 + F - f, \\ C &= C_0 - \frac{g}{a}(F + f), \end{aligned} \quad (363)$$

In the above Equations we have omitted, for simplicity, the arguments at the denotations of the functions.

According to Equation (363) pressure and velocity are determined by two systems of waves which move in opposite directions and are added together. The second system f is the wave reflected from the upstream end of the pipe. Both functions F and f depend upon the limiting conditions at both ends of the pipe, i. e. upon the method of closure and upon the method of the reflection at the inlet respectively.

Allievi calls a water hammer at which no reflection of the pressure wave occurs – i. e. the case of infinitely long pipe or the case where the closure time $T_s < \frac{2L}{a}$ – a direct water hammer. Let us determine for this case the functions F and f from the limit conditions. As far as function f is concerned we can state immediately, that it is non-existent, because there is no reflection of the pressure wave and no reverse sweep of the water hammer.

Let us denote (Fig. 480) C_A the flow velocity in cross section A (for $x = 0$), V the outlet velocity at the gate and y_A the pressure head in cross section A . As we consider an efflux from the gate as a free jet, the following limit condition holds good:

$$V = \sqrt{2g \left(y_A + \frac{C_A^2}{2g} \right)} \quad \text{or} \quad V^2 - C_A^2 = 2gy_A.$$

The state of equilibrium before closure can be described by the equation $V_0^2 - C_{A0}^2 = 2 \cdot g \cdot y_0$. During closure the velocity C_A changes with time. This can be expressed generally as $C_A = V \cdot \psi(t)$; for $t = 0$, $C_0 = C_{A0} = V \cdot \psi(0)$.

During closure velocity decreases and pressure rises before the gate. This disturbance spreads only in one direction. As the reflected wave does not return to the gate before maximum pressure is attained, we are presented here with a direct function $F\left(t - \frac{x}{a}\right)$ and therefore the following holds good:

$$y = y_0 + F\left(t - \frac{x}{a}\right),$$

$$C = C_0 - \frac{g}{a} F\left(t - \frac{x}{a}\right).$$

By elimination of the unknown function F we receive:

$$y - y_0 = F\left(t - \frac{x}{a}\right) = -\frac{a}{g} (C - C_0)$$

or we can write also

$$h = y - y_0 = \frac{a}{g} (C_0 - C).$$

This relation is identical with that obtained directly at the beginning of this expression (352).

Let us consider now the case when the reflected pressure wave – indirect water

hammer – returns to the gate before the closure is terminated, i. e. before the maximum pressure has been attained.

For the first period, i. e. up to the moment at which the pressure waves reaches the inlet cross section, only the first function F holds good in Equations (363). The duration of this period is $T_L = \frac{L}{a}$. In accordance with the relation $y = y_0 + F$ pressure in the inlet cross section then should rise; however, this is not possible, because the pressure in this place is determined by the free level of the reservoir. Therefore the Equation (363) must contain an additional function, so that:

$$y = y_0 + F - f$$

and for the inlet cross section with the abscissa $x = L$, there must be $F = f$, because $y_B = Y_{B0}$. This means that a reflected wave of the same value as the original wave, is formed, but with an opposite sign (the opposite sign has been introduced in the equations). The reflected wave is diagrammatically illustrated in Fig. 481.

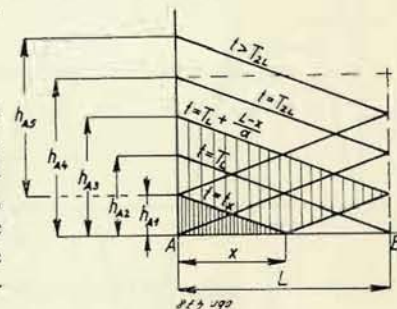


Fig. 481

In Fig. 481 the movement of the pressure wave from the gate to the inlet is clearly illustrated. In a time $t = t_x$ the disturbance reaches a place with the abscissa x , and the pressure rise at the gate is h_{A1} . In a time $t = T_L = \frac{L}{a}$ the disturbance reaches the inlet and the pressure rise at the gate is h_{A2} . At this moment the pressure wave is reflected and, in a time $t = T_L + \frac{L-x}{a}$ the reflected wave arrives into x ; pressure rise at the gate still increases and attains the value h_{A3} . The pressure rise caused by the reflected wave must be deducted from that caused by the original wave in all places through which the reflected wave has passed. The shaded portion of the picture shows the actual pressure increase along the whole pipe at the moment considered. In place B (inlet) no pressure rise exists. In time $t = T_{2L}$ the pressure rise at the gate reaches its maximum value h_{A4} ; it cannot increase any more, because the value of the reflected wave rises in the same way as that of the primary wave ($h_{A5} = h_{A4}$). After closure has been terminated, the cause of the primary wave formation disappears. However, the reflected wave still exists and causes a pressure drop. Pressure disturbances are present at both ends of the pipe and a periodic oscillation of pressure appears throughout the whole pipe length. This oscillation is gradually damped down by the friction between water and pipe walls. Fig. 482 shows the whole process in the form of the developed time curve.¹⁾

¹⁾ Mostkov, Bashkirov: Razchoty gidravlicheskovo udara, Gosudarstvennoye energeticheskoye izdatelstvo, Moscow-Leningrad, 1952.

We can see in Fig. 481 that the value of the reflected wave in an arbitrarily selected cross section x equals the value which the primary wave attained in the same cross section a certain time ago. This time is $\left(t - 2\frac{L-x}{a}\right)$, i. e. minus the time required by the primary wave to travel from x to the inlet and that required by the reflected wave to travel from the inlet to x . Thus we can write the following relation:

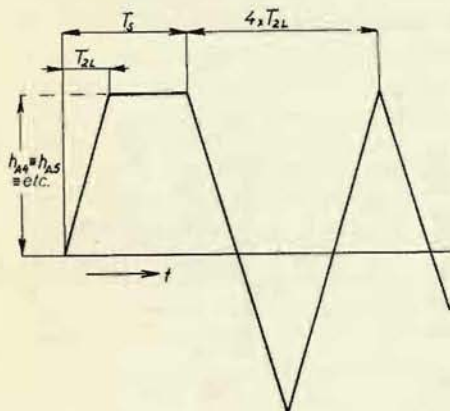


Fig. 482

$$\begin{aligned} f\left(t + \frac{x}{a}\right) &= \\ &= F\left(t - 2\frac{L-x}{a} - \frac{x}{a}\right) = \\ &= F\left(t - \frac{2L-x}{a}\right) \end{aligned}$$

or

$$f\left(t + \frac{x}{a}\right) = F\left(\Phi - \frac{x}{a}\right),$$

after having introduced the denotation $\Phi = t - 2\frac{L-x}{a}$. Equations (363) may be written in the following form:

$$y = y_0 + F\left(t - \frac{x}{a}\right) - F\left(\Phi - \frac{x}{a}\right), \quad (364)$$

$$C = C_0 - \frac{g}{a} \left[F\left(t - \frac{x}{a}\right) + F\left(\Phi - \frac{x}{a}\right) \right].$$

By this procedure we have eliminated by application of the limit condition ($y_B = y_{B0}$), the function f , so that only one unknown function F remains in the equations. This function must be determined from the limit condition valid for the efflux end of the pipe.

In order to determine the maximum value of the pressure rise, Allievi has developed the functions in Equations (364) into Taylor's series as follows:

$$F\left(t - \frac{x}{a}\right) = F(t) - \frac{x}{a \cdot 1!} F'(t) + \sum_1,$$

$$F\left(\Phi - \frac{x}{a}\right) = F\left(t - \frac{2L-x}{a}\right) = F(t) - \frac{2L-x}{a \cdot 1!} F'(t) + \sum_2.$$

If $F'(t) = \text{const.}$, the higher derivations of the series contained in the sums \sum_1 ,

and \sum_2 equal zero. This first derivation will be of constant value if the efflux velocity will be reduced uniformly, i. e. the gate will be closed proportionately.¹⁾ If we assume that closure proceeds in this way, Equations (364) are simplified as follows:

$$y - y_0 = 2 \frac{L-x}{a} F'(t), \quad (365)$$

$$C - C_0 = -2 \frac{g}{a} \left[F(t) - \frac{L}{a} F'(t) \right].$$

By neglecting the velocity head in the full cross section before the gate, we may write the limit condition for the efflux as:

$$V^2 = 2g y_A,$$

and from this it follows:

$$2V \frac{\partial V}{\partial t} = 2g \frac{\partial y_A}{\partial t}. \quad (366)$$

As $F'(t) = \text{const.}$, it follows from the first Equation (365) that $\frac{\partial y}{\partial t} = 0$, and for an outlet cross section of the abscissa $x = 0$ it follows also, that $\frac{\partial y_A}{\partial t} = 0$. This means that pressure rise will stop at the moment, when Equation (364) becomes valid and this occurs at the moment, when the reflected wave arrives at the gate.

By inserting into Equation (366) the condition $\frac{\partial y_A}{\partial t} = 0$ and the relation $C_A = V \cdot \psi(t)$ or in another form $V = \frac{C_A}{\psi(t)}$, we may write:

$$2 \frac{C_A}{\psi(t)} \frac{\psi(t)}{\psi^2(t)} \frac{\partial C_A}{\partial t} - C_A \psi'(t) = 0$$

and also

$$C_A \left[\psi(t) \frac{\partial C_A}{\partial t} - C_A \cdot \psi'(t) \right] = 0$$

or

$$\frac{\partial C_A}{\partial t} = C_A \frac{\psi'(t)}{\psi(t)} = \psi'(t) V,$$

and finally

$$\frac{\partial C_A}{\partial t} = \psi'(t) \sqrt{2g y_A}. \quad (367)$$

¹⁾ Allievi, Dubs, Battaillard, p. 64.

By differentiating the second of the Equations (365) and relating it to the outlet cross section ($x = 0$) and with regard to $F'(t) = \text{const.}$, we receive:

$$\frac{\partial C_A}{\partial t} = -\frac{2g}{a} F'(t)$$

and by comparing this Equation (367), it follows:

$$F'(t) = -\frac{a}{2g} \psi'(t) \sqrt{2gy_A},$$

$$F'(t) = -\frac{a}{2} \psi'(t) \sqrt{\frac{2y_A}{g}}.$$

From the limiting condition valid for the outlet we have thus received the first derivation of the unknown function F which we require for the Equation (365). By inserting this value into the first Equation (365) applied for $x = 0$, it follows:

$$y_A = y_0 - L\psi'(t) \sqrt{\frac{2y_A}{g}}, \quad (368)$$

which, for the investigated y_A , is an equation of the second order which must be further modified.

If, according to the former assumption, the closure of the gate is linear and the time of closure is denoted again T_s , it follows (Fig. 483):

$$\psi'(t) = -\frac{1}{T_s} \psi(0),$$

and because $\psi(0) = \frac{C_0}{V_0}$ it further follows:

$$\psi'(t) = -\frac{1}{T_s} \frac{C_0}{V_0}.$$

Before closure begins, the following relation holds good: $V_0 = \sqrt{2gy_0}$, so that we may write

$$\psi'(t) = -\frac{1}{T_s} \frac{C_0}{\sqrt{2gy_0}}.$$

By inserting this value into Equation (368) it follows:

$$y_A = y_0 + \frac{LC_0}{T_s \sqrt{2gy_0}} \sqrt{\frac{2y_A}{g}},$$

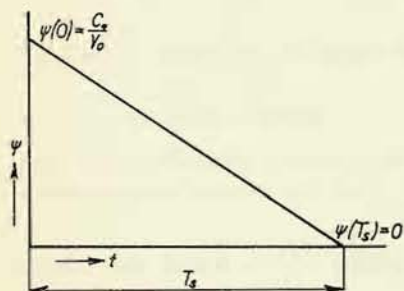


Fig. 483

or in another form

$$\frac{y_A}{y_0} = 1 + \frac{LC_0}{T_s g y_0} \sqrt{\frac{y_A}{y_0}}.$$

The expression $\frac{LC_0}{g y_0}$ is the known starting time of the pipe T_l and by introducing further denotations $\frac{T_l}{T_s} = n$ and $\frac{y_A}{y_0} = z$, we receive the following simple equation:

$$z - 1 = n \sqrt{z},$$

which can be written as

$$z^2 - 2z + 1 = n^2 z$$

or

$$z^2 - z(2 + n^2) + 1 = 0,$$

and finally

$$z = 1 + \frac{1}{2} n [n \pm \sqrt{n^2 + 4}],$$

$$\frac{y_A}{y_0} = 1 + \frac{1}{2} \frac{T_l}{T_s} \left[\frac{T_l}{T_s} \pm \sqrt{\left(\frac{T_l}{T_s} \right)^2 + 4} \right]. \quad (369)$$

Thus we have determined the value of the maximum relative pressure $\frac{y_A}{y_0}$ (carrying the sign +) for a linear closure of the efflux at the end of the closure time T_s , or the minimum relative pressure (carrying the sign -) for a linear opening at the end and of the opening time T_s .

As explained before, the expression (369) is valid only if $T_{2L} = \frac{2L}{a} < T_s$; in case that $T_s < T_{2L}$, Joukovski's expression $y_A = y_0 + \frac{a}{g} \Delta C$ or $\frac{y_A}{y_0} = 1 + \frac{a}{g y_0} \Delta C$ is valid. Even if $T_s > T_{2L}$ we must check according to Joukovski's expression, the value of the water hammer in time $t = T_{2L}$, i. e. in the time in which the reflected wave reaches the gate, because this value may be higher, than the final value according to Equation (369).

In actual practice the closure is never exactly linear; therefore in Equation (369) we use the coefficient 0.8 instead of 1/2 (as we have used in Michaud's expression 2.2 instead of 2).

Fig. 484 is an example of an arrangement which permits to explain the great importance of the mechanism of the pressure wave reflections.

Two vertical pipes are connected with the container and joined at the lower end into one single pipe with a closing

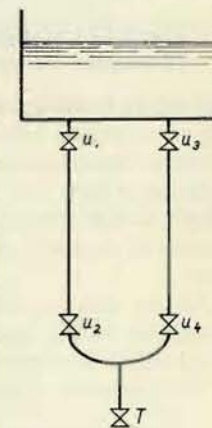


Fig. 484

organ (turbine) T . (This arrangement actually exists in Czechoslovakia. The power house is located in a mine and the penstock is mounted in the pit. For a better utilization of the pit profile the penstock consists of two pipes which are joined into one at the bottom of the pit). Each branch of the pipe has at the upper and lower end a (manipulating) closing valve $u_1 \dots u_4$. During operation the inlet valve of one branch (u_1 or u_3) must never be closed without closing simultaneously

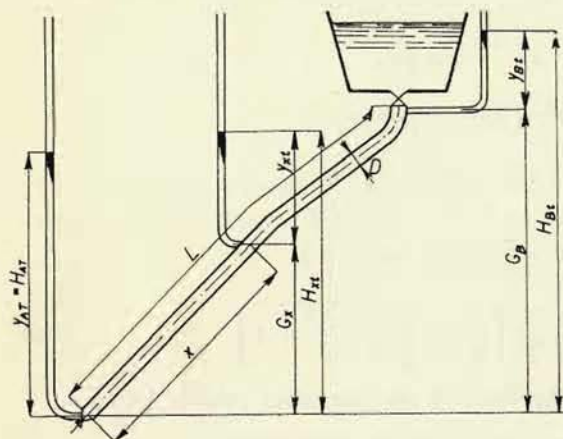


Fig. 485

In this chapter we have derived only the maximum value of the water hammer. The course of pressures has not been investigated analytically, because it can be followed more suitably in the graphical method discussed in the following chapter.

2. Graphical Method of Water Hammer Analysis (Schnyder-Bergeron method.)

Analytic investigation of the water hammer becomes difficult after the simplifying assumptions have been abandoned and some actual conditions are taken into account. Such conditions to be considered are: the actual conditions at the inlet (relation of inlet loss to velocity), the pipe has not the same diameter in the whole length, sound velocity is not identical throughout the whole length of the pipe, the process of closure is not linear or we want to establish the total course of pressure rise.

All the above conditions can be well considered in a graphical analysis. The principles of this analysis are explained in this chapter and some examples are given which illustrate the actual application of the method.

The method is derived for a general case of an inclined pipe.¹⁾

¹⁾ According to Schnyder: *Über Druckstöße in Rohrleitungen, Wasserkraft und Wasserwirtschaft*, 1932, p. 49.

Let us start from the basic Equations (363) which were derived in the previous paragraph. With the application of the denotations from Fig. 485, these equations are written in the following form (the former denotation y has been related to the pipe axis, the new denotation H represents the total head; subscript x is introduced because later on we shall consider two more points with the co-ordinates X and X'):

$$\begin{aligned} y_{xt} - y_{x_0} &= H_{xt} - H_{x_0} = F\left(t - \frac{x}{a}\right) - f\left(t + \frac{x}{a}\right), \\ C - C_0 &= C_{xt} - C_{x_0} = -\frac{g}{a} \left[F\left(t - \frac{x}{a}\right) + f\left(t + \frac{x}{a}\right) \right]. \end{aligned} \quad (370)$$

In the analysis we must respect the limiting conditions at the pipe inlet and outlet. These conditions determine how the pressure (or pressure head) at both ends of the pipe depends upon velocity and time. Therefore we may state generally, that

$$H_{At} = A(C_{At}, t)$$

for the outlet end of the pipe,

$$H_{Bt} = B(C_{Bt}, t)$$

for the inlet end of the pipe. (371)

The conditions are graphically shown as pressure plotted against velocity, while time is given as a parameter.

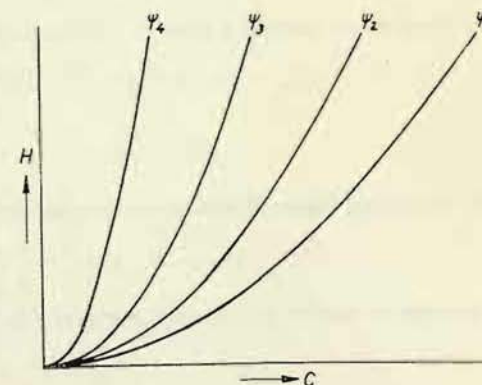


Fig. 486

For example, if water flows as a free jet from a closing valve the opening of which changes with time, the dependence is represented by a system of parabolas

$$C^2 = k \cdot 2 \cdot g \cdot H$$

Where each parabola corresponds to a certain opening of the valve which in turn corresponds to a certain time – see Fig. 486.

For a graphical investigation of the water hammer in one system of co-ordinates the second Equation (370) must be multiplied by the value $-\frac{a}{g}$ and the equations are added together as follows:

$$\frac{H_{xt} - H_{x_0} = F\left(t - \frac{x}{a}\right) - f\left(t + \frac{x}{a}\right) - \frac{a}{g}(C_{xt} - C_{x_0}) = F\left(t - \frac{x}{a}\right) + f\left(t + \frac{x}{a}\right)}{H_{xt} - H_{x_0} = \frac{a}{g}(C_{xt} - C_{x_0}) + 2F\left(t - \frac{x}{a}\right)}. \quad (372)$$

These equations hold good generally: thus they are valid also for a point with the abscissa X in time T . Thus we can write:

$$H_{XT} - H_{X0} = \frac{a}{g} (C_{XT} - C_{X0}) + 2F \left(T - \frac{X}{a} \right).$$

By selecting time T for point X in such relation to the time t for point x , that

$$t - \frac{x}{a} = T - \frac{X}{a},$$

function F has an identical value in both equations and by its elimination we receive the following equation

$$H_{xt} - H_{XT} - (H_{x0} - H_{X0}) = \frac{a}{g} (C_{xt} - C_{XT}) - \frac{a}{g} (C_{x0} - C_{X0}),$$

As long as we assume a pipe of unchanging diameter the following holds good:

$$H_{x0} = H_{X0} \text{ and } C_{x0} = C_{X0} \text{ and } T - \frac{X}{a} = t - \frac{x}{a},$$

$$H_{xt} = H_{XT} = \frac{a}{g} (C_{xt} - C_{XT}). \quad (373)$$

By deducting the equations we receive the following relation:

$$H_{xt} - H_{X'T'} = -\frac{a}{g} (C_{xt} - C_{X'T'}). \quad (374)$$

In order to receive an identical function f in both equations, we have substituted

$$t + \frac{x}{a} = T' + \frac{X'}{a}.$$

The above procedure means, that we are comparing states of flow in different places of the pipe at different times. The difference in time equals the time required by the pressure wave to travel from one place of observation to the next one, because

$$\begin{aligned} t - T &= \frac{x}{a} - \frac{X}{a} = \frac{x - X}{a}, \\ t - T' &= \frac{X'}{a} - \frac{x}{a} = \frac{X' - x}{a}. \end{aligned} \quad (375)$$

For states at both ends of the pipe, i. e. for $x = 0$ and $X = L$ we can write then:

$$\begin{aligned} H_{At} - H_{B,t-T_L} &= -\frac{a}{g} (C_{At} - C_{B,t-T_L}), \\ H_{Bt} - H_{A,t-T_L} &= +\frac{a}{g} (C_{Bt} - C_{A,t-T_L}) \end{aligned} \quad (376)$$

(the sign $+$ is applied if the second observed point lies in a downstream direction from the first one — see Equations (375) and (373, 374)).

Equations (376) can be used for a graphical investigation of the water hammer; see the following example in Fig. 487.

In Fig. 487 flow velocities C are marked on the horizontal axis, pressure heads H are on the vertical axis. Curves representing the limiting conditions for the outlet (A) and inlet (B) are drawn for times equal to the half-time of one interval of the pressure wave $\frac{L}{a} = T_L$. This means that we assume the case of a simultaneous

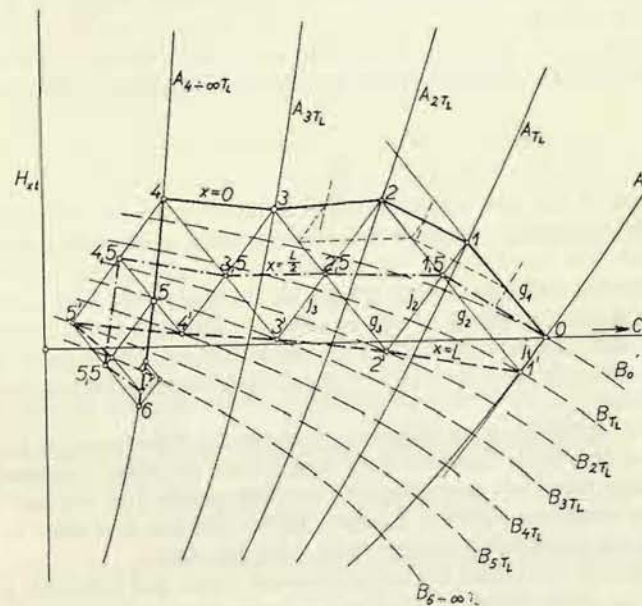


Fig. 487

start of closure of the inlet and outlet valve. At the start, in a state of continuous flow, conditions prevailing in the whole pipe are represented by one single point O which is the intersection of the curves A_0 and B_0 . Now let us assume that the closure of both valves starts simultaneously. After time T_L the inlet valve is closed to such an extent, that the state of flow is represented by the curve B_{1T_L} , the outlet valve is closed so that the respective flow is shown by curve A_{1T_L} . After time $2 \cdot T_L$ both valves are closed more and the respective states are represented by the curves B_{2T_L} and A_{2T_L} , etc.

After time $t = T_L$ the state at the efflux end of the pipe is represented by the curve A_{1T_L} and also by the straight line g_1 which is a graphical representation of the first Equation of the system (376):

$$H_{A,T_L} - H_{B,0} = -\frac{a}{g} (C_{A,T_L} - C_{B,0}),$$

This line has a slope $-\frac{a}{g}$ and the state at the efflux end (after time T_L) is determined by the intersection 1. In a similar way the straight line j_2 represents the equation

$$H_{B,2T_L} - H_{A,T_L} = \frac{a}{g} (C_{B,2T_L} - C_{A,T_L}),$$

The intersection of this line and the curve B_{2T_L} represents the state at the inlet end after time $2 T_L$, etc. etc.

After the time $t = T_L$ the state at the inlet end is determined by the curve B_{1T_L} and by the straight line j_1 which represents the second Equation of the system (376):

$$H_{B,1T_L} - H_{A,0} = \frac{a}{g} (C_{B,1T_L} - C_{A,0}),$$

so that the state at the inlet (after time T_L) is represented by the intersection 1'. The line g_2 and curve A_{2T_L} determine further the state at the outlet end after the time $2 \cdot T_L$, etc. etc. In this way we construct the whole course of the pressure change. We assume that the closing process at the outlet end is terminated after a time equalling four halftimes of one interval ($4 \cdot T_L$) and at the inlet end after $6 \cdot T_L$, so that after this time the curves $A_{4T_L-\infty}$ and $B_{6T_L-\infty}$ hold good. The water hammer lines always reverse at these curves and their slopes represent the damping of the oscillations.

The course of pressure at an arbitrary place can be determined as the locus of intersections of the water hammer lines which start at points representing flow states at the pipe terminals prevailing one interval earlier. For the half length of the pipes these times are identical for both halves and the flow state is therefore determined by the intersection of these lines. (See Fig. 487.)

It is advantageous to replace the actual pressure heads and velocities by relative values which can be obtained by dividing the pressure head by a significant pressure head H_0 (total head) and the velocity by a significant velocity C_0 (normal velocity at fully opened valves). The relative values obtained in this way are the following:

$$h_{xt} = \frac{H_{xt}}{H_0}, h_{x0} = \frac{H_{x0}}{H_0}, c_{xt} = \frac{C_{xt}}{C_0}, c_{x0} = \frac{C_{x0}}{C_0} \text{ etc.}$$

Equations (373) and (374) are transformed into:

$$\begin{aligned} h_{xt} - h_{XT} &= \frac{a}{g} \frac{C_0}{H_0} (c_{xt} - c_{XT}), \\ h_{xt} - h_{X'T'} &= -\frac{a}{g} \frac{C_0}{H_0} (c_{xt} - c_{X'T'}). \end{aligned} \quad (377)$$

The expression $\frac{a \cdot C_0}{g \cdot H_0} = \varrho$ is called the characteristic of the pipe.

The application of these transformed equations is demonstrated on the following example of a free efflux from a nozzle with a full consideration of pressure losses.

Let us first establish the relations which determine the limiting conditions. The ratio of the outlet cross section of the nozzle to the cross section of the pipe is denoted as ψ (we still consider a pipe of a uniform cross section), for an arbitrary opening of the nozzle, and as ψ_0 the same ratio for a full (maximum) opening of the nozzle. The pressure loss in the nozzle is expressed as $\xi_A \cdot \frac{V^2}{2g}$ (V is the velocity in the nozzle), so that we can write

$$y_{At} + \frac{C_{At}^2}{2g} = \frac{V^2}{2g} + \xi_A \frac{V^2}{2g}$$

or

$$H_{At} = y_{At} = \frac{C_{At}^2}{2g} \left[\frac{1}{\psi^2} (1 + \xi_A) - 1 \right], \quad (378)$$

This equation represents the limiting condition for the downstream end of the pipe.

We assume, that the inlet end of the pipe is connected with a reservoir sufficiently large in which the water level does not change at all and the actual inlet is placed below the level, so that the inlet pressure is proportional to the pressure head y_B .

Losses in the grid and inlet valve can be expressed as $\mp \xi_B \frac{C_{Bt}^2}{2g}$.

Then we can write the following limiting condition for the inlet:

$$y_{Bt} = y_B - \frac{C_{Bt}^2}{2g} (1 \pm \xi_B). \quad (379)$$

If we consider the general case of an inclined pipe (Fig. 485), Equation (379) changes as follows:

$$H_{Bt} = G_B + y_{Bt} = G_B + y_B - \frac{C_{Bt}^2}{2g} (1 \pm \xi_B). \quad (380)$$

In order to introduce relative values let us select as a reference head the static head from the upper level of the reservoir to the outlet opening of the nozzle $H_0 = y_B + G_B$ and as a reference velocity the flow velocity C_0 which corresponds with the reference head in the case of a fully opened nozzle. According to (378):

$$H_0 = \frac{C_0^2}{2g} \left[\frac{1}{\psi_0^2} (1 + \xi_A) - 1 \right].$$

We further substitute

$$\frac{1}{\varphi^2} = \frac{\frac{1}{\psi^2} (1 + \xi_A) - 1}{\frac{1}{\psi_0^2} (1 + \xi_A) - 1}$$

and

$$\frac{C_0^2}{2g} = k \cdot H_0$$

$$\left[\text{where } k = \frac{1}{\frac{1}{\psi_0^2} (1 + \xi_A) - 1} \right],$$

we arrive at the limiting conditions

$$h_{At} = \alpha(c_{At}, t) = \left(\frac{c_{At}}{\varphi} \right)^2$$

where φ is the function of time $\varphi = f(t)$

$$h_{Bt} = \eta(c_{Bt}, t) = 1 - k c_{Bt}^2 (1 \pm \xi_B). \quad (381)$$

The limiting conditions are drawn in the diagram Fig. 488. The relative flow velocity c is marked on the axis X , the relative pressure head h on the axis Y . The

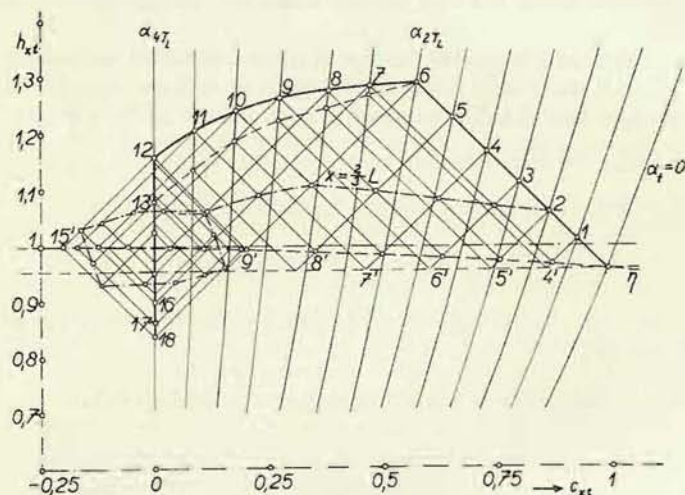


Fig. 488

condition valid for the inlet is, therefore, represented by the parabola η which does not depend on time. The outlet condition changes with time and, when plotting φ as a parameter, it is represented by a system of parabolas.

The course of the pressure rise is then constructed by the application of the Equations (377). The slope of the water hammer lines is given by the characteristic of the pipe $\varrho = \frac{a \cdot C_0}{g \cdot H_0}$; with reference to the prior explanation, further procedure is easily comprehensible from the picture. We assume that closure is

terminated after four half-intervals of the pressure wave, after which the water hammer lines turn about on the vertical line $\alpha_t = 4 \cdot T_L$. Six parabolas α are drawn for the total time of interval $2 T_L$ and therefore, the intersections of the water hammer lines represent pressure changes in places located at a distance of $1/6$ pipe length. The dot and dash line in Fig. 488 represents the pressure course at a place which is at $2/3$ pipe length from the outlet.

Errors caused by the omission of the inlet loss and velocity head are shown in Fig. 488 by the dash line which represents $h_B = \text{const}$, and from which the course of the water hammer is analyzed.

If we want to consider also pipe friction losses, we may concentrate them into the inlet cross section and increase the inlet loss by the value of friction. This is a simple way how to approach actual conditions.

The course of pressure changes established in this way is redrawn in Fig. 489,

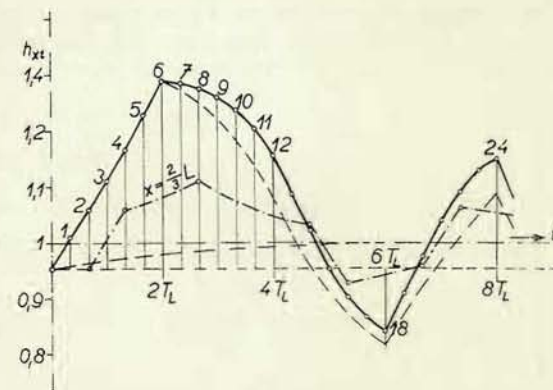


Fig. 489

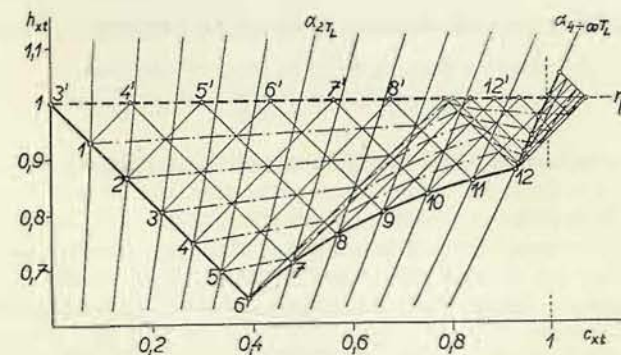


Fig. 490

where time is marked on the axis X . The diagram 489 is then the time diagram of the course of the water hammer.

Pressure drop during nozzle opening is investigated in Fig. 490. The time considered equals again four half-intervals of the pressure wave. Inlet losses and velo-

city head are not considered. During the investigation of the pressure drop we are very interested in the course of the drop in the whole length of the pipe. It is necessary to determine whether pressure decreases at any place to zero. This would mean a disruption of the water column. The dot and dash line in Fig. 490 shows the pressure course in places located at a distance of $1/6$ of the pipe length.

A changing cross section of the pipe is easy to consider in the graphical analysis.

During the analysis the time interval for each individual section of a uniform

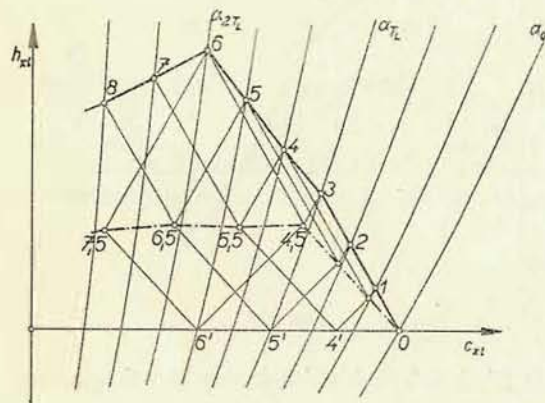


Fig. 491

cross section is established and the resultant times are round, so that they are either equal or whole multiples of each other. Equations (377) are applied to the individual pipe sections of a uniform cross section. By denoting the contact cross sections as S_1 , S_2 , we can write for the pipe section between the outlet and contact S_1 the following equations:

$$\begin{aligned} h_{At} - h_{S_1, t-T_L} &= \\ &= -\rho_1 (c_{At} - c_{S_1, t-T_L}) \\ h_{S_1, t} - h_{A, t-T_L} &= \\ &+ \rho_1 (c_{S_1, t} - c_{A, t-T_L}), \quad (382) \end{aligned}$$

In a similar way for the section between S_1 and S_2 we can write:

$$\begin{aligned} h_{S_1, t} - h_{S_2, t-T_L} &= -\rho_2 (c_{S_1, t} - c_{S_2, t-T_L}) \\ h_{S_2, t} - h_{S_1, t-T_L} &= +\rho_2 (c_{S_2, t} - c_{S_1, t-T_L}) \quad (383) \end{aligned}$$

and so forth.

As stated before, we must bear in mind that individual points of the diagram can be valid at different times for various places of the pipe. Fig. 491 shows the analysis of water hammer in a pipe composed of two sections of different diameters and thus also of different characteristics ρ . The lower part of the pipe has the characteristic ρ_1 which determines the slope of the water hammer line $0-1-2-3$, the second section has a characteristic ρ_2 which determines the water hammer line $0-4.5$.

During closure water hammer is formed in the lower part with the characteristic ρ_1 . Let us denote the half-time of interval of the whole pipe as T_L , the same time for an individual section as $\frac{T_L}{2}$ and let us consider a time $2 \left(\frac{T_L}{2} \right)$.

The first Equation (382) applied to this time is written as follows:

$$h_{A, 2 \frac{T_L}{2}} - h_{S_1, \frac{T_L}{2}} = \rho_1 \left(c_{A, 2 \frac{T_L}{2}} - c_{S_1, \frac{T_L}{2}} \right).$$

Pressure rise in time $\frac{T_L}{2}$ has not yet reached the point S_1 , because there is no change of conditions (pressure and velocity) and the state is represented in the diagram by the point O . Therefore, according to the above equation, conditions valid for point A (efflux end of the pipe) will be represented by a point which belongs to the water hammer line of a slope $-\rho_1$, i. e. on the line $0-1, 2, 3$. The point representing these conditions must belong also to the curve of the limiting conditions of the outlet end, i. e. to the parabola $A_{T_L} = 2 \frac{T_L}{2}$. The investigated point is therefore identical with point 3.

Now let us consider the time $3 \frac{T_L}{2}$ and use the first Equation of the system (383). As point S_2 in our example is identical with the inlet, we shall use the denotation B instead of S_2 . It follows:

$$h_{S_1, 3 \frac{T_L}{2}} - h_{B, 2 \frac{T_L}{2}} = -\rho_2 \left(c_{S_1, 3 \frac{T_L}{2}} - c_{B, 2 \frac{T_L}{2}} \right).$$

Pressure change has not yet reached the inlet (B) in time $2 \frac{T_L}{2}$; the state is represented here by the point O . According to the equation the state valid for the point S_1 in time $3 \frac{T_L}{2}$ must be determined by a point of the water hammer line starting from point O and having a slope $-\rho_2$, i. e. on the line $O-4.5$ (the figures give the time in seconds for $T_L = 3$ sec.).

Let us apply for the same interval $3 \frac{T_L}{2}$ the second Equation (382) as follows:

$$h_{S_1, 3 \frac{T_L}{2}} - h_{A, 2 \frac{T_L}{2}} = +\rho_1 \left(c_{S_1, 3 \frac{T_L}{2}} - c_{A, 2 \frac{T_L}{2}} \right).$$

We know the state of point A in time $2 \frac{T_L}{2}$; it is determined by point 3. According to the Equation the state of point S_1 in time $3 \frac{T_L}{2}$ must be represented by a point of the water hammer line starting from point 3 and having a slope $+\rho_1$, i. e. the line $3-4.5$ and it will be determined by the intersection with the water hammer line $0-4.5$ mentioned before. The investigated point is identical with the point 4.5.

By a similar application of Equations (382), (383) to time $4 \frac{T_L}{2}$ we receive the points 6 and 6', then 7.5, etc. For a more exact determination of the pressure course we must divide the basic time $2 \frac{T_L}{2}$ so as to obtain more points (In the given example the basic time has been divided into three equal time intervals). The construction appears to be almost a mechanically drawn "reflection" of water hammer lines.

In this graphical method we can respect without difficulties conditions which in the numerical analysis are often impossible to handle. Therefore this graphical method is widely used.¹⁾

III. SURGE TANKS

1. Purpose of Surge Tanks and Stability of the Supply System

Long closed conduits are generally interrupted by a surge tank as shown schematically in Fig. 492.

Surge tanks are placed as near to the power station as possible; the water supply conduit should be always horizontal. Water hammer cannot spread from the turbine into the conduit between the surge tank and reservoir, because the free level in the surge tank causes a reflection of the pressure wave. The conduit between the surge tank and reservoir is thus subjected to a lower pressure head and is constructed as a tunnel. The pipe length between the turbine and the place of reflection is shortened (without surge tank the pressure wave would be reflected from the reservoir); the water hammer is reduced. Conditions for proper automatic control are improved, because the starting time of the pipe T_l is reduced. Fig. 492 shows the most simple arrangement: the surge tank is located in the penstock. The surge tank can be placed also beyond the turbine, if a discharge tunnel is used in an underground power station, see Fig. 493. If no surge tank is arranged in an underground power station, flow rate changes cause great pressure fluctuations beyond the runner and turbine regulation becomes very difficult (increase of T_l).

Combinations of two surge tanks either according to Fig. 493 or according to Fig. 494 constitute a hydraulically very complicated case, because both surge tanks are mutually influenced.

¹⁾ For further applications see the cited article of Schnyder as well as the following works: Mostkov, Bashkurov: Raschoty gidravlicheskovo udara, Gosud. energeticheskoye izdatelstvo, Moscow-Leningrad, 1952. Bergeron L.: Du coup de bélier en hydraulique au coup de foudre en electricité, Paris, Dunod, 1950, Jäger: Technische Hydraulik, Basel, 1949.

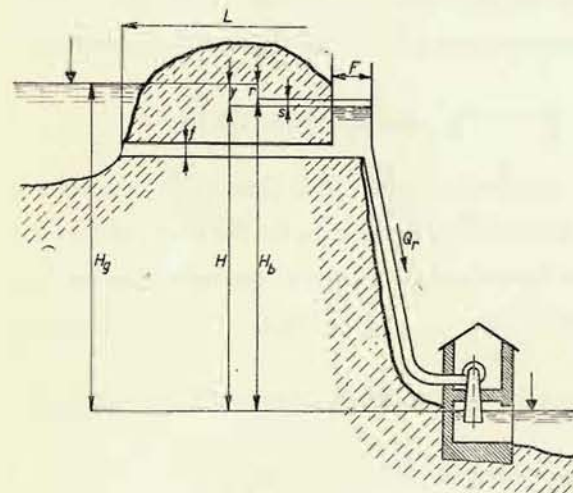


Fig. 492

Fig. 492 shows that the surge tank and reservoir form a system of interconnected vessels which is capable to oscillate. Let us imagine that the pressure pipe leading to the turbine is shut off and the water level in the surge tank is pressed down (by

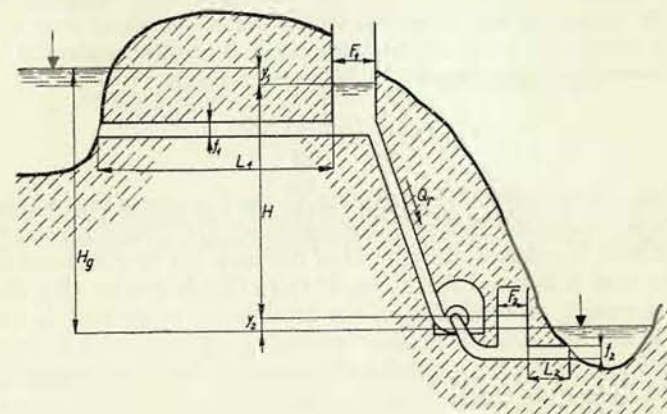


Fig. 493

any pressure exerting installation). It is obvious that by a sudden relief of the pressure in the surge tank the water level in the tank starts to oscillate. Water will flow in the tunnel alternately in both directions, this turbulent flow will cause friction losses which are proportionate to the square of velocity and the movement

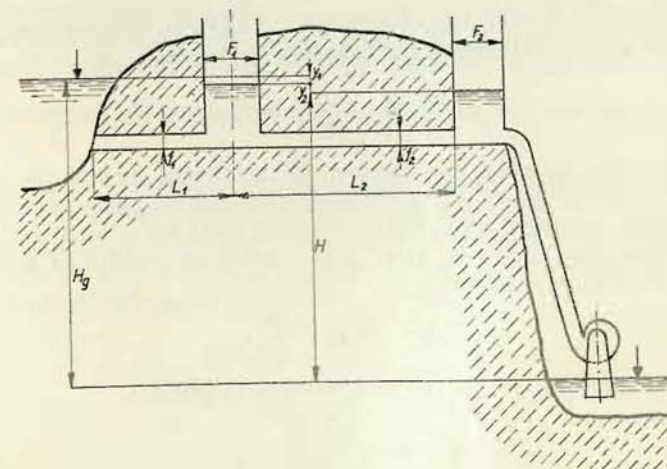


Fig. 494

will be damped down gradually. If no water flows from the surge tank to the turbine, the water level in the surge tank will be stabilised. In the case of an open penstock and with an automatically controlled turbine, conditions can arise, at which more energy is supplied to the surge tank, than delivered from the surge tank to the turbine. The surplus energy causes an oscillation of the water level in the surge tank which gradually increases. An automatic controller maintains a constant output of the turbine according to the following formula

$$N = \frac{Q_r H \eta}{75} \cdot 1000$$

where N is the output in metric horse power, Q_r the flow rate of the turbine in m^3/sec . This output is maintained even at a changing head. If the level in the surge tank is lowered the head is reduced, the controller increases the flow rate and so the level in the surge tank is lowered still more. If this effect is greater than the damping effect of the tunnel, an oscillation of the level in the surge tank is started. The amplitude of this oscillation is steadily increasing, the oscillation is transmitted to the controller and finally the operation of the turbine becomes untenable.

In order to prevent an increasing oscillation of the system and to reduce the level fluctuation caused by the changing flow rate of the turbine, certain conditions of stability must be fulfilled.

Let us derive the basic equations valid for the movement of the system (using denotations according to Fig. 492).

The level difference y reduced by friction losses in the tunnel $z = k \cdot v^2/v$ is the velocity of water in the tunnel) accelerates in the tunnel a water column of the mass $m = \frac{f \cdot L \cdot \gamma}{g}$, where f is the cross section area of the tunnel, L its length, γ the specific weight of water and g the gravity acceleration. The pressure $(y - z) \cdot \gamma$ acts upon the area f and therefore the following holds good:

$$f L \frac{\gamma}{g} \frac{dv}{dt} = (y - kv^2) \gamma f.$$

Apart from this equation, the equation of continuous flow is also valid; the difference between the quantity of water flowing through the penstock to the turbine and the quantity flowing through the tunnel must equal the reduction of the water content of the surge tank (the value y is considered positive in a downward direction). We may thus write:

$$Q_r - fv = F \frac{dy}{dt}.$$

The quantity flowing from the surge tank to the turbine is:

$$Q_r = \frac{N \cdot 75}{H \cdot 1000 \cdot \eta}.$$

The water level in the surge tank differs from that in the reservoir by y . If we

denote the difference between head-race and tail-race as the geodetic head H_g , we may write:

$$H = H_g - y,$$

and by substituting

$$A = \frac{N \cdot 75}{1000},$$

we can express Q_r by the following relation:

$$Q_r = \frac{A}{(H_g - y) \cdot \eta}.$$

By substituting this relation into the above derived equation of continuous flow, we receive the following two equations which are sufficient for the solution of the problem:

$$\begin{aligned} \frac{L}{g} \frac{dv}{dt} &= y - kv^2 \\ F \frac{dy}{dt} &= \frac{A}{(H_g - y)\eta} - fv. \end{aligned} \quad (384)$$

By assuming that the amplitude of the level oscillation is small in comparison with the total head¹⁾ we receive the following two conditions of the stability from the above equations:

$$\begin{aligned} kv_s^2 &= r < \frac{H_b}{2} \frac{\eta_s}{\eta_s - i \cdot H_b} \\ \left(\frac{2kFg}{fL} - \frac{i}{\eta_s} \right) H_b &> 1. \end{aligned} \quad (385)$$

Symbols used are taken from Fig. 492: v_s is the medium velocity of flow in the tunnel (at the load considered), η_s medium efficiency of the system at the flow rate considered and i is the ratio of change of the efficiency in dependence on head: $i = \frac{d\eta}{dH}$. Change of efficiency in dependence on the flow rate does not effect stability.

The first criterion demands, that tunnel losses r should be smaller than half of the difference between the surge tank level and tail-race level.

The second condition determines the size of the level area F in the surge tank.

If the value of the ratio: change of efficiency in dependence on head is small, and thus $i \doteq 0$, both criteria can be simplified as follows:

$$\begin{aligned} kv_s^2 &= r < \frac{H_b}{2} = \frac{H_g}{3} \\ \frac{2kFgH_b}{Lf} &> 1. \end{aligned} \quad (386)$$

¹⁾ See e. g. Nechleba: *Theorie indirektní regulace rychlosti* (Theory of indirect speed control), Technicko-vědecké vydavatelství, Prague, 1952.

The second condition is often called Thoma's condition, because Thoma was the first who investigated the stability of surge tanks¹⁾ and the area complying with this condition is called Thoma's area:

$$F_{Th} = \frac{Lf}{2kgH_b}$$

From Equations (384) we can calculate also the maximum amplitude of the level oscillation occurring at a flow rate change ΔQ in a surge tank with a constant cross section F :

$$S_{max} = \frac{\Delta Q}{\sqrt{fF}} \sqrt{\frac{L}{g}} \sqrt{\frac{H_b}{H_b - 2r}} \quad (387)$$

and the time of one oscillation wave:²⁾

$$T = 2\pi \sqrt{\frac{FH_b L}{fg(H_b - 2r)}} \quad (388)$$

2. Dimensioning of Surge Tanks

In the preceding chapter we have dealt with the basic values for the dimensioning of surge tanks. In this connection we have discussed first of all the minimum surface area of the water level in the surge tank, Thoma's area, which forms a limiting condition of stability. Actual cross section of the surge tank must be greater than this calculated limiting value. We must respect the condition $F > F_{Th}$ or $F = n \cdot F_{Th}$ and $n > 1$.

We introduce the safety coefficient n in order to ensure a sufficient damping effect and also to compensate for risks occurring in the selection of the tunnel coefficient k . The latter must be introduced in calculations before the tunnel begins to operate and thus there is no possibility of checking by actual measurements.

As stated before, the critical surface area F_{Th} has been determined under the assumption that the level amplitude of the surge tank is negligible in comparison with the total head. This assumption holds good only for high heads. For lower heads we must introduce a certain correction which will be dealt with further on.

The second directional value for the dimensioning of the surge tank is the amplitude of the level oscillation, i. e. the sum of the maximum rise and maximum fall of the water level in the surge tank. For this value we have introduced the expression (387) from which it can be seen that the amplitude rises with an increasing change of the flow rate ΔQ . Level rise attains the highest value in the case of a complete load rejection in all turbines connected with the surge tank. This extreme case must be considered when determining the height of the surge

¹⁾ Thoma R.: Zur Theorie des Wasserschlosses, Oldenbourg, Berlin, 1910.

²⁾ For the derivation of both expressions see e. g. Nechleba: Theorie indirektní regulace rychlosti (Theory of indirect speed control), Technicko-vědecké vydavatelství, Praha, 1952.

tank. On the contrary a maximum fall of the level occurs in the event of full load being suddenly applied to all turbines running hitherto without load. Theoretically we should consider this case for the determination of the bottom of the surge tank. A careful analysis of the operating conditions of the system will show, if this extreme case must be considered. However, an increase of load amounting to the half of the maximum load occurring simultaneously in all turbines is generally counted with.

Value (387) has been derived under certain simplifying assumptions and therefore it does not give exact results; we have assumed a case of undamped oscillation ($F = F_{Th}$), the amplitude is smaller in the event of a damped oscillation. The construction of a surge tank is expensive and we must try to determine the most exact dimensions necessary for the proper function.

Rise and fall of the level in the surge tank can be best determined by graphical methods worked out e. g. by Braun, Calame-Gaden and Schoklitsch. The latter is the most simple and it will be described in a later paragraph. It has a further advantage that it can be applied for an analysis of the more complicated surge tank arrangements which are used for a reduction of level variations, i. e. reducing surge tank dimensions and first costs.

3. More Complicated Surge Tanks

Special designs of surge tanks are made in order to reduce the dimensions. The underlying idea applied in these designs is the following: the retardation of the flow in the tunnel (at a decrease of the flow rate) is the more effective, the more rapid will be the pressure rise in the lower part of the surge tank, and on the other hand acceleration of the flow in the tunnel (at an increased flow rate) will be the more effective, the more rapid will be the pressure drop in the lower part of the surge tank. The desired rate of pressure change can be achieved by a special shape of the surge tank or by a suitable throttling of the water inlet into the tank.

a) *Surge tanks with an upper and lower chamber* according to Fig. 495 are used in cases when rock excavation is appropriate. The cross section area F_s of the central part is rather small but always larger than the above defined critical area F_{Th} . Cross section areas F_1 and F_2 of the upper and lower chambers are larger and dimensioned by a detailed investigation. It is obvious, that e. g. at a sudden reduction of the flow rate of the turbine the level in the surge tank rises almost to the maximum and immediately has a retarding effect upon the flow

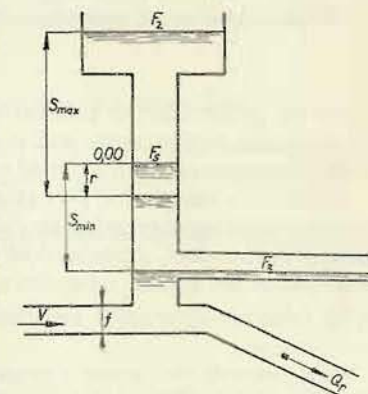


Fig. 495

in the tunnel. Level oscillation formulas mentioned above are not valid for this type of surge tanks and the case must be analysed by a graphical method.¹⁾

b) *The restricted orifice surge tank.* The same effect (intensive retardation or acceleration in the tunnel) can be achieved by restricting the orifice, i. e. by

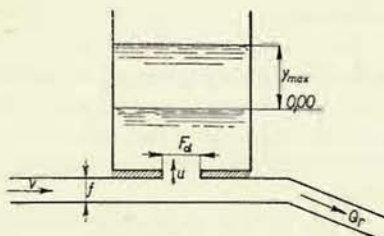


Fig. 496

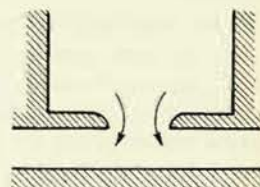


Fig. 497

throttling the inlet into the surge tank according to Fig. 496. During a change of the level in the surge tank, water flows through the orifice at a speed $u = k \frac{dy}{dt}$ and a throttling loss $\pm \frac{\Delta p}{\gamma}$ occurs. The throttling has, therefore, a favourable effect

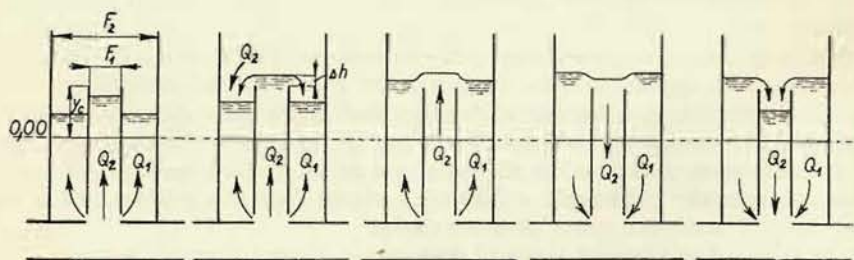


Fig. 498

upon the acceleration or retardation of the flow in the tunnel, but stresses caused by increased overpressure and underpressure represent an adverse effect. Generally these stresses in the tunnel construction are not very high.

It has been stated, that flow rate changes during reduction are generally greater, than those occurring during an increase of the flow rate. The throttling orifice is designed, therefore, asymmetrically according to Fig. 497. Friction losses during the inlet period are higher (reduction of the central flow area), than those during outlet.

c) *Johnson's differential surge tank.* This is a variation of the restricted orifice

¹⁾ In literature we encounter sometimes the idea of an „idealized surge tank“. By this a surge tank is understood where the total volume of the tank is concentrated in the extreme positions of the water level.

surge tank. It consists of an internal riser chamber of a smaller cross section area F_1 and of an outer chamber of a cross section area $F_2 - F_1$. The lower part of the riser contains throttling ports through which the water flows (Q_1) into or from the outer chamber or, after having reached the maximum level y_c , the water overflows into the outer chamber. The function of the surge tank is illustrated schematically in Fig. 498 with all phases of inlet and emptying.

This type of surge tank requires a rather great restriction of the orifice in order to secure a rapid increase of the water column in the riser. Pressure rise cannot reach dangerous values, because of the overflow arrangement.

Fig. 499 shows an arrangement which is a variety of Johnson's differential tank. The riser is substituted by the side-duct II which has been originally a lifting pit during the excavation of the tunnel Q . The arrangement may be considered as a differential tank only if the distance $A - A'$ is short so that the mass of water in this short connecting duct may be neglected. Otherwise the arrangement represents a system of surge tanks according to Fig. 494.

It must be born in mind, that the restricted orifice does not increase the stability of the system and the cross section area of differential surge tanks must be also greater, than the critical value of Thoma. We must remember, that at small changes of the flow, velocity in the orifice is so small, that practically no pressure loss occurs and stability is not effected at all. In Johnson's differential surge tank the cross section area of the riser must be greater than Thoma's value, because at larger surges water level in the riser is different from that in the outer chamber and the important factor is the level head of the riser.

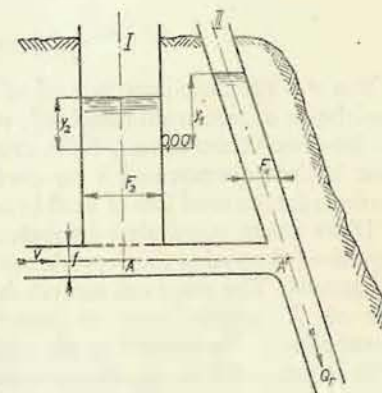


Fig. 499

4. Graphical Method to Determine Level Changes in the Surge Tank

Level changes in complicated surge tanks are very difficult to determine by numerical analysis. They can be analysed very exactly and clearly by the graphical method of Schoklitsch¹⁾.

First of all the basic Equations (384) are taken as a starting point. The equation for the acceleration in the tunnel reads:

$$\frac{L}{g} \frac{dv}{dt} = y - kv^2 \quad (389)$$

¹⁾ Jäger: Technische Hydraulik, Birkhäuser, Basel, 1949, p. 232 - also Schoklitsch: Spiegelbewegung in Wasserschlossern, Schweizerische Bauzeitung, 1923, p. 129-146.

and the equation of continuous flow is:

$$Q_r - fv = F \frac{dy}{dt}. \quad (390)$$

By substituting the differentials by differences, i. e. by values very small but not infinitesimal, we can re-write these equations in the following way:

$$\Delta v = -\frac{g}{L} \Delta t (kv^2 - y), \quad (391)$$

$$vf \Delta t = Q_r \Delta t - F \Delta y, \quad (392)$$

where y is the difference in level of the reservoir and the surge tank (counted as positive in a downward direction), v the flow velocity in the tunnel, f the cross section area of the tunnel, F the cross section area of the surge tank, Q_r the flow rate in the penstock and k the coefficient of friction in the tunnel used in the formula for the total loss of head in conduit from reservoir to surge tank $r = k \cdot v^2$.

If we select equal time intervals Δt , the value Δt becomes constant and the equations determine the dependence of the velocity v upon the level drop y in the surge tank. The graphical analysis is shown in Fig. 500. Velocity v is marked on the axis X (positive values to the left i. e. direction of flow into the surge tank). Level change y is marked on the axis Y (positive values downward in accordance with actual conditions - y is a level drop.)

First of all we draw the following auxiliary lines:

$r = \pm k \cdot v^2$ marked in the picture as 1;

$\Delta v = +\frac{g}{L} \cdot \Delta t \cdot y$, this equation is illustrated by the straight line 2; Δt is selected as an arbitrary value, but equal throughout the whole analysis, so that it represents a constant value;

$v \cdot f \cdot \Delta t = V_f$ is plotted in the positive direction of y , see the straight line 3;

$\Delta V = F \cdot \Delta y$, representing the volume of the surge tank at different levels. ΔV is plotted in the direction of the X axis and the starting point is arbitrarily selected (however, sufficiently low so, as to be lower than the expected lowest level), see line 4.

Finally we must draw the line $Q_r \cdot \Delta t$, where Q_r is the flow rate after the turbine load has been changed. E. g. if we investigate a level change for the event of a load rejection corresponding to a flow rate reduction from maximum to one third, we calculate with a value $Q_r = \frac{1}{3} \cdot Q_{\max}$. Simultaneously we can take into account that flow rate changes as a function of the head. E. g. for a constant outlet orifice of a cross section area f_e we can write the following equation:

$$Q_r \Delta t = f_e \sqrt{2g(H - y)} \cdot \Delta t.$$

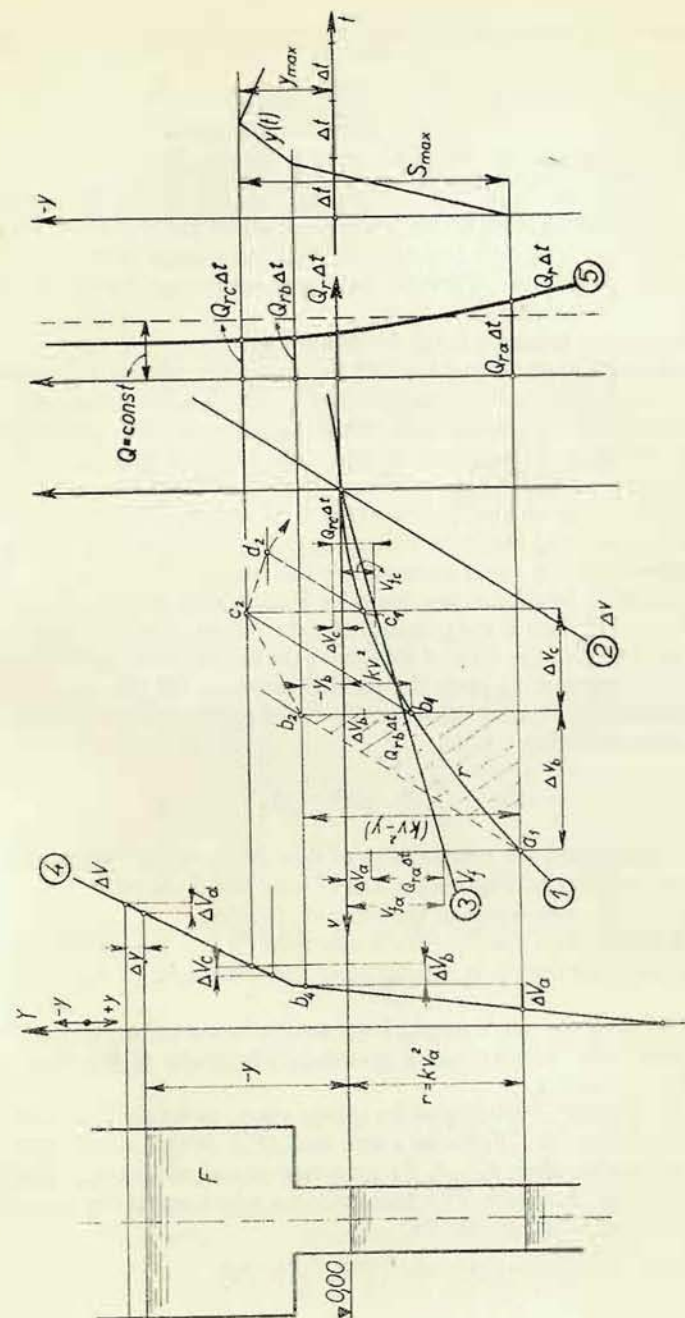


Fig. 500

For the automatically controlled constant output the following equation holds good:

$$Q_r \Delta t = \frac{N}{H-y} \frac{75}{1000 \cdot \eta} \cdot \Delta t.$$

The line representing this function in the picture is the hyperbola 5.

Note: We do not consider how flow rate changes proceed during the regulating process after a load rejection, because the time required by the controller is of the order of several seconds. The time required for the level change in the surge tank is of the order of several minutes. Therefore the flow rate change during regulation may be considered as instantaneous.

The analysis (Fig. 500) proceeds in the following way:

Let us start from point a_1 on the line 1, which represents the velocity in the tunnel at the initial level position in the surge tank, i. e. at a state of continuous flow in the tunnel prior to the change of the flow rate. Through this point we draw a parallel to the line 2; the end point of the parallel is not known yet. This parallel represents the Equation (391) as we shall see later on. We apply now the Equation of continuous flow (392), i. e.: $v \cdot f \cdot \Delta t = Q_r \cdot \Delta t - F \cdot \Delta y$. The values $v \cdot f \cdot \Delta t = V_f$ are represented by the line 3 and the value belonging to the velocity of the point a_1 is given by the ordinate of this point extended to the line 3. The value $Q_r \cdot \Delta t$ is represented by the line 5. By subtracting this value from V_f (as shown in the picture) we receive $F \cdot \Delta y = \Delta V$. This is the quantity of water which enters the surge tank during the time interval Δt and on line 4 we receive the corresponding level position as point b_4 . Point b_4 is projected upon the parallel drawn at the point a_1 and thus we receive on the ordinate axis the value Δv . From the shaded triangle we can see, that the following relation holds good:

$$-\Delta v = \frac{g}{L} \Delta t \cdot (kv^2 - y).$$

Thus we have determined the new velocity of flow in the tunnel which belongs to point b_2 . To this velocity belongs on the loss of head line 1 the point b_1 which is the starting point for the next cycle of the repeated plotting.

By plotting the values y on the equal time segments Δt (see the right hand side of Fig. 500) we construct the curve representing the movement of water level in time.

If time intervals Δt are small enough, level oscillations or the curve of level movement are established with sufficient accuracy. The shape of the surge tank does not cause any difficulties.

The analysis can be easily applied also for special cases, as we shall demonstrate on the example of Johnson's differential surge tank (Fig. 501). Let us denote F_1 the cross section area of the riser, $F_2 - F_1$ the cross section area of the outer chamber, f_e the area of the connecting ports. The water volume which enters the surge tank must be divided into two parts as follows:

$$vf \Delta t - Q_r \Delta t = -(V' \Delta t + V'' \Delta t)$$

Further the following relations hold good:

$$V' \Delta t = F_1 \Delta y_1 \quad \text{and} \quad V'' \Delta t = (F_2 - F_1) \Delta y_2,$$

Δy are the level differences in different parts of the surge tank from the reservoir level. The volume $V_f = v \cdot f \cdot \Delta t$ is represented, as before, by the line 3. Instead of the former volume line 4 we must draw two lines 4' and 4'' for both parts of the surge tank (riser and outer chamber). The volume entering the surge tank is divided

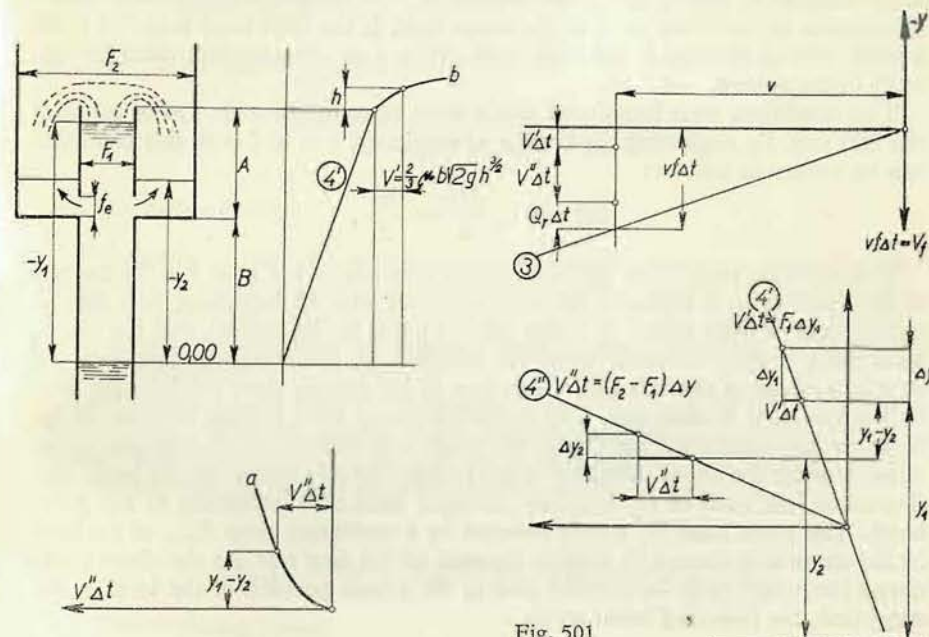


Fig. 501

into V' and V'' ; for this purpose we use the line a representing the port flow f_e . It follows:

$$V'' \Delta t = f_e \sqrt{2g(y_1 - y_2)} \cdot \Delta t.$$

It is obvious that we must proceed empirically. If the level in the riser reaches the overflow edge, we use for the overflow the line b :

$$V' = \frac{2}{3} \mu b \sqrt{2g} h^{\frac{3}{2}} \quad \text{and} \quad V'' \Delta t = f_e \sqrt{2g(y_1 - y_2)} \cdot \Delta t + \frac{2}{3} \mu b \sqrt{2g} \cdot h^{\frac{3}{2}}.$$

In order to ensure a rapid rise of the level in the riser and also to ensure a rapid emptying of the outer chamber, non-return flaps were mounted in the ports f_e . These flaps were worn out very quickly; they were abandoned and the ports are now made with rounded off outer edges and sharp inner edges (similar section as in Fig. 497) ensuring a smaller flow rate during the inlet period and more rapid emptying.

5. Stability in Case of Great Level Oscillations

We have shown in the first section of this chapter that certain conditions must be fulfilled in order to ensure a stable position of the level in a surge tank from which water is supplied to a turbine with an automatically controlled output.

These conditions have been established for the case of level changes which were negligibly small in comparison with the total head. We have seen, however, that great changes of output and consequently of flow rates can cause considerable movements of the water level in the surge tank. If the total head is rather small a great drop of the level in the surge tank can have an adverse effect upon the stability of the system.

Two conditions were introduced which must be complied with. Let us consider the first one. By neglecting the change of efficiency, i. e. at $i = 0$, this condition can be written as follows:

$$kv_s^2 = r < \frac{H_b}{2} = \frac{H_g}{3}.$$

This equation determines the maximum admissible loss of head r in the tunnel. If this limit value is exceeded the head decreases with an increasing flow rate so rapidly (loss of head caused by rising friction losses in the tunnel), that the loss of head has a greater influence upon the output than the increased flow rate. At further increase of the flow rate the output of the turbine does not increase, but, on the contrary, it decreases. The controller reacts by a further increase of the flow rate and complete emptying of the surge tank takes place. It amounts to the same, whether the above inequality is not fulfilled by increasing the left hand side (increased flow rate) or by reducing the right hand side (reduction of the gross head). The gross head H_b is here reduced by a maximum drop S_{\max} of the level in the surge tank caused by sudden increase of the flow rate. As the above mentioned inequality must be fulfilled also at the lowest position of the level in the surge tank, the following holds good:

$$kv_s^2 < \frac{H_b - S_{\max}}{2} = \frac{H_g - r - S_{\max}}{2}. \quad (393)$$

The second condition of stability has been established as

$$\left(\frac{2kFg}{fL} - \frac{i}{\eta_s} \right) \cdot H_b > 1,$$

or written in a different form:

$$F > \frac{fL}{2kgH_b} + \frac{ifL}{\eta_s \cdot 2kg}.$$

The fulfillment of this condition means that the movements of the water level caused by a change of the turbine output are being gradually reduced. At conditions represented by a reverse direction of the above inequality the level movements would gradually increase.

The direction of the inequality can be reversed also by reduction of the gross head H_b caused by the level drop of S_{\max} . If the head reduced in this way would reach a value which is smaller than that at which the inequality is transformed into equality, the drop of the level could be increased to the extent of a total emptying of the surge tank. Therefore the above condition must be fulfilled also for the greatest level drop, i. e. for the lowest head $H_g - r - S_{\max}$ and it follows, that:

$$F > \frac{fL}{2kg(H_g - r - S_{\max})} + \frac{ifL}{\eta_s 2kg}, \quad (394)$$

or for $i = 0$ the following holds good:

$$F > \frac{fL}{2kg(H_g - r - S_{\max})}.$$

6. The Safety Factor

Surge tanks dimensioned according to these considerations, i. e. inequalities just changing into equalities, would operate on the limits of stability. A deviation of the surface once formed would not increase, but would not decrease either. The greater the actual surface area (compared with the calculated area), the more rapid the damping of the level fluctuation.

Generally it is sufficient to multiply the calculated area by the safety factor $n = 1.5$ to 2 .¹⁾ However, in cases of non-uniform load demands in the system which entail frequent changes of flow rate, we must ensure a rapid damping of level fluctuations and the value of the safety factor is increased up to $n > 2$.

IV. CLOSING ORGANS FOR CONDUITS

1. Quick-Closing Device

Turbine feed must be quickly closed particularly in the following two instances:

a) in the event of the turbine unit running at runaway speed caused by a fault of the speed controller,

b) in the event of flood danger caused by a burst spiral or pipe line.

The first possibility must be considered with high-head turbines as well as with low-head turbines. Quick-closing devices may be omitted only in turbines equipped with automatically operated double controls (Pelton turbines controlled by needle and deflector, Kaplan turbines with regulated guide blades and runner blades). If, e. g., the speed of a Kaplan turbine increases above the admissible r. p. m., the emergency governor closes the runner blades regardless to the open guide apparatus. In a similar way in a Pelton turbine the deflector changes the direction of the jet without regard to the opening of the needle. For meeting the first type

¹⁾ See also Jäger: Technische Hydraulik, Birkhäuser, Basel, 1949, p. 228.

of emergency, quick-closing devices are used mainly in Francis turbines. The closing organs are actuated by an electrically connected remote control emergency governor. (A safe source of current must be provided for this connection). It should be noted, that in the case of the turbine running at runaway speed the unit need not be closed instantaneously; according to the valid standard specifications

all revolving parts of the turbine – including the alternator – must withstand the runaway speed.¹⁾ However the runaway speed must be reduced to normal or slightly above normal in a time interval which is of the order of a few seconds or some tens of seconds. Longer runs at runaway speed may cause the bearings to be seized or melted out and thus cause catastrophic consequences.

The second possibility must be considered mainly in high-head turbines. Bursting of pipes or spiral casings occurs only very rarely, because pressure rise during closure is correctly calculated and the minimum time of closure is controlled by the orifice plate in the servomotor pipe. However, this emergency cannot be excluded entirely because faults of material and unforeseen operational conditions may be the cause of bursting. (Air from the pressure vessel penetrating into the servomotor is particularly dangerous in this respect). Fig. 502 shows the consequences of a similar breakdown in a rather small unit.

In the event of a breakdown of the type described, the water feed to the turbine must be closed in the shortest possible time. For this purpose a quick-closing device is mounted at the intake, i. e. a gate at the entrance of the conduit or a valve at the inlet end of the pipe. In the event of a break down, the device is closed automatically.

Quick-closing devices are actuated either by installations reacting when the maximum velocity at the pipe inlet is exceeded (the so called maximal protection), or by those reacting to different flow rates at the pipe inlet and spiral inlet (the so called differential protection). Because the differential protection does not protect the spiral, it is sometimes combined with the maximal protection.

Maximal protection is not suitable particularly in arrangements where a common pipe line carries water to several turbine units. The protection must then be set

¹⁾ See ČSN (Czechoslovak Standard Specification) 085010 – 1951, paragraph 22.



Fig. 502

for a flow rate which is slightly greater than the sum of the flow rates of all turbines running at full load. If, on the contrary, some of the turbines are out of operation, the protection does not react at leakages where the total flow rate is below the value set and great damage can be caused even at this state of leakages. The impulse relays consists of a target plate projecting into the pipe and counterbalanced by a weight

(Fig. 503). For a set velocity the dynamic pressure $k \cdot \frac{C^2}{2g}$ is counterbalanced by the weight of the relays. If the set velocity is increased the lever is slanted, an electric contact is established (battery D. C.) and the quick-closing device is actuated. The principle of the Pitot tube can be applied too.

In the case of differential protection – more advantageous, but hitherto scarcely used – the flow rate at the pipe inlet and the spiral inlet is measured by orifice plates or by Pitot tubes and the results are compensated (electrically or hydraulically) at an equal flow rate. If a greater flow rate is measured at the pipe inlet (compared with the flow rate at the spiral inlet), the quick-closing device is actuated electrically or hydraulically.

Quick-closing devices consist of gates or valves. In both cases opening is carried out by outside energy (electrically), while closure is done either by the own weight of the gate or by a weight mounted for this purpose. Thus closure by gravitation ensures a reliable function of the closing organ; the last phase of the closure is retarded by hydraulic breaking.

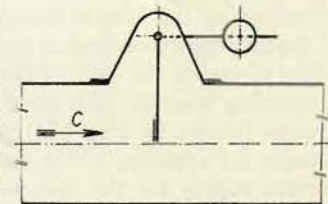


Fig. 503

2. Quick-Closing gates

Low and medium pressure hydro-stations are equipped with quick-closing gates; in high pressure installations these gates are used only when they are built-in into the intake canals (valves are preferred for these installations).

Gates of small dimensions are made of wood and they have an additional weight in order to ensure reliable contact with the seat in spite of the hydraulic lift and friction in the guides existing during closure (when the gate is subjected to water pressure acting upon one side of the gate).

Large gates made of steel ensure a reliable seat contact by their own weight.

The space beyond the gate must have a well designed air-inlet in order to prevent increased stresses in the gate and spiral flume caused by a vacuum by the inertia of the moving water mass (also a disruption of the water column and reflected pressure wave can be caused by the same reason).

Fig. 504 shows the lifting mechanism of a small gate. The gate is lifted mechanically: either by hand or by an electric motor *E*. After lifting, the gate rests upon the support *Z* and the gear coupling *S* of the hoisting mechanism is relieved. When the

necessity arises, the support *Z* is unlocked by remote control and the gate falls downward by its own weight. The fall is retarded by the oil brake *B*, particularly towards the end.

The suspension of the gate is arranged so, that the gate remains suspended as long as the coil of the magnet *M* has a current supply. By breaking the circuit either by a manual switch or by the remote action of the emergency controller the weight *G* opens the lock of the supporting lever *Z*. This arrangement (shown in Fig. 504) is suitable for systems, where the current supply for the magnet coil is not always reliably secured (e. g. current is supplied by the alternator of the turbine set). The gate is thus closed whenever the current supply is cut off. — A reversely acting arrangement is applied in cases where the magnet coil receives current from an independent, absolutely safe source, (e. g. storage batteries). In this arrangement

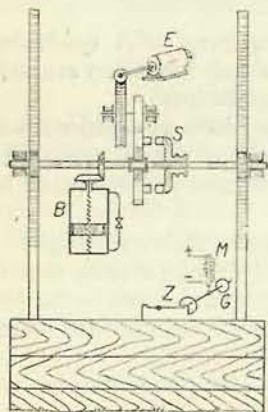


Fig. 504

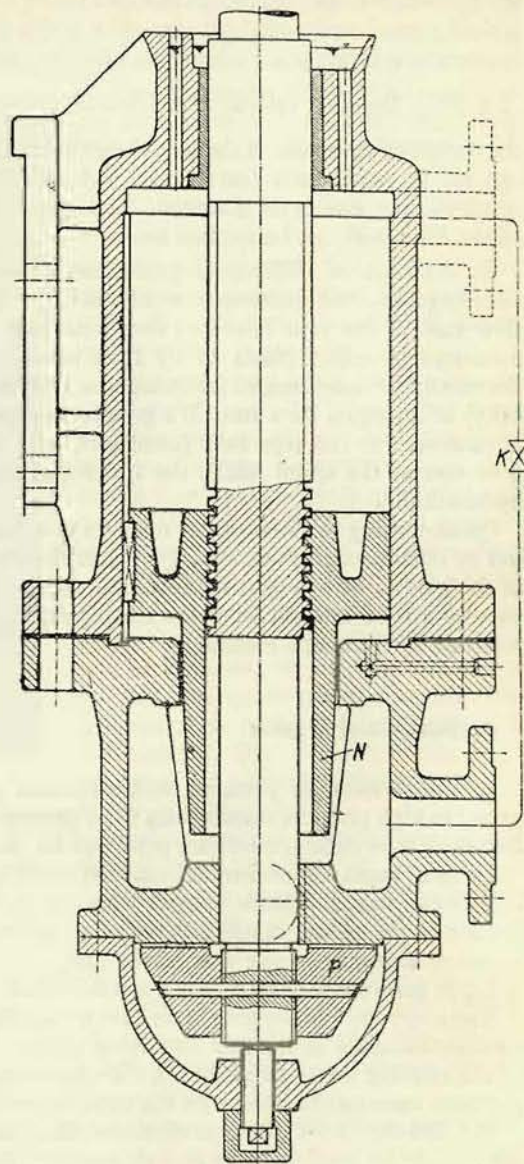


Fig. 505

gement the gate is held in a lifted position when the weight *G* is in a low position. By switching on the current circuit, the magnet is activated, it lifts the weight *G* and the gate is unlocked.

The braking oil dashpot *B* (Fig. 505 – system ČKD Blansko) consists of a piston moved by a threaded spindle and bevel gear driven by the lifting mechanism of the gate. Oil is pressed from one side of the piston to the other and throttled by

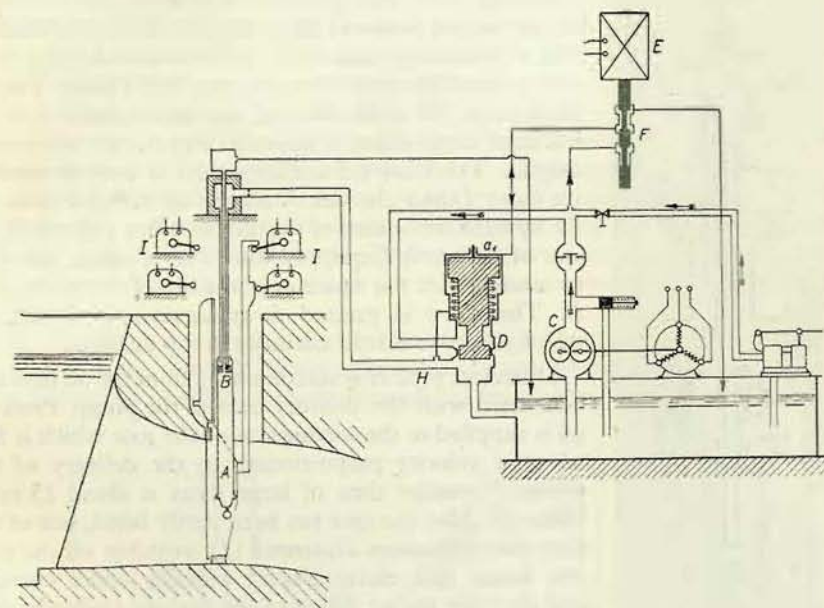


Fig. 506

an adjustable orifice or by the cock *K*. The required falling speed of the gate is obtained by the proper adjustment of the orifice or cock. Near the lower dead-point (which corresponds to the closed position of the gate) oil discharge from the space below the piston is prevented by the piston sleeve *N* and thus the fall of the gate is damped down. The course of oil pressure is checked by a pressure gauge connected to the space under the piston by an indicating boring. Axial forces acting upon the spindle are taken up by the thrust bearing *P*.

It is possible to damp the fall of the gate also by other means: e. g. the Escher – Wyss Works use a gearwheel pump for this purpose.

Hydraulic lifting mechanism are used for the lifting of large gates made of steel. The mechanism is rather simple, does not require large space and develops a considerable lifting force. A schematic illustration of this arrangement is shown in Fig. 506. The lifting cylinder *A* is firmly connected with the gate construction. The cylinder contains the piston *B*, the piston rod is hinged on a rigid construction.

The hollow piston rod serves as an inlet pipe for pressure oil entering the space above the piston and also as a discharge pipe for the leakage oil from the space below the piston. When pressure oil (at 40—90 atm. g.) supplied by the gear-wheel pump *C* enters the space above the piston, the gate is lifted. The gate is closed by discharging the pressure oil through the valve *D*.

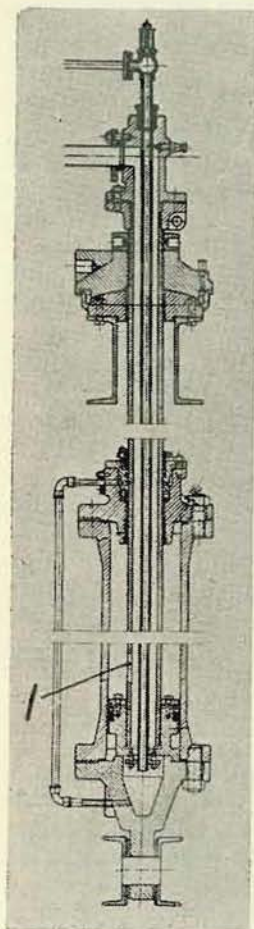


Fig. 507

Lifting of the gate proceeds as follows. By switching on the electric motor of the pump, the coil of the magnet *E* is activated simultaneously and the auxiliary gate valve *F* is moved upwards. For the required closure time of large gates (10 to 20 seconds) the main control valve *D* has large dimensions, if operated directly by an electromagnet. Therefore the auxiliary valve is used to operate the valve *D* and the size of magnet is reduced also. By the upward movement of the control valve *F* the delivery side of the pump (equipped also with a safety valve) is connected with the space a_1 at the top of the main valve *D*. The valve is pressed down against the spring by which the valve is held normally in top position.

Discharge pipe *H* is disconnected from the oil tank and connected with the delivery side of the pump. Pressure oil is supplied to the servomotor of the gate which is lifted at a velocity proportionate to the delivery of the pump. (Opening time of large gates is about 15 to 30 minutes). After the gate has been partly lifted, one of the four circuit breakers illustrated (*I*) switches off the electric motor (the electromagnet remains under current) and the gate stops; filling of the turbine casing begins. After filling has been completed — it is checked in the powerhouse e. g. by a pressure gauge — circuit breaker *I* is switched on again by hand and pumping continues. The gate is lifted to the highest position. In this position the second switch breaks the circuit of the driving electromotor (but not that of the electromagnet). The gate is held in highest position by the pressure of the servomotor oil, because the delivery branch of the pump is equipped with a non-return valve. Because of various leakages the gate begins to descend slowly. After it has been lowered by 10—20 cm the circuit breaker for the

top position is switched on and the gate is lifted again to top position. In this way the gate is maintained open (the secondary pumping takes place in intervals of 10—30 minutes).

The designer must take into account also the possibility that the circuit breaker for the top position is out of order and does not cut off the pump. For this emer-

gency the gate has the possibility to travel to such a height that the piston of the servomotor impinges upon the cylinder lid, the lifting of the gate is stopped and the oil returns through the relief valve into the oil tank. The cylinder lid must be dimensioned so, as to carry the whole lifting force reduced by the weight of the gate.

The remaining two circuit breakers are used for signalisation. One sends optical signals to the power house when the gate is closed and the other signalises the open position of the gate. The "gate open" signal is extinguished even when the gate passes the prescribed limit for the periodical lowering caused by leakages.

Closure of the gate takes place in the following way. The current circuit of the electromagnet *E* and the electromotor is broken by a press button or automatically. No pressure is in space a_1 and the main control valve *D* is pushed to top position by the pressure in pipe *H* and by the spring which holds the valve in top position even if there is no oil pressure in the pipe *H*. Oil is discharged from the servomotor at a speed proportionate to the orifice in the pipe. The gate falls and in the last phase the fall is damped by the braking effect caused by the gradual closing of gate *I* (Fig. 507) in the piston rod. The piston rod passes through the cylinder cover with a protruding sleeve, which at a certain position overlaps the gate *I* of the piston rod.

Fig. 507 shows an actual design of the lifting cylinder (Escher-Wyss). Leather cup sealing of the piston is clearly visible and so is the arrangement for the disposal of the leakage oil as well as the hollow piston rod functioning as an oil pipe. Oil which

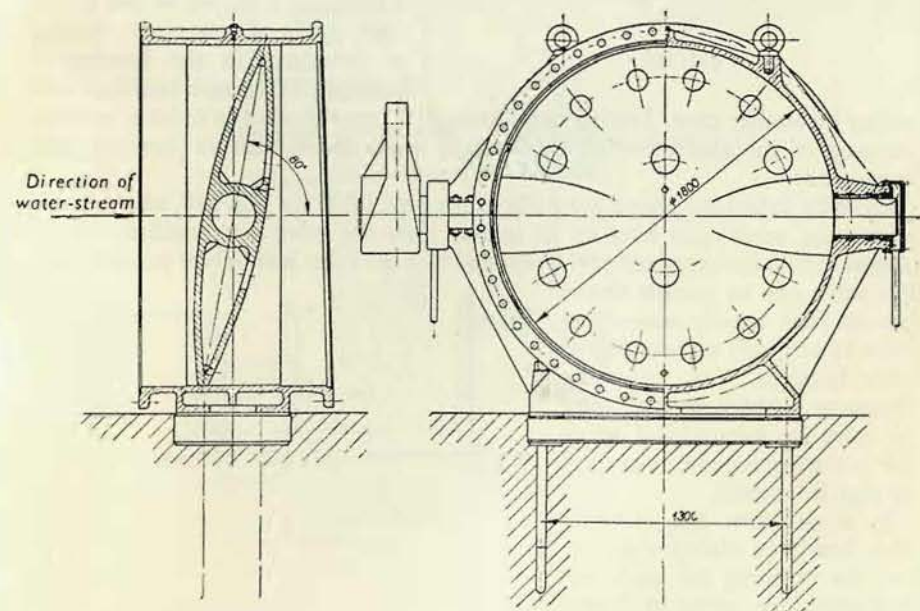


Fig. 508

percolates through the sealing leather cups is removed from below the piston by an inserted pipe which is clearly visible. The piston rod is suspended on a spherical hinge. Sometimes Cardan hinges (ČKD) are used for this purpose.

The arrangement is sometimes reversed. The cylinder is attached to the rigid construction (tiltably) and the piston rod is fixed on the gate (see examples of gate valve arrangements).

3. Quick-Closing Devices for Pipes

Quick-closing devices for pipes are generally made as butterfly valves. (See Fig. 508.) They are in principle lense-shaped discs seated in a split housing which

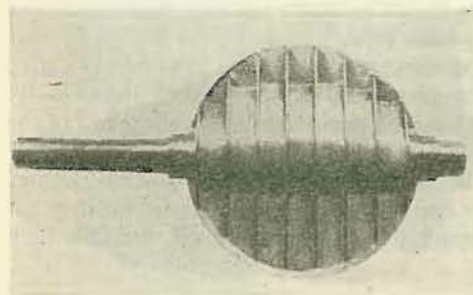


Fig. 509

forms a section of the pipe-line. The lense is either cast (grey cast iron or cast steel) or welded.

It must have a sufficient moment of resistance in order to withstand maximum pressure and for this reason it is cast into a lense shape. Welded valves are reinforced by ribs located in the direction of the flow surfaces – see Fig. 509. The lense is keyed – on to the shaft made of one piece. Seating of the shaft in the housing is arranged in bronze bushings and

sealing by leather cups. Seating must have sufficient clearance in order to prevent jamming of the shaft, caused by bending under water pressure (bending must be checked).

Butterfly valves are placed generally at the pipe inlet, see Fig. 510, and the pipe beyond the valve must have an air intake. Here the valve is exposed to smaller stresses than at the lower end of the pipe and thus the valve is of lighter construction. The valve can be quickly closed (closure time usually amounts to about 10 seconds) without fear of water hammer. The only disadvantage is the fact, that after the valve has been closed water flow to the turbine continues until the pipe is emptied.

In some cases the butterfly valve has been placed close before the turbine; for such arrangements the course of closure must be exactly calculated and

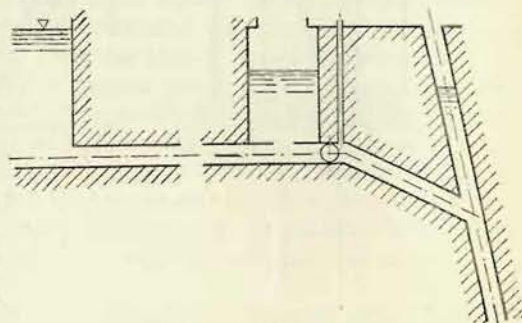


Fig. 510

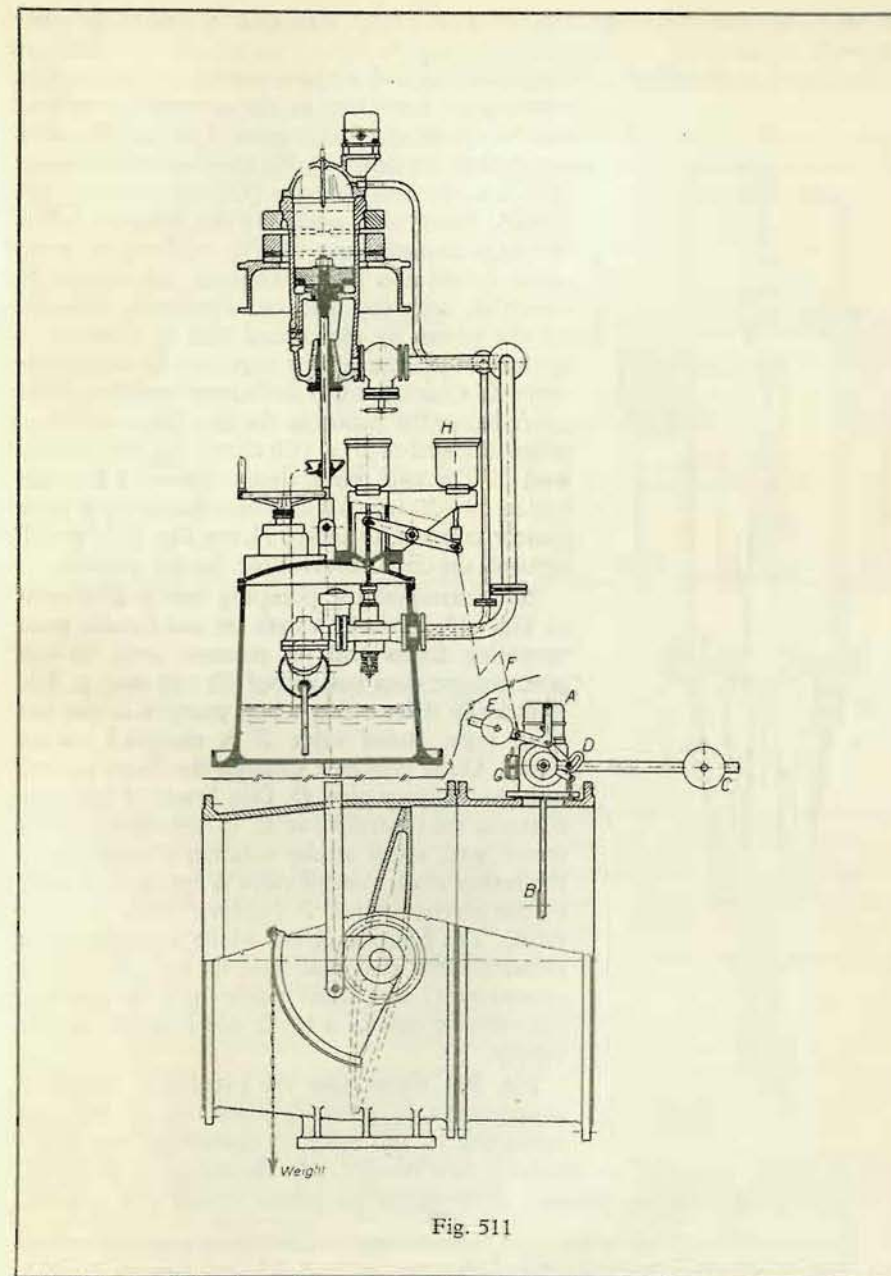


Fig. 511

ensured, because otherwise the valve is easily damaged by water hammer surges.¹⁾

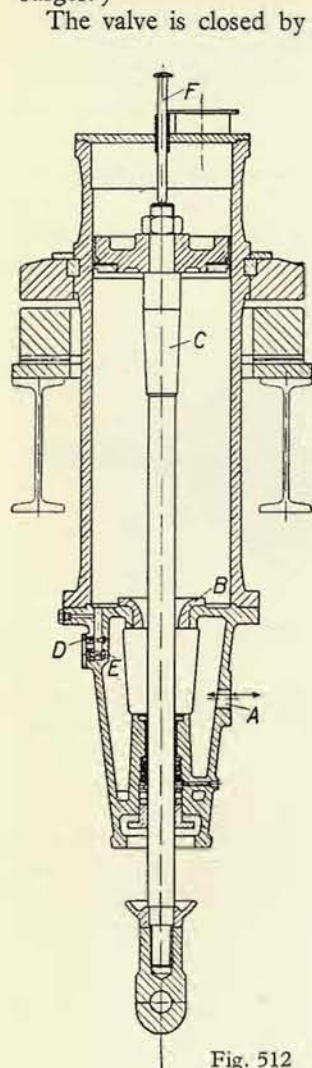


Fig. 512

plate *B* which, in case of an excessive flow velocity, lifts the weight *C*. Weight *C* in a lifted position opens the latch *D* by which the second weight *E* is relieved.

¹⁾ Thomann: Über Drucksteigerung in Rohrleitungen bei Betätigung von Absperrorganen, Wasserkraft und Wasserwirtschaft, 1936.

The valve is closed by a weight and opened by pressure oil by means of a servomotor according to the principle described for the operation of large gates. Fig. 511 illustrates a complete lay-out. Fig. 512 shows the servomotor with a suspended cylinder (Cardan hinge system ČKD). Inlet and outlet of the pressure oil is arranged in the flange *A*. The oil flows from the space below the piston through the orifice *B*, which is, near the dead point position, throttled by the piston by the conical part *C*. Velocity to the end of closure can be regulated by the needle valve *D*. Check valve *E* facilitates the filling of the space below the piston in the first phase of lifting when the orifice *B* is still closed by the conical part *C*. The total falling time of the valve amounting to 10–20 seconds can be adjusted by a valve closely attached to flange *A*, see Fig. 511. Bolt *F* actuates the circuit breaker for the top position.

The corresponding pumping unit is illustrated in Fig. 513. Butterfly valves do not require great operating forces and oil pressure used in this arrangement does not exceed 30–40 atm. g. The electrically driven gear-wheel pump is of the one stage type. Relief valve *B* is mounted on the casing. Oil is delivered through the check valve *C* into the delivery pipe *D*. One branch of this pipe connects the control valve *E*. In this case a servomotor with small stroke volumes is used and so the rather small control valve is operated directly by the electromagnet *F* (without using a pilot valve). The function of the whole arrangement is identical with that described in the case of gate operation. *G* is a hand pump used for opening the valve in case of a break down of the current supply.

Fig. 511 shows also the previously described arrangement of maximal protection of the pipe consisting of the relay *A* containing the target

Weight *E* actuates the control valve by means of the cord *F* and simultaneously transmits an impulse to the electromagnet through the connecting switch *G*. Apart from this, weight *E* actuates also the signalisation. Electromagnet *H* is used for a remote control adjustment of the relay.

Fig. 514 shows a complete lay-out of the intake of a large high-pressure power station. The inlet is protected by racks. The pipe end can be closed for repairs by

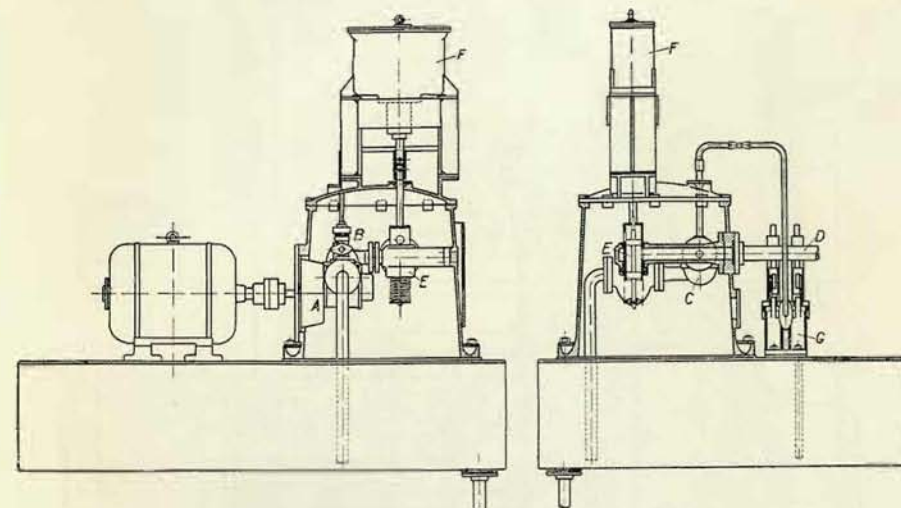


Fig. 513

a blind flange. Beyond the intake an emergency butterfly valve, operated by electric motor and reduction gear, is mounted. Then follows a hydraulically operated butterfly valve. Between both valves a relay is mounted which is an emergency protection for the event of pipe bursting. Mud discharge pipe branches are located beyond each valve. The air intake pipe is arranged behind the quick-closing butterfly valve. The picture of the layout shows also the location of the servomotors, closing weights and pumping units.

For a safe design of the butterfly valve and the operating mechanism we must know the forces developed by the water flow which act upon the valve. We must know these forces in order to determine the moment which the servomotor piston must develop to keep the valve safely in any required position and under any conceivable operational condition without damaging the mechanism of the valve. At first sight it seems, that the lense-shaped disc of the valve is hydraulically well balanced and no moment is formed by the flow around the lense. Further it seems, that reactions in the bearings and friction in them attain their maximum value in the case of a completely closed valve when the force acting upon the valve equals the cross section area multiplied by the difference of pressures on both sides of the valve.

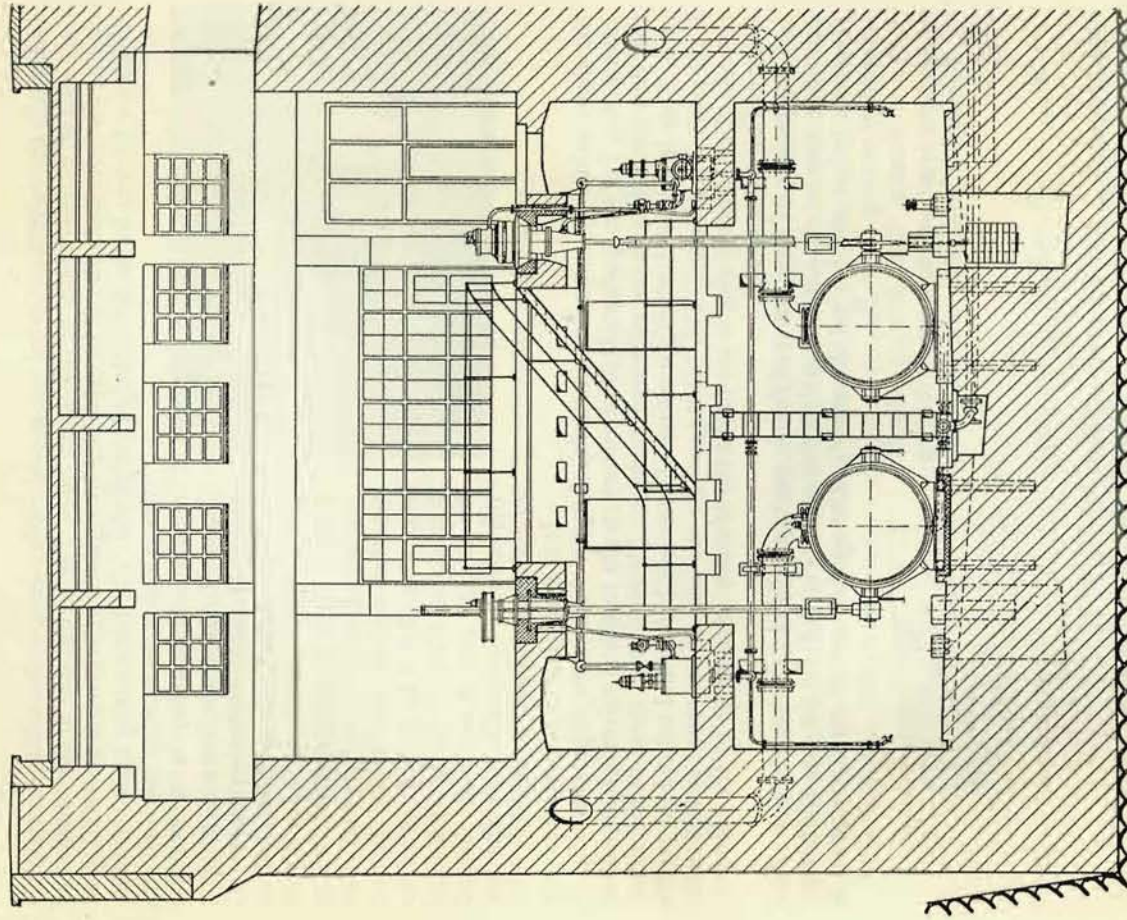


Fig. 514b

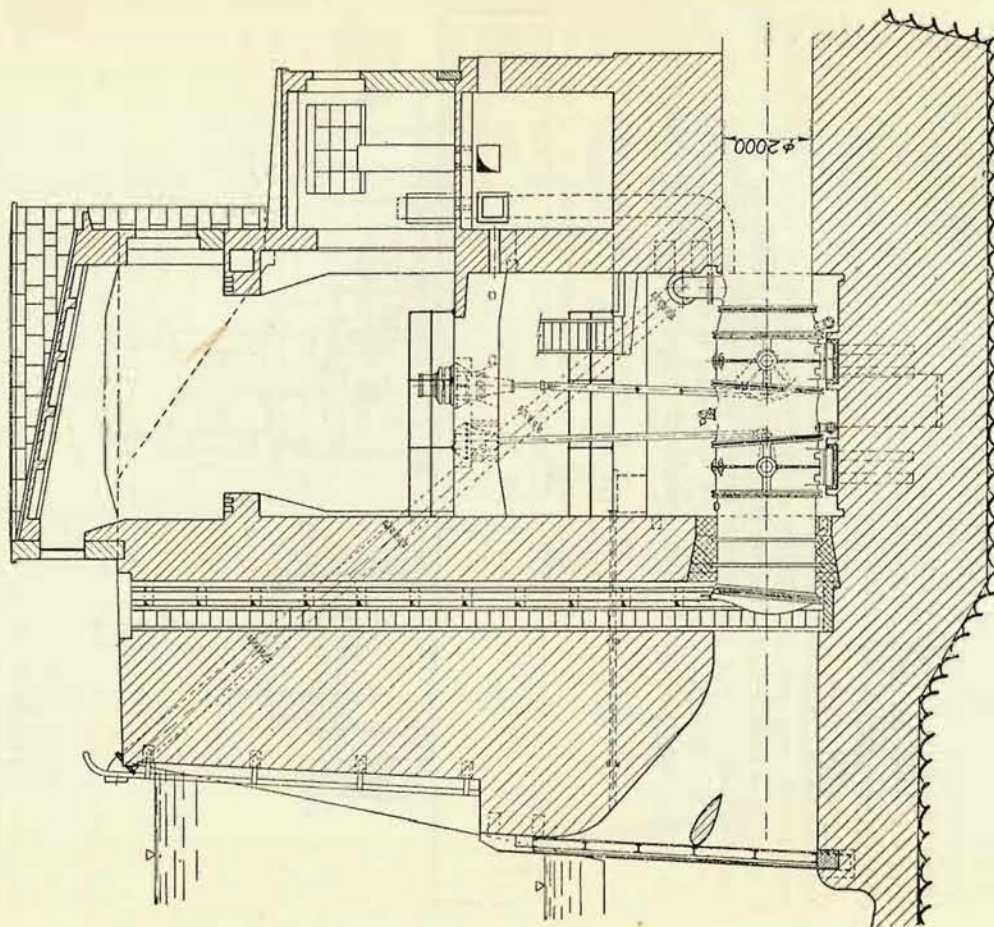


Fig. 514a

Actually the valve is subjected to a considerable torque action which is negligible only with an entirely closed or fully open valve. The torque acts in the direction of closing the valve and this can be explained by regarding the lense as an airfoil upon which the lift acts in the first third of the profile. The force acting upon the valve

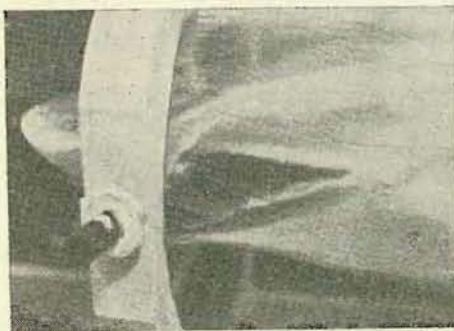


Fig. 515

(from which the bearing reactions are determined) can be, in a position inclined by 45° to the flow axis, greater, than in the completely closed position.

These values, the torque and the force, depend largely upon the conditions of flow. It is important whether the flow around the lense is perfect or whether cavities are formed behind the valve. See Fig. 515. It is of no importance whether the cavity is filled by air (the case of air intake behind the valve) or by water vapour (the case of cavitation behind the valve).

It is impossible to determine exactly the above values by numerical methods, they are determined experimentally in laboratories. For the application of laboratory results to actual valves it is important that flow conditions in the measured model are identical with those in the actual pipe. This is achieved when the course of pressures before and behind the profile is the same in both cases. This holds good for the case of cavitation as well as for the case of air intake (owing to the formation of water vapours or to the compressibility of air respectively).

A comparison of these states of flow is made possible by the introduction of the cavitation number σ^1 . Let us establish this value (Fig. 516) for the case of different diameters before and behind the valve². The special case of equal diameters is covered by putting $D_1 = D_2$.

For a stream line flowing closely around the lense we can write, according to Bernoulli's equation, the following relation:

$$H_{\min} + \frac{V_M^2}{2g} = H_2 + \frac{V_2^2}{2g}. \quad (395)$$

Denotations H_{\min} and V_M represent the pressure and velocity in point M which is the selected point of lowest pressure, the suffixes 2 apply to the cross section D_2 .

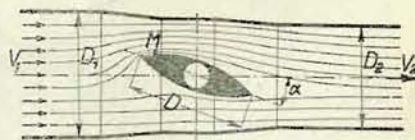


Fig. 516

For similar flows in a model and in an actual valve, the following conditions must be fulfilled:

$$V_M = aV_2 \quad \text{and} \quad \frac{V_2^2}{2g} = bH_k, \quad (396)$$

where values a and b must be identical in both cases.

H_k is the valve head which is defined as the energy difference before and behind the valve increased by the velocity head belonging to the velocity in the cross section of the valve. It follows, that:

$$H_k = \left(H_1 + \frac{V_1^2}{2g} \right) - \left(H_2 + \frac{V_2^2}{2g} \right) + \frac{V_D^2}{2g} \quad (397)$$

$$\left(\text{for } D_1 = D_2 \text{ then holds good } H_k = H_1 - H_2 + \frac{V^2}{2g} \right).$$

We have selected this definition, because the coefficient of the valve resistance is generally related to the velocity head in the valve cross section, i. e.:

$$\xi = \frac{\left(H_1 + \frac{V_1^2}{2g} \right) - \left(H_2 + \frac{V_2^2}{2g} \right)}{\frac{V_D^2}{2g}} = \frac{H_k}{\frac{V_D^2}{2g}} - 1 = \frac{1}{K_D^2} - 1,$$

where $K_D = \frac{V_D}{\sqrt{2gH_k}}$ is the coefficient of velocity.

The second reason justifying this definition is the requirement, that the head defined for an open position of the valve should not be zero, because it could not be used for the calculation of forces and moments acting upon the valve.

From Equation (395) it follows for a minimum pressure:

$$\begin{aligned} H_{\min} &= H_2 + \frac{V_2^2}{2g} - \frac{V_M^2}{2g} = H_2 + bH_k - \frac{a^2 \cdot V_2^2}{2g} = H_2 + b \cdot H_k - a^2 b H_k = \\ &= H_2 - H_k b (a^2 - 1) = H_2 - H_k \cdot \sigma, \end{aligned}$$

where we have substituted $b \cdot (a^2 - 1) = \sigma$, so that it follows:

$$\sigma = \frac{H_2 - H_{\min}}{H_k}.$$

In this cavitation number we can see the analogy of the cavitation coefficient of hydraulic turbines.

If there is no air intake, underpressure is limited by the tension of water vapour, so that the maximum value of $H_{\min} = -H_b$ (pressure is measured as overpressure in relation to the atmosphere), where $H_b = H_B - H_k$, where H_B is the barometric

¹) Ackeret: Experimentale und theoretische Untersuchung über Hohlraumbildung im Wasser, Techn. Mechanik und Thermodynamik, 1936, Number 1—2.

²) Keller, Vushkovich: Strömungsversuche an Sicherheitsorganen von Wasserkraftanlagen, EWAG Mitteilungen, 1942/43 — Hundert Jahre Turbinenbau, p. 191.

pressure (in the water column) and H_t is the water vapour tension at water temperature, so that it follows:

$$\sigma = \frac{H_2 + H_b}{H_k}$$

It has been stated that it is of no importance whether the cavity behind the valve is filled by air or by vapour, so that the cavitation number may be applied also in the case of an air intake. For differently executed air intakes we receive different values of σ .

Figs. 517, 518 and 519 show how the values of the moment M acting upon the valve, the force P (valve resistance) and the flow rate

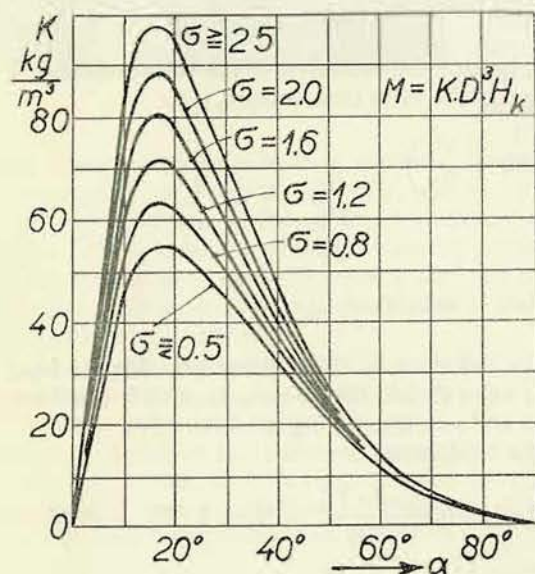


Fig. 517

(expressed by the velocity V_D) depend upon the cavitation number σ . Fig 517 shows the course of the coefficient

$$K = \frac{M}{D^3 H_k}$$

for various openings of the valve ($\alpha = 0$ for a fully opened valve!) and for different values of σ . We can see that at a perfect air intake the value of K is reduced to half (the cavity formed by a perfect air intake is the same as full cavitation, when

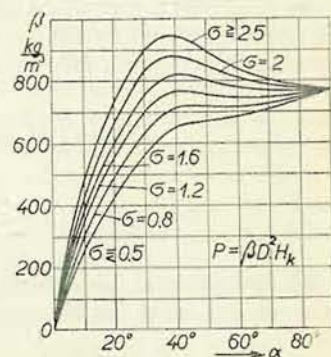


Fig. 518

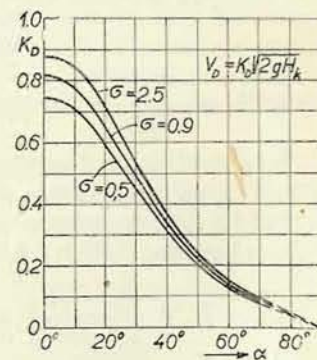


Fig. 519

$\sigma \leq 0.5$). Similar considerations apply to the other values. Therefore, as a matter of principle, the space behind the valve receives a rich air intake, see Fig. 514.

Values included in Figs. 517 and 519 are results obtained from measurements carried out on a valve of a certain shape¹⁾ and we can use them for an approximate calculation of the moment $M = K \cdot D^3 \cdot H_k$, they differ slightly for different valve designs. For an exact determination of these values we must carry out measurements on a model which is geometrically similar to the valve under investigation. The servomotor must be able to evolve a braking effect which safely compensates this moment (acting in the direction of closing) reduced by the bearing friction due to the reactions to the force $P = \beta \cdot D^2 \cdot H_k$. The size of the servomotor is calculated from this moment. The weight used for valve closure in normal operation must produce a moment of the same order, so that the time of closure should not depend upon the flow rate too much.

4. High-Pressure Inlet Valves

Tight closing organs are used in high-head installations and located in front of the spiral casing. Formerly wedge type gate valves were used most frequently for this purpose. These valves are used even to-day by some manufacturers of turbines. They are now, however, hydraulically operated, with servomotors using water from pressure pipes (filtered) as a pressure fluid.

Nowadays plug-valves are used most extensively in Europe. These valves have several advantages: they require smaller space, have better strength properties, need smaller operating forces and thus smaller servomotors and they offer to water a completely uninterrupted passage when in open position.

Fig. 520 shows the section of a plug valve (ČKD). The valve is drawn in a closed position. Flow direction is from left to right, closure is carried out by the plate B which is pressed to the seat in the casing A by the water pressure. The closing plate is seated in the internal rotating plug C which can be turned around the screwed-on pivots D by means of a geared segment and servomotors. Servomotors are operated either by water delivered through filters from the main pressure pipe or by oil delivered by a special pumping unit. In open position the plug is turned by 90° from the position shown in the picture, so that the closing plate is on the top. We can see, that in an open position the rotating plug forms a continuation of the pipe with no hindrance to the flow.

Before the plug can be rotated, the closing plate must be relieved from the seat. If there is no pressure behind the valve, the plate is pressed to the seat by the full pressure and friction is so great, that it is impossible to turn the plug. Generally the valve is equipped with a by-pass, but, owing to leakages existing in turbine installations, it is not possible to equalize pressures on both sides of the plate. Apart from this, there must be a possibility to close the valve in cases of controller failure when the runner of the turbine cannot be closed at all.

¹⁾ Bleuler: Strömungsvorgänge an hydraulischen Drosselklappen bei Hohlrambildung, EWAG-Forschung an Turbomaschinen, p. 31.

The valve is, therefore, designed so, that even if there is no pressure behind the valve, the plate can be relieved and the valve operated.

Fig. 521 shows schematically the method of relieving the closing plate. The space before the plate is connected through the hollow journal of the plug and the pipe (see the dot and dash line in the picture) containing the valve V with the space

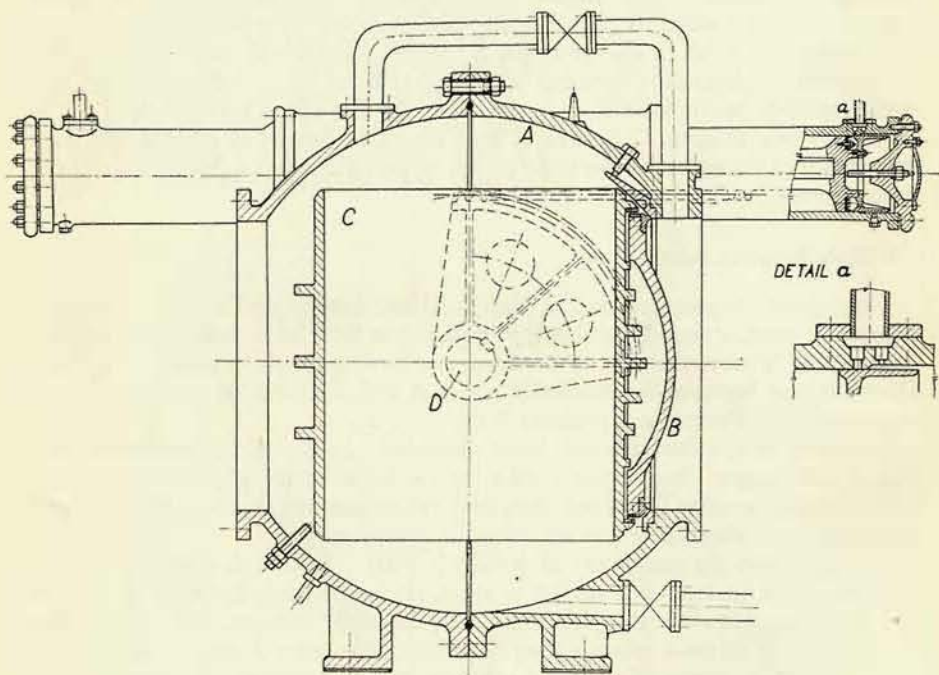


Fig. 520

behind the plate. By opening the valve V in the relief pipe, pressure before the plate is reduced to a lower value h and the force acting upon the plate is reduced considerably. The plate has a larger diameter than the seat. The full pressure of the pipe acts upon the area B (Fig. 521) and this force acts against the force which presses the plate against the seat. If valve V is fully opened the counterforce should be greater than the pressing force acting upon the plate, so that the plate can be fully relieved. For normal operation the valve V is adjusted so, that the pressing force is slightly greater than the counterforce in order to prevent a vibration of the plate¹⁾.

¹⁾ The correct opening of the valve V is established in the following way: at an open turbine the valve, V is gradually opened until the plate begins to vibrate audibly; then the valve is closed so that vibration cannot be heard any more.

In order to relieve the plate, the valve must be designed so that certain surface areas must be in definite relations to each other. The areas concerned are the following: 1. The area of water supply to the space before the plate, i. e. the gap cross section of the plate guide $\pi \cdot \Phi_1 \cdot s$ (see Fig. 521) increased (eventually) by the supplementing gate area of a diameter d , 2. the minimum area f in the relief pipe — this is usually in the duct of the plug, provided that the valve V is fully open;

3. the area upon which the counterforce acts, i. e. $(\Phi_v^2 - \Phi_m^2) \frac{\pi}{4}$. If H is the pressure in the main pipe line and $\pi \cdot \Phi_1 \cdot s +$

$\frac{\pi d^2}{4} = f_1$ the pressure before the plate h (at a fully open relief valve) is thus determined by the following relations:

$$f_1 \sqrt{2g(H-h)} = f_2 \sqrt{2gh}$$

$$\frac{H-h}{h} = \left(\frac{f_2}{f_1}\right)^2,$$

$$h = \frac{H}{1 + \left(\frac{f_2}{f_1}\right)^2}.$$

The pressing force acting upon the plate (at a fully open relief valve) is then:

$$P_1 = \frac{\pi \Phi_m^2}{4} h \gamma,$$

whereas the counterforce acting upon the annular surface B is:

$$P_2 = \frac{\pi(H-h)}{4} (\Phi_v^2 - \Phi_m^2) \gamma.$$

The relief force should be slightly greater, than the pressing force.

If the valve V is closed (at a closed position of the plug) the pressure before the plate is increased through the area f_1 to the initial value H and the bronze sealing ring of the plate is pressed against the bronze seat by the following force:

$$P_3 = H \frac{\pi \Phi_m^2}{4} \gamma.$$

The sealing area should be dimensioned so that the specific pressure:

$$p_3 = \frac{P_3}{\frac{\pi}{4} (\Phi_m^2 - \Phi_t^2)}$$

should not exceed the value 500 kg/cm².

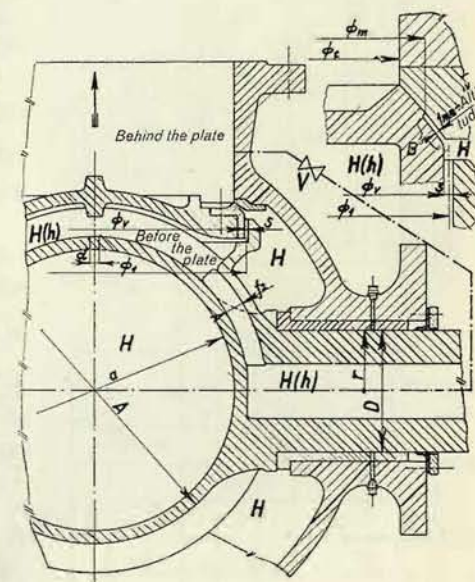


Fig. 521

Thus we can relieve the closing plate so, that no friction opposes the turning of the plug. However the force P_3 formerly taken up by the seat is now transmitted into the bearings. The corresponding bearing friction must be overcome during the turning of the plug. Apart from this the bearings are subjected to hydraulic forces causing a loading of the journals and a torque according to the position of the plug.

Fig. 522 shows diagrams of the values¹⁾: coefficient K of the torque, coefficient K_p of the flow rate, the angle φ of the force P_3 and the coefficient of this force β . All values are shown for different positions of the plug.

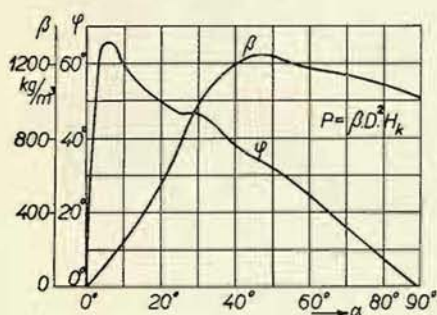
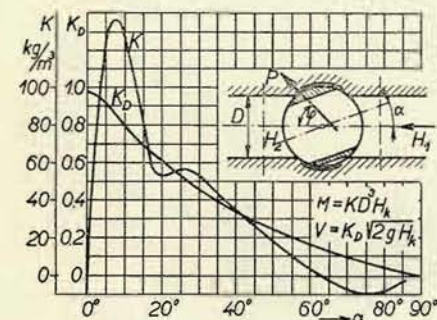


Fig. 522

is very important with regard to water hammer effects if the valve is closed at full flow rate.²⁾

As in butterfly valves, clearances in the bearings must be sufficient to prevent jamming due to bending moments.

¹⁾ Keller, Vushkovich: Strömungsversuche an Sicherheitsorganen von Wasserkraftanlagen, EWAG Mitteilungen 1942/43, Hundert Jahre Turbinenbau, p. 192.

²⁾ When determining the time of closure we must bear in mind that flow rate reduction takes place only during the last third of the closure; until then flow rate remains unchanged and only flow velocity is changed on account of the turbine head. For this reason the total closing time of the valve must equal, at least, three times the critical time determined from the admissible water hammer.

From these values we determine:

the torque $M = K D^3 H_k$,

the flow rate $Q = K_p F \sqrt{2g H_k}$,

The force acting upon the plug

$$P_3 = \beta D^2 H_k,$$

where $H_k = H_1 - H_2 + \frac{V^2}{2g}$, as defined in the case of the butterfly valve.

The rotating plug is operated by hydraulic servomotors (Fig. 520) by means of a geared segment. Pistons of the servomotors have leather cup packings. Time of opening and of closure amounts to about 15–30 seconds and depends upon the area of the orifice in the inlet flange to both chambers of the servomotor. There are two orifices and one is overlapped by the piston when the latter reaches a position near the dead point. The rate of closure of the plug-valve is thus reduced in the last phase. This

V. PRESSURE REGULATORS

Pressure regulators should prevent the formation of water hammer at a rapid closure of the turbine during automatic control. They are used for high heads only; for smaller heads (up to 50–60 m) water hammer can be reduced to an acceptable value by increasing the closure time of the controller and the starting time of the unit (by an increased GD^2 of the set), so that the temporary speed increase remains within acceptable limits also.

With high heads and long penstocks the above arrangements are not suitable and for Francis turbines we use pressure regulators (called also auxiliary discharge or synchronized valve).

Formerly valves have been used which acted as relief valves. They have been actuated by pilot valves and opened an outlet in the spiral casing or in the pipe before the spiral whenever a pressure rise has occurred. However, they acted late, i. e. after the pressure has been increased. This is their marked disadvantage. Therefore in new installations we use valves operated by the regulating ring. If the regulating ring moves in the direction of opening the turbine, the pressure regulator remains out of action. If the control mechanism moves in the opposite direction, i. e. in the direction of closing the

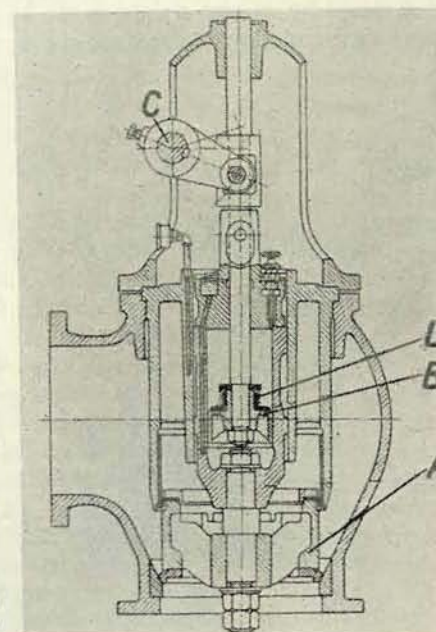


Fig. 523

turbine, the pressure regulator is opened in proportion to the closure of the turbine. The same quantity of water, by which the controller has reduced the flow rate in the turbine is discharged by the pressure regulator, so that the flow rate in the pressure pipe remains unchanged and no water hammer occurs; the pressure regulator is then automatically steadily closed.

Fig. 523 shows a simple design of a smaller valve. The main valve A is completely relieved and demands only small operating forces. The valve has an oil dashpot

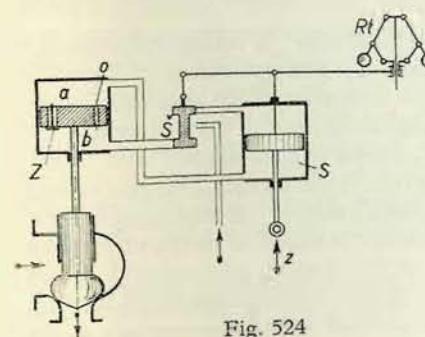


Fig. 524

with piston *B*, piston rod and a crank on the shaft *C*. The piston of the dashpot has a check valve (*D*). Shaft *C* is connected with the mechanism of the controller so, that during closure of the turbine the crank is turned upwards and the piston of the dashpot moves upwards also. Oil moving from one side of the piston to the other is throttled and the valve *A* is lifted. After the crank has stopped, the valve *A* is closed by its own weight or the by action of a spring. When the crank moves downwards, oil flows through the check valve *D*. (Voith's design).

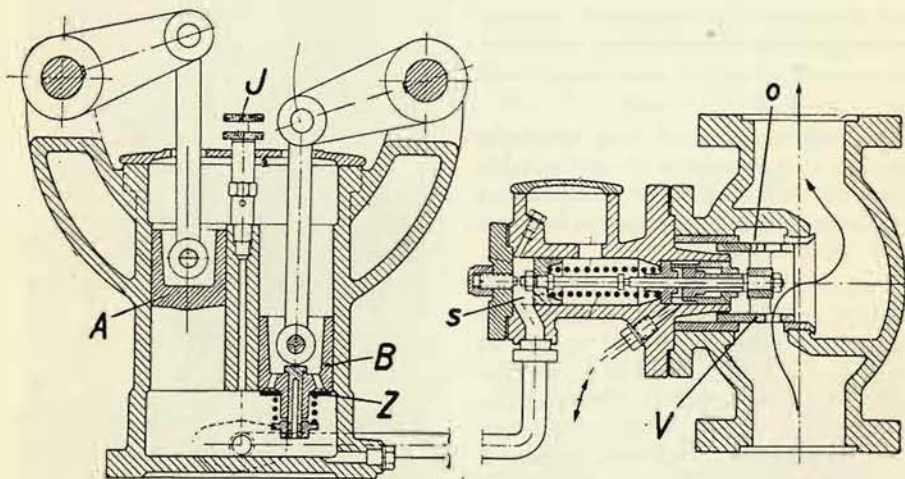


Fig. 525

This arrangement, though very simple, has the disadvantage that in case of a fault of the valve (when the valve does not open) a dangerous water hammer can be formed. For this reason an arrangement is sought where in case of a valve failure the closure time of the controller is increased and the effect of the water hammer reduced. This can be attained with a valve operated hydraulically by a special servomotor.

An example of a similar "interlocking of the controller" is illustrated schematically in Fig. 524. (Design of Ateliers Charmilles). *S* is the servomotor of the guide apparatus of the turbine, *Rt* the governor of the controller, *S* the gate valve of the governor. The restoring mechanism between the servomotor of the turbine and the floating lever of the governor is, for simplicity, drawn as a stabilisator with droop, though actually it is an elastic compensating device. It can be seen, that gate valve *S* can supply pressure oil directly only to the opening side of the servomotor. Pressure oil to the closing side of the turbine servomotor is supplied by the servomotor of the pressure regulator. If the turbine is to be opened, gate valve *S* moves upwards and pressure oil flows to the opening side of the servomotor of the turbine. Oil from the other side of the servomotor *S* is pressed into the servomotor of the

pressure regulator, it flows freely through the check valve *Z* to the control valve *S* and hence to the discharge tank. If the turbine is to be closed, pressure oil from the control valve *S* flows to the opening chamber *b* of the servomotor of the pressure regulator, the latter starts to open and oil from the chamber *a* is pressed to the closing side of the turbine servomotor *S* which in turn starts to close the guide apparatus. After the movement has been completed the pressure regulator returns to the closed position by its own weight or by an additional (generally hydraulic) pressure, because the small communicating gate *o* in the piston of the servomotor permits the flow of oil from one chamber of the servomotor to the other. It is obvious, that in this arrangement the guide apparatus cannot be closed without a prior opening of the pressure regulator, except the closure at a very low velocity proportionately to the flow rate through the gate *o*.

A disadvantage of this arrangement lies in the fact, that the relation between the strokes of both servomotor is different from the relation between the quantity of water discharged by the pressure regulator and that eliminated by the closure of the guide apparatus. The flow rate of the pressure regulator is related to the stroke of the servomotor by a different relation, than that expressing the dependence of the flow rate of the guide apparatus; the respective water quantities are bound to be different and some water hammer effect appears.

Fig. 525 shows another arrangement of interlocking which eliminates the above described disadvantage. The valve illustrated on the right hand side of the picture is inserted into the oil pipe of the turbine servomotor. In the position shown in the picture oil passes without hindrance through the large gates of the closing cylinder *V*. In closed position the large gates are overlapped and oil can pass only through the small opening *o* and this means a prolonged time of closure. The valve is actuated by the device shown on the left hand side of the picture. The device has two pistons; piston *A* is moved by the mechanism of the turbine controller and the second piston *B* is actuated by the piston of the pressure regulator. During closure of the turbine piston *A* moves downwards; if a simultaneous opening of the pressure regulator takes place, piston *B* moves upwards. Stroke volumes are mutually compensated, so that no oil is pressed from the piston chambers to the servomotor *s* of the interlocking valve. If the pressure regulator is not opened, oil is pressed into the servomotor *s* of the valve, the interlocking valve is closed (the lift is limited by an overflow gate) and the movement of the turbine guide apparatus is slowed down. During opening of the turbine the pressure regulator remains in position, piston *A* moves upwards and oil is recirculated through the check valve *Z* of the piston *B*. In order not to waste pressure water, pressure regulators are generally adjusted so, that they do not open at small movements of the shifting ring of the turbine (a pressure rise of 20 % is allowed); the by-pass with the adjustable needle valve *f* prevents in this case a premature interlocking of the turbine controller.¹⁾

Appendix VIII is a drawing of a large size pressure regulator designed and manu-

¹⁾ This method of interlocking the controller is purposeful only in case that the time interval from the start of closing the controller to the shifting of the interlocking orifice is shorter than the time T_{sl} (see Fig. 482).

factured by the ČKD Works. Water is lead into the bulb-like casing of the valve.

The outlet opening of the valve is closed by a needle similar to that used in Pelton turbines. The nozzle is exchangeable and permits dismantling after excessive wear. The discharge space behind the nozzle, into which the water jet is directed, is intensively aerated in order to prevent cavitations which cause strong shocks.¹⁾ The jet is aerated in a cylindrical chamber containing the orifice of the air intake

pipe. The bulb-like chamber must be connected with the air chamber and discharge pipe by joints which withstand the force evolved by the reaction of the water jet. The needle has a bronze sleeve and is seated in bronze bushings equipped with tecalamite grease lubricators. Packing is provided by two leather cups.

The needle is connected with the piston rod of the oil operated servomotor. The piston rod passes through the lid of the servomotor cylinder and is connected with the restoring mechanism of the controller located separately on the ground floor of the power house. The pressure regulator is mounted in the basement of the power house.

In closed position the needle is pressed by the oil pressure to the seat of the nozzle. The joint of the nozzle must be dimensioned to withstand this force. The controlling mechanism of this pressure regulator is illustrated in Appendix IX. The movement of the restoring mechanism of the turbine controller is transmitted to shaft 1. The movement is transmitted by a slotted link which we shall describe later on. To shaft 1 a lever carrying the oil dashpot 2 is keyed on. Transmission is arranged so, that during the opening of the turbine the cylinder of the dashpot 2 moves downwards. Underpressure is created underneath the piston 3 which separates from the plate valve 4 and

through the gap thus formed oil flows freely from the space above the piston into the space below it. Lever 5 remains in position. If the turbine is closed, cylinder 2 moves upwards, oil communication does not exist and piston 3 as carried upwards. By this the left end of lever 5 is lifted. As pivot 6 is the floating fulcrum of the lever 5, the right end of the lever moves downwards and control valve 7 is pushed downwards too.

Control valve 7 opens the inlet of pressure oil or pressure water to the opening side of the servomotor of the pressure regulator, the closing side is connected to the discharge and the pressure regulator begins to open. Pressure oil flows from

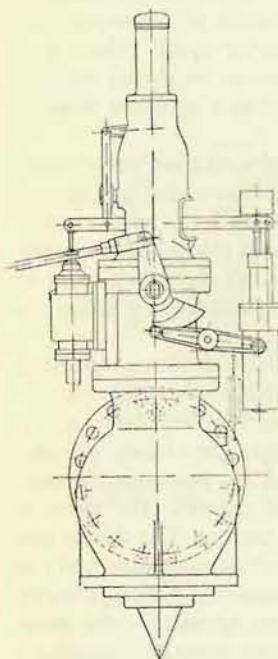


Fig. 526

¹⁾ See also Kratochvíl: Kavitační zjevy u výpustného potrubí a uzávěrů přehradních. (Cavitation phenomena in discharge pipes and dam gates). Stroj. Obzor, 1937. Nos. 7 and 9.

the air pressure vessel of the pumping unit (similar to the pumping unit of the turbine controller). Pressure water flows from the main pressure pipe. (This applies in cases where the pressure regulator is operated by a servomotor using pressure water as an operating fluid. The pressure water supplied from the main pipe is filtered before it enters the servomotor. This system is used for smaller pressure regulators and with water containing no scale.).

Note: It is worth while to note, that the control valve is operated by a pilot valve (as in large controllers), because of the great dimensions of the control valve; smaller control valves are operated directly by the floating lever.

Simultaneously with the pressure controller also the restoring mechanism 8 begins to move and the slotted link 8' actuates a system of levers which in turn move the fulcrum 6 in an upward direction and so the control valve 7 is always returned to the neutral position. This means that a given degree of closure of the turbine corresponds to a certain opening of the pressure regulator.

If the closure of the turbine stops, the cylinder 2 of the dashpot stops too and the pressure regulator is no more opened. Weight 9 presses the piston of the dashpot downward and valve 10 in the piston of the dashpot is opened by the lever 5, oil flow from the lower part to the space above the piston, the piston descends steadily and the pressure regulator is closed again. The closing velocity depends upon the flow area of the valve 10 and it can be regulated by inserting a suitably dimensioned lug into the valve 10. In this arrangement (ČKD design) the by-pass is opened only after the pressure regulator has been opened. By this we can reduce or adjust the slip of the pressure regulator, i. e. the stroke of the controller mechanism at which the pressure regulator remains still closed. Frequently the valve 10 has a constant flow area. Time of closure of the pressure regulator is 20 to 60 seconds according to the length of the pipe.

Further we can see that the stroke of the control valve can be adjusted in the closing direction by the nut 11. The adjustment is arranged so, that under no circumstances (not even at a break down of the lever system which actuates the control valve) can the pressure regulator close more quickly than the adjustment permits. Controllers of high pressure turbines are generally so adjusted, that opening time is twice as long as the time of closure. The adjusted time of closure of the pressure regulator equals then the opening time of the turbine, i. e. the double time of closure of the turbine. By this arrangement the water hammer effect, occurring in the case of an unexpected break down of the operating mechanism of the pressure regulator, is considerably reduced.

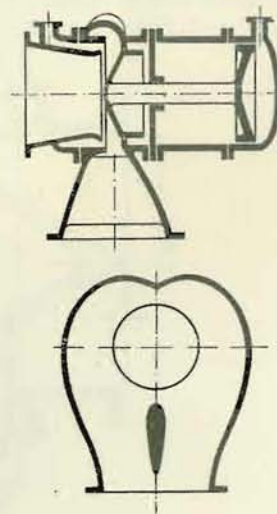


Fig. 527

The picture shows also the interconnecting arrangement described before according to Fig. 525.

Shaft 12 revolves due to the movement of the mechanism of the pressure regulator. Shaft 13 revolves due to the movement of the controller mechanism of the turbine. (The above mentioned slotted link is keyed on this shaft.) Owing to the different stroke volumes the surplus oil actuates the auxiliary gate valve 14 through which pressure oil passes from the air pressure vessel of the pumping unit to the closing side of the servomotor of the interlocking orifice.

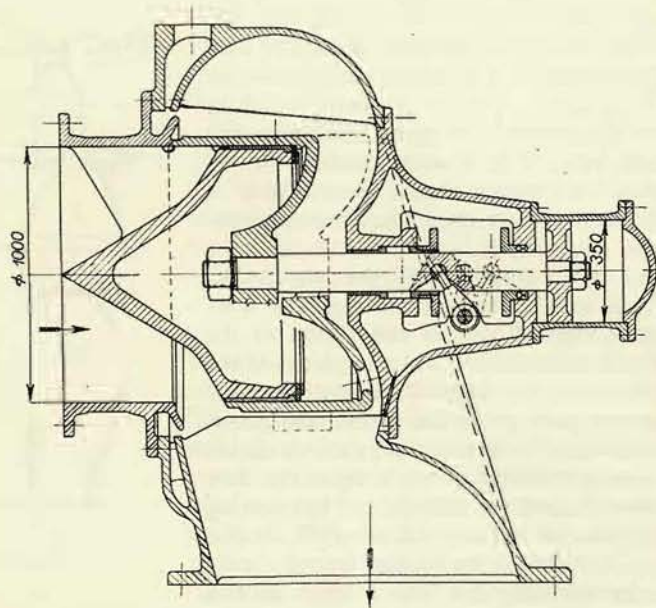


Fig. 528

Fig. 526 shows the assembly of a smaller pressure regulator operated by pressure water. The control valve of the servomotor and the operating mechanism are combined into one unit. Particularly well visible are: the slotted link, the operation of the dashpot and the drive of the slotted link (by the controller shaft).

In spite of the fact, that relation between flow rate and stroke is different for the turbine and for the pressure regulator a suitably shaped slotted piece permits to arrange that the pressure regulator discharges the same quantity of water as eliminated by the closure of the guide apparatus.

In pressure regulators just described (arranged as Pelton nozzles) the rather large chamber is under full pressure and is very heavy owing to the particular shape causing an unfavourable distribution of stresses. Therefore pressure regu-

lators are produced presently where the direction of flow is reversed and the chamber is thus relieved.

Fig. 527 is a schematic illustration of this design (Escher-Wyss). Pressure is applied to the cylindrical part which is very suitable from the point of view of stress distribution and the chamber is used only for the collecting of splash water. Water flow is transformed into a shape of two vortex streams, by which the kinetic energy of water is suitably destroyed.

Fig. 528 shows a similar modern pressure regulator (ČKD). The valve proper is hydraulically entirely relieved, so that minimum operational force is required. The servomotor has also small dimensions and no separate pumping unit is needed for the oil supply. Pressure oil is delivered from the air pressure vessel of the controller.

STARTING OPERATION AND GUARANTEE MEASUREMENTS

I. STARTING OPERATION

Turbine unit and equipment properly assembled are generally neither tested for proper functioning nor exactly adjusted. Only controllers and oil pumping units are adjusted – as far, as it is possible – in the manufacturer's workshop, but they must be also tested for proper functioning after their installation has been completed.

As protecting devices (pipe protection, etc.) are also not adjusted, we must proceed with great care and consider the safety of the personnel present as well as the safety of machinery and equipment. First of all we shall carry out all adjustment which can be completed with the turbine at a standstill and at a closed water flow. Operation will then start with the plant partially adjusted, so that no catastrophe can occur by starting the unit under operating conditions. Final tests and adjustments are made on the running plant.

Safety devices and emergency installations are prepared and adjusted first. Before the conduit is filled with water, the quick-closing device is put into operation, closing and opening times are set and its remote (from the power house) and local (in the intake object) controls are tested and adjusted. Times of closure and opening of the controller and of the pressure regulator are set and tested before the turbine is put into operation. Air intake of the draft tube is checked at the same time. Emergency installation for excessive speed regulation is adjusted at least to such an extent that it function by manual actuation, because we cannot yet adjust the emergency governor for the maximum admissible speed.

The procedure of starting operation is explained for the following cases:

A. *High-pressure plant.* Apart from the turbine set proper, the plant consists of the following equipment; quick-closing device at the intake (generally a butterfly valve), plug valve at the turbine inlet, controller, eventually controller with a separate pumping unit for pressure oil, in the case of Francis turbines pressure regulator operated by pressure water or by pressure oil from a separate pumping unit. The pressure oil supply may serve also the operating mechanism of the plug valve or the pressure regulator may have a common oil supply with the controller. Large plants have separate pumping units for bearing lubrication and compressors for the air pressure vessels of the pumping units.

An emergency closing organ is normally mounted in the upstream direction from

the butterfly valve at the tunnel entrance or at the orifice of an open canal. The function of this organ is tested „in a dry state“, without water.

First of all the electrical part of the quick-closing device is tested. The coupling between the electric motor and oil pump is disconnected. We ascertain if the electric motor and electromagnet are operated in the proper direction by the impulses prescribed, if the electric motor stops by lifting the circuit breaker for the filling position and the top position (see chapter C-IV). If the electric installation is in order, the electric motor and the pump are connected. The spring of the relief-valve is completely relieved and the pump is started by pressing the proper button. After the pump has been started, the spring of the relief-valve is gradually put under stress and oil pressure is increased to the value required for the opening of the butterfly valve.

The prescribed time of closure is set on the orifice in the pipe (see Part III, Chap. C-IV). The opening of the orifice for the first test can be determined from the relation for the flow velocity:

$$V = \varphi \sqrt{2g \frac{p}{\gamma}}$$

Where p is the pressure in the servomotor; flow coefficient φ is taken at a value of about 0.7. The first closure is carried out from the filling position. Braking during the final phase is adjusted and by a pressure gauge (connected with the space below the servomotor piston) we check the pressures evolved. In the case of adjustable orifices, the set opening is safely secured.

In this way we test „in a dry state“ the complete function of the quick-closing valve and particularly the closure after pressing the respective push buttons.

Closure in case of pipe failure is also tested – the necessary impulse movement is initiated by hand.

Finally the relief-valve is set for a pressure calculated for the case of full water pressure acting upon the lense of the butterfly valve or the gate. For this purpose the circuit breaker for the top position is over-bridged and the piston is pressed up to the upper flange of the servomotor or the servomotor pipe is closed by a blind flange. If a hand operated gate valve is inserted into the pipe, the operational pressure is adjusted, the valve is opened again and its position is firmly fixed so that it cannot be closed (not even by a mistake of the attendant). Final oil pressure can be adjusted also during the opening of the butterfly valve when the pipe is first filled with water.

After the intake valve has been adjusted and tested, the pipe is not filled with water until the plug valve at the downstream end of the pipe has been adjusted and tested. This test must be carried out also at a de-watered pipe (at least if the valve is operated by pressure oil). The main task here is the adjustment of the time of closure established according to the directions described in Chapter C-IV.

If the servomotor of the plug valve is operated by pressure water, the pipe must be filled with water prior to the valve test.

Filling of the pipe can start only after we have ascertained that the plug valve is

in a closed position and its relief, by-pass and mud valves are closed. At the same time all auxiliary water off-takes are closed. Filling starts by opening the butterfly valve into filling position and proceeds slowly; simultaneously pipe expansion and flange tightness is checked along the whole pipe. After the pipe has been filled, closure time of the butterfly valve and function of plug valve are checked again. In the latter we must adjust now the relief installation of the closing plate (see Chapter C/IV - 3).

When the plug valve is tested and the pipe filled with water, the turbine must be ready to start, because selfstarting can occur if the pull rods of the regulating ring are not set right. Selfstarting, therefore, can occur even if the regulating ring is properly secured in a closed position.

Therefore all bearings are filled with oil and the lubricating installation is tested prior to the filling of the pipe. It is recommended to rinse the bearings for several hours by operating the lubrication system. After this rinsing, oil is to be filtered before it is returned for operation.

As far as controllers are concerned, most important is the adjustment of the correct time of closure and opening. Small size controllers, where all parts are built in one unit these times are usually adjusted in the manufacturer's shop and adjustment on the spot is not necessary. If the oil pump of the controller is driven by the main shaft, a provisional electrically driven pump is installed for testing-purposes.

Times of large size controllers with separately located servomotors are generally adjusted after mounting in the power house. Adjustment is carried out either by limiting the stroke of the control valve or more suitably by inserting orifice plates into the pipe which connects the control valve and the servomotor. Checking is done either by a sudden movement of the governor sleeve from one extreme position to the other or by adjusting the pilot valve of the control valve. At this occasion the pilot valve is disconnected from all operating levers. When adjusting the governor sleeve (or the pilot valve of the governor), the restoring mechanism is disconnected or its acceleration is set for a value $\beta = 0$, so that the time of closure and opening were not prolonged by the influence of the feed-back.

It is obvious that prior to the above tests the pumping unit of the controller is put into operation and the required quantity of air is delivered to the pressure tank either from a permanent compressor (if installed for this purpose) or by running the unit for a time sufficiently long to build up the air content by quantities supplied by the air chamber of the unit. All controller times are set at the final operational oil pressure.

Governor speed droop and neutral position of the governor sleeve are normally set and adjusted in the factory. We must adjust, however, the acceleration of the restoring mechanism, the value of which can be easily determined from the ratio of transmission. Falling time of the isodrome must be also adjusted; it is calculated as the time in which the displaced piston of the isodrome falls by one third of the displacement.

Times of the pressure regulator are equally important, they must be properly

adjusted and the function of the valve tested. If the pressure regulator is operated by pressure water, the water is drawn from the inlet pipe in front of the plug valve, to enable it.

In pressure regulators we adjust first of all the operational time (see Chapter V) of closure which is about 20 to 60 seconds (with regard to the starting time of the pipe). The closure time is adjusted by the oil dashpot. Further we adjust the minimum time of closure which equals the opening time of the turbine. This time is adjusted by an orifice between the mechanism and servomotor or by limiting the stroke of the control valve. This minimum time guarantees, that the pressure regulator will never close in a shorter time (not even if the operating lever system is out of order) and so no damaging of the pipe can occur.

The pressure regulator is tested also in co-operation with the turbine. The turbine is quickly closed and opened by the controller and the function of the pressure regulator is observed simultaneously. We use the characteristics of the turbine and the pressure regulator to establish the relation between the opening of the pressure regulator and closing of the turbine in order to secure that the same quantity of water is discharged by the pressure regulator as eliminated by the turbine. In this way it is possible to check the shape of the slotted link of the pressure regulator.

With Pelton turbines closing and opening times of the deflector are adjusted (they equal about one second) as well as the closing and opening times of the needle. Closing time of the needle is according to the length of the pipe 15 to 30 seconds. Opening time is selected so, that pressure reduction should not exceed 30 %.

After having completed the above tests, we begin to fill the spiral and start the turbine. The lubricating system, the pumping unit of the controller and that of the pressure regulator are put into operation before the spiral is filled with water. After the spiral is filled and de-aerated, the guide apparatus is opened by the controller, and the runner is started at one third of the rated speed. The starting speed must not be lower, because a lower speed does not guarantee the formation of an oil film on the sliding surfaces of the thrust bearing. At this first test run the thermometers of the bearings are observed and temperature curves (plotted against time) are drawn. With bearings properly functioning the rate of temperature rise must decrease with increasing temperature. If the temperature rise does not follow this rule or if the temperature of a bearing rises too quickly, the test run must be interrupted and a close inspection of the bearing must take place. After the operating temperature of the bearings has been reached, the flow rate of cooling water for the oil is adjusted and speed is step by step increased up to the rated r. p. m. The turbine is then running for several hours in order to observe the stabilisation of all temperatures.

The turbine can be considered as run-in; now the safety governor is adjusted for a speed increase of 6—10 % above the value of the supposed temporary speed increase for a full load rejection. During testing the governor is disconnected from the operating parts of the emergency installation in order to avoid frequent stops of the turbine. After the adjustment of the governor is completed, the whole function of the safety installation is subjected to a final test, including the shut down of the turbine.

Then usually follows the drying of the alternator winding and exciting to the rated current value. The time spent for testing the alternator is utilized for a simultaneously observation of the automatic control and its adjustment at a no-load run. After the alternator has been dried and the protections adjusted, circuit breaking tests are carried out, during which also the function of the controller is tested.

During these tests the set is loaded by a specially built water resistance or by the actual net (if this is feasible). The alternator is loaded and then cut off by a switch from the resistance or network and the run controller is observed. Speed changes are recorded by a tachograph, pressure changes in the spiral are recorded by a pressure recorder; the controller is adjusted accordingly (acceleration of the restoring mechanism and falling time of the isodrome). Tests start with a load of about 25 % which is increased step by step up to the full rated load. If the set is loaded by a water resistance and during the test the alternator is suddenly connected to the resistance, these tests are carried out to a 50 % load.

After the circuit breaking tests it is necessary to adjust the pipe protecting installations. In the case of a maximal protection all machines connected to a common pipe line are brought under full load and the flow rate is still increased by opening the pressure regulator. The protection must properly operate even under these conditions. If no pressure regulator is installed in the plant, protection is adjusted so, that its function is secured at a maximum load of all machines working at the same pipe branch and afterwards the compensating weight is shifted by about 20 % from the fulcrum of the lever.

B. Low-pressure plants. The testing procedure is based upon the same principles. Adjustment of the pressure regulator is omitted. However, with Kaplan turbines we must test the slotted link which interconnects the setting of the runner blades with that of the guide blades. This adjustment is made again "in a dry state". Time of closure of the runner is set (see Chapter A-III) to about 60 to 120 seconds.

Function of the air supply valves for the aeration of the draft tube must be carefully checked. Times of closure and opening of the guide apparatus are tested simultaneously.

These are carried out at a closed intake gate or quick-closing device. Adjustment of the quick-closing device is carried out only after the turbine is ready for starting. At the time of adjustment water in the forebya is usually at a high level and during manipulation of the gate water is let into the turbine casing. Therefore we must be prepared for an unforeseen start of the turbine. After adjustment and testing of the quick-closing device all tests and inspections are carried out in the same order as in the case of high-pressure plants.

After terminating the switching tests of the controller, the wheel for setting the control valve must be adjusted to a value corresponding to maximum load at slightly increased frequencies, so that it is not possible that the wheel for setting the speed control valve reaches a position at which the controller would not close. Also the servomotor of the guide apparatus must be adjusted to a stroke corresponding to maximum output of the turbine (at lowest operational head).

II. GUARANTEE MEASUREMENTS

Apart from controller switching tests also output, head and flow rate are measured in the course of guarantee tests. These value are needed for efficiency calculations. Methods and evaluations of measurements are prescribed by the Czechoslovak Standard Specification ČSN 085010-1951. Therefore we shall not discuss these tests in detail. We shall present only examples of measurements carried out in large power stations where special and expensive adaptations were made for this purpose.¹⁾

One of the most important measurements is the determination of the head. We must measure also the position of the ground-water level. If the ground-water level beyond the draft tube is not calm, but changes irregularly due to the outlet from the draft tube, measuring grids are suspended and placed upon the level; their basic position is determined by levelling of their top plane. Distances from this basic position are measured by marks on the ropes when the grids are suspended in a position, at which water in the grid openings is at level with the top plane of the grids. Fig. 529. illustrates such arrangement schematically and Fig. 530 shows an actual measurement carried out in a large power station. In larger power station three grids were used for a simultaneous measurement.

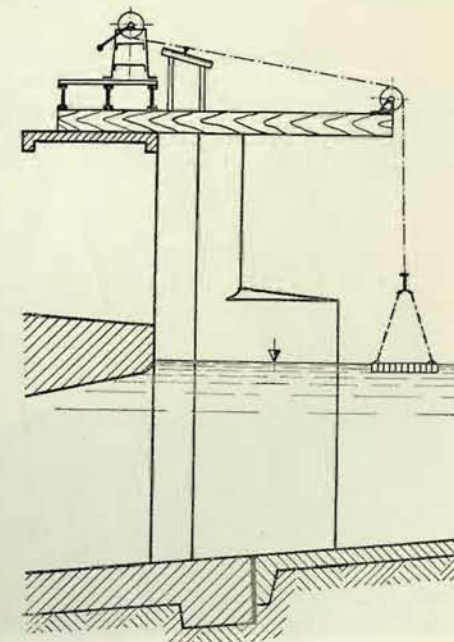


Fig. 529

Flow rate is measured most frequently by measuring propellers. In large plants measurements by one propeller suspended on a rod are not sufficient, because deep water is involved and measurement takes a long time. Therefore a special cart travelling on rollers is used. The rollers are placed in slots of the pillars of the intake structure. Fig. 531 illustrates a cart with mounted propellers. In this particular case seven propellers were used, lowered into different positions determined before the operation of the cart had started.

¹⁾ A. Wasserbauer: Zkoušky na velkých vodních elektrárnách. (Testing in large hydraulic power stations). Strojnický obzor 24 (1944) No 7, p. 99.
J. H. Lieber: Procédé de jaugeage d'une installation à basse chute et gros débit. Informations techniques Charmilles, No 2 (1947), p. 36.



Fig. 530

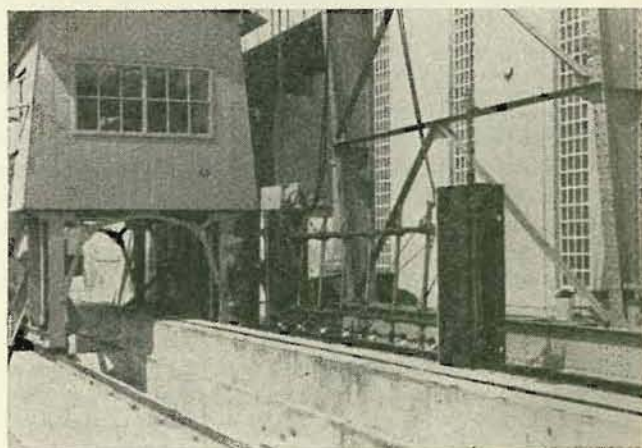


Fig. 531

During measurement the intake has been equipped with a provisional guide wall made of timber¹⁾. (See Fig. 532.) The intake may then be considered as a nozzle with parallel walls and of a rectangular cross section. The propeller were mounted so, that their axes were parallel to the upper and lower wall. The profile of velocities is also shown in the picture. The influence of the concrete supports of the racks can be clearly seen, because the racks were very near to the nozzle. In spite of the airfoil shape these supports cause hydraulic "shadows" and velocity losses. This is caused by the fact, that the socket of the nozzle deflected the stream lines, so that their course differed from that for which the supports were designed. The upper part of the diagram shows also a clear influence of the socket. It is obvious, that the length of the socket should have been increased. For this reason the horizontal measuring lines were close to each other but the stream lines did not run parallel to the propeller axes, as they were supposed to do.

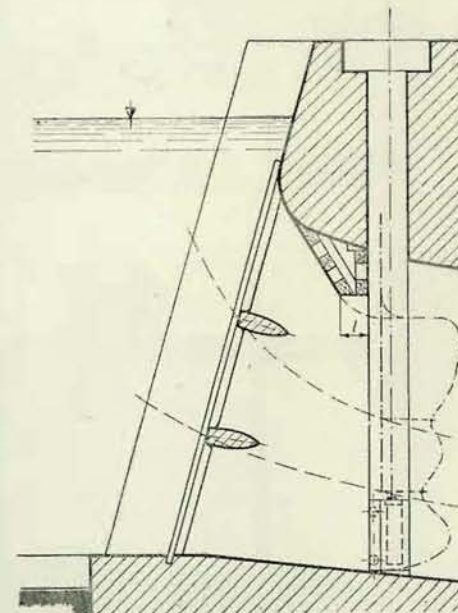


Fig. 532

Fig. 533 shows another type of a propeller cart used in a hydro plant where the high socle is before the intake. To eliminate its influence the measuring profile had to be shifted backward. The cart was guided in emergency gate slots and propellers were mounted on supports which protruded in the downstream direction. During lowering the cart the supports were slanted (Fig. 534) in order to pass through the opening and only afterwards they were fixed in position. The cart was shifted vertically to horizontal levels, which were determined in advance. Velocity was measured at 6 places simultaneously. Altogether the cart covered 8—11 horizontal levels. One turbine intake was divided by a pillar into two sections and the measurement was carried out in both sections separately. By this 96—154 measured points have been determined. The velocities measured were evaluated according to the above mentioned Standard Specification.²⁾

Gibson's method is suitable for measuring large flow rates at medium and high heads. Here flow rates are determined according to the pressure rise in the inlet pipe

¹⁾ Design of Ott (Kempten).

²⁾ See also Teyssler V.: Výkonnost a množství (Output and Quantity) Praha, 1935.

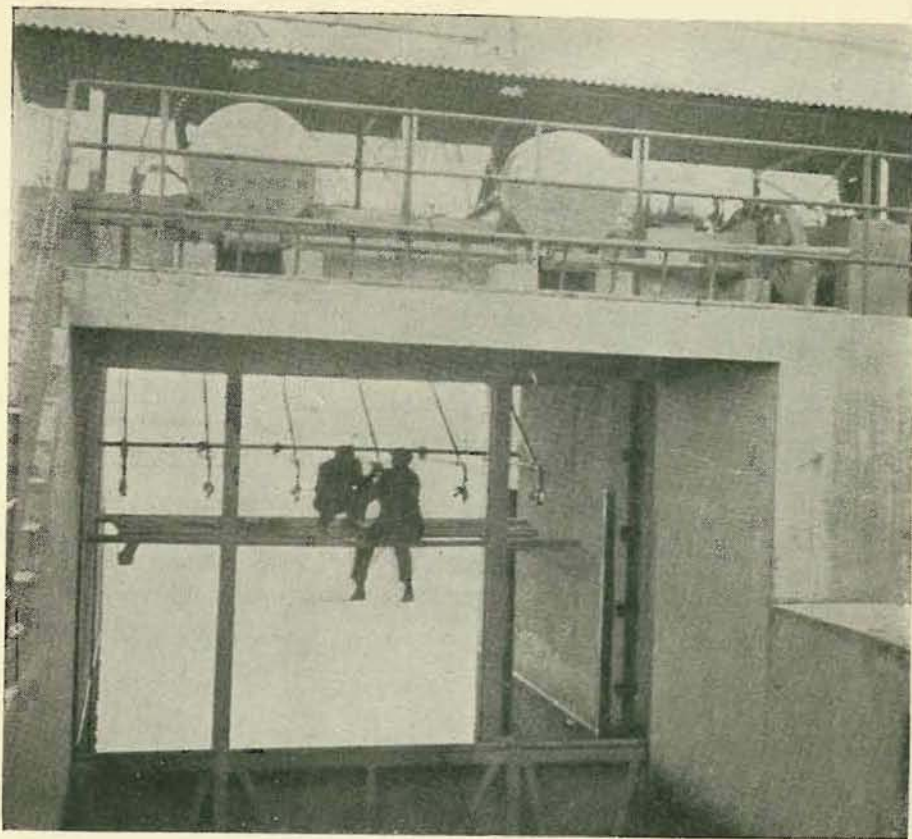


Fig. 533

after closing the guide apparatus.¹⁾ Poirson's method is suitable for measurements at high heads, where efficiency is determined by the increase of water temperature during passage through the turbine.²⁾

As we have no experience with these methods, we make no use of them.

¹⁾ Addison H.: Hydraulic Measurements, London, Chapman and Hall, 1946.

²⁾ Fontaine M.: Quelques applications de la méthode thermométrique Poirson. L'Houill: Blanche, 1951, p. 12.

Fig. 534



LITERATURE

BOOKS

- Addison H.: Hydraulic Measurements. London, Chapman and Hall, 1946.
- Alexeev A. E.: Konstruktsia elektricheskikh mashin. Moskva-Leningrad, Gosenergoizdat, 1949.
- Allievi-Dubs-Bataillard: Allgemeine Theorie über die veränderliche Bewegung des Wassers in Rohrleitungen. Berlin, Springer, 1909.
- Allievi-Gaden: Theorie du coup de bélier. Paris, Dunod, 1921.
- Bergeron L.: Du coup de bélier en hydraulique au coup de foudre en électricité. Paris, Dunod, 1950.
- Bosch V.: Vorlesungen über Maschinenelemente. Berlin, Springer, 1929.
- Camerer: Vorlesungen über Wasserkraftmaschinen. Leipzig, Engelmann, 1924.
- Černoch: Strojné technická příručka. (Mechanical Engineering Handbook.) Prague, Práce, 1947.
- ČSN 085010-1951, (Czechoslovak Standard): Vodní turbíny, předpisy pro zkoušení a záruky hydraulických a regulačních vlastností. II. revidované vydání normy ČSN 1021. (Hydraulic Turbines, Regulations for Tests and Guarantees of hydraulic and regulating properties. 2nd revised Edition of Standard ČSN 1021.) Prague, Průmyslové vydavatelství, 1951.
- Dobrovolný: Pružnost a pevnost. (Strength of Materials.) Prague, Ústav pro učební pomůcky, 1944.
- Dubbl H.: Taschenbuch für den Maschinenbau. Part II. Berlin, 1943.
- Dubs R.: Angewandte Hydraulik. Zurich, Rascher, 1947.
- Ergebnisse der Aerodynamischen Versuchsanstalt zu Göttingen, 1.—4. Lieferung. Berlin, Oldenbourg 1925—1932.
- Erhart F.: Kritická a zvuková rychlost média. (Critical and sonic Velocity of Medium.) Prague, Technické knihkupectví, 1937.
- Escher R.: Die Theorie der Wasserturbinen. Berlin, Springer, 1924.
- Fabritz G.: Die Regelung der Kraftmaschinen. Wien, Springer, 1940.
- Falz: Grundzüge der Schmiertechnik. Berlin, Springer, 1926.
- Föppl: Drang und Zwang, I.—II. Berlin, Oldenbourg, 1928.
- Gamze-Goldsher: Tekhnologiya proizvodstva krupnikh ghidroturbin. Moskva-Leningrad, Gosnautchtechizdat, 1950.
- Granovskiy-Orgo-Smolyarov: Konstruktsiyi ghidroturbin i roztchet yikh detailei. Moskva-Leningrad, Mashgiz, 1935.
- Grimm L.: Přednášky o vodních motorech na býv. čes. vys. škole techn. v Brně. (Lectures on Hydraulic Motors, Techn. Univers., in Brno.)
- Havliček: Mazání strojů a hospodaření oleji v průmyslových podnicích. (Machine Lubrication and Lubricant Economy in Industrial Plants.) Prague, Práce, 1947.
- Hoeck: Druckverluste in Druckleitungen großer Kraftwerke. Zurich, Leemann u. Co.
- Hruschka A.: Druckrohrleitungen der Wasserkraftwerke. Wien-Berlin, 1929.
- Hütte, des Ingenieurs Taschenbuch, I.—II., Berlin, Ernst u. Sohn, 1925, 1926.
- Hýbl J.: Vodní motory, I.—III. (Hydraulic Motors, Parts I to III), Prague, Česká matice technická, 1922, 1924, 1928.
- Jäger: Technische Hydraulik. Basel, Birkhäuser, 1949.
- Joukovski, see Zhukovski.
- Kaplan-Lechner: Theorie und Bau von Turbinen-Schnellläufern. München-Berlin, Oldenbourg, 1931.
- Keyl-Häckert: Wasserkraftmaschinen und Wasserkraftanlagen. Leipzig, Fachbuchverlag, 1951.
- Kieswetter J.: Vodní stroje lopatkové, přednášky. (Hydraulic Turbomachinery. Lectures.) Brno, Donátův fond, 1939.

- Kvyatkovskiy*: Maliye ghidroturbiny. Moskva, Gosnautchtechizdat, Mashinostroy. lit., 1950.
Letecký průvodce, 2. díl. (Aerial Guide, Part 2.) Prague, Česká matice technická, 1939.
Mashinostroyeniye. Part 12. Moskva, Gosnautchtechizdat, 1948.
Morozov: Ispolzovaniye vodyanoy enyergiyi. Moskva-Leningrad, Gosenergoizdat, 1952.
Mostkov and Bashkirov: Roztchety ghidravlicheskogo udara. Moskva-Leningrad, Gosenergoizdat, 1952.
Nechleba M.: Theorie indirektní regulace rychlosti. (Theory of Indirect Speed Regulation, 2nd Edition. (Prague, Technickovědecké vydavatelství, 1952.
Nowotny: Werkstoffzerstörung durch Kavitation. Berlin, VDI-Verlag, 1942.
Oguey Mamin: Étude théorique et expérimentale de la dispersion du jet... Lausanne, 1944.
Petrov N. P.: Ghidrodinamicheskaya teoriya smazki. Leningrad, Izdatelstvo Akademiyi Nauk SSSR, 1948.
Pfarr: Die Turbinen für Wasserkraftbetrieb. Berlin, 1912.
Prandtl L.: Führer durch die Strömungslehre. Braunschweig, Vieweg, 1944.
Proskura: Ghidrodinamika turbomashin. Moskva, Energoizdat, 1934.
Sokolov: Ghidravlicheskiye turbiny dlya malykh GES. Moskva, Gosenergoizdat, 1951.
Spannhake: Kreisräder als Pumpen und Turbinen. Berlin, Springer, 1931.
Stodola A.: Die Dampf- und Gasturbinen. Berlin, Springer, 1922.
Šmerák V.: Kluzná ložiska. (Slide bearings.) Prague, Průmyslové vydavatelství, 1950.
Technický průvodce - Části strojů. Sv. 6, část II. (Technical Guide - Machine Parts. Vol. 6, Part II.) Prague, Česká matice technická, 1951.
Technický průvodce - Pružnost a pevnost. (Technical Guide - Strength of Materials.) Prague, Česká matice technická, 1944.
Ténot A.: Turbines hydrauliques et régulateurs de vitesse. Part I—III. Paris, Eyrolles, 1935.
Teyssler: Výkonnost a množství. (Output and Quantity.) Prague, Česká matice technická, 1935.
Thoma D.: Zur Theorie des Wasserschlosses. Berlin, Oldenbourg, 1910.
Thomann R.: Die Wasserturbinen und Turbinenpumpen. Part I and II. Stuttgart, K. Wittwer, 1924 and 1931.
Tietjens: Hydro- und Aeromechanik nach Vorlesungen von L. Prandtl. Berlin, Springer, 1929—1931.
Timoshenko S.: Pružnost a pevnost. (Strength of Materials. [Translated from Russian].) Prague, Vědeckotechnické vydavatelství, 1952.
Weinig: Strömung um die Schaufeln von Turbomaschinen. Leipzig, Barth, 1935.
Zhukovskiy: Aérodynamique, Paris, 1916.

PERIODICALS

- Ackeret*: Experimentale und theoretische Untersuchung über Hohlraumbildung im Wasser. Technische Mechanik und Thermodynamik I, (1930).
Ackeret, de Haller: Über die Zerstörung von Wasserstoffen durch Tropfenschlag und Kavitation. Schweizerische Bauzeitung 108 (1936), p. 105.
Armanet: Quelques applications des lois de similitudes... Informations techniques Charmilles No. 3.
Bleuler: Strömungsvorgänge an hydraulischen Drosselklappen bei Hohlraumbildung. EWAG - Forschung an Turbomaschinen, p. 31.
Boyle, White: 62,000 h. p. Vertical Six-Nozzle Impulse Turbines for the Bridge River Hydrodevelopment. ASME (1951), p. 289.
Bovet: Contribution au calcul de la résistance mécanique d'une bache spirale. Informations techniques Charmilles No. 1, (1945).
Braun E.: Über Turbinendiagramme. Zeitschrift für das gesamte Turbinenwesen, (1909).
Bundschuh: Wirtschaftlicher Entwurf von Turbinenrohrleitungen. Wasserkraft und Wasserwirtschaft, (1931), p. 56.
Casacci, Jarriaud: Mesure des poussées hydrauliques des turbines Francis à axe vertical. La Houille Blanche, (1950), p. 326.

- Casacci, Peuchmaur*: Études expérimentales sur le fonctionnement des pivoteries industrielles. La Houille Blanche, 1951, p. 23.
Dahl: Die Strömungs- und Druckverhältnisse in schnellaufenden Wasserturbinen. Wasserkraft und Wasserwirtschaft, 1940, p. 1.
Druckmüller M.: Důsledky změny počtu lopatek Kaplanových turbin. (Consequences of Blade Number Variations in Kaplan Turbines.) Strojirenství 2, (Mechanical Engineering) No. 7, 1952, p. 295.
Dubs R.: Die Bedeutung des Saugrohres. Wasserkraftjahrbuch (1924), p. 437.
Dubs R.: Die Beeinflussung des Wirkungsgrades durch das Saugrohr. Wasserkraftjahrbuch (1925/26), p. 338.
Federhofer: Zur strengen Berechnung liegender weiter Rohre. Wasserkraft und Wasserwirtschaft (1943), No. 10, p. 237.
Ferrand: La conduite forcée unique pour hautes chutes à grande puissance. La Houille Blanche (1946), p. 245.
Foltýn V.: Kavitační zkoušky na modelech vodních turbin. (Cavitation Tests on Models of Hydraulic Turbines.) Strojnický obzor (Mechanical Engineering Review), 1950, No. 12.
Foltýn V.: Kathodická ochrana proti kavitační korozi. Strojirenství 2. (Cathodic Protection against Cavitation Corrosion. Mechanical Engineering 2.) 1952.
Fontaine M.: Quelques applications de la méthode thermométrique Poirson. La Houille Blanche (1951), p. 12.
Föttinger: Untersuchungen über Kavitation und Korrosion bei Turbinen, Turbopumpen und Propellern. Hydraulische Probleme VDI (1925).
Gynt S.: Recent Development of Bearings and Lubrication Systems for Vertical Generators. ASEA-Journal (1947), p. 72.
Joukovskiy, see Zhukovskiy.
Keller, Vuskovic: Strömungsversuche an Sicherheitsorganen von Wasserkraftanlagen. EWAG-Mitteilungen (1942/43) - 100 Jahre Turbinenbau, p. 191.
Kieswetter J.: Kavitační jevy na lopatkách vodních turbin. (Cavitation Phenomena on Blades of Hydraulic Turbines.) Strojnický obzor (Mechanical Engineering Review), 1937.
Kieswetter J.: Ustálení vodního proudu v kanálech lopatkových strojů. (Stabilization of the Water Flow in Passages of Turbomachinery.) Strojnický obzor (Mechanical Engineering Review), 1941, p. 105.
Kieswetter J.: Výpočet a konstrukce zubových pump. (Calculation and Design of Gear Pumps.) Technické zprávy Škodových závodů (Technical Reports of Skoda-Works), 1939, (No. 3), 1940, (No. 1), 1942, (No. 1).
Knapp, Hollander: Laboratory Investigation of the Mechanism of Cavitation. Transaction ASME, (1948).
Kohn F.: Uzavírací orgány vodních turbin. (Closing Organs of Hydraulic Turbines.) Strojirenství 2 (Mechanical Engineering 2), 1952, p. 24.
Kratochvíl St.: Kavitační jevy u výpustného potrubí a u uzavěrů přehradních. (Cavitation Phenomena in Outlet Pipes and Closures of Dams.) Strojnický obzor (Mechan. Engin. Rev.) 1937, Nos. 7 and 9.
Kraus H.: Strömung in Spiralgehäusen. Zeitschrift VDI 79 (1935), No. 44, p. 1345.
Kutta: Auftriebskräfte in strömenden Flüssigkeiten. Illustrierte Aeronautische Mitteilungen (1902).
Kutta: Über ebene Zirkulationsströmungen. Müncher Ber. (1910 und 1911).
Lafoon: Hydraulic Turbine Generators. Water Power (1949), p. 64.
Lieber J. H.: Procédé de jaugeage d'une installation à base chute et gros débit. Informations techniques Charmilles (1947), No. 2, p. 36.
Meissner L.: Die Kaplanturbinen des Wasserkraftwerks Neu-Ötting. VDI-Zeitschrift 93 (1951), p. 868.
Meissner, Rudert: Einige Konstruktionsmerkmale neuerzeitlicher Großfreistrahlturbinen. Wasserkraft und Wasserwirtschaft 38 (1943), p. 153.

- Meyer H.: Calcul des cercles de vannage des turbines hydrauliques. Bulletin technique de la Suisse romande (1932).
- Michalec J.: Vliv použitých energetických zdrojů na hospodářské utváření krajů. (Influence of the Power Sources on the Economic Development of the Country.) Strojnický obzor 29 (Mech. Engin. Rev. 29), 1949, No. 12.
- Mühlemann E.: Zur Aufwertung des Wirkungsgrades von Überdruck-Wasserturbinen. Schweizerische Bauzeitung 66 (1948), p. 331.
- Nechleba M.: Cirkulace kolem lopatky vodní turbíny. (Circulation around the Blades of a Hydraulic Turbine.) Strojnický obzor (Mech. Engin. Rev.), 1943, No. 15/16.
- Nechleba M.: Doplnění diagramu Višněgradského a jeho aplikace na regulaci vodních turbin. (Supplement of Vishnyegrad-Diagram and Its Application to the Regulation of Hydraulic Turbines.) Strojirenství 3 (Mechanical Engineering 3), 1953, p. 787.
- Nechleba M.: Kaplan Turbine Blading. 4th World Congress of Energy, London, 1950.
- Nechleba M.: Nový hydraulický regulátor vodních turbin ČKD. (New Hydraulic Regulator of the Hydraulic Turbines of Type ČKD.) Strojirenství 1 (Mechanical Engineering 1), 1951, No. 7/8, p. 264.
- Nechleba M.: Sur la fonction de cavitation, La Houille Blanche 1947, p. 117.
- Nechleba M.: Pevnostní výpočet oběžného kola Francisovy turbíny. (Strength Calculation of a Francis Turbine Runner.) Strojirenství 2 (Mechan. Engineering 2), 1952, No. 7, p. 292.
- Nechleba M.: Pevnostní výpočet regulačního kruhu o dvou táhlech. (Strength Calculation of a Regulating Ring with Two Pull Rods.) Strojnický obzor (Mech. Eng. Rev.), 1941, p. 317.
- Nechleba M.: K zákonu o mechanické podobnosti vodních turbin. (On the Law of Hydraulic Similarity of Hydr. Turbines.) Technický sborník pro odbor strojně elektrotechniky, SAVU, Bratislava. (Technical Review of Mechanical and Electrical Engineering, Slovak Academy of Science and Arts.) Bratislava, 1952, No. 3, p. 33.
- Nekolný J.: Výpočet a návrh zubové pumpy. (Calculation and Design of a Gear Pump.) Strojnický obzor (Mech. Eng. Rev.), 1941, p. 260.
- Němec K.: Konstrukční provedení hydraulického regulátoru vodních turbin ČKD. (Design and Construction of the Hydraulic Regulator for Hydraulic Turbines of Type ČKD.) Strojirenství 1 (Mechanical Engineering 1), 1951, No. 7/8, p. 268.
- Osobennosti technologii odlivky pracovního kola i statora ghidroturbíny Francisovy dlya Dnieprovskoy GES. Vyestnik mashinostroyeniya (1947), p. 59.
- Performance of Vertical Water Wheel Thrust Bearing during the Starting Period. Transaction ASME 68 (1947), No. 40, p. 543.
- Poulter: The Mechanism of Cavitation Erosion. Journal of Applied Mechanics, 1942.
- Pozdunin: Základy teorie, konstrukce, a práce superkavitujících lodních šroubů. (Fundamentals of Theory, Design, and Function of Supercavitating Ship Propellers.) Czech Translation from Izvestiya Akademii Nauk SSSR (1945), No. 10/11.
- Prášil: Über die Flüssigkeitsströmungen in Rotationshöhlräumen. Schweizerische Bauzeitung 41, 1903.
- Pressure Pipe Lines. Water Power, 1950.
- Ribaux A.: Pompes à vis. Bulletin technique de la Suisse romande, 1943, p. 256.
- Roberts: The 103,000 hp Turbines at Shasta Dam. Transaction ASME (1948), p. 217.
- Salto de Castro: Water Power (1953), p. 84.
- Salzmann, Süß: Festigkeitsuntersuchungen an Spiralgehäusen. EWAG-Mitteilungen (1942/43) - 100 Jahre Turbinenbau, p. 164.
- Schauta: Der geometrische Zusammenhang der Betriebskurven. Wasserkraft und Wasserwirtschaft, 1935, p. 222.
- Schnyder: Über Druckstöße in Rohrleitungen. Wasserkraft und Wasserwirtschaft, 1932, p. 49.
- Schnyder: Die Festigkeitsberechnung der Regulierringe für Wasserturbinen und Pumpen. Dissertation ETH-Zürich, (1930).
- Schoklitsch: Spiegelbewegung in Wasserschlössern, Schweizerische Bauzeitung 1923, p. 129.

- Smirnov: Zakon podobiya i modelirovaniya ghidroturbin. Kotloturbostroyeniye, 1947, No. 3.
- Stein T.: Die optimale Regelung von Wasserturbinen. Schweizerische Bauzeitung 70, 1952, p. 287.
- Sylvestre V.: Contribution à l'histoire de la houille blanche et le part de la Savoie dans la conquête de l'énergie hydroélectrique. La Houille Blanche, 1946, p. 293.
- Shalnev: Shchelevaya Kavitatsiya. Inzheneriy Sbornik, Akademiya Nauk SSSR, book VIII, 1950.
- Šmerák: Prüfung und Bewertung von Lagerwerkstoffen. Škoda-Mitteilungen (1943), Nos. 1 and 2.
- Thoma D.: Zur Theorie des Wasserstoßes in Rohrleitungen. Zeitschrift für das gesamte Turbinenwesen, 1918, p. 293.
- Thomann R.: Über Drucksteigerung in Rohrleitungen bei Betätigung von Absperrorganen. Wasserkraft und Wasserwirtschaft, 1936.
- Turbina LMZ typ Francisovy, mozhnosty 102,000 HP. Vyestnik mashinostroyeniya, 1947, p. 25.
- Wasserbauer A.: Zkoušky na velkých vodních elektrárnách. (Tests in Large Hydraulic Power Stations.) Strojnický obzor (Mech. Eng. Rev.) 24, (1944), No. 7, p. 99.
- Zhukovski (Joukovski): Über die Konturen der Tragflächen der Drachenflieger. Zeitschrift für Flugtechnik und Motorluftschiffahrt, (1919).
- Zhukovski N. E.: O ghidravlicheskom udare v vodoprovodnikh trubakh. Trudy IV ruskogo vodoprovodnogo syezda, Odessa, 1901.

INDEX

A

Absolute velocity 17, 36
Acceleration of water in discharge duct 578
— of restoring mechanism 438, 468
Aerodynamic properties in airfoils 328
Air chamber 442
Airfoil (see geometric characteristics of airfoils) 330
Air pressure tank of controller 445
Allievi - water hammer 554
Anchorage of pipes (see pipe seating) 539, 545
Angle of attack 345, 347
Angular velocity 39
Aspect ratio of wing 346
Axial deformation, effect of, in water hammer 555
Axial-flow turbine 17
Axial load (axial force) 189, 359

B

Ball valve 607
Bandage 540, 551
Bánki turbine 23
Bearing 60, 301, 360, 512
Bernoulli equation 31
— — for relative motion 313
Biel expression (for loss coefficient in pipes) 85
Blade angles 36, 75
Bladeless space 37, 138
Blasius expression (for loss coefficient in pipes) 81
Blocking of controller (by pressure regulator) 610
Boundary layer 320
Brakes 62, 478
Braun's turbine diagrams 106
By-pass valve 612, 617

C

Calculation, energy 30, 32
— volume 30
—, of control 466
Camerer formula (for recalculation of efficiency) 83
Casing of Pelton turbine 426
Cavitation 54
— coefficient 54, 97, 235
Centrifugal force 48, 400
— turbine 18, 90

Centripetal turbine 18
Change of speed of controllers 460
Characteristics of controller 433, 609
— of pipe 566
— of turbine 97
Classification of turbines 23, 80
Closure 593, 620
Circulation 209, 313
Circular projection 142, 352
Coefficient of friction, f 481, 484
— of lift and drag, c_z , c_x , k_z , k_x ; 327, 345
Compressor, air, for pressure vessel 439
Conformal representation 146, 151
Conical turbine 18
Constant-pressure (impulse) turbine 49
Controller of air content 445
— of flow 440
— of speed 439
— with air pressure tank 445
Control of pressure wave 560, 565
— of runner 427
Coriolis force 41
Critical speed 243
Curvature of blade 392

D

Deflector 63, 441
— of jet 411, 432
Deformation of pipes (water hammer) 552
Design units 224, 359, 423
Deviation angle (effective blade angle) 37, 345
Deviator 63, 411
Direct impact (see total impact)
Discharge loss 29, 43
Distributing head 60, 478
Double regulation (of speed) 411, 462
Draft tube 50, 132, 218, 305
Driving pressure (overpressure, underpressure) on blade 54, 178
Dynamic viscosity 481

E

Economical diameter of pipes 535
Effective output (see Output, effective)
Efficiency, hydraulic 26, 43, 51, 81
—, mechanical 26
—, of draft tube 50
—, of pump 439
— turbine, total, 24, 26, 87
—, volumetric 24

Electric drive of governor 453
Elementary turbines 114, 123
Emergency governor, safety governor 555, 591
Energy 15, 26
— equation 36, 57, 72
Entrance shock 44, 88, 94, 108
Euler energy equation (see Energy equation)
Exaggeration of blade angles 157
Expansion joint 540
Extension of regulation 278

F

Filling of turbine 86, 112, 116
Filter 61
Fink regulation 58
Flow fields 123, 125
Flow in stationary ducts 30
Flow-rate equation 31, 45, 57
— of turbine 86, 92, 417
— under head of lm 67
— unit 69
Flow surface 114, 123
Force acting on blade 180, 204, 325
— of inertia 438
Fournayon turbine 22
Francis turbine 22, 57, 112, 123
Friction (see coefficient of friction)
Froude number 64

G

Gap (clearance) of runner 58, 192, 241
— cavitation 347
Gate hoist oil pump 439
Gates 589, 604
Gear case 309
Geodetic head 28
Geometric characteristics of airfoils 329
— similarity 64, 85
Girard turbine 23, 49
Governor of controller 434, 450
—, safety 584
Graphical method of water hammer analysis (Schnyder-Bergeron) 566
— — of surge tank analysis 583
Grids 28
Gross head (see Head, gross)
Guarantee measurement 623
— tests 623
Guide apparatus (see Guide wheel)
— blade 58, 200, 250
— wheel 200

H

Hanger structure 478, 526
Head, H 24, 26
—, geodetic 28
—, gross 26
—, hydraulic 26
—, indicated 72
—, net 26, 28
—, of ball valve 609
—, of valve 602
—, usable 26, 28
Head race level control 460
Helmholtz-Thomson theorem 317
High-pressure turbine 80, 309
Hub of runner 123
Hydracone 219
Hydraulic governor 454
— head (see Head, hydraulic)
— load (see Axial load)
— pull (see Axial load)
— similarity 64, 103, 118
— theory of lubrication 481

I

Idealized surge tank 581
Indicated head (see Head, indicated)
— (specific) velocity 72, 385
Indirect impact 560
Induced angle of attack 337
— drag 337
Inlet valve 596, 601, 615
— velocity 36, 37
Insulation of thrust bearing 526
Isodrome 435
— control 435

J

Johnson's surge tank 582, 585
Joints of pipes 539
Joukowski expression for water hammer (see also Zhukovski) 552
— lift 320

K

Kaplan draft tube 222
— turbine 23, 61, 312, 344
Kinematic viscosity 83, 482
Kutta-Joukowski (also Kutta-Zhukovski) theorem 320

L

Labyrinth 60, 242, 245
Laminar flow 126
Lattice 340

Lid of turbine 58, 293
 Lift 320, 321, 327
 Load, axial (see Axial load)
 Losses 24, 27, 44, 87
 Loss in pipes 82
 — head 82
 Lubrication 301, 511, 529
 Lubricating installation 529

M

Magnus effect 317
 Mechanical losses 96
 Mechanism of gate hoists 596
 — of rapid closure valves 593
 Measurable width 162
 Measurement of flow rate 623
 — of head 623
 Meridional velocity (subscript m) 44, 124, 200
 — sections 140
 Michaud's formula (water hammer) 555
 Mises expression (for loss coefficient in pipes) 83
 Mixed-flow (radiaxial) turbine 17
 Model turbine 97, 118
 Modulus of elasticity of cast iron 555
 — — of steel 543, 555
 — — water 555
 Moment of blade 44
 — of duct 35
 — of momentum 36
 — of turbine 96, 105
 —, starting 97
 — unit, M_1 70
 Moody expression (for recalculation of efficiency) 83
 Mud valve 617

N

NACA airfoils 331
 Needle (of Pelton turbine) 62, 415
 — (of pressure regulator) 612
 — balancing (Pelton turbine) 62, 431
 Newton equation 32
 Nozzle 415, 431
 Number of blades 153, 200, 389

O

Oblique discharge from guide apparatus 157, 159
 Oil cooling 527
 — dash pot 435, 592
 — film 490, 503, 515
 — vessel 61, 450

Oil pump for bearing 61
 — — — controller 439
 — — — gate hoist 593
 Oscillation of surge tank level 580
 Outlet velocity 37, 134, 144, 158
 Output, effective 24, 90, 379
 — for head of 1 m 67
 —, hydraulic 26, 96
 —, theoretical 24
 —, unit 70
 — of turbine 24, 89, 379
 Overpressure of runner 45, 132, 190, 325

P

Parallel run of alternators 472
 Partial admission turbine 22
 Pelton turbine 23, 62, 374, 425
 Peripheral velocity, U 36, 381
 — component of velocity (subscript n) 42
 Pilot valve 434, 446
 Pipe protection, differential 590
 — —, maximal 590
 Pipes 533, 547
 —, burst of 590
 —, connections (flanges) 538
 —, high pressure 550
 —, starting time of 467, 470, 554
 Pit of turbine 209
 Potential of velocity (see Velocity potential)
 — — flow 129
 — — whirl 316
 Pressure drop 239, 307, 469
 — rise (see water hammer)
 — (reaction) turbine 17, 49
 — regulator 609
 Propeller turbine 23, 62, 344
 Proskura diagram 341, 342
 Pumping unit of bearings 527, 615
 — — of ball valve 606
 — — of controller 450, 459
 — — of gate hoist 593, 598
 — — of pressure regulator 613

Q

Quick-closing device 591
 — — devices for pipes 598
 — — gates 593

R

Radial-flow turbine 17
 Radiaxial (mixed-flow) turbine 17
 Reciprocating motors 15
 Reduced cross section 211, 286

Reflection of pressure wave 560, 564
 Regulating heart 282
 — (shifting) ring 59, 257
 — shaft 278
 — mechanism 59, 259, 278
 Regulation, internal, external, 61, 253, 257
 —, work of, A 259
 Reiffenstein turbine 23
 Relative velocity, W 17, 36, 382
 Relative change of speed 466
 Relief of runner 58, 60
 — valve 609, 612, 615, 618
 Representation of blade sections 140
 Restoring mechanism 435
 Return motion gear (see Restoring mechanism)
 Reverse shock 61
 Reynold's number, Re 82, 83
 Runaway speed, n_p (see Speed, runaway)
 Runner blades of Francis turbine 77, 140, 179, 225
 — — — Kaplan turbine 349, 355, 359
 — — — Pelton turbine 390
 Runner duct (see Blade duct)
 — of Francis turbine (see also Split runners) 57, 163, 225
 — — Kaplan turbine (see also Hub of runner) 344, 359
 — — Pelton turbine 62, 381, 427
 Rupture of water column 61

S

Safety devices 358, 615
 Schnyder-Bergeron (see graphical analysis of water hammer)
 Schoklitsch's method (see graphical analysis of surge tank)
 Seating of pipes 538, 541
 Segment bearing (see thrust bearing)
 Segments 499, 505, 513
 Servomotor of ball valve 609
 — — controller 279, 433
 — — guide wheel 279
 — — rapid closure valve 593, 598
 — — runner 363
 Shaft 59, 242, 248, 363
 Shell turbine 21
 Shut down tests of controllers 443, 475
 Similarity, hydraulic (see Hydraulic similarity)
 — of cavitation 105, 239
 — with regard to strength 100
 Sliding surface of thrust bearings (see Segments)
 Slot link of runner 462

Space of turbine 131, 342
 Spacing of blades, t , 147, 327
 Span of wing 339
 Specific gravity of water 24
 — load of blade 180, 327
 — speed 70, 99, 374
 — velocities 71
 Speed, for head of 1 m 66
 —, normal 477
 —, runaway 95
 —, specific (see Specific speed)
 —, unit of 69
 — of sound (pressure wave in pipes) 552, 557
 Spiral 209, 284
 Split runners 231
 Stability of controller 435, 469
 — of flow 354
 — of large swings 587
 — of surge tanks 576
 Standard CSN 085010-1951 30, 476, 621
 Starting whirl 322
 Start of operation 616
 Stay blades of spiral 217, 284
 Stopping whirl 322
 Stream line 123
 Stuffing box 15, 59, 296, 362
 Suction head 54, 177
 Surface area of surge tanks 576
 Surge tank 532, 576, 580
 — —, Johnson's 582, 585
 — —, with throttled flow 581
 — — — upper and lower level 581
 — —, swing of level of 580
 Synchronous speed 119, 472, 477
 Swing of level (see Surge tank)

T

Tail race 26
 Tangential turbine 18
 Tank 61, 450
 Test pressure 547
 Thoma's surface area 579
 Throttled flow of surge tank 581
 Through flow resistance 31, 534
 — — velocity 16, 534, 617
 Thrust bearing, sliding surface of (see Segments)
 Time of closure of ball valve 609
 — — closure (opening) of controller 467
 — — — of gate hoist 593, 595
 — — — of pressure regulator 613
 — — falling of isodrome 467
 — — level oscillation of surge tank 580

— — one interval of pressure wave 552
— — starting of pipe 467, 470, 554
— — — the machine 467
Total impact (water hammer) 554, 559
Triangle of velocities, 36, 65
Turbines, classification and development
(see Classification of turbines)
Turbulent flow 127
Type series of turbines 119

U

Unit, running in of 532
Unit values 69, 102
Unloading valve of pump 443

V

Valve, ball 605, 616
—, by-pass 607, 617
—, control 433
—, mud 617

—, of turbine air supply 61, 305
—, relief 607, 617
Velocity diagram 157, 384
— potential 130, 314
— triangle 36, 65
Viscosity (dynamic) 481

W

Water hammer 551
— —, linear course of 553, 558
— jet (Pelton turbine) 374, 380
— wheel 15
Whirl fibre 317, 318
Work of regulation (see Regulation work)
— — — in connection with turbine 42

Z

Zhukovski expression for water hammer 552
— lift 320

UNIVERSITY OF ILLINOIS-URBANA

621.24N28VEM C001
HYDRAULIC TURBINES\$PRAGUE



3 0112 007957308